PROGRESS TOWARD THE SYNTHESIS OF (+)-ZOANTHENOL

AND

THE DEVELOPMENT OF AN ASYMMETRIC TSUJI ALLYLATION REACTION

Thesis by

Douglas Carl Behenna

In Partial Fulfillment of the Requirements

for the Degree of

Doctor of Philosophy

California Institute of Technology

Pasadena, California

2007

(Defended November 6, 2006)

To my parents

for their constant support

ACKNOWLEDGEMENTS

There are several people without whom this thesis would not have been possible. Brian is first among these. In addition to his impressive knowledge of science, Brian's enthusiasm, creativity, and dedication have been an inspiration to me during my successes and failures in graduate school. His guidance and support have been indispensable. I learn something every time he picks up a piece of chalk. I'm grateful for the latitude he's allowed me in pursuing some of my own ideas. I'm only beginning to appreciate how much moxie that requires when one is an assistant professor trying to get tenure. It's been a luxury to have an advisor whose door is always open to discuss problems or new ideas. Moreover, Brian and Erna are really nice people. They made the group feel like a family in the early days of the lab, frequently hosting parties at their apartment.

I also want to thank my committee members. Professor Dave MacMillan and Professor John Bercaw have been on my committee from the beginning. I'm grateful for the time and effort they clearly put into reviewing my work. Their insights and critique of my candidacy report and research proposals encouraged me to think about the big picture as well as details. More recently, Professor Bob Grubbs has added a valued perspective. Our group has benefited from collaborations with Professor Bill Goddard for several years, and I am particularly thankful that he was willing to join my committee with such little notice.

As an undergraduate at the University of Pennsylvania, Professor Dewey McCafferty took me into his lab and got me excited about research. Dewey allowed me to work on meaningful aspects of very interesting projects. I benefited from his broad

perspective in science and his belief in my abilities. Dewey was tremendously important in my decision to go to graduate school, and my decision to work for Brian was in no small part due to their many similarities. As a chemist at the bench, I was fortunate to learn much from a true master, Professor Predrag Cudic, then a postdoc in the McCafferty group.

I've benefited greatly from the support of the Fannie and John Hertz Foundation during my time in graduate school. In addition to essential financial support, I have greatly enjoyed the opportunities to attend the Foundation's conferences, and camaraderie of the other fellows.

I've been fortunate to collaborate with some truly exceptional chemists in the Stoltz group. Dr. Jeff Bagdanoff did important work in the early phases of the zoanthenol project. Jenn Stockdill and I have toiled together for three years to make the quaternary stereocenters in zoanthenol. Through good and bad results she's kept me motivated in the dog days of grad school. I'm lucky to be leaving that project in the hands of someone as talented and hardworking as she is. Additionally, her editing has kept the majority of this thesis from reading like a Borat skit.

One of the most rewarding aspects of grad school for me has been watching others in the group extend the Tsuji allylation project in creative ways. JT Mohr was my closest collaborator on the allylation chemistry. The "protonation bet" is sure to go down in Stoltz group lore. Besides being a creative chemist, he's always good for engaging discussion, obscure music (at least to me), and the occasional game of dry ice hockey. There is always room for more people on "Team Tsuji" these days. Dr. Kousuke Tani, Dr. Toyoki Nishimata, Nat Sherden, Dr. Dave White, Dr. Zoli Novák, and Smaranda

Marinescu have all contributed substantially to the development of the method. John Keith has been a great help as our computational collaborator and adopted member of Team Tsuji. It's difficult to draw a line in our group between methodology development and application in total synthesis. Sandy Ma, Dr. Andy Harned, John Enquist, and Jenny Roizen have made strides in both areas. Ryan McFadden, Mike Krout, Dr. Jeff Servesko, and Brinton Seashore-Ludlow have taken on the challenge of applying this work to natural products synthesis. Sandy Ma deserves special recognition as my longest tenured baymate and as an aficionado of 80s music. I've also had the good fortune to work with Megumi Abe, James Hegeman, and Eric Kwei while they were undergraduates. I learned a lot from the experience. I hope they did too.

In my mind all the Stoltz group plank owners stand out. Eric Ashley was my roommate for several years, and our late-night discussions on chemistry, politics, and life were a great frustration reliever. He and Jenn were always willing to get whichever was warranted, coffee or beer. In the early days of 204 Church, Dr. Jeremy May and Sarah Spessard were always the bay to visit for a good conversation. I always took inspiration from the work ethic of Professor Richmond Sarpong and Dr. Eric Ferreira.

While all the research groups in Church, Crellin, and Noyes were generous in donating chemicals and know-how in the early days of the Stoltz group, the Berkeley-era MacMillan group members deserve special mention. Professor Tehshik Yoon, Professor Vy Dong, Dr. Jake Wiener, and Dr. Chris Borths understood the pressure of working in a new lab, and were always willing to help. More recently, it was nice to hear a familiar accent in Dr. Nikki Goodwin's voice.

In addition to the faculty and students there are a number of people that make Caltech's chemistry department a great place to do science. I might be the last grad student that can remember a time before Dr. Mona Shahgholi and Dr. Scott Ross took over in the mass spectral and NMR facilities, respectively. Trust me, we are lucky to have them. Dr. Mike Day and Larry Henling did all the hard work of obtaining the X-ray structures in this thesis. They have an amazing ability to wring good data from the poor crystals I invariably grow. Six years of experience have convinced me that if Dana Roth can't find it, it doesn't exist. Dian Buchness has probably untangled more red tape for me than I even know about. Her efforts will be missed by the graduate students in this department.

My parents were my first teachers and continue to be my most stalwart supporters. I can only hope to live up to the role model they provided. Finally, I can't imagine going through grad school without my fiancée, Angela. Her encouragement, patience, and proofreading made this thesis possible. Somehow, I hope I can give her as much as she's given me.

ABSTRACT

The stereoselective synthesis of all carbon quaternary stereocenters is an important problem in synthetic chemistry due to their common occurrence in bioactive compounds. The zoanthamine class of marine natural products highlights the challenge in constructing such stereocenters. After a summary of the isolation, structure determination, and biological activities of the zoanthamine natural products, published approaches toward their chemical synthesis are reviewed.

Synthetic strategies toward the carbocyclic portion of zoanthenol focus on the synthesis of the three challenging quaternary stereocenters located on the central C ring. An unusual acid-mediated S_N' cyclization of a nucleophilic arene with an allylic alcohol forms the B ring and diastereoselectively constructs the benzylic C(12) quaternary stereocenter. However, difficulties with late-stage installation of the remaining C(9) quaternary stereocenter compelled the use of C ring synthons containing the vicinal C(9) and C(22) stereocenters installed at an early stage in the synthesis. Desymmetrization of a *meso*-anhydride containing vicinal quaternary stereocenters accomplishes this goal in an enantioselective fashion. Several C ring synthons bearing the vicinal quaternary stereocenters are elaborated with A ring fragments, and several methods for the formation of the C(11)-C(12) bond in these systems are explored. Ultimately, a radical conjugate addition strategy provides the carbocyclic core of zoanthenol with the correct relative configuration of all three quaternary stereocenters.

These efforts toward the synthesis of zoanthenol highlight the difficulty in generating enantioenriched α-quaternary cycloalkanones derived from ketones with multiple acidic α-hydrogens. The first direct catalytic enantioselective access to such products is achieved by the application of chiral bidentate phosphinooxazoline (PHOX) ligands to Tsuji's non-enantioselective allylation reactions. Cyclic allyl enol carbonates, silyl enol ethers, and allyl β-ketoesters all provide uniformly excellent yields and high enantioselectivity in the reaction. The limitations on the substrate scope of the reaction are discussed. Preliminary studies into the mechanism of these allylation reactions with prochiral enolate fragments suggest that they occur by a different mechanism than the outer-sphere nucleophilic attack commonly proposed in the alkylation of prochiral allyl fragments.

TABLE OF CONTENTS

LIST OF FIGURES

List of Schemes

LIST OF TABLES

List of Abbreviations

$[\alpha]_D$	specific rotation at wavelength of sodium D line
Ac	acetyl
ACN	acetonitrile
Ad	adamantyl
app	apparent
aq	aqueous
Ar	aryl group
atm	atmosphere
BBN	borabicyclo[3.3.1]nonane
BHT	2,6-di-*tert*-butyl-4-methylphenol
BINAP	2,2'-Bis(diphenylphosphino)-1,1'-binaphthyl
Bn	benzyl
Boc	*tert*-butoxycarbonyl
BOM	benzyloxymethyl
bp	boiling point
br	broad
BSA	*N*,*O*-bis(trimethylsilyl)acetamide
Bu	butyl
n-Bu	*n*-butyl
t-Bu	*tert*-butyl
Bz	benzoyl
c	concentration for optical rotation measurement

^{13}C	carbon 13, isotope
/C	supported on activated carbon
°C	degrees Celsius
cat.	catalytic
calc'd	calculated
CAM	ceric ammonium molybdate stain
CAN	ammonium cerium (IV) nitrate
Cbz	benzyloxycarbonyl
CCDC	Cambridge Crystallographic Data Centre
comp	complex
CSA	camphorsulfonic acid
conv	conversion
Cy	cyclohexyl
d	doublet
dba	dibenzylideneacetone
DBU	1,8-diazabicyclo[5.4.0]undec-7-ene
DCC	1,3-dicyclohexylcarbodiimide
DCE	1,2-dichloroethane
DCM	dichloromethane or methylene chloride
DEAD	diethyl azodicarboxylate
DIBAL	diisobutylaluminum hydride
DIOP	2,3-O-isopropylidene-2,3-dihydroxy-1,4-bis(diphenylphosphino)butane
DIPA	diisopropyl amine

DMA	N,N’-dimethylacetamide
DMAP	4-dimethylaminopyridine
dmdba	3,5,3’,5’-dimethoxydibenzylideneacetone
DME	1,2-dimethoxyethane
DMF	dimethylformamide
DMP	Dess-Martin periodinane
DMPU	N,N'-dimethyl propylene urea
DMS	dimethylsulfide
DMSO	dimethylsulfoxide
DNA	deoxyribonucleic acid
DPPB	1,4-bis(diphenylphosphino)butane
DPPE	1,2-bis(diphenylphosphino)ethane
dr	diastereomeric ratio
ee	enantiomeric excess
E	entgegen olefin geometry
EI	electrospray ionization
equiv	equivalent(s)
Et	ethyl
EtOAc	ethyl acetate
FAB	fast atom bombardment
g	gram
GC	gas chromatography
Grubbs II	Grubbs’ second generation metathesis catalyst

[H]	reduction
h	hour(s)
hν	light
^{1}H	proton
^{3}H	tritium
HMDS	hexamethyldisilazide or hexamethyldisilizane
HMPA	hexamethylphosphoramide
HPLC	high performance liquid chromatography
HRMS	high resolution mass spectroscopy
Hz	hertz
η^n	eta; n = number of atoms coordinated to metal
IC_{50}	concentration required for 50% growth inhibition
imid.	imidazole
IR	infrared spectroscopy
J	coupling constant
k_n	rate constant, n refers to various reactions, negative n indicates reverse reaction
kcal	kilocalories
KHMDS	potassium hexamethyldisilazide
L	liter
LAH	lithium aluminum hydride
LDA	lithium diisopropylamide
LD_{50}	Lethal Dosage to kill 50% of test population
LiHMDS	lithium hexamethyldisilazide

m	meta
m	multiplet or milli
μ	micro
M	mega, metal, or molar
m/*z*	mass to charge ratio
m-CPBA	*meta*-chloroperbenzoic acid
Me	methyl
(*R*,*R*)-Me-DUPHOS	(-)-1,2-Bis((2R,5R)-2,5-dimethylphospholano)benzene
MEK	methyl ethyl ketone
MH-60	mouse myelohybridoma cells
MIC	minimal inhibitory concetration
min	minute(s)
mol	mole(s)
mol%	percentage used based on moles
MOM	methoxymethyl
(*R*)-MOP	(R)-(+)-2-(Diphenylphosphino)-2'-methoxy-1,1'-binaphthyl
mp	melting point
Ms	methanesulfonyl
MS	molecular sieves
MTPA	α-methoxy-α-(trifluoromethyl)phenylacetic acid
MVK	methyl vinyl ketone
N	normal

NBS	*N*-bromosuccinimide
NMR	nuclear magnetic resonance
NOE	nuclear Overhauser effect
o	ortho
[O]	oxidation
p	para
PCC	pyridinium chlorochromate
PDC	pyridinium dichromate
PG	prostaglandin
Ph	phenyl
pH	hydrogen ion concentration in aqueous solution
Ph-H	benzene
PHOX	phosphinooxazoline
Phth	phthalamidyl
Piv	pivaloyl
PMA	phorbol myristate acetate
PMB	*p*-methoxybenzyl
PMBM	*p*-methoxybenzyloxymethyl
p.o.	administered orally
ppm	parts per million
PPTS	pyridinium *p*-toluenesulfonate
Pr	propyl
i-Pr	isopropyl

psi	pounds per square inch
Py or Pyr	pyridine
q	quartet
QUINAP	(R)-(+)-1-(2-Diphenylphosphino-1-naphthyl)isoquinoline
R	alkyl group
R	rectus (configurational)
Red-Al	sodium bis(2-methoxyethoxy)aluminum hydride
R_f	retention factor
RNA	ribonucleic acid
s	singlet
S	sinister (configurational)
SAR	structure-activity relationship
sat.	saturated
stoich.	stoichiometric
t	triplet
TBAF	tetrabutylammonium fluoride
TBAT	tetrabutylammonium triphenyldifluorosilicate
TBDPS	*tert*-butyldiphenylsilyl
TBS	*tert*-butyldimethylsilyl
temp	temperature
TEA	triethylamine
TES	triethylsilyl
Tf	trifluoromethanesulfonyl

TFA	trifluoroacetic acid
THF	tetrahydrofuran
TIPS	triisopropylsilyl
TLC	thin-layer chromatography
TMEDA	tetramethylethylenediamine
TMS	trimethylsilyl
TOF	turnover frequency
TON	turnover number
TPAP	tetrapropylammonium perruthenate
TROC	trichloroethoxycarbonyl
Ts	*p*-toluenesulfonyl or *p*-toluenesulfonic
UV	ultraviolet
Vis	visual wavelength
v/v	volume per volume
w/v	weight per volume
X	halide or trifluoromethanesulfonate
Z	zusammen olefin geometry

CHAPTER ONE

A Biological and Chemical Introduction to the Zoanthamine Alkaloids

1.1 Isolation of Zoanthamine Alkaloids

1.1.1 *The Order Zoantharia*

The order zoantharia comprises an intriguing group of marine polyps. This order has been morphologically classified into at least a dozen genera, and recent analysis of their respective mitochondrial DNA has elucidated the relationships between them.[1] Species in this order are widely dispersed throughout the temperate and tropical littoral regions of the Indian, Pacific, and Atlantic Oceans. These soft corals are generally aggressive colonizers of reef environments. In the wild, they are known to reproduce both sexually[2] and by asexual budding of new polyps.

Figure 1.1 Representative Zoanthids

The polyps have a tube-shaped body and are radially symmetric. Atop the body are tentacles that guide food to the central orifice for digestion. Additionally, zoanthids frequently contain symbiotic microalgae, which provide energy via photosynthesis. These dinoflagellate algae also play an important role in the biosynthesis of secondary metabolites originally isolated from the zoanthids.[3] When alarmed, the polyps contract their tentacles inward, and some species also expel from their bodies a stream of water laden with powerful toxins as a means of defense from predators. As a result of their vibrant pigmentation, zoanthids are prized as specimens for marine aquariums and are commonly sold as "sea mats."

1.1.2 *Natural Products Isolated from the Order Zoantharia*

A rich diversity of natural product archetypes has been isolated from species in the order zoantharia (Figure 1.2). Zoanthusterone (**1**) is a representative ecdysteroid isolated from a *Zoanthus sp*.[4] Prostaglandins like PGA_2 (**2**), isolated from *Palythoa kochii*, have been shown to stabilize microtubules in a manner similar to paclitaxel.[5] A family of more than a dozen natural products based on the highly fluorescent zoanthoxanthin (**3**) skeleton has been isolated from *Parazoanthus axinellae*.[6] A related demethylated structure, parazoanthoxanthin A, has shown significant anticholinesterase activity.[7] Both red[8] and yellow[9] fluorescent proteins containing novel chromophores have been isolated and crystallographically studied. Perhaps the best known compound isolated from these marine organisms is palytoxin (**4**). Palytoxin was isolated from *Palythoa sp*. in the Hawaiian islands and remains one of the most toxic compounds

known, with an LD_{59} of 15 μg/kg in mice.[10] The structure of palytoxin was determined and later synthesized by Kishi.[11]

Figure 1.2 Representative Natural Products from Zoanthids

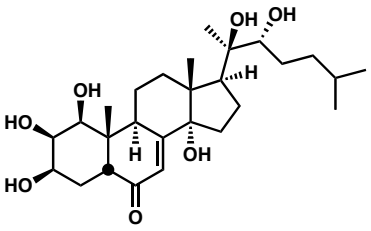

Zoanthusterone ***(1)***

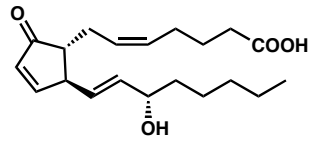

PGA_2 ***(2)***

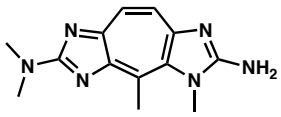

Zoanthoxanthin ***(3)***

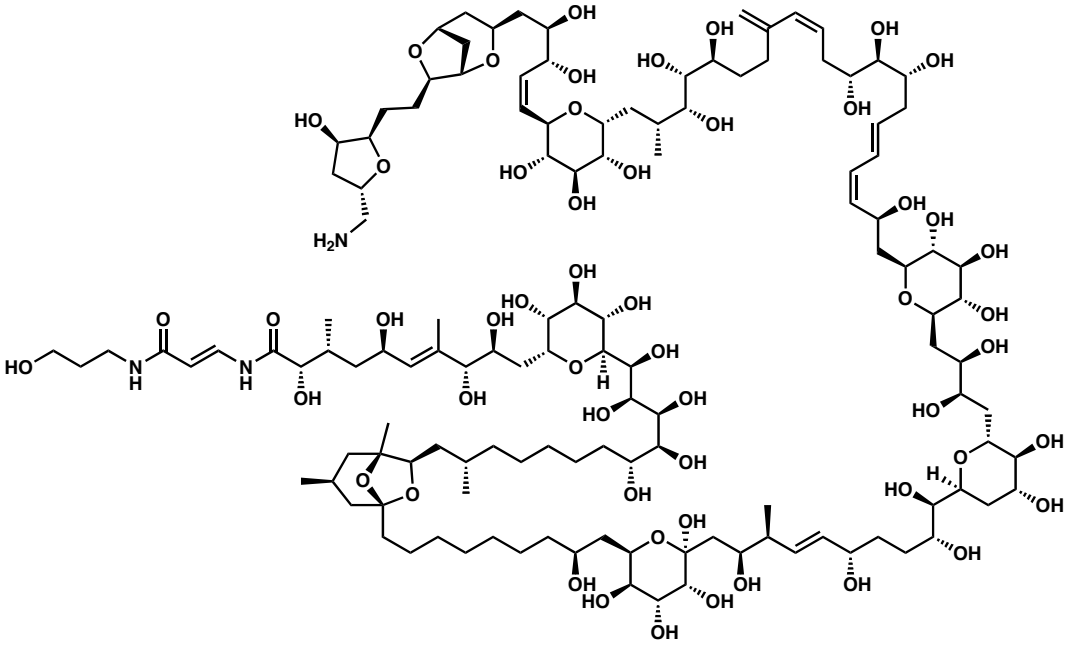

Palytoxin ***(4)***

1.2 The Zoanthamine Natural Products

1.2.1 *Isolation and Structural Characterization*

In 1984, the isolation of the natural product zoanthamine (**5**) from a species of the genus Zoanthus off the Visakhapatnam coast of India was disclosed. The connectivity

and relative stereochemistry of the previously unknown alkaloid skeleton was unambiguously determined by single crystal X-ray diffraction.[12] This isolation effort also afforded the related natural products zoanthenamine (**6**) and zoanthenamide (**7**).[13] The same group later described 28-deoxyzoanthenamine (**8**) and 22-*epi*-28-deoxyzoanthenamine (**9**) from a Zoanthus species isolated in the Bay of Bengal.[14] The latter four structures were deduced by comparison with zoanthamine's spectroscopic data. Originally, this isolation effort was undertaken in search of a known eye irritant produced by the Zoanthus species. However, all five of the isolated alkaloids showed some inhibition of phorbol myristate acetate (PMA) inflammation in mouse ears. The function of the zoanthamine alkaloids in the producing organisms is unknown.

Figure 1.3 Zoanthamine Natural Products Isolated by Rao

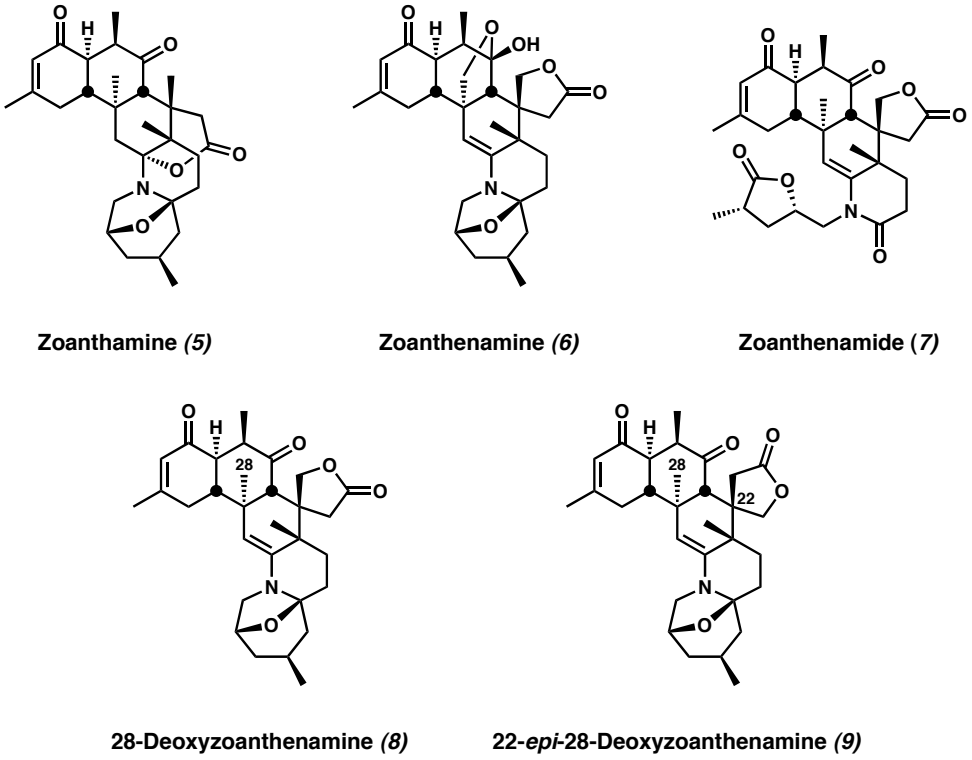

In 1995, Uemura and coworkers identified five new zoanthamine natural products isolated from a Zoanthus species collected off the Ayamaru coast of the Amami Islands south of Japan.[15] Among these, norzoanthamine (**10**) and norzoanthaminone (**11**) lack the C(26) methyl group, while in oxyzoanthamine (**12**) the C(26) methyl group has been oxidized. The relative configuration of norzoanthamine was confirmed by X-ray diffraction.[15] The absolute configuration of norzoanthamine, later determined by NMR analysis of MTPA derivatives, is shown in Figure 1.4.[16] The C_{30} alkaloid related to norzoanthaminone (**11**), zoanthaminone (**13**), was amenable to X-ray crystal structure determination as disclosed by Clardy.[17] Cyclozoanthamine (**14**) and epinorzoanthamine (**15**) represent intriguing modifications to the enone functionality typical of zoanthamines. Both structures were assigned by extensive NOE experiments.[15]

Figure 1.4 Zoanthamine Natural Products Isolated by Uemura and Clardy

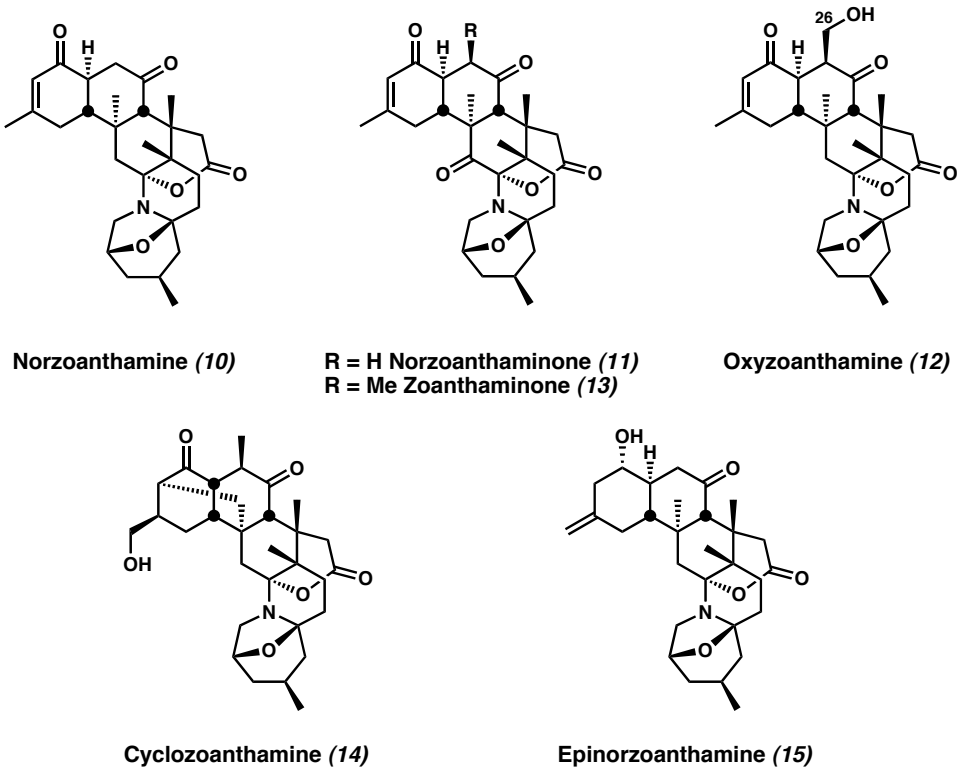

Zoanthids isolated from the Canary Islands by Norte and coworkers in 1996 provide zoanthamine natural products with several interesting oxidation patterns (Figure 1.5). Epioxyzoanthamine (**16)** is unique in its C(19) stereochemistry, which was determined by comparison with NMR data for oxyzoanthamine.[18] 3-Hydroxyzoanthamine (**17)** and 30-hydroxyzoanthamine (**18)** show novel sites of oxidation, while 11-hydroxyzoanthamine (**19)** and 11-hydroxynorzoanthamine (**20)** are presumably related to zoanthaminone and norzoanthamineone. Finally, zoanthenol (**21**) has a unique oxidized aromatic A ring, which removes the C(13) and C(18) stereocenters. As a result of the structural change, extensive HMBC and ROESY correlation experiments were performed to confirm its structure and relative stereochemistry.[19]

Figure 1.5 Zoanthamine Natural Products Isolated by Norte

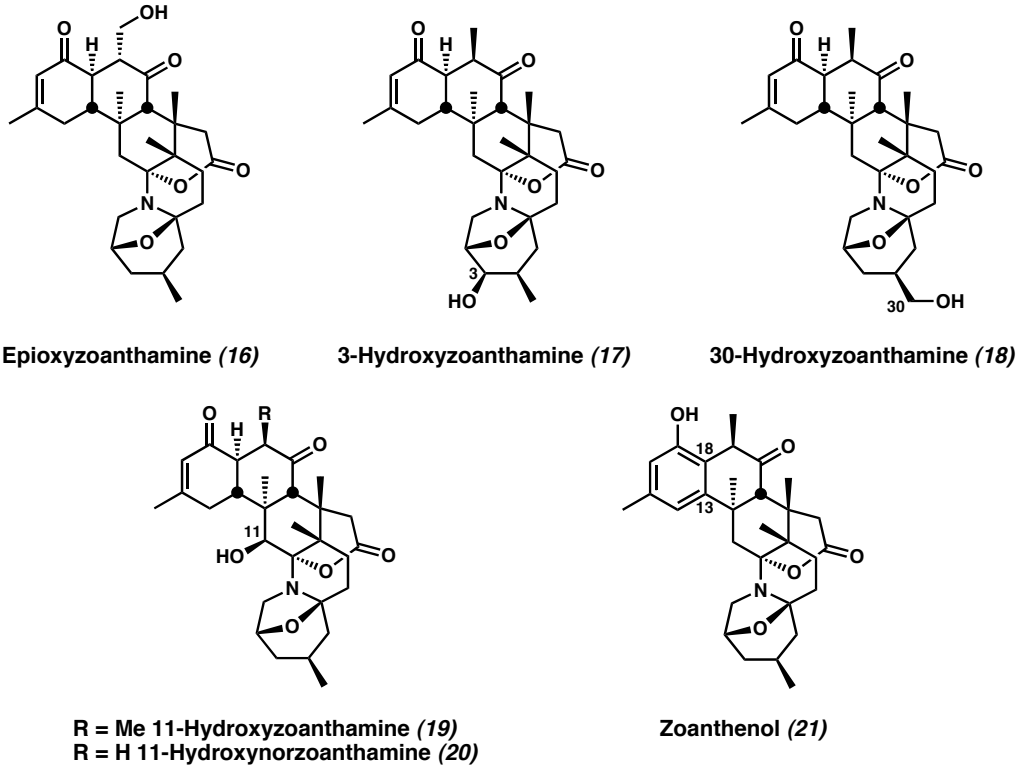

1.2.2 *Biosynthesis of the Zoanthamine Natural Products*

The C_{30} skeleton of the zoanthamine natural products led to initial biosynthetic speculation focused on triterpene precursors.[12] However, no normal head-to-tail isoprene connectivity could account for the zoanthamine skeleton. More recently, Uemura has proposed that the zoanthamine natural products may arise via a polyketide construction (Scheme 1.1).[16,20] The proposed intermediate **22** accounts for most of the oxygenation found in the zoanthamines. While no definitive statement can be made about biosynthesis, there appears to be support for the polyketide hypothesis.[18]

Scheme 1.1 Hypothetical Polyketide Precursor

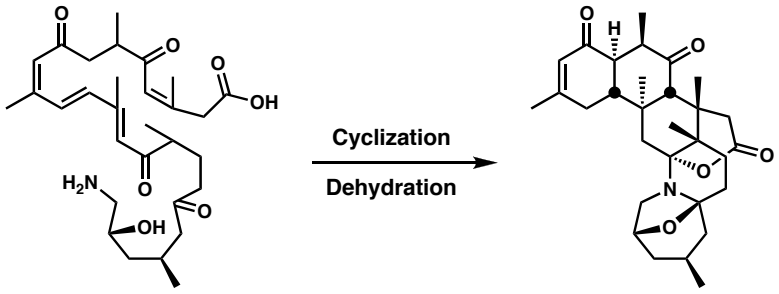

Hypothetical Polyketide Precursor *(22)* **Zoanthamine *(5)***

Another factor complicating the understanding of zoanthamine alkaloid biosynthesis is the role of the symbiotic dinoflagellate algae that are commonly contained in zoanthids. Although such symbiotic strains are difficult to culture in isolation, Nakamura and coworkers have been able to produce quantities of *Symbiodinium sp*. free of zoanthids.[21] Algae of the genus *Symbiodinium* have been isolated from zoanthids of the genus Zoanthus.[22] While the algae produced different distributions of metabolites depending on the media used, Nakamura's group was able to isolate a new C_{30} alkaloid

they named zooxanthellamine (**23)** after significant experimentation with culture conditions. Zooxanthellamine exists as a mixture of imine and lactone forms (Figure 1.6). Its structure and relative configuration were delineated from extensive NMR studies. Zooxanthellamine was shown to have the same sense of absolute configuration as the zoanthamine alkaloids by NMR comparison of its MTPA esters.[21] The remarkable similarity between zooxanthellamine and zoanthamine has called into question the role of the zoanthids in producing the zoanthamine natural products.[23] It may be that the zoanthids play only a small role in adjusting the oxidation state of the completed zoanthamine skeleton. The subtle variations in the alkaloids' structures could be determined by factors in the marine environment or by the host zoanthid species. Alternatively, different algae species may be involved in the production of different zoanthamines.

Figure 1.6 Structure of Zooxanthellamine

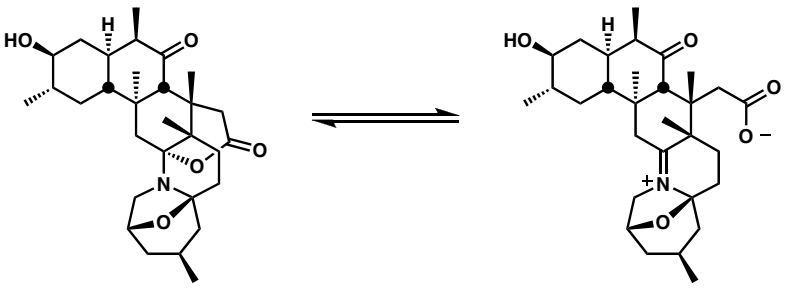

Zooxanthellamine *(23)*

Another intriguing biosynthetic question involving the zoanthamine natural products is the origin of the norzoanthamine-type alkaloids, which lack the C(26) methyl group. The isolation of oxyzoanthamine prompted Uemura and coworkers to propose a

mechanism for the demethylation of zoanthamines (Scheme 1.2). They propose oxidation of the zoanthamine to the intermediate oxyzoanthamine, which then undergoes a retro aldol, formally releasing formaldehyde and the noralkaloid.[15]

Scheme 1.2 Proposed Biosynthesis of the Norzoanthamines

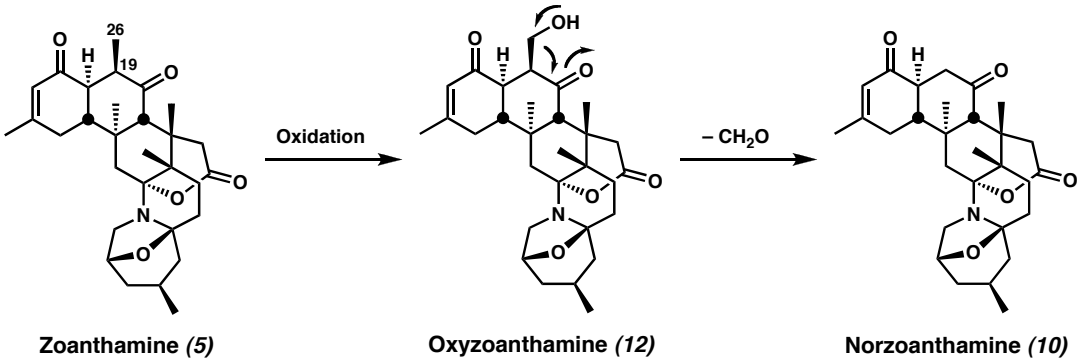

1.2.3 *Chemical Reactivity of the Zoanthamine Natural Products*

Fluxion between lactone and imine isomers, similar to the equilibration observed with zooxanthellamine, has been demonstrated in several zoanthamine natural products (Scheme 1.3). Norzoanthamine forms iminium **24** under acidic conditions and reverts upon neutralization.[20] Under neutral to basic conditions, elimination forms enamine **25**. The equilibrium between norzoanthamine and enamine **25** was demonstrated by the conversion of norzoanthamine to methyl ester **26** in minutes upon exposure to diazomethane.[20] Furthermore, NMR spectra of norzoanthamine in D_2O show specific and complete deuterium incorporation at the 11β position to give deuteride **27** in minutes.[18,19] Similar rates of deuterium incorporation were observed with zoanthenol, 3-hydroxynorzoanthamine, and 30-hydroxnorzoanthamine. In contrast, the 11β-hydroxyzoanthamines did not show significant deuterium incorporation, suggesting that

the elimination to an enamine is inaccessible.[19] This fluxional behavior in aqueous media at physiologically relevant pHs may play an important role in determining the bioactivities of these molecules.

Scheme 1.3 Equilibria Between Lactone and Enamine Isomers of Norzoanthamine

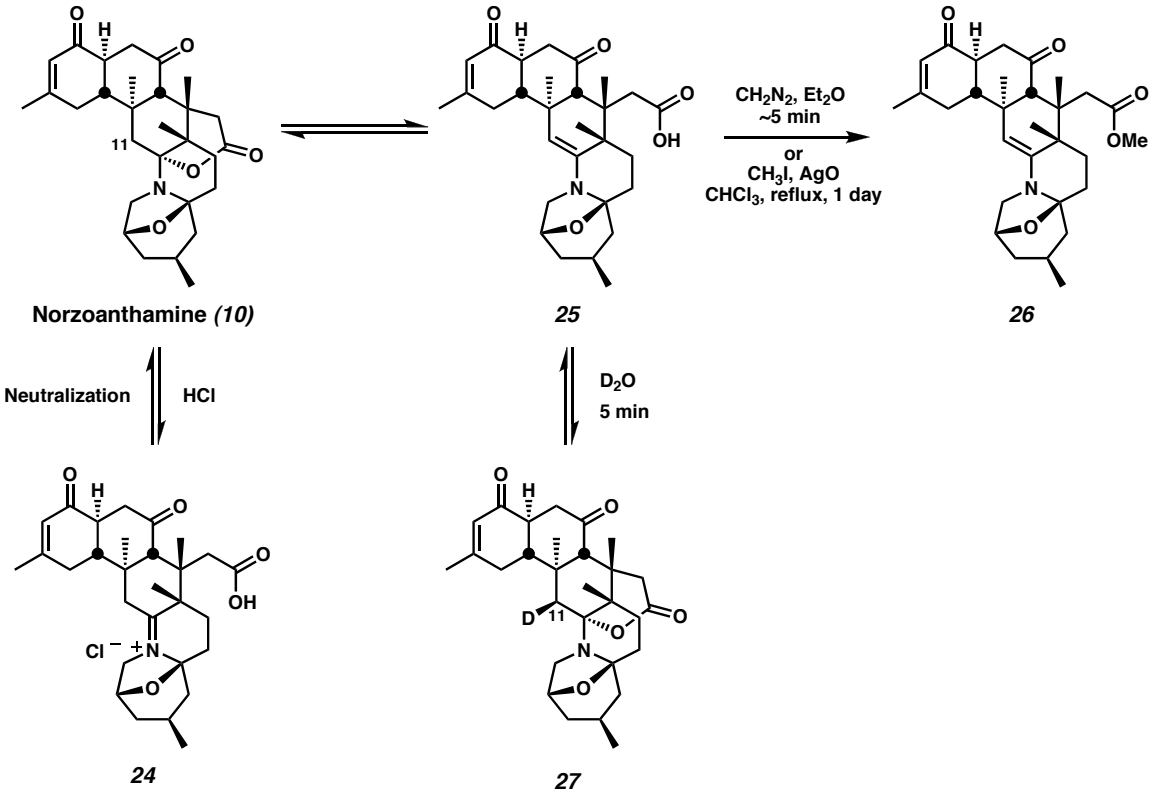

The hemiaminal region of the zoanthamine alkaloids also shows intriguing reactivity under reductive conditions. Treatment of norzoanthamine with sodium borohydride generates two anomalous products, enone **28** and allylic alcohol **29** (Scheme 1.4).[20,16] Under the reaction conditions, enamine **31** is believed to attack the lactone in an intramolecular fashion to afford keto-iminium **32**. Dehydration generates iminium **33**, which undergoes reduction to give enone **28**. Further reduction affords allylic alcohol **30**.

Scheme 1.4 Anomalous Reduction of Norzoanthamine

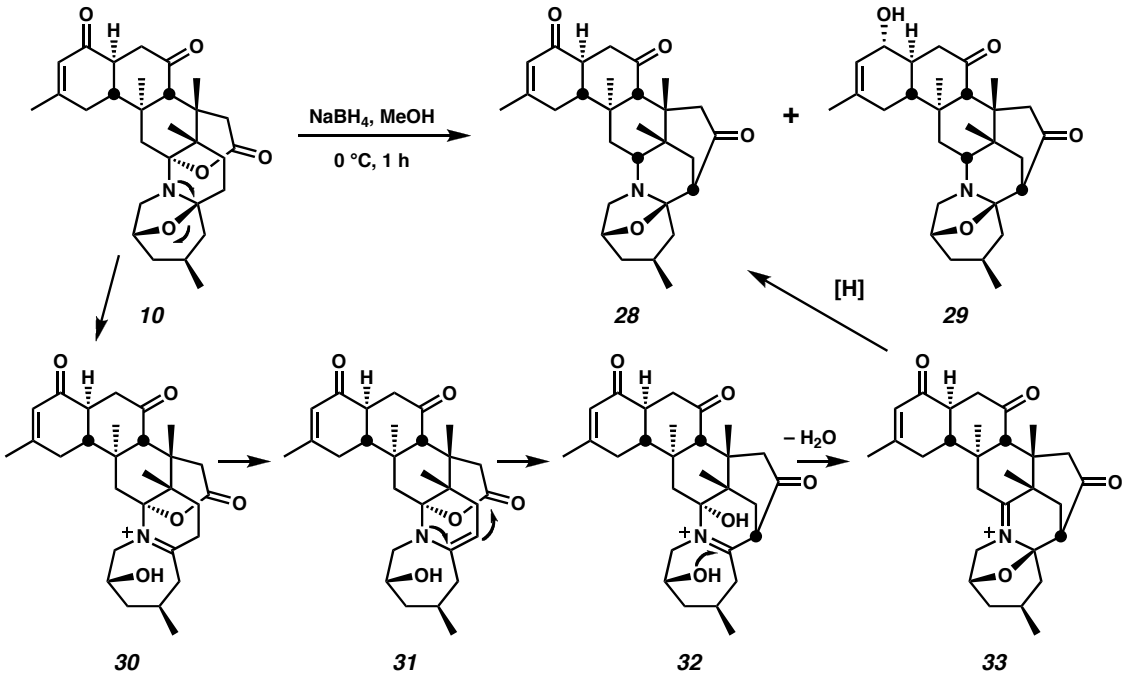

1.3 Biological Activities of Zoanthamine Alkaloids

1.3.1 *Antiosteoporotic Activity*

Perhaps the best studied and most well-known biological activity of the zoanthamine alkaloids is the antiosteoporotic effect first reported by Uemura in 1996.[24] Norzoanthamine and its hydrochloride salt have been shown in vivo to prevent the symptoms of osteoporosis in ovariectomized mice, a pharmaceutical model for postmenopausal osteoporosis. Osteoporosis is a loss of bone mineral density that often results when osteoclasts reabsorb bone tissue at a rate faster than it is regenerated.[25] In the model, ovariectomized mice, lacking in estrogen, quickly lose bone mass and strength. At doses of 0.4 and 2.0 mg/kg/d (five days a week for 4 weeks, *p.o.*) of norzoanthamine hydrochloride, the ovariectomized mice retained femur weight at statistically higher rates than untreated ovariectomized mice.[26] Additionally, with doses

from 0.016-0.4 mg/kg/d of norzoanthamine hydrochloride the femurs of ovariectomized mice maintained strength, as measured by failure load, nearly comparable to unovariectomized control mice.[27] Finally, mice treated with norzoanthamine hydrochloride were observed to possess cortical bone significantly thicker than that found in the control animals.[28]

In analogy to estrogen replacement therapy in postmenopausal women, ovariectomized mice can be rescued from the effects of osteoporosis by treatment with 17β-estradiol. However, treatment with norzoanthamine hydrochloride shows interesting differences from estrogen therapy. Uterine atrophy, a side effect of estrogen deficiency after ovariectomy, is not affected by treatment with norzoanthamine hydrochloride.[28] This ability to restore bone strength without eliciting other side effects associated with steroid hormone receptors is a highly desirable property.

The origin of norzoanthamine's antiosteoporotic effect may lie in its ability to suppress the production of interleukin 6 (IL-6). Norzoanthamine and its hydrochloride salt **24** have been shown to suppress the excretion of IL-6 from preosteoblastic cells at concentrations of 13 and 4.6 μg/ml, respectively, in vitro.[29] IL-6 is in turn involved in stimulating the generation of osteoclasts, which reabsorb bone tissue. Estrogen derives its antiosteoporotic properties from the inhibition of IL-6 production.[30] However, in vitro studies on osteoblasts with norzoanthamine hydrochloride showed no effect on osteoclast formation. Also, the suppression of IL-6 secretion has not yet been demonstrated in vivo.[28] These last two points, along with the lack of uterine weight gain in ovariectomized mice, suggest that the zoanthamine alkaloids may act by a mechanism distinct from estrogen's.[31]

The need to find non-estrogen therapies to prevent the onset of osteoporosis has spurred considerable effort to define a structure activity relationship (SAR) for norzoanthamine's antiosteoporotic effects, despite its unclear molecular target. Via semi-synthesis, Uemura and coworkers produced and tested a number of norzoanthamine derivatives.[20,29] It should be noted that all of the derivatives assayed were significantly less efficacious (higher IC_{50} values) in limiting IL-6 production than norzoanthamine (Figure 1.7).[32] The removal of the olefin (ketone **35** and diol **36**) caused some loss in activity. However, disruption of the lactone/hemiaminal functionality (carboxylic acid **37** and ester **27**) caused the greatest drops in activity.[20]

Figure 1.7 SAR Study of Norzoanthamine's Ability to Inhibit IL-6 Production

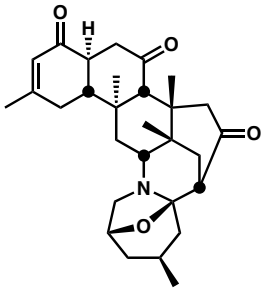

28

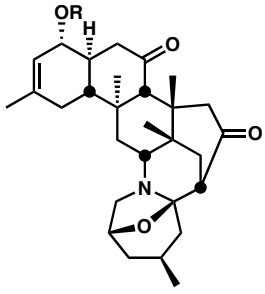

29, R = H
34, R = OAc

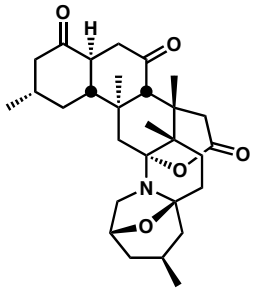

35

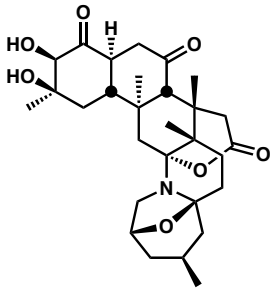

36

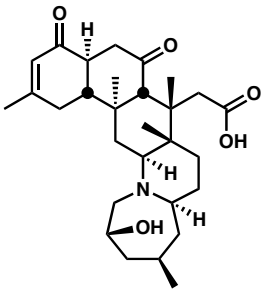

37

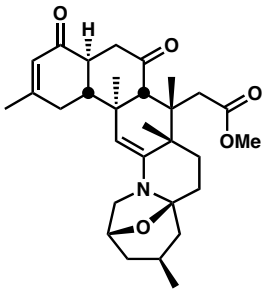

26

Compound	IC_{50} (μg/mL) for Suppression of IL-6 Production
Norzoanthamine *(10)*	13
28	25
29	30
34	23
35	45
36	35
37	42
26	>100

More recently, Hirama and coworkers have studied the SAR of zoanthenol-related molecules to inhibit the growth of IL-6 dependent MH-60 cells (Figure 1.8). In their assays, the zoanthamine hydrochloride salts **24** and **38** showed the strongest inhibition of IL-6 production with IC_{50} values of 13 and 26 μM, respectively. A truncated mimic of zoanthenol's "northern" carbocyclic region **39** and a mimic of the zoanthamine "southern" heterocyclic region **40** both showed very poor activity. However, iminium **41**, the hydrochloride salt of heterocycle **40**, demonstrated a significant amount of the activity found in the zoanthamine hydrochlorides.[33] This result provides further support for two trends: (a) the hydrochloride salt form of a zoanthamine molecule is a more active inhibitor of IL-6 production than the natural product, and (b) the heterocyclic portion of the molecule contains a large part of the pharmacophore for IL-6 inhibition.

Figure 1.8 SAR of Zoanthenol Analogues' Inhibition of IL-6 Dependent Cell Growth

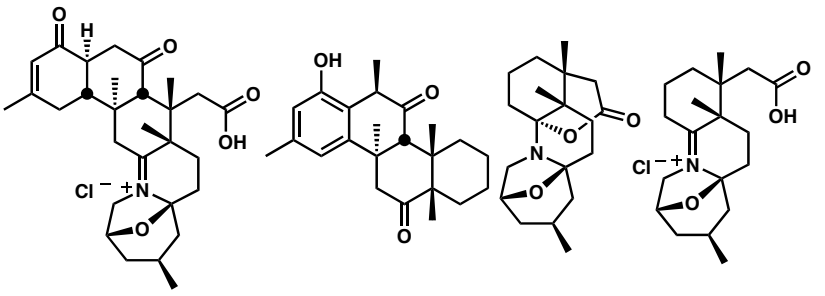

Compound	IC_{50} (μM) for IL-6 Dependent Cell Growth
24	13
38	26
39	>100
40	>100
41	~70

1.3.2 *Miscellaneous Biological Activities*

A multitude of other biological activities have been discovered for molecules in the zoanthamine family. As previously mentioned, zoanthamine, zoanthenamine, and zoanthamide were found to be inhibitors of PMA-induced inflammation in mouse ear.[12,13]

In addition to the isolation of norzoanthamine, norzoanthamineone, oxyzoanthamine, cyclozoanthamine, and epinorzoanthamine, Uemura and coworkers reported that these structures had significant cytotoxicity against P388 murine leukemia cells (Table 1.1).[15] The most potent cytotoxicity was displayed by norzoanthaminone. The antibacterial properties of zoanthamine and several of its reduced derivatives have been investigated.[34] In disk susceptibility experiments, the zoanthamine alkaloids showed broad spectrum activity against both Gram negative and Gram positive bacteria (Table 1.1). More recently the effect of zoanthamine alkaloids on human platelet aggregation has been investigated.[35] These experiments showed that at concentrations of 0.5 mM 11-hydroxyzoanthamine and methyl ester **26** prevent the majority of platelet aggregation caused by collagen, arachidonic acid, and thrombin. In contrast, oxyzoanthamine and zoanthenol were highly effective inhibitors of aggregation in the presence of collagen at 0.5 mM, but showed almost no activity in the presence of arachidonic acid or thrombin.

Table 1.1 Summary of Miscellaneous Biological Activities

Cytotoxicity		**Antibacterial Activity**				
			Inhibition Zone (dia. in mm)			
Compound	**IC_{50} (μg/ml) for Inhibition of P388 Murine Leukemia Cells**	**Compound**	**Gram Negative**		**Gram Positive**	
			S. typhimurium	***E. coli***	***B. sphaericus***	***S. aureus***
Norzoanthamine *(10)*	**24.0**	**Zoanthamine *(5)***	**6**	**6**	**8**	**7**
Norzoanthaminone *(11)*	**1.0**	***42***	**12**	**6**	**8**	**10**
Oxyzoanthamine *(12)*	**7.0**	***43***	**7**	**6**	**8**	**10**
Cyclozoanthamine *(14)*	**24.0**	***44***	**6**	**7**	**7**	**9**
Epinorzoanthamine *(15)*	**2.6**					

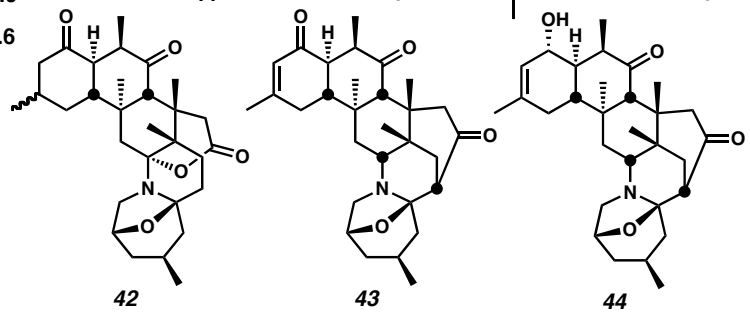

42 ***43*** ***44***

1.4 Approaches Toward the Synthesis of Zoanthamine Natural Products

1.4.1 *General Remarks*

The intriguing diversity of biological activities and the challenging structures of the zoanthamine alkaloids have inspired no fewer than seven synthetic chemistry groups to publish strategies toward the total synthesis of these molecules. Carbon numbering and ring naming will refer to the zoanthamine numbering scheme throughout this thesis (Figure 1.9). Though the focus of the work in our laboratories has been toward the synthesis of zoanthenol, a survey of the synthetic work toward any of the zoanthamines is instructive due to the similar challenges posed by all the molecules in this family. Many researchers have focused their efforts on the synthesis of the ABC rings, which poses a significant synthetic challenge due to its stereochemical density. For example, the C ring contains three quaternary stereocenters in vicinal and non-vicinal relationships. In addition to the difficulty of synthesizing quaternary centers, their steric bulk also renders even routine transformations on nearby functionally recalcitrant. Other researchers have focused on the synthesis of the heterocyclic DEFG rings. DEFG ring synthesis presents the challenge of forming the heterocycles with the correct hemiaminal connectivity.

Figure 1.9 Carbon Numbering and Ring Naming Scheme for the Zoanthamine Alkaloids

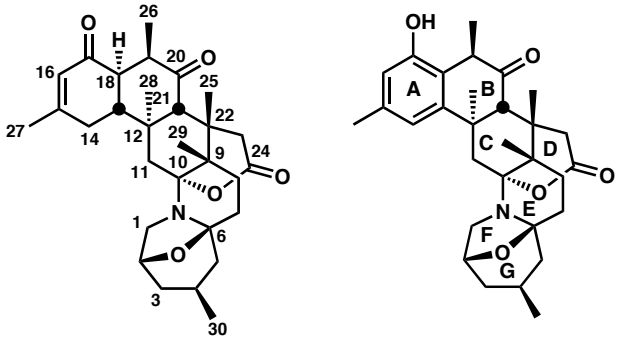

Zoanthamine *(5)* **Zoanthenol *(21)***

1.4.2 *Miyashita's Synthesis of Norzoanthamine*

Twenty years after the isolation of the first zoanthamine alkaloids, Miyashita and coworkers reported the only completed total synthesis to date of a zoanthamine alkaloid with their synthesis of norzoanthamine.[36] This impressive 41-step effort included several creative solutions to problems that likely arose during the execution of the synthesis. Their Diels-Alder strategy for the construction of the ABC ring system of norzoanthamine was disclosed in 2002 (Scheme 1.5).[37] Addition of cuprate **45** to enantiopure enone **46** followed by aldol reaction with aldehyde **47** provided ketone **48**. This efficient three component coupling sequence established all the carbons of the ABC ring system. After further manipulation, furan **49** was oxidized and its enone silylated to give Diels-Alder substrate **50**. Upon heating to 240 °C, the Diels-Alder reaction proceeded predominantly through the desired *exo* transition state **51** (72:28). After silyl cleavage, diastereomerically pure ketone **53** was isolated in 51% yield. This impressive Diels-Alder reaction sets both the C(12) and C(22) quaternary centers of norzoanthamine with the correct relative stereochemistry. However, this strategy provided little functionality to aid in the construction of the C(9) quaternary stereocenter. After significant functional group manipulation, ketone **53** was converted to ketoalcohol **54**.

Ketoalcohol **54** contains suitable functionality to attempt the formation of the C(9) quaternary center (Scheme 1.6). To that end, acylation of ketoalcohol **54** with dimethyl carbonate and lithium *tert*-butoxide proceeded regioselectively, presumably due to lactone formation, and was followed by quenching with methyl iodide to give *O*-alkylated β-ketolactone **55**. Upon treatment with lithium *tert*-butoxide and methyl iodide in DMPU, the *O*-alkylated β-ketolactone **55** underwent C-alkylation to give quaternized

δ-lactone **56**. Impressively, this difficult transformation was accomplished in 83% yield as a single diastereomer.

Scheme 1.5 Miyashita's Diels-Alder Construction of the ABC Rings of Norzoanthamine

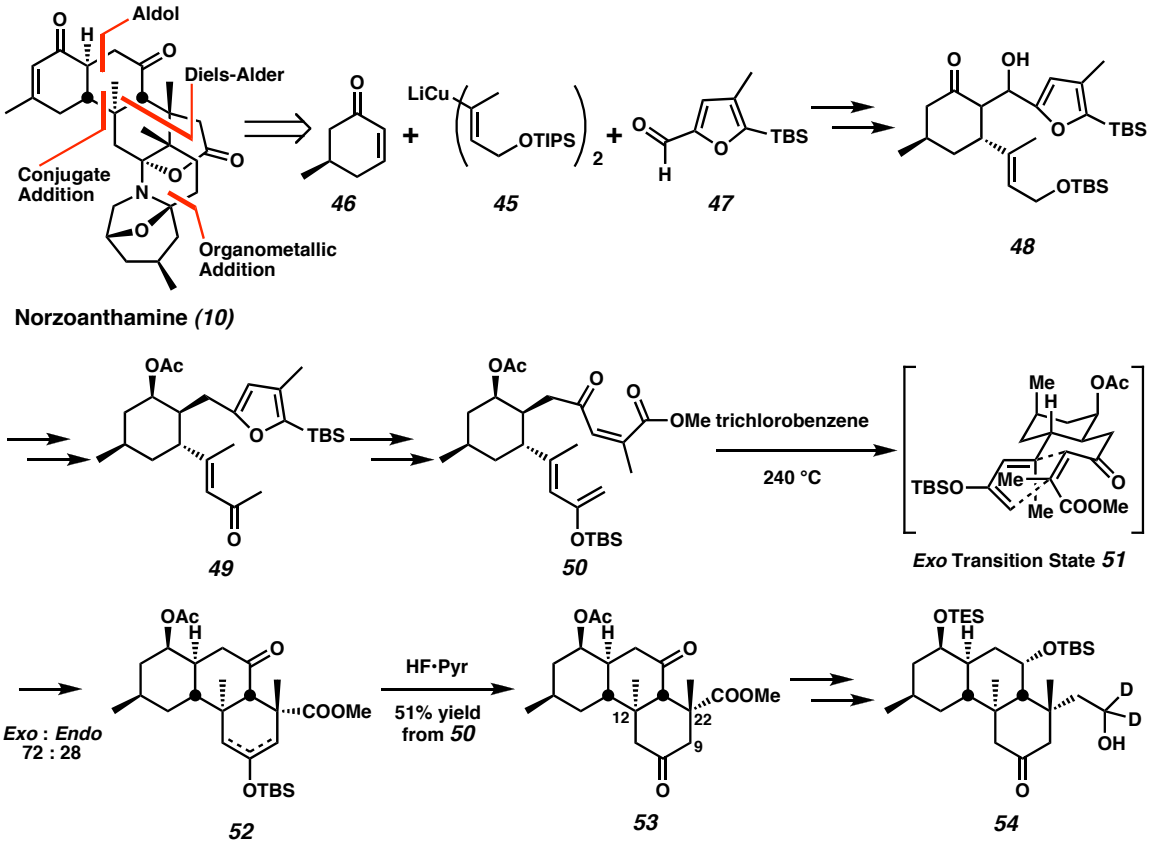

The next challenge lay in converting δ-lactone **56** to acetylene **57** (Scheme 1.6). The addition of methyl lithium with subsequent silylation converted δ-lactone **56** to ketone **58**. While the dehydration of ketone **58** appeared routine, it was at this point that Miyashita's clever incorporation of deuterium proved necessary. When the hydrido equivalent of ketone **58** was treated with triflic anhydride, the intermediate carbocation was predominantly intercepted by intramolecular hydride addition leading to

dihydropyran **59**. However, deuteride transfer proved much slower, and the deutero ketone **58** could be dehydrated to alkyne **57** with only minor amounts of the dihydropyran formed.

The carbon skeleton of norzoanthamine was completed by the addition of aldehyde **60** to the lithium salt of alkyne **57** and oxidation of the resulting alcohol to ynone **61**. Completion of the target required a further twelve steps of deprotection, oxidation state adjustment, and dehydration. In addition to the impressive synthetic accomplishment, this synthesis also served to unambiguously confirm the absolute stereochemistry of norzoanthamine that had been deduced from NMR experiments.

Scheme 1.6 The Completion of Norzoanthamine

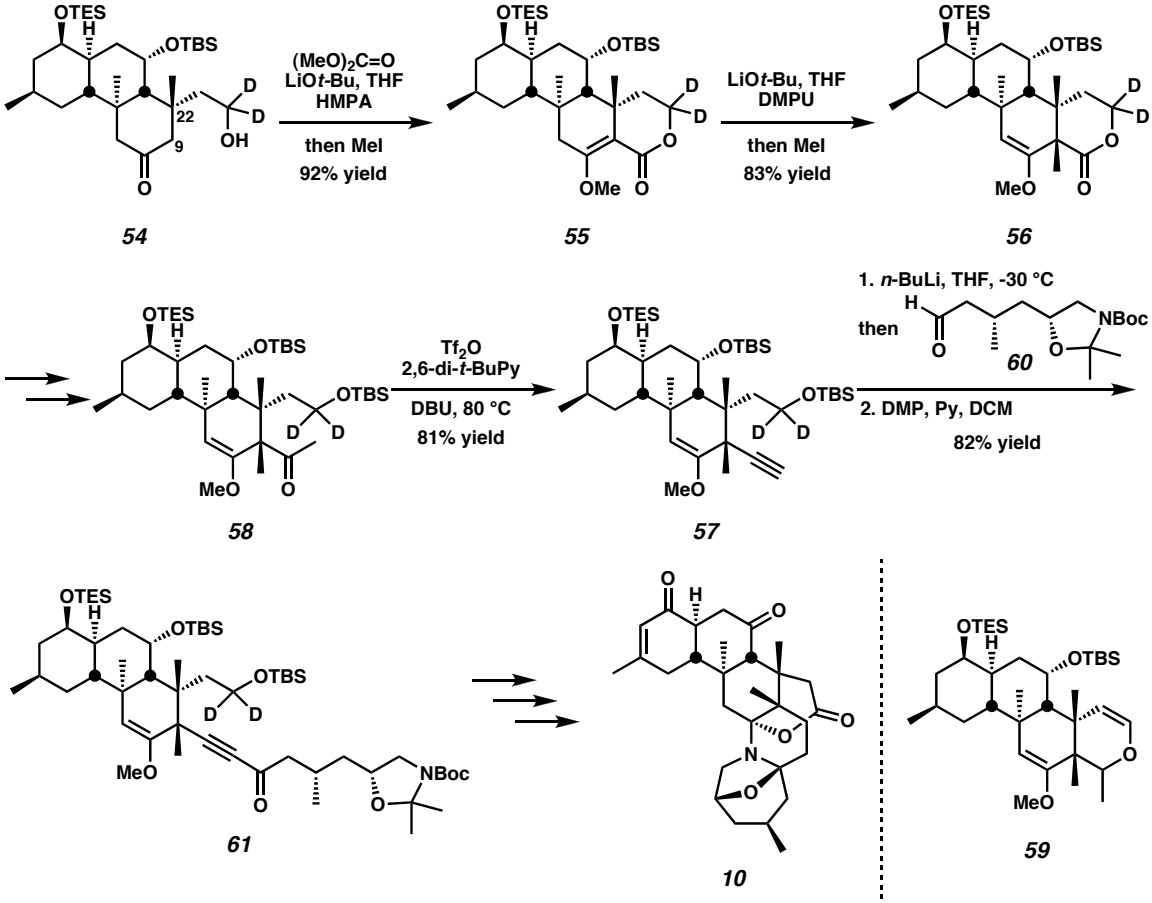

1.4.3 *Tanner's Diels-Alder Approach to the Zoanthamine ABC Ring System*

Tanner and coworkers also chose to assemble the ABC rings via a Diels-Alder approach (Scheme 1.7). Their synthesis began with (*S*)-(–)-perillyl alcohol **62** as a chiral synthon for the A ring.[38] After numerous steps, (*S*)-(–)-perillyl alcohol was transformed into iodide **63**.[39] Stille coupling with stannane **64** proved difficult and required conditions reported by Corey to afford reasonable yields of the Diels-Alder substrate **65**.[40,41] Though not the originally conceived or most direct substrate, diene **65** evolved through significant experimentation.[42] The alcohol oxidation state at C(20) was found to be necessary to prevent elimination of the primary TBS group at C(24), which occurred from the corresponding ketone. However, without the C(20) carbonyl, the diene was no longer electron deficient enough to support the desired inverse demand Diels-Alder reaction. Thus the stannane fragment was redesigned to stannane **64**, incorporating an ester moiety at the C(10) position that would need to be excised later in the synthesis. Of the two C(20) alcohol diastereomers isolated, only diene **65** underwent thermal Diels-Alder reaction. The reaction proceeded with high diastereoselectivity to afford β,γ unsaturated ester **66**, albeit in modest yield. The major product isolated involved displacement of C(17) methoxymethyl ether to give tetrahydrofuran **67**. This problem can likely be circumvented with a more robust protecting group at C(17) or protection of the C(20) alcohol. While this Diels-Alder strategy nicely establishes the quaternary center at C(12), it requires the formation of the difficult vicinal C(9) and C(22) quaternary centers at a late stage. Tanner proposes to carryout this transformation by conjugate addition into the latent C(10) enone, which is to be revealed by oxidative cleavage of the ethyl ester in

Diels-Alder adduct **66**, followed by methyl iodide trapping. No model studies were presented to demonstrate this strategy's ability to form vicinal quaternary stereocenters.[43]

Scheme 1.7 Tanner's Approach to the ABC Ring System

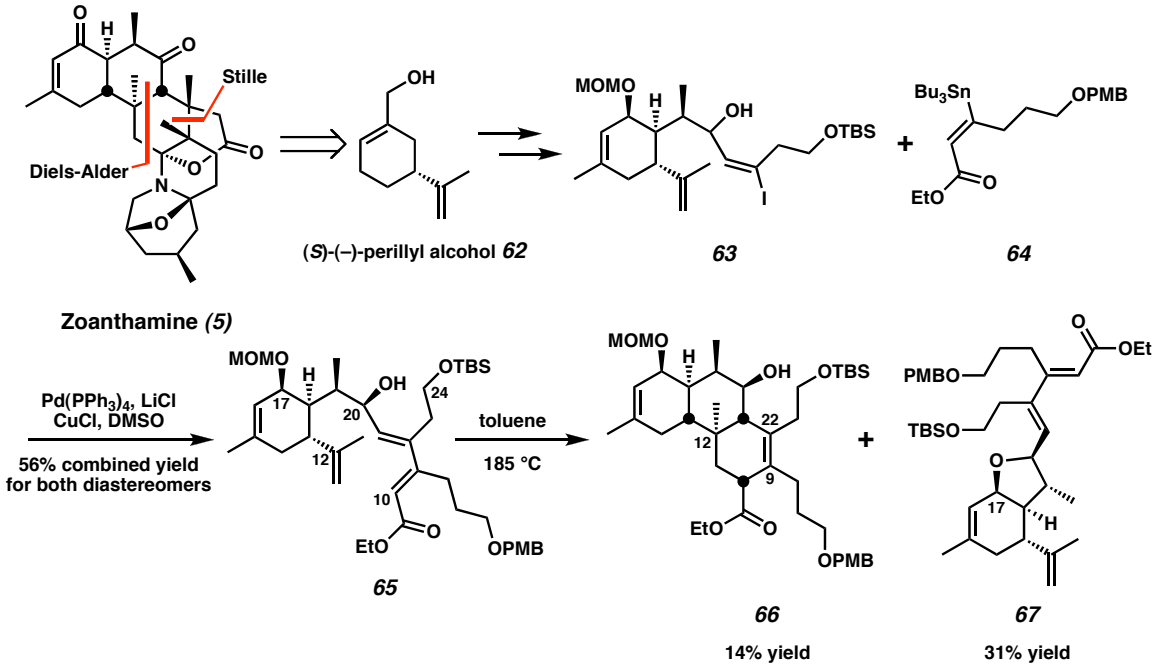

1.4.4 *Uemura's Biomimetic Approach to the Norzoanthamine ABC Ring System*

Recently, Uemura and coworkers have proposed a synthetic strategy based on their biosynthetic hypothesis, which purports that the zoanthamine alkaloids arise from a linear polyketide skeleton, which then undergoes numerous cyclizations.[44] To support this hypothesis, they endeavored to synthesize and cyclize polyene **68**, which would in turn arise from enyne **69** (Scheme 1.8). Vinyl iodide **70** and alkyne **71** were efficiently assembled by Sonogashira coupling[45] and conversion to enyne **69** was completed by oxidation and methylation. No report has appeared on the selective reduction of enyne **69** to the linear polyene **68** or on attempts to cyclize polyene **68**.

Scheme 1.8 Uemura's Biomimetic Cyclization Approach to Norzoanthamine

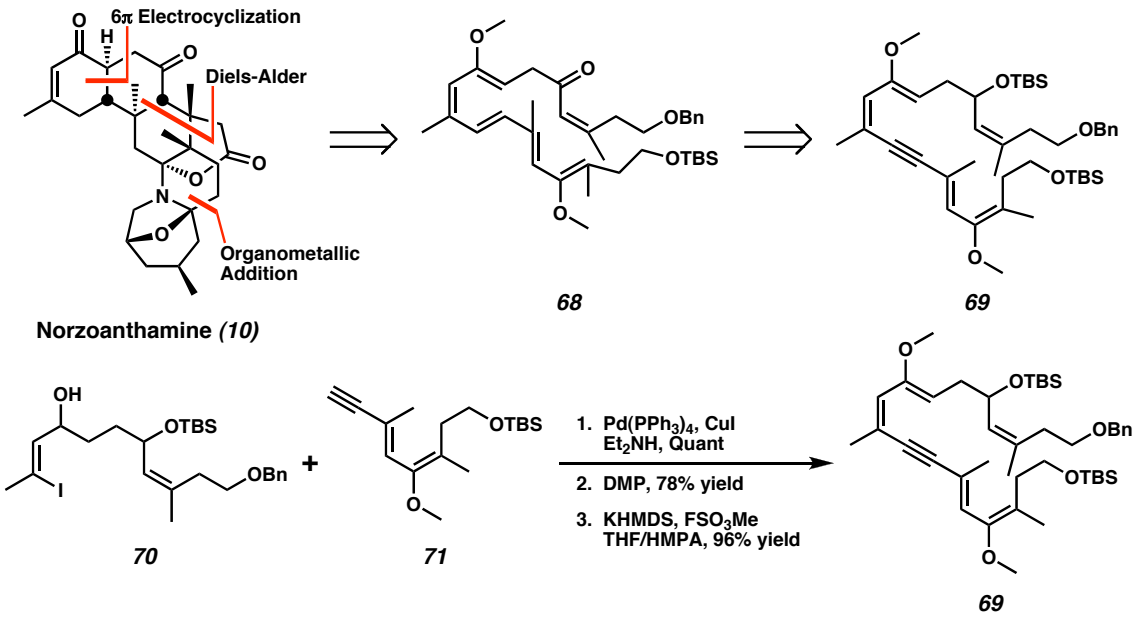

1.4.5 *Williams's Approach to the Norzoanthamine AB and EFG Ring Systems*

Williams and coworkers have contributed approaches to both the synthesis of the carbocyclic AB rings and the heterocyclic EFG rings. Their Diels-Alder strategy constructs the AB rings and subsequently appends the C ring (Scheme 1.9).[46] In the event, nitro alkene **72** underwent reaction in refluxing benzene via an *endo* transition state to afford decalin **73** in good yield and 10:1 dr. A Nef reaction[47] converted the nitro moiety to the desired ketone and facilitated olefin migration. The product enone **74** has the necessary stereochemistry and functionality to begin C ring annulation.

In addition, the Williams group demonstrated an efficient strategy to append the C(1)-C(8) fragment to the ABC ring system and stereospecifically establish the C(9) quaternary center.[48] When heated with zinc (II) chloride, chiral imine **75** generates a significant amount of enamine **76** at equilibrium. The enamine **76** undergoes conjugate addition from the β-face (over the smaller methyl group) of the energy minimized

conformation depicted. Enone **77** was prepared in enantioenriched form using the Evans chiral oxazolidinone.[49] Hydrolysis of the intermediate imine affords diketone **78** with excellent diastereoselectivity (22:1). Upon Staudinger reduction and silyl deprotection of azide **78**, the desired imine formation, ketalization, and dehydration occur without further intervention to give the EFG model enamine **79**.

Scheme 1.9 William's Efforts Toward Norzoanthamine

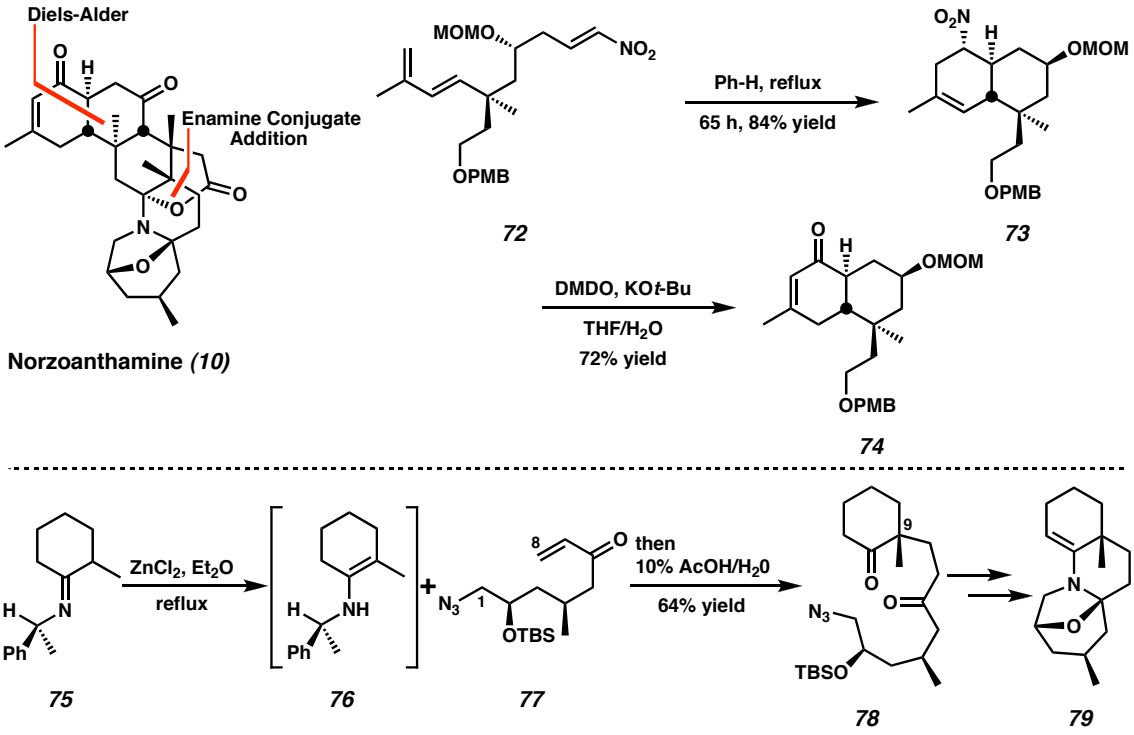

1.4.6 *Theodorakis's Annulation Approach to the Norzoanthamine ABC Ring System*

The annulation strategy proposed by Theodorakis and coworkers is unique in that it starts with the B ring intact and sequentially appends the C and A rings.[50] Condensation of diketone **80** and ketoester **81** with potassium fluoride conditions previously described by their group afforded enone **82** (Scheme 1.10).[51] The formation of

the quaternary stereocenter at C(22) was the next challenge. Treatment of α,β unsaturated ketoester **83** with potassium *tert*-butoxide and methyl iodide produced the quaternized ketoester **84** with complete diastereomeric control. After significant functional group modification, hydroxymethylene-ketone **86** was ready for A ring annulation. A two-step Robinson annulation[52] protocol gave enone **87** as a single isomer at the newly formed C(18) center. After straightforward transformation to enone **88**, methyl lithium addition and PCC oxidation afforded the transposed enone **89**, which contained all the functionality and stereochemistry in the AB rings.

Scheme 1.10 Theodorakis's Annulation Approach to the ABC Ring System

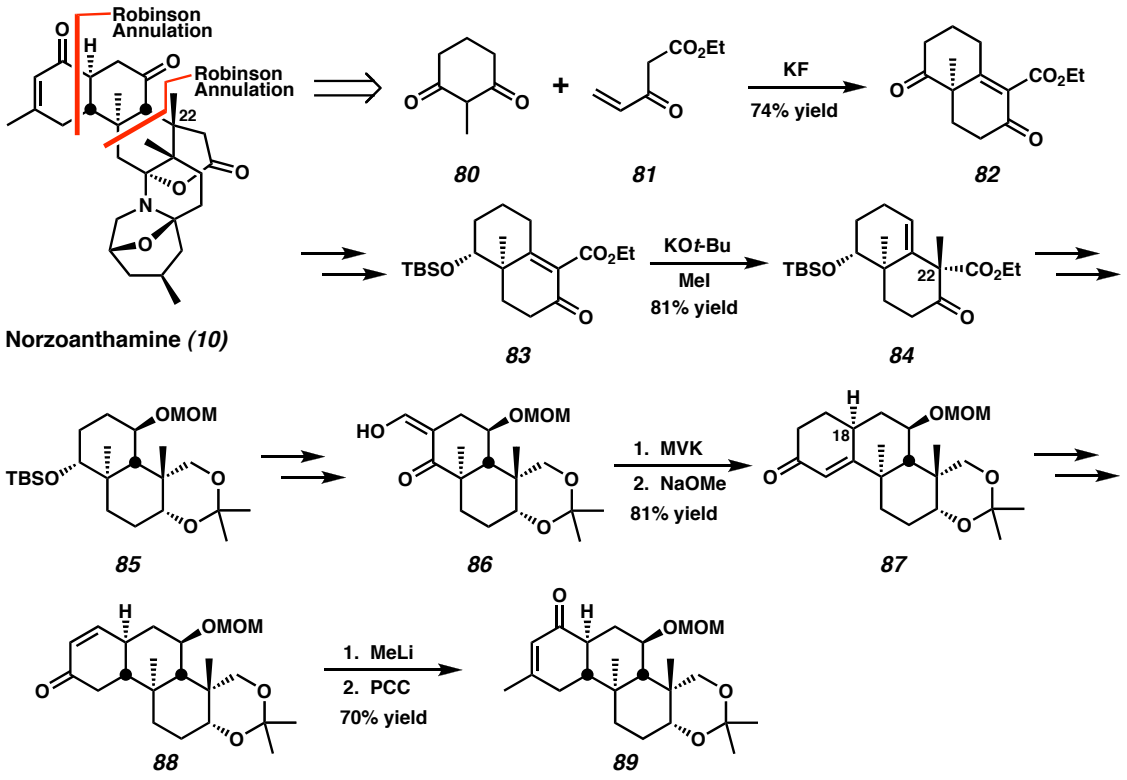

In a related study, Theodorakis demonstrated that the installation of the difficult C(9) quaternary center was possible from intermediate acetonide **85** (Scheme 1.11).[53] Acetonide **85** was advanced by selective protection to give alcohol **90**, which could in turn be converted to methyl ketone **91**. Acetal formation between Stork's dibromo-acetal reagent **92**[54] and the alcohol moiety of methyl ketone **91** produced bromide **93**. Exposure of bromide **93** to base gave a single intramolecular alkylation product **94** in 71% yield. The efficiency of this protocol is impressive given the difficulty of establishing vicinal quaternary centers. Additionally, the alkylation gave complete selectivity for the desired C(9) diastereomer of acetal **94**, as affirmed by X-ray structure determination. Taken in conjunction with Theodorakis's other work, this strategy solved the difficult problem of generating all three of the C ring quaternary centers and produced a norzoanthamine ABC ring system well accoutered for the completion of the total synthesis.

Scheme 1.11 Theodorakis's Installation of the C(9) Quaternary Center

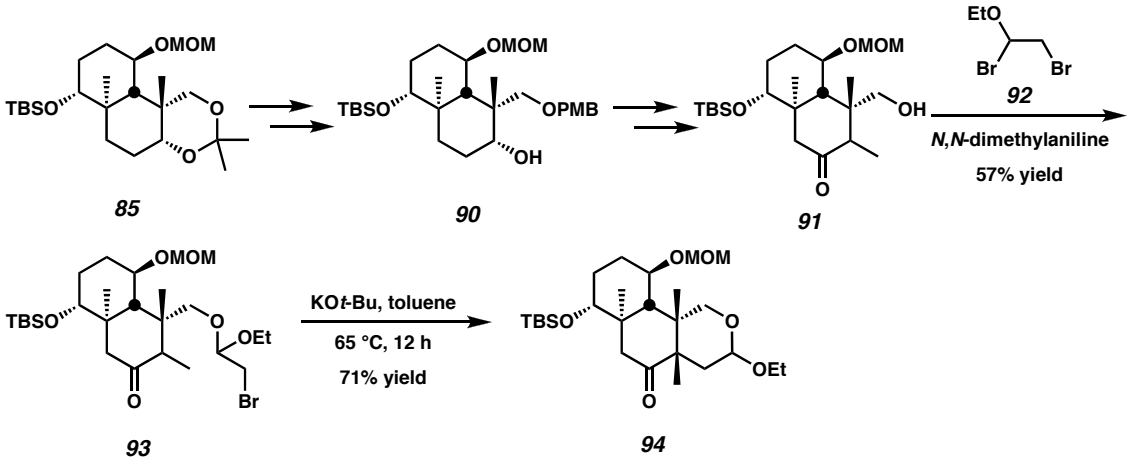

1.4.7 *Kobayashi's Synthesis of the Heterocyclic CDEFG Zoanthamine Ring System*

In 1998 Kobayashi and coworkers disclosed an enantioselective route to the complete CDEFG ring system.[55] The Wieland-Miescher ketone **95**[56] served as the starting material to produce aldehyde **96** (Scheme 1.12). The coupling of sulfone **97**'s lithium salt to aldehyde **96** and oxidation state adjustment completed the Cbz protected cyclization substrate **98**. Treatment with hydrochloric acid removed the acetonide and formed the FG rings. Tricyclic intermediate **99** underwent hydrogenolysis and dehydration to complete the pentacyclic hemiaminal **100**. A one-pot, two-step protocol for cyclization, using Boc protected substrate **101** and acidic conditions, was subsequently investigated and gave an excellent yield of the hemiaminal **100**.[57]

Scheme 1.12 Kobayashi's Sulfone Approach to the Heterocyclic DCEFG Ring System

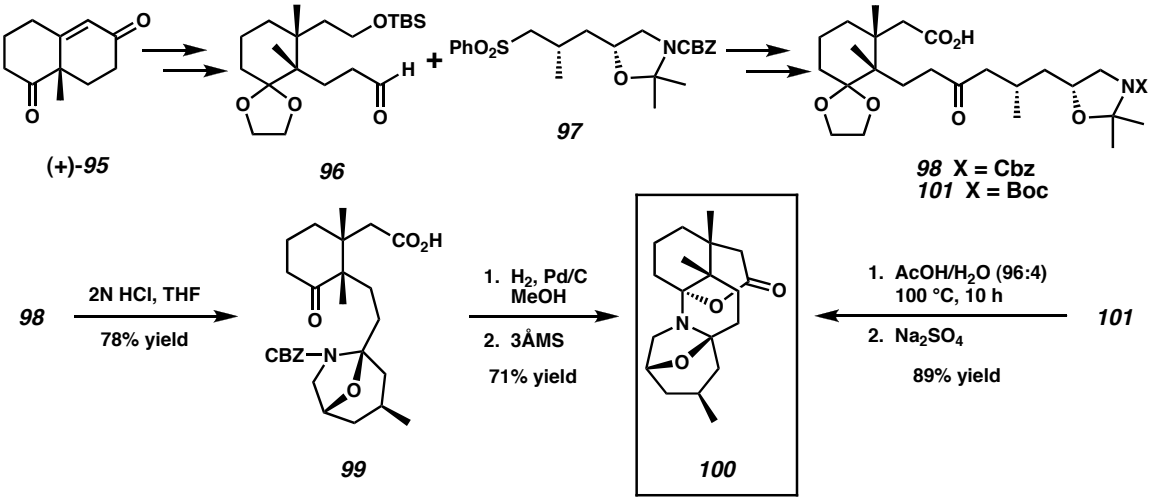

1.4.8 *Hirama's Strategy for the Zoanthenol ABC Ring System*

The strategy proposed by Hirama and coworkers is uniquely geared toward the synthesis of zoanthenol's ABC ring system. The key Heck[58] disconnection of the C(12)-

C(13) bond relies on the aromatic A ring unique to zoanthenol (Scheme 1.13). Further disconnection of the B ring at the C(20)-C(21) bond reveals stannane **102** and enone **103** as appropriate fragments. The C ring synthon, enone **103**, was envisioned to arise in enantioenriched form from an asymmetric quinone Diels-Alder reaction also developed in the Hirama group.[59] In practice, transmetallation of stannane **102** and addition into enone **103** afforded tertiary alcohol **104** as a mixture of diastereomers at C(20). Straightforward conversion of tertiary alcohol **104** to triflate **105** allowed for the investigation of the key intramolecular Heck reaction. After significant optimization, conditions were discovered to produce the desired enol ether **106** in modest yield.[60] Though the reaction did proceed with excellent diastereoselectivity, it had several drawbacks, including reduction of the substrate, high palladium loading, and long reaction times.

Scheme 1.13 Hirama's Heck Strategy for the Zoanthenol ABC Ring System

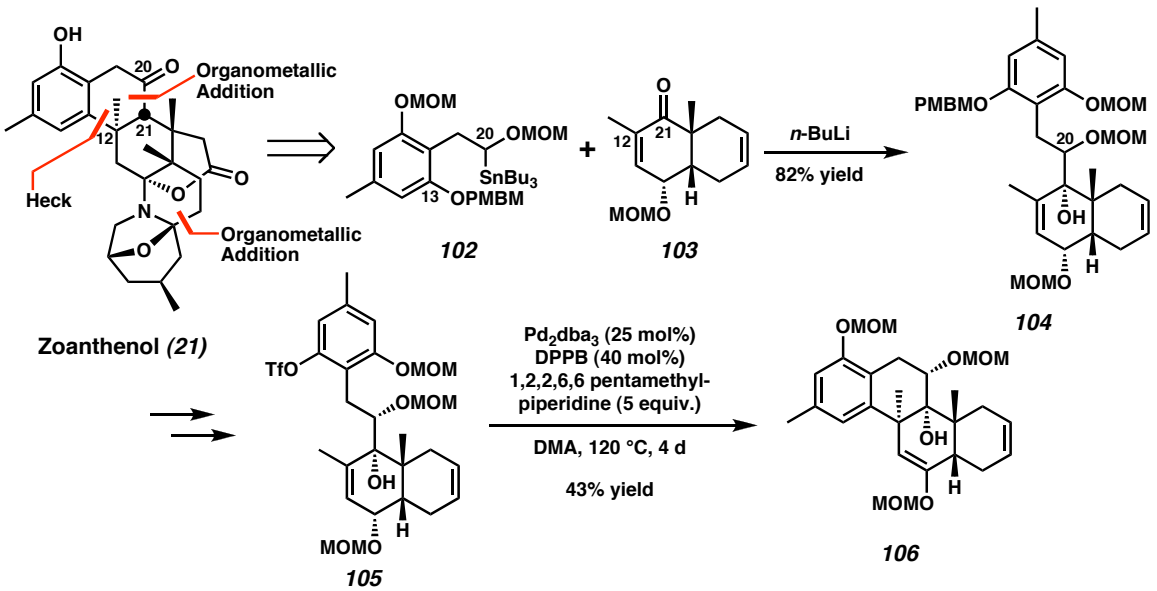

In light of these problems, Heck substrate **105** was altered to increase the electrophilicity of the accepting olefin. As shown in Scheme 1.14, exposure of enone **107** to reductive Heck conditions produced ketone **108** in excellent yield. With the difficult C(12) stereocenter established, their next goal was the reduction of the tertiary alcohol moiety of ketone **109**. Samarium (II) iodide gave the reduced ketone **110** as a single diastereomer and in good yield.[61]

Scheme 1.14 Hirama's Alternate Heck Strategy

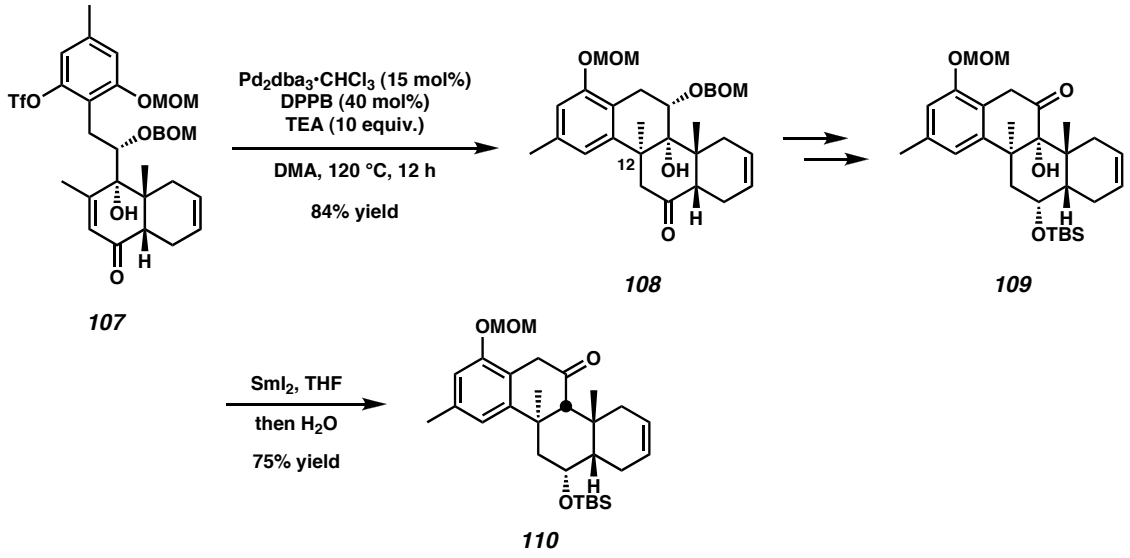

107 *108* *109* *110*

The largest challenge that remains in Hirama's synthesis is the establishment of the C(9) quaternary stereocenter. However, his group has already demonstrated a highly diastereoselective methylation of silyl enol ether **111** as a model of methylation at C(9) (Scheme 1.15).[62] The methylation was achieved by samarium (II) iodide promoted cyclopropanation and acid-mediated ring opening to give methyl ketone **113** and its C(9) epimer with a favorable 3:1 dr.

Scheme 1.15 Hirama's Installation of the C(9) Methyl

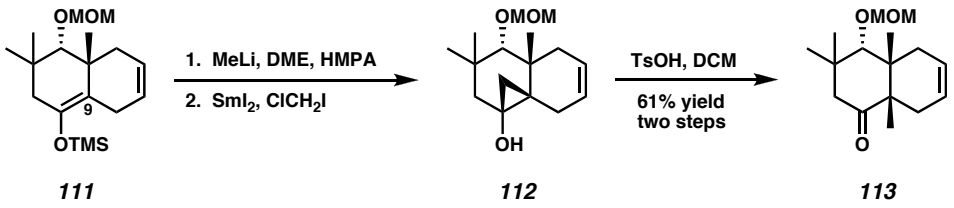

111 *112* *113*

Recently, Hirama and coworkers have disclosed an alternate strategy for the assembly of zoanthenol's ABC ring system. This strategy reverses the order in which the B ring bonds are formed.[63] As depicted in Scheme 1.16, Suzuki coupling of aryl triflate **114** and borane **115** unite the A and C ring synthons via the C(12)-C(13) bond to yield biaryl **116**. Upon the elaboration of Diels-Alder adduct **119**, the final B ring bond, C(20)-C(21), will likely be constructed by an organometallic addition analogous to the synthesis of tertiary alcohol **104**.

Scheme 1.15 Hirama's Alternate Heck Strategy

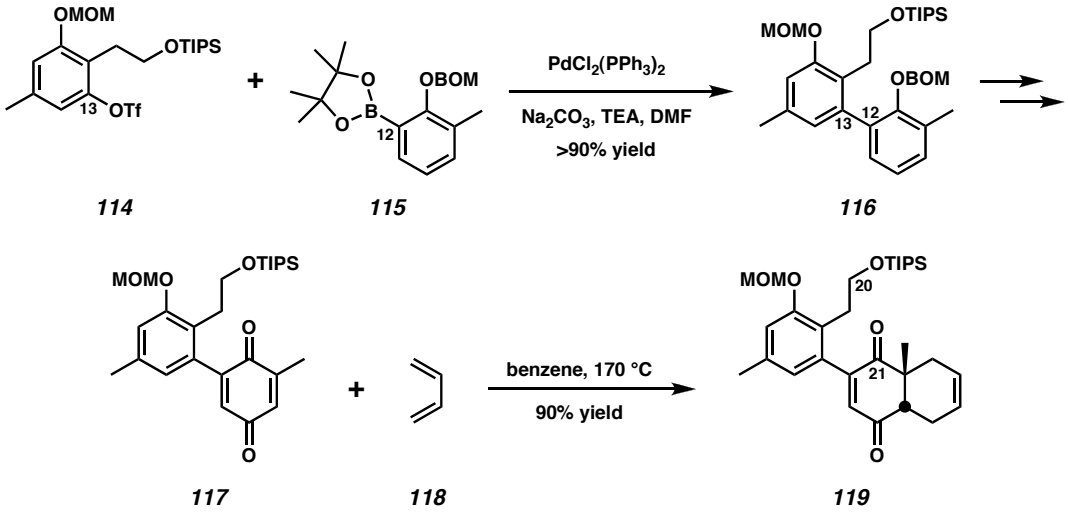

114 *115* *116*

117 *118* *119*

1.5 Conclusion

The zoanthamine alkaloids are a structurally unique family of natural products. Though they are isolated from soft coral of the order zoantharia, it may be that symbiotic algae play a large role in the biosynthesis of these secondary metabolites. Their biosynthesis is believed to be polyketide in origin, but no specifics of the pathway are known. The benefit of these complicated natural products to the producing organisms is unknown, but the isolation of various zoanthamine alkaloids in the Indian, Pacific, and Atlantic Oceans suggests that these widespread metabolites may have an important function. Species in the order zoantharia have produced several classes of biologically active natural products. The zoanthamines are no exception. Antiosteoporotic, antibiotic, anti-inflammatory, and cytotoxic biological activities have been discovered in various zoanthamines. As a result, these molecules have garnered increasing attention from synthetic chemists.

As synthetic targets, the zoanthamine alkaloids are a challenge to current synthetic methods and an inspiration for the creation of new reactions. In the contemporary era, it is common for newly isolated natural products of interesting structure or biological significance to succumb to total synthesis in one to two years' time. By comparison, twenty years passed between the isolation of zoanthamine and Miyashita's total synthesis of norzoanthamine in 2004. Any successful synthesis of these alkaloids requires expertise in both carbocyclic and heterocyclic chemistry. Construction of the carbocyclic ABC rings is hindered by the stereochemical density of this tricycle. In particular, the three quaternary centers of the C ring represent a major challenge. This challenge has inspired a number of creative annulation strategies utilizing Diels-Alder,

Heck, and Robinson annulation reactions. The heterocyclic DEFG rings are topographically complex and contain a number of sensitive functional groups. Pioneering syntheses of the heterocyclic region of these molecules determined the feasibility of different cyclization strategies.

1.6 Notes and Citations

(1) Sinniger, F.; Montoya-Burgos, J. I.; Chevaldonné, P.; Pawlowski, J. *Marine Biology* **2005**, *147*, 1121-1128.

(2) Ono, S.; Reimer, J. D.; Tsukahara, J. *Zoological Science* **2005**, *22*, 247-255.

(3) Nakamura, H.; Kawase, Y.; Maruyama, K.; Muria, A. *Bull. Chem. Soc. Jpn.* **1998**, *71*, 781-787.

(4) (a) Suksamrarn, A.; Jankam, A.; Tarnchompoo, B.; Putchakarn, S. *J. Nat. Prod.* **2002**, *65*, 1194-1197. (b) Shigemori, H.; Sato, Y.; Kagata, T.; Kobayashi, J. *J. Nat. Prod.* **1999**, *62*, 372-374.

(5) Han, C.; Qi, J.; Shi, X.; Sakagami, Y.; Shibata, T.; Uchida, K.; Ojika, M. *Biosci. Biotechnol. Biochem.* **2006**, *70*, 706-711.

(6) Fernández, J. J.; Souto, M. L.; Daranas, A. H.; Norte, M. *Current Topics in Phytochemistry* **2000**, *4*, 106-119.

(7) Sepcic, K.; Turk, T.; Macek, P. *Toxicon* **1998**, *36*, 93-940.

(8) Pletneva, N.; Pletnev, S.; Tikhonova, T.; Popov, V.; Martynov, V.; Pletnev, V. *Acta Cryst. Sec. D* **2006**, *62*, 527-532.

(9) Remington, S. J.; Wachtner, R. M.; Yarbrough, D. K.; Branchaud, B.; Anderson, D. C.; Kallio, K.; Lukyanov, K. A. *Biochemistry* **2005**, *44*, 202-212.

(10) Moore, R. E.; Scheuer, P. J. *Science* **1971**, *172*, 495-498.

(11) For structure determination see: Cha, J. K.; Christ, W. J.; Finan, J. M.; Fujioka, H.; Kishi, Y.; Klein, L. L.; Ko, S. S.; Leder, J.; McWhorter, W. W.; Pfaff, K.-P.; Yonaga, M.; Uemura, D.; Hirata, Y. *J. Am. Chem. Soc.* **1982**, *104*, 7369-7371. For

total synthesis see: Suh, E. M.; Kishi, Y. *J. Am. Chem. Soc.* **1994**, *116*, 11205-11206.

(12) Roa, C. B.; Anjaneyula, A. S. R.; Sarma, N. S.; Venkatateswarlu, Y.; Rosser, R. M.; Faulkner, D. J.; Chen, M. H. M.; Clardy, J. *J. Am. Chem. Soc.* **1984**, *106*, 7983-7984.

(13) Roa, C. B.; Anjaneyula, A. S. R.; Sarma, N. S.; Venkatateswarlu, Y. *J. Org. Chem.* **1985**, *50*, 3757-3760.

(14) Roa, C. B.; Roa, D. V.; Raju, V. S. N. *Heterocycles* **1989**, *28*, 103-106.

(15) Fukuzawa, S.; Hayashi, Y.; Uemura, D.; Nagatsu, A.; Yamada, K.; Ijuin, Y. *Heterocyclic Communications* **1995**, *1*, 207-214.

(16) Kuramoto, M.; Hayashi, K.; Fujitani, Y.; Yamaguchi, K.; Tsuji, T.; Yamada, K.; Ijuin, Y.; Uemura, D. *Tetrahedron Lett.* **1997**, *38*, 5683-5686.

(17) Atta-ur-Rahman; Alvi, K. A.; Abbas, S. A.; Choudhary, M. I.; Clardy, J. *Tetrahedron Lett.* **1989**, *30*, 6825-6828.

(18) Daranas, A. H.; Fernández, J. J.; Gavín, J. A.; Norte, M. *Tetrahedron* **1998**, *54*, 7891-7896.

(19) Daranas, A. H.; Fernández, J. J.; Gavín, J. A.; Norte, M. *Tetrahedron* **1999**, *55*, 5539-5546.

(20) Kuramoto, M.; Hayashi, K.; Yamaguchi, K.; Yada, M.; Tsuji, T.; Uemura, D. *Bull. Chem. Soc. Jpn.* **1998**, *71*, 771-779.

(21) Nakamura, H.; Kawase, Y.; Maruyama, K.; Murai, A. *Bull. Chem. Soc. Jpn.* **1998**, *71*, 781-789.

(22) Trench, R. K. *Pure Appl. Chem.* **1981**, *53*, 819-835.

(23) Also in this study, a molecule closely related to palytoxin, zooxanthellatoxin, was isolated. See ref. 21 for details.

(24) Kuramoto, M.; Arimoto, H.; Hayashi, K.; Hayakawa, I.; Uemura, D.; Chou, T.; Yamada, K.; Tsuji, T.; Yamaguchi, K.; Yazawa, K. *Symposium Papers, 38th Symposium on the Chemistry of Natural Products*, **1996**, 79-84.

(25) Chambers, T. J. *J. Cell Sci.* **1982**, *57*, 247-260.

(26) The dose given in the text (0.4 mg/kg/d) for $p < 0.05$ is from ref. 27. However, in ref. 20, when the femur weight is analyzed per body mass (mg/g), a dose of 0.08 mg/kg/d is sufficient to give $p < 0.05$.

(27) The dose range given in the text (0.016-0.4 mg/kg/d) for $p < 0.05$ is from ref. 20. However, in ref. 27 only dosing at 0.4 mg/kg/day gave a significant ($p < 0.05$) increase in failure load. No explanation for this disparity is given.

(28) Yamaguchi, K.; Yada, M.; Tsuji, T.; Kuramoto, M.; Uemura, D. *Biol. Pharm. Bull.* **1999**, *22*, 920-924.

(29) Kuramoto, M.; Yamaguchi, K.; Tsuji, T.; Uemura, D. Zoanthamines, Antiosteoporotic Alkaloids. In *Drugs from the Sea*, Fusetani, N., Ed.; Karger: Basel, 2000, 98-106.

(30) Bodine, P. V. N.; Harris, H. A.; Komm, B. S. *Endocrinology* **1999**, *140*, 2439-2451.

(31) For other descriptions of this activity, see: (a) Kuramoto, M.; Arimoto, H.; Uemura, D. *J. Synth. Org. Chem., Jpn.* **2003**, *61*, 59-65. (b) Kuramoto, M.; Arimoto, H.; Uemura, D. *Mar. Drugs* **2004**, *1*, 39-54. (c) Kita, M.; Uemura, D.

Chem. Lett. **2005**, *34*, 454-459. (d) Yamada, K.; Kuramoto, M.; Uemura, D. *Recent Res. Devel. Pure & Applied Chem.* **1999**, *3*, 245-254.

(32) The IC_{50} values are for inhibition of IL-6 production from preosteoblastic MC3T3-E1 cells stimulated by parathyroid hormone. See ref. 28.

(33) Hirai, G.; Oguri, H.; Hayashi, M.; Koyama, K.; Koizumi, Y.; Moharram, S. M.; Hirama, M. *Bioorg. Med. Chem. Lett.* **2004**, *14*, 2647-2651.

(34) Venkateswarlu, Y.; Reddy, N. S.; Ramesh, P.; Reddy, P. S.; Jamil, K. *Heterocyclic Communications* **1998**, *4*, 575-580.

(35) Villar, R. M.; Gil-Longo, J.; Daranas, A. H.; Souto, M. L.; Fernández, J. J.; Peixinho, S.; Barral, M. A.; Santafé, G.; Rodríguez, J.; Jiménez, C. *Bioorg. Med. Lett.* **2003**, *11*, 2301-2306.

(36) Miyashita, M.; Sasaki, M.; Hattori, I.; Sakai, M.; Tanino, K. *Science* **2004**, *305*, 495-499.

(37) Sakai, M.; Sasaki, M.; Tanino, K.; Miyashita, M. *Tetrahedron Lett.* **2002**, *43*, 1705-1708.

(38) Tanner, D.; Anderson, P. G.; Tedenborg, L.; Somfai, P. *Tetrahedron* **1994**, *50*, 9135-9144.

(39) (a) Tanner, D.; Tedenborg, L.; Somfai, P. *Acta Chem. Scand.* **1997**, *51*, 1217-1223. (b) Nielsen, T. E.; Tanner, D. *J. Org. Chem.* **2002**, *67*, 6366-6371.

(40) Nielsen, T. E.; Le Quement, S.; Juhl, M.; Tanner, D. *Tetrahedron* **2005**, *61*, 8013-8024.

(41) Han, X.; Stoltz, B. M.; Corey, E. J. *J. Am. Chem. Soc.* **1999**, *121*, 7600-7605.

(42) Juhl, M.; Nielsen, T. E.; Le Quement, S.; Tanner, D. *J. Org. Chem.* **2006**, *71*, 265-280.

(43) Beilstein searches reveal only seven such examples of conjugate additions into tetrasubstituted enones to form quaternary centers, none of which involved addition to a cyclic system.

(44) Irifune, T.; Ohashi, T.; Ichino, T.; Sakia, E.; Suenaga, K.; Uemura, D. *Chem. Lett.* **2005**, *34*, 1058-1059.

(45) Sonogashira, K.; Tohdo, Y.; Hagihara, N. *Tetrahedron Lett.* **1975**, *16*, 4467-4470.

(46) Williams, D. R.; Brugel, T. A. *Org. Lett.* **2000**, *2*, 1023-1026.

(47) For a review of Nef reactions see: Pinnick, H. W. *Org. React.* **1990**, *38*, 655-792.

(48) Williams, D. R.; Cortez, G. A. *Tetrahedron Lett.* **1998**, *39*, 2675-2678.

(49) For a review of Evans aldol methodology see: Ager, D. J.; Prakash, I.; Schaad, D. R. *Aldrichimica Acta* **1997**, *30*, 3-12.

(50) Ghosh, S.; Rivas, F.; Fischer, D.; González, M. A.; Theodorakis, E. A. *Org. Lett.* **2004**, *6*, 941-944.

(51) (a) Ling, T.; Chowdhury, C.; Kramer, B. A.; Vong, B. G.; Palladino, M. A.; Theodorakis, E. A. *J. Org. Chem.* **2001**, *66*, 8843-8853. (b) Ling, T.; Kramer, B. A.; Palladino, M. A.; Theodorakis, E. A. *Org. Lett.* **2000**, *2*, 2073-2076.

(52) For a review of Robinson annulations see: Gawley, R. E. *Synthesis* **1976**, 777-794.

(53) Rivas, F.; Ghosh, S.; Theodorakis, E. A. *Tetrahedron Lett.* **2005**, *46*, 5281-5284.

(54) The use of dibromide **92** for radical cyclizations was explored by Stork, see: (a) Stork, G.; Mook, R.; Biller, S. A.; Rychnovsky, S. D. *J. Am. Chem. Soc.* **1983**,

105, 3741-3742. (b) Stork, G.; Sher, P. M. *J. Am. Chem. Soc.* **1983**, *105*, 6765-6766.

(55) (a) Hikage, N.; Furukawa, H.; Takao, K.; Kobayashi, S. *Tetrahedron Lett.* **1998**, *39*, 6237-6240. (b) Hikage, N.; Furukawa, H.; Takao, K.; Kobayashi, S. *Tetrahedron Lett.* **1998**, *39*, 6241-6244.

(56) Weiland, P.; Miescher, K. *Helv. Chim. Acta* **1950**, *33*, 2215-2228. For enantioselective preparation see: Buchschacher, P.; Fürst, A.; Gutzwiller, J. *Org. Synth.* **1985**, *63*, 37-43.

(57) Hikage, N.; Furukawa, H.; Takao, K.; Kobayashi, S. *Chem. Pharm. Bull.* **2000**, *48*, 1370-1372.

(58) (a) Heck, R. F.; Nolley, J. P. *J. Am. Chem. Soc.* **1968**, *90*, 5518-5526. (b) Heck, R. F. *Acc. Chem. Res.* **1979**, *12*, 146-151. (c) Heck, R. F. *Org. React.* **1982**, *27*, 345-390.

(59) Moharram, S. M.; Hirai, G.; Koyama, K.; Oguri, H.; Hirama, M. *Tetrahedron Lett.* **2000**, *41*, 6669-6673.

(60) Hirai, G.; Oguri, H.; Moharram, S. M.; Koyama, K.; Hirama, M. *Tetrahedron Lett.* **2001**, *42*, 5783-5787.

(61) Hirai, G.; Koizumi, Y.; Moharram, S. M.; Oguri, H.; Hirama, M. *Org. Lett.* **2002**, *4*, 1627-1630.

(62) Hirai, G.; Oguri, H.; Hirama, M. *Chem. Lett.* **1999**, *28*, 141-142.

(63) Moharram, S. M.; Oguri, H.; Hirama, M. *Egypt. J. Pharm. Sci.* **2003**, *44*, 177-193.

CHAPTER TWO

Early Approaches to the Synthesis of Zoanthenol

2.1 Synthetic Planning

2.1.1 *Introduction*

In late 2000, our laboratory became interested in the total synthesis of the zoanthamine alkaloids. At that time, Tanner[1] and Williams[2] had published the most comprehensive strategies toward the total synthesis of these natural products. In 1998, Kobayashi[3] and Williams[4] had described routes for the construction of the heterocyclic portion of these molecules. No work had yet been published toward the total synthesis of zoanthenol. Our interest in zoanthenol was piqued by its unique aromatic A ring. Aromatization of the A ring removes the C(13) and C(18) stereocenters from the zoanthamine skeleton (Figure 2.1). Despite this simplification, we felt that zoanthenol still embodied the core challenges of the zoanthamines. Additionally, the aromatic A ring allowed us to consider a number of disconnections of the C(12)-C(13) bond that were not readily applicable to the non-aromatic zoanthamines.

Figure 2.1 Zoanthamine and Zoanthenol

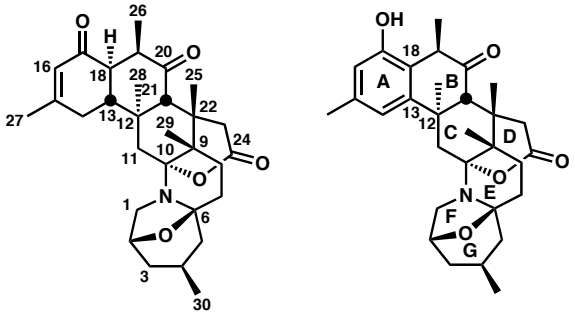

Zoanthamine *(5)* **Zoanthenol *(21)***

2.1.2 *Retrosynthesis*

Zoanthenol is a densely functionalized, topographically complex target molecule. Though only a C_{30} molecule, it is comprised of seven rings and nine stereocenters. The C ring poses the single greatest stereochemical challenge with three quaternary centers and five contiguous stereocenters (Scheme 2.1). The quaternary stereocenters are disposed in vicinal (C(9) and C(22)) and remote (C(12) and C(22)) relationships. Our overarching strategy in assembling the C ring was to generate one of these quaternary centers in enantioenriched fashion, and then derive the rest of the stereocenters in a highly diastereoselective manner. Another design feature common to all our strategies was to unite A and C ring synthons in a convergent manner by forging the B ring. With respect to the heterocyclic portion of the molecule, our goal was to introduce all the functionality of the C(1) to C(8) fragment in a single operation.

Our disconnections began with the heterocyclic portion of the molecule. Previous work had demonstrated that the complicated hemiaminals forming the DEFG rings were thermodynamically favored.[3,4] Thus, retrosynthetically, the heterocycles could be unraveled to give triketone **120** with a linear C(1) to C(8) side chain (Scheme 2.1). Disconnection of the C(8)-C(9) bond in the sense of a conjugate addition of an enamine affords methyl ketone **121** and enone **122**. Enone **122** may be derived from a vinyl anion addition to the amide carbonyl of caprolactam **123**. Caprolactam **123** may be simplified to lactone **124** by conjugate methyl addition and amination. Ultimately, lactone **124** may arise in enantioenriched form via an asymmetric hetero Diels-Alder reaction pioneered by Jacobsen and coworkers.[5] The synthesis of optically active caprolactam **123** was carried

out by Dr. Jeffrey Bagdanoff, a former graduate student in the lab, and has been detailed elsewhere.[6]

Scheme 2.1 Retrosynthetic Analysis of Zoanthenol

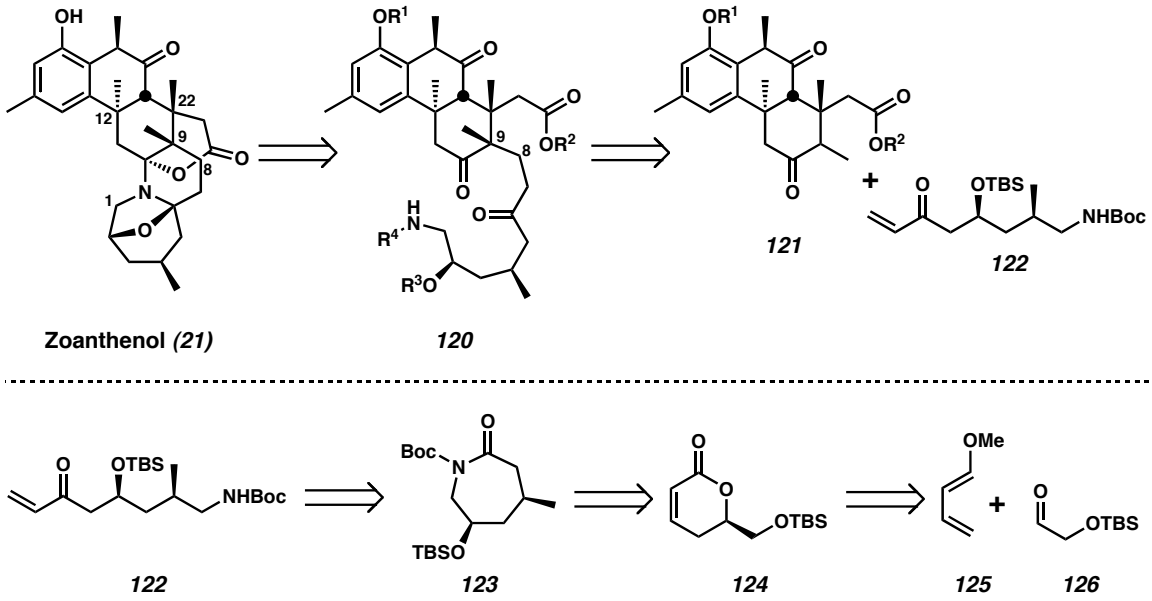

Further simplification of methyl ketone **121** commences by removing the methyl group at C(9) to afford tricyclic diketone **127** (Scheme 2.2). Oxidation state adjustment and Diels-Alder disconnection across the B ring of diketone **127** yields the known mono-protected quinone **128**[7] and diene **129** as target fragments. Diene **129** could be assembled by Stille coupling involving enol triflate **130**, which could in turn be derived from ketoester **131**. Finally, asymmetric deprotonation of meso ketone **132** and reaction with an appropriate electrophile could afford ketoester **131** in enantioenriched form.

Scheme 2.2 Retrosynthetic Analysis of Zoanthenol's ABC Ring System

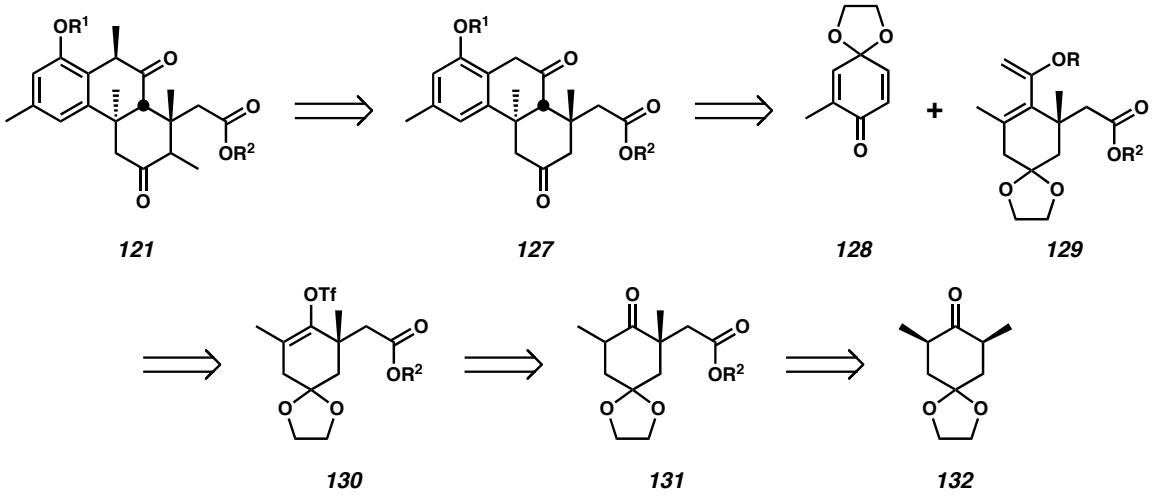

2.2 A Diels-Alder Approach to the Zoanthenol ABC Ring System

2.2.1 *Racemic Synthesis of the Substrate Diene*

In order to determine the feasibility of the quinone Diels-Alder strategy, the target diene was synthesized racemically (Scheme 2.3). Known dimethyl ketone **133**[8,9] was deprotonated with LiHMDS and alkylated with *t*-butyl bromoacetate in the presence of HMPA to give ketoester **134** in excellent yield as a mixture of diastereomers. Low temperature deprotonation of ketoester **134** with KHMDS and quenching with $PhNTf_2$ afforded enol triflate **135**, which underwent Stille coupling with vinyl stannane **136** to produce a diene **137** in excellent yield. The use of copper (I) chloride promoted Stille coupling conditions, reported by Corey, was essential.[10] Numerous other conditions failed to give significant amounts of diene **137**.

Scheme 2.3 Diene Synthesis

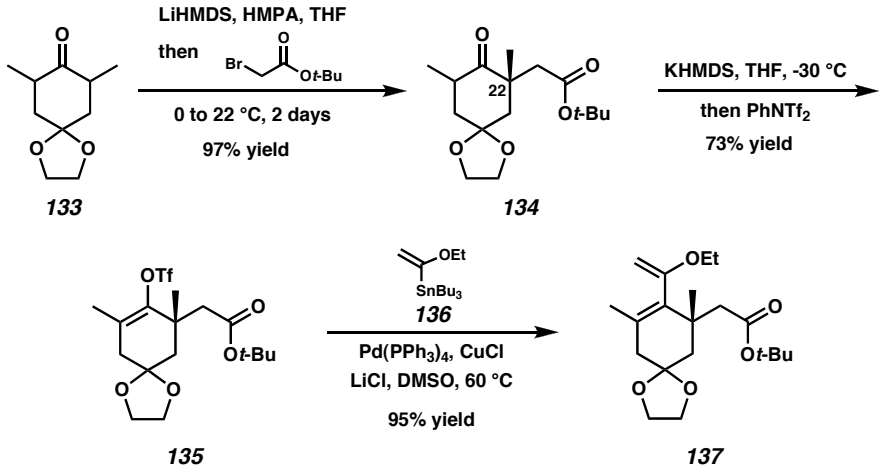

2.2.2 *Diels-Alder Reactions for B Ring Synthesis*

With quantities of both quinone **128** and diene **137** in hand, numerous trials to effect Diels-Alder reaction were performed. Thermal reaction of the two reactants up to 180 °C failed to give any Diels-Alder adducts. Treatment with Lewis acids including tin (IV) chloride, titanium (IV) chloride, ethyl aluminum dichloride, TBSOTf, methyl aluminum dichloride, and $TiCl_2(O\textit{i}\text{-}Pr)_2$ also failed to give a productive reaction.[11] More asynchronous or stepwise versions of the reaction that replaced ethyl enol ether **137** with its enolate equivalent did not produce any of the desired C-C bonds.

Scheme 2.4 Attempted Diels-Alder Reactions

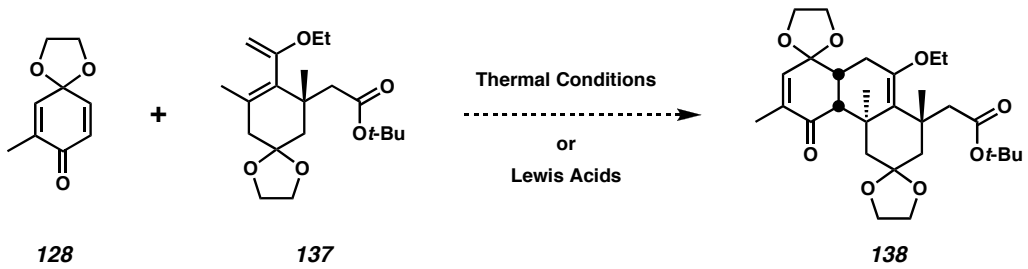

2.3 An Intramolecular Conjugate Addition Approach to the Zoanthenol ABC Rings

2.3.1 *Revised Retrosynthetic Analysis*

As a result of our inability to construct the B ring in a single Diels-Alder reaction, we considered strategies that would construct the B ring in a stepwise manner. One such strategy with good historical precedent was the intramolecular conjugate addition of electron-rich arenes into enones. This reaction has been demonstrated with steric environments as demanding as zoanthenol, as shown with enones **139** and **140** (Scheme 2.5).[12] These cyclizations were commonly employed in syntheses of Abietane natural products.[13] This Friedel-Crafts cyclization has been shown to proceed under either strongly Lewis acidic or Brønsted acidic conditions, but the reaction does require an extremely electron-rich arene for effective cyclization.[14]

Scheme 2.5 Intramolecular Conjugate Additions in the Synthesis of Abietane Skeleton

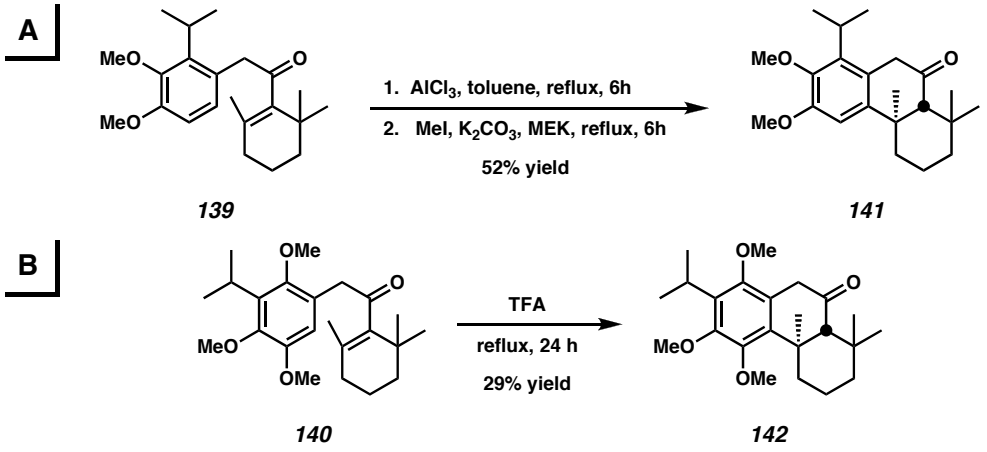

Encouraged by the ability of such intramolecular 6-*endo* conjugate additions to form difficult benzylic quaternary centers, analogous to zoanthenol's C(12) stereocenter, we altered our retrosynthesis of diketone **127** to incorporate this disconnection (Scheme

2.6). In order to increase the nucleophilicity of the aromatic ring and facilitate conjugate addition, oxygenation was incorporated at C(16) of enone **143**. In turn, we envisioned enone **143** could arise by 1,2-addition of organometallic reagent **144** into enal **145**.

Scheme 2.6 Intramolecular Conjugate Addition Approach

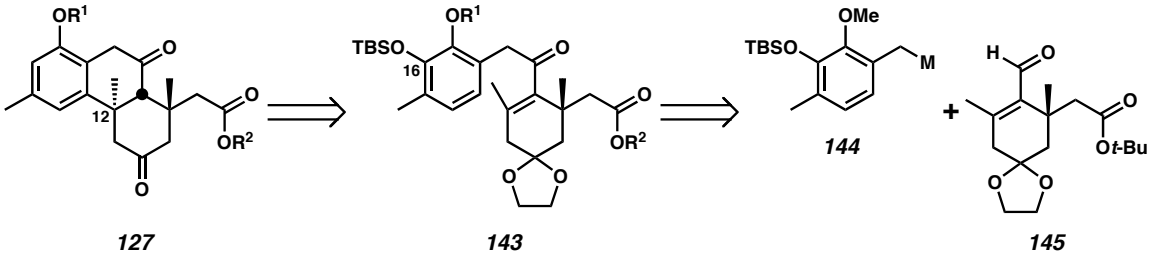

2.3.2 *Synthesis of A Ring Fragment*

The synthesis of the A ring synthon commenced with Wolff-Kishner reduction[15] of *o*-vanillin (**146**) and silyl protection to afford arene **147** in 84% yield over two steps after distillation (Scheme 2.7). Methoxy-directed *ortho*-lithiation of arene **147** and quenching with N,N′-dimethylformamide (DMF) afforded a mixture of the desired benzaldehyde **148** and desilylated benzaldehyde **149**. After chromatographic separation, phenol **149** was readily resilylated under standard conditions to provide additional benzaldehyde **148**. Carefully monitored reduction of benzaldehyde **148** with 10% Pd/C under a balloon of hydrogen afforded an excellent yield of benzylic alcohol **150**. If alcohol **150** was allowed to persist under the reaction conditions for several additional hours after the consumption of benzaldehyde **148**, significant over-reduction was observed. Benzylic alcohol **150** was converted with phosphorus tribromide and pyridine to benzyl bromide **151** in 92% yield after distillation. Benzyl bromide **151** was

anticipated to allow for the synthesis of several potential organometallic nucleophiles. Overall, the synthesis of the A ring synthon was efficient and scalable. We routinely produced 20-25 g of benzyl bromide **151** per batch.

Scheme 2.7 Synthesis of A Ring Benzyl Bromide

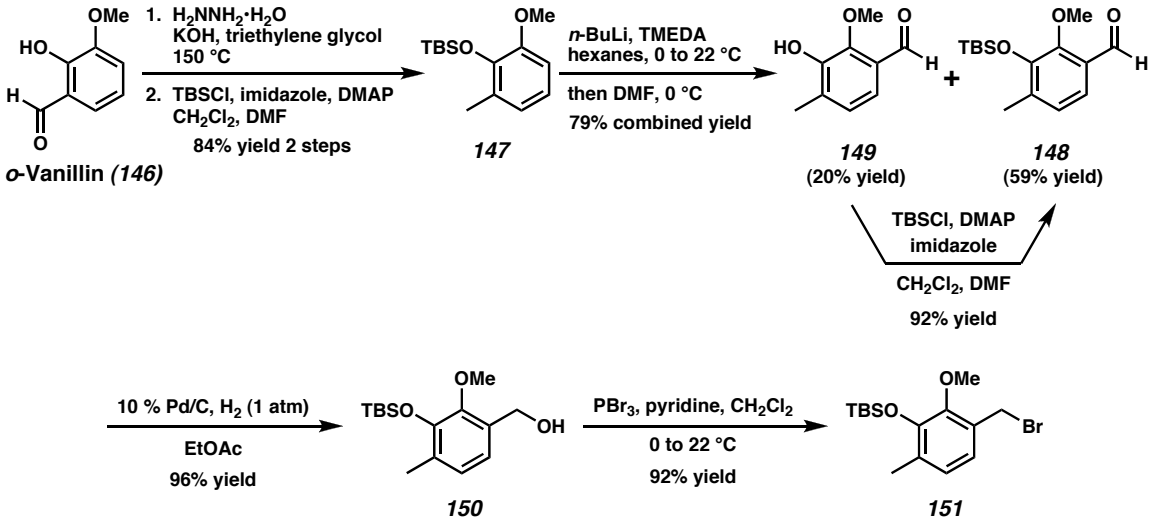

2.3.3 *Synthesis of the C Ring Synthon*

Two syntheses of the desired enal **145** were developed starting from intermediate triflate **135** (Scheme 2.8). A two-step approach involved Stille coupling with vinyl tributyltin to produce an intermediate diene. Oxidative cleavage with osmium (VIII) tetraoxide (OsO_4) and sodium periodate gave enal **145** (Reaction A). This route had several disadvantages. The oxidative cleavage required a minimum of 5 mol% of the expensive and toxic OsO_4 to consume all the hindered diene. In addition, modest yields in the oxidative cleavage resulted from poor olefin selectivity during the dihydroxylation.

As a result of these difficulties, a one-step palladium-catalyzed carbonylation method was developed for the synthesis of enal **145** (Reaction B). Treatment of triflate

135 under an atmosphere of carbon monoxide with palladium (II) acetate, 1,4-bis-(dicyclohexylphosphino)butane as a ligand, and TES-H as a reducing agent afforded the desired enal **145** in good yield. The use of this bulky, electron-rich bisphosphine ligand was essential. For example, the use of 1,4-bis(diphenylphosphino)butane (DPPB) afforded significant amounts of the corresponding reduced olefin. Additionally, the slow addition of the hydride source, TES-H, was necessary to minimize direct reduction of triflate **135**. While operationally demanding, this reaction greatly improved the efficiency and throughput in making enal **145**.[16]

Scheme 2.8 Syntheses of C Ring Enal

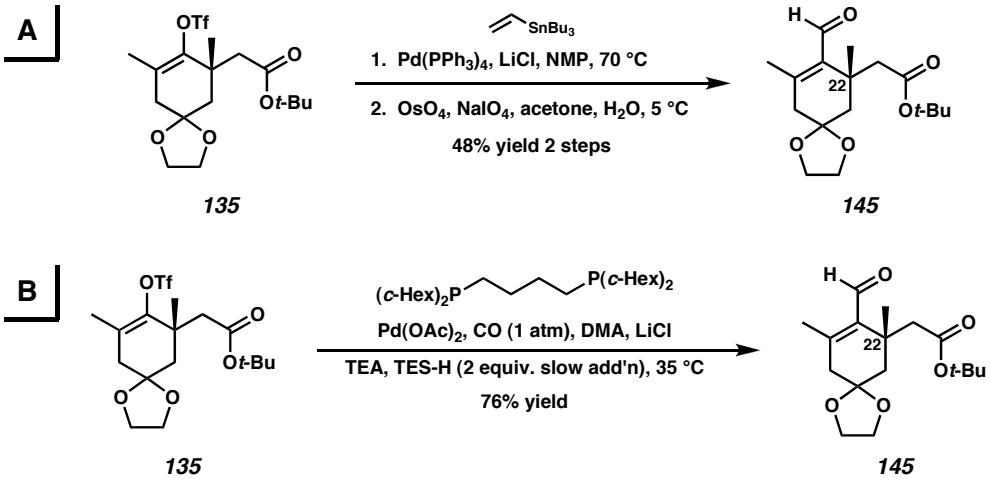

2.3.4 *Asymmetric Tsuji Allylation for the Synthesis of C Ring Enal **145***

Although racemic material was adequate for exploratory studies, our goal from the outset was the catalytic asymmetric total synthesis of zoanthenol. In accord with our strategy to set a single enantiopure stereocenter and relay that stereochemistry

diastereoselectively throughout the structure, we considered several approaches to set the C(22) quaternary stereocenter in ketoester **134** enantioselectively (Scheme 2.3).

Our first strategy was based on the enantioselective deprotonation of *meso*-ketones. The use of chiral lithium amides for asymmetric deprotonation of ketones was pioneered by Koga[17] and refined by Simpkins.[18] While we had some success in the desymmetrization of *meso*-ketone **132**, the use of stoichiometric amounts of chiral lithium amides seemed impractical on scale.[19]

Ultimately, we found that the asymmetric Tsuji allylation methodology developed in our laboratory was a reliable and efficient method to produce enantioenriched ketoester **134** (Scheme 2.9). Quaternary (*S*)-(–)-ketone **152** could be produced in good ee from several enolate precursors by a palladium (0) phosphinooxazoline catalyst.[20] Oxidative olefin cleavage and esterification gave (+)-*t*-butyl ester **153** in 51% yield over two steps. Methylation of (+)-*t*-butyl ester **153** under standard conditions gave a separable mixture of diastereomeric methyl ketoesters **134**, an intermediate in our racemic C ring synthesis.

Scheme 2.9 Asymmetric Synthesis of Ketoester **134**

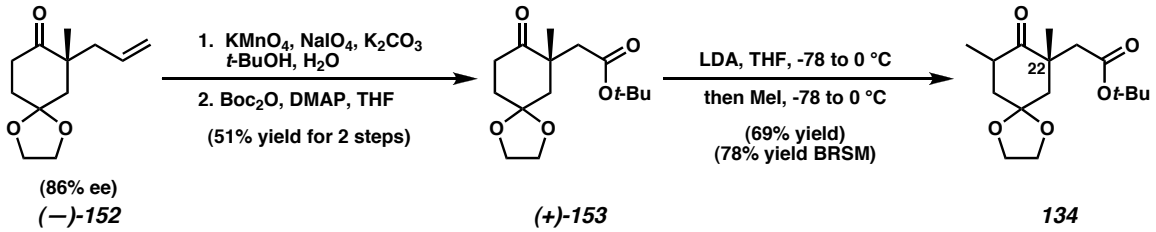

2.3.5 *Fragment Coupling and Cyclization Attempts*

With the new A and C ring fragments available, work to complete an intramolecular conjugate addition substrate began (Scheme 2.10). Treatment of benzyl

bromide **151** with magnesium turnings in refluxing ethyl ether afforded good conversion to Grignard reagent **154**. While the generation of Grignard reagent **154** was highly reproducible, it should be noted that analogous benzyl bromides with different protecting groups (e.g., methoxy replaced with BOM) afforded very poor yields of organomagnesium and organozinc reagents. Grignard reagent **154** was added immediately upon generation to enal **145** to produce allylic alcohol **155**. We found that the use of methylene chloride as a cosolvent improved the diastereoselectivity of the 1,2-addition and minimized the formation of lactone **156** in situ. Fortuitously, lactone **156**, which could be intentionally formed by deprotonation in ethereal solvents, was amenable to X-ray structure determination and established the relative configuration of the newly formed alcohol stereocenter. Simple Dess-Martin oxidation of allylic alcohol **155** provided the desired enone **157**.

Scheme 2.10 Grignard Addition

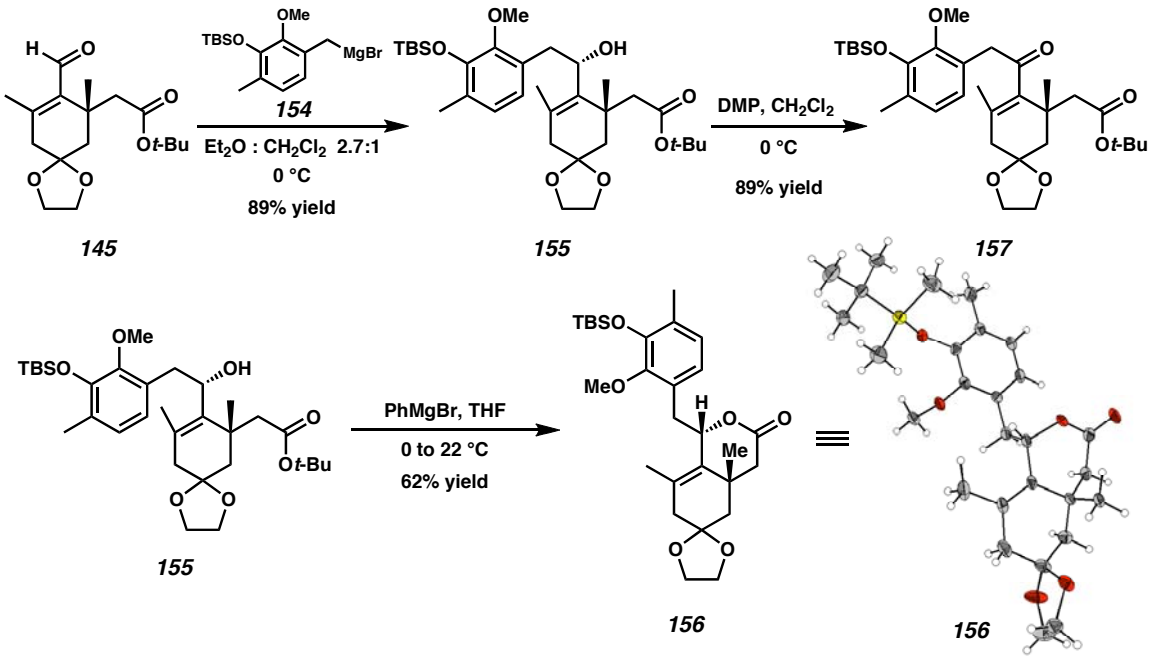

Enone **157** was subjected to numerous acidic conditions that were precedented to affect intramolecular cyclization (Scheme 2.11). However, none produced the desired C(12)-C(13) bond.[21] Treatment with trifluoroacetic acid (TFA) followed by methylation afforded a mixture of products resembling enone **158**. This tentative structural assignment piqued our interest in the possibility of a 6-*exo* acid-mediated cyclization.

Scheme 2.11 Attempted Cyclization

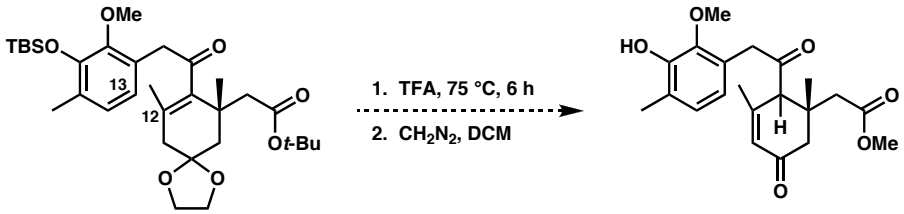

157 *158*

2.4 Development of an S_N' Strategy for the Zoanthenol ABC Ring System

In order to examine the possibility of 6-*exo* cyclization, allylic alcohol **155** was exposed to refluxing TFA (Scheme 2.12). We anticipated the loss of protecting groups and olefin migration would afford enone **159**. Enone **159** could then undergo 6-*exo* conjugate addition giving keto alcohol **160**. The major product isolated from the reaction contained a single aromatic C-H by ^{1}H NMR, suggesting that cyclization had occurred. However, the presence of another olefinic proton in the NMR suggested an elimination had occurred. Proton NMR also showed a roughly 5:1 mixture of diastereomeric acids, which were chromatographically separable. To our delight, upon standing in $CDCl_3$, the major product formed crystals suitable for X-ray diffraction. Cyclization of allylic alcohol **155** had indeed occurred, but not by the anticipated 6-*exo* mechanism. Instead,

an S_N' cyclization had produced acid **161**.[22] The solid state structure confirmed the desired *trans* disposition of the methyl groups at C(12) and C(22). Optimized conditions, including lowering the temperature to 50 °C and desilylation of the crude reaction mixture with TBAF afforded a 49% yield of diastereomerically pure acid **161**.[23]

Scheme 2.12 Trifluoroacetic Acid-Mediated Cyclization

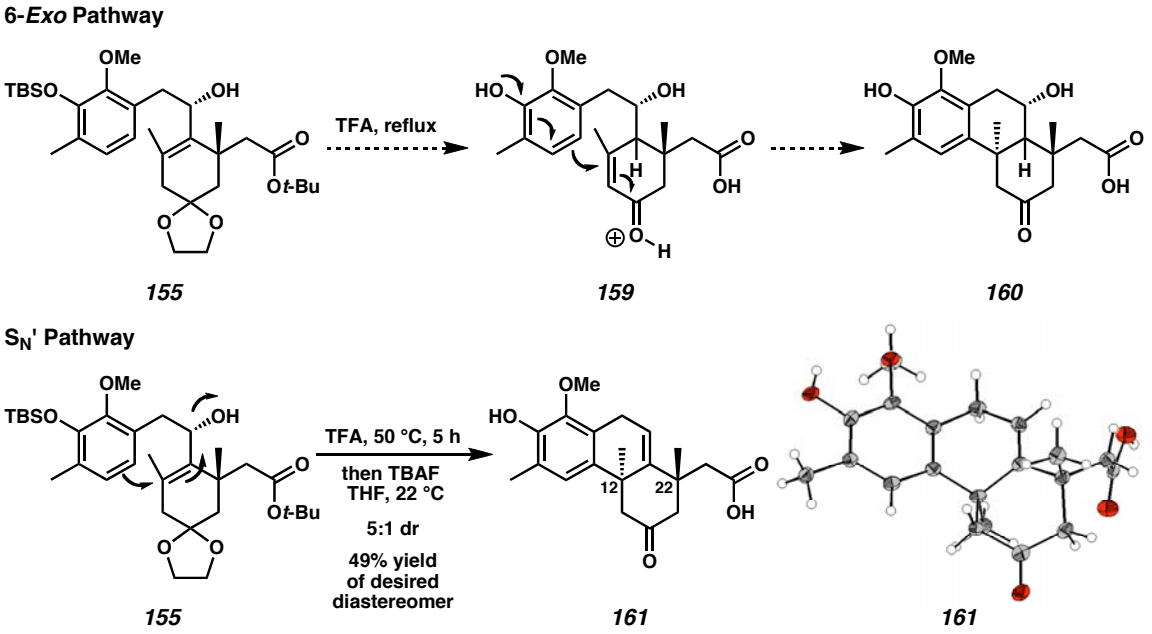

The S_N' Friedel-Crafts reaction to produce carboxylic acid **161** achieved the important goal of generating the C(12) quaternary stereocenter with the desired relative configuration. In order to improve the yield and better understand the reaction pathway, a number of modifications were evaluated. The choice of acid in the reaction is crucial. Trifluoroacetic acid was unique in promoting S_N' cyclization. Both stronger acids (e.g., triflic acid) and weaker acids (e.g., acetic acid) failed to produce carboxylic acid **161**. Even the dilution of neat TFA with methylene chloride, benzene, or acetic acid caused

nearly complete inhibition of cyclization. Interestingly, both lactone **156** and allylic acetate **162**[24] underwent cyclization in TFA to give acid **161** with similar yields and diastereoselectivities as allylic alcohol **155** (Scheme 2.13).[25] The des-oxy arene **163** failed to generate any cyclized products, even under forcing conditions. This confirmed the importance of the arene nucleophilicity imparted by C(16) oxygenation. Additionally, compounds analogous to lactone **156** and allylic alcohol **155**, but epimeric at C(20), failed to cyclize when treated under the same conditions.

Scheme 2.13 Further Substrates for TFA-Mediated S_N' Cyclization

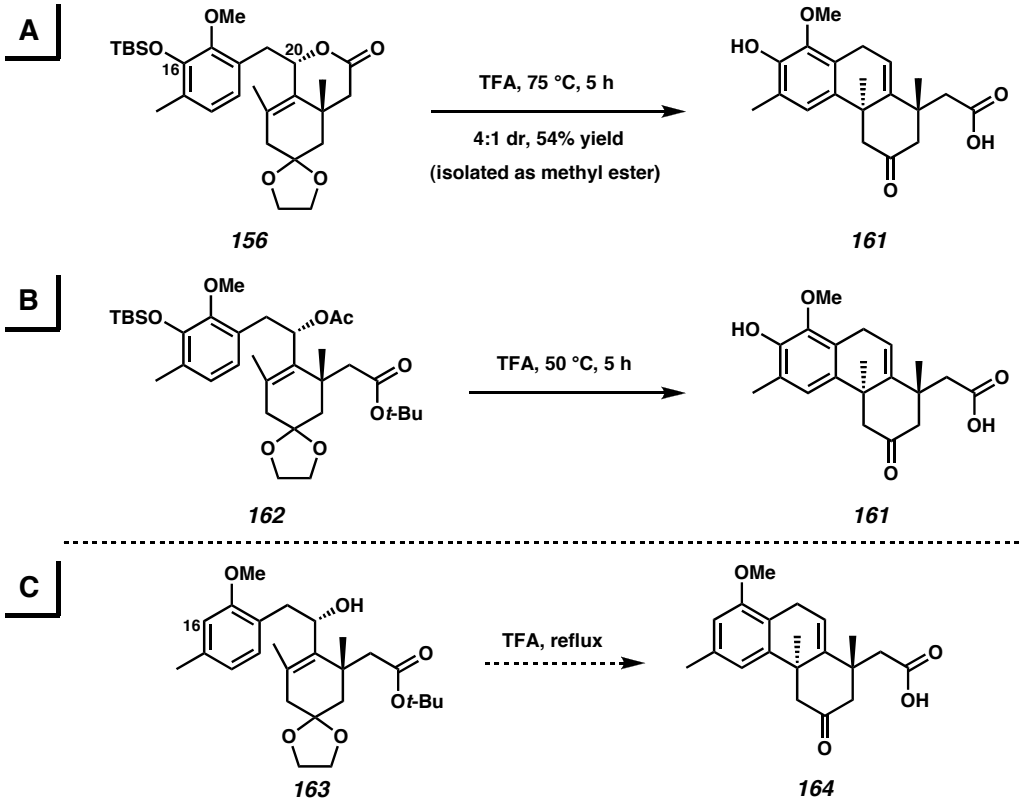

Taken together, these experiments give some insight into the likely pathways for the S_N' reaction (Scheme 2.14). The unique ability of TFA, among numerous other Lewis and Brønsted acids, to mediate the reaction suggests that its properties as a strong acid, a

dehydrating agent, and a good leaving group (as a trifluoroacetate) are important to the reaction mechanism. It seems likely that all three substrates proceed through an intermediate with a leaving group at C(20). Allylic alcohol **155** may be converted to intermediate trifluoroacetate **165** in situ,[26] while the other substrates already contain good leaving groups. Because the C(20) epimers of the substrates do not readily undergo cyclization, it seems likely that the reactions proceed via a concerted displacement that relies on the trajectory of the leaving group, rather than through a full allyl cation.

Scheme 2.14 Possible Pathways in the S_N' Reaction

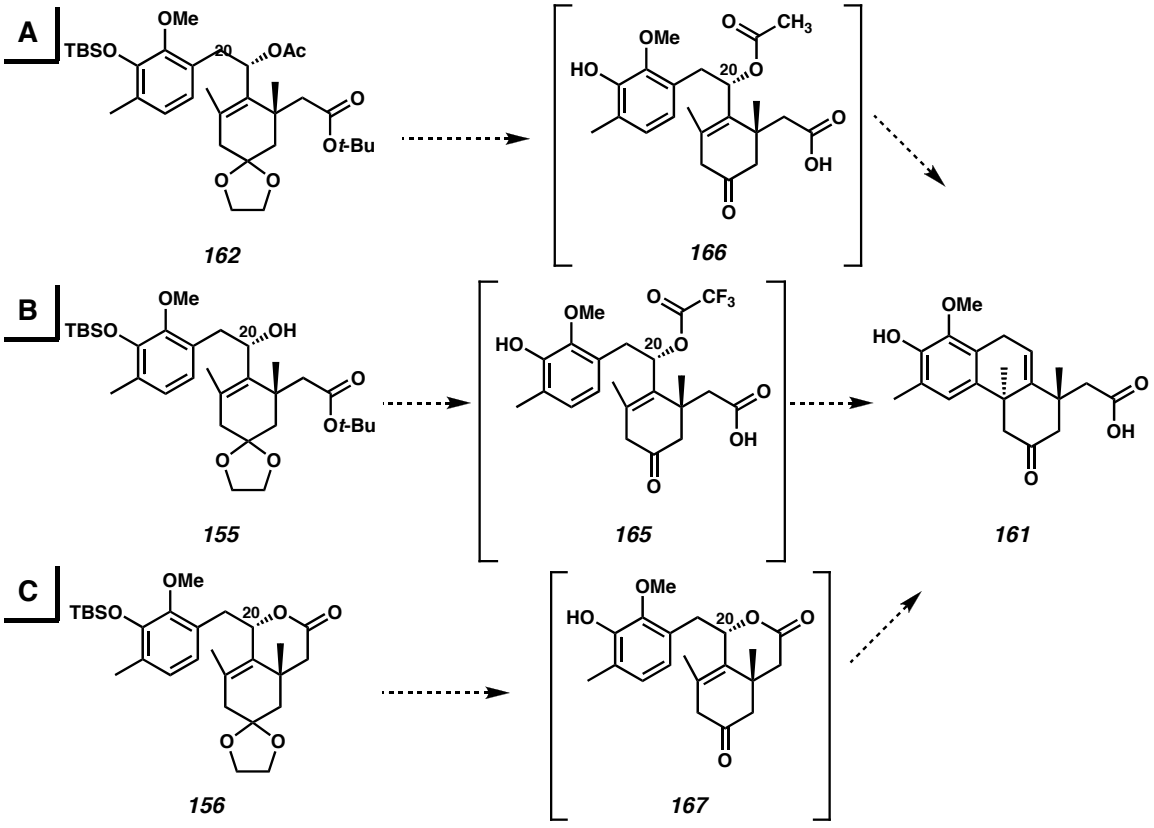

2.5 Elaboration Toward the Zoanthenol ABC Ring System

2.5.1 *General Remarks*

With an efficient route in hand to construct the zoanthenol ABC ring system with two of the three quaternary stereocenters, we turned our attention to adjusting the functionality on the rings to complete the synthesis. Our objectives were the removal of the now superfluous phenol and the reoxygenation of the olefin in carboxylic acid **161**.

2.5.2 *Reduction of the Phenol*

The C(16) phenol moiety had served only to increase the nucleophilicity of the arene in the cyclization. With that complete, our next task was its deoxygenation (Scheme 2.15). Esterification of carboxylic acid **161** with diazomethane followed by treatment with triflic anhydride and pyridine afforded aryl triflate **168** in good yield for the two steps. The reduction of congested bis-*ortho* substituted aryl triflates are typically difficult. However, conditions specifically designed for such substrates,[27] involving a number of potential hydride sources, proved highly effective in producing deoxygenated ketoester **169**. Ketoester **169** was an important branch point. It provided a suitable substrate to investigate both the installation of the C(9) substituents and the olefin oxygenation.

Scheme 2.15 A Ring Deoxygenation

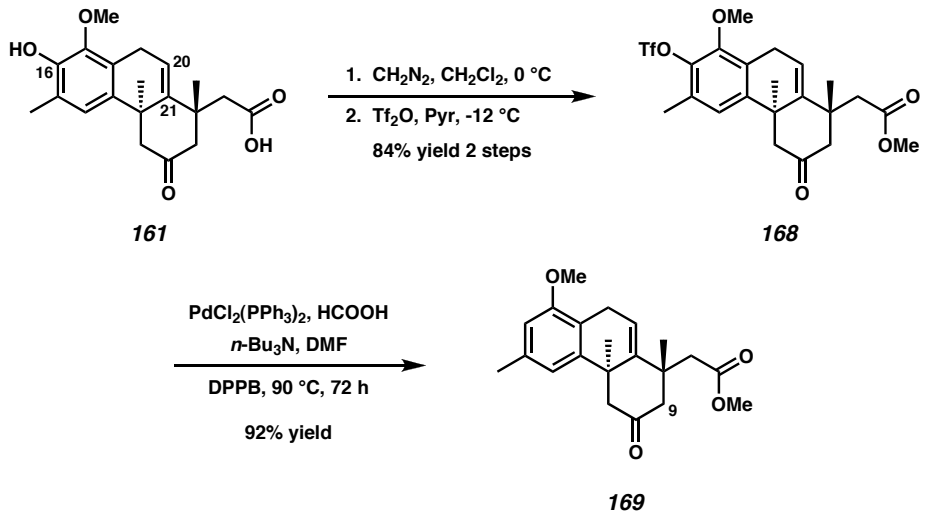

2.5.3 *Olefin Refunctionalization*

Due to our serendipitous discovery of the S_N' reaction, we had not anticipated the reoxygenation of the olefin in our retrosynthetic planning. Significant experimentation was required to find a synthetic strategy to reoxygenate the olefin of ketoester **169**. A number of atom-transfer oxidations were considered. Epoxidation conditions based on *m*CPBA, DMDO, UHP,[28] iron (III) acetylacetate and hydrogen peroxide,[29] hexafluoroacetone and hydrogen peroxide,[30] potassium permanganate and copper (II) sulfate,[31] and methyltrioxorhenium and hydrogen peroxide[32] all failed to give the desired oxidation.[33] Hydroboration of ester **170** with BH_3•THF did appear to affect hydroboration from both faces of the olefin. However, the products also seemed to have undergone reduction of the ester functionality and were inseparable (Scheme 2.16). Milder and more sterically demanding hydroborating reagents either caused ester reduction or failed to react at all.

Scheme 2.16 Hydroboration of Ester **170**

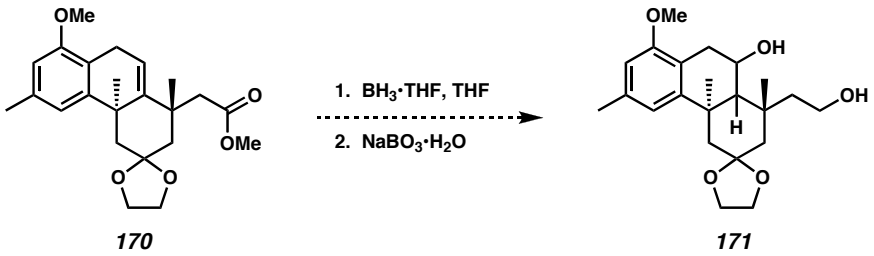

170 *171*

These difficulties were largely attributed to steric encumbrance around the C(20)-C(21) olefin. Figure 2.2 shows representations of the solid state structure of carboxylic acid **161**. While it is often problematic to infer solution conformations from solid state structures, the rigid nature of the carbocyclic system found in carboxylic acid **161** and ketoester **169** make it reasonable to assume that they will have conformations similar to one another in solution and in the solid state. The ball and stick model demonstrates that the C ring methyl groups are disposed in a nearly axial manner on either face of the olefin. The space-filling model demonstrates that a significant portion of the olefin is obstructed. In light of this, we chose to pursue a more classical, and importantly intramolecular, method of olefin oxygenation.

Figure 2.2 Ball and Stick and Space-Filling Representations of Carboxylic Acid **161**'s Solid State Structure

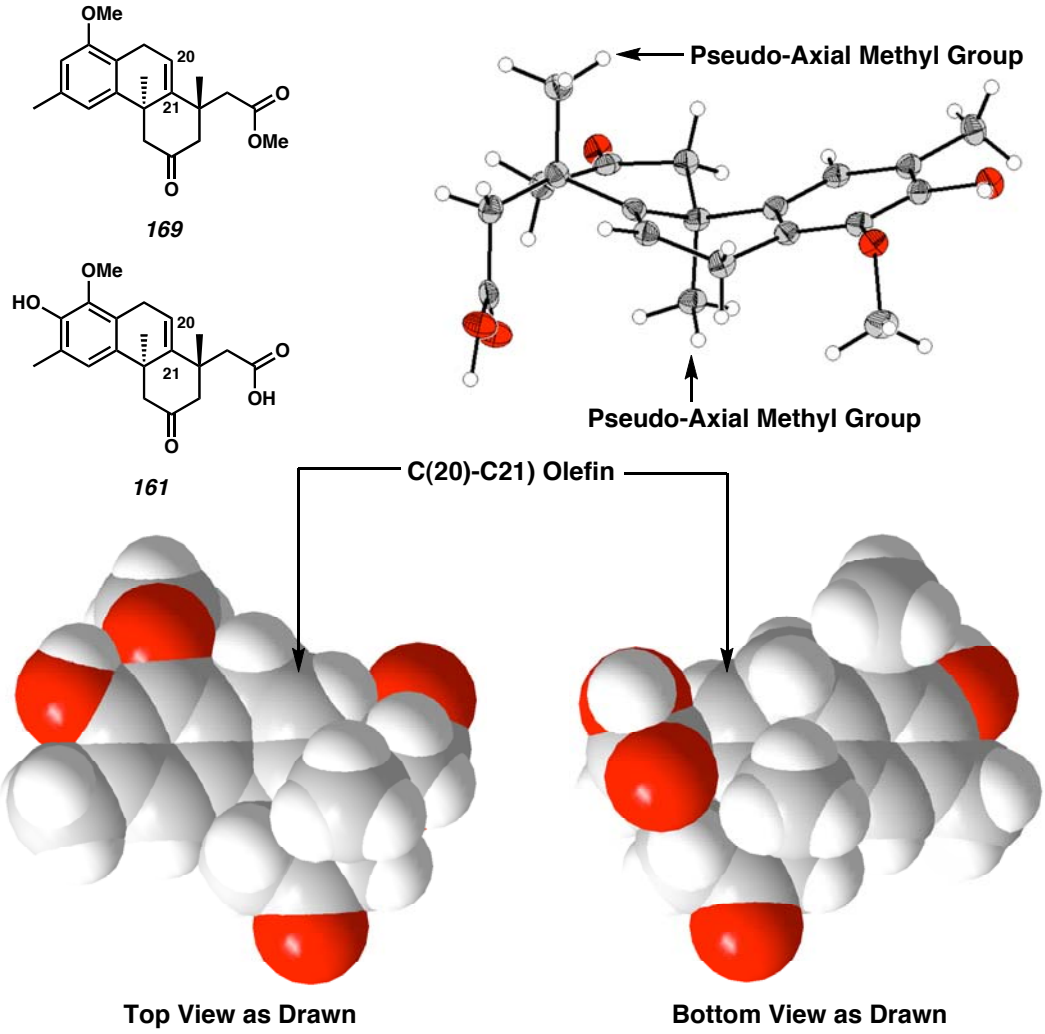

Our intramolecular functionalization began with saponification of ketoester **169** followed by ketalization under Dean-Stark conditions (Scheme 1.17). Although the two operations could be performed in either order, the rate of ketalization was greatly improved when the carboxylic acid was present in the molecule. Treatment of the crude ketalized acid with potassium iodide and iodine under mildly basic conditions gave iodolactone **172** in 85% yield for three steps after recrystallization. Treatment with

cesium carbonate in methanol afforded smooth conversion to epoxide **173**. Hydride migration from C(20) was affected by heating epoxide **173** in nonpolar solvents with magnesium chloride.[34,35] Though the reaction was somewhat sluggish, it gave clean conversion to rearranged ketoester **174** in 73% yield.

Scheme 2.17 Reoxygenation of the C(20)-C(21) Olefin

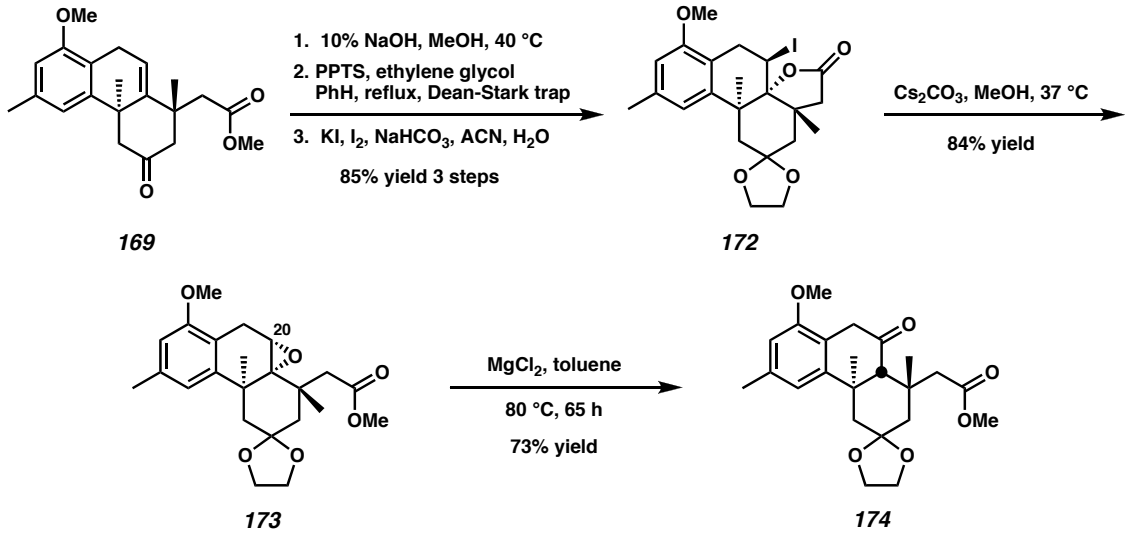

Typically, rearrangements of epoxides to carbonyl compounds give products of *syn*-hydride migration due to a concerted hydride shift, but anomalous products are known.[36] As a result, we wished to confirm the stereochemical outcome of the hydride migration (Scheme 2.18). Exposure of ketoester **174** to tosic acid in acetone produced diketone **175**, which gave crystals from acetone/heptane suitable for X-ray structure determination. The structure confirmed the desired C(21) stereochemistry from the hydride shift. With a successful strategy in hand for olefin refunctionalization, our next major objective was the synthesis of the final quaternary stereocenter.

Scheme 2.18 Confirmation of the Hydride Migration Stereochemistry

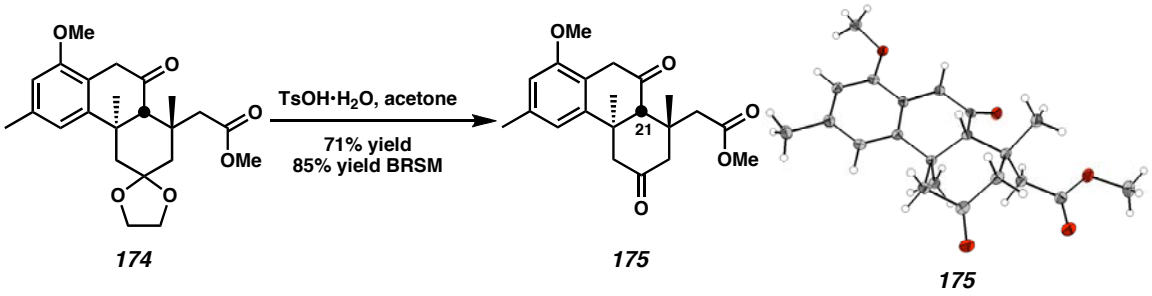

2.6 Introduction of the C(9) Quaternary Stereocenter

As shown in Scheme 2.19, our initial strategy for constructing the C(9) quaternary center involved three steps: (1) position-selective methylation at C(9), (2) condensation with an amine to give an enamine, and (3) conjugate addition of the enamine **177** or deprotonated metalloenamine into enone **178**. This strategy was closely modeled on the work of Williams.[37]

Scheme 2.19 Initial Strategy for Functionalization at C(9)

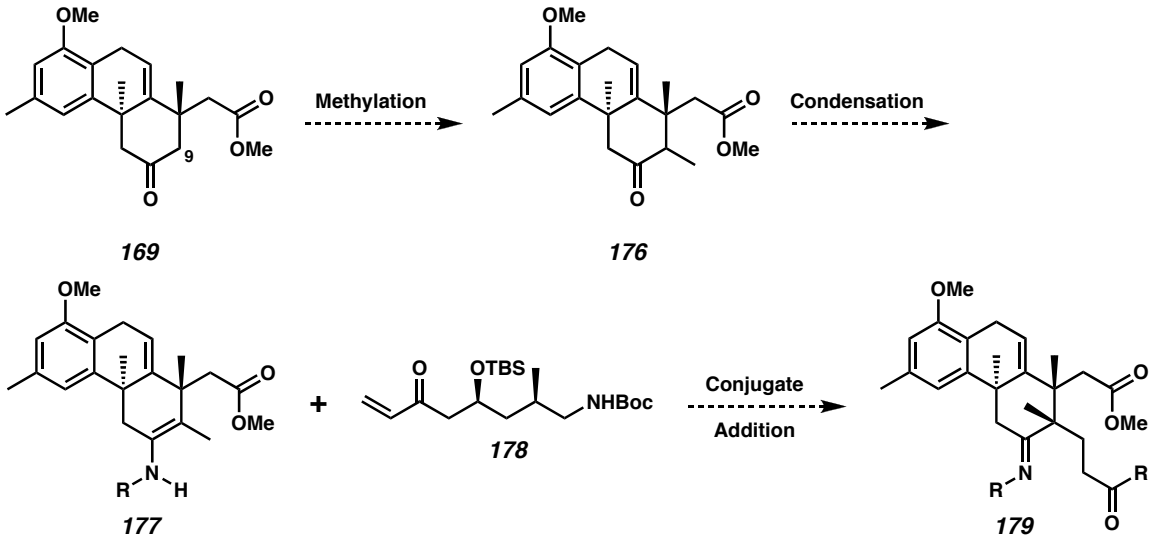

Selective enolization of C(9) over C(11) proved difficult (Scheme 2.20). When treated under kinetic conditions, ketoester **169** showed an unfavorable 4:1 ratio of silyl enol ethers. Though the silyl enol ethers were not separable, the major product was identified as silyl enol ether **180** due to a strong NOE interaction between vinylic enol proton and the arene proton. Analogous silylation with diketone **175** afforded an improved 1:1 mixture of silyl enol ethers **182** and **183**.[38] The bis silyl enol ethers were again inseparable and significant experimentation failed to improve the ratio. Under thermodynamic enolization conditions, nearly exclusive enolization was obtained at C(11) with ketoester **169**.[39]

Scheme 2.20 Positional Selectivity in Kinetic Silyl Enol Ether Formation

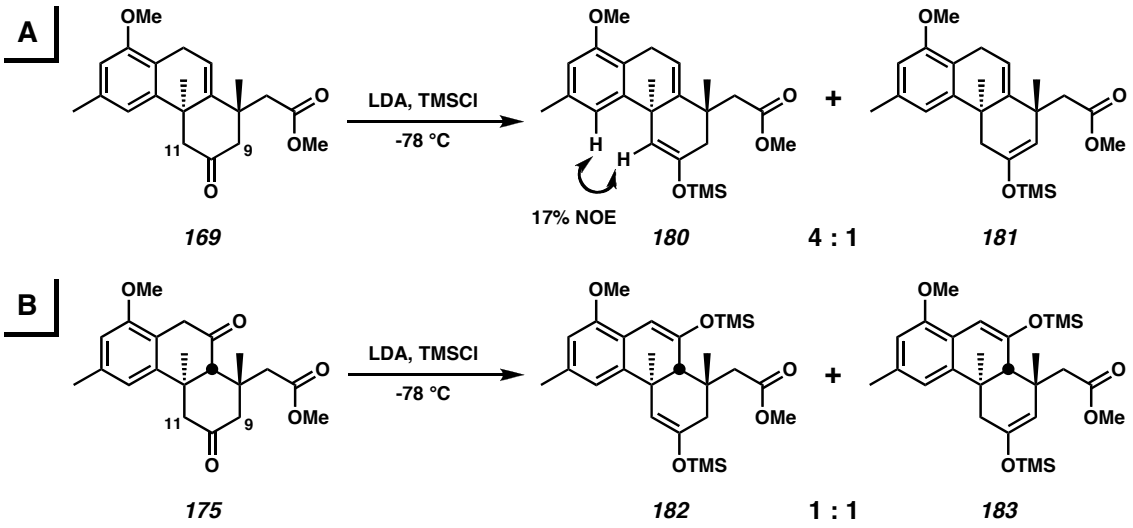

Further difficulties were encountered when trying to model the condensation to form the required imine (Scheme 2.21). Known ketone **184**[40] was treated with Dean-Stark dehydration conditions in the presence of benzyl amine, but afforded only trace amounts of what appeared to be the desired imine **185**.

Scheme 2.21 Amine Condensation with a Sterically Demanding Ketone

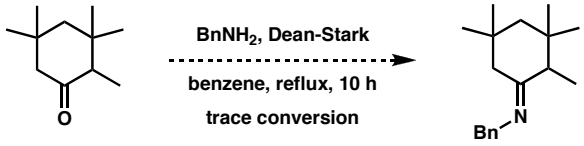

184 *185*

Our difficulty in modeling the conjugate addition strategy led us to consider other strategies to generate the C(9) quaternary stereocenter. Specifically, we examined a cyclopropanation approach,[41] similar to Hirama's strategy,[42] and a Tsuji allylation-based approach.[43] Ultimately, due to the lack of success with these additional strategies, we made the strategic decision to install the difficult vicinal quaternary stereocenters (i.e., C(9) and C(22)) early in the synthesis.

2.7 Concluding Remarks

A concise method for the construction of the zoanthenol ABC ring system was developed. Common to all our routes was the underlying strategy of combining A and C ring synthons and in the process generating the B ring. The final convergent strategy generated a fully functionalized A ring synthon from *o*-vanillin in six steps. Racemic synthesis of the C ring synthon was completed in just three steps from known materials. Of note is the carbonylation of hindered triflate **135** to enal **145**. Addition of the A ring Grignard **154** to enal **145** proceeded in a highly diastereoselective manner to combine the A and C ring fragments.

In the key step of the synthesis, allylic alcohol **155** underwent a S_N' Friedel-Crafts reaction in TFA. This diastereoselective transformation forms the B ring, sets the

difficult benzylic quaternary stereocenter, and removes three protecting groups in a single step. Only eight linear steps were required to establish the ABC ring system of zoanthenol. To our knowledge, this represents the first use of such an S_N' cyclization in total synthesis. Significant progress was made in advancing the ABC ring system to include all the functionality needed to complete the synthesis. Ultimately, difficulties in forming the final quaternary stereocenter at a late stage forced us to re-evaluate our retrosynthetic path. The route did not allow us to complete the total synthesis, but experience with the advanced ABC carbocycles taught us invaluable lessons about the difficulty of generating quaternary stereocenters and the increased challenge of performing otherwise standard chemistries adjacent to them.

2.8 Experimental Procedures

2.8.1 *Materials and Methods*

Unless otherwise stated, reactions were performed at ambient temperature (typically 19-24 °C) in flame-dried glassware under an argon or nitrogen atmosphere using dry, deoxygenated solvents. Solvents were dried by passage through an activated alumina column under argon. TMEDA, HMPA, TEA, DIPA and pyridine were freshly distilled from CaH. KHMDS (95%) was purchased from Aldrich and stored in a glovebox until use. Trifluoroacetic acid (99%) was purchased from Aldrich. Tf_2O was freshly distilled from P_2O_5. Magnesium chloride (~325 mesh, <1.5% H_2O) was purchased from Aldrich. All other commercially obtained reagents were used as received. Reaction temperatures were controlled by an IKAmag temperature modulator. Thin-layer chromatography (TLC) was performed using E. Merck silica gel 60 F254

precoated plates (0.25 mm) and visualized by UV fluorescence quenching, anisaldehyde, $KMnO_4$, or CAM staining. ICN silica gel (particle size 0.032-0.063 mm) was used for flash chromatography. Optical rotations were measured with a Jasco P-1010 polarimeter at 589 nm. ^{1}H and ^{13}C NMR spectra were recorded on a Varian Mercury 300 (at 300 MHz and 75 MHz, respectively), or a Varian Inova 500 (at 500 MHz and 125 MHz, respectively) and are reported relative to Me_4Si (δ 0.0). Data for ^{1}H NMR spectra are reported as follows: chemical shift (δ ppm) (multiplicity, coupling constant (Hz), integration). Multiplicities are reported as follows: s = singlet, d = doublet, t = triplet, q = quartet, sept. = septet, m = multiplet, comp. m = complex multiplet, app. = apparent, bs = broad singlet. IR spectra were recorded on a Perkin Elmer Paragon 1000 spectrometer and are reported in frequency of absorption (cm^{-1}). High resolution mass spectra were obtained from the California Institute of Technology Mass Spectral Facility. Crystallographic analyses were performed at the California Institute of Technology Beckman Institute X-Ray Crystallography Laboratory. Crystallographic data have been deposited at the CCDC, 12 Union Road, Cambridge CB2 1EZ, UK, and copies can be obtained on request, free of charge, from the CCDC by quoting the publication citation and the deposition number (see Appendix Three for deposition numbers).

2.8.2 *Preparation of Compounds*

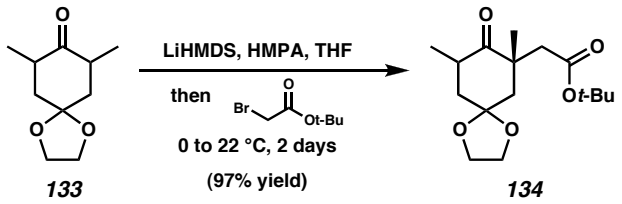

Ketoester 134. To a cooled (0 °C) 1.00 M LiHMDS (52.2 mL, 52.2 mmol, 1.20 equiv) solution in THF was added ketone **133** (8.00 g, 43.5 mmol, 1.00 equiv) in THF (50 mL) in a dropwise manner over 30 min. After an additional 30 min at 0 °C, HMPA (8.31 mL, 47.8 mmol, 1.10 equiv) was added and maintained at 0 °C for 1 h. *t*-butyl bromoacetate (10.6 mL, 69.5 mmol, 1.60 equiv) was added in portions over 1 h and, after a further 2 h at 0 °C, allowed to warm to ambient temperature. After 48 h, the reaction mixture was poured into H_2O (300 mL), extracted with Et_2O (6 x 150 mL), dried ($MgSO_4$), and concentrated to an oil, which was purified by flash chromatography on silica gel (7 to 10% EtOAc in hexanes) to provide ketoester **134** (12.5 g, 97% yield) as a pale yellow oil (as a ~3:1 mixture of diastereomers). See below for full characterization of both methyl diastereomers, synthesized in enantioenriched form via asymmetric allylation.

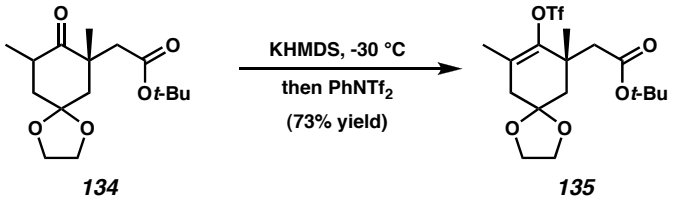

Triflate 135. To a cooled (-30 °C) solution of KHMDS (4.41 g, 22.1 mmol, 1.20 equiv) in THF (35 mL) was added ketoester **134** (5.50 g, 18.5 mmol, 1.00 equiv) in THF (30 mL) in a dropwise manner over 10 min. After 5 h at -30 °C, $PhNTf_2$ (7.20 g, 20.2

mmol, 1.09 equiv) in THF (30 mL) was added, maintained for an additional 30 min at -30 °C, and warmed to 0 °C for 2 h. The reaction mixture was diluted with Et_2O (200 mL), poured into a mixture of brine (150 mL), H_2O (150 mL), and 1 M NaOH (50 mL), and extracted with Et_2O (3 x 50 mL). The organic layers were washed with 1 M NaOH (6 x 50 mL), H_2O (50 mL), and brine (3 x 50 mL), dried (Na_2SO_4), and concentrated to an oil, which was purified by flash chromatography on silica gel (7 to 10% EtOAc in hexanes and 0.5 % TEA) to provide triflate **135** (5.74 g, 73% yield) as a pale yellow oil: R_f 0.63 (35% EtOAc in hexanes); ^{1}H NMR (300 MHz, $CDCl_3$) δ 4.02-3.92 (comp. m, 4H), 2.71 (d, J = 14.5 Hz, 1H), 2.45 (s, 2H), 2.42 (d, J = 13.5 Hz, 1H), 2.30 (d, J = 14.7 Hz, 1H), 1.78 (s, 3H), 1.70 (d, J = 13.8 Hz, 1H), 1.42 (s, 9H), 1.32 (s, 3H); ^{13}C NMR (75 MHz, $CDCl_3$) δ 70.2, 146.9, 124.5, 118.7 (q, $J_{C\text{-}F}$ = 319 Hz), 106.2, 80.5, 64.4, 64.3, 43.1, 42.0, 41.9, 39.2, 28.0, 25.0, 17.8; IR (Neat film NaCl) 2980, 2935, 2888, 1726, 1403, 1212, 1142, 1007, 862 cm^{-1}; HRMS (FAB) $[M+H]^+$ calc'd for $[C_{17}H_{25}SF_3O_7+H]^+$: m/z 431.1351, found 431.1365.

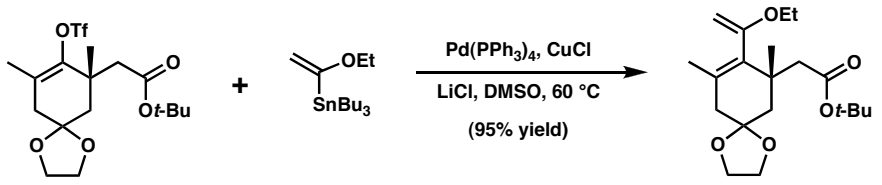

135 *136* *137*

Diene 137. A solution of triflate **135** (azeotroped from PhH, 717 mg, 1.67 mmol, 1.0 equiv) in DMSO (17 mL) was added to an argon-filled, flame-dried Schlenk flask (50 mL) charged with LiCl (flamed-dried under vacuum, 422 mg, 10.0 mmol, 6.0 equiv), $Pd(PPh_3)_4$ (193 mg, 0.167 mmol, 0.10 equiv), and CuCl (825 mg, 8.33 mmol, 5.0 equiv). The flask was purged (5 x) with argon, and vinyl stannane **136** (1.02 g, 2.83 mmol, 1.70

equiv) was added as a neat liquid. The resulting mixture was degassed (3 x) by the freeze/pump-thaw process (-78 to 25 °C, Ar), and stirred at ambient temperature for 1 h, then for a further 12 h at 60 °C. The reaction mixture was quenched with Et_2O (30 mL), brine (120 mL), and 5% aq. NH_4OH (30 mL), and the aqueous layer was further extracted with Et_2O (4 x 30 mL). The combined organic layers were washed with H_2O (4 x 30 mL), then brine (2 x30 mL), dried ($MgSO_4$), and concentrated to give an oil, which was purified by flash chromatography on silica gel (5% EtOAc in hexanes) to give diene **137** (557 mg, 95% yield) as a pale yellow oil: R_f 0.59 (20% EtOAc in hexanes developed twice); ^{1}H NMR (300 MHz, $CDCl_3$) δ 4.18 (d, *J* = 1.8 Hz, 1H), 4.08-3.90 (comp. m, 4H), 3.84 (d, *J* = 1.8 Hz, 1H), 3.72 (dq, *J* = 1.5, 6.9 Hz, 2H), 2.62 (d, *J* = 14.4 Hz, 1H), 2.39 (d, *J* = 13.8 Hz, 1H), 2.35 (d, *J* = 17.7 Hz, 1H), 2.28 (dd, *J* = 1.0, 13.7 Hz, 1H), 2.25 (d, *J* = 18.0 Hz, 1H), 1.67 (s, 3H), 1.56 (d, *J* = 13.8 Hz, 1H), 1.43 (s, 9H), 1.29 (t, *J* = 7.0 Hz, 3H), 1.18 (s, 3H); ^{13}C NMR (75 MHz, $CDCl_3$) δ 171.9, 158.9, 135.7, 130.3, 107.6, 86.3, 79.7, 64.2, 64.0, 62.5, 44.5, 41.6, 40.3, 38.4, 28.2, 26.6, 21.1, 14.5; IR (Neat film NaCl) 2978, 2930, 2879, 1722, 1606, 1368, 1268, 1142, 1093, 977, 806 cm^{-1}; HRMS (FAB) $[M+H]^+$ calc'd for $[C_{20}H_{32}O_5+H]^+$: *m/z* 353.2328, found 353.2334.

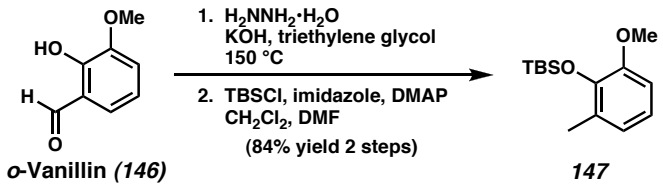

Arene 147. To a warmed solution (110 °C for 45 min) of *o*-vanillin (60.0 g, 0.394 mol, 1.00 equiv) and NH_2NH_2•H_2O (53.6 mL, 1.10 mol, 2.79 equiv) in triethylene glycol (320 mL) in a 1 L round bottom flask was added KOH (132 g, 2.37 mol, 6.02

equiv) [*Caution: gas evolution and exotherm*] in portions over 20 min. The reaction mixture was maintained at 150 °C under a reflux condenser for 5 h, cooled to ambient temperature, and poured into H_2O (750 mL), ice (200 g), and 6 M HCl (500 mL). The mixture was further acidified to pH 2 with 6 M HCl, then extracted with $CHCl_3$ (7 x 200 mL), dried ($MgSO_4$), and evaporated to give a green solid (~60 g) that was immediately used in the next step without further purification.

To a solution of this crude solid in DMF (300 mL) and CH_2Cl_2 (300 mL) were added imidazole (53.6 g, 0.788 mol, 2.00 equiv), DMAP (62.5 g, 0.512 mol, 1.30 equiv), and TBSCl (62.1 g, 0.414 mol, 1.05 equiv). After 4 h at ambient temperature, the reaction mixture was poured into H_2O (1.3 L), extracted with CH_2Cl_2 (3 x 150 mL), and the combined organic layers were washed with cold 0.25 M HCl (2 x 250 mL), 1 M NaOH (250 mL), and brine (2 x 200 mL). Evaporation of the organics gave an oil, which was purified by distillation at reduced pressure (~2 mmHg) to give arene **147** (83.6 g, bp 120-127 °C at 2 mmHg, 84% yield over 2 steps) as a colorless oil: R_f 0.74 (10% EtOAc in hexanes); ^{1}H NMR (300 MHz, $CDCl_3$) δ 6.83-6.69 (comp. m, 3H), 3.78 (s, 3H), 2.24 (s, 3H), 1.01 (s, 9H), 0.18 (s, 6H); ^{13}C NMR (75 MHz, $CDCl_3$) δ 150.0, 143.1, 129.6, 122.8, 120.5, 109.1, 54.8, 26.1, 18.9, 17.1, -3.9; IR (Neat film NaCl) 2955, 2930, 1488, 1280, 1251, 1233, 1086, 920, 781 cm^{-1}; HRMS (FAB) $[M+H]^+$ calc'd for $[C_{14}H_{24}SiO_2+H]^+$: *m/z* 253.1624, found 253.1633.

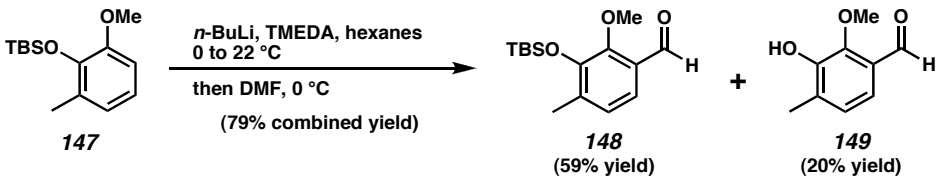

Benzaldehyde 148 from arene **147**. To a cooled (0 °C) solution of arene **147** (30.0 g, 119 mmol, 1.00 equiv), and TMEDA (25.1 mL, 166 mmol, 1.40 equiv) in hexanes (200 mL) was added *n*-BuLi (2.25 M in hexanes, 63.4 mL, 142 mmol, 1.20 equiv) in a dropwise manner over 15 min. After 1 h at 0 °C, the reaction mixture was allowed to warm to ambient temperature for 6 h. The reaction mixture was cooled (0 °C) again and DMF (15.6 mL, 202 mmol, 1.70 equiv) was added dropwise over 10 min. After an additional 1 h at 0 °C, saturated aqueous NH_4Cl (100 mL) was added, and the mixture was allowed to warm to ambient temperature overnight. The mixture was poured into H_2O (200 mL) and Et_2O (200 mL), then extracted with Et_2O (2 x 100 mL). The aqueous layers were then acidified with 2 M HCl to pH 1, and further extracted with Et_2O (5 x 150 mL). The combined organic layers were washed with brine (50 mL), dried (Na_2SO_4), and evaporated to give an oil that was purified by gradient flash chromatography on silica gel (2 to 20% EtOAc in hexanes) to give benzaldehyde **148** (19.7 g, 59% yield) as a colorless oil: R_f 0.67 (20% EtOAc in hexanes); ^{1}H NMR (300 MHz, $CDCl_3$) δ 10.28 (s, 1H), 7.36 (d, J = 7.5 Hz, 1H), 6.98 (d, J = 8.1 Hz, 1H), 3.81 (s, 3H), 2.28 (s, 3H), 1.03 (s, 9H), 0.20 (s, 6H); ^{13}C NMR (75 MHz, $CDCl_3$) δ 189.7, 154.2, 147.2, 138.4, 128.1, 126.4, 120.7, 62.5, 26.0, 18.6, 17.9, -4.1; IR (Neat film NaCl) 2957, 2932, 2859, 1691, 1464, 1273, 1255, 838 cm^{-1}; HRMS (FAB) $[M+H]^+$ calc'd for $[C_{15}H_{24}SiO_3+H]^+$: m/z 281.1573, found 281.1572 and phenol **149** (3.9 g, 20% yield) as a white solid: mp 90.0-91.0 °C; R_f 0.25 (20% EtOAc in hexanes); ^{1}H NMR (300 MHz,

$CDCl_3$) δ 10.18 (s, 1H), 7.27 (d, *J* = 8.1 Hz, 1H), 7.01 (d, *J* = 8.1 Hz, 1H), 6.02 (bs, 1H), 3.95 (s, 3H), 2.32 (s, 3H); ^{13}C NMR (75 MHz, $CDCl_3$) δ 189.4, 148.4, 147.5, 132.8, 126.7, 126.5, 121.3, 63.8, 16.3; IR (Neat film NaCl) 3410, 2938, 2857, 1686, 1466, 1261, 1061, 782 cm^{-1}; HRMS (FAB) $[M+H]^+$ calc'd for $[C_9H_{10}O_3+H]^+$: *m/z* 167.0708, found 167.0708.

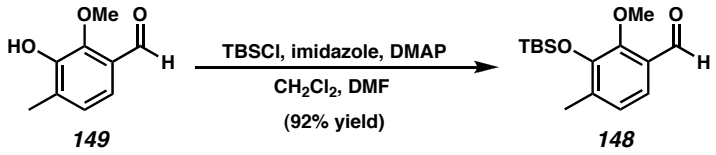

149 ***148***

Benzaldehyde 148 from phenol **149**. To a solution of phenol **149** (10.0 g, 60.2 mmol, 1.00 equiv) in DMF (60 mL) and CH_2Cl_2 (60 mL) were added imidazole (8.20 g, 120 mmol, 2.00 equiv), DMAP (9.55 g, 78.3 mmol, 1.30 equiv), and TBSCl (11.7 g, 78.3 mmol, 1.30 equiv). After 36 h, the reaction mixture was quenched with H_2O (200 mL) and CH_2Cl_2 (200 mL), and extracted with CH_2Cl_2 (3 x 50 mL) The combined organics were washed with H_2O (200 mL) and then brine (100 mL), dried ($MgSO_4$), and concentrated to an oil, which was purified by flash chromatography on silica gel (2% EtOAc in hexanes) to provide benzaldehyde **148** (15.5 g, 92% yield).

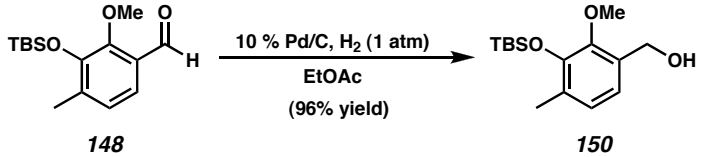

148 ***150***

Benzyl alcohol 150. A flame-dried 100 mL round-bottom flask was charged with 10% Pd/C (270 mg), EtOAc (55 mL), and benzaldehyde **148** (2.0 g, 7.13 mmol, 1.00 equiv) under an N_2 atmosphere. The reaction mixture and head space were sparged with

H_2 (5 min) and stirred vigorously under an atmosphere of H_2 (balloon) for 3 h. Immediately following the completion of the reaction, as indicated by TLC, the reaction mixture was sparged with N_2 for 15 min then concentrated to an oil, which was purified by flash chromatography on silica gel (10 to 15% EtOAc in hexanes) to provide benzyl alcohol **150** (1.93 g, 96% yield) as a colorless oil: R_f 0.33 (20% EtOAc in hexanes); ^{1}H NMR (300 MHz, $CDCl_3$) δ 6.88 (d, *J* = 7.5 Hz, 1H), 6.83 (d, *J* = 8.1 Hz, 1H), 4.65 (d, *J* = 6.3 Hz, 2H), 3.75 (s, 3H), 2.25 (t, *J* = 6.3 Hz, 1H), 2.21 (s, 3H), 1.03 (s, 9H), 0.18 (s, 6H); ^{13}C NMR (75 MHz, $CDCl_3$) δ 49.4, 147.0, 132.4, 130.6, 126.1, 121.1, 61.7, 60.5, 26.0, 18.6, 17.2, -4.2; IR (Neat film NaCl) 3340, 2956, 2931, 2859, 1464, 1420, 1285, 839, 782 cm^{-1}; HRMS (FAB) $[M+H-H_2]^+$ calc'd for $[C_{15}H_{25}SiO_3]^+$: m/z 281.1573, found 281.1564.

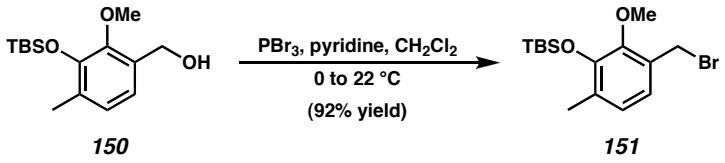

150 ***151***

Benzyl bromide 151. To a cooled (0 °C) solution of benzyl alcohol **150** (16.0 g, 56.7 mmol, 1.00 equiv) and pyridine (4.36 mL, 53.9 mmol, 0.95 equiv) in CH_2Cl_2 (200 mL) was added PBr_3 (4.84 mL, 51.0 mmol, 0.90 equiv) in CH_2Cl_2 (50 mL) over 30 min. After stirring an additional 30 min at 0 °C, the reaction mixture was allowed to come to ambient temperature and stirred for a further 2.5 h. The reaction mixture was diluted with CH_2Cl_2 (300 mL), brine (500 mL), and H_2O (250 mL), then extracted with Et_2O (2 x 150 mL), dried over Na_2SO_4, and concentrated. The resulting oil was passed through a plug of silica gel (10 cm h x 5.5 cm d) (1:1 hexanes:CH_2Cl_2), concentrated, and the resultant oil was purified by distillation at reduced pressure (~2 mmHg) to provide benzyl bromide **151** (27.4 g, bp 146-147 °C at ~2 mmHg, 92% yield) as a colorless oil: R_f 0.50

(2.5% EtOAc in hexanes); ^{1}H NMR (300 MHz, $CDCl_3$) δ 6.91 (d, *J* = 8 Hz, 1H), 6.87 (d, *J* = 8 Hz, 1H), 4.56 (s, 2H), 3.83 (s, 3H), 2.23 (s, 3H), 1.04 (s, 9H), 0.18 (s, 6H); ^{13}C NMR (75 MHz, $CDCl_3$) δ 49.7, 147.2, 131.9, 129.6, 126.2, 123.2, 60.4, 28.8, 26.0, 18.6, 17.3, -4.2; IR (Neat film NaCl) 2957, 2931, 2859, 1464, 1421, 1289, 1259, 1239, 1072, 840, 782 cm^{-1}; HRMS (FAB) $[M+H]^+$ calc'd for $[C_{15}H_{25}SiBrO_2+H]^+$: *m/z* 345.0885, found 345.0885.

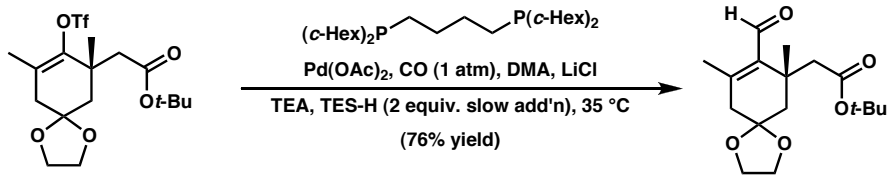

135 ***145***

Enal 145. A solution of flame-dried LiCl (600 mg, 14.2 mmol, 2.69 equiv), $Pd(OAc)_2$ (156 mg, 0.695 mmol, 0.132 equiv), and 1,4-bis-(dicyclohexylphosphino)butane (314 mg, 0.695 mmol, 0.132 equiv) in DMA (16 mL) was sparged with CO and warmed to 90 °C until a color change from red/orange to pale yellow was observed, at which point the reaction mixture was cooled to 35 °C. To the homogenous reaction mixture was added TEA (2.60 mL, 18.6 mmol, 3.53 equiv) and enol triflate **135** (2.27 g, 5.27 mmol, 1.00 equiv) in DMA (16 mL). A solution of Et_3SiH (1.47 mL, 9.28 mmol, 1.76 equiv) in DMA (8.5 mL) was added by syringe pump to the reaction over 10 h. After an additional 14 h at 35 °C, the reaction mixture was cooled to ambient temperature, $KF•2H_2O$ (2.00 g) was added, the mixture was stirred for 45 min, and then poured into ice water (200 mL). This mixture was extracted with 1:1 Et_2O:hexanes (5 x 100 mL). The combined organic layers were washed with brine (2 x 100 mL), dried (Na_2SO_4), and concentrated to give an oil, which was purified by gradient

flash chromatography on silica gel (10 to 20% EtOAc in hexanes) to give enal **145** (1.24 g, 76% yield) as a pale yellow oil: R_f 0.42, 0.41 (35% EtOAc in hexanes, 20% EtOAc in hexanes developed twice); ^{1}H NMR (300 MHz, $CDCl_3$) δ 10.13 (s, 1H), 4.00-3.90 (comp. m, 4H), 3.04 (d, *J* = 14.4 Hz, 1H), 2.54 (app. dt, *J* = 1.0, 19.2 Hz, 1H), 2.37 (dd, *J* = 1.8, 18.9 Hz, 1H), 2.34 (d, *J* = 14.7 Hz, 1H), 2.15 (d, *J* = 13.6 Hz, 1H), 2.12 (s, 3H), 1.53 (dd, *J* = 2, 13.6 Hz, 1H), 1.35 (s, 9H), 1.33 (s, 3H); ^{13}C NMR (75 MHz, $CDCl_3$) δ 91.0, 171.3, 152.8, 137.4, 106.5, 79.8, 64.3, 64.0, 44.7 (2C), 42.4, 38.3, 28.0, 26.5, 19.3; IR (Neat film NaCl) 2977, 2932, 2884, 1721, 1673, 1368, 1161, 1141, 1079 cm^{-1}; HRMS (FAB) $[M+H]^+$ calc'd for $[C_{17}H_{26}O_5+H]^+$: *m/z* 311.1858, found 311.1849.

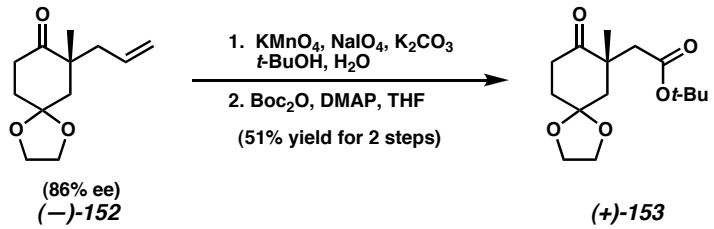

(+)-*t*-Butyl ester 153. A solution of ketone (–)-**152** (1.00 g, 4.76 mmol, 1.00 equiv) and K_2CO_3 (987 mg, 7.14 mmol, 1.5 equiv) in *t*-BuOH (60 mL) was treated (slight exotherm) with a premixed (30 min) solution of $NaIO_4$ (8.14 g, 38.1 mmol, 8.00 equiv) and $KMnO_4$ (113 mg, 0.714 mmol, 0.15 equiv) in H_2O (100 mL) and stirred in a room temperature bath for 3 h. The reaction mixture was diluted with CH_2Cl_2 (100 mL) and H_2O (100 mL), extracted with CH_2Cl_2 (6 x 50 mL), dried ($MgSO_4$), and concentrated to an oil, which was used immediately in the next step.

A solution of the above crude carboxylic acid in THF (40 mL) was treated with Boc_2O (3.40 g, 15.6 mmol, 3.27 equiv) and DMAP (200 mg, 1.64 mmol, 0.344 equiv). After 12 h, additional Boc_2O (2.00 g, 9.16 mmol, 1.93 equiv) and DMAP (175 mg, 1.43 mmol,

0.30 equiv) were added, and the reaction was stirred for a further 3 h. The reaction mixture was concentrated and purified by gradient flash chromatography on silica gel (5 to 25% Et_2O in hexanes) to give (+)-*t*-butyl ester **153** (688 mg, 51% yield) as a colorless oil: R_f 0.27 (10% EtOAc in hexanes developed 2 times); ^{1}H NMR (300 MHz, $CDCl_3$) δ 4.03-3.94 (comp. m, 4H), 2.70 (d, *J* = 15.9 Hz, 1H), 2.63 (d, *J* = 6.6 Hz, 1H), 2.60 (d, *J* = 6.0 Hz, 1H), 2.49 (d, *J* = 15.9 Hz, 1H), 2.22 (dd, *J* = 1.4, 14.0 Hz, 1H), 2.20-2.08 (m, 1H), 2.04-1.92 (m, 1H), 1.78 (dd, *J* = 2.4, 14.1 Hz, 1H), 1.40 (s, 9H), 1.20 (s, 3H); ^{13}C NMR (75 MHz, $CDCl_3$) δ 212.7, 170.7, 107.6, 80.7, 64.4, 64.2, 46.0, 44.7, 44.5, 35.6, 33.9, 28.0, 25.1; IR (Neat film NaCl) 2976, 2935, 2885, 1725, 1714, 1368, 1157, 1120, 1074 cm^{-1}; HRMS (EI) $[M]^+$ calc'd for $[C_{15}H_{24}O_5]^+$: *m/z* 284.1624, found 284.1633; $[\alpha]_D^{26}$ +45.63 (c 1.89, CH_2Cl_2, 86% ee).

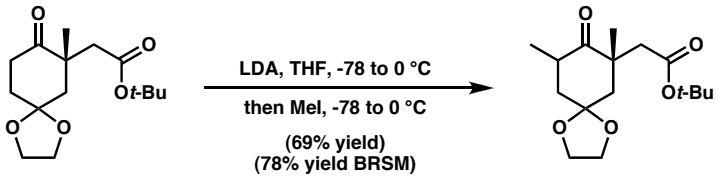

(+)-153 *134*

Methyl ketones 134a and 134b. A solution of LDA in THF was prepared by dropwise addition of 2.45 M *n*-BuLi solution in hexanes (787 μL, 1.93 mmol, 1.4 equiv) to diisopropylamine (290 μL, 2.07 mmol, 1.5 equiv) in THF (20.7 mL) at 0 °C, followed by stirring for 1 h. Upon cooling the solution to -78 °C, a solution of (+)-*t*-butyl ester **153** (392 mg, 1.38 mmol, 1.00 equiv) in THF (2.00 mL) was added in a dropwise manner, and the reaction mixture was stirred at -78 °C for 1 h, then 0 °C for 1 h. After cooling again to -78 °C, the reaction mixture was treated with MeI (258 μL, 4.13 mmol, 3.00 equiv), allowed to warm to ambient temperature slowly over 5 h, and stirred for an

additional 12 h at ambient temperature. The reaction mixture was quenched with saturated aqueous $NaHCO_3$ (10 mL), extracted with CH_2Cl_2 (6 x 30 mL), dried ($MgSO_4$), and concentrated to an oil, which was purified by gradient flash chromatography on silica gel (3 to 10% EtOAc in hexanes) to give diastereomeric methyl ketones **134a** and **134b** (284 mg, 69% combined yield) as colorless oils and recovered *t*-butyl ester **153** (43.2 mg, 11% yield). High R_f diastereomer **134a**: R_f 0.43 (10% EtOAc in hexanes developed 2 times); ^{1}H NMR (300 MHz, $CDCl_3$) δ 4.10-3.90 (comp. m, 4H), 2.89 (app. d of sept., J = 1.2, 6.6 Hz, 1H), 2.73 (d, J = 16.5 Hz, 1H), 2.36 (d, J = 13.8 Hz, 1H), 2.16 (d, J = 16.2 Hz, 1H), 2.06-1.96 (comp. m, 1H), 1.93 (d, J = 13.5 Hz, 1H), 1.85 (dd, J = 3.3, 13.8 Hz, 1H), 1.42 (s, 9H), 1.29 (s, 3H), 1.07 (d, J = 6.9 Hz, 3H); ^{13}C NMR (75 MHz, $CDCl_3$) δ 214.0, 170.9, 107.5, 80.4, 64.6, 64.0, 46.0, 44.5, 44.3, 41.9, 38.0, 28.1, 26.4, 14.7; IR (Neat film NaCl) 2976, 2932, 2880, 1726, 1710, 1367, 1146, 1080 cm^{-1}; HRMS (EI) $[M]^+$ calc'd for $[C_{16}H_{26}O_5]^+$: m/z 298.1780, found 298.1791; $[\alpha]_D^{26}$ +45.13 (c 1.06, CH_2Cl_2, 86% ee). Low R_f diastereomer **134b**: R_f 0.32 (10% EtOAc in hexanes developed 2 times); ^{1}H NMR (300 MHz, $CDCl_3$) δ 4.10-3.85 (comp. m, 4H), 3.21 (d, J = 14.7 Hz, 1H), 3.09 (app. d of sept., J = 1.5, 6.6 Hz, 1H), 2.32 (d, J = 14.4 Hz, 1H), 2.14-2.00 (comp. m, 2H), 1.76 (d, J = 14.7 Hz, 1H), 1.68 (app. t, J = 14.0 Hz, 1H), 1.36 (s, 9H), 1.08 (s, 3H), 1.03 (d, J = 6.3 Hz, 3H); ^{13}C NMR (75 MHz, $CDCl_3$) δ 213.8, 170.4, 107.2, 80.8, 64.6, 64.0, 46.8, 46.1, 45.2, 43.9, 37.7, 27.9, 23.0, 14.4; IR (Neat film NaCl) 2976, 2933, 2884, 1726, 1717, 1457, 1367, 1232, 1160, 1141, 1084, 979 cm^{-1}; HRMS (EI) $[M]^+$ calc'd for $[C_{16}H_{26}O_5]^+$: m/z 298.1780, found 298.1775; $[\alpha]_D^{26}$ –25.44 (c 1.17, CH_2Cl_2, 86% ee).

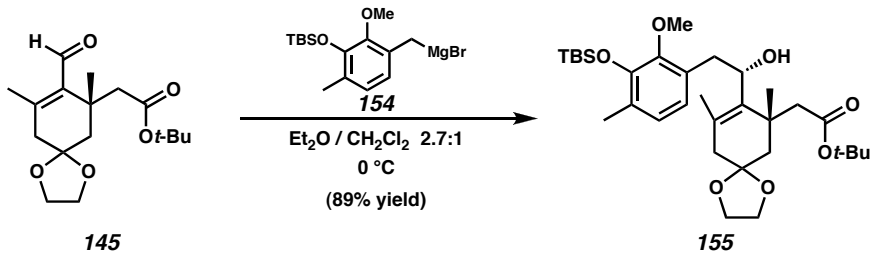

Allylic alcohol 155. A flame-dried two-neck round-bottom flask equipped with a reflux condenser and septum was charged with magnesium turnings (9.00 g, 370 mmol, 34.6 equiv) and Et_2O (120 mL) under an N_2 atmosphere and heated to reflux. To this mixture was added 1,2-dibromoethane (1.53 mL, 17.8 mmol, 1.66 equiv) in a dropwise manner [*Caution: gas evolution!*]. When gas evolution ceased, a solution of benzyl bromide **151** (5.91 g, 17.1 mmol, 1.60 equiv) in Et_2O (50 mL) was added in a dropwise manner over 30 min and heating was continued for an additional 30 min. The Grignard reagent was then cooled (0 °C), and added to a cooled (0 °C) solution of enal **145** (3.32 g, 10.7 mmol, 1.00 equiv) in Et_2O (100 mL) and CH_2Cl_2 (100 mL). After 1 h, the reaction mixture was quenched with H_2O (200 mL) and saturated aqueous NH_4Cl (100 mL), extracted with Et_2O (3 x 200 mL), dried ($MgSO_4$), and concentrated to an oil, which was purified by gradient flash chromatography on silica gel (7.5 to 20% EtOAc in hexanes) to give allylic alcohol **155** (5.51 g, 89% yield) as a thick syrup: R_f 0.59 (20% EtOAc in hexanes developed twice); ^{1}H NMR (300 MHz, $CDCl_3$) δ 6.83 (s, 2H), 4.43 (dd, J = 2.1, 9.9 Hz, 1H), 4.04-3.90 (comp. m, 4H), 3.68 (s, 3H), 3.22 (bs, 1H), 3.17 (dd, J = 9.9, 13.8 Hz, 1H), 2.84 (dd, J = 3.3, 13.8 Hz, 1H), 2.64 (d, J = 13.5 Hz, 1H), 2.31 (d, J = 17.4 Hz, 1H), 2.24-2.04 (comp. m, 3H), 2.19 (s, 3H), 2.07 (s, 3H), 1.57 (dd, J = 2.3, 13.8 Hz, 1H), 1.40 (s, 9H), 1.12 (s, 3H), 1.02 (s, 9H), 0.18 (s, 3H), 0.16 (s, 3H); ^{13}C NMR (75 MHz, $CDCl_3$) δ 72.1, 149.6, 147.0, 136.7, 131.3, 130.5, 128.7, 125.7, 123.5, 107.6, 80.9, 70.6,

64.2, 63.9, 59.9, 46.4, 43.3, 42.0, 41.3, 36.6, 28.0, 26.8, 26.0, 21.1, 18.6, 17.0, -4.1 (2C); IR (Neat film NaCl) 3499, 2957, 2931, 2896, 2859, 1706, 1462, 1419, 1368, 1286, 1075, 840 cm^{-1}; HRMS (FAB) $[M+H]^+$ calc'd for $[C_{32}H_{52}SiO_7+H]^+$: *m/z* 577.3561, found 577.3543.

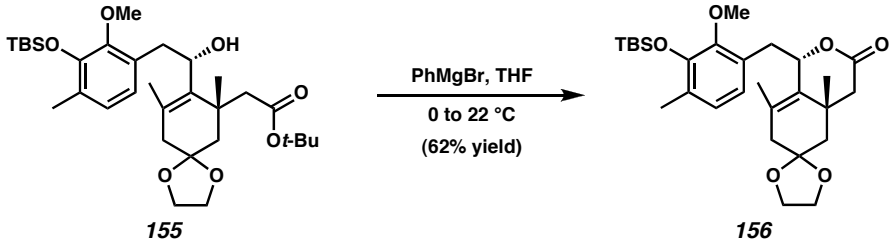

155 *156*

Lactone 156. To a cooled (0 °C) solution of allylic alcohol **155** (108 mg, 0.187 mmol, 1.00 equiv) in THF (12 mL) was added 3.0 M PhMgBr in Et_2O (68.6 μL, 0.206 mmol, 1.10 equiv). Additional 3.0 M PhMgBr in Et_2O (85.0 μL, 0.255 mmol, 1.36 equiv) was added in portions over 4 h. The reaction mixture was quenched into H_2O (30 mL) and EtOAc (30 mL), acidified to pH 2 with 0.1 M HCl, extracted with EtOAc (3 x 20 mL), dried over Na_2SO_4, and concentrated to an oil, which was purified by gradient flash chromatography on silica gel (10 to 20% EtOAc in hexanes) to give lactone **156** (58.5 mg, 62% yield) as white solid. Crystals suitable for X-ray analysis were obtained by crystallization from hexanes at ambient temperature: mp 139-140 °C (hexanes); R_f 0.40 (35% EtOAc in hexanes); ^{1}H NMR (300 MHz, $CDCl_3$) δ 6.83 (d, *J* = 7.8 Hz, 1H), 6.66 (d, *J* = 8.1 Hz, 1H), 5.40 (d, *J* = 9.0 Hz, 1H), 4.08-3.95 (m, 2H), 3.95-3.86 (m, 2H), 3.67 (s, 3H), 3.07 (dd, *J* = 3.5, 14.3 Hz, 1H), 2.75 (dd, *J* = 10.2, 14.4 Hz, 1H), 2.48 (s, 2H), 2.43 (s, 2H), 2.19 (s, 3H), 1.82 (d, *J* = 13.2 Hz, 1H), 1.71 (d, *J* = 13.2 Hz, 1H), 1.71 (s, 3H), 1.22 (s, 3H), 1.03 (s, 9H), 0.18 (s, 3H), 0.15 (s, 3H); ^{13}C NMR (75 MHz, $CDCl_3$) δ 71.4, 149.7, 147.0, 131.2, 129.8, 128.1, 126.0, 125.5, 123.5, 107.8, 80.0, 64.4, 63.6,

60.0, 45.7, 44.1, 43.4, 38.2, 35.9, 26.0, 25.9, 19.0, 18.5, 17.1, -4.2 (2C); IR (Neat film NaCl) 2957, 2931, 2886, 2859, 1751, 1463, 1419, 1251, 1237, 1078, 841 cm^{-1}; HRMS (FAB) $[M+H]^+$ calc'd for $[C_{28}H_{42}SiO_6+H]^+$: *m/z* 503.2829, found 503.2809.

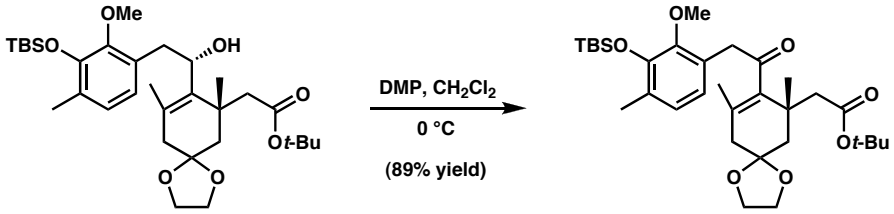

155 *157*

Enone 157. To a cooled (0 °C) solution of allylic alcohol **155** (200 mg, 0.347 mmol, 1.00 equiv) in CH_2Cl_2 (22 mL) was added Dess-Martin periodinane (221 mg, 0.521 mmol, 1.50 equiv) and the resulting mixture was stirred for 2 h. The reaction mixture was diluted with Et_2O (75 mL), filtered, and concentrated to an oil, which was purified by gradient flash chromatography on silica gel (7.5 to 20% Et_2O in hexanes) to give enone **157** (177 mg, 89% yield) as a pale yellow oil: R_f 0.37 (25% Et_2O in hexanes developed twice); ^1H NMR (500 MHz, $CDCl_3$) δ 6.85 (d, *J* = 8.0 Hz, 1H), 6.66 (d, *J* = 7.0 Hz, 1H), 4.08-4.02 (m, 1H), 4.02-3.92 (comp. m, 3H), 3.92 (d, *J* = 18.5 Hz, 1H), 3.84 (d, *J* = 18.0 Hz, 1H), 3.65 (s, 3H), 2.76 (d, *J* = 14.5 Hz, 1H), 2.46 (d, *J* = 14.5 Hz, 1H), 2.37 (d, *J* = 18.0 Hz, 1H), 2.35 (dd, *J* = 1.5, 13.5 Hz, 1H), 2.28 (d, *J* = 18.0 Hz, 1H), 2.21 (s, 3H), 1.75 (s, 3H), 1.57 (d, *J* = 13.5 Hz, 1H), 1.43 (s, 9H), 1.30 (s, 3H), 1.03 (s, 9H), 0.16 (s, 6H); ^{13}C NMR (125 MHz, $CDCl_3$) δ 207.3, 171.3, 150.0, 147.0, 140.9, 129.9, 128.1, 125.8, 125.5, 123.4, 107.4, 80.0, 64.3, 64.0, 59.9, 47.3, 44.1, 41.6, 40.5, 38.4, 28.2, 26.6, 26.1, 20.8, 18.6, 17.1, -4.2; IR (Neat film NaCl) 2959, 2931, 2886, 2860, 1724, 1699,

1463, 1421, 1368, 1286, 1253, 1234, 1145, 1075, 1014, 857, 839, 782 cm^{-1}; HRMS (FAB) $[M+H]^+$ calc'd for $[C_{32}H_{50}SiO_7+H]^+$: *m/z* 575.3404, found 575.3394.

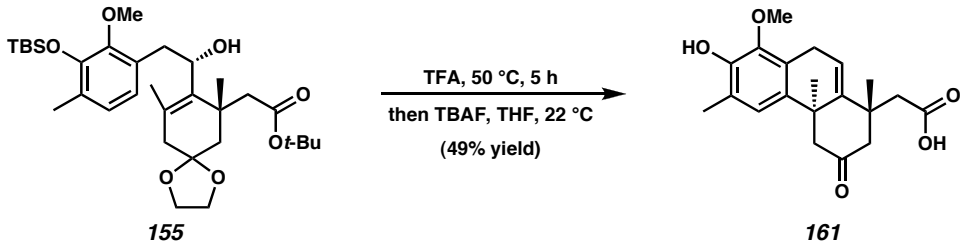

155 *161*

Acid 161. A solution of allylic alcohol **155** (5.50 g, 9.53 mmol, 1.00 equiv) in TFA (240 mL) was warmed to 50 °C for 5 h. The reaction mixture was concentrated and the resulting residue was dissolved in THF (100 mL) and 1.0 M TBAF (12.0 mL, 12.0 mmol, 1.26 equiv) in THF was added. After 1 h, the reaction mixture was concentrated to ~25 mL, quenched with H_2O (100 mL), brine (100 mL), and 3 M HCl (100 mL), and extracted with EtOAc (6 x 100 mL). The organic layers were concentrated to an oil, which was purified by flash chromatography on silica gel (1:1 CH_2Cl_2:$CHCl_3$ + 1% AcOH) to give acid **161** (1.62 g, 49% yield) as a white foam. Crystals suitable for X-ray analysis were obtained by crystallization from $CDCl_3$ at ambient temperature: mp 112-113 °C ($CDCl_3$); R_f 0.32 (1:1 CH_2Cl_2 : $CHCl_3$ + 3% MeOH developed twice); ^{1}H NMR (300 MHz, $CDCl_3$) δ 6.76 (s, 1H), 6.05 (dd, *J* = 1.8, 6.3 Hz, 1H), 5.63 (bs, 1H), 3.78 (s, 3H), 3.58 (dd, *J* = 6.6, 20.7 Hz, 1H), 3.47 (d, *J* = 17.7 Hz, 1H), 3.17 (d, *J* = 18.3 Hz, 1H), 3.11 (d, *J* = 17.4 Hz, 1H), 2.93 (d, *J* = 15.9 Hz, 1H), 2.76 (d, *J* = 17.4 Hz, 1H), 2.50 (d, *J* = 15.6 Hz, 1H), 2.34 (d, *J* = 17.1 Hz, 1H), 2.24 (s, 3H), 1.24 (s, 3H), 1.17 (s, 3H); ^{13}C NMR (75 MHz, CD_2Cl_2) δ 210.8, 176.8, 146.0, 145.4, 143.9, 137.6, 125.3, 123.1, 121.6, 120.6, 61.2, 50.1, 49.2, 46.2, 39.5, 39.0, 33.3, 30.7, 24.9, 16.0; IR (Neat film NaCl) 3500-

2500, 2963, 2926, 1707, 1489, 1461, 1422, 1360, 1295, 1228, 1071, 955, 711 cm^{-1}; HRMS (FAB) $[M+H]^+$ calc'd for $[C_{20}H_{24}O_5+H]^+$: *m/z* 345.1702, found 345.1709.

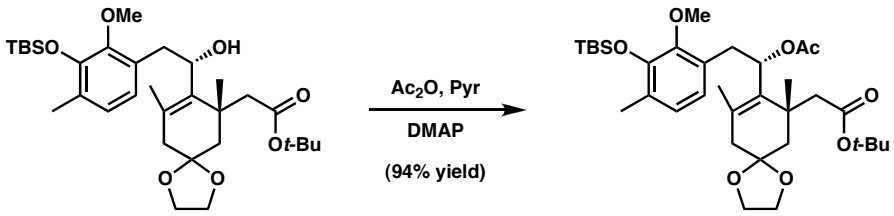

155 *162*

Allylic acetate 162. To a solution of allylic alcohol **155** (88.0 mg, 0.153 mmol, 1.00 eq) in pyridine (250 μL) and acetic anhydride (3.00 mL) was added DMAP (28.0 mg, 0.229 mmol, 1.50 equiv). After 2 h, the reaction mixture was concentrated to an oil, which was purified by gradient flash chromatography on silica gel (5 to 10% EtOAc in hexanes) to give allylic acetate **162** (89.3 mg, 94% yield) as a colorless oil: R_f 0.68 (20% EtOAc in hexanes developed twice); ^{1}H NMR (500 MHz, $CDCl_3$) δ 6.76 (d, *J* = 7.5 Hz, 1H), 6.69 (d, *J* = 7.5 Hz, 1H), 5.73 (dd, *J* = 2.8, 10.8 Hz, 1H), 4.12-4.04 (m, 1H), 4.00-3.90 (comp. m, 3H), 3.70 (s, 3H), 3.07 (app. t, *J* = 12.5 Hz, 1H), 2.97 (dd, *J* = 3.3, 13.8 Hz, 1H), 2.66 (d, *J* = 15.0 Hz, 1H), 2.57 (d, *J* = 14.5 Hz, 1H), 2.38 (d, *J* = 17.5 Hz, 1H), 2.26 (d, *J* = 13.0 Hz, 1H), 2.24 (d, *J* = 17.5 Hz, 1H), 2.18 (s, 3H), 1.97 (s, 3H), 1.80 (s, 3H), 1.48 (d, *J* = 14.5 Hz, 1H), 1.42 (s, 9H), 1.28 (s, 3H), 1.03 (s, 9H), 0.19 (s, 3H), 0.14 (s, 3H); ^{13}C NMR (125 MHz, $CDCl_3$) δ 171.8, 169.3, 150.0, 146.9, 135.0, 131.1, 129.3, 129.2, 125.3, 123.4, 107.3, 79.7, 71.5, 64.3, 63.9, 59.9, 43.5, 40.7, 39.9, 35.9, 28.2, 26.2, 26.1, 21.3, 21.0, 18.5, 17.1, -4.2, -4.4; IR (Neat film NaCl) 2958, 2931, 2896, 2860, 1740, 1463, 1419, 1368, 1287, 1235, 1147, 1079, 1014, 854, 841, 783, 734 cm^{-1}; HRMS (FAB) $[M+H-H_2]^+$ calc'd for $[C_{34}H_{53}O_8Si]^+$: *m/z* 617.3510, found 617.3487.

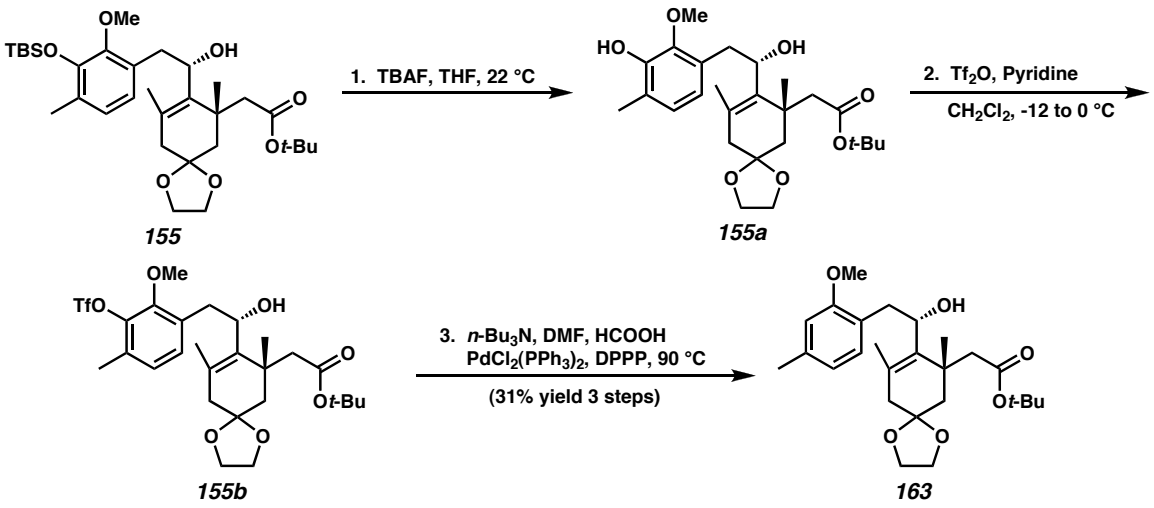

Arene 163. To a solution of allylic alcohol **155** (554 mg, 0.962 mmol, 1.0 equiv) in THF (10 mL) was added 1.00 M TBAF in THF (1.50 mL, 1.50 mmol, 1.56 equiv). After 5 min, the reaction mixture was concentrated to ~5 mL and was purified by gradient flash chromatography on silica gel (20 to 40% EtOAc in hexanes) to give phenol **155a** (223 mg, 52% yield).

To a cooled (-12 °C) solution of phenol **155a** (202 mg, 0.438 mmol, 1.00 equiv) and pyridine (142 μL, 1.75 mmol, 4.0 equiv) in CH_2Cl_2 (5 mL) was added Tf_2O (74.3 μL, 0.526 mmol, 1.2 equiv). After 2 h, additional Tf_2O (10.0 μL, 0.071 mmol, 0.16 equiv) was added. After a further 2 h, the reaction mixture was quenched into a mixture of H_2O (10 mL), brine (10 mL), and CH_2Cl_2 (10 mL), then extracted with CH_2Cl_2 (3 x 10 mL). The combined organic layers were dried (Na_2SO_4), and concentrated to an oil, which was purified by gradient flash chromatography on silica gel (15 to 25% EtOAc in hexanes + 1% TEA) to give triflate **155b** (193 mg, 75% yield).

A flame-dried 25 mL Schlenk flask was charged with triflate **155b** (193 mg, 0.325 mmol, 1.00 equiv), $PdCl_2(PPh_3)_2$ (27.3 mg, 0.0389 mmol, 0.12 equiv), 1,4-bis-(diphenylphosphino)butane (40.2 mg, 0.0974 mmol, 0.30 equiv), DMF (4 mL), *n*-Bu_3N

(650 μL, 2.73 mmol, 8.40 equiv), and HCOOH (61.3 μL, 1.62 mmol, 5.00 equiv) under an Ar atmosphere and heated to 90 °C. After 22 h, the reaction mixture was quenched with H_2O (40 mL), extracted with Et_2O (5 x 15 mL), dried ($MgSO_4$), and concentrated to a residue, which was purified by gradient flash chromatography on silica gel (10 to 15% acetone in hexanes) to give arene **163** (117 mg, 80% yield) as a white solid: mp 135-136 °C; R_f 0.50 (35% EtOAc in hexanes); ^{1}H NMR (300 MHz, $CDCl_3$) δ 7.15 (d, *J* = 7.5 Hz, 1H), 6.73 (d, *J* = 7.5 Hz, 1H), 6.68 (s, 1H), 4.46 (dd, *J* = 2.3, 10.1 Hz, 1H), 4.02-3.90 (comp. m, 4H), 3.80 (s, 3H), 3.08 (dd, *J* = 10.2, 13.8 Hz, 1H), 3.07 (s, 1H), 2.94 (dd, *J* = 3.0, 13.8 Hz, 1H), 2.65 (d, *J* = 13.5 Hz, 1H), 2.33 (s, 3H), 2.30-2.10 (comp. m, 3H), 2.07 (s, 3H), 1.58 (dd, *J* = 2.1, 13.8 Hz, 1H), 1.40 (s, 9H), 1.16 (s, 3H); ^{13}C NMR (75 MHz, $CDCl_3$) δ 72.1, 157.3, 137.3, 136.8, 131.4, 130.3, 125.1, 121.0, 111.2, 107.6, 80.8, 69.5, 64.2, 63.9, 55.0, 46.4, 43.3, 42.0, 41.3, 36.7, 28.0, 26.7, 21.5, 21.1; IR (Neat film NaCl) 3501, 2974, 2934, 1705, 1368, 1259, 1155, 1126, 1080, 1042 cm^{-1}; HRMS (FAB) $[M+H]^+$ calc'd for $[C_{26}H_{38}O_6+H]^+$: *m/z* 447.2747, found 447.2749.

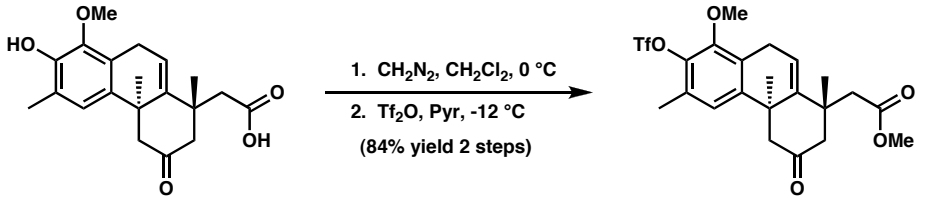

161 *168*

Triflate 168. To a cooled (0 °C) solution of acid **161** (994 mg, 2.88 mmol, 1.00 equiv) in CH_2Cl_2 (30 mL) was added a cooled (0 °C) solution of CH_2N_2 in Et_2O (~0.2 M, 18.7 mL, 1.30 equiv) in a dropwise manner over 10 min. After 20 min, TLC analysis indicated complete consumption of the starting material and the reaction mixture was concentrated *in vacuo*. To a cooled (-12 °C) solution of the crude reaction mixture and

pyridine (2.45 mL, 28.8 mmol, 10.0 equiv) in CH_2Cl_2 (50 mL) was added Tf_2O (1.01 mL, 7.20 mmol, 2.50 equiv) in a dropwise manner over 5 min. After 30 min, additional Tf_2O (1.01 mL, 7.20 mmol, 2.50 equiv) was added. After a further 1 h at -12 °C, the reaction mixture was allowed to warm to 0 °C, stirred for 1 h, and quenched with saturated aqueous $NaHCO_3$ (30 mL). The reaction mixture was poured into half saturated aqueous $NaHCO_3$ (60 mL), extracted with CH_2Cl_2 (5 x 30 mL), dried over K_2CO_3, and concentrated to an oil, which was purified by gradient flash chromatography on silica gel (10 to 25% EtOAc in hexanes) to give triflate **168** (1.18 g, 84% yield) as an off-white solid: mp 123-125 °C (decomp.) (benzene); R_f 0.45 (35% EtOAc in hexanes); ^{1}H NMR (300 MHz, $CDCl_3$) δ 6.89 (s, 1H), 6.03 (dd, J = 2.0, 6.5 Hz, 1H), 3.82 (s, 3H), 3.67 (s, 3H), 3.66 (dd, J = 6.3, 21.0 Hz, 1H), 3.50 (d, J = 17.7 Hz, 1H), 3.17 (app. d, J = 21.9 Hz, 1H), 3.09 (d, J = 17.4 Hz, 1H), 2.91 (d, J = 15.3 Hz, 1H), 2.76 (d, J = 17.4 Hz, 1H), 2.46 (d, J = 15.6 Hz, 1H), 2.34 (s, 3H), 2.33 (d, J = 17.4 Hz, 1H), 1.29 (s, 3H), 1.16 (s, 3H); ^{13}C NMR (75 MHz, $CDCl_3$) δ 210.1, 171.5, 148.5, 146.0, 144.7, 140.0, 129.4, 127.6, 121.9, 119.7, 118.6 (q, $J_{C\text{-}F}$ = 318 Hz), 61.0, 51.5, 49.3, 48.8, 45.9, 39.4, 38.5, 33.1, 30.3, 24.3, 16.5; IR (Neat film NaCl) 2960, 1735, 1715, 1417, 1210, 1138, 1072, 903, 856 cm^{-1}; HRMS (FAB) $[M+H]^+$ calc'd for $[C_{22}H_{25}SO_7F_3+H]^+$: m/z 491.1351, found 491.1363.

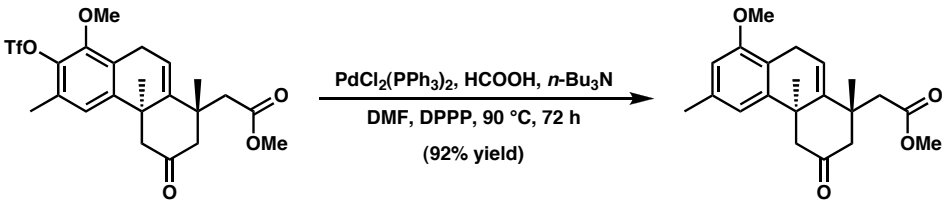

168 *169*

Ketoester 169. A flame-dried 250 mL Schlenk flask was charged with triflate **168** (azeotroped from PhH solution, 1.150 g, 2.34 mmol, 1.00 equiv), $PdCl_2(PPh_3)_2$ (198 mg, 0.282 mmol, 0.12 equiv), 1,4-bis-(diphenylphosphino)butane (290 mg, 0.704 mmol, 0.30 equiv), DMF (20 mL), *n*-Bu_3N (4.70 mL, 19.7 mmol, 8.40 equiv), and HCOOH (443 μL, 11.7 mmol, 5.00 equiv) under an N_2 atmosphere and heated to 90 °C. After 72 h, the reaction mixture was quenched with H_2O (150 mL) and Et_2O (40 mL), extracted with Et_2O (6 x 50 mL), dried ($MgSO_4$), and concentrated to a residue, which was purified by gradient flash chromatography on silica gel (5 to 10% acetone in hexanes) to give ketoester **169** (735 mg, 92% yield) as a colorless oil: R_f 0.53 (35% acetone in hexane); ^{1}H NMR (300 MHz, $CDCl_3$) δ 6.68 (s, 1H), 6.57 (s, 1H), 6.04 (dd, *J* = 1.8, 6.3 Hz, 1H), 3.83 (s, 3H), 3.66 (s, 3H), 3.64 (dd, *J* = 6.3, 21.8 Hz, 1H), 3.47 (d, *J* = 17.4 Hz, 1H), 3.14 (d, *J* = 17.7 Hz, 1H), 3.02 (app. d, *J* = 21.6 Hz, 1H), 2.89 (d, *J* = 15.6 Hz, 1H), 2.77 (d, *J* = 17.4 Hz, 1H), 2.46 (d, *J* = 15.6 Hz, 1H), 2.35 (s, 3H), 2.32 (d, *J* = 17.4 Hz, 1H), 1.28 (s, 3H), 1.17 (s, 3H); ^{13}C NMR (75 MHz, $CDCl_3$) δ 211.2, 171.6, 156.1, 146.0, 144.0, 136.9, 120.8, 119.7, 116.3, 108.4, 55.3, 51.4, 49.6, 49.1, 46.2, 39.2, 38.5, 33.2, 30.9, 24.1, 21.9; IR (Neat film NaCl) 2956, 1735, 1711, 1584, 1462, 1314, 1198, 1134, 1064 cm^{-1}; HRMS (FAB) $[M+H]^+$ calc'd for $[C_{21}H_{26}O_4+H]^+$: *m/z* 343.1909, found 343.1894.

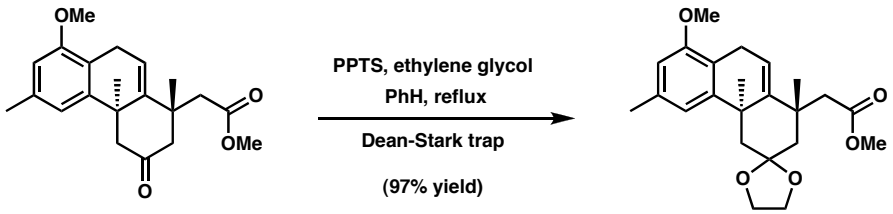

169 ***170***

Ester 170. To a solution of ketoester **169** (200 mg, 0.581 mmol, 1.00 equiv), ethylene glycol (4.00 mL, 71.7 mmol, 124 equiv), and pyridinium *p*-toluenesulfonate (2.00 g, 7.96 mmol, 13.7 equiv) in benzene (70 mL) was fitted with a Dean-Stark apparatus and refluxed at 95 °C for 10 h. The reaction mixture was allowed to cool to ambient temperature, diluted with H_2O (50 mL), and CH_2Cl_2 (50 mL), and extracted with CH_2Cl_2 (5 x 30 mL). The combined organics were washed with a 1:1:1 solution of brine, H_2O, and sat. aq. $NaHCO_3$ (4 x 20 mL), dried (K_2CO_3), and concentrated to a oil, which was purified by gradient flash chromatography on silica gel (30% Et_2O in hexanes) to give ester **170** (217 mg, 97% yield) as a colorless oil: R_f 0.48 (50% Et_2O in hexane); ^1H NMR (300 MHz, $CDCl_3$) δ 6.77 (s, 1H), 6.54 (s, 1H), 6.00 (dd, *J* = 2.3, 6.2 Hz, 1H), 4.18-4.04 (m, 2H), 4.02-3.89 (m, 2H), 3.81 (s, 3H), 3.64 (s, 3H), 3.55 (dd, *J* = 6.2, 21.8 Hz, 1H), 2.96 (d, *J* = 21.8 Hz, 1H), 2.91 (d, *J* = 14.1 Hz, 1H), 2.73 (d, *J* = 14.1 Hz, 1H), 2.52 (dd, *J* = 2.0, 13.7 Hz, 1H), 2.34 (s, 3H), 2.32 (dd, *J* = 2.1, 14.1 Hz, 1H), 2.11 (d, *J* = 13.8 Hz, 1H), 1.56 (d, *J* = 14.1 Hz, 1H), 1.38 (s, 3H), 1.29 (s, 3H); ^{13}C NMR (75 MHz, $CDCl_3$) δ 172.5, 155.9, 148.3, 144.8, 136.6, 121.2, 119.4, 116.6, 108.6, 107.9, 64.7, 63.2, 55.3, 51.1, 46.5, 45.4, 43.0, 39.3, 38.7, 30.8, 30.2, 24.0, 21.9; IR (Neat film NaCl) 2956, 2883, 1733, 1462, 1348, 1199, 1135, 1067, 1018 cm^{-1}; HRMS (FAB) $[M+H]^+$ calc'd for $[C_{23}H_{30}O_5+H]^+$: *m/z* 387.2171, found 387.2179.

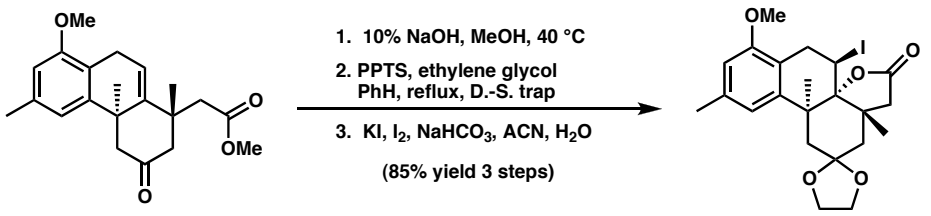

169 *172*

Iodolactone 172. A solution of ketoester **169** (200 mg, 0.581 mmol, 1.00 equiv) in MeOH (13 mL), and 10% w/v aqueous NaOH (13 mL) was heated at 40 °C for 10 h. The reaction mixture was cooled to ambient temperature, poured into brine (50 mL) and H_2O (10 mL), acidified with 3 M HCl to pH 0, extracted with EtOAc (6 x 20 mL), dried (Na_2SO_4), concentrated, and used in the next step without further purification.

A solution of the above crude carboxylic acid, ethylene glycol (500 μL, 8.97 mmol, 15.4 equiv), and pyridinium *p*-toluenesulfonate (500 mg, 1.99 mmol, 3.42 equiv) in benzene (50 mL) was fitted with a Dean-Stark apparatus and refluxed at 100 °C for 2 h. The cooled (0 °C) reaction mixture was diluted with H_2O (25 mL), brine (25 mL), and CH_2Cl_2 (50 mL), and extracted with CH_2Cl_2 (6 x 30 mL). The combined organics were dried (Na_2SO_4), concentrated, and used immediately in the next step without further purification.

To a solution of the crude ketal and $NaHCO_3$ (68.4 mg, 0.814 mmol, 1.4 equiv) in H_2O (5 mL) and acetonitrile (5 mL) was added KI (125 mg, 0.756 mmol, 1.3 equiv) and I_2 (192 mg, 0.756 mmol, 1.3 equiv). The reaction mixture was stirred in the dark for 30 h and quenched with saturated aqueous $Na_2S_2O_3$ (10 mL), H_2O (20 mL), and brine (20 mL). The reaction mixture was extracted with EtOAc (8 x 20 mL), dried (Na_2SO_4), concentrated, and recrystallized (15% acetone in hexanes, ~25 mL, from 80 to –20 °C) to give iodolactone **172** (247 mg, 85% yield) as a white solid: mp 155-160 °C (decomp.)

(acetone/hexanes); R_f 0.37 (35% EtOAc in hexanes); ^{1}H NMR (500 MHz, C_6D_6) δ 6.92 (s, 1H), 6.22 (s, 1H), 5.29 (app. t, *J* = 10.0 Hz, 1H), 3.75 (dd, *J* = 10.0, 19.3 Hz, 1H), 3.52-3.34 (comp. m, 3H), 3.34-3.26 (comp. m, 2H), 3.24 (s, 3H), 3.01 (d, *J* = 18.0 Hz, 1H), 2.76 (d, *J* = 16.0 Hz, 1H), 2.49 (d, *J* = 16.0 Hz, 1H), 2.45 (d, *J* = 18.0 Hz, 1H), 2.12 (s, 3H), 1.54 (d, *J* = 14.5 Hz, 1H), 1.13 (s, 3H), 0.98 (d, *J* = 14.5 Hz, 1H), 0.95 (s, 3H); ^{13}C NMR (125 MHz, C_6D_6) δ 173.5, 156.9, 143.6, 138.1, 121.2, 117.6, 109.4, 107.2, 87.2, 64.5, 64.2, 55.1, 46.1, 45.8, 45.4, 43.2, 42.6, 36.5, 30.9, 30.8, 25.2, 22.2; IR (Neat film NaCl) 2964, 2881, 1790, 1461, 1229, 1203, 1071, 1023 cm^{-1}; HRMS (FAB) $[M+H]^+$ calc'd for $[C_{22}H_{27}IO_5+H]^+$: *m/z* 499.0982, found 499.0986.

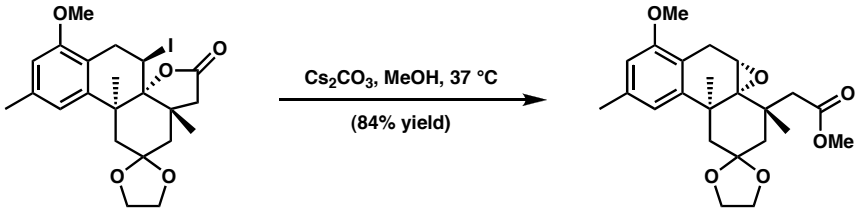

172 ***173***

Epoxide 173. To a solution of iodolactone **172** (75.0 mg, 0.151 mmol, 1.00 equiv) in MeOH (15 mL) was added Cs_2CO_3 (981 mg, 3.01 mmol, 20.0 equiv). The reaction mixture was warmed to 37 °C and vigorously stirred for 19 h. The reaction mixture was cooled to ambient temperature, diluted with H_2O (20 mL), brine (20 mL), and CH_2Cl_2 (20 mL), extracted with CH_2Cl_2 (5 x 20 mL) and EtOAc (5 x 25 mL), dried (Na_2SO_4), and concentrated. The resulting residue was purified by flash chromatography on silica gel (15% EtOAc in hexanes + 1% TEA) to give epoxide **173** (51.0 mg, 84% yield) as a colorless oil: R_f 0.54, 0.28 (35% EtOAc in hexanes, 10% EtOAc in hexanes developed 3 times); ^{1}H NMR (500 MHz, $CDCl_3$) δ 6.72 (s, 1H), 6.45 (s, 1H), 4.12-4.08

(m, 1H), 4.06-4.01 (m, 1H), 3.94-3.86 (comp. m, 2H), 3.78 (s, 3H), 3.66 (s, 3H), 3.58 (d, J = 2.5 Hz, 1H), 3.24 (d, J = 19.5 Hz, 1H), 2.90 (dd, J = 3.5, 20.0 Hz, 1H), 2.80 (dd, J = 1.0, 14.5 Hz, 1H), 2.79 (d, J = 14.5 Hz, 1H), 2.37 (d, J = 14.0 Hz, 1H), 2.31 (dd, J = 1.0, ~15 Hz, 1H), 2.30 (s, 3H), 2.03 (d, J = 15.0 Hz, 1H), 1.72 (d, J = 15.0 Hz, 1H), 1.63 (s, 3H), 1.11 (s, 3H); ^{13}C NMR (125 MHz, C_6D_6) δ 172.8, 157.5, 144.9, 136.6, 120.4, 116.1, 108.9, 108.2, 65.7, 64.8, 63.7, 57.1, 55.2, 51.1, 48.8, 43.4, 41.7, 39.7, 38.3, 27.5, 26.7, 24.4, 22.2; IR (Neat film NaCl) 2950, 1734, 1590, 1462, 1360, 1196, 1135, 1075, 1017 cm^{-1}; HRMS (FAB) $[M+H]^+$ calc'd for $[C_{23}H_{30}O_6+H]^+$: m/z 403.2121, found 403.2113.

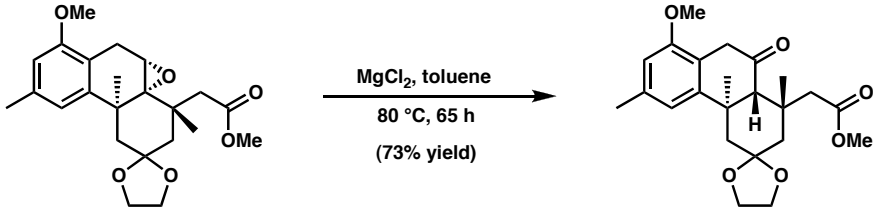

173 *174*

Ketone 174. A solution of epoxide **173** (49.0 mg, 0.122 mmol, 1.00 equiv) in toluene (30 mL) in a flame-dried Schlenk flask under an N_2 atmosphere was treated with magnesium chloride (2.00 g, 21.0 mmol, 172 equiv) and heated to 80 °C for 65 h. After cooling to ambient temperature, the reaction mixture was filtered and the filter cake was washed with toluene (2 x 25 mL). The filter cake was partitioned between EtOAc (20 mL) and ice cold water (20 mL), and further extracted with EtOAc (3 x 20 mL). The combined organics were dried (Na_2SO_4), and concentrated to an oil, which was purified by gradient flash chromatography on silica gel (10 to 20% EtOAc in hexanes) to give ketone **174** (36.0 mg, 73% yield) as a colorless oil: R_f 0.55, 0.33 (35% EtOAc in hexanes, 10% EtOAc in hexanes developed 3 times); ^{1}H NMR (500 MHz, $CDCl_3$) δ 6.73

(s, 1H), 6.57 (s, 1H), 4.15-4.05 (m, 2H), 4.00-3.88 (m, 2H), 3.80 (s, 3H), 3.67 (s, 3H), 3.64 (d, *J* = 22.5 Hz, 1H), 3.47 (dd, *J* = 1.5, 14.5 Hz, 1H), 3.34 (d, *J* = 22.0 Hz, 1H), 3.23 (d, *J* = 14.5 Hz, 1H), 2.58 (dd, *J* = 2.5, 14.5 Hz, 1H), 2.56 (s, 1H), 2.45 (dd, *J* = 2.5, 13.5 Hz, 1H), 2.35 (s, 3H), 2.13 (d, *J* = 13.0 Hz, 1H), 1.30 (s, 3H), 1.21 (s, 3H), 1.14 (dd, *J* = 1.5, 14.5 Hz, 1H); ^{13}C NMR (125 MHz, $CDCl_3$) δ 209.0, 173.9, 156.4, 149.4, 137.6, 117.3, 116.1, 108.7, 108.3, 65.2, 63.0, 62.8, 55.3, 50.9, 46.4, 42.5, 42.3, 40.0, 36.0, 35.6, 28.9, 25.6, 21.9; IR (Neat film NaCl) 2953, 2885, 1731, 1713, 1586, 1462, 1360, 1193, 1065 cm^{-1}; HRMS (EI) $[M]^+$ calc'd for $[C_{23}H_{30}O_6]^+$: *m/z* 402.2042, found 402.2027.

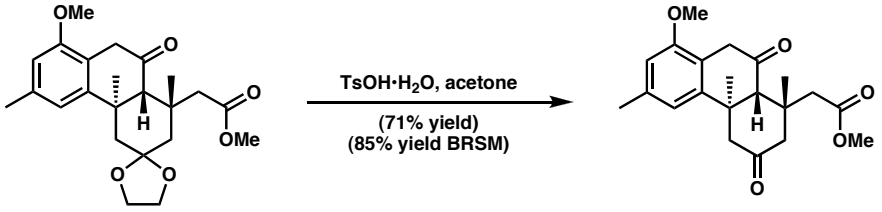

174 ***175***

Diketone 175. A solution of ketone **174** (29.3 mg, 0.728 mmol, 1.00 equiv) in acetone (10 mL) was treated with TsOH•H_2O (100 mg, 0.526 mmol, 7.22 equiv) and stirred at ambient temperature for 4 h. The reaction mixture was poured into saturated aqueous $NaHCO_3$ (25 mL), extracted with CH_2Cl_2 (6 x 15 mL), dried (Na_2SO_4), and concentrated to an oil, which was purified by gradient flash chromatography on silica gel (7.5 to 12.5% EtOAc in hexanes) to give starting ketone **164** (4.6 mg, 16% yield) and diketone **175** (18.6 mg, 71% yield) as a white solid. Crystals suitable for X-ray analysis were obtained by crystallization from acetone/heptanes at ambient temperature: mp 184-186 °C (acetone/heptanes); R_f 0.40 (35% EtOAc in hexanes); ^{1}H NMR (500 MHz, $CDCl_3$) δ 6.61 (s, 1H), 6.59 (s, 1H), 3.82 (s, 3H), 3.71 (d, *J* = 22.0 Hz, 1H), 3.69 (s, 3H),

3.46 (dd, *J* = 1.5, 14.5 Hz, 1H), 3.39 (d, *J* = 22.5 Hz, 1H), 3.08 (s, 1H), 2.99 (dd, *J* = 2.3, 12.8 Hz, 1H), 2.93 (dd, *J* = 2.3, 12.8 Hz, 1H), 2.89 (d, *J* = 12.5 Hz, 1H), 2.36 (s, 3H), 2.33 (d, *J* = 14.5 Hz, 1H), 2.21 (d, *J* = 12.5 Hz, 1H), 1.36 (s, 3H), 1.16 (s, 3H); ^{13}C NMR (125 MHz, $CDCl_3$) δ 208.7, 207.8, 171.9, 156.6, 147.6, 138.2, 117.1, 115.5, 109.3, 62.7, 55.4, 53.6, 52.2, 51.4, 45.7, 40.1, 39.5, 37.6, 28.0, 26.6, 21.9; IR (Neat film NaCl) 2953, 1732, 1713, 1586, 1462, 1331, 1194, 1063, 731 cm^{-1}; HRMS (EI) $[M]^+$ calc'd for $[C_{21}H_{26}O_5]^+$: *m/z* 358.1780, found 358.1774.

2.9 Notes and Citations

(1) (a) Tanner, D.; Anderson, P. G.; Tedenborg, L.; Somfai, P. *Tetrahedron* **1994**, *50*, 9135-9144. (b) Tanner, D.; Tedenborg, L.; Somfai, P. *Acta Chem. Scand.* **1997**, *51*, 1217-1223.

(2) Williams, D. R.; Brugel, T. A. *Org. Lett.* **2000**, *2*, 1023-1026.

(3) (a) Hikage, N.; Furukawa, H.; Takao, K.; Kobayashi, S. *Tetrahedron Lett.* **1998**, *39*, 6237-6240. (b) Hikage, N.; Furukawa, H.; Takao, K.; Kobayashi, S. *Tetrahedron Lett.* **1998**, *39*, 6241-6244.

(4) Williams, D. R.; Cortez, G. A. *Tetrahedron Lett.* **1998**, *39*, 2675-2678.

(5) Dossetter, A. G.; Jamison, T. F.; Jacobsen, E. N. *Angew. Chem. Int. Ed.* **1999**, *38*, 2398-2400.

(6) Bagdanoff, J. T. Development of the Enantioselective Oxidation of Secondary Alcohols and Natural Products Total Synthesis. Ph.D., California Institute of Technology, Pasadena, CA, August 2005.

(7) (a) Breuning, M.; Corey, E. J. *Org. Lett.* **2001**, *3*, 1559-1562. (b) Rose, P. A.; Lei, B.; Shaw, A. C.; Abrams, S. R.; Walker-Simmons, M. K.; Napper, S.; Quail, J. W. *Can. J. Chem.* **1996**, *74*, 1836-1843.

(8) Franck-Neumann, M.; Miesch, M.; Barth, F. *Tetrahedron* **1993**, *49*, 1409-1420.

(9) In our experience, the dimethyl ketone **133** was best prepared by iodobenzene diacetate oxidation of 2,6 dimethylphenol **i** to give quinone **ii**. Quinone **ii** was readily reduced to ketone **133** with Pd/C under hydrogen (60 psi).

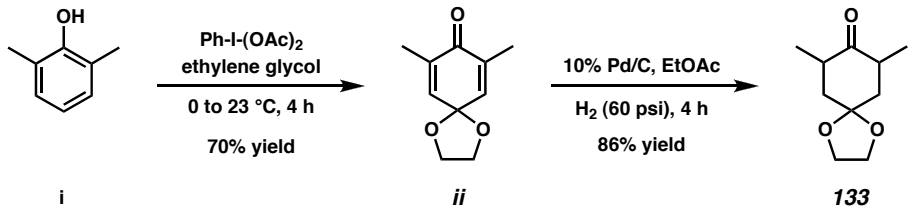

i *ii* ***133***

(10) Han, X.; Stoltz, B. M.; Corey, E. J. *J. Am. Chem. Soc.* **1999**, *121*, 7600-7605.

(11) The use of TBS enol ether **iii** analogous to ethyl enol ether **137** in either thermal or Lewis acid-promoted reactions gave none of the desired reaction. Frequently enone **iv** was observed.

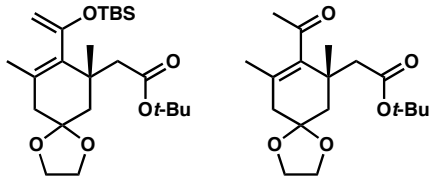

iii ***iv***

(12) (a) Matsumoto, T.; Ohmura, T. *Chem. Lett.* **1977**, 335-338. (b) Liebeskind, L. S.; Chidambaram, R.; Nimkar, S.; Liotta, D. *Tetrahedron Lett.* **1990**, *31*, 3723-3726.

(13) (a) Schmidt, C.; Thazhuthaveetil, J. *Can. J. Chem.* **1973**, *51*, 3620-3624. (b) Matsumoto, T.; Usui, S.; Morimoto, T. *Bull. Chem. Soc. Jpn.* **1977**, *50*, 1575-1579. (c) Matsumoto, T.; Usui, S. *Chem. Lett.* **1978**, 897-900. (d) Stevens, R. V.; Bisacchi, G. S. *J. Org. Chem.* **1982**, *47*, 2396-2399.

(14) This was confirmed by cyclization of enones **v** and **vi**. Ketone **vii** was produced in only ~10% yield, while ketone **viii** was produced in ~40% yield. X-ray structure determination confirmed the relative configuration between the stereocenters in ketone **viii**.

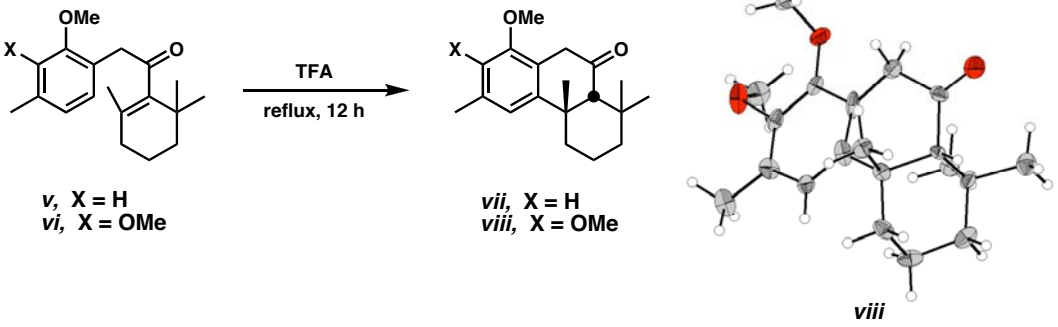

v, X = H
vi, X = OMe

vii, X = H
viii, X = OMe

viii

(15) Stevens, R. V.; Angle, S. R.; Kloc, K.; Mak, K. F.; Trueblood, K. N.; Liu, Y.-X. *J. Org. Chem.* **1986**, *51*, 4347-4353.

(16) To our knowledge this is the first time that such a hindered enol triflate was carbonylated directly to the enal oxidation state.

(17) (a) Shirai, R.; Tanaka, M.; Koga, K. *J. Am. Chem. Soc.* **1986**, *108*, 543-545. (b) Sato, D.; Kawasaki, H.; Shimada, I,; Arata, Y.; Okamura, K.; Date, T.; Koga, K. *J. Am. Chem. Soc.* **1992**, *114*, 761-763. (c) Aoki, K.; Noguchi, H.; Tomioka, K.; Koga, K. *Tetrahedron Lett.* **1993**, *34*, 5105-5108.

(18) (a) Cox, P.; Simpkins, N. S. *Tetrahedron Asymmetry* **1991**, *2*, 1-26. (b) Cox, P.; Simpkins, N. S. *Synlett* **1991**, 321-323. (c) Bunn, B. J.; Simpkins, N. S. *J. Org. Chem.* **1993**, *58*, 533-534.

(19) Using chiral lithium amide **ix** we demonstrated that *meso*-ketone **132** could be desymmetrized in up to 91% ee by deprotonation and trapping with TMSCl. We planned to react the silyl enol ether **x** with an allyl electrophile to generate the quaternary center in ketone **xi**. Oxidative cleavage and esterification would complete the asymmetric synthesis of ketoester **134**. However, our experience in alkylating ketone **133** under non-enantioselective conditions suggested that

asymmetric allylation would be slow as well. This would provide ample time for racemization of the intermediate chiral enolate to occur.

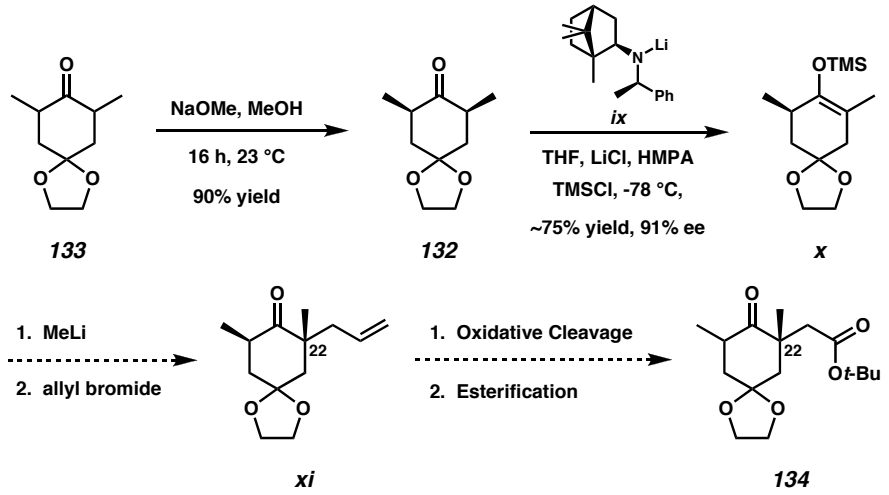

(20) See Chapter 4 for details.

(21) Other acidic conditions included polyphosphoric acid, phosphoric acid/formic acid, and $AlCl_3$.

(22) For an excellent review of S_N' reactions, see: Paquette, L. A.; Stirling, C. J. M.; *Tetrahedron* **1992**, *48*, 7383-7423.

(23) Subsequent to, and independent of, our own studies of the S_N' cyclization of allylic alcohols and arenes under acid conditions, a similar report appeared in the literature, see: Ma, S.; Zhang, J. *Tetrahedron Lett.* **2002**, *43*, 3435-3438.

(24) Reaction of allylic acetate **162** in TFA produced more side products than the other substrates. This prevented quantification of dr and yield.

(25) Additionally, the analogous trifluoroacetate **xii** underwent cyclization in TFA to give comparable yields and diastereoselectivities as allylic alcohol **155**.

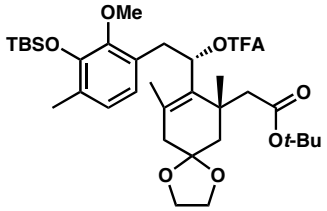

xii

(26) The formation of trifluoroacetates in situ is supported by the isolation of minor amounts of trifluoroacetylated product **xiii** from S_N' reactions in TFA.

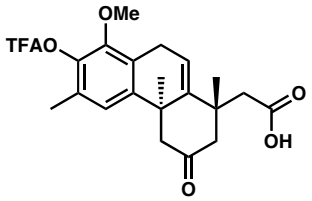

xiii

(27) Saá, J. M.; Dopico, M.; Martorell, G.; García-Raso, A. G. *J. Org. Chem.* **1990**, *55*, 991-995.

(28) Cooper, M. S.; Heaney, H.; Newbold, A. J.; Sanderson, W. R. *Synlett.* **1990**, 533-535.

(29) Tohma, M.; Tomita, T.; Kimura, M. *Tetrahedron Lett.* **1973**, *14*, 4359-4362.

(30) van Vliet, M. C. A.; Arends, I. W. C. E.; Sheldon, R. A. *Synlett.* **2001**, 1305-1307.

(31) (a) Syamala, M. S.; Das, J.; Baskaran, S.; Chandrasekaran, S. *J. Org. Chem.* **1992**, *57*, 1928-1930. (b) Salvador, J. A. R.; Melo, M. L. S.; Neves, A. S. *Tetrahedron Lett.* **1996**, *37*, 687-690.

(32) Rudolph, J.; Reddy, K. L.; Chiang, J. P.; Sharpless, K. B. *J. Am. Chem. Soc.* **1997**, *119*, 6189-6190.

(33) A number of oxidation conditions gave oxidation at the benzylic C(19) position.

(34) The use of magnesium chloride was critical as use of magnesium bromide afforded the halogen exchange product. Treatment with BF_3•Et_2O gave the desired hydride shift with concomitant deketalization.

(35) Naqvi, S. M.; Horwitz, J. P.; Filler, R. *J. Am. Chem. Soc.* **1957**, *79*, 6283-6286.

(36) (a) House, H. O. *J. Am. Chem. Soc.* **1955**, *77*, 5083-5089. (b) House, H. O. *J. Am. Chem. Soc.* **1955**, *77*, 3070-3075.

(37) Williams, D. R.; Cortez, G. A. *Tetrahedron Lett.* **1998**, *39*, 2675-2678.

(38) Under other kinetic enolate trapping conditions, fragmentation of ketoester **169** occurred to give the extended enone **xiv**.

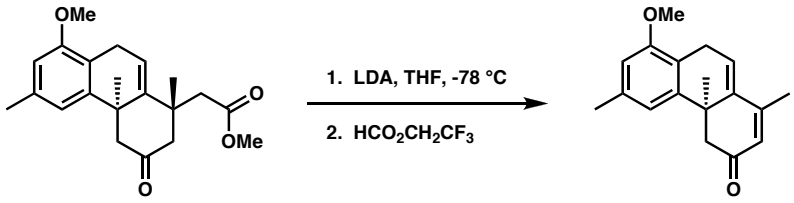

169 ***xiv***

(39) The ability to selectively deprotonate at C(11) led us to pursue a strategy to "protect" C(11). Ketoester **169** was condensed with methyl formate at C(11) and then successfully methylated at C(9). Unfortunately, despite extensive experimentation, no reagents could be found that were capable of removing the hydroxymethylene from methyl ketone **xvi** in greater than ~20% yield.

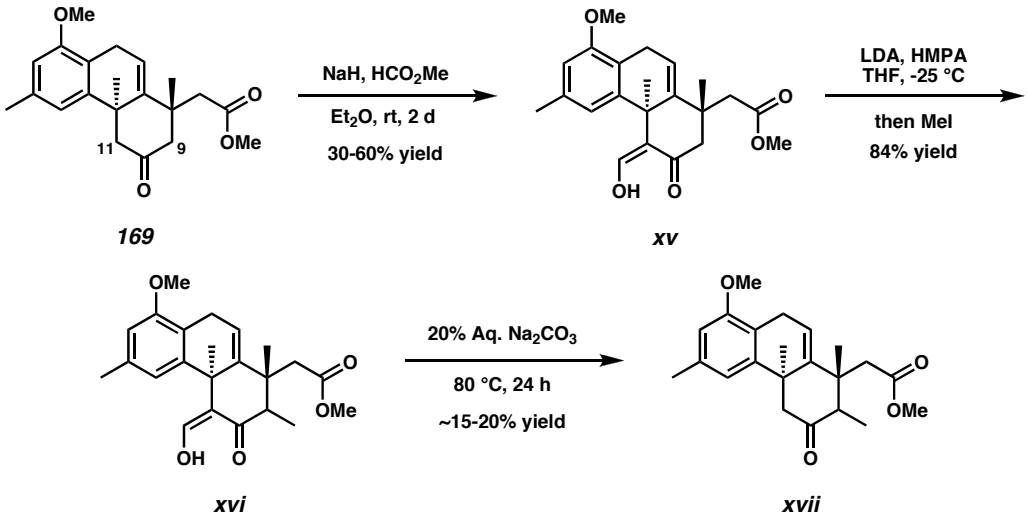

(40) Bofinger, K. R.; Hanack, M. *Chem. Ber.* **1985**, *118*, 2993-3003.

(41) Since selective enolization had proved difficult, we hoped to separate the isomers and cyclopropanate the C(9)-C(10) enol. To that end, cyclopropanation of steric model methyl enol ether **xviii** was attempted with diethyl zinc and methylene iodide. Treatment with tosic acid in benzene opened the cyclopropane **xix** to the desired methyl ketone **xx**. However, in our hands it was difficult to drive the reaction to more than ~60% conversion under optimized conditions.

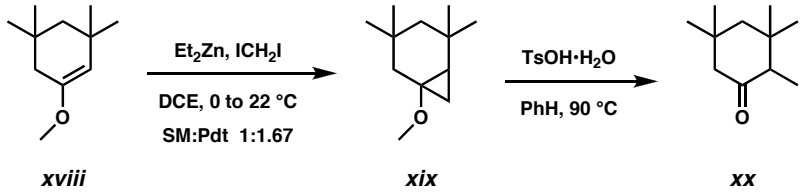

(42) Hirai, G.; Oguri, H.; Hirama, M. *Chem. Lett.* **1999**, *28*, 141-142.

(43) We were delighted to find that pentamethyl β-ketoester **xxi** underwent allylation selectively at the more substituted α-site with Tsuji's conditions. We envisioned this method as a late-stage means to install the C(9) quaternary stereocenter in the presence of the other C ring quaternary stereocenters. In this case, chiral ligands

may have been used to override the inherent diastereoselectivity of the allylation. These allylation methods have the additional advantage of forming quaternary centers at room temperature in a few hours or less under neutral conditions.

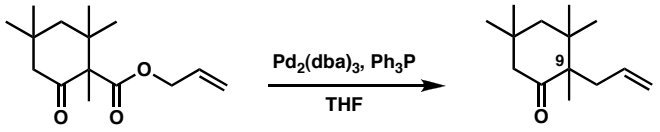

xxi ***xxii***

APPENDIX ONE

Synthetic Summary of the S_N' Approach to Zoanthenol

Scheme A1.1: Synthesis and Coupling of A and C Ring Synthons

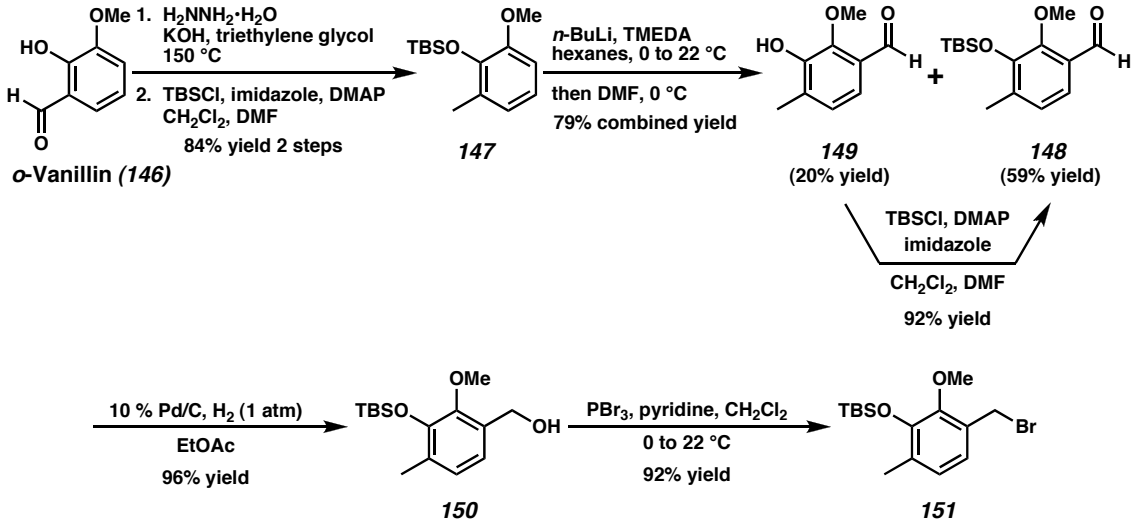

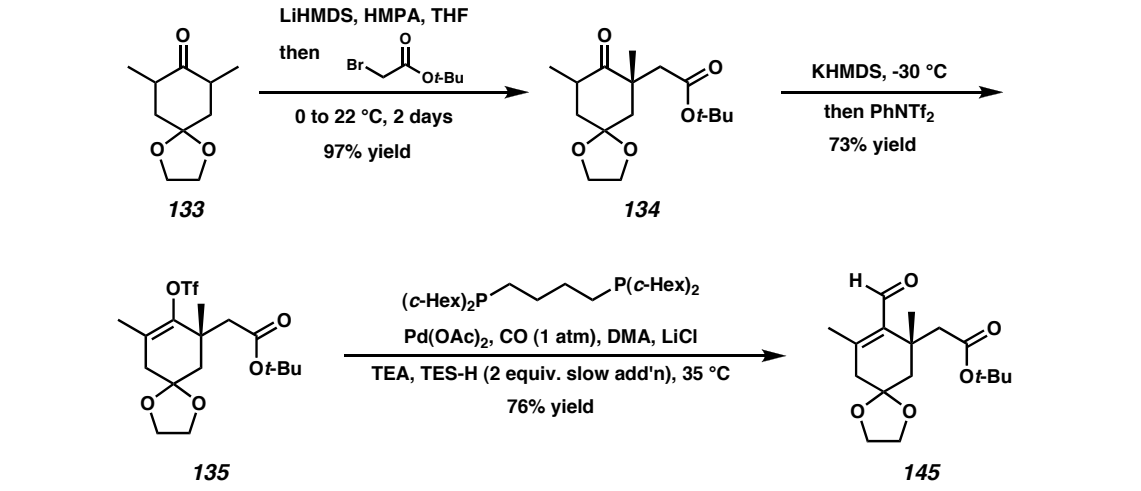

Scheme A1.2 Asymmetric Synthesis of C Ring Intermediate

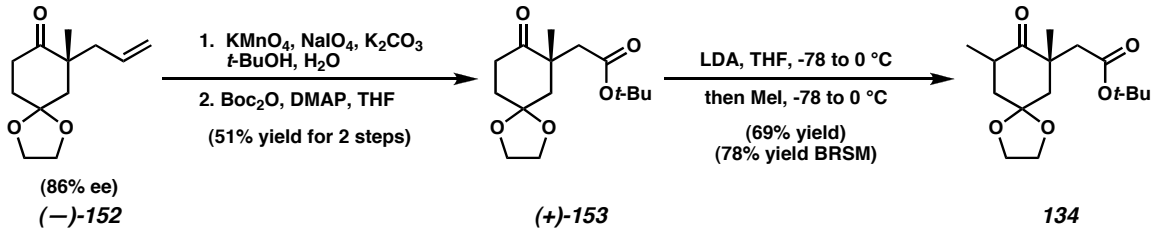

Scheme A1.3 S_N' Cyclization and Elaboration of the Zoanthenol ABC Rings

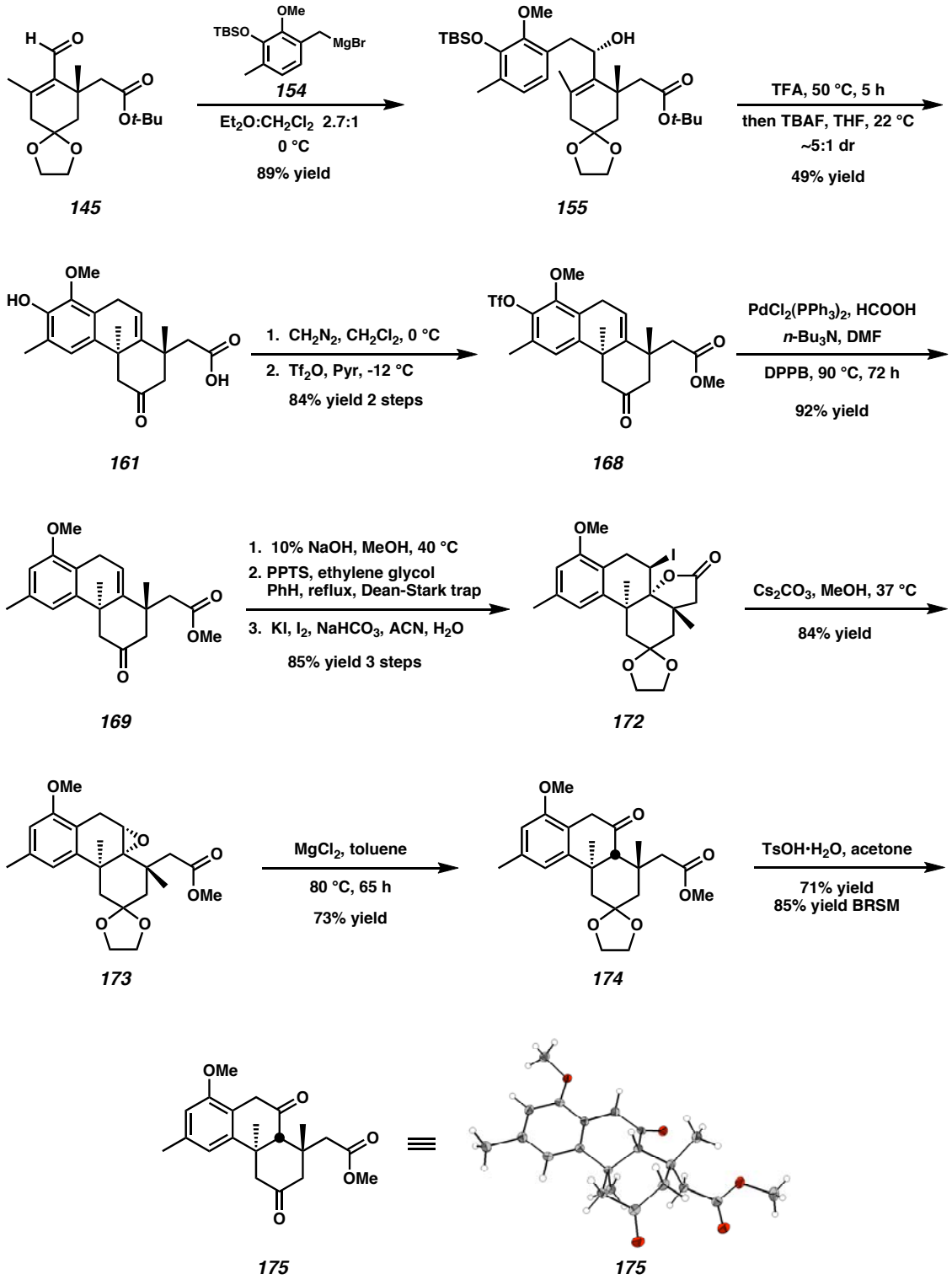

APPENDIX TWO

Spectra of Compounds Relevant to Chapter Two

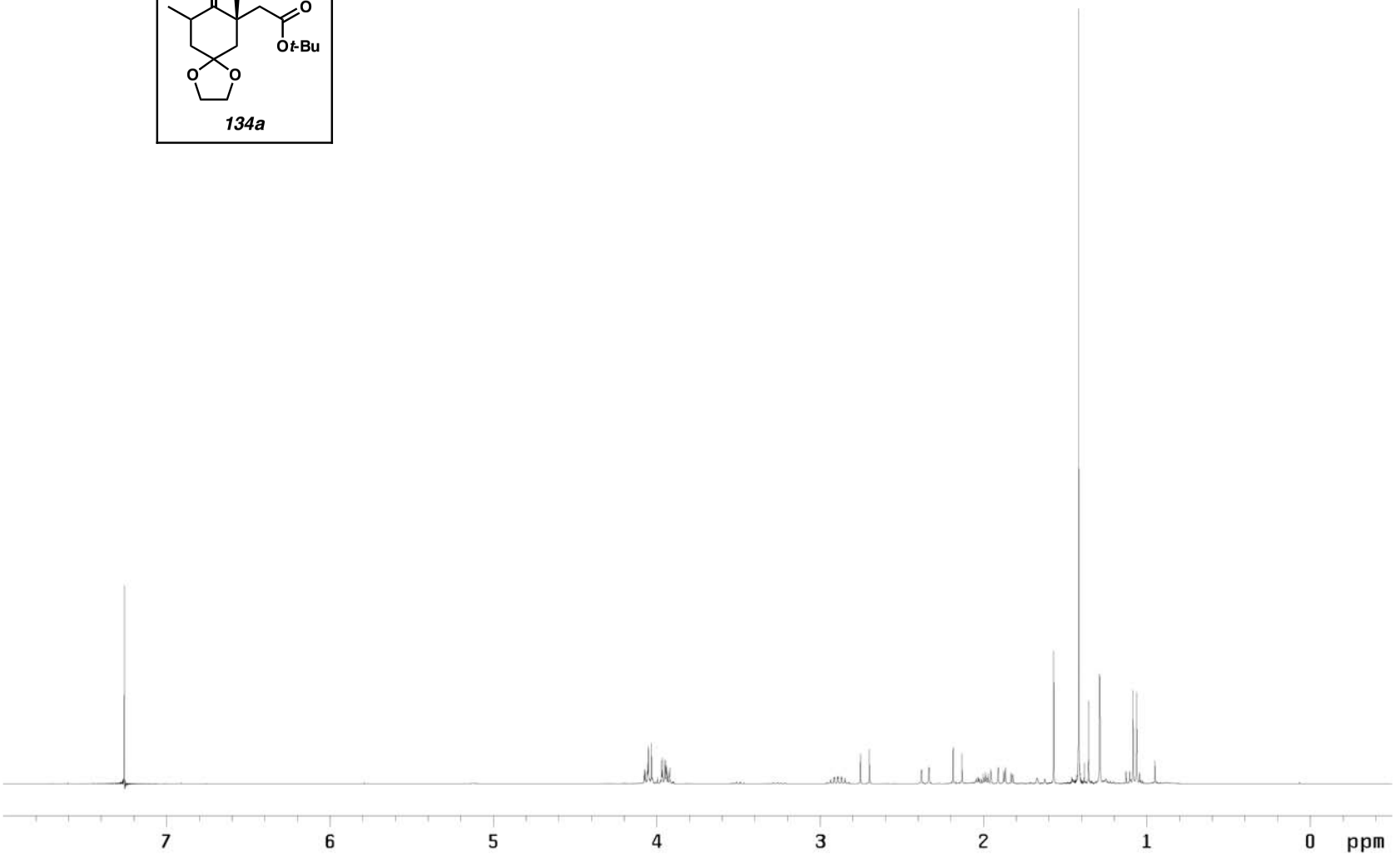

Figure A2.1 ^{1}H NMR of compound **(+)-134a** (300 MHz, $CDCl_3$)

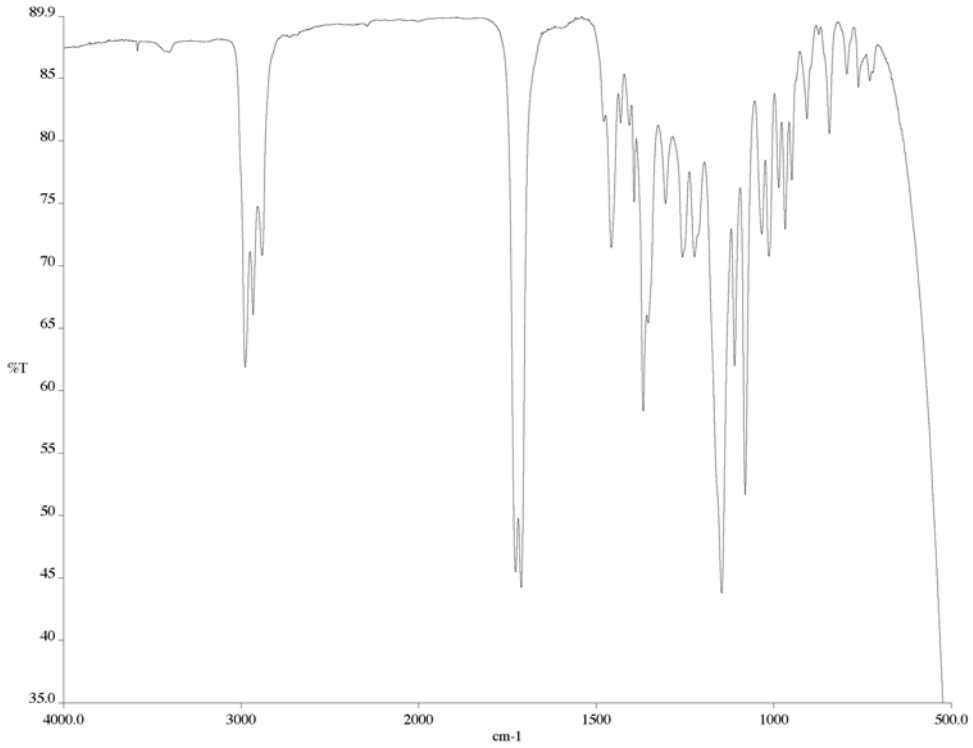

Figure A2.2 IR of compound **(+)-134a** (NaCl/film)

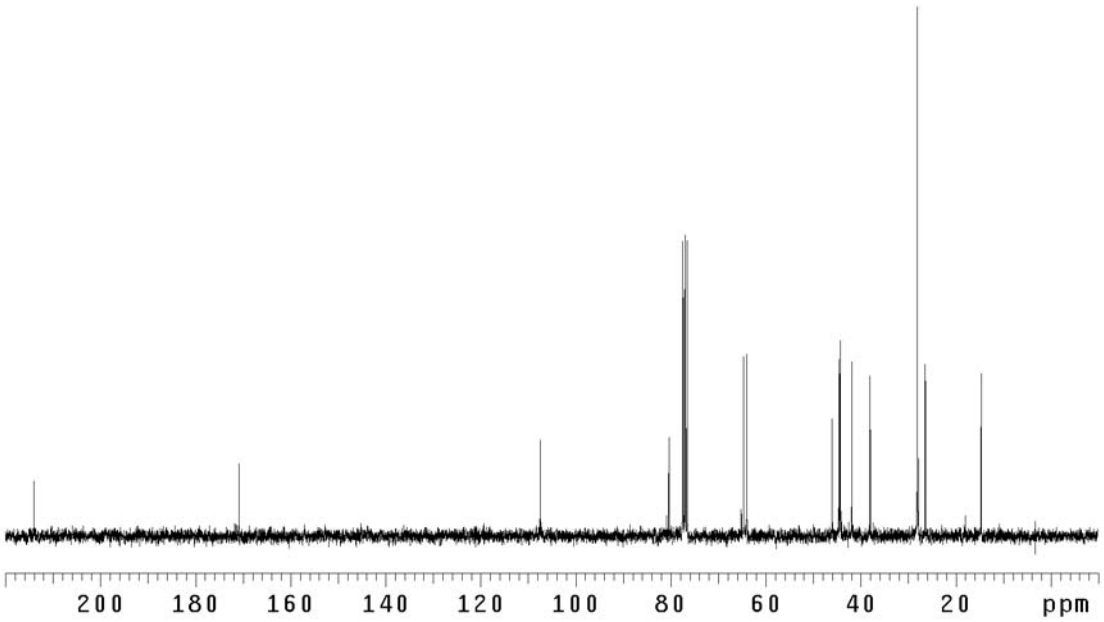

Figure A2.3 ^{13}C NMR of compound **(+)-134a** (75 MHz, $CDCl_3$)

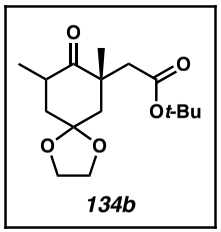

Figure A2.4 ^{1}H NMR of compound **(–)-134b** (300 MHz, $CDCl_3$)

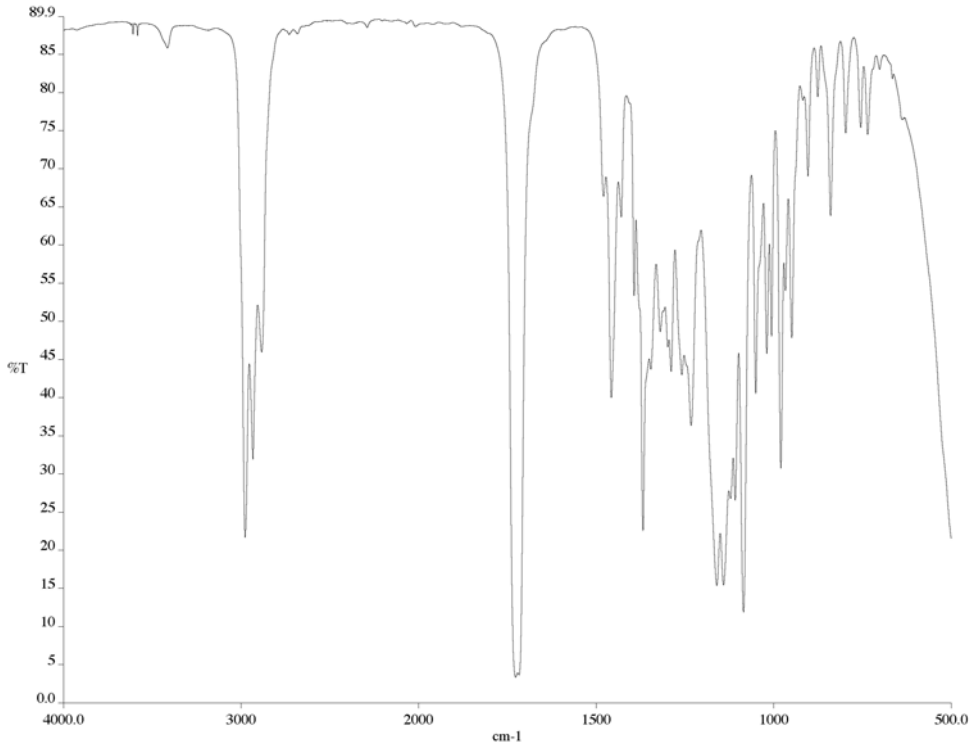

Figure A2.5 IR of compound **(–)-134b** (NaCl/film)

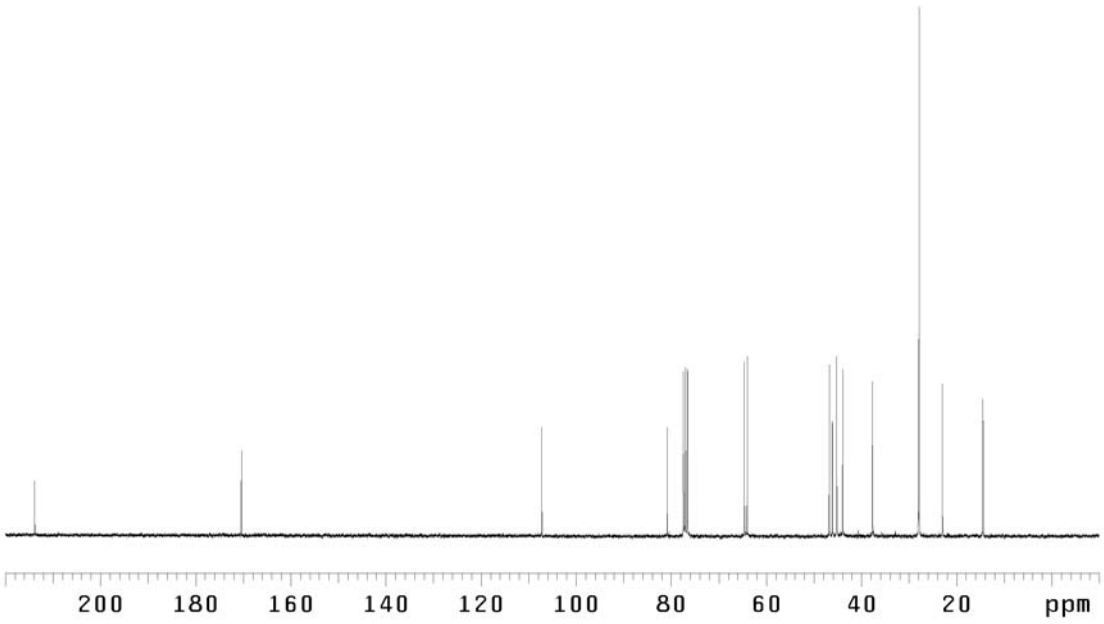

Figure A2.6 ^{13}C NMR of compound **(–)-134b** (75 MHz, $CDCl_3$)

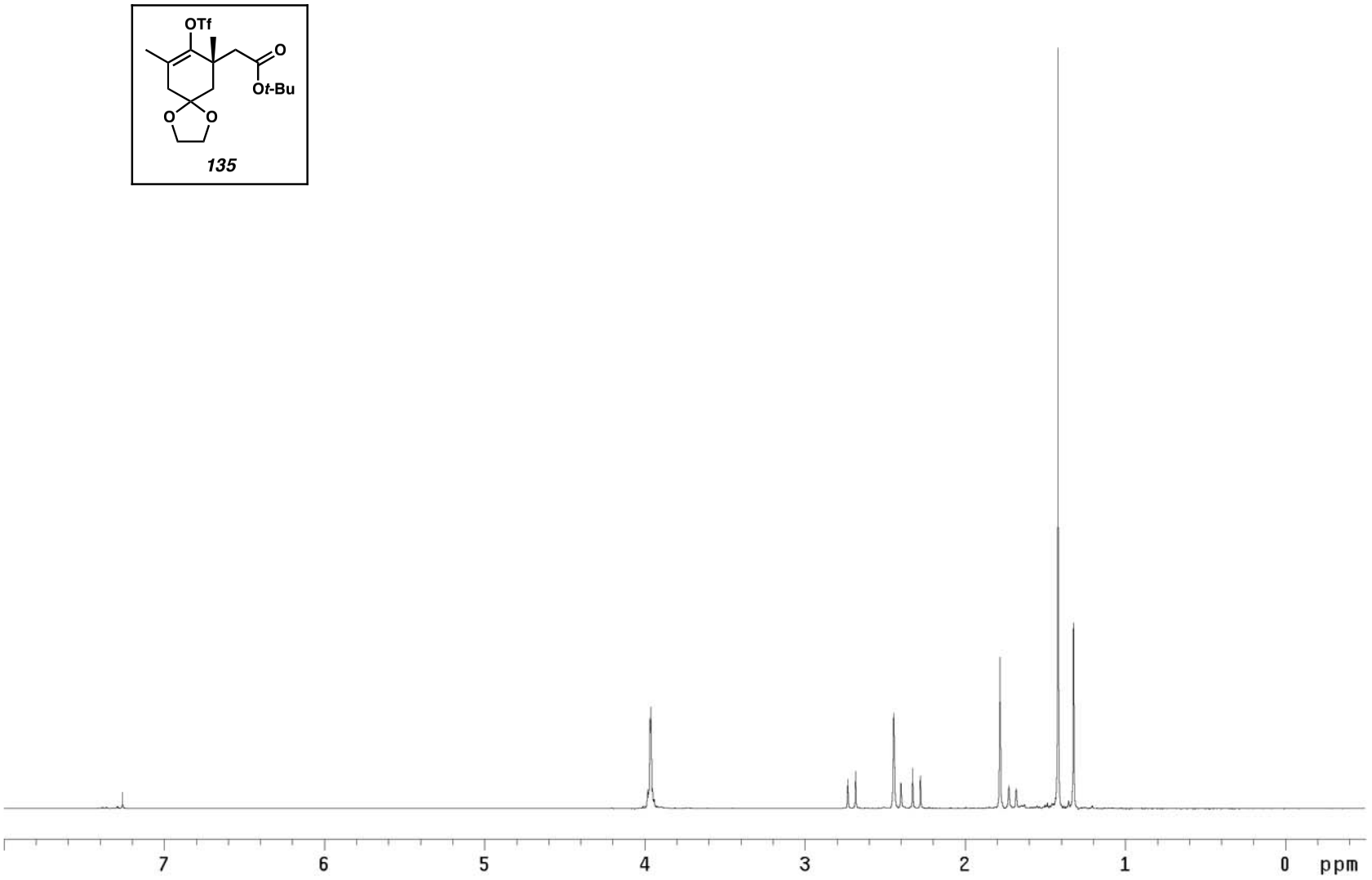

Figure A2.7 ^{1}H NMR of compound **135** (300 MHz, $CDCl_3$)

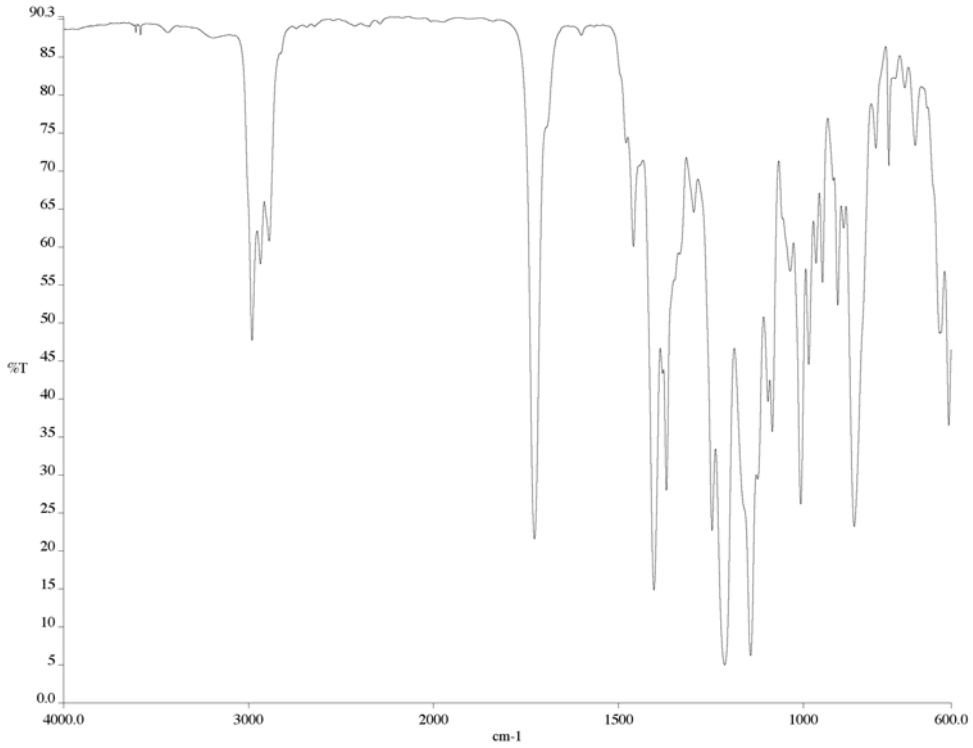

Figure A2.8 IR of compound **135** (NaCl/film)

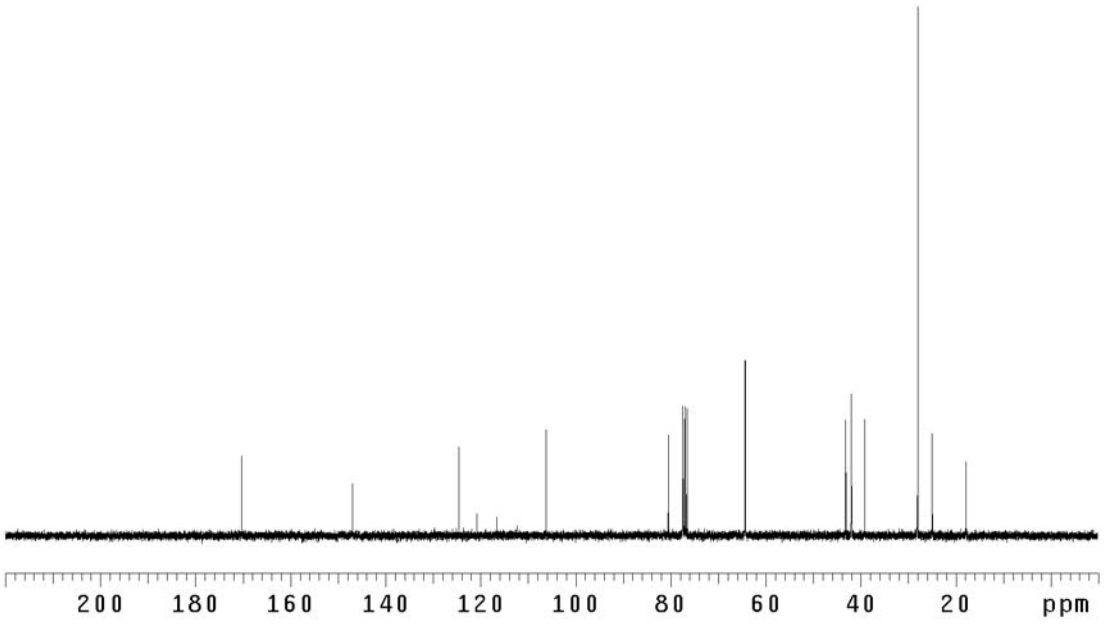

Figure A2.9 ^{13}C NMR of compound **135** (75 MHz, $CDCl_3$)

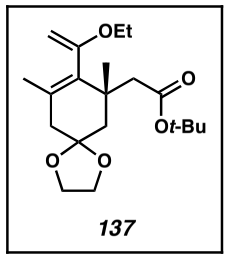

137

Figure A2.10 ^{1}H NMR of compound **137** (300 MHz, $CDCl_3$)

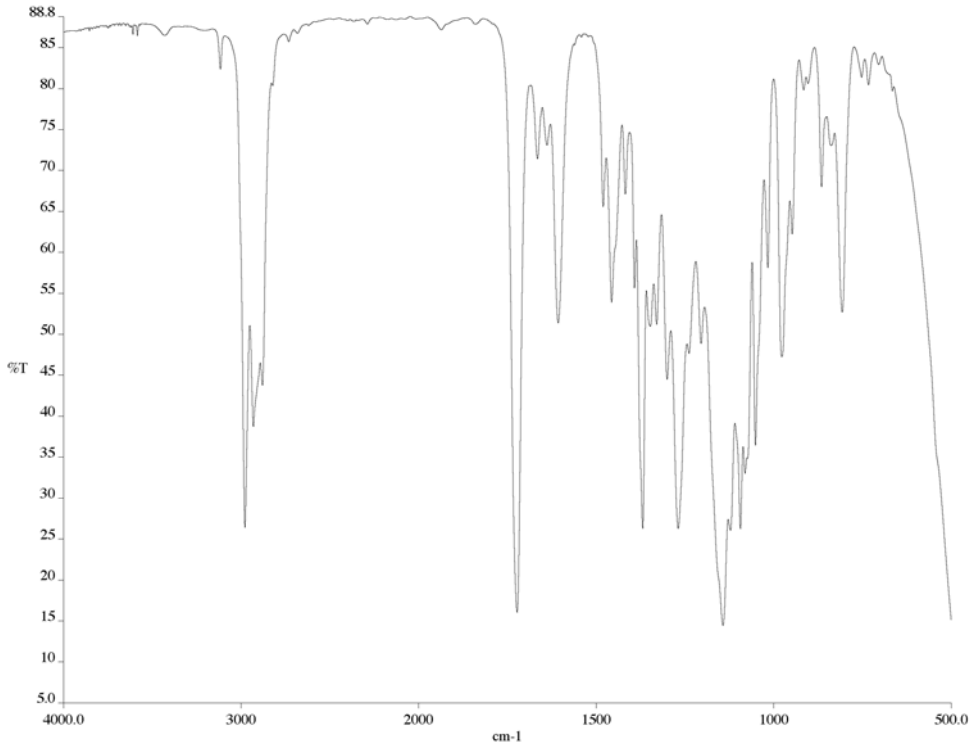

Figure A2.11 IR of compound **137** (NaCl/film)

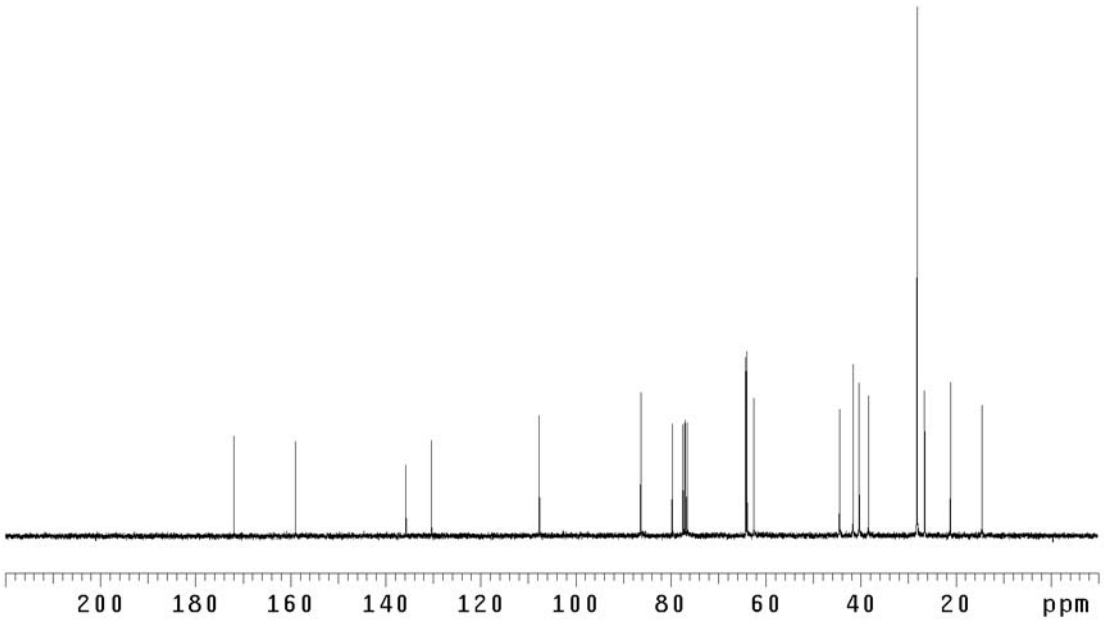

Figure A2.12 ^{13}C NMR of compound **137** (75 MHz, $CDCl_3$)

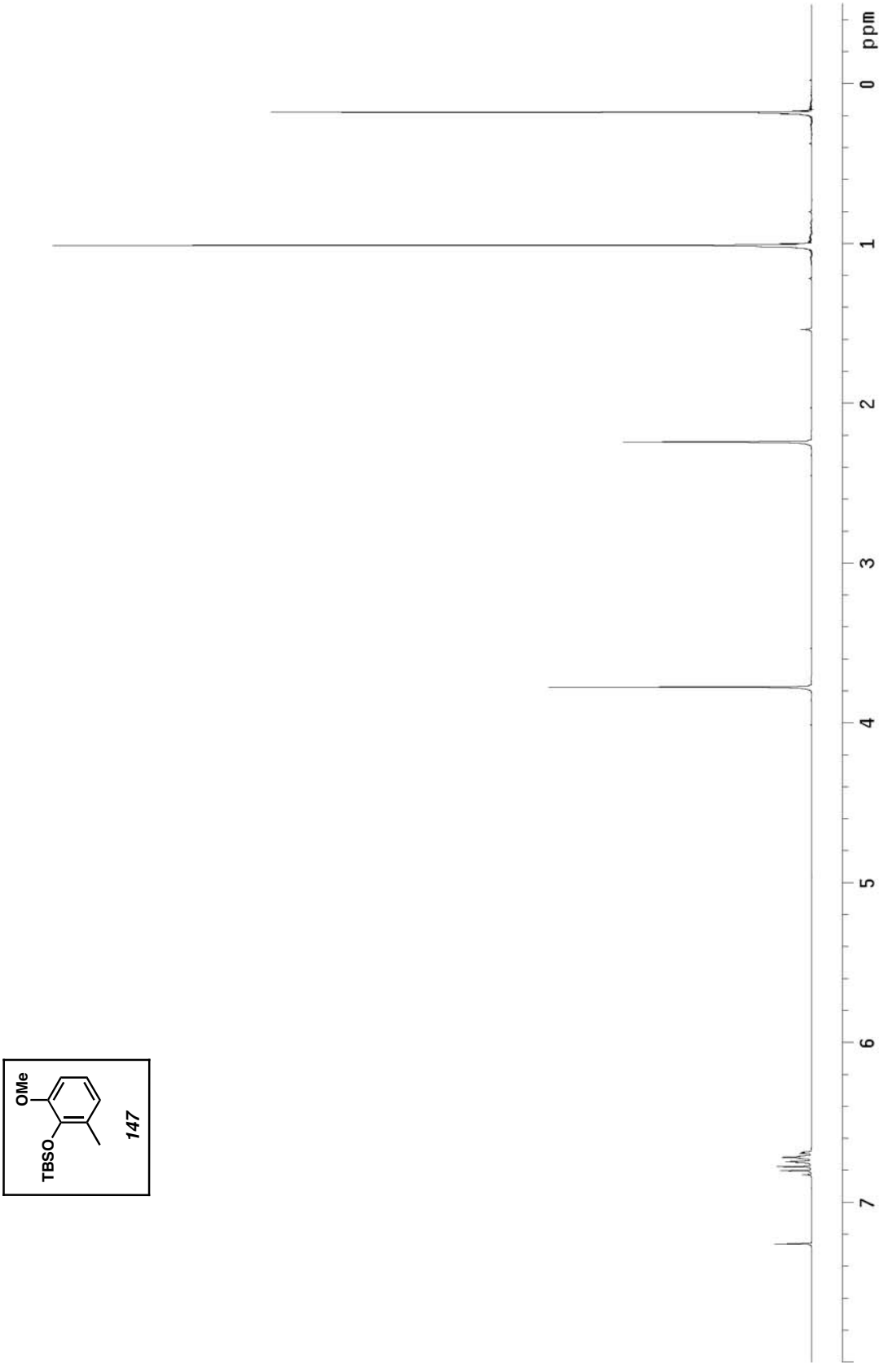

Figure A2.13 ^{1}H NMR of compound **147** (300 MHz, $CDCl_3$)

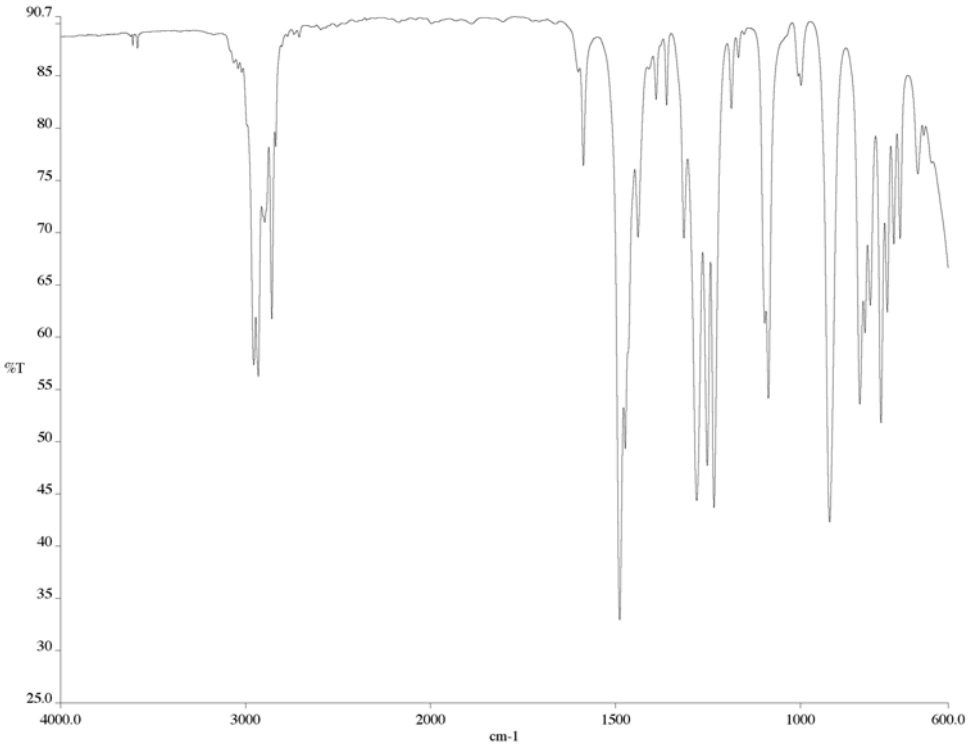

Figure A2.14 IR of compound **147** (NaCl/film)

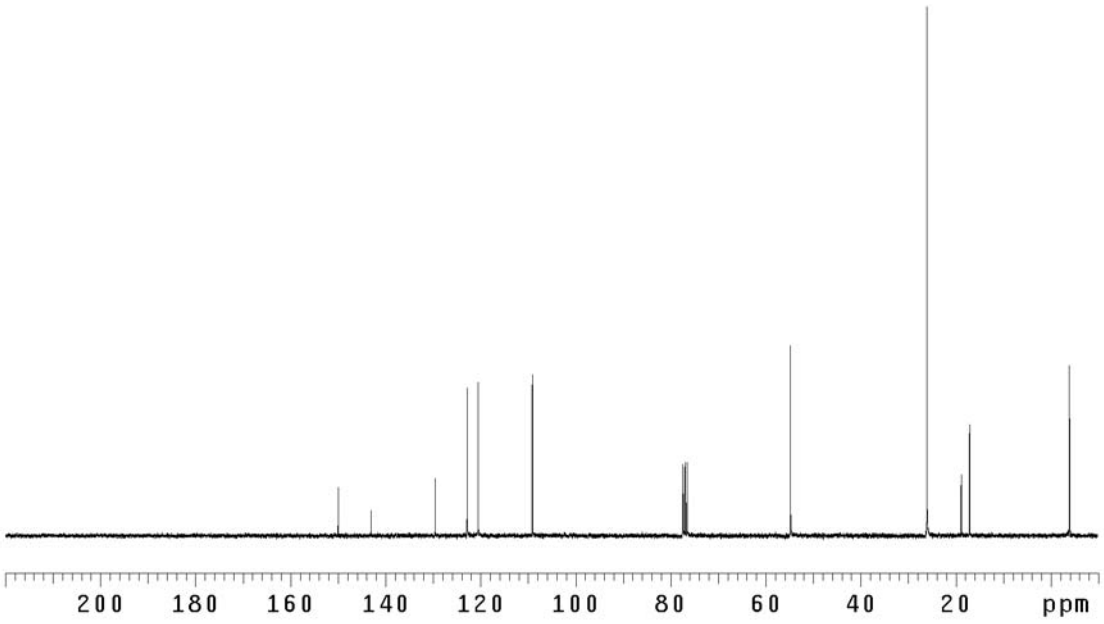

Figure A2.15 ^{13}C NMR of compound **147** (75 MHz, $CDCl_3$)

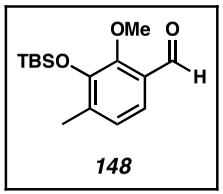

Figure A2.16 ^{1}H NMR of compound **148** (300 MHz, $CDCl_3$)

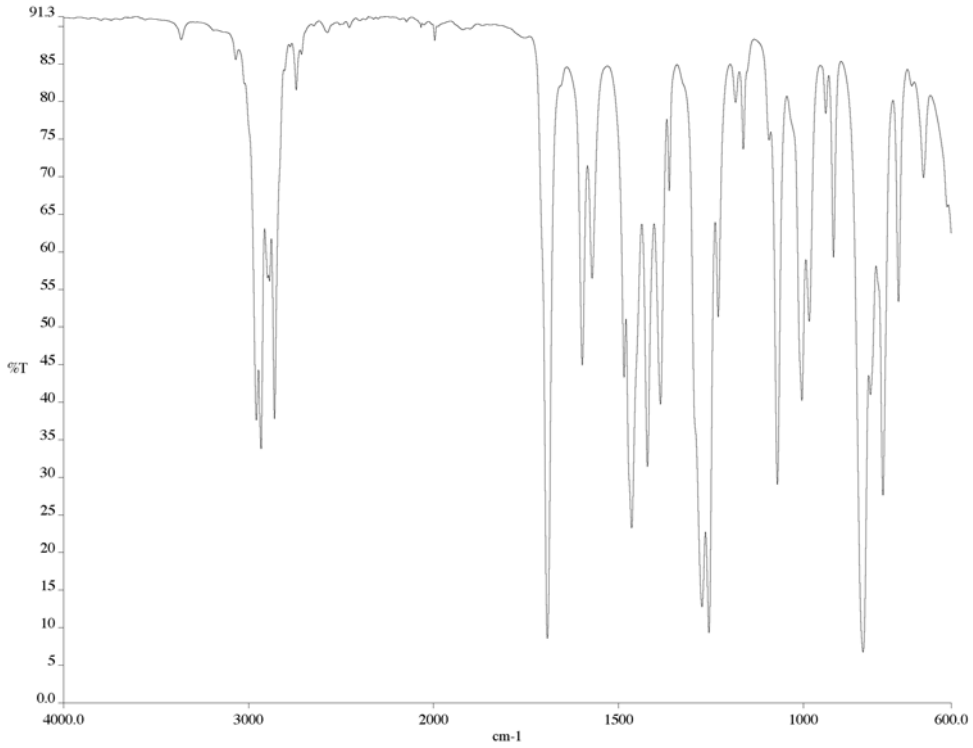

Figure A2.17 IR of compound **148** (NaCl/film)

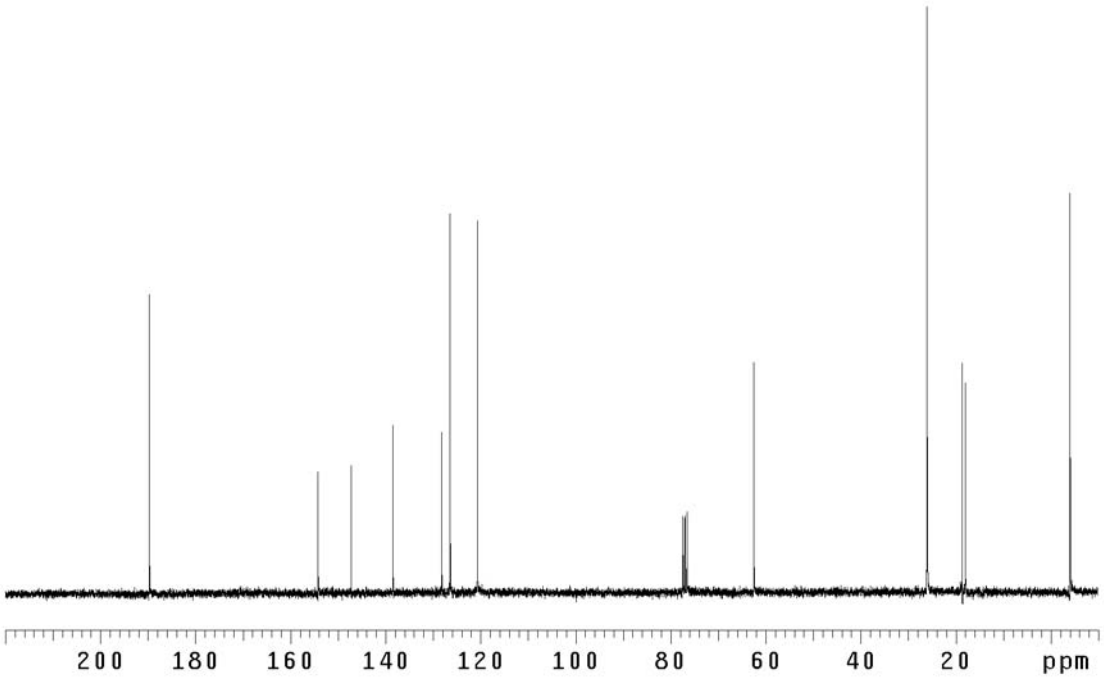

Figure A2.18 ^{13}C NMR of compound **148** (75 MHz, $CDCl_3$)

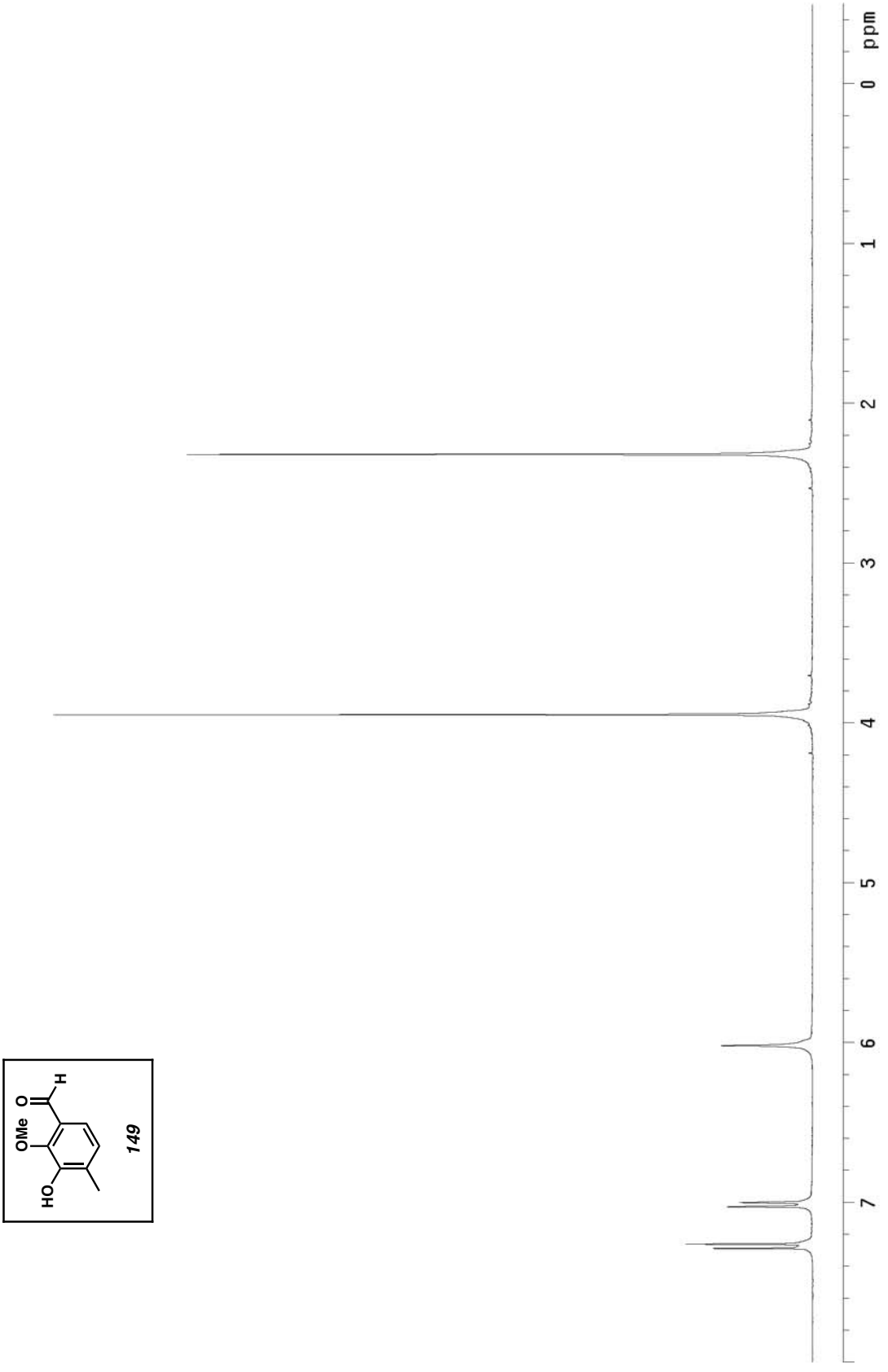

Figure A2.19 ^{1}H NMR of compound **149** (300 MHz, $CDCl_3$)

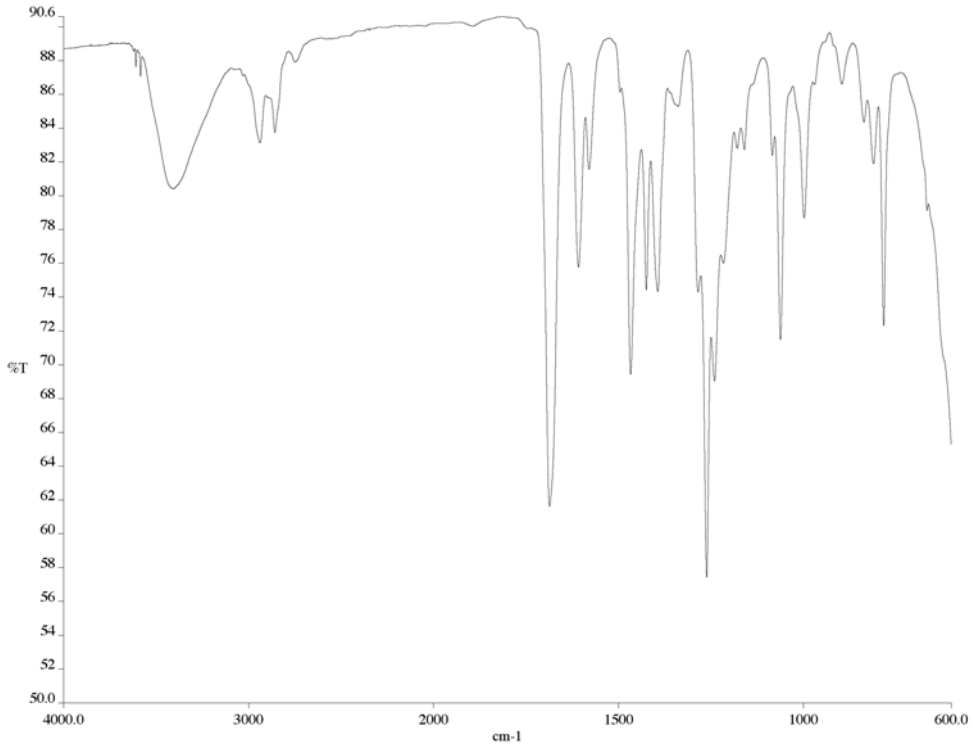

Figure A2.20 IR of compound **149** (NaCl/film)

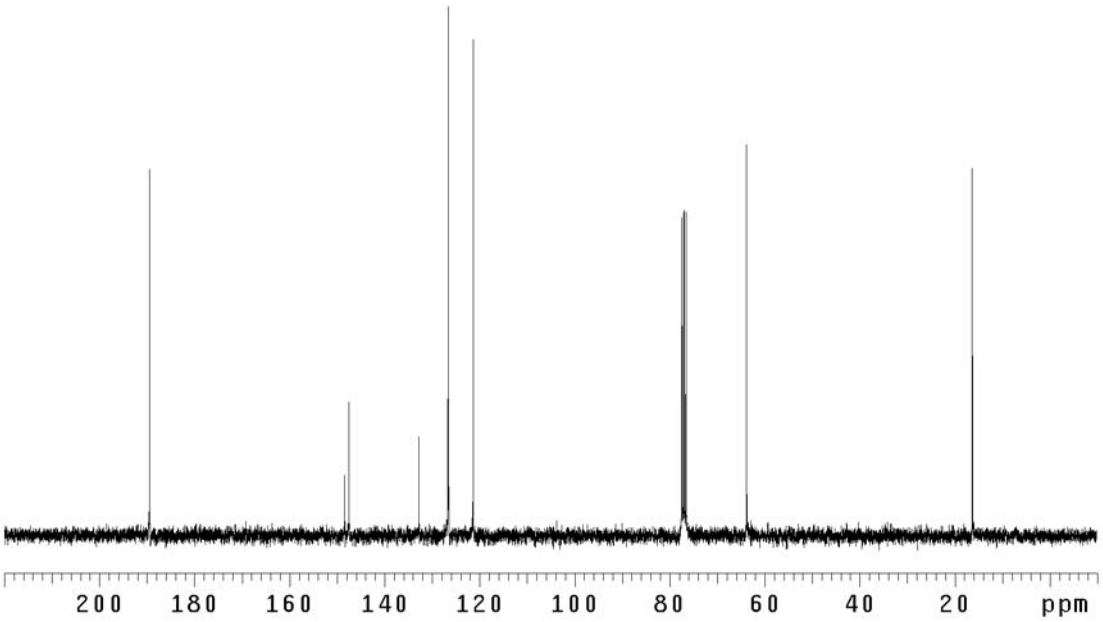

Figure A2.21 ^{13}C NMR of compound **149** (75 MHz, $CDCl_3$)

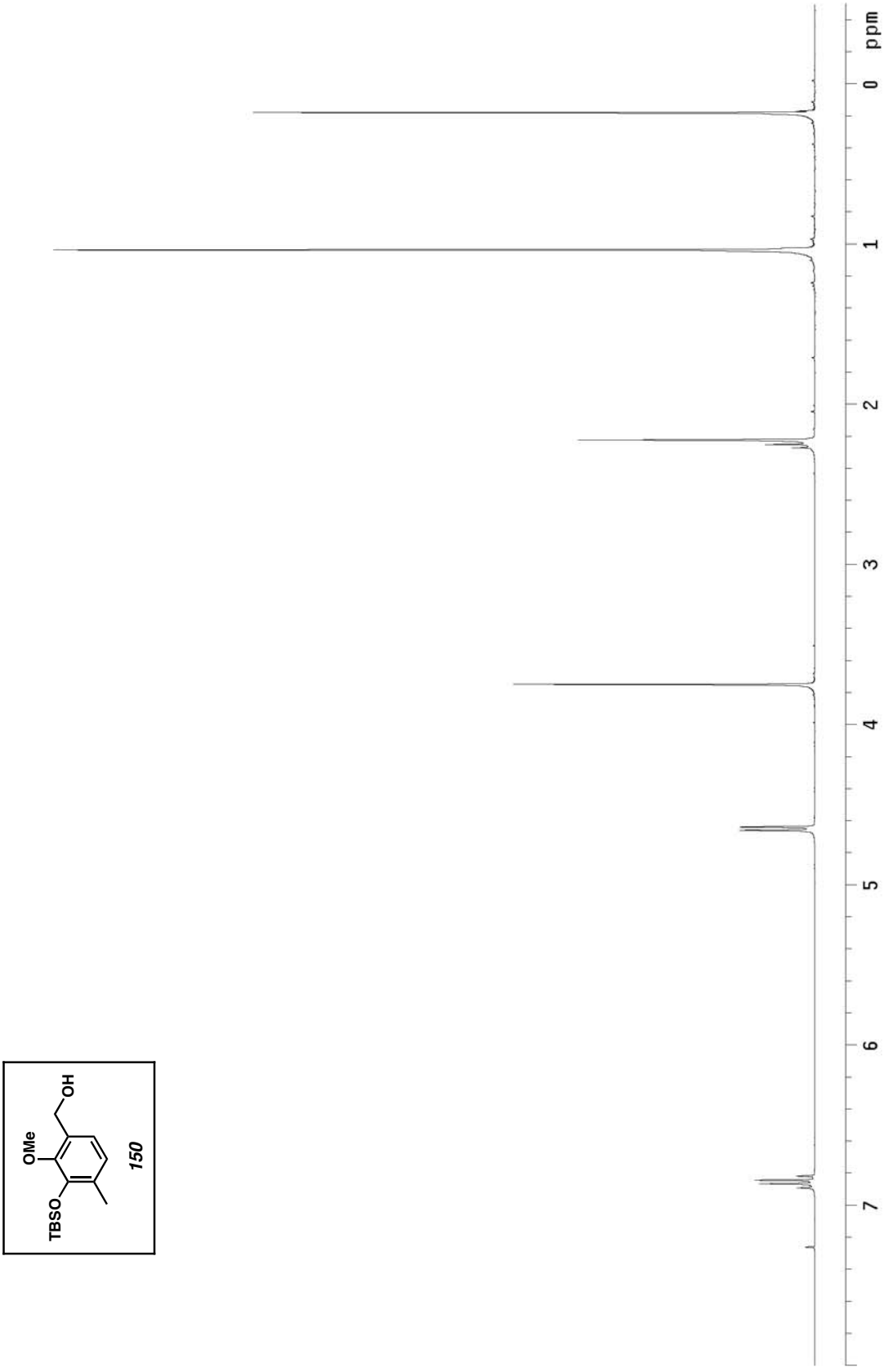

Figure A2.22 ^{1}H NMR of compound **150** (300 MHz, $CDCl_3$)

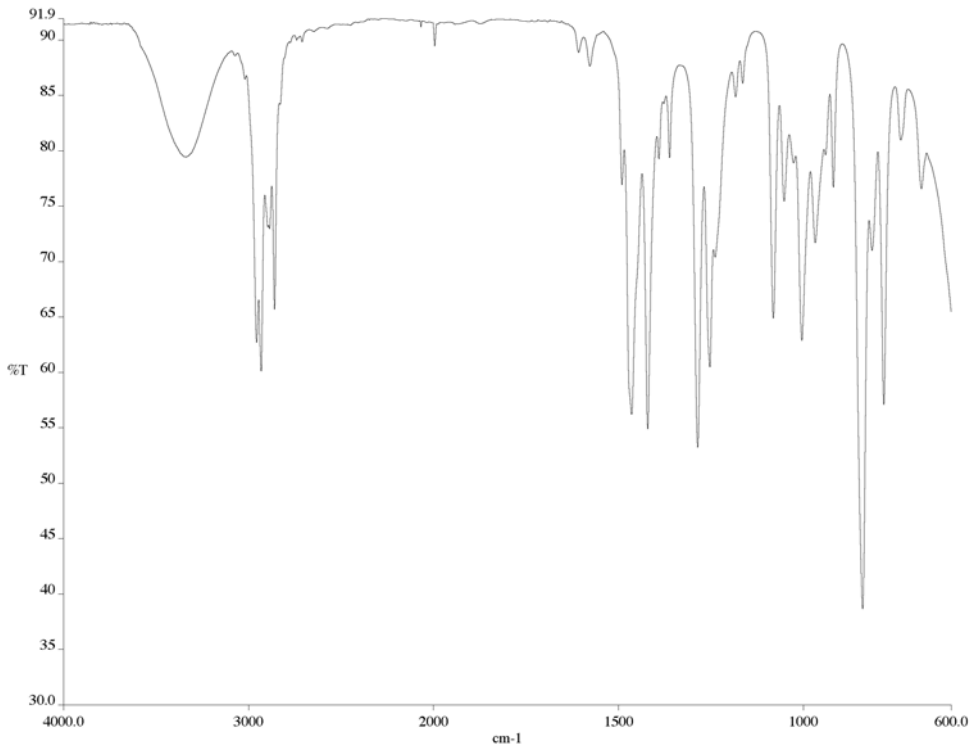

Figure A2.23 IR of compound **150** (NaCl/film)

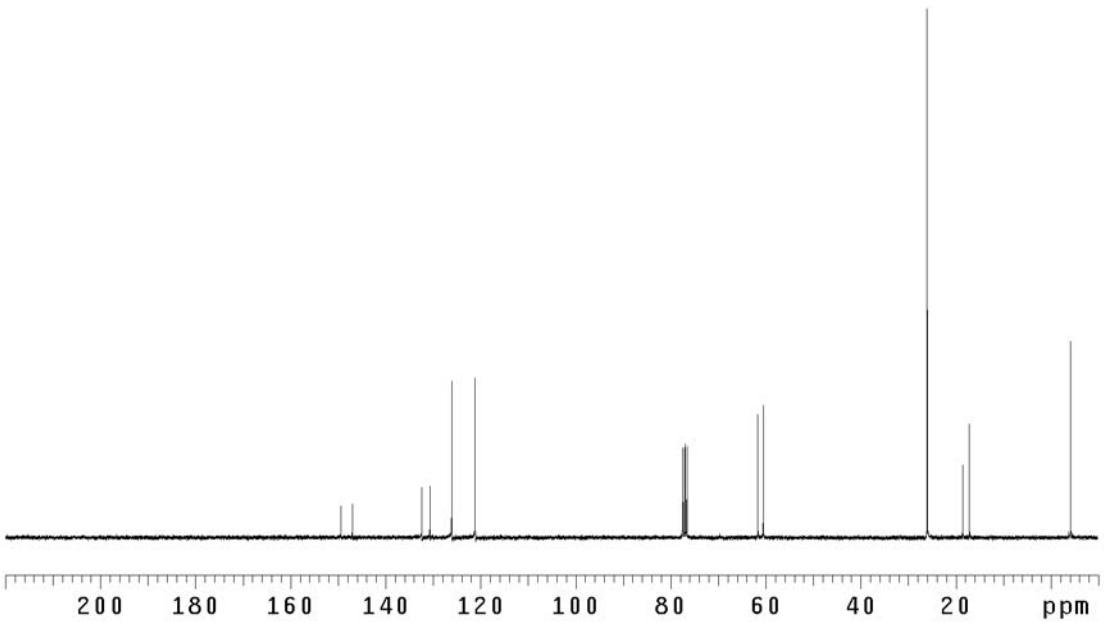

Figure A2.24 ^{13}C NMR of compound **150** (75 MHz, $CDCl_3$)

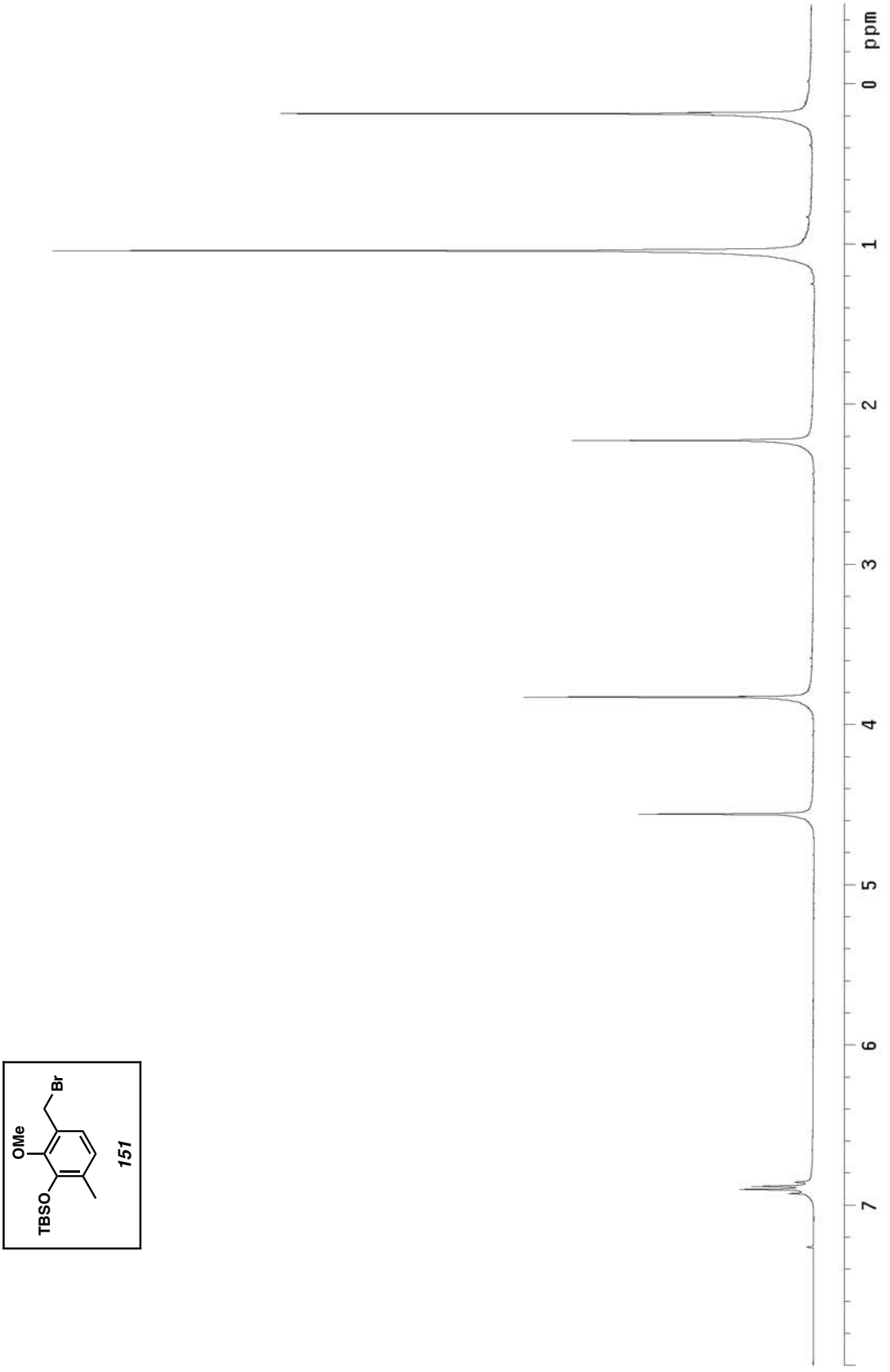

Figure A2.25 ^{1}H NMR of compound **151** (300 MHz, $CDCl_3$)

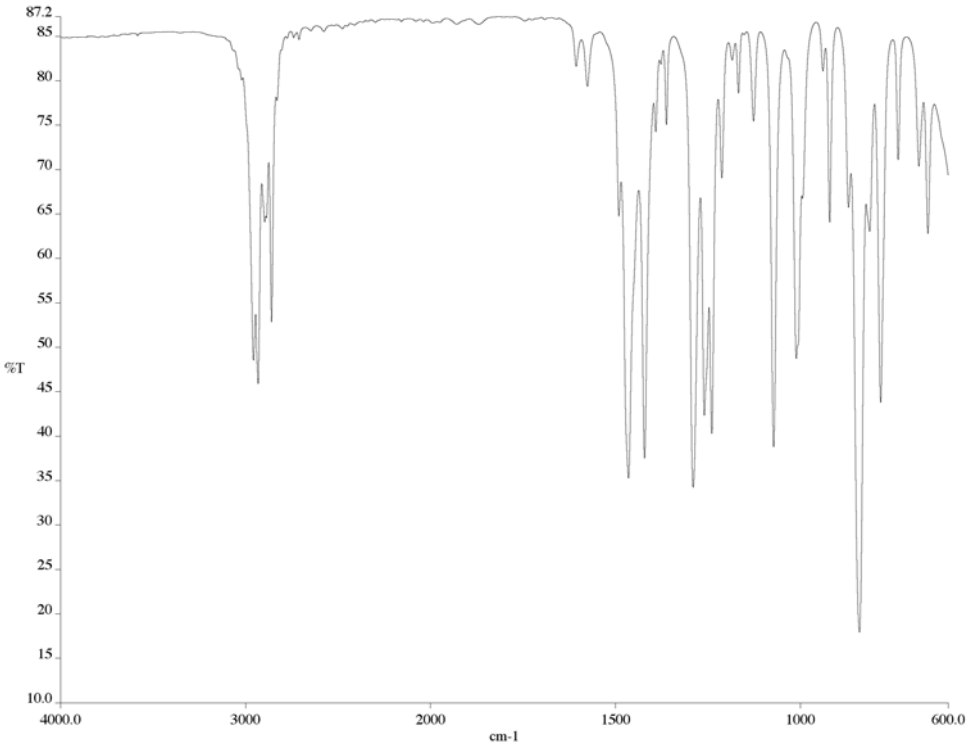

Figure A2.26 IR of compound **151** (NaCl/film)

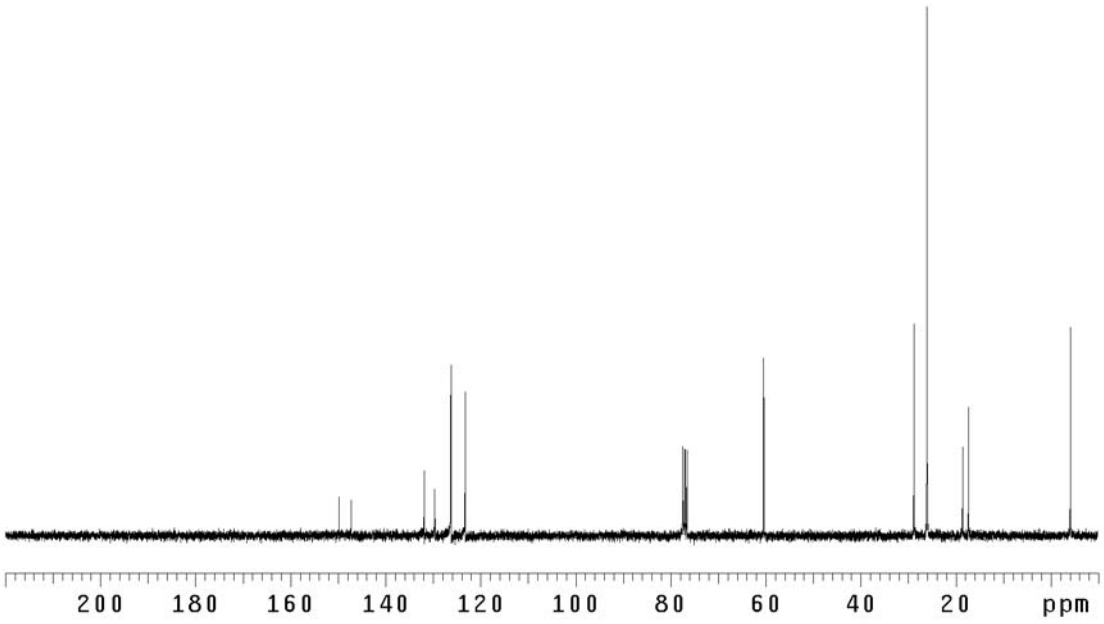

Figure A2.27 ^{13}C NMR of compound **151** (75 MHz, $CDCl_3$)

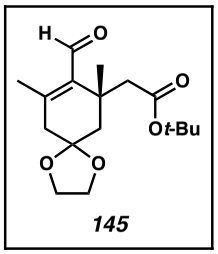

Figure A2.28 ^{1}H NMR of compound **145** (300 MHz, $CDCl_3$)

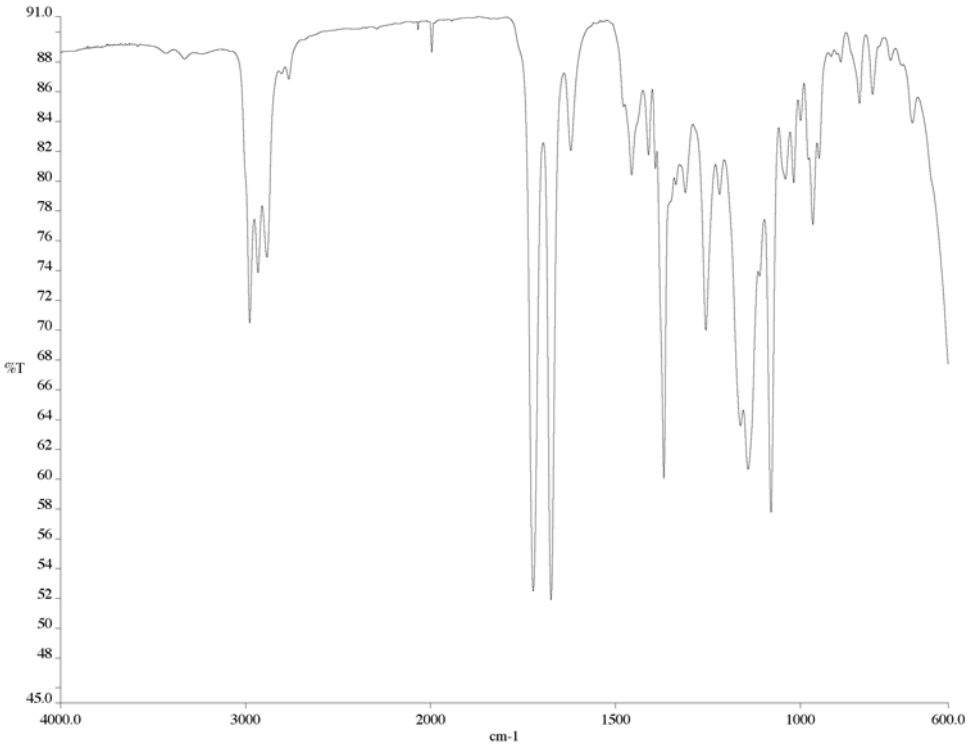

Figure A2.29 IR of compound **145** (NaCl/film)

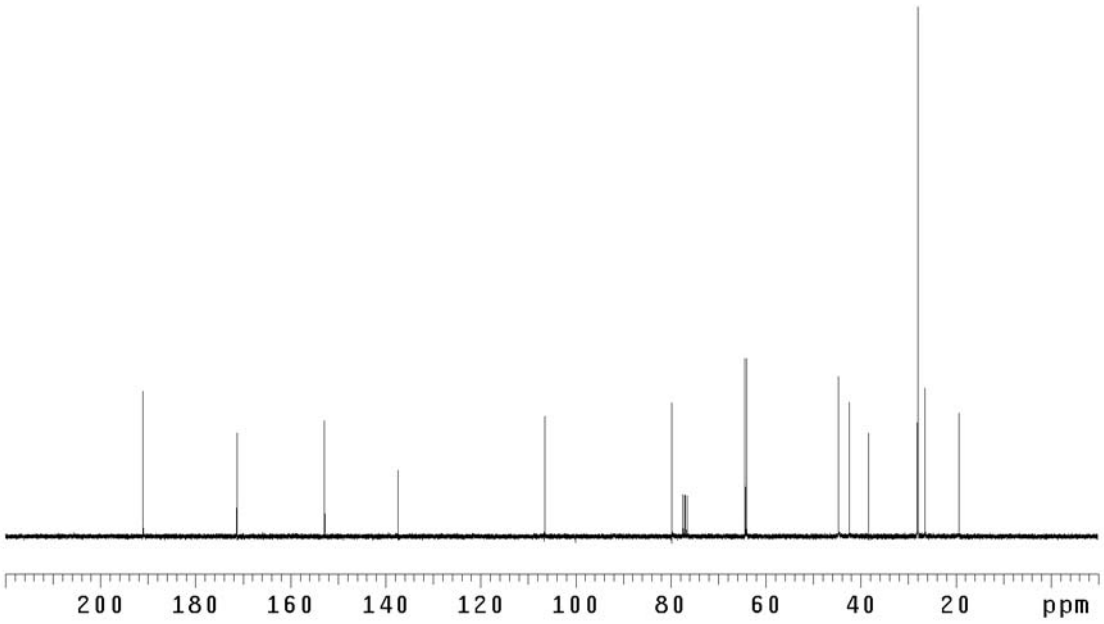

Figure A2.30 ^{13}C NMR of compound **145** (75 MHz, $CDCl_3$)

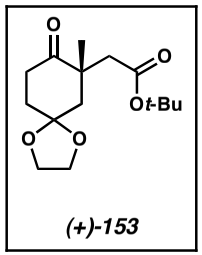

Figure A2.31 ^{1}H NMR of compound **(+)-153** (300 MHz, $CDCl_3$)

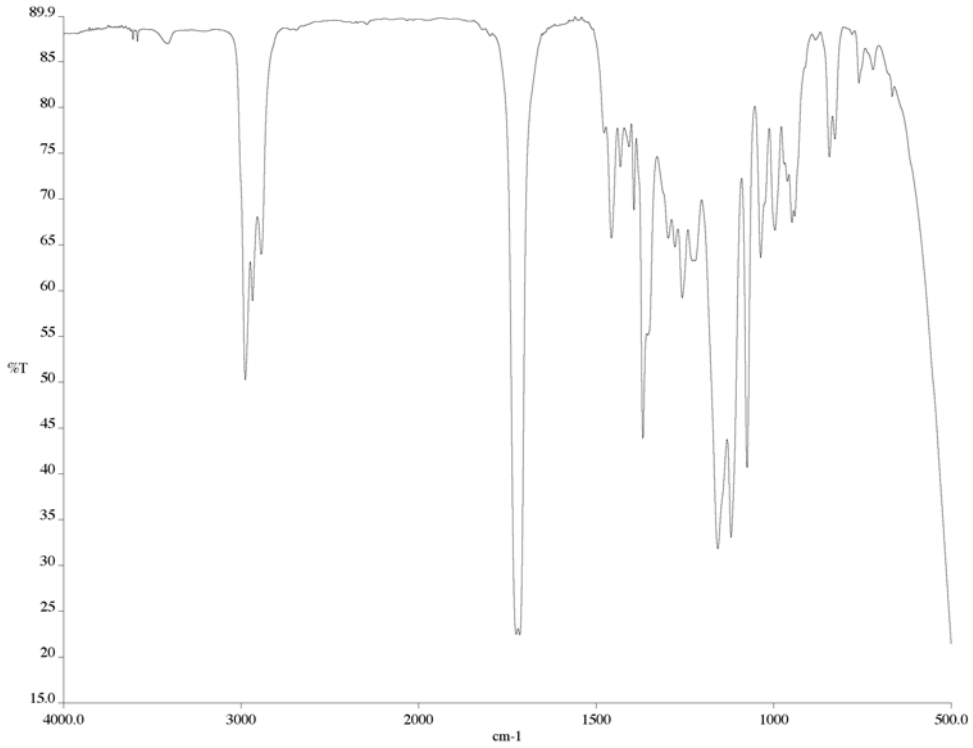

Figure A2.32 IR of compound **(+)-153** (NaCl/film)

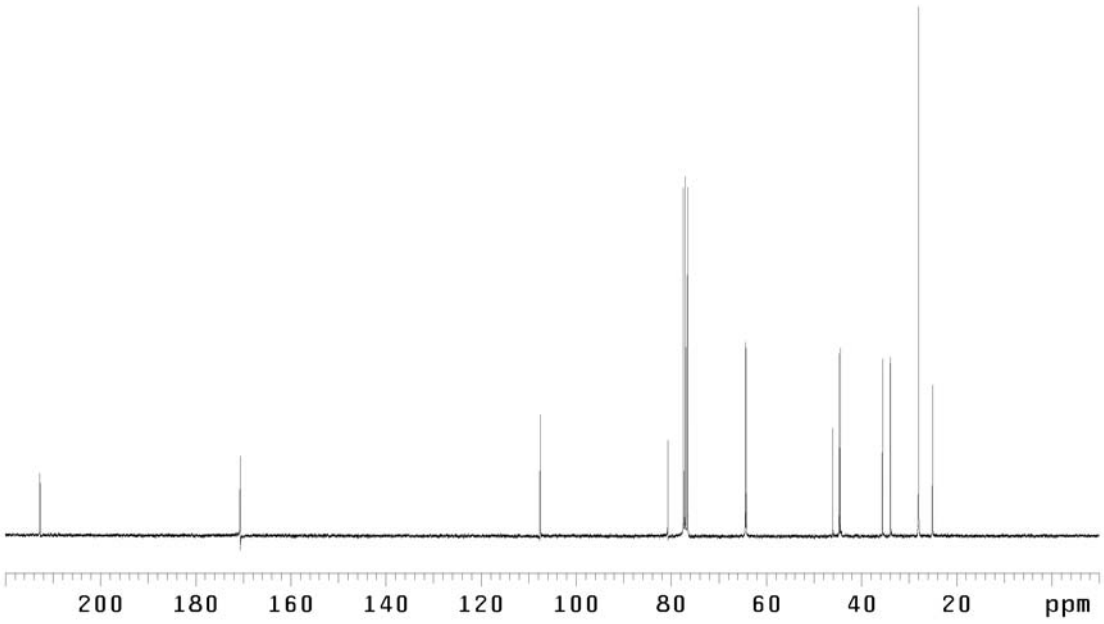

Figure A2.33 ^{13}C NMR of compound **(+)-153** (75 MHz, $CDCl_3$)

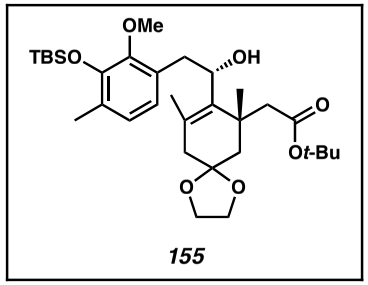

155

Figure A2.34 ^{1}H NMR of compound **155** (300 MHz, $CDCl_3$)

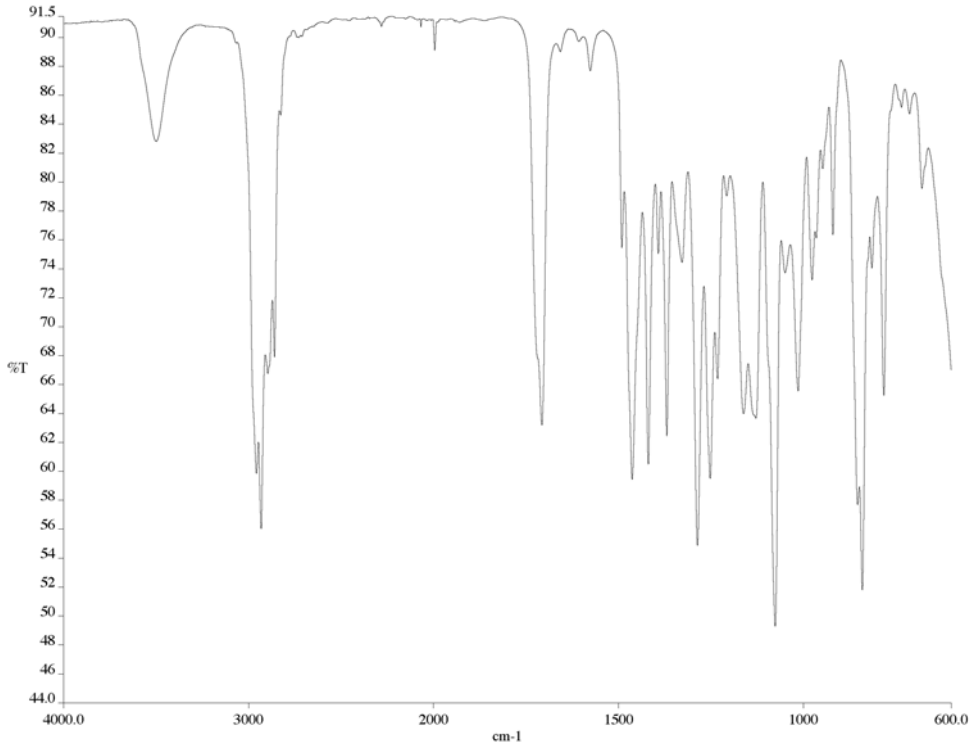

Figure A2.35 IR of compound **155** (NaCl/film)

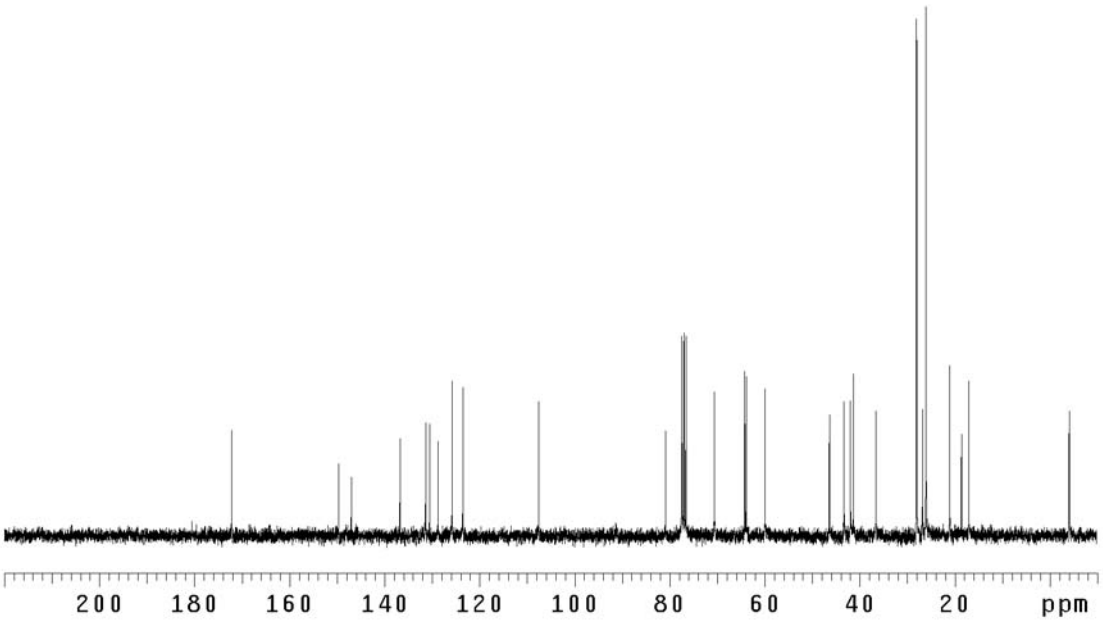

Figure A2.36 ^{13}C NMR of compound **155** (75 MHz, $CDCl_3$)

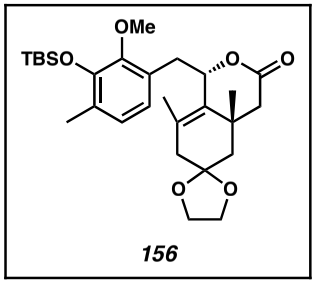

Figure A2.37 ^{1}H NMR of compound **156** (300 MHz, $CDCl_3$)

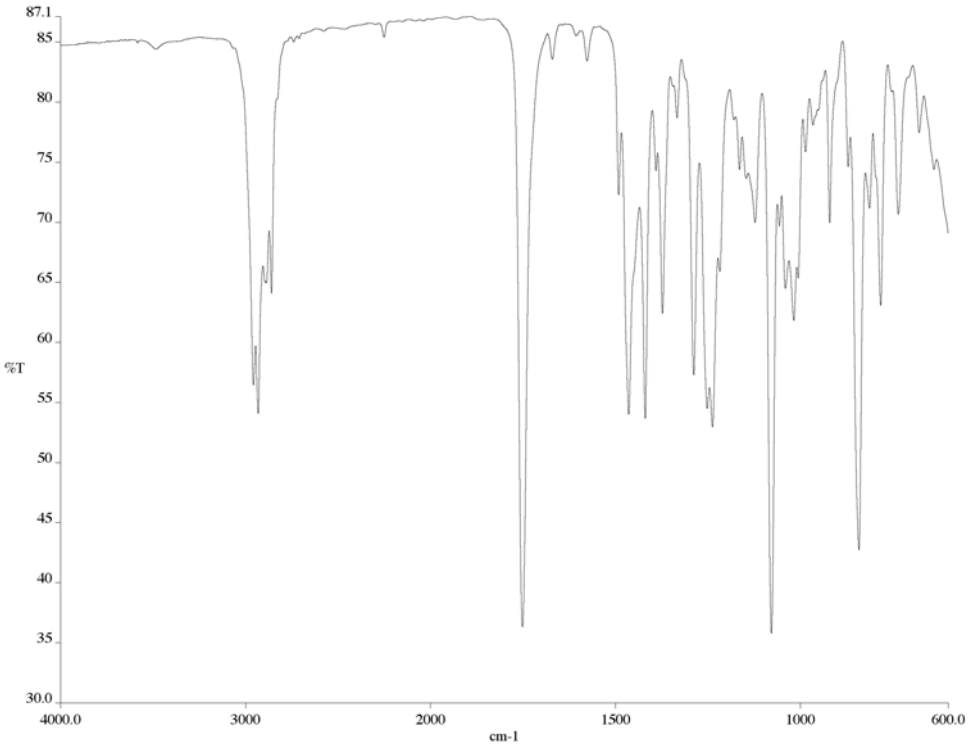

Figure A2.38 IR of compound **156** (NaCl/film)

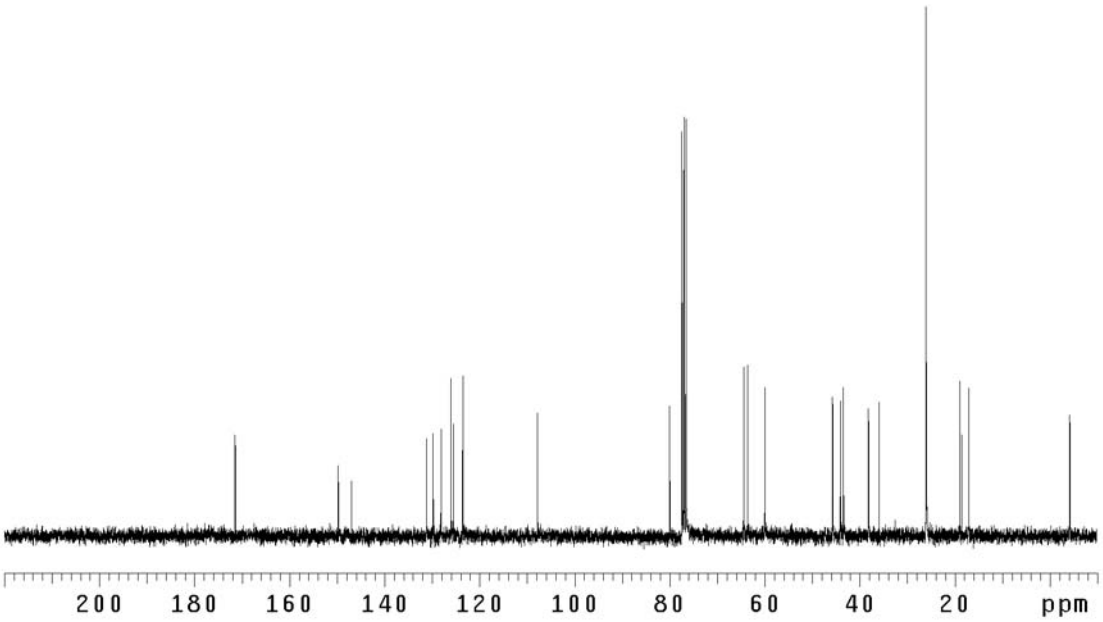

Figure A2.39 ^{13}C NMR of compound **156** (75 MHz, $CDCl_3$)

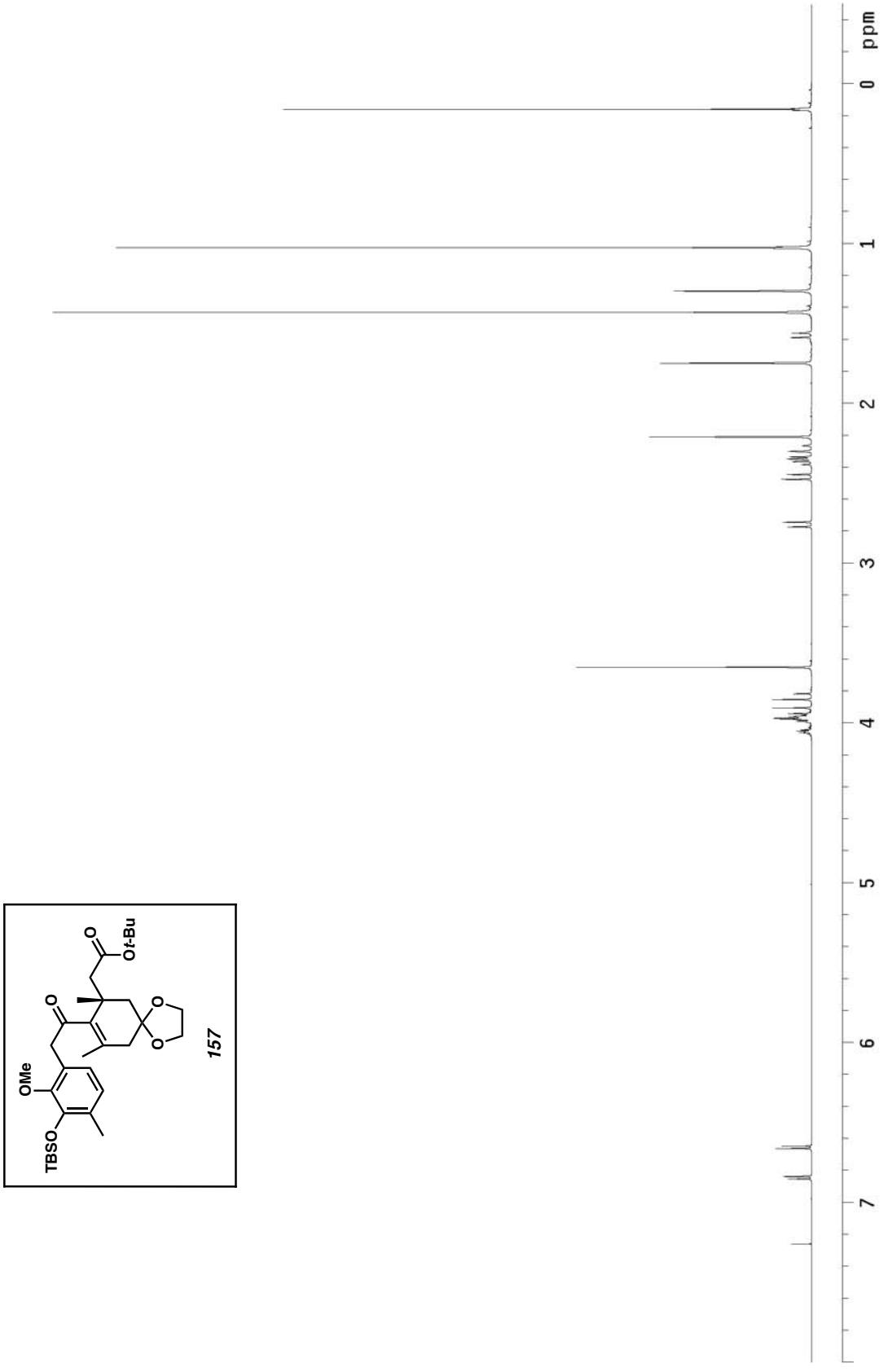

Figure A2.40 ^{1}H NMR of compound **157** (500 MHz, $CDCl_3$)

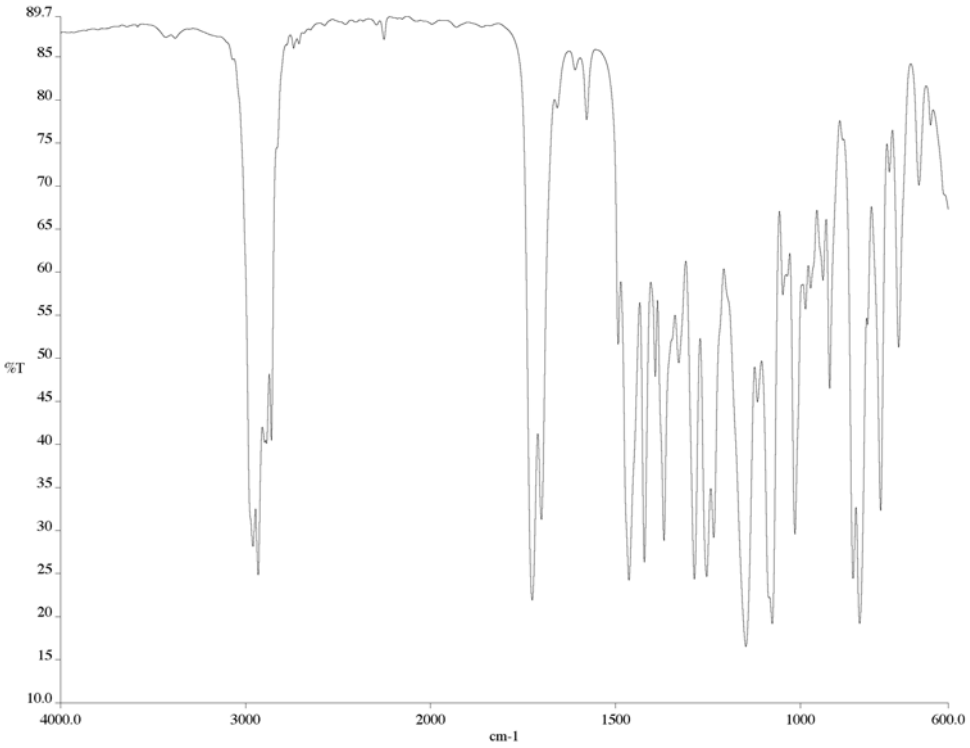

Figure A2.41 IR of compound **157** (NaCl/film)

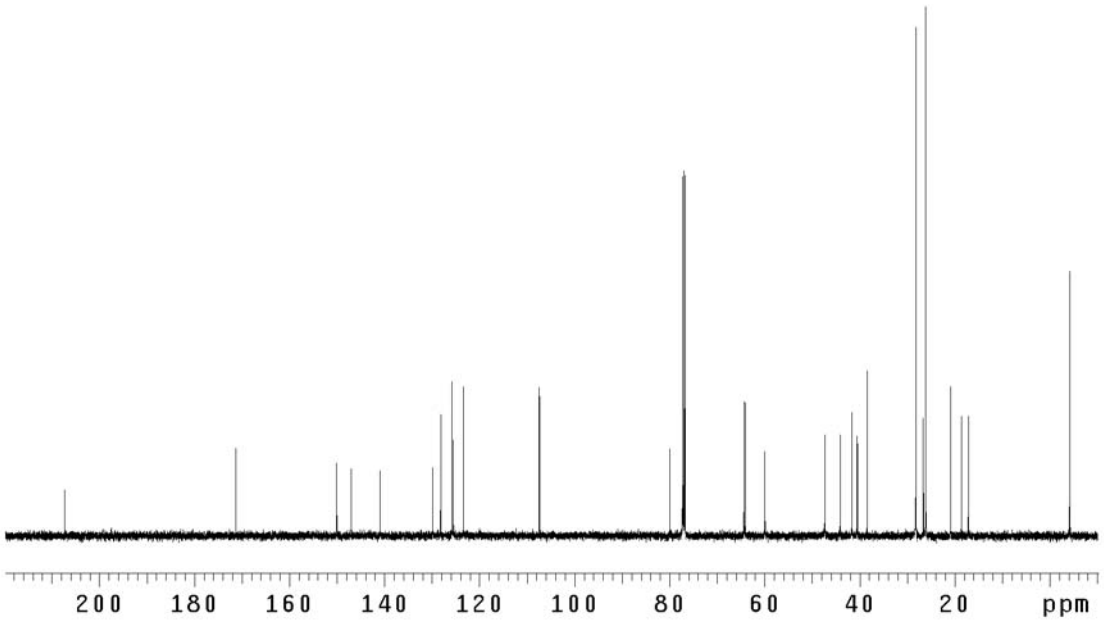

Figure A2.42 ^{13}C NMR of compound **157** (125 MHz, $CDCl_3$)

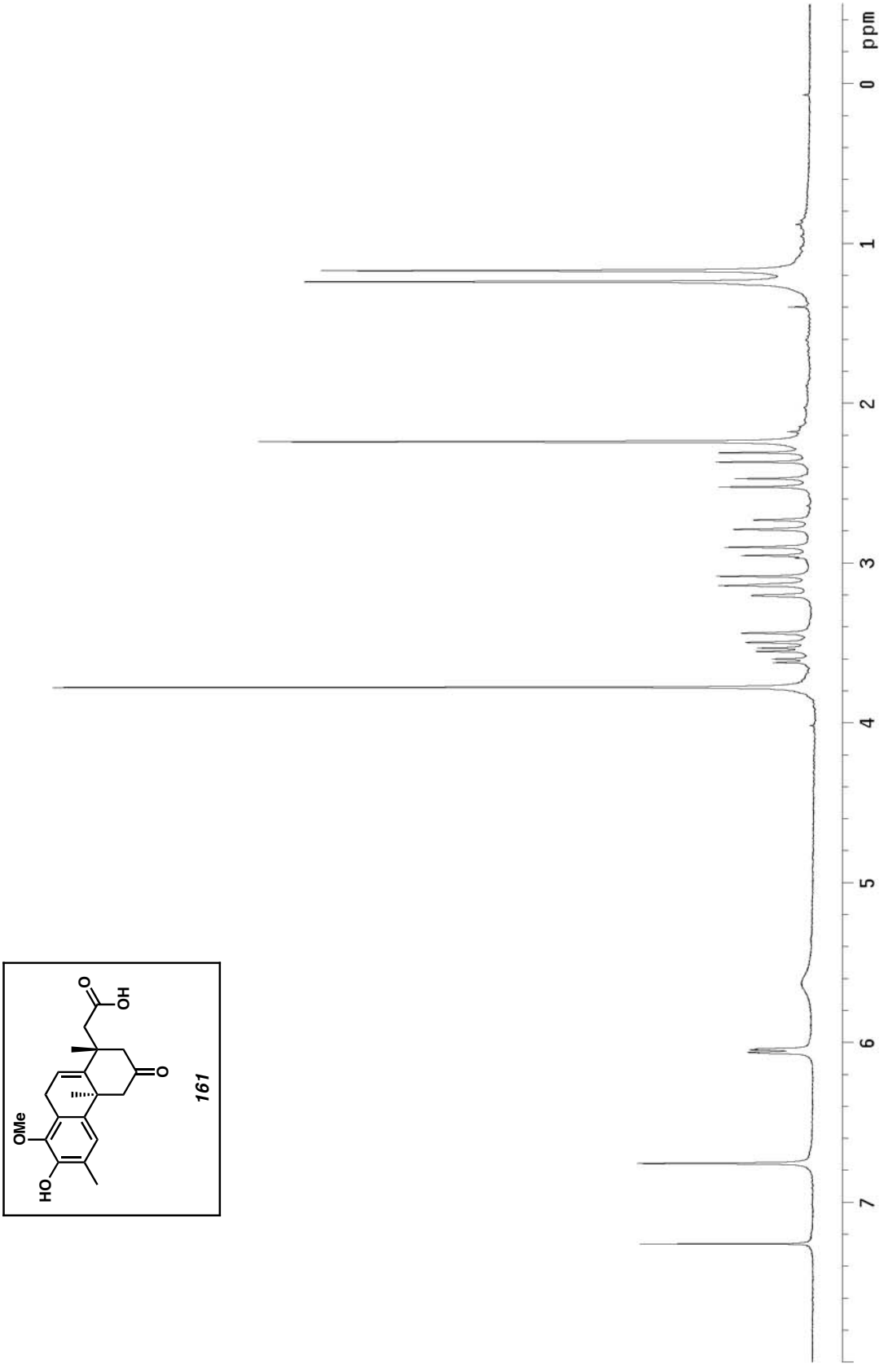

Figure A2.43 ^{1}H NMR of compound **161** (300 MHz, $CDCl_3$)

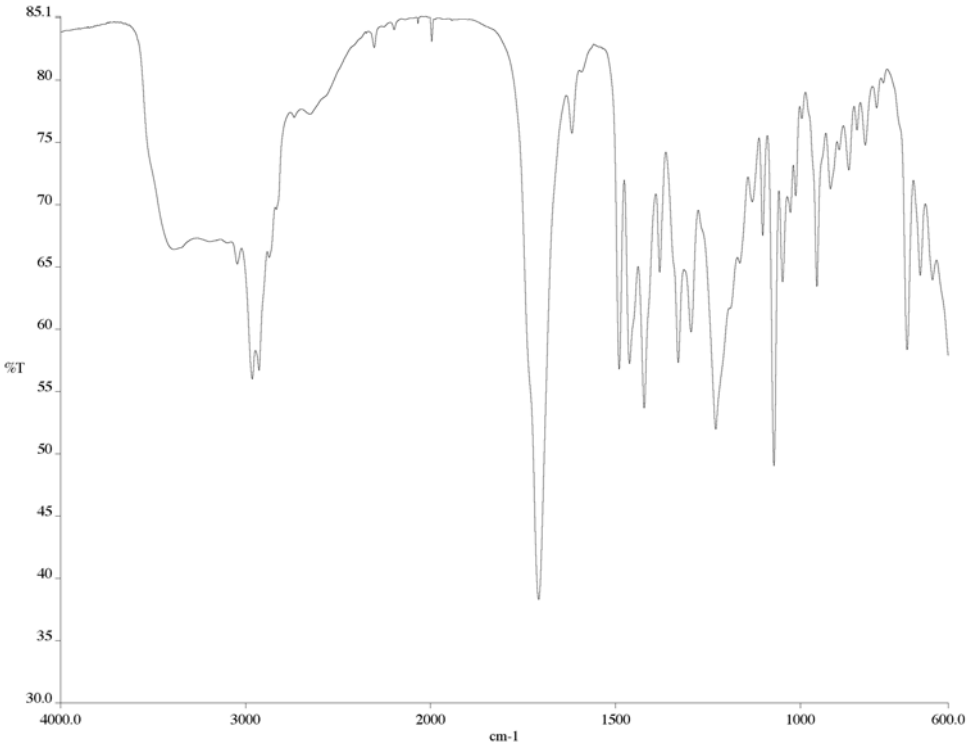

Figure A2.44 IR of compound **161** (NaCl/film)

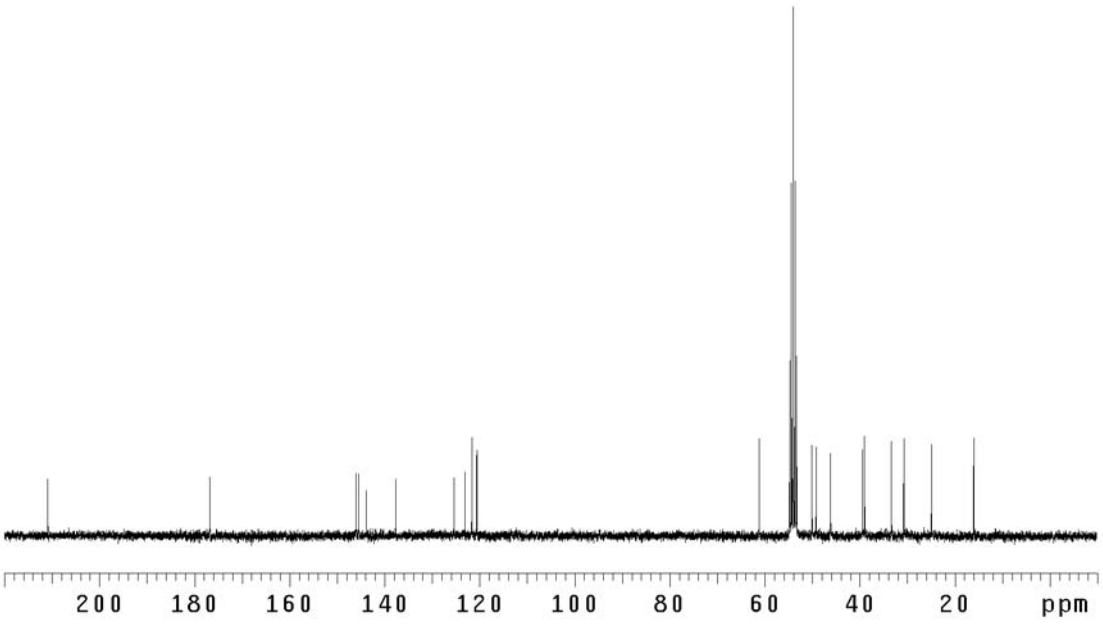

Figure A2.45 ^{13}C NMR of compound **161** (75 MHz, CD_2Cl_2)

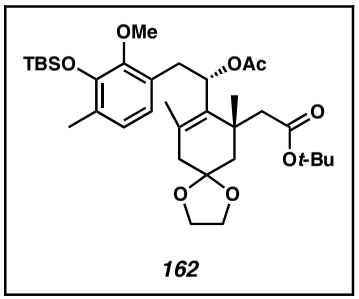

162

Figure A2.46 ^{1}H NMR of compound **162** (500 MHz, $CDCl_3$)

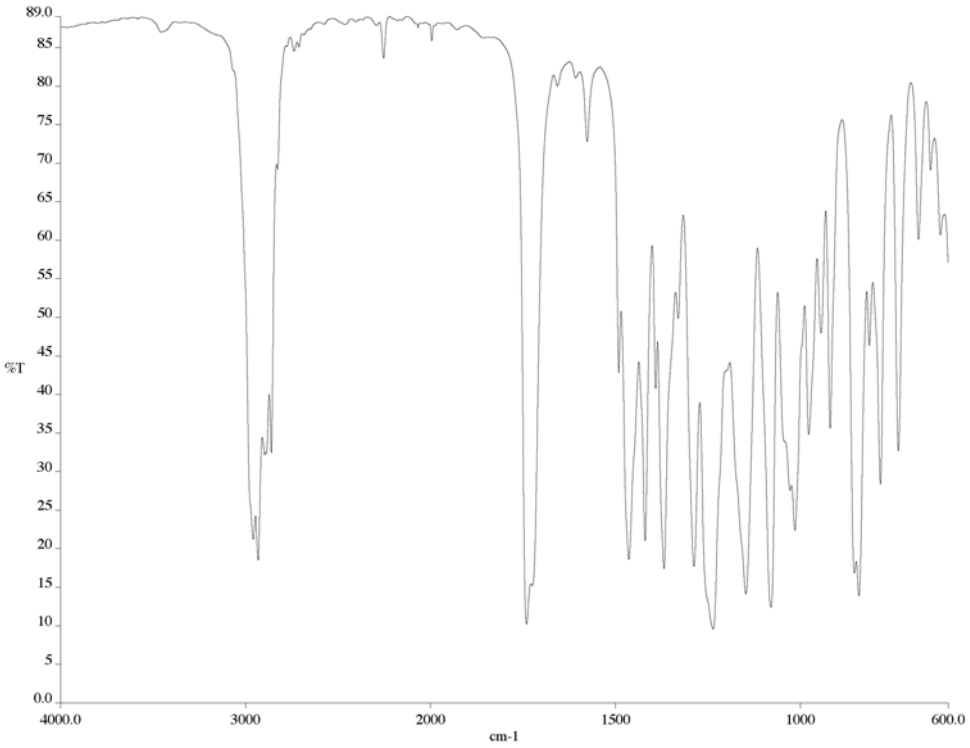

Figure A2.47 IR of compound **162** (NaCl/film)

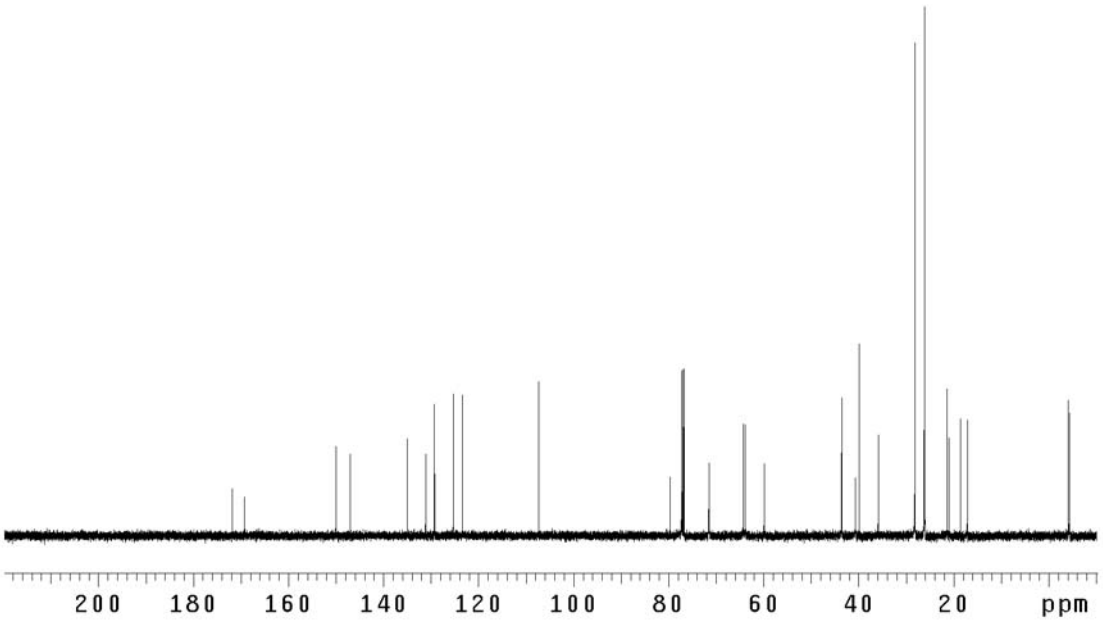

Figure A2.48 ^{13}C NMR of compound **162** (125 MHz, $CDCl_3$)

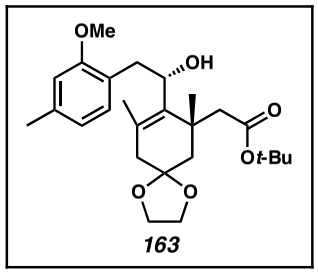

163

Figure A2.49 ^{1}H NMR of compound **163** (300 MHz, $CDCl_3$)

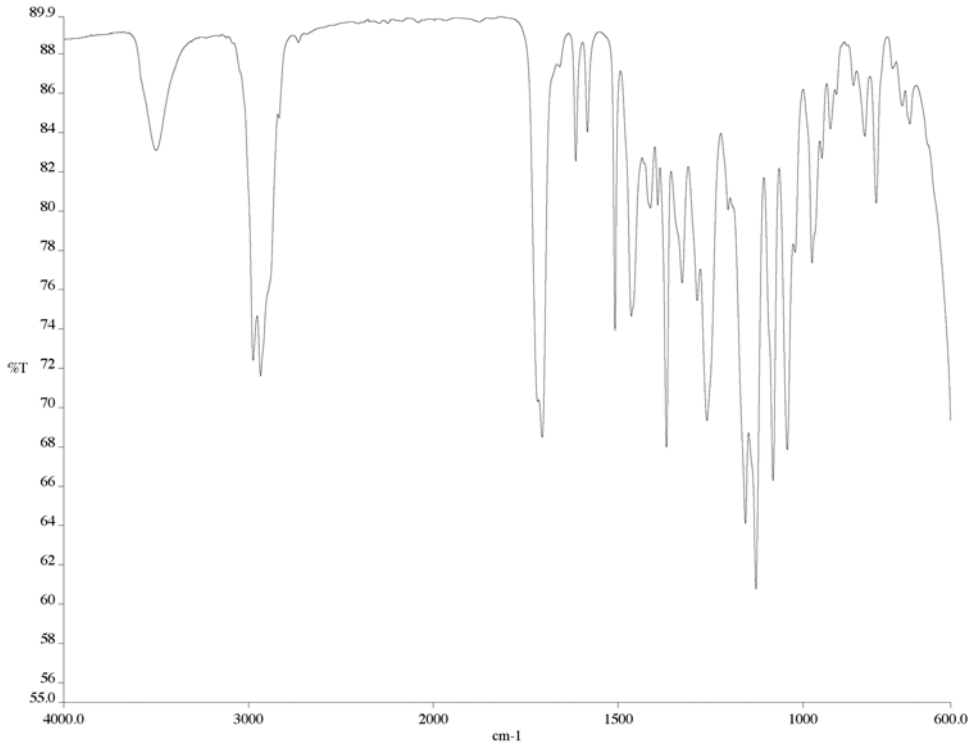

Figure A2.50 IR of compound **163** (NaCl/film)

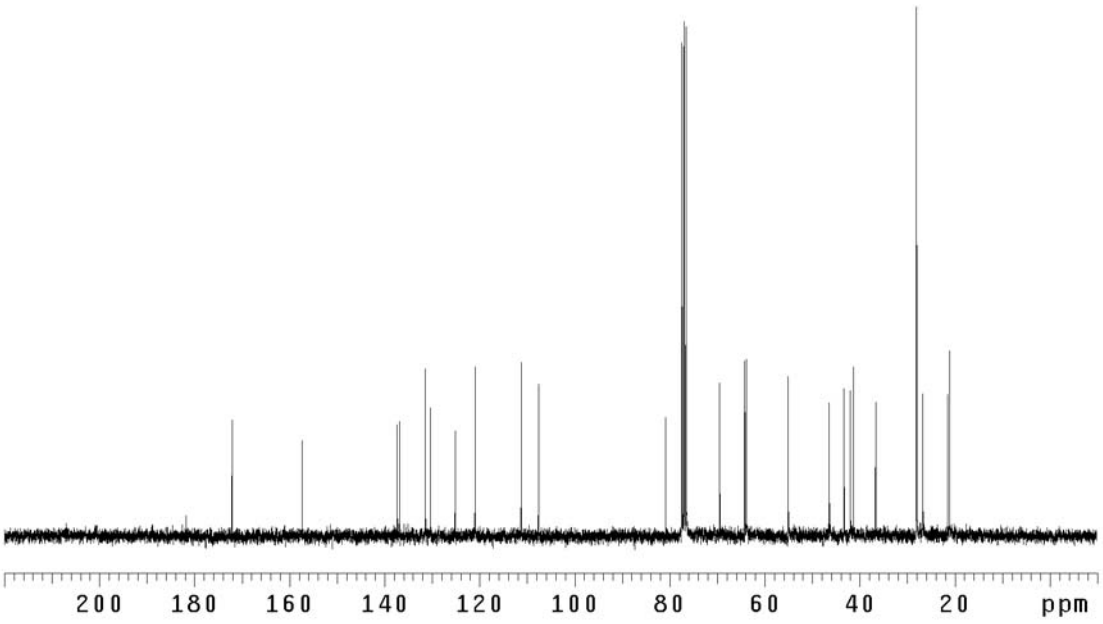

Figure A2.51 ^{13}C NMR of compound **163** (75 MHz, $CDCl_3$)

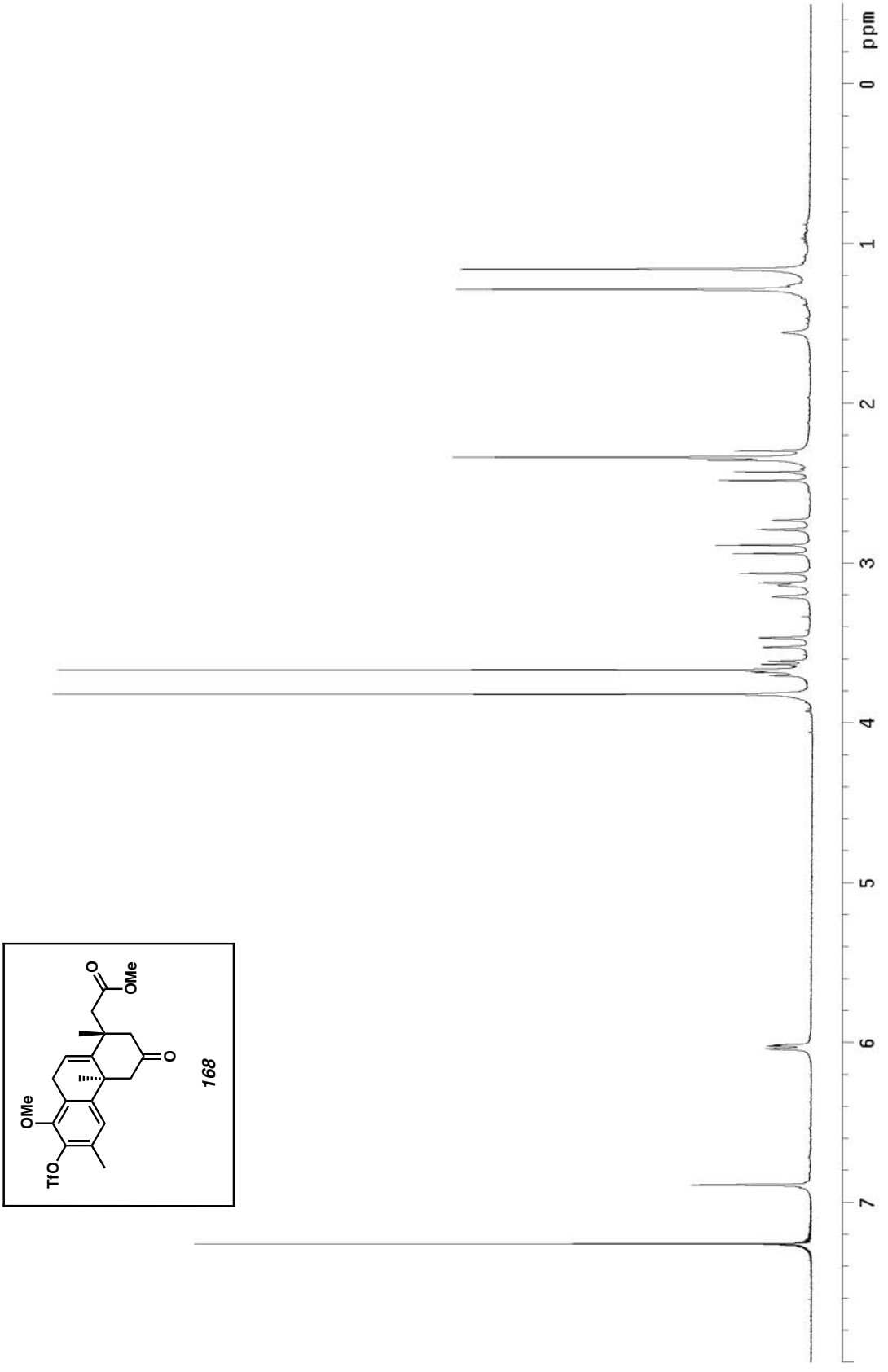

Figure A2.52 ^{1}H NMR of compound **168** (300 MHz, $CDCl_3$)

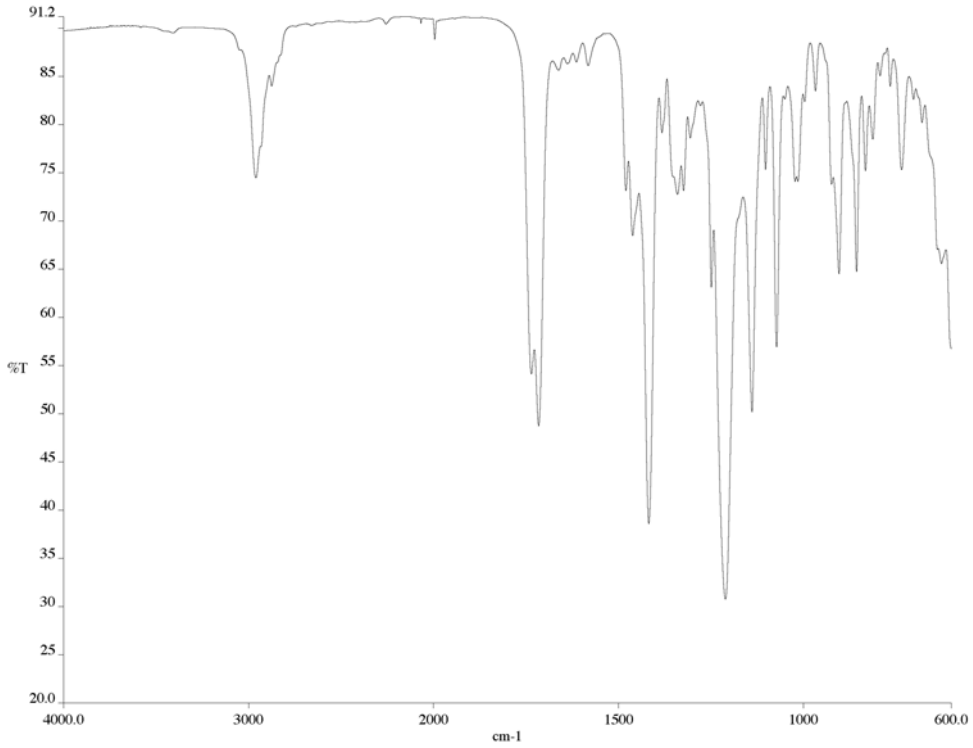

Figure A2.53 IR of compound **168** (NaCl/film)

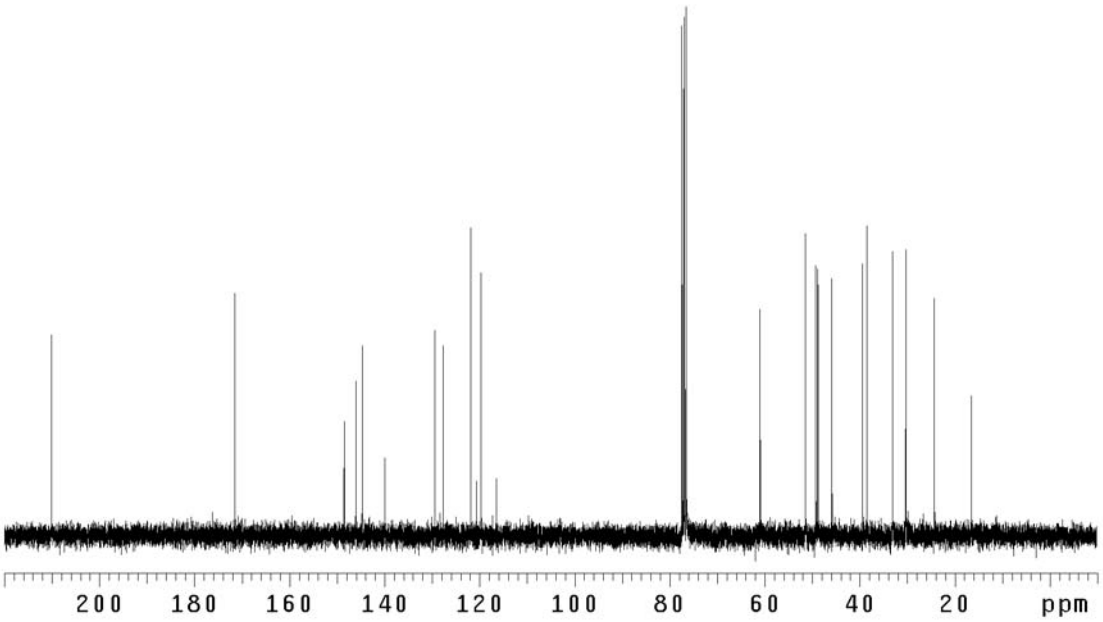

Figure A2.54 ^{13}C NMR of compound **168** (75 MHz, $CDCl_3$)

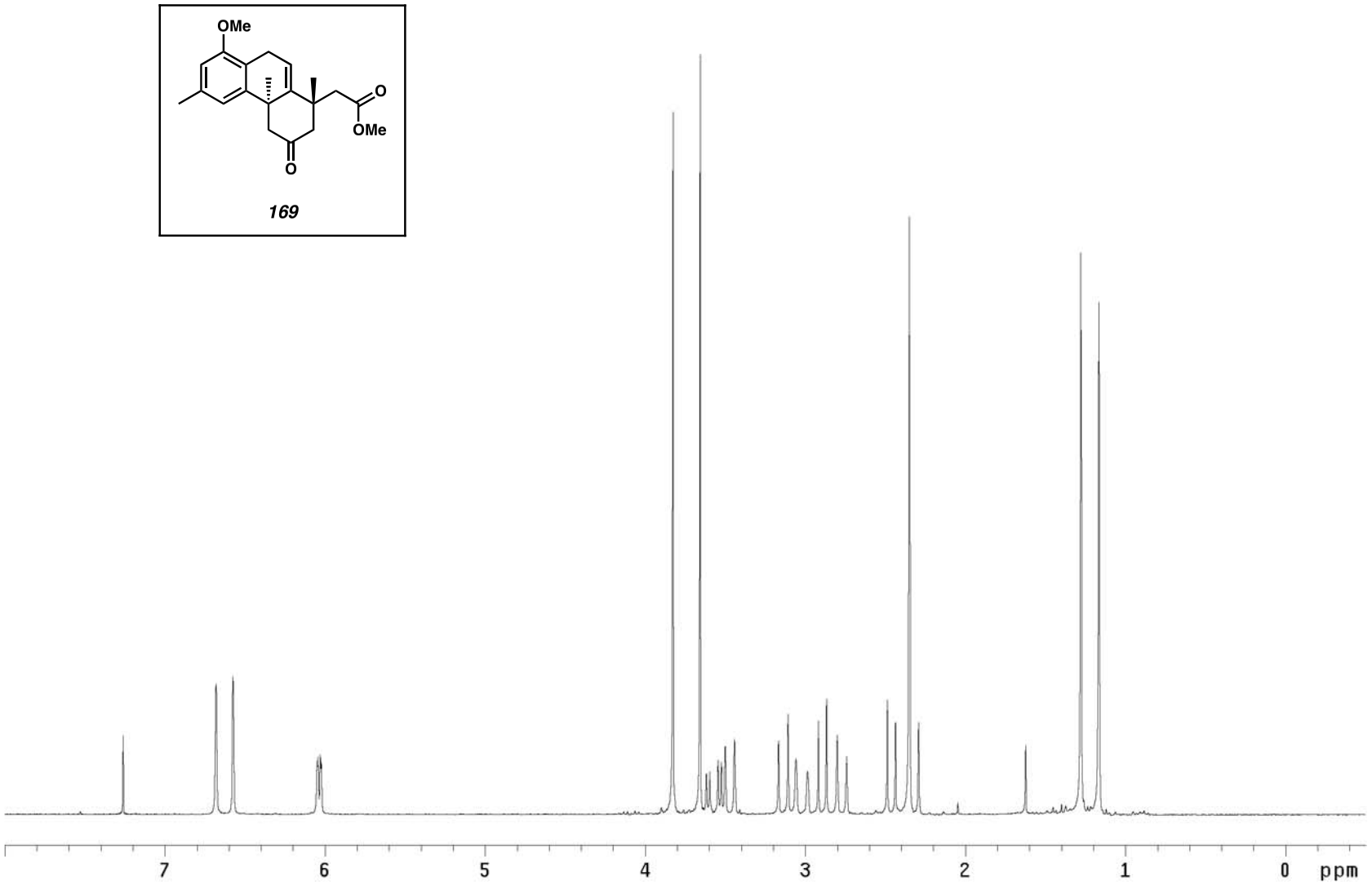

Figure A2.55 ^{1}H NMR of compound **169** (300 MHz, $CDCl_3$)

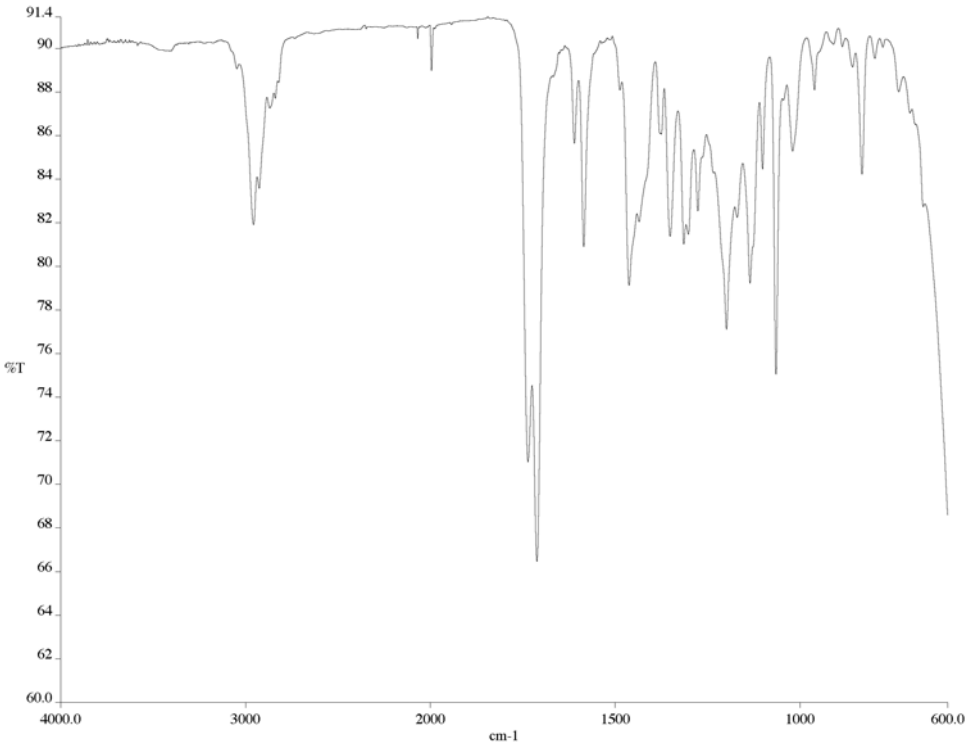

Figure A2.56 IR of compound **169** (NaCl/film)

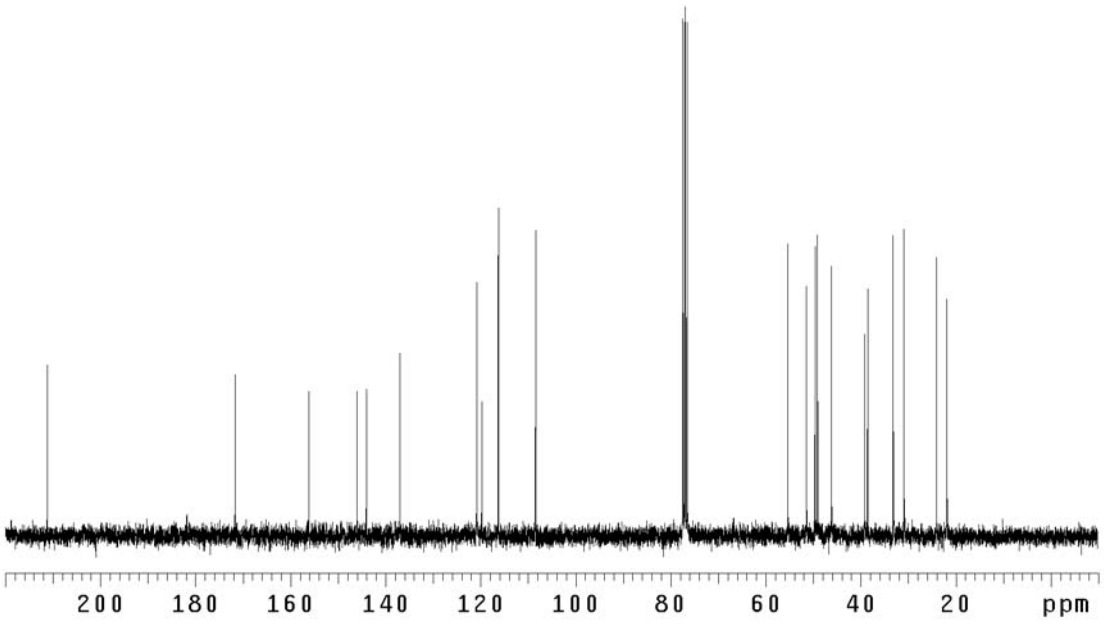

Figure A2.57 ^{13}C NMR of compound **169** (75 MHz, $CDCl_3$)

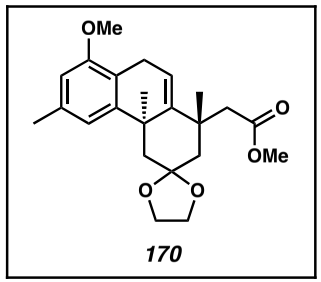

170

Figure A2.58 ^{1}H NMR of compound **170** (300 MHz, $CDCl_3$)

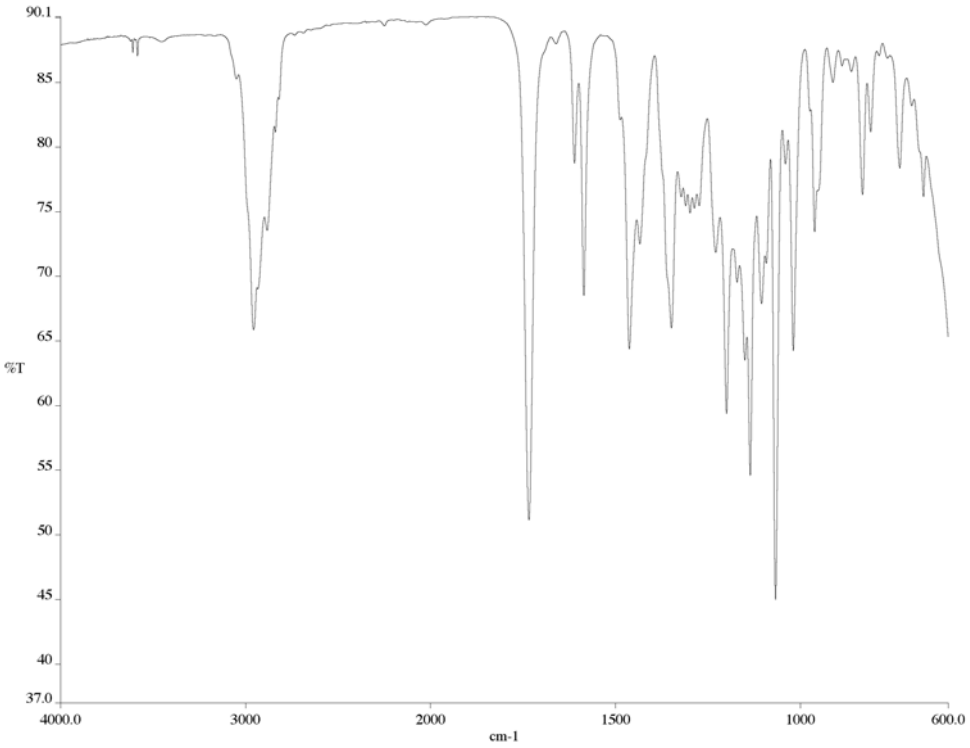

Figure A2.59 IR of compound **170** (NaCl/film)

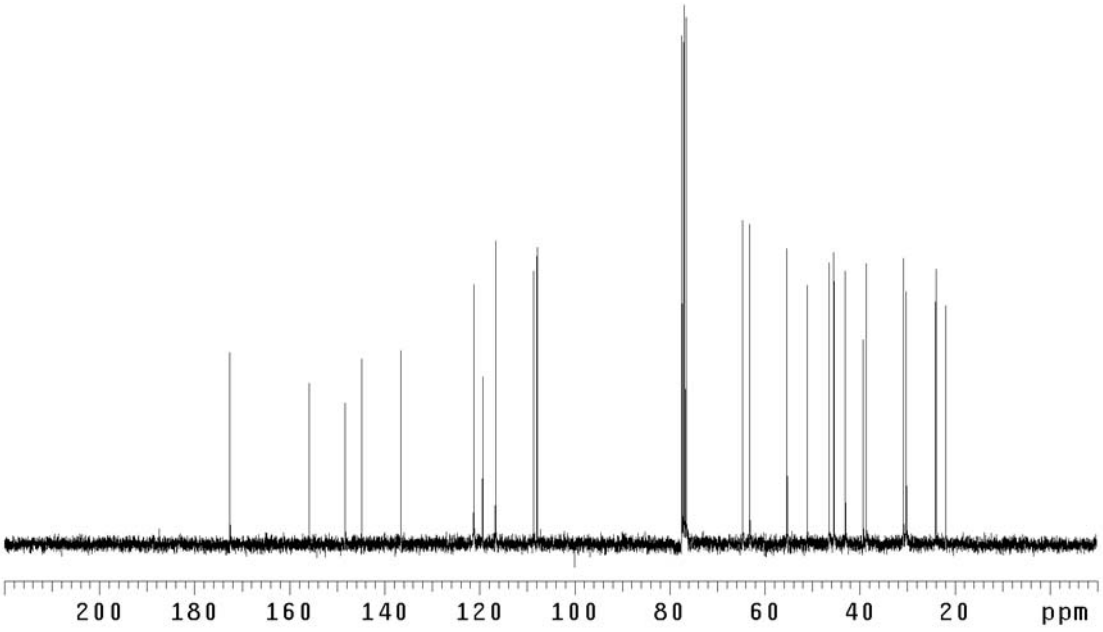

Figure A2.60 ^{13}C NMR of compound **170** (75 MHz, $CDCl_3$)

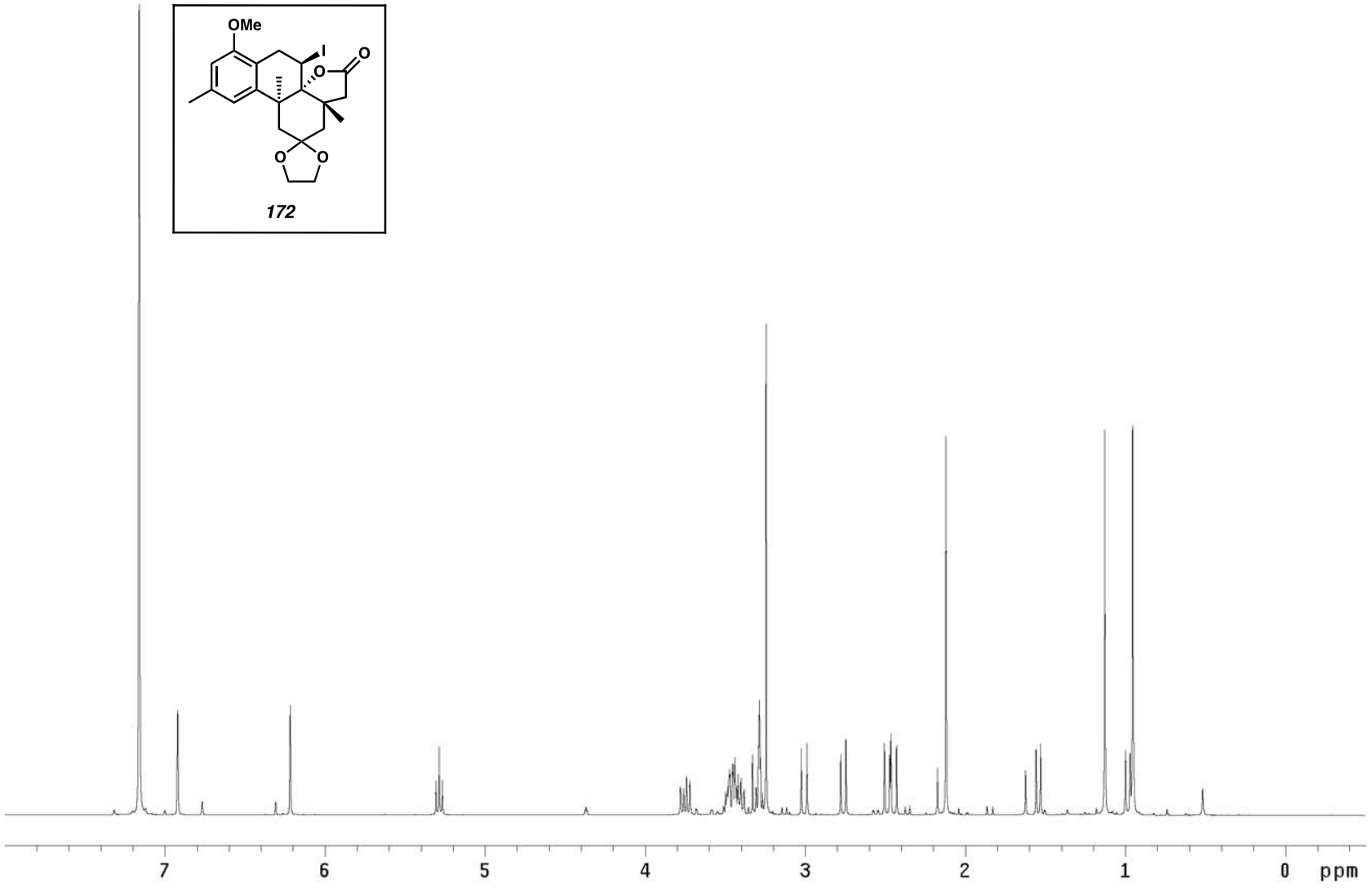

Figure A2.61 ^{1}H NMR of compound **172** (500 MHz, C_6D_6)

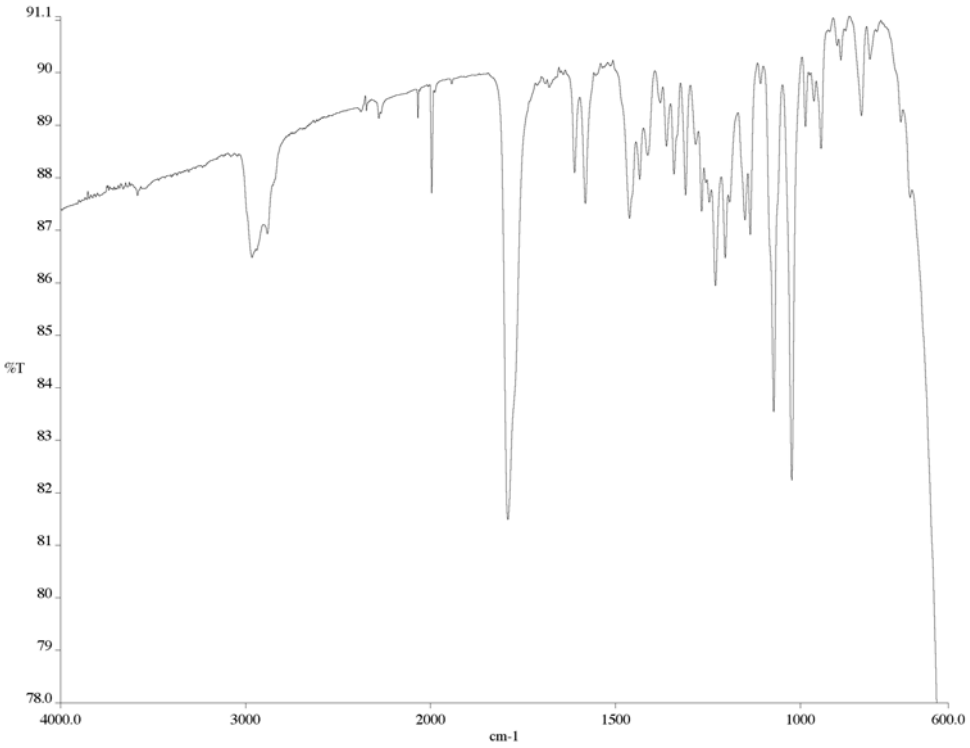

Figure A2.62 IR of compound **172** (NaCl/film)

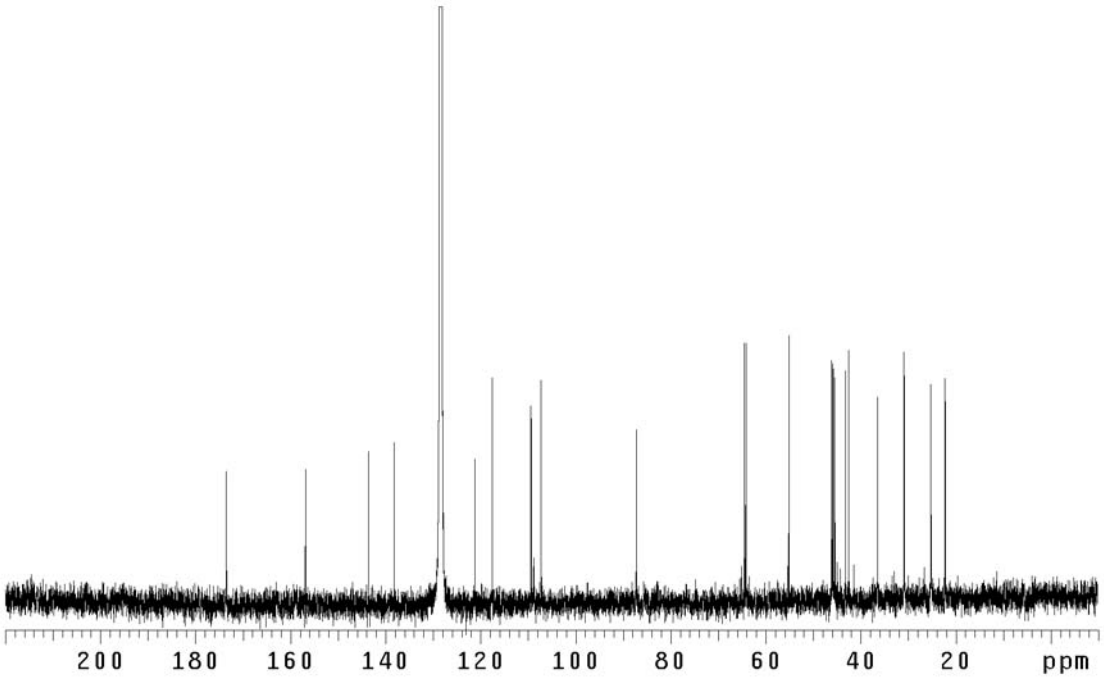

Figure A2.63 ^{13}C NMR of compound **172** (125 MHz, C_6D_6)

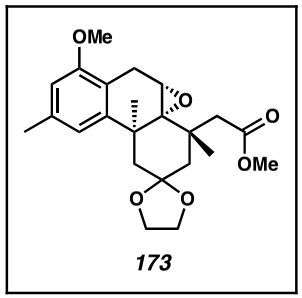

Figure A2.64 ^{1}H NMR of compound **173** (500 MHz, $CDCl_3$)

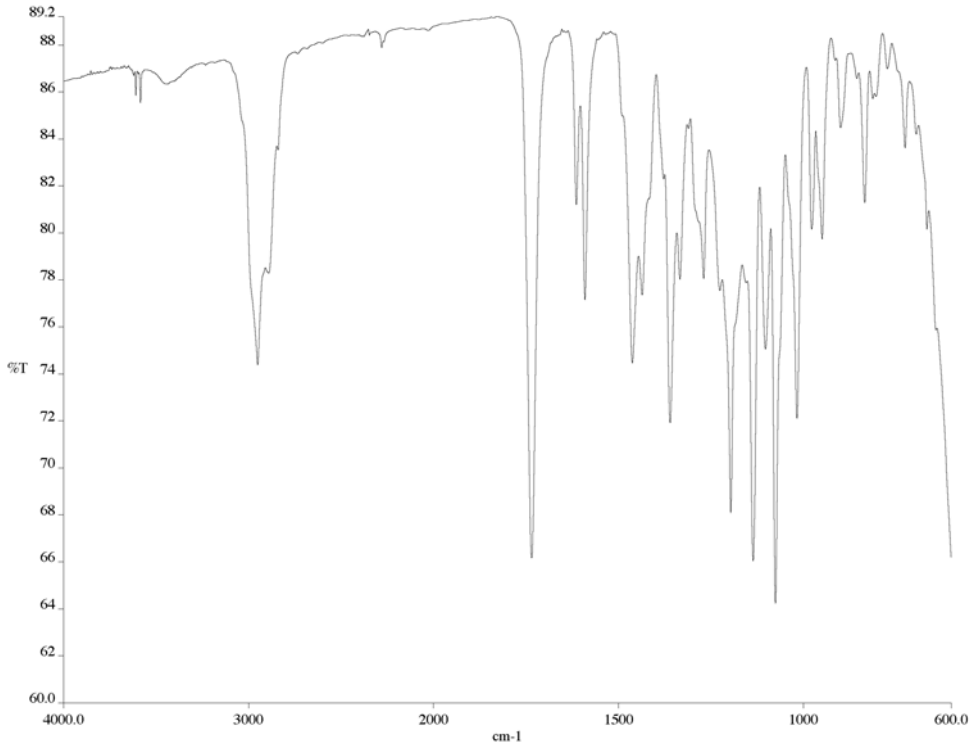

Figure A2.65 IR of compound **173** (NaCl/film)

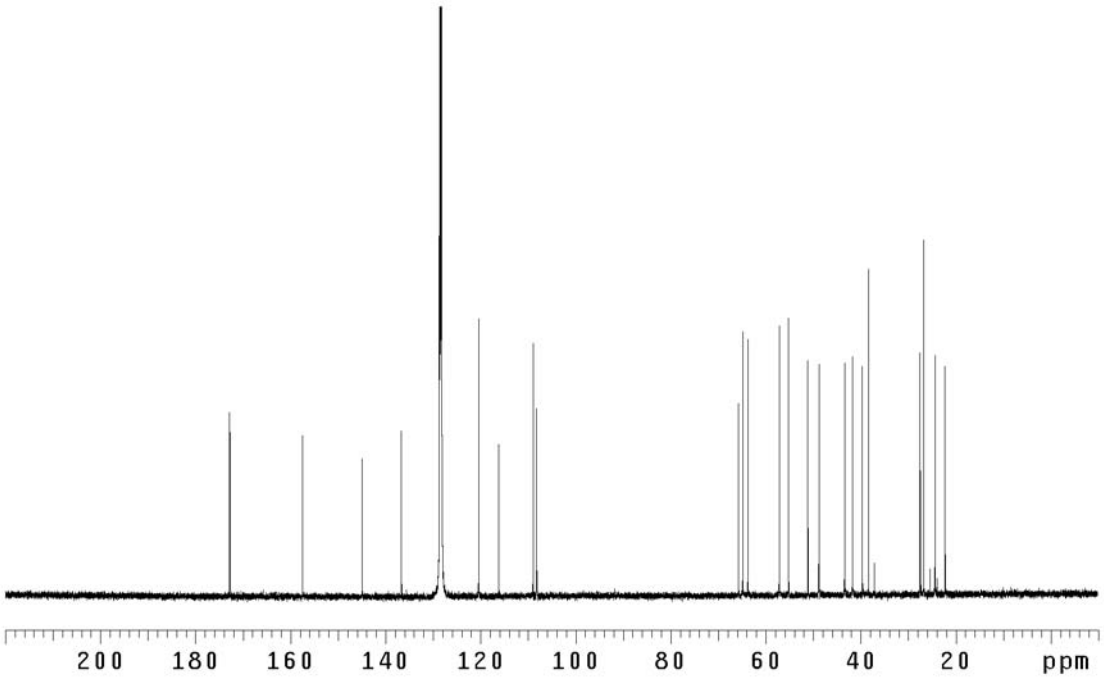

Figure A2.66 ^{13}C NMR of compound **173** (125 MHz, C_6D_6)

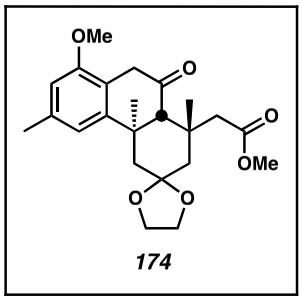

Figure A2.67 ^{1}H NMR of compound **174** (500 MHz, $CDCl_3$)

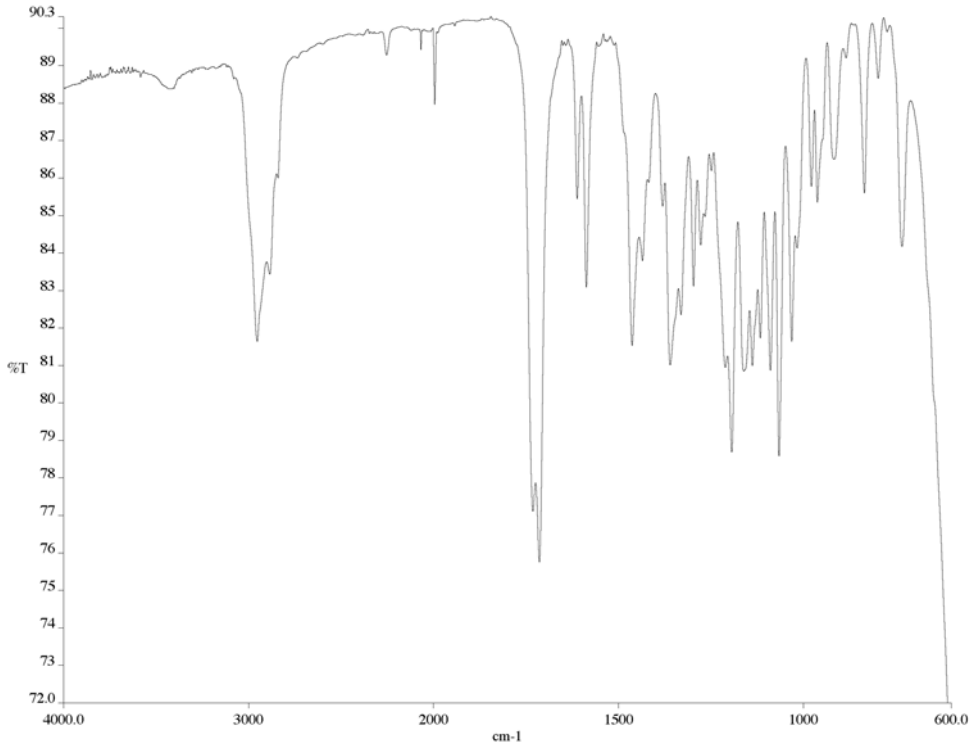

Figure A2.68 IR of compound **174** (NaCl/film)

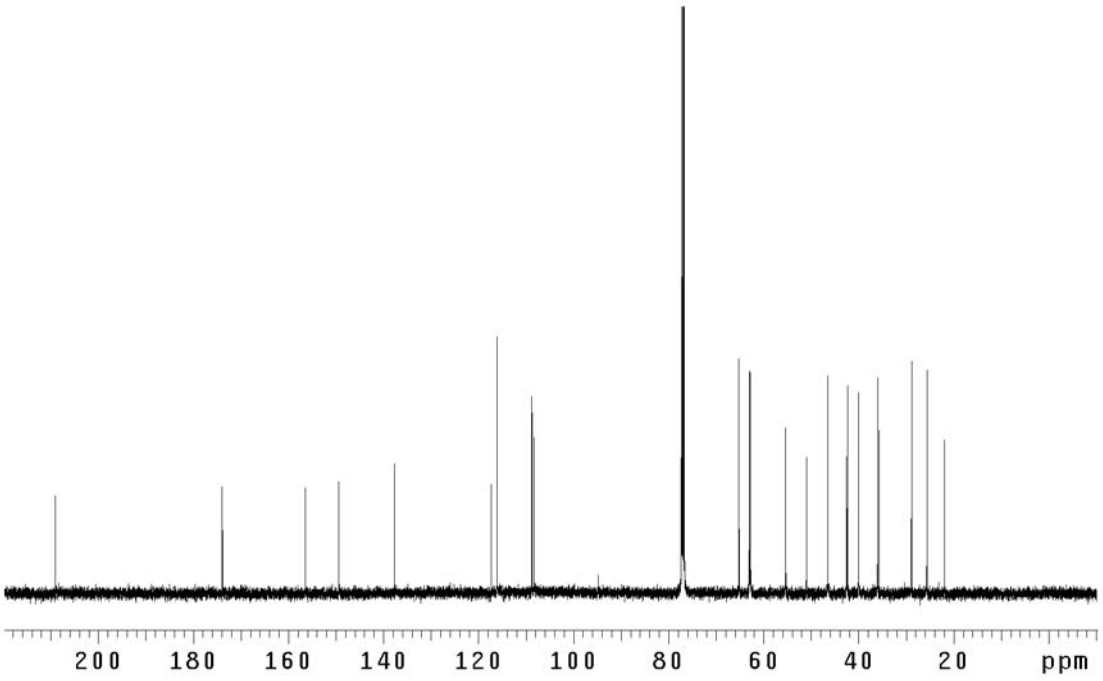

Figure A2.69 ^{13}C NMR of compound **174** (125 MHz, $CDCl_3$)

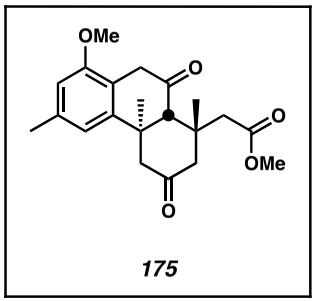

175

Figure A2.70 ^{1}H NMR of compound **175** (500 MHz, $CDCl_3$)

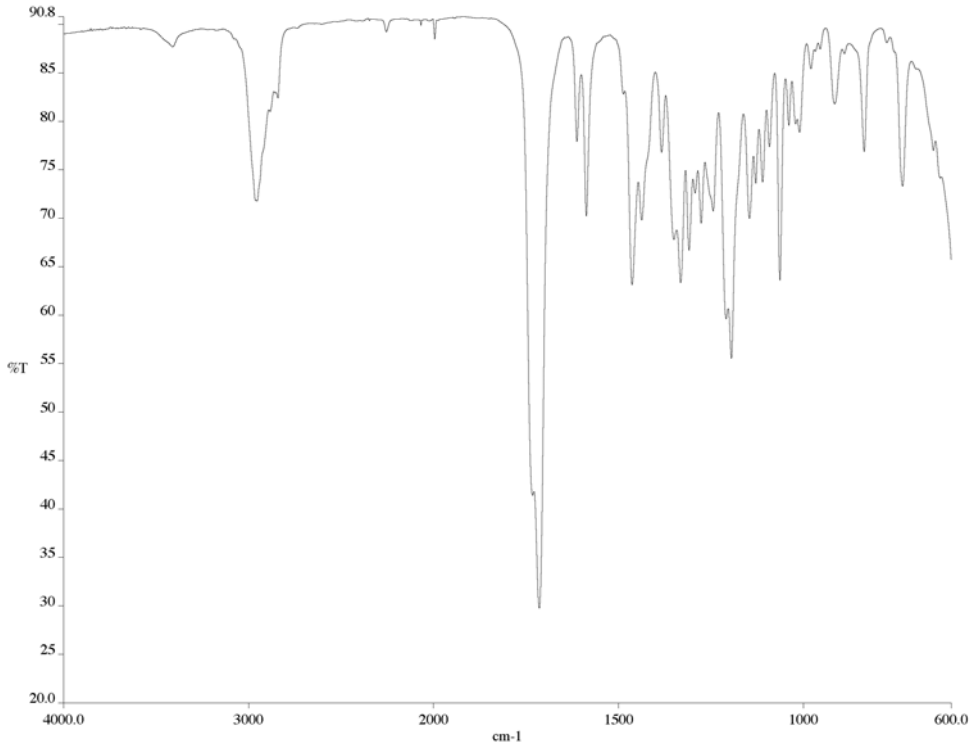

Figure A2.71 IR of compound **175** (NaCl/film)

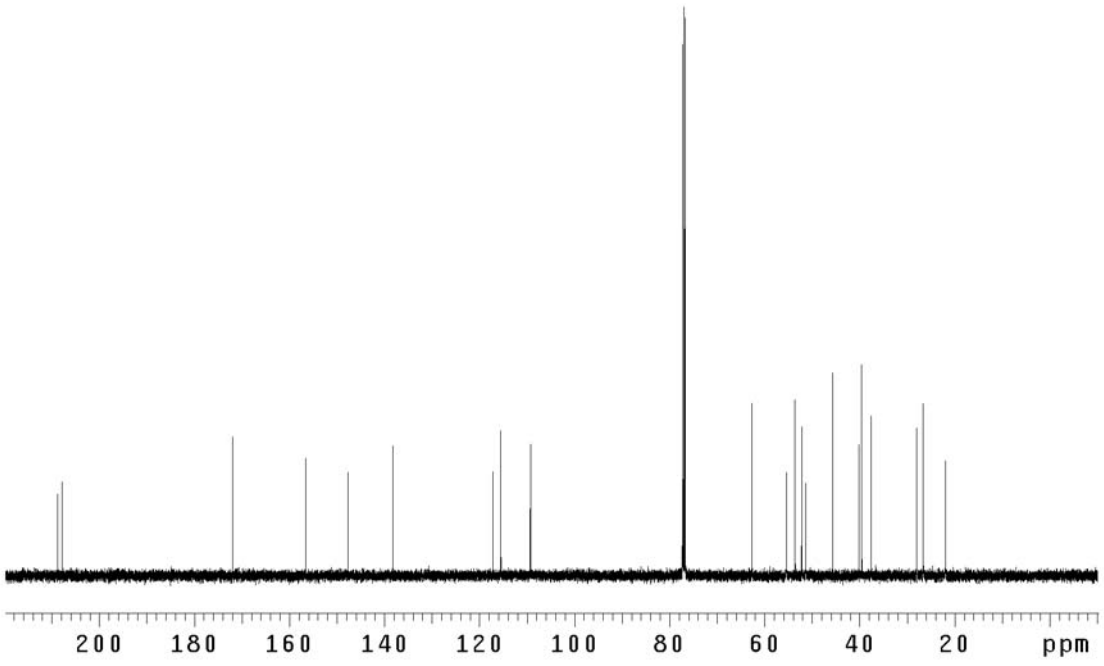

Figure A2.72 ^{13}C NMR of compound **175** (125 MHz, $CDCl_3$)

APPENDIX THREE

X-Ray Crystallographic Data Relevant to Chapter Two

CALIFORNIA INSTITUTE OF TECHNOLOGY

BECKMAN INSTITUTE

X-RAY CRYSTALLOGRAPHY LABORATORY

Crystal Structure Analysis of:

Ketone viii (DCB03)

(CCDC 172324)

Contents

Figure A3.1 Representation of Ketone **viii**

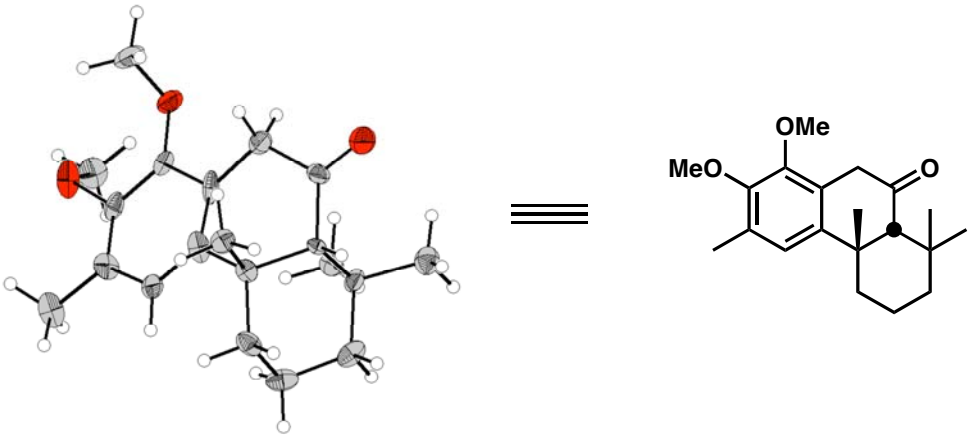

Table 1. Crystal data and structure refinement for DCB03 (CCDC 172324).

Empirical formula	$C_{20}H_{28}O_3$
Formula weight	316.42
Crystallization Solvent	Hexanes
Crystal Habit	Block
Crystal size	0.30 x 0.22 x 0.19 mm^3
Crystal color	Colorless

Data Collection

Preliminary Photos	Rotation
Type of diffractometer	CCD area detector
Wavelength	0.71073 Å MoKα
Data Collection Temperature	98(2) K
θ range for 9714 reflections used in lattice determination	2.60 to 28.29°
Unit cell dimensions	a = 7.900(3) Å b = 8.104(5) Å β= 97.212(6)° c = 13.664(4) Å
Volume	867.8(7) $Å^3$
Z	2
Crystal system	Monoclinic
Space group	$P2_1$
Density (calculated)	1.211 Mg/m^3
F(000)	344
Data collection program	Bruker SMART
θ range for data collection	2.93 to 28.38°
Completeness to θ = 28.38°	29.9 %
Index ranges	$-9 \le h \le 9$, $-10 \le k \le 10$, $-18 \le l \le 17$
Data collection scan type	ω scans at 7 ϕ settings
Data reduction program	Bruker SAINT v6.2
Reflections collected	4065
Independent reflections	4065 [R_{int}= 0.0000]
Absorption coefficient	0.080 mm^{-1}
Absorption correction	None
Max. and min. transmission	0.9854 and 0.9768

Table 1 (cont.)

Structure solution and Refinement

Structure solution program	SHELXS-97 (Sheldrick, 1990)
Primary solution method	Direct methods
Secondary solution method	Difference Fourier map
Hydrogen placement	Geometric positions
Structure refinement program	SHELXL-97 (Sheldrick, 1997)
Refinement method	Full matrix least-squares on F^2
Data / restraints / parameters	4065 / 1 / 215
Treatment of hydrogen atoms	Riding
Goodness-of-fit on F^2	0.983
Final R indices [$I>2\sigma(I)$, 2775 reflections]	R1 = 0.0513, *w*R2 = 0.0823
R indices (all data)	R1 = 0.0790, *w*R2 = 0.0900
Type of weighting scheme used	Sigma
Weighting scheme used	$w=1/\sigma^2(Fo^2)$
Max shift/error	0.001
Average shift/error	0.000
Absolute structure parameter	2(3)
Largest diff. peak and hole	0.110 and -0.108 e.Å^{-3}

Special Refinement Details

The crystals are twinned. The twinning is non-merohedral and therefore (since the reciprocal lattices don't overlap exactly) the data required special handling. An orientation matrix was identified for each twin and each matrix was used to integrate the data for each twin component. The two resulting data sets were merged into one set that contained reflections unique to each twin component and reflections exactly overlapping between the two twin components. For component one there were 3057 exact overlaps, 14021 partial overlaps and 538 unique, for component two the corresponding numbers are 3060, 14136 and 505. The data set used for least squares refinement contained only 696 reflections after merging equivalents from both twin components into a single reflection..

Refinement of F^2 against ALL reflections. The weighted R-factor (*w*R) and goodness of fit (S) are based on F^2, conventional R-factors (R) are based on F, with F set to zero for negative F^2. The threshold expression of $F^2 > 2\sigma(F^2)$ is used only for calculating R-factors(gt) etc. and is not relevant to the choice of reflections for refinement. R-factors based on F^2 are statistically about twice as large as those based on F, and R-factors based on ALL data will be even larger.

All esds (except the esd in the dihedral angle between two l.s. planes) are estimated using the full covariance matrix. The cell esds are taken into account individually in the estimation of esds in distances, angles and torsion angles; correlations between esds in cell parameters are only used when they are defined by crystal symmetry. An approximate (isotropic) treatment of cell esds is used for estimating esds involving l.s. planes.

Table 2. Atomic coordinates (x 10^4) and equivalent isotropic displacement parameters ($Å^2$x 10^3) for DCB03 (CCDC 172324). U(eq) is defined as the trace of the orthogonalized U^{ij} tensor.

	x	y	z	U_{eq}
O(1)	5945(12)	3813(7)	2029(5)	33(1)
O(2)	3847(9)	5388(4)	564(3)	34(1)
O(4)	4869(8)	-122(3)	4754(2)	37(1)
C(1)	4219(13)	3657(8)	2004(6)	16(2)
C(2)	3094(15)	4363(9)	1223(8)	24(2)
C(3)	1350(19)	4257(9)	1208(7)	26(2)
C(4)	745(12)	3298(5)	1930(5)	27(1)
C(5)	1789(17)	2637(11)	2680(7)	23(2)
C(6)	1034(11)	1640(7)	3497(5)	20(1)
C(7)	1112(10)	2803(4)	4392(3)	27(1)
C(8)	-797(10)	1109(7)	3252(4)	27(1)
C(9)	-1031(8)	-266(5)	2461(3)	30(1)
C(10)	64(12)	-1751(6)	2817(5)	29(2)
C(11)	1952(10)	-1365(6)	3057(4)	25(1)
C(12)	2789(11)	-2888(3)	3597(3)	31(1)
C(13)	2752(8)	-1097(5)	2147(3)	24(1)
C(14)	2119(9)	111(5)	3821(4)	18(1)
C(15)	3981(10)	547(6)	4091(4)	24(1)
C(16)	4684(10)	1943(5)	3536(5)	28(1)
C(17)	3524(18)	2647(10)	2719(7)	26(3)
C(18)	6548(9)	5292(5)	2521(5)	41(1)
C(19)	4648(11)	4484(7)	-129(3)	35(1)
C(20)	190(13)	5086(7)	378(4)	34(2)

Table 3. Bond lengths [Å] and angles [°] for DCB03 (CCDC 172324).

O(1)-C(1)	1.365(12)	C(20)-H(20A)	0.9800
O(1)-C(18)	1.426(7)	C(20)-H(20B)	0.9800
O(2)-C(2)	1.410(12)	C(20)-H(20C)	0.9800
O(2)-C(19)	1.409(8)		
O(4)-C(15)	1.203(7)	C(1)-O(1)-C(18)	111.3(7)
C(1)-C(2)	1.421(16)	C(2)-O(2)-C(19)	112.6(5)
C(1)-C(17)	1.435(14)	O(1)-C(1)-C(2)	120.7(9)
C(2)-C(3)	1.378(17)	O(1)-C(1)-C(17)	120.1(10)
C(3)-C(4)	1.387(13)	C(2)-C(1)-C(17)	119.0(10)
C(3)-C(20)	1.522(15)	C(3)-C(2)-O(2)	121.9(12)
C(4)-C(5)	1.343(15)	C(3)-C(2)-C(1)	121.1(11)
C(4)-H(4)	0.9500	O(2)-C(2)-C(1)	116.3(10)
C(5)-C(17)	1.365(19)	C(2)-C(3)-C(4)	117.2(12)
C(5)-C(6)	1.557(11)	C(2)-C(3)-C(20)	119.4(11)
C(6)-C(8)	1.506(11)	C(4)-C(3)-C(20)	123.3(12)
C(6)-C(7)	1.539(6)	C(5)-C(4)-C(3)	122.2(11)
C(6)-C(14)	1.539(9)	C(5)-C(4)-H(4)	118.9
C(7)-H(7A)	0.9800	C(3)-C(4)-H(4)	118.9
C(7)-H(7B)	0.9800	C(4)-C(5)-C(17)	123.0(11)
C(7)-H(7C)	0.9800	C(4)-C(5)-C(6)	120.0(10)
C(8)-C(9)	1.547(6)	C(17)-C(5)-C(6)	116.7(12)
C(8)-H(8A)	0.9900	C(8)-C(6)-C(7)	107.1(6)
C(8)-H(8B)	0.9900	C(8)-C(6)-C(14)	108.6(5)
C(9)-C(10)	1.525(9)	C(7)-C(6)-C(14)	107.4(5)
C(9)-H(9A)	0.9900	C(8)-C(6)-C(5)	115.6(8)
C(9)-H(9B)	0.9900	C(7)-C(6)-C(5)	105.7(5)
C(10)-C(11)	1.520(10)	C(14)-C(6)-C(5)	111.9(7)
C(10)-H(10A)	0.9900	C(6)-C(7)-H(7A)	109.5
C(10)-H(10B)	0.9900	C(6)-C(7)-H(7B)	109.5
C(11)-C(13)	1.479(8)	H(7A)-C(7)-H(7B)	109.5
C(11)-C(12)	1.544(7)	C(6)-C(7)-H(7C)	109.5
C(11)-C(14)	1.582(6)	H(7A)-C(7)-H(7C)	109.5
C(12)-H(12A)	0.9800	H(7B)-C(7)-H(7C)	109.5
C(12)-H(12B)	0.9800	C(6)-C(8)-C(9)	112.9(6)
C(12)-H(12C)	0.9800	C(6)-C(8)-H(8A)	109.0
C(13)-H(13A)	0.9800	C(9)-C(8)-H(8A)	109.0
C(13)-H(13B)	0.9800	C(6)-C(8)-H(8B)	109.0
C(13)-H(13C)	0.9800	C(9)-C(8)-H(8B)	109.0
C(14)-C(15)	1.513(9)	H(8A)-C(8)-H(8B)	107.8
C(14)-H(14)	1.0000	C(10)-C(9)-C(8)	109.4(5)
C(15)-C(16)	1.506(8)	C(10)-C(9)-H(9A)	109.8
C(16)-C(17)	1.468(14)	C(8)-C(9)-H(9A)	109.8
C(16)-H(16A)	0.9900	C(10)-C(9)-H(9B)	109.8
C(16)-H(16B)	0.9900	C(8)-C(9)-H(9B)	109.8
C(18)-H(18A)	0.9800	H(9A)-C(9)-H(9B)	108.2
C(18)-H(18B)	0.9800	C(11)-C(10)-C(9)	114.1(5)
C(18)-H(18C)	0.9800	C(11)-C(10)-H(10A)	108.7
C(19)-H(19A)	0.9800	C(9)-C(10)-H(10A)	108.7
C(19)-H(19B)	0.9800	C(11)-C(10)-H(10B)	108.7
C(19)-H(19C)	0.9800	C(9)-C(10)-H(10B)	108.7

H(10A)-C(10)-H(10B)	107.6	H(20B)-C(20)-H(20C)	109.5
C(13)-C(11)-C(10)	111.1(6)		
C(13)-C(11)-C(12)	108.5(5)		
C(10)-C(11)-C(12)	106.8(6)		
C(13)-C(11)-C(14)	115.8(5)		
C(10)-C(11)-C(14)	107.2(6)		
C(12)-C(11)-C(14)	107.1(4)		
C(11)-C(12)-H(12A)	109.5		
C(11)-C(12)-H(12B)	109.5		
H(12A)-C(12)-H(12B)	109.5		
C(11)-C(12)-H(12C)	109.5		
H(12A)-C(12)-H(12C)	109.5		
H(12B)-C(12)-H(12C)	109.5		
C(11)-C(13)-H(13A)	109.5		
C(11)-C(13)-H(13B)	109.5		
H(13A)-C(13)-H(13B)	109.5		
C(11)-C(13)-H(13C)	109.5		
H(13A)-C(13)-H(13C)	109.5		
H(13B)-C(13)-H(13C)	109.5		
C(15)-C(14)-C(6)	111.8(5)		
C(15)-C(14)-C(11)	109.6(5)		
C(6)-C(14)-C(11)	115.0(5)		
C(15)-C(14)-H(14)	106.7		
C(6)-C(14)-H(14)	106.7		
C(11)-C(14)-H(14)	106.7		
O(4)-C(15)-C(16)	120.0(7)		
O(4)-C(15)-C(14)	122.4(7)		
C(16)-C(15)-C(14)	117.5(6)		
C(17)-C(16)-C(15)	116.2(8)		
C(17)-C(16)-H(16A)	108.2		
C(15)-C(16)-H(16A)	108.2		
C(17)-C(16)-H(16B)	108.2		
C(15)-C(16)-H(16B)	108.2		
H(16A)-C(16)-H(16B)	107.4		
C(5)-C(17)-C(1)	116.4(13)		
C(5)-C(17)-C(16)	123.7(11)		
C(1)-C(17)-C(16)	118.9(11)		
O(1)-C(18)-H(18A)	109.5		
O(1)-C(18)-H(18B)	109.5		
H(18A)-C(18)-H(18B)	109.5		
O(1)-C(18)-H(18C)	109.5		
H(18A)-C(18)-H(18C)	109.5		
H(18B)-C(18)-H(18C)	109.5		
O(2)-C(19)-H(19A)	109.5		
O(2)-C(19)-H(19B)	109.5		
H(19A)-C(19)-H(19B)	109.5		
O(2)-C(19)-H(19C)	109.5		
H(19A)-C(19)-H(19C)	109.5		
H(19B)-C(19)-H(19C)	109.5		
C(3)-C(20)-H(20A)	109.5		
C(3)-C(20)-H(20B)	109.5		
H(20A)-C(20)-H(20B)	109.5		
C(3)-C(20)-H(20C)	109.5		
H(20A)-C(20)-H(20C)	109.5		

Table 4. Anisotropic displacement parameters ($Å^2 x 10^4$) for DCB03 (CCDC 172324). The anisotropic displacement factor exponent takes the form: $-2\pi^2 [h^2 a^{*2} U^{11} + ... + 2 h k a^* b^* U^{12}]$

	U^{11}	U^{22}	U^{33}	U^{23}	U^{13}	U^{12}
O(1)	230(30)	240(20)	520(30)	-2(18)	90(30)	-50(30)
O(2)	500(40)	275(16)	307(19)	80(13)	280(40)	130(30)
O(4)	370(30)	356(13)	372(15)	109(13)	-10(30)	-60(30)
C(1)	220(40)	150(20)	150(30)	-4(19)	170(30)	-20(30)
C(2)	310(50)	120(20)	330(40)	-10(20)	180(40)	20(30)
C(3)	350(50)	330(30)	70(30)	20(20)	-10(40)	10(40)
C(4)	230(30)	147(19)	420(30)	-56(19)	40(40)	40(30)
C(5)	350(50)	260(20)	130(40)	20(20)	170(40)	130(40)
C(6)	190(30)	220(30)	180(30)	-20(20)	70(40)	50(30)
C(7)	330(30)	224(18)	240(20)	-92(16)	-10(30)	-10(30)
C(8)	180(30)	360(30)	270(30)	60(20)	60(30)	60(30)
C(9)	240(30)	430(20)	250(20)	-58(18)	60(30)	-90(30)
C(10)	300(40)	320(30)	280(30)	40(20)	170(40)	-120(40)
C(11)	220(40)	130(20)	410(30)	-11(18)	60(40)	-10(30)
C(12)	380(40)	252(19)	300(20)	-23(15)	30(40)	10(30)
C(13)	240(30)	228(19)	236(18)	-72(15)	10(30)	30(30)
C(14)	150(30)	180(20)	190(30)	17(17)	-60(30)	0(30)
C(15)	200(30)	210(20)	280(30)	-62(19)	-60(40)	30(30)
C(16)	170(30)	190(20)	490(30)	-20(20)	100(40)	20(30)
C(17)	430(60)	110(20)	280(50)	0(20)	160(50)	110(40)
C(18)	240(30)	266(19)	720(30)	-120(20)	100(40)	-90(30)
C(19)	380(40)	400(20)	290(20)	24(16)	110(40)	0(40)
C(20)	440(50)	370(30)	220(30)	40(20)	140(40)	150(40)

Table 5. Hydrogen coordinates (x 10^4) and isotropic displacement parameters ($Å^2$x 10^3) for DCB03 (CCDC 172324).

	x	y	z	U_{iso}
H(4)	-447	3103	1893	32
H(7A)	796	2194	4961	40
H(7B)	316	3722	4237	40
H(7C)	2274	3235	4547	40
H(8A)	-1494	2076	3011	32
H(8B)	-1224	706	3860	32
H(9A)	-2246	-596	2340	36
H(9B)	-688	149	1833	36
H(10A)	-357	-2206	3414	35
H(10B)	-80	-2615	2301	35
H(12A)	2521	-3874	3193	46
H(12B)	2350	-3021	4232	46
H(12C)	4029	-2734	3710	46
H(13A)	2606	-2088	1734	36
H(13B)	3971	-872	2322	36
H(13C)	2207	-156	1784	36
H(14)	1703	-311	4436	21
H(16A)	5041	2838	4011	33
H(16B)	5719	1545	3270	33
H(18A)	6205	5309	3186	61
H(18B)	6058	6248	2149	61
H(18C)	7795	5335	2566	61
H(19A)	3814	3748	-498	53
H(19B)	5580	3827	216	53
H(19C)	5106	5247	-586	53
H(20A)	624	6194	264	51
H(20B)	-967	5170	562	51
H(20C)	167	4430	-226	51

CALIFORNIA INSTITUTE OF TECHNOLOGY

BECKMAN INSTITUTE

X-RAY CRYSTALLOGRAPHY LABORATORY

Crystal Structure Analysis of:

Lactone 156 (DCB06)

(CCDC 175859)

Contents:

Figure A3.2 Representation of Lactone **156**

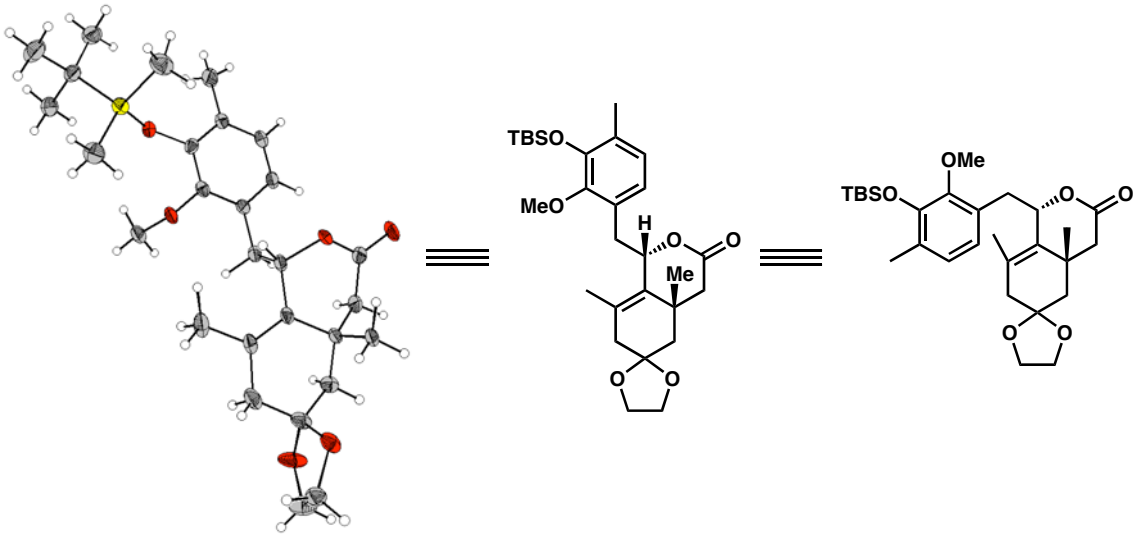

Table 1. Crystal data and structure refinement for DCB06_(CCDC_175859).

Empirical formula	$C_{28}H_{42}O_6Si$
Formula weight	502.71
Crystallization Solvent	Hexanes
Crystal Habit	Block
Crystal size	0.33 x 0.17 x 0.14 mm^3
Crystal color	Colorless

Data Collection

Type of diffractometer	Bruker P4
Wavelength	0.71073 Å MoKα
Data Collection Temperature	96(2) K
θ range for 8201 reflections used in lattice determination	2.79 to 26.49°
Unit cell dimensions	a = 29.220(3) Å b = 6.7215(8) Å β= 90.035(2)° c = 14.4249(17) Å
Volume	2833.0(6) $Å^3$
Z	4
Crystal system	Monoclinic
Space group	$P2_1/c$
Density (calculated)	1.179 Mg/m^3
F(000)	1088
Data collection program	Bruker SMART v5.054
θ range for data collection	1.39 to 28.38°
Completeness to θ = 28.38°	93.9 %
Index ranges	$-37 \le h \le 38$, $-8 \le k \le 8$, $-19 \le l \le 19$
Data collection scan type	ω scans at 5 ϕ settings
Data reduction program	Bruker SAINT v6.22
Reflections collected	38935
Independent reflections	6656 [R_{int}= 0.0985]
Absorption coefficient	0.120 mm^{-1}
Absorption correction	None
Max. and min. transmission	0.9829 and 0.9610

Table 1 (cont.)

Structure solution and Refinement

Structure solution program	Bruker SHELXTL
Primary solution method	Direct methods
Secondary solution method	Difference Fourier map
Hydrogen placement	Difference Fourier map
Structure refinement program	Bruker SHELXTL
Refinement method	Full matrix least-squares on F^2
Data / restraints / parameters	6656 / 0 / 484
Treatment of hydrogen atoms	Unrestrained
Goodness-of-fit on F^2	1.403
Final R indices [I>2σ(I), 3988 reflections]	R1 = 0.0584, *w*R2 = 0.0804
R indices (all data)	R1 = 0.1062, *w*R2 = 0.0844
Type of weighting scheme used	Sigma
Weighting scheme used	$w=1/\sigma^2(Fo^2)$
Max shift/error	0.001
Average shift/error	0.000
Largest diff. peak and hole	0.333 and -0.349 e.Å^{-3}

Special Refinement Details

Refinement of F^2 against ALL reflections. The weighted R-factor (*w*R) and goodness of fit (S) are based on F^2, conventional R-factors (R) are based on F, with F set to zero for negative F^2. The threshold expression of $F^2 > 2\sigma(F^2)$ is used only for calculating R-factors(gt) etc. and is not relevant to the choice of reflections for refinement. R-factors based on F^2 are statistically about twice as large as those based on F, and R-factors based on ALL data will be even larger.

All esds (except the esd in the dihedral angle between two l.s. planes) are estimated using the full covariance matrix. The cell esds are taken into account individually in the estimation of esds in distances, angles and torsion angles; correlations between esds in cell parameters are only used when they are defined by crystal symmetry. An approximate (isotropic) treatment of cell esds is used for estimating esds involving l.s. planes.

Table 2. Atomic coordinates (x 10^4) and equivalent isotropic displacement parameters ($Å^2$x 10^3) for DCB06_(CCDC_175859). U(eq) the trace of the orthogonalized U^{ij} tensor.

	x	y	z	U_{eq}
Si(1)	6142(1)	3545(1)	4087(1)	25(1)
O(1)	6571(1)	5169(2)	4135(1)	23(1)
O(2)	7293(1)	2606(2)	3725(1)	23(1)
O(3)	8211(1)	1108(2)	6169(1)	28(1)
O(4)	8640(1)	2202(2)	7317(1)	44(1)
O(5)	9414(1)	-4435(2)	4438(1)	30(1)
O(6)	9725(1)	-2363(2)	3364(1)	45(1)
C(1)	5665(1)	5006(3)	3527(1)	27(1)
C(2)	5841(1)	5905(4)	2608(2)	35(1)
C(3)	5260(1)	3633(5)	3329(2)	43(1)
C(4)	5503(1)	6694(4)	4154(2)	36(1)
C(5)	6282(1)	1358(4)	3362(2)	34(1)
C(6)	5995(1)	2734(5)	5291(2)	39(1)
C(7)	6962(1)	5171(3)	4672(1)	21(1)
C(8)	6990(1)	6481(3)	5429(1)	24(1)
C(9)	6595(1)	7823(4)	5660(2)	37(1)
C(10)	7397(1)	6526(4)	5928(1)	27(1)
C(11)	7762(1)	5352(3)	5700(1)	26(1)
C(12)	7740(1)	4049(3)	4942(1)	22(1)
C(13)	7334(1)	3973(3)	4446(1)	20(1)
C(14)	7349(1)	3475(4)	2815(1)	32(1)
C(15)	8145(1)	2785(3)	4670(1)	22(1)
C(16)	8169(1)	761(3)	5164(1)	22(1)
C(17)	8623(1)	1598(3)	6522(1)	28(1)
C(18)	9030(1)	1238(4)	5922(2)	26(1)
C(19)	8979(1)	-684(3)	5354(1)	19(1)
C(20)	8948(1)	-2437(4)	6036(1)	24(1)
C(21)	9394(1)	-899(3)	4715(1)	24(1)
C(22)	9349(1)	-2544(3)	4006(1)	28(1)
C(23)	9638(1)	-5668(3)	3767(2)	29(1)
C(24)	9927(1)	-4215(4)	3241(2)	39(1)
C(25)	8901(1)	-2427(4)	3480(2)	33(1)
C(26)	8502(1)	-1441(3)	3960(1)	24(1)
C(27)	8074(1)	-1401(5)	3388(2)	35(1)
C(28)	8545(1)	-548(3)	4787(1)	19(1)

Table 3. Bond lengths [Å] and angles [°] for DCB06_(CCDC_175859).

Si(1)-O(1)	1.6629(15)	C(16)-C(28)	1.510(3)
Si(1)-C(5)	1.849(3)	C(16)-H(16)	0.995(16)
Si(1)-C(6)	1.872(2)	C(17)-C(18)	1.490(3)
Si(1)-C(1)	1.887(2)	C(18)-C(19)	1.538(3)
O(1)-C(7)	1.379(2)	C(18)-H(18A)	0.96(2)
O(2)-C(13)	1.392(2)	C(18)-H(18B)	0.96(2)
O(2)-C(14)	1.446(2)	C(19)-C(28)	1.512(3)
O(3)-C(17)	1.350(2)	C(19)-C(21)	1.531(3)
O(3)-C(16)	1.473(2)	C(19)-C(20)	1.538(3)
O(4)-C(17)	1.218(2)	C(20)-H(20A)	0.987(19)
O(5)-C(22)	1.428(2)	C(20)-H(20B)	1.016(18)
O(5)-C(23)	1.433(2)	C(20)-H(20C)	1.003(19)
O(6)-C(24)	1.389(3)	C(21)-C(22)	1.512(3)
O(6)-C(22)	1.443(2)	C(21)-H(21A)	0.99(2)
C(1)-C(4)	1.527(3)	C(21)-H(21B)	0.99(2)
C(1)-C(3)	1.528(3)	C(22)-C(25)	1.516(3)
C(1)-C(2)	1.545(3)	C(23)-C(24)	1.498(3)
C(2)-H(2A)	1.05(2)	C(23)-H(23A)	0.98(2)
C(2)-H(2B)	0.99(2)	C(23)-H(23B)	0.940(19)
C(2)-H(2C)	1.00(2)	C(24)-H(24A)	0.86(3)
C(3)-H(3A)	0.98(2)	C(24)-H(24B)	0.97(3)
C(3)-H(3B)	0.95(2)	C(25)-C(26)	1.509(3)
C(3)-H(3C)	1.04(2)	C(25)-H(25A)	0.99(2)
C(4)-H(4A)	0.99(2)	C(25)-H(25B)	0.98(2)
C(4)-H(4B)	0.99(2)	C(26)-C(28)	1.340(2)
C(4)-H(4C)	0.99(2)	C(26)-C(27)	1.498(3)
C(5)-H(5A)	0.97(2)	C(27)-H(27A)	0.95(2)
C(5)-H(5B)	1.01(2)	C(27)-H(27B)	0.97(2)
C(5)-H(5C)	0.98(2)	C(27)-H(27C)	1.06(2)
C(6)-H(6A)	1.03(3)		
C(6)-H(6B)	0.98(3)	O(1)-Si(1)-C(5)	112.26(10)
C(6)-H(6C)	0.98(2)	O(1)-Si(1)-C(6)	109.05(11)
C(7)-C(13)	1.392(3)	C(5)-Si(1)-C(6)	110.16(13)
C(7)-C(8)	1.405(3)	O(1)-Si(1)-C(1)	103.44(9)
C(8)-C(10)	1.389(3)	C(5)-Si(1)-C(1)	109.60(11)
C(8)-C(9)	1.503(3)	C(6)-Si(1)-C(1)	112.21(11)
C(9)-H(9A)	1.02(2)	C(7)-O(1)-Si(1)	130.34(12)
C(9)-H(9B)	0.92(2)	C(13)-O(2)-C(14)	113.73(17)
C(9)-H(9C)	0.95(2)	C(17)-O(3)-C(16)	118.89(15)
C(10)-C(11)	1.369(3)	C(22)-O(5)-C(23)	106.28(14)
C(10)-H(10)	0.98(2)	C(24)-O(6)-C(22)	109.25(17)
C(11)-C(12)	1.403(3)	C(4)-C(1)-C(3)	108.6(2)
C(11)-H(11)	0.965(19)	C(4)-C(1)-C(2)	108.7(2)
C(12)-C(13)	1.388(3)	C(3)-C(1)-C(2)	109.5(2)
C(12)-C(15)	1.508(3)	C(4)-C(1)-Si(1)	111.25(15)
C(14)-H(14A)	0.99(2)	C(3)-C(1)-Si(1)	109.77(18)
C(14)-H(14B)	1.00(2)	C(2)-C(1)-Si(1)	108.96(15)
C(14)-H(14C)	1.05(2)	C(1)-C(2)-H(2A)	113.2(11)
C(15)-C(16)	1.538(3)	C(1)-C(2)-H(2B)	109.5(13)
C(15)-H(15A)	1.047(18)	H(2A)-C(2)-H(2B)	106.4(17)
C(15)-H(15B)	0.950(18)	C(1)-C(2)-H(2C)	108.6(12)

H(2A)-C(2)-H(2C)	108.2(18)	H(14A)-C(14)-H(14C)	108.8(17)
H(2B)-C(2)-H(2C)	110.9(18)	H(14B)-C(14)-H(14C)	114.6(17)
C(1)-C(3)-H(3A)	110.1(14)	C(12)-C(15)-C(16)	114.35(16)
C(1)-C(3)-H(3B)	110.8(14)	C(12)-C(15)-H(15A)	112.3(10)
H(3A)-C(3)-H(3B)	108.4(19)	C(16)-C(15)-H(15A)	104.7(10)
C(1)-C(3)-H(3C)	113.7(12)	C(12)-C(15)-H(15B)	109.6(11)
H(3A)-C(3)-H(3C)	108.5(18)	C(16)-C(15)-H(15B)	108.4(11)
H(3B)-C(3)-H(3C)	105.0(19)	H(15A)-C(15)-H(15B)	107.1(14)
C(1)-C(4)-H(4A)	109.9(14)	O(3)-C(16)-C(28)	112.77(15)
C(1)-C(4)-H(4B)	112.8(12)	O(3)-C(16)-C(15)	108.69(16)
H(4A)-C(4)-H(4B)	110.7(17)	C(28)-C(16)-C(15)	112.34(16)
C(1)-C(4)-H(4C)	115.2(12)	O(3)-C(16)-H(16)	101.4(9)
H(4A)-C(4)-H(4C)	104.1(17)	C(28)-C(16)-H(16)	113.5(10)
H(4B)-C(4)-H(4C)	103.8(18)	C(15)-C(16)-H(16)	107.4(10)
Si(1)-C(5)-H(5A)	113.1(14)	O(4)-C(17)-O(3)	118.11(19)
Si(1)-C(5)-H(5B)	112.4(13)	O(4)-C(17)-C(18)	124.7(2)
H(5A)-C(5)-H(5B)	108(2)	O(3)-C(17)-C(18)	117.06(17)
Si(1)-C(5)-H(5C)	110.5(14)	C(17)-C(18)-C(19)	111.65(18)
H(5A)-C(5)-H(5C)	106.6(19)	C(17)-C(18)-H(18A)	109.4(12)
H(5B)-C(5)-H(5C)	106.0(18)	C(19)-C(18)-H(18A)	112.2(12)
Si(1)-C(6)-H(6A)	110.3(13)	C(17)-C(18)-H(18B)	111.5(11)
Si(1)-C(6)-H(6B)	114.0(13)	C(19)-C(18)-H(18B)	111.1(12)
H(6A)-C(6)-H(6B)	107(2)	H(18A)-C(18)-H(18B)	100.5(16)
Si(1)-C(6)-H(6C)	107.1(13)	C(28)-C(19)-C(21)	110.20(15)
H(6A)-C(6)-H(6C)	111.0(19)	C(28)-C(19)-C(18)	108.56(17)
H(6B)-C(6)-H(6C)	108(2)	C(21)-C(19)-C(18)	108.89(16)
O(1)-C(7)-C(13)	120.97(17)	C(28)-C(19)-C(20)	110.06(16)
O(1)-C(7)-C(8)	119.01(17)	C(21)-C(19)-C(20)	111.11(17)
C(13)-C(7)-C(8)	119.93(18)	C(18)-C(19)-C(20)	107.94(16)
C(10)-C(8)-C(7)	117.79(19)	C(19)-C(20)-H(20A)	111.0(10)
C(10)-C(8)-C(9)	121.9(2)	C(19)-C(20)-H(20B)	108.3(10)
C(7)-C(8)-C(9)	120.24(19)	H(20A)-C(20)-H(20B)	107.8(14)
C(8)-C(9)-H(9A)	109.2(13)	C(19)-C(20)-H(20C)	110.5(11)
C(8)-C(9)-H(9B)	112.5(13)	H(20A)-C(20)-H(20C)	104.4(15)
H(9A)-C(9)-H(9B)	111.6(18)	H(20B)-C(20)-H(20C)	114.8(14)
C(8)-C(9)-H(9C)	112.0(13)	C(22)-C(21)-C(19)	113.99(17)
H(9A)-C(9)-H(9C)	106.5(18)	C(22)-C(21)-H(21A)	107.4(12)
H(9B)-C(9)-H(9C)	104.8(19)	C(19)-C(21)-H(21A)	112.5(11)
C(11)-C(10)-C(8)	122.0(2)	C(22)-C(21)-H(21B)	107.6(10)
C(11)-C(10)-H(10)	120.2(12)	C(19)-C(21)-H(21B)	110.2(10)
C(8)-C(10)-H(10)	117.8(12)	H(21A)-C(21)-H(21B)	104.7(16)
C(10)-C(11)-C(12)	120.8(2)	O(5)-C(22)-O(6)	104.75(15)
C(10)-C(11)-H(11)	120.4(11)	O(5)-C(22)-C(21)	110.15(16)
C(12)-C(11)-H(11)	118.8(11)	O(6)-C(22)-C(21)	107.79(17)
C(13)-C(12)-C(11)	117.63(19)	O(5)-C(22)-C(25)	112.29(19)
C(13)-C(12)-C(15)	121.07(18)	O(6)-C(22)-C(25)	109.41(17)
C(11)-C(12)-C(15)	121.30(19)	C(21)-C(22)-C(25)	112.09(19)
C(12)-C(13)-C(7)	121.79(18)	O(5)-C(23)-C(24)	102.91(18)
C(12)-C(13)-O(2)	118.78(17)	O(5)-C(23)-H(23A)	110.8(11)
C(7)-C(13)-O(2)	119.39(17)	C(24)-C(23)-H(23A)	113.5(12)
O(2)-C(14)-H(14A)	107.7(11)	O(5)-C(23)-H(23B)	109.3(12)
O(2)-C(14)-H(14B)	103.7(13)	C(24)-C(23)-H(23B)	112.7(12)
H(14A)-C(14)-H(14B)	111.7(17)	H(23A)-C(23)-H(23B)	107.6(17)
O(2)-C(14)-H(14C)	109.9(11)	O(6)-C(24)-C(23)	106.3(2)

O(6)-C(24)-H(24A)	111(2)
C(23)-C(24)-H(24A)	121(2)
O(6)-C(24)-H(24B)	107.4(15)
C(23)-C(24)-H(24B)	109.6(15)
H(24A)-C(24)-H(24B)	101(2)
C(26)-C(25)-C(22)	117.35(18)
C(26)-C(25)-H(25A)	105.2(13)
C(22)-C(25)-H(25A)	103.6(13)
C(26)-C(25)-H(25B)	109.0(12)
C(22)-C(25)-H(25B)	108.3(12)
H(25A)-C(25)-H(25B)	113.4(18)
C(28)-C(26)-C(27)	124.0(2)
C(28)-C(26)-C(25)	122.27(19)
C(27)-C(26)-C(25)	113.50(18)
C(26)-C(27)-H(27A)	111.8(14)
C(26)-C(27)-H(27B)	110.0(13)
H(27A)-C(27)-H(27B)	108.2(19)
C(26)-C(27)-H(27C)	118.2(11)
H(27A)-C(27)-H(27C)	102.5(18)
H(27B)-C(27)-H(27C)	105.5(18)
C(26)-C(28)-C(16)	120.96(18)
C(26)-C(28)-C(19)	122.09(18)
C(16)-C(28)-C(19)	116.83(16)

_____

Table 4. Anisotropic displacement parameters ($Å^2 x 10^4$) for DCB06_(CCDC_175859). The anisotropic displacement factor exponent takes the form: $-2\pi^2 [h^2 a^{*2} U^{11} + ... + 2 h k a^* b^* U^{12}]$

	U^{11}	U^{22}	U^{33}	U^{23}	U^{13}	U^{12}
Si(1)	252(3)	279(4)	224(3)	4(3)	10(3)	-5(3)
O(1)	223(8)	280(9)	195(7)	-17(6)	-35(6)	7(6)
O(2)	277(8)	286(9)	134(7)	-31(6)	-19(6)	-16(7)
O(3)	292(9)	444(10)	110(7)	15(7)	31(6)	67(7)
O(4)	623(12)	535(12)	148(8)	-121(7)	-86(7)	211(9)
O(5)	483(10)	221(9)	186(7)	34(7)	67(7)	24(7)
O(6)	607(11)	324(10)	426(9)	130(8)	373(8)	165(8)
C(1)	206(12)	327(14)	273(12)	19(10)	-8(10)	-14(10)
C(2)	339(16)	452(18)	257(13)	51(12)	-44(12)	55(14)
C(3)	243(15)	500(19)	547(18)	-31(17)	-58(13)	-29(14)
C(4)	287(15)	436(17)	370(15)	43(13)	11(12)	69(14)
C(5)	344(16)	311(15)	366(15)	-48(12)	17(12)	-74(14)
C(6)	465(18)	396(17)	313(14)	73(13)	77(13)	51(15)
C(7)	190(12)	250(13)	199(11)	50(9)	-14(9)	-7(10)
C(8)	254(12)	283(13)	190(10)	6(10)	-4(9)	29(10)
C(9)	400(17)	389(17)	309(15)	-133(14)	-63(12)	122(14)
C(10)	315(14)	336(14)	170(11)	-59(11)	-37(10)	-4(11)
C(11)	274(14)	329(14)	165(11)	3(10)	-41(10)	-10(11)
C(12)	225(12)	279(13)	143(10)	36(9)	23(9)	1(9)
C(13)	237(12)	217(13)	151(10)	13(9)	9(9)	-59(10)
C(14)	336(16)	453(16)	160(11)	-4(12)	-1(10)	-19(14)
C(15)	208(13)	273(13)	170(11)	13(10)	-15(9)	-33(10)
C(16)	202(12)	323(14)	128(10)	10(9)	-18(9)	-19(10)
C(17)	328(14)	308(14)	207(11)	3(10)	-45(10)	114(11)
C(18)	266(14)	297(15)	202(11)	-55(11)	-68(10)	5(11)
C(19)	191(11)	245(12)	126(10)	-11(9)	3(8)	-18(9)
C(20)	228(14)	356(15)	125(11)	21(11)	-11(10)	15(11)
C(21)	253(13)	218(14)	240(12)	33(10)	54(10)	-15(10)
C(22)	378(14)	250(13)	209(11)	52(10)	128(10)	45(11)
C(23)	364(15)	201(13)	292(13)	-18(11)	14(12)	51(12)
C(24)	351(17)	247(15)	576(18)	-68(13)	127(15)	-24(12)
C(25)	501(16)	330(16)	164(12)	6(12)	1(11)	53(13)
C(26)	318(13)	239(12)	150(10)	21(10)	-44(9)	-16(10)
C(27)	458(17)	310(16)	269(13)	-22(13)	-157(12)	-2(13)
C(28)	208(12)	244(13)	125(10)	42(9)	2(9)	-23(9)

Table 5. Hydrogen coordinates (x 10^4) and isotropic displacement parameters ($Å^2$x 10^3) for DCB06_(CCDC_175859).

	x	y	z	U_{iso}
H(2A)	6133(7)	6800(30)	2693(13)	38(6)
H(2B)	5928(7)	4820(40)	2180(15)	49(7)
H(2C)	5594(8)	6750(40)	2334(15)	49(7)
H(3A)	5005(8)	4400(40)	3059(15)	54(8)
H(3B)	5343(7)	2620(40)	2906(15)	47(8)
H(3C)	5141(7)	2890(30)	3909(15)	48(7)
H(4A)	5371(7)	6140(40)	4734(15)	53(7)
H(4B)	5749(7)	7660(30)	4298(13)	29(6)
H(4C)	5256(7)	7520(30)	3897(14)	38(6)
H(5A)	6544(8)	620(40)	3588(15)	55(8)
H(5B)	6018(8)	410(40)	3306(15)	53(7)
H(5C)	6356(8)	1770(40)	2728(16)	53(7)
H(6A)	5864(8)	3910(40)	5662(16)	68(8)
H(6B)	5767(8)	1660(40)	5317(15)	60(8)
H(6C)	6278(8)	2230(30)	5577(15)	50(7)
H(9A)	6319(8)	6970(30)	5851(14)	47(7)
H(9B)	6667(7)	8740(30)	6106(14)	36(7)
H(9C)	6499(7)	8590(30)	5140(16)	48(7)
H(10)	7416(7)	7440(30)	6454(14)	36(6)
H(11)	8045(6)	5450(30)	6044(12)	27(6)
H(14A)	7663(7)	4000(30)	2774(12)	28(6)
H(14B)	7302(7)	2330(40)	2385(15)	49(7)
H(14C)	7118(7)	4650(30)	2727(13)	39(6)
H(15A)	8144(6)	2430(30)	3962(13)	27(5)
H(15B)	8421(6)	3490(30)	4792(11)	16(5)
H(16)	7859(6)	150(20)	5125(10)	8(4)
H(18A)	9081(6)	2380(30)	5535(13)	31(6)
H(18B)	9308(7)	1230(30)	6276(13)	31(6)
H(20A)	8897(6)	-3700(30)	5704(12)	18(5)
H(20B)	9252(6)	-2550(30)	6377(12)	21(5)
H(20C)	8673(7)	-2290(30)	6446(12)	26(5)
H(21A)	9683(7)	-1130(30)	5063(13)	34(6)
H(21B)	9448(6)	360(30)	4373(12)	24(5)
H(23A)	9815(7)	-6710(30)	4072(13)	34(6)
H(23B)	9417(6)	-6290(30)	3393(13)	24(6)
H(24A)	9995(11)	-4420(50)	2670(20)	112(14)
H(24B)	10229(9)	-4160(40)	3514(16)	64(9)
H(25A)	8972(7)	-1560(30)	2948(15)	51(7)
H(25B)	8812(7)	-3770(30)	3298(14)	39(7)
H(27A)	8088(8)	-420(40)	2917(16)	56(8)
H(27B)	8027(7)	-2690(40)	3096(15)	48(7)
H(27C)	7762(7)	-1060(30)	3722(13)	43(7)

CALIFORNIA INSTITUTE OF TECHNOLOGY

BECKMAN INSTITUTE

X-RAY CRYSTALLOGRAPHY LABORATORY

Crystal Structure Analysis of:

Acid 161•$CHCl_3$ (DCB05)

(CCDC 175588)

Contents:

Figure A3.3 Representation of Acid **161•$CHCl_3$**

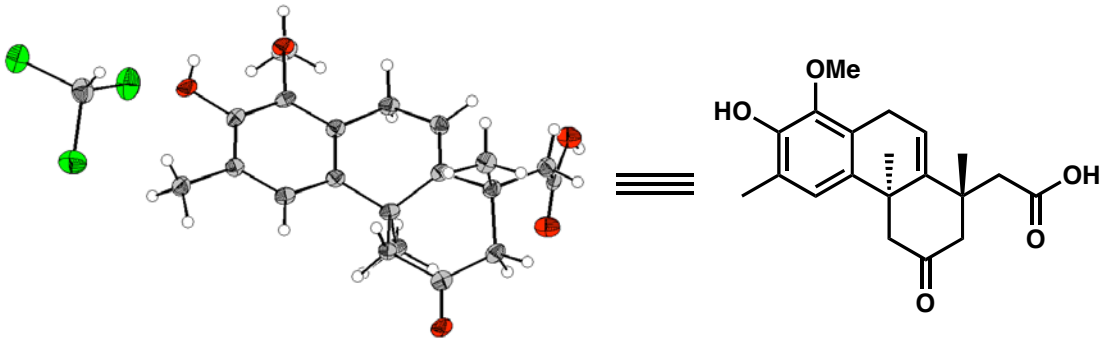

Table 1. Crystal data and structure refinement for DCB05 (CCDC 175588).

Empirical formula	$C_{20}H_{24}O_5 \cdot CHCl_3$
Formula weight	463.76
Crystallization Solvent	Chloroform
Crystal Habit	Fragment
Crystal size	0.22 x 0.15 x 0.15 mm^3
Crystal color	Colorless

Data Collection

Preliminary Photos	Rotation
Type of diffractometer	Bruker SMART 1000
Wavelength	0.71073 Å MoKα
Data Collection Temperature	98(2) K
θ range for 4336 reflections used in lattice determination	2.47 to 25.80°
Unit cell dimensions	a = 11.137(3) Å b = 13.282(3) Å β= 98.762(4)° c = 15.008(4) Å
Volume	2194.3(10) $Å^3$
Z	4
Crystal system	Monoclinic
Space group	$P2_1/n$
Density (calculated)	1.404 Mg/m^3
F(000)	968
Data collection program	Bruker SMART v5.054
θ range for data collection	2.06 to 28.36°
Completeness to θ = 28.36°	93.7 %
Index ranges	$-14 \le h \le 14$, $-17 \le k \le 17$, $-19 \le l \le 19$
Data collection scan type	ω scans at 5 ϕ settings
Data reduction program	Bruker SAINT v6.22
Reflections collected	32070
Independent reflections	5144 [R_{int}= 0.1503]
Absorption coefficient	0.447 mm^{-1}
Absorption correction	None
Max. and min. transmission	0.9368 and 0.9072

Table 1 (cont.)

Structure solution and Refinement

Structure solution program	SHELXS-97 (Sheldrick, 1990)
Primary solution method	Direct methods
Secondary solution method	Difference Fourier map
Hydrogen placement	Difference Fourier map
Structure refinement program	SHELXL-97 (Sheldrick, 1997)
Refinement method	Full matrix least-squares on F^2
Data / restraints / parameters	5144 / 0 / 362
Treatment of hydrogen atoms	Unrestrained
Goodness-of-fit on F^2	1.064
Final R indices [$I>2\sigma(I)$, 2718 reflections]	R1 = 0.0468, *w*R2 = 0.0744
R indices (all data)	R1 = 0.1218, *w*R2 = 0.0862
Type of weighting scheme used	Sigma
Weighting scheme used	$w=1/\sigma^2(Fo^2)$
Max shift/error	0.000
Average shift/error	0.000
Largest diff. peak and hole	0.402 and -0.348 e.Å^{-3}

Special Refinement Details

Refinement of F^2 against ALL reflections. The weighted R-factor (*w*R) and goodness of fit (S) are based on F^2, conventional R-factors (R) are based on F, with F set to zero for negative F^2. The threshold expression of $F^2 > 2\sigma(F^2)$ is used only for calculating R-factors(gt) etc. and is not relevant to the choice of reflections for refinement. R-factors based on F^2 are statistically about twice as large as those based on F, and R-factors based on ALL data will be even larger.

All esds (except the esd in the dihedral angle between two l.s. planes) are estimated using the full covariance matrix. The cell esds are taken into account individually in the estimation of esds in distances, angles and torsion angles; correlations between esds in cell parameters are only used when they are defined by crystal symmetry. An approximate (isotropic) treatment of cell esds is used for estimating esds involving l.s. planes.

Table 2. Atomic coordinates (x 10^4) and equivalent isotropic displacement parameters ($Å^2$x 10^3) for DCB05 (CCDC 175588). U(eq) is defined as the trace of the orthogonalized U^{ij} tensor.

	x	y	z	U_{eq}
O(1)	2996(2)	1246(2)	424(1)	23(1)
O(2)	3667(2)	289(1)	2011(1)	23(1)
O(3)	10816(2)	767(1)	809(1)	24(1)
O(4)	10340(2)	21(1)	3988(1)	28(1)
O(5)	9289(2)	-1153(1)	4583(1)	27(1)
C(1)	4196(2)	1102(2)	735(2)	20(1)
C(2)	4579(2)	649(2)	1547(2)	19(1)
C(3)	5789(2)	489(2)	1874(2)	19(1)
C(4)	6178(2)	-65(2)	2727(2)	22(1)
C(5)	7352(2)	-608(2)	2734(2)	20(1)
C(6)	8184(2)	-314(2)	2243(2)	18(1)
C(7)	9343(2)	-929(2)	2231(2)	20(1)
C(8)	9093(3)	-1750(2)	1504(2)	25(1)
C(9)	9748(3)	-1452(2)	3131(2)	22(1)
C(10)	9824(2)	-789(2)	3926(2)	21(1)
C(11)	10377(2)	-254(2)	2003(2)	23(1)
C(12)	10036(2)	410(2)	1214(2)	21(1)
C(13)	8738(2)	652(2)	926(2)	19(1)
C(14)	7993(2)	658(2)	1710(2)	18(1)
C(15)	8424(3)	1530(2)	2337(2)	22(1)
C(16)	6654(2)	805(2)	1345(2)	18(1)
C(17)	6244(2)	1260(2)	531(2)	19(1)
C(18)	5037(2)	1421(2)	199(2)	19(1)
C(19)	4615(3)	1892(3)	-688(2)	24(1)
C(20)	3502(3)	888(3)	2774(2)	28(1)
C(21)	1118(3)	3109(2)	603(2)	31(1)
Cl(1)	1475(1)	3147(1)	1778(1)	41(1)
Cl(2)	2089(1)	3910(1)	117(1)	45(1)
Cl(3)	-397(1)	3458(1)	263(1)	39(1)

Table 3. Bond lengths [Å] and angles [°] for DCB05 (CCDC 175588).

O(1)-C(1)	1.361(3)	C(21)-Cl(3)	1.749(3)
O(1)-H(1)	0.72(3)	C(21)-Cl(1)	1.749(3)
O(2)-C(2)	1.401(3)	C(21)-Cl(2)	1.753(3)
O(2)-C(20)	1.428(3)	C(21)-H(21)	0.91(3)
O(3)-C(12)	1.230(3)		
O(4)-C(10)	1.216(3)	C(1)-O(1)-H(1)	107(3)
O(5)-C(10)	1.319(3)	C(2)-O(2)-C(20)	113.6(2)
O(5)-H(5A)	0.97(4)	C(10)-O(5)-H(5A)	111.0(18)
C(1)-C(2)	1.368(4)	O(1)-C(1)-C(2)	121.6(2)
C(1)-C(18)	1.390(3)	O(1)-C(1)-C(18)	118.2(2)
C(2)-C(3)	1.378(3)	C(2)-C(1)-C(18)	120.3(2)
C(3)-C(16)	1.403(3)	C(1)-C(2)-C(3)	122.7(2)
C(3)-C(4)	1.483(4)	C(1)-C(2)-O(2)	116.2(2)
C(4)-C(5)	1.492(4)	C(3)-C(2)-O(2)	120.9(2)
C(4)-H(4A)	0.94(3)	C(2)-C(3)-C(16)	118.1(2)
C(4)-H(4B)	0.96(3)	C(2)-C(3)-C(4)	121.7(2)
C(5)-C(6)	1.328(3)	C(16)-C(3)-C(4)	120.1(2)
C(5)-H(5)	0.97(3)	C(3)-C(4)-C(5)	112.8(2)
C(6)-C(14)	1.516(4)	C(3)-C(4)-H(4A)	108.3(16)
C(6)-C(7)	1.529(3)	C(5)-C(4)-H(4A)	109.2(15)
C(7)-C(9)	1.525(4)	C(3)-C(4)-H(4B)	108.8(16)
C(7)-C(8)	1.538(4)	C(5)-C(4)-H(4B)	107.1(16)
C(7)-C(11)	1.539(3)	H(4A)-C(4)-H(4B)	111(2)
C(8)-H(8A)	0.95(3)	C(6)-C(5)-C(4)	122.6(3)
C(8)-H(8B)	1.02(3)	C(6)-C(5)-H(5)	119.0(14)
C(8)-H(8C)	1.03(3)	C(4)-C(5)-H(5)	118.4(14)
C(9)-C(10)	1.475(4)	C(5)-C(6)-C(14)	119.3(2)
C(9)-H(9A)	0.92(3)	C(5)-C(6)-C(7)	120.7(2)
C(9)-H(9B)	0.93(2)	C(14)-C(6)-C(7)	119.97(19)
C(11)-C(12)	1.478(4)	C(9)-C(7)-C(6)	111.69(19)
C(11)-H(11A)	0.99(3)	C(9)-C(7)-C(8)	107.6(2)
C(11)-H(11B)	1.00(3)	C(6)-C(7)-C(8)	109.0(2)
C(12)-C(13)	1.480(4)	C(9)-C(7)-C(11)	109.4(2)
C(13)-C(14)	1.541(3)	C(6)-C(7)-C(11)	110.7(2)
C(13)-H(13A)	0.94(2)	C(8)-C(7)-C(11)	108.4(2)
C(13)-H(13B)	1.00(2)	C(7)-C(8)-H(8A)	108.3(15)
C(14)-C(16)	1.520(4)	C(7)-C(8)-H(8B)	107.9(16)
C(14)-C(15)	1.523(4)	H(8A)-C(8)-H(8B)	109(2)
C(15)-H(15A)	1.00(2)	C(7)-C(8)-H(8C)	113.1(14)
C(15)-H(15B)	1.00(2)	H(8A)-C(8)-H(8C)	106(2)
C(15)-H(15C)	1.01(3)	H(8B)-C(8)-H(8C)	113(2)
C(16)-C(17)	1.378(4)	C(10)-C(9)-C(7)	114.7(2)
C(17)-C(18)	1.377(4)	C(10)-C(9)-H(9A)	111.5(15)
C(17)-H(17)	0.97(2)	C(7)-C(9)-H(9A)	114.9(16)
C(18)-C(19)	1.481(4)	C(10)-C(9)-H(9B)	105.6(15)
C(19)-H(19A)	0.94(3)	C(7)-C(9)-H(9B)	111.0(15)
C(19)-H(19B)	0.92(3)	H(9A)-C(9)-H(9B)	97(2)
C(19)-H(19C)	1.03(2)	O(4)-C(10)-O(5)	122.0(2)
C(20)-H(20A)	1.00(3)	O(4)-C(10)-C(9)	123.9(2)
C(20)-H(20B)	0.95(2)	O(5)-C(10)-C(9)	114.2(2)
C(20)-H(20C)	0.99(3)	C(12)-C(11)-C(7)	114.6(2)

C(12)-C(11)-H(11A)	106.0(16)
C(7)-C(11)-H(11A)	112.5(15)
C(12)-C(11)-H(11B)	113.7(14)
C(7)-C(11)-H(11B)	108.6(15)
H(11A)-C(11)-H(11B)	101(2)
O(3)-C(12)-C(11)	120.7(2)
O(3)-C(12)-C(13)	120.3(2)
C(11)-C(12)-C(13)	119.0(2)
C(12)-C(13)-C(14)	113.2(2)
C(12)-C(13)-H(13A)	109.8(13)
C(14)-C(13)-H(13A)	108.8(12)
C(12)-C(13)-H(13B)	110.1(13)
C(14)-C(13)-H(13B)	109.3(12)
H(13A)-C(13)-H(13B)	105.3(19)
C(6)-C(14)-C(16)	110.5(2)
C(6)-C(14)-C(15)	108.5(2)
C(16)-C(14)-C(15)	108.9(2)
C(6)-C(14)-C(13)	110.5(2)
C(16)-C(14)-C(13)	109.8(2)
C(15)-C(14)-C(13)	108.6(2)
C(14)-C(15)-H(15A)	109.5(14)
C(14)-C(15)-H(15B)	111.6(14)
H(15A)-C(15)-H(15B)	107.9(18)
C(14)-C(15)-H(15C)	116.1(16)
H(15A)-C(15)-H(15C)	111(2)
H(15B)-C(15)-H(15C)	100(2)
C(17)-C(16)-C(3)	118.0(2)
C(17)-C(16)-C(14)	123.4(2)
C(3)-C(16)-C(14)	118.6(2)
C(18)-C(17)-C(16)	124.3(2)
C(18)-C(17)-H(17)	117.2(15)
C(16)-C(17)-H(17)	118.6(15)
C(17)-C(18)-C(1)	116.7(2)
C(17)-C(18)-C(19)	123.3(2)
C(1)-C(18)-C(19)	120.0(2)
C(18)-C(19)-H(19A)	114.1(17)
C(18)-C(19)-H(19B)	111.4(17)
H(19A)-C(19)-H(19B)	109(2)
C(18)-C(19)-H(19C)	109.9(15)
H(19A)-C(19)-H(19C)	104(2)
H(19B)-C(19)-H(19C)	107(2)
O(2)-C(20)-H(20A)	111.9(14)
O(2)-C(20)-H(20B)	104.7(14)
H(20A)-C(20)-H(20B)	108(2)
O(2)-C(20)-H(20C)	112.1(16)
H(20A)-C(20)-H(20C)	108(2)
H(20B)-C(20)-H(20C)	111(2)
Cl(3)-C(21)-Cl(1)	110.32(16)
Cl(3)-C(21)-Cl(2)	110.32(17)
Cl(1)-C(21)-Cl(2)	109.98(17)
Cl(3)-C(21)-H(21)	109.2(19)
Cl(1)-C(21)-H(21)	105.5(19)
Cl(2)-C(21)-H(21)	111.4(16)

Table 4. Anisotropic displacement parameters ($Å^2 x 10^4$) for DCB05 (CCDC 175588). The anisotropic displacement factor exponent takes the form: $-2\pi^2 [h^2 a^{*2} U^{11} + ... + 2 h k a^* b^* U^{12}]$

	U^{11}	U^{22}	U^{33}	U^{23}	U^{13}	U^{12}
O(1)	149(10)	334(13)	235(11)	33(9)	80(9)	-25(9)
O(2)	182(10)	311(11)	210(10)	7(9)	113(8)	-10(8)
O(3)	154(10)	348(11)	253(11)	24(9)	102(8)	-2(8)
O(4)	324(11)	318(12)	214(10)	-30(9)	98(9)	-60(9)
O(5)	325(11)	325(12)	182(11)	-13(10)	95(9)	-42(9)
C(1)	142(14)	230(15)	221(15)	-30(12)	23(11)	8(12)
C(2)	142(14)	248(15)	205(15)	-29(12)	82(11)	-27(11)
C(3)	174(15)	228(15)	167(14)	-8(12)	58(11)	4(11)
C(4)	183(15)	279(17)	222(16)	16(14)	92(12)	-9(13)
C(5)	223(15)	228(16)	165(15)	17(13)	41(12)	4(12)
C(6)	155(14)	222(15)	159(14)	-23(11)	31(11)	-4(11)
C(7)	164(14)	230(15)	198(15)	8(12)	36(11)	1(11)
C(8)	240(17)	298(18)	208(16)	-20(14)	47(13)	18(14)
C(9)	190(16)	242(16)	242(16)	20(13)	49(12)	24(14)
C(10)	148(14)	267(17)	208(15)	27(13)	-21(12)	41(12)
C(11)	150(15)	294(17)	243(16)	-13(14)	53(12)	15(13)
C(12)	216(15)	196(15)	230(16)	-72(12)	56(12)	-7(12)
C(13)	175(15)	235(16)	172(15)	24(13)	71(12)	9(12)
C(14)	158(14)	222(15)	186(14)	-19(12)	92(11)	-10(11)
C(15)	192(15)	254(16)	217(16)	-18(13)	85(12)	-7(13)
C(16)	169(14)	203(14)	180(14)	-3(11)	79(11)	13(11)
C(17)	176(14)	229(15)	194(15)	-22(12)	92(12)	-2(12)
C(18)	184(14)	216(15)	191(14)	-5(12)	67(11)	22(11)
C(19)	181(16)	298(18)	228(16)	44(15)	29(13)	-2(14)
C(20)	237(18)	400(20)	250(17)	-48(15)	140(15)	-19(15)
C(21)	345(18)	274(18)	296(17)	-15(15)	10(14)	23(15)
Cl(1)	443(5)	519(5)	245(4)	-55(4)	17(3)	122(4)
Cl(2)	415(5)	447(5)	491(5)	63(4)	117(4)	-38(4)
Cl(3)	331(4)	475(5)	339(4)	-10(4)	21(3)	69(4)

Table 5. Hydrogen coordinates (x 10^4) and isotropic displacement parameters ($Å^2$x 10^3) for DCB05 (CCDC 175588).

	x	y	z	U_{iso}
H(1)	2670(30)	960(20)	710(20)	37(11)
H(4A)	6260(20)	400(20)	3203(17)	23(7)
H(4B)	5570(20)	-560(20)	2799(17)	29(7)
H(5)	7500(20)	-1210(20)	3098(17)	29(8)
H(5A)	9470(30)	-750(30)	5120(20)	60(10)
H(8A)	8480(20)	-2180(20)	1656(18)	30(8)
H(8B)	9870(30)	-2160(20)	1514(18)	40(8)
H(8C)	8770(20)	-1467(19)	875(19)	30(7)
H(9A)	9340(20)	-2040(20)	3214(16)	19(7)
H(9B)	10520(20)	-1729(19)	3152(16)	22(7)
H(11A)	10710(20)	190(20)	2508(19)	39(8)
H(11B)	11100(20)	-680(20)	1959(16)	29(7)
H(13A)	8666(18)	1287(17)	642(14)	3(6)
H(13B)	8370(20)	165(18)	456(16)	16(7)
H(15A)	8294(19)	2176(18)	1999(15)	11(6)
H(15B)	7970(20)	1565(18)	2856(17)	22(7)
H(15C)	9280(30)	1480(20)	2670(19)	39(8)
H(17)	6830(20)	1466(18)	154(16)	23(7)
H(19A)	4240(20)	2520(20)	-652(18)	31(8)
H(19B)	4110(20)	1470(20)	-1056(19)	33(8)
H(19C)	5350(20)	2042(19)	-1011(17)	32(7)
H(20A)	4260(30)	910(20)	3234(18)	29(8)
H(20B)	2880(20)	553(17)	3031(15)	14(6)
H(20C)	3270(20)	1590(20)	2602(19)	38(9)
H(21)	1220(20)	2450(20)	447(19)	39(9)

Table 6. Hydrogen bonds for DCB05 (CCDC 175588) [Å and °].

D-H...A	d(D-H)	d(H...A)	d(D...A)	<(DHA)
O(1)-H(1)...O(3)#1	0.72(3)	2.10(3)	2.656(2)	135(3)
O(1)-H(1)...O(2)	0.72(3)	2.28(3)	2.703(3)	119(3)
O(5)-H(5A)...O(4)#2	0.97(4)	1.64(4)	2.600(3)	175(3)

Symmetry transformations used to generate equivalent atoms:
#1 x-1,y,z #2 -x+2,-y,-z+1

CALIFORNIA INSTITUTE OF TECHNOLOGY

BECKMAN INSTITUTE

X-RAY CRYSTALLOGRAPHY LABORATORY

Crystal Structure Analysis of:

Diketone 175 (DCB11)

(CCDC 201187)

Contents:

Figure A3.4 Representation of Diketone **175**.

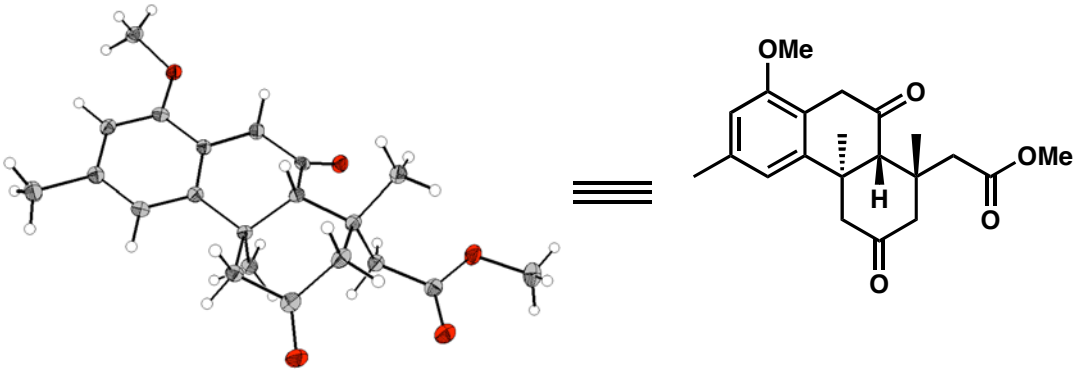

Table 1. Crystal data and structure refinement for DCB11 (CCDC 201187).

Empirical formula	$C_{21}H_{26}O_5$
Formula weight	358.42
Crystallization Solvent	Acetone/heptane
Crystal Habit	Fragment
Crystal size	0.26 x 0.22 x 0.17 mm^3
Crystal color	Colorless

Data Collection

Preliminary Photos	Rotation
Type of diffractometer	Bruker SMART 1000
Wavelength	0.71073 Å MoKα
Data Collection Temperature	98(2) K
θ range for 11980 reflections used in lattice determination	2.28 to 28.32°
Unit cell dimensions	a = 9.0211(6) Å b = 11.3617(7) Å β= 97.5510(10)° c = 17.9596(12) Å
Volume	1824.8(2) $Å^3$
Z	4
Crystal system	Monoclinic
Space group	$P2_1/n$
Density (calculated)	1.305 Mg/m^3
F(000)	768
Data collection program	Bruker SMART v5.054
θ range for data collection	2.13 to 28.32°
Completeness to θ = 28.32°	93.0 %
Index ranges	$-11 \le h \le 11$, $-14 \le k \le 14$, $-23 \le l \le 23$
Data collection scan type	ω scans at 5 ϕ settings
Data reduction program	Bruker SAINT v6.022
Reflections collected	25862
Independent reflections	4226 [R_{int}= 0.0517]
Absorption coefficient	0.092 mm^{-1}
Absorption correction	None
Max. and min. transmission	0.9845 and 0.9764

Table 1 (cont.)

Structure solution and Refinement

Structure solution program	SHELXS-97 (Sheldrick, 1990)
Primary solution method	Direct methods
Secondary solution method	Difference Fourier map
Hydrogen placement	Difference Fourier map
Structure refinement program	SHELXL-97 (Sheldrick, 1997)
Refinement method	Full matrix least-squares on F^2
Data / restraints / parameters	4226 / 0 / 339
Treatment of hydrogen atoms	Unrestrained
Goodness-of-fit on F^2	2.153
Final R indices [$I>2\sigma(I)$, 3426 reflections]	R1 = 0.0404, *w*R2 = 0.0704
R indices (all data)	R1 = 0.0511, *w*R2 = 0.0715
Type of weighting scheme used	Sigma
Weighting scheme used	$w=1/\sigma^2(Fo^2)$
Max shift/error	0.001
Average shift/error	0.000
Largest diff. peak and hole	0.326 and -0.254 e.Å^{-3}

Special Refinement Details

Refinement of F^2 against ALL reflections. The weighted R-factor (*w*R) and goodness of fit (S) are based on F^2, conventional R-factors (R) are based on F, with F set to zero for negative F^2. The threshold expression of $F^2 > 2\sigma(F^2)$ is used only for calculating R-factors(gt) etc. and is not relevant to the choice of reflections for refinement. R-factors based on F^2 are statistically about twice as large as those based on F, and R-factors based on ALL data will be even larger.

All esds (except the esd in the dihedral angle between two l.s. planes) are estimated using the full covariance matrix. The cell esds are taken into account individually in the estimation of esds in distances, angles and torsion angles; correlations between esds in cell parameters are only used when they are defined by crystal symmetry. An approximate (isotropic) treatment of cell esds is used for estimating esds involving l.s. planes.

Table 2. Atomic coordinates (x 10^4) and equivalent isotropic displacement parameters ($Å^2$x 10^3) for DCB11 (CCDC 201187). U(eq) is defined as the trace of the orthogonalized U^{ij} tensor.

	x	y	z	U_{eq}
O(1)	7731(1)	4507(1)	529(1)	19(1)
O(2)	4749(1)	8200(1)	472(1)	21(1)
O(3)	9216(1)	11345(1)	2166(1)	25(1)
O(4)	3377(1)	11397(1)	1288(1)	24(1)
O(5)	5418(1)	12446(1)	1710(1)	29(1)
C(1)	10631(1)	7158(1)	1330(1)	16(1)
C(2)	11220(1)	6047(1)	1256(1)	16(1)
C(3)	12869(2)	5814(1)	1455(1)	23(1)
C(4)	10262(1)	5133(1)	986(1)	16(1)
C(5)	8757(1)	5346(1)	789(1)	15(1)
C(6)	8217(2)	3305(1)	562(1)	20(1)
C(7)	8162(1)	6478(1)	851(1)	14(1)
C(8)	6510(1)	6650(1)	623(1)	18(1)
C(9)	5914(1)	7834(1)	811(1)	15(1)
C(10)	6851(1)	8484(1)	1442(1)	14(1)
C(11)	6098(1)	9579(1)	1751(1)	15(1)
C(12)	4682(1)	9175(1)	2071(1)	19(1)
C(13)	5708(1)	10548(1)	1148(1)	17(1)
C(14)	4865(1)	11569(1)	1417(1)	18(1)
C(15)	2478(2)	12330(1)	1540(1)	31(1)
C(16)	7204(1)	10084(1)	2400(1)	18(1)
C(17)	8678(1)	10359(1)	2139(1)	18(1)
C(18)	9450(1)	9319(1)	1844(1)	18(1)
C(19)	8466(1)	8626(1)	1220(1)	14(1)
C(20)	8500(2)	9259(1)	463(1)	19(1)
C(21)	9104(1)	7387(1)	1138(1)	14(1)

Table 3. Bond lengths [Å] and angles [°] for DCB11 (CCDC 201187).

O(1)-C(5)	1.3673(13)	C(20)-H(20A)	0.996(14)
O(1)-C(6)	1.4332(14)	C(20)-H(20B)	0.987(13)
O(2)-C(9)	1.2162(13)	C(20)-H(20C)	0.985(13)
O(3)-C(17)	1.2186(13)		
O(4)-C(14)	1.3457(14)	C(5)-O(1)-C(6)	117.41(9)
O(4)-C(15)	1.4438(16)	C(14)-O(4)-C(15)	115.32(10)
O(5)-C(14)	1.2036(14)	C(2)-C(1)-C(21)	121.54(11)
C(1)-C(2)	1.3828(16)	C(2)-C(1)-H(1)	118.7(7)
C(1)-C(21)	1.3997(16)	C(21)-C(1)-H(1)	119.8(7)
C(1)-H(1)	1.006(12)	C(1)-C(2)-C(4)	118.97(11)
C(2)-C(4)	1.3963(16)	C(1)-C(2)-C(3)	121.17(11)
C(2)-C(3)	1.5069(17)	C(4)-C(2)-C(3)	119.86(11)
C(3)-H(3A)	0.967(14)	C(2)-C(3)-H(3A)	109.9(8)
C(3)-H(3B)	0.963(16)	C(2)-C(3)-H(3B)	111.4(9)
C(3)-H(3C)	0.980(15)	H(3A)-C(3)-H(3B)	109.7(12)
C(4)-C(5)	1.3783(16)	C(2)-C(3)-H(3C)	111.9(9)
C(4)-H(4)	0.958(11)	H(3A)-C(3)-H(3C)	108.7(12)
C(5)-C(7)	1.4037(15)	H(3B)-C(3)-H(3C)	105.1(12)
C(6)-H(6A)	0.978(12)	C(5)-C(4)-C(2)	120.19(11)
C(6)-H(6B)	0.973(12)	C(5)-C(4)-H(4)	119.0(7)
C(6)-H(6C)	0.999(13)	C(2)-C(4)-H(4)	120.8(7)
C(7)-C(21)	1.3926(16)	O(1)-C(5)-C(4)	124.44(10)
C(7)-C(8)	1.5051(16)	O(1)-C(5)-C(7)	114.64(10)
C(8)-C(9)	1.5034(16)	C(4)-C(5)-C(7)	120.92(11)
C(8)-H(8A)	0.993(13)	O(1)-C(6)-H(6A)	105.1(7)
C(8)-H(8B)	0.996(13)	O(1)-C(6)-H(6B)	110.4(7)
C(9)-C(10)	1.5144(16)	H(6A)-C(6)-H(6B)	110.7(10)
C(10)-C(11)	1.5546(16)	O(1)-C(6)-H(6C)	111.8(7)
C(10)-C(19)	1.5679(16)	H(6A)-C(6)-H(6C)	110.0(10)
C(10)-H(10)	0.982(11)	H(6B)-C(6)-H(6C)	108.8(10)
C(11)-C(12)	1.5377(16)	C(5)-C(7)-C(21)	119.20(11)
C(11)-C(13)	1.5525(16)	C(5)-C(7)-C(8)	118.20(10)
C(11)-C(16)	1.5420(16)	C(21)-C(7)-C(8)	122.58(10)
C(12)-H(12A)	0.986(12)	C(7)-C(8)-C(9)	115.21(10)
C(12)-H(12B)	1.025(12)	C(7)-C(8)-H(8A)	112.9(8)
C(12)-H(12C)	0.993(12)	C(9)-C(8)-H(8A)	106.4(7)
C(13)-C(14)	1.5018(16)	C(7)-C(8)-H(8B)	109.6(8)
C(13)-H(13A)	0.986(12)	C(9)-C(8)-H(8B)	105.9(8)
C(13)-H(13B)	0.957(11)	H(8A)-C(8)-H(8B)	106.3(11)
C(15)-H(15A)	0.969(14)	O(2)-C(9)-C(10)	124.61(11)
C(15)-H(15B)	0.980(15)	O(2)-C(9)-C(8)	120.35(11)
C(15)-H(15C)	0.989(15)	C(10)-C(9)-C(8)	115.03(10)
C(16)-C(17)	1.4999(17)	C(9)-C(10)-C(11)	115.52(10)
C(16)-H(16A)	0.980(12)	C(9)-C(10)-C(19)	107.82(9)
C(16)-H(16B)	0.982(12)	C(11)-C(10)-C(19)	118.21(9)
C(17)-C(18)	1.5039(17)	C(9)-C(10)-H(10)	104.1(6)
C(18)-C(19)	1.5492(16)	C(11)-C(10)-H(10)	105.7(6)
C(18)-H(18A)	0.966(12)	C(19)-C(10)-H(10)	103.8(6)
C(18)-H(18B)	0.996(12)	C(12)-C(11)-C(10)	108.53(9)
C(19)-C(21)	1.5357(15)	C(12)-C(11)-C(13)	110.46(10)
C(19)-C(20)	1.5424(16)	C(10)-C(11)-C(13)	112.81(9)

C(12)-C(11)-C(16)	108.40(10)
C(10)-C(11)-C(16)	107.36(9)
C(13)-C(11)-C(16)	109.15(10)
C(11)-C(12)-H(12A)	109.5(7)
C(11)-C(12)-H(12B)	110.2(7)
H(12A)-C(12)-H(12B)	109.2(9)
C(11)-C(12)-H(12C)	109.5(7)
H(12A)-C(12)-H(12C)	108.7(10)
H(12B)-C(12)-H(12C)	109.7(9)
C(14)-C(13)-C(11)	113.64(10)
C(14)-C(13)-H(13A)	104.7(7)
C(11)-C(13)-H(13A)	110.9(7)
C(14)-C(13)-H(13B)	108.1(7)
C(11)-C(13)-H(13B)	109.4(7)
H(13A)-C(13)-H(13B)	110.0(10)
O(5)-C(14)-O(4)	122.87(11)
O(5)-C(14)-C(13)	125.55(12)
O(4)-C(14)-C(13)	111.58(10)
O(4)-C(15)-H(15A)	107.3(8)
O(4)-C(15)-H(15B)	109.3(9)
H(15A)-C(15)-H(15B)	110.0(12)
O(4)-C(15)-H(15C)	110.6(8)
H(15A)-C(15)-H(15C)	111.5(12)
H(15B)-C(15)-H(15C)	108.1(12)
C(17)-C(16)-C(11)	110.67(10)
C(17)-C(16)-H(16A)	108.5(7)
C(11)-C(16)-H(16A)	111.5(7)
C(17)-C(16)-H(16B)	108.4(7)
C(11)-C(16)-H(16B)	107.5(7)
H(16A)-C(16)-H(16B)	110.2(9)
O(3)-C(17)-C(18)	122.40(11)
O(3)-C(17)-C(16)	122.92(11)
C(18)-C(17)-C(16)	114.67(11)
C(17)-C(18)-C(19)	113.93(10)
C(17)-C(18)-H(18A)	109.0(7)
C(19)-C(18)-H(18A)	110.2(7)
C(17)-C(18)-H(18B)	105.8(7)
C(19)-C(18)-H(18B)	109.9(7)
H(18A)-C(18)-H(18B)	107.8(9)
C(21)-C(19)-C(20)	106.90(9)
C(21)-C(19)-C(18)	110.43(9)
C(20)-C(19)-C(18)	108.92(10)
C(21)-C(19)-C(10)	107.65(9)
C(20)-C(19)-C(10)	113.48(10)
C(18)-C(19)-C(10)	109.42(9)
C(19)-C(20)-H(20A)	108.7(7)
C(19)-C(20)-H(20B)	111.1(7)
H(20A)-C(20)-H(20B)	107.8(10)
C(19)-C(20)-H(20C)	112.4(7)
H(20A)-C(20)-H(20C)	107.0(10)
H(20B)-C(20)-H(20C)	109.7(10)
C(1)-C(21)-C(7)	119.14(11)
C(1)-C(21)-C(19)	121.02(10)
C(7)-C(21)-C(19)	119.82(10)

Table 4. Anisotropic displacement parameters ($Å^2 x\ 10^4$) for DCB11 (CCDC 201187). The anisotropic displacement factor exponent takes the form: $-2\pi^2 [h^2 a^{*2} U^{11} + ... + 2 h k a^* b^* U^{12}]$

	U^{11}	U^{22}	U^{33}	U^{23}	U^{13}	U^{12}
O(1)	179(5)	129(4)	246(5)	-34(4)	5(4)	-8(3)
O(2)	175(5)	198(5)	252(5)	-10(4)	-23(4)	19(4)
O(3)	239(5)	164(5)	340(5)	-50(4)	-12(4)	-28(4)
O(4)	181(5)	202(5)	316(5)	-22(4)	1(4)	57(4)
O(5)	270(5)	197(5)	396(6)	-85(4)	44(4)	-6(4)
C(1)	170(6)	162(6)	152(6)	-5(5)	26(5)	-28(5)
C(2)	160(6)	188(7)	140(6)	12(5)	29(5)	5(5)
C(3)	165(7)	220(8)	302(8)	-28(7)	7(6)	13(6)
C(4)	189(7)	140(6)	158(6)	10(5)	43(5)	31(5)
C(5)	176(6)	159(6)	118(6)	-7(5)	29(5)	-31(5)
C(6)	223(8)	142(7)	237(7)	-9(6)	13(6)	-2(6)
C(7)	145(6)	157(6)	123(6)	7(5)	31(5)	4(5)
C(8)	162(7)	168(7)	209(7)	-33(6)	8(5)	0(5)
C(9)	142(6)	161(6)	161(6)	30(5)	48(5)	-18(5)
C(10)	151(6)	128(6)	143(6)	26(5)	21(5)	7(5)
C(11)	173(6)	128(6)	153(6)	1(5)	32(5)	14(5)
C(12)	202(7)	167(7)	216(7)	13(6)	73(6)	27(6)
C(13)	185(7)	159(7)	171(7)	4(5)	29(5)	13(5)
C(14)	209(7)	164(7)	163(6)	30(5)	19(5)	19(5)
C(15)	218(8)	287(9)	419(10)	-13(7)	64(7)	94(7)
C(16)	241(7)	145(7)	153(7)	-7(5)	26(5)	29(5)
C(17)	203(7)	172(7)	130(6)	-11(5)	-53(5)	9(5)
C(18)	158(7)	159(7)	206(7)	-1(5)	4(5)	-17(5)
C(19)	139(6)	125(6)	166(6)	0(5)	15(5)	-6(5)
C(20)	196(7)	182(7)	201(7)	18(5)	58(6)	0(6)
C(21)	162(6)	150(6)	114(6)	8(5)	37(5)	3(5)

Table 5. Hydrogen coordinates (x 10^4) and isotropic displacement parameters ($Å^2$x 10^3) for DCB11 (CCDC 201187).

	x	y	z	U_{iso}
H(1)	11324(13)	7813(10)	1530(6)	16(3)
H(3A)	13385(15)	6538(12)	1604(7)	35(4)
H(3B)	13289(17)	5469(13)	1039(9)	50(5)
H(3C)	13068(16)	5243(13)	1865(9)	48(5)
H(4)	10635(12)	4351(10)	941(6)	13(3)
H(6A)	7338(14)	2849(10)	357(7)	21(3)
H(6B)	8556(13)	3077(10)	1078(7)	18(3)
H(6C)	9048(14)	3171(10)	254(7)	19(3)
H(8A)	6202(14)	6529(11)	77(8)	29(4)
H(8B)	5944(15)	6062(11)	886(7)	33(4)
H(10)	6980(11)	7914(9)	1856(6)	9(3)
H(12A)	4310(12)	9821(10)	2363(6)	17(3)
H(12B)	3867(14)	8942(10)	1643(7)	22(3)
H(12C)	4927(13)	8491(11)	2410(7)	20(3)
H(13A)	6623(14)	10898(10)	997(6)	18(3)
H(13B)	5112(12)	10214(10)	719(6)	12(3)
H(15A)	1440(17)	12099(12)	1419(8)	38(4)
H(15B)	2664(16)	13060(13)	1277(8)	43(4)
H(15C)	2744(16)	12466(12)	2086(9)	44(4)
H(16A)	6816(13)	10804(10)	2604(6)	16(3)
H(16B)	7366(13)	9478(10)	2792(7)	18(3)
H(18A)	10357(14)	9583(10)	1663(6)	16(3)
H(18B)	9741(13)	8799(10)	2285(7)	22(3)
H(20A)	9509(15)	9153(10)	304(7)	26(3)
H(20B)	7759(14)	8917(10)	69(7)	22(3)
H(20C)	8331(13)	10112(11)	498(6)	21(3)

CHAPTER THREE

Current Approaches to the Synthesis of Zoanthenol: Synthesis of the ABC Ring System Containing All of the Quaternary Stereocenters[†]

3.1 Revised Retrosynthetic Plan

Our early efforts outlined an expeditious synthesis of the ABC rings of zoanthenol. However, selective late-stage alkylation to form the final quaternary stereocenter proved difficult by a number of strategies. As a result, we decided to alter our retrosynthetic analysis to incorporate the formation of the C(9) quaternary stereocenter early in the synthesis (Scheme 3.1). We envisioned that with the vicinal C(9) and C(22) stereocenters established, we would be able to apply our previously developed methods for cyclization, either S_N' cyclization or Friedel-Crafts type conjugate addition, to directly generate a zoanthenol ABC ring system with all three quaternary centers. In accordance with this plan, we targeted alkyne **186** as an intermediate. Retrosynthetic disconnection of the C(1)-C(6) fragment of alkyne **186** was envisioned to occur by addition of the anion of alkyne **187** into caprolactam **123**. Caprolactam **123** was a previously projected intermediate and had been already synthesized in our laboratories.[1] ABC ring fragment **187** would be simplified to enone **188** via one of our cyclization methods. Using methods analogous to those demonstrated in Chapter Two, enone **188** would be reduced in complexity to ketone **190**. Oxidation state adjustment and a one-carbon homologation of *meso*-anhydride **191** could afford ketone **190**. We targeted *meso*-anhydride **191** as an opportunity to generate enantioenriched intermediates by desymmetrization. Finally, *meso*-anhydride **191** could arise via a Diels-Alder reaction of

[†] This work was performed in collaboration with Ms. Jennifer Stockdill, a graduate student in the Stoltz group.

1,4-oxygenated diene **192** and 2,3-dimethylmaleic anhydride (DMMA, **193**). Although challenging, such a Diels-Alder reaction would generate both the C(9) and C(22) quaternary stereocenters in a single step with reliable relative stereochemistry.

Scheme 3.1 Revised Retrosynthetic Plan for Zoanthenol

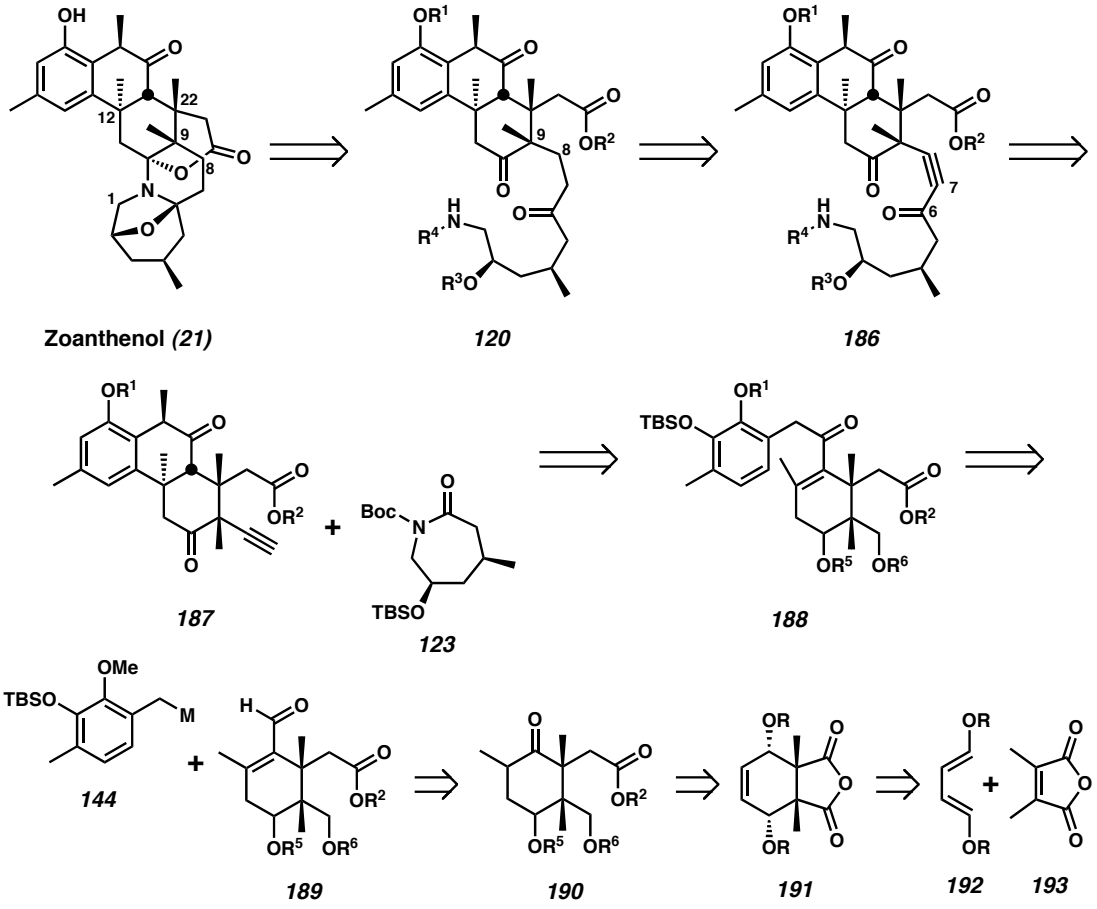

3.2 Synthesis of a C Ring Synthon Containing Vicinal Quaternary Stereocenters

3.2.1 *Diels-Alder Reactions of DMMA*

The preceding plan relies on a Diels-Alder reaction of DMMA. Such reactions are rare and difficult to accomplish.[2] However, the difficulty of generating compounds containing vicinal quaternary stereocenters with predictable relative stereochemistry has

stimulated significant work on the problem of DMMA Diels-Alder reactions. In particular, sulfur heterocycle **195** has been developed as a surrogate for DMMA (Scheme 3.2).[3] The sulfur atom is believed to constrain what would be the methyl groups in DMMA, making them both sterically smaller and less electron donating to the olefin. Dihydrothiophene **195** has been successfully applied in an elegant Diels-Alder strategy to synthesize cantharidin, where DMMA failed to react.[4] It's noteworthy that diydrothiophene **195** still required extremely high pressure (15 kbar) to successfully react with furan.

Scheme 3.2 Dauben's Synthesis of Cantharidin

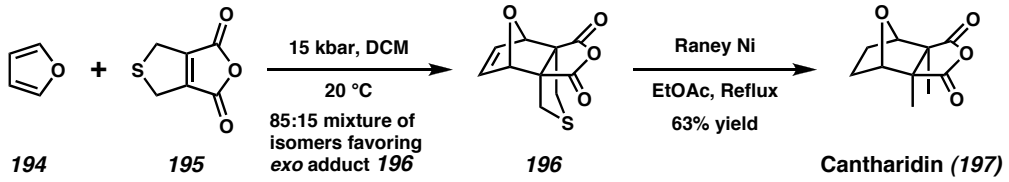

Despite these difficulties, we were encouraged by Danishefsky and Birman's use of a DMMA Diels-Alder reaction in their recent synthesis of merrilactone A (Scheme 3.3).[5] The first step of their synthesis combines oxygenated diene **198** and DMMA in good yield. We hoped to react an even more electron rich 1,4-dioxygenated diene **200**[6] in a similar manner to give the *meso*-Diels-Alder adduct **201**. However, despite the similarity of the reactions, less than 20% yield of Diels-Alder adducts were produced under thermal conditions. This yield of Diels-Alder adducts consisted of similar amounts of three diastereomers. Furthermore, NMR studies with 1,4-dioxygenated diene **200**

showed that isomerization of olefin geometry was favorable and occurred faster than the Diels-Alder reaction. As a result, the use of diene **200** seemed impractical.

Scheme 3.3 Diels-Alder Reactions of DMMA

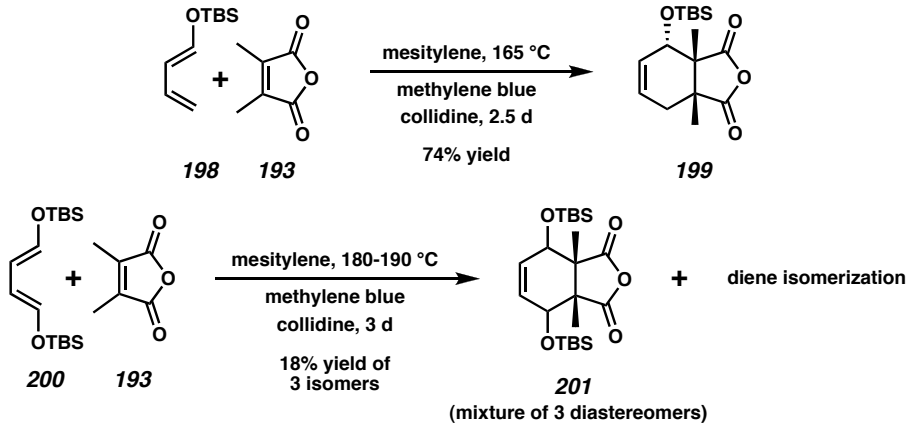

3.2.2 *Advancing Danishefsky's DMMA Diels-Alder Adduct*

Alternatively, we decided to advance Danishefsky's Diels-Alder adduct **199**. Rather than desymmetrize a bisoxygenated Diels-Alder adduct (i.e., **201**), our strategy was to deprotect silyl ether **199** and eliminate it to a *meso*-diene (i.e., **203**) anhydride suitable for desymmetrization. We were encouraged to find the reaction that Danishefsky reported between silyloxy diene **198**[7] and DMMA[8] to be highly reproducible and amenable to scale (Scheme 3.4). Typically, we carried out the reaction on a 0.350 mol scale to give an isolated yield of more than 70 g of *endo*-Diels-Alder product **199**. Treatment of the Diels-Alder adduct with sulfuric acid in refluxing dichloroethane caused TBS deprotection and elimination to *meso*-diene **203** in excellent yield. Additionally, significant amounts of *exo*-Diels-Alder adduct **202** were isolated in the Diels-Alder reaction and underwent elimination to *meso*-diene **203** under identical conditions. Unlike

Danishefsky's synthesis, our route eliminates the allylic stereocenter, thus the *exo*-Diels-Alder adduct **202** improved the overall throughput of the route. With diene **203** in hand, our next goal was to effectively desymmetrize it.

Scheme 3.4 Diels-Alder Route to *meso*-Diene **203**

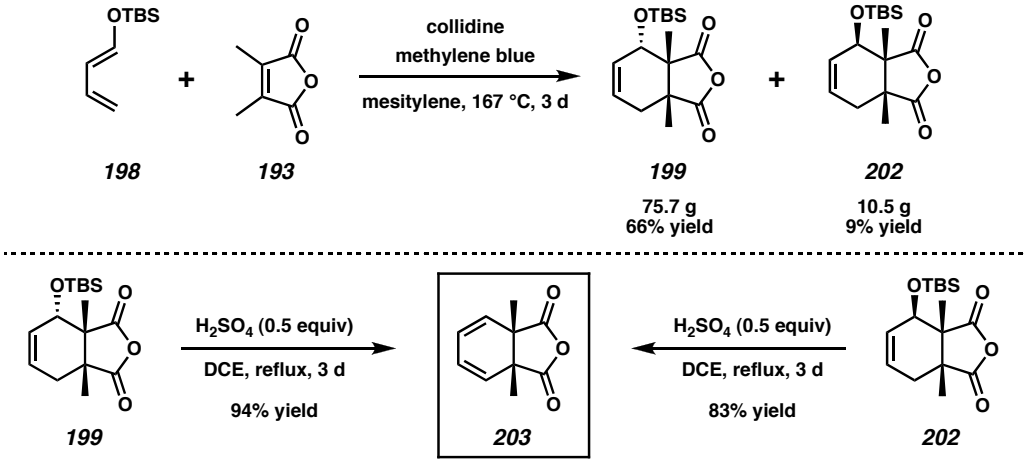

The desymmetrization of cyclic *meso*-anhydrides to chiral monoesters has been studied by Fujisawa,[9] Bolm,[10] and Deng.[11] Such asymmetric alcoholysis of cyclic anhydrides with cinchona alkaloids has been reviewed.[12] However, prior to our work this strategy had never been applied to set multiple quaternary stereocenters. To our delight, we found that with slight modifications to Bolm's conditions excellent chemical yields and good enantioselectivities could be achieved (Scheme 3.5). Typically, for material throughput purposes, we performed the reaction with catalytic quinine (**204**) and stoichiometric DBU, which gave quick conversion but racemic product. However, with judicious choice of the stoichiometric achiral base, pempidine, the reaction could be completed catalytically with good enantioselectivity (Entry 2). In general, lowering the reaction temperature did cause a significant increase in ee, but also drastically increased

reaction time. Because some of the potential routes we considered to complete zoanthenol reorient monoester **205**, it is noteworthy that the use of quinidine (**206**) provides access to the opposite enantiomer obtained from quinine with similar ee (Entry 3). Additionally, we have found that menthol derivatives **207** and **208** give superior chiral induction.[13] To date, our best results are from quinine derivative **208**, which gave monoester **205** in 85% ee (Entry 5). Likely we will be able to increase the ee of this material by recrystallization. To our knowledge, this is the first desymmetrization of an anhydride to set the absolute configuration of vicinal quaternary stereocenters and is one of only a handful methods available to do so.

Scheme 3.5 Desymmetrization of *meso*-Anhydride **203**

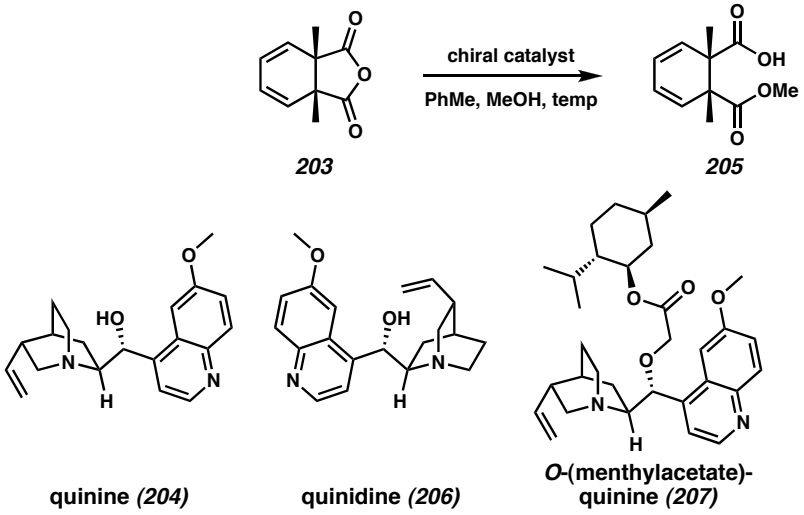

Entry	Chiral Controller (mol%)	Other Conditions	Temperature (°C)	Time (d)	Sign of Rotation	%ee (% yield)
1	*204* (105)	MeOH (5 equiv)	22	0.3	–	50
2	*204* (10)	MeOH (3 equiv) pempidine (1 equiv) 50% CCl_4 v/v	-50	18	–	70 (88)
3	*206* (100)	MeOH (3 equiv)	-50	6	+	70
4	*207* (105)	MeOH (10 equiv)	-25	3	–	72
5	*208* (101)	MeOH (3 equiv)	-50	10	+	85

3.2.3 *C Ring Synthon Reoxygenation*

Due to the difficulty of performing the DMMA Diels-Alder reaction with a 1,4-dioxygenated diene and our desire to desymmetrize a *meso*-diene, we were faced with the problem of reoxygenating the C ring (Scheme 3.6). Selenolactonization and halolactonization were both explored. Classical iodolactonization conditions proved most advantageous, giving predominantly a single iodolactone isomer by the end of the reaction.[14] Typically, the reaction was performed as a two-step sequence without purification of the intermediate monoester **205**. The bridged bicyclic nature of iodolactone **209** hinders S_N2 displacement of the iodide from the concave face, but is well disposed for S_N2' displacement. Treatment of iodolactone **209** with silver (I) acetate in pyridine at 35 °C afforded selectively S_N2' displacement to give allylic acetate **210** with the desired 1,4 oxygenation pattern. Selective acetate cleavage from bicyclic lactone **211** was accomplished by brief treatment with potassium carbonate in methanol. The stereochemical course of this sequence was confirmed by X-ray structure determination of allylic alcohol **211**. This efficient three-step sequence achieves stereospecific 1,4-reoxygenation of the C ring synthon and has proved robust and amenable to scale. Allylic alcohol **211** represents an important branch point in our synthetic efforts. Several increasingly functionalized C ring equivalents were derived from allylic alcohol **211**.

Scheme 3.6 Installation of 1,4-Oxygenation on Diene **203**

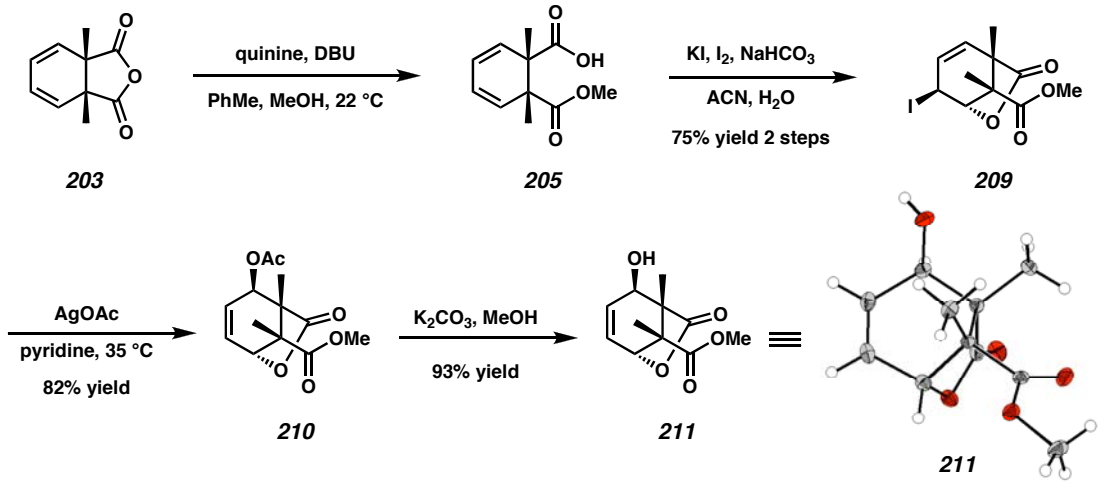

203 ***205*** ***209*** ***210*** ***211*** ***211***

3.3 The Lactone C Ring Synthon Approach

3.3.1 *Completion of the Lactone C Ring Synthon*

The most straightforward elaboration of allylic alcohol **211**, namely leaving its ester and lactone functionality unmodified, gave us speedy access to molecules containing coupled A and C ring synthons. In turn, we could quickly begin experimentation with key B ring cyclization reactions. The sequence began with the conversion of allylic alcohol **211** to ketone **212** (Scheme 3.7). In theory, this transformation could be achieved by transition metal-catalyzed olefin isomerization. Isomerizations were attempted with a large number of catalysts, but all showed insufficient reactivity.[15] In practice, a two-step procedure consisting of manganese (IV) oxide oxidation and olefin reduction to give ketone **212** was superior. Direct methylation of ketone **212** with LDA and methyl iodide in THF consistently gave a surprising mixture of bismethylation and the starting ketone **212**. As a result, a two-step protocol of methylene installation with *N*,*N*,*N*',*N*'-tetramethyldiaminomethane and hydrogenation

with Adams catalyst gave good yields of separable methyl ketones **213**. Triflate formation from both methyl ketone diastereomers occurred under standard conditions. Unfortunately, enol triflate **214** failed to undergo carbonylation when submitted to the one-step palladium-catalyzed carbonylation conditions we developed for hindered enol triflates.[16] However, Stille coupling of enol triflate **214** with vinyl tributyltin followed by oxidative cleavage by osmium (VIII) tetroxide and sodium periodate did afford acceptable yields of enal **216**.

Scheme 3.7 Elaboration to the Complete Lactone C Ring Synthon.

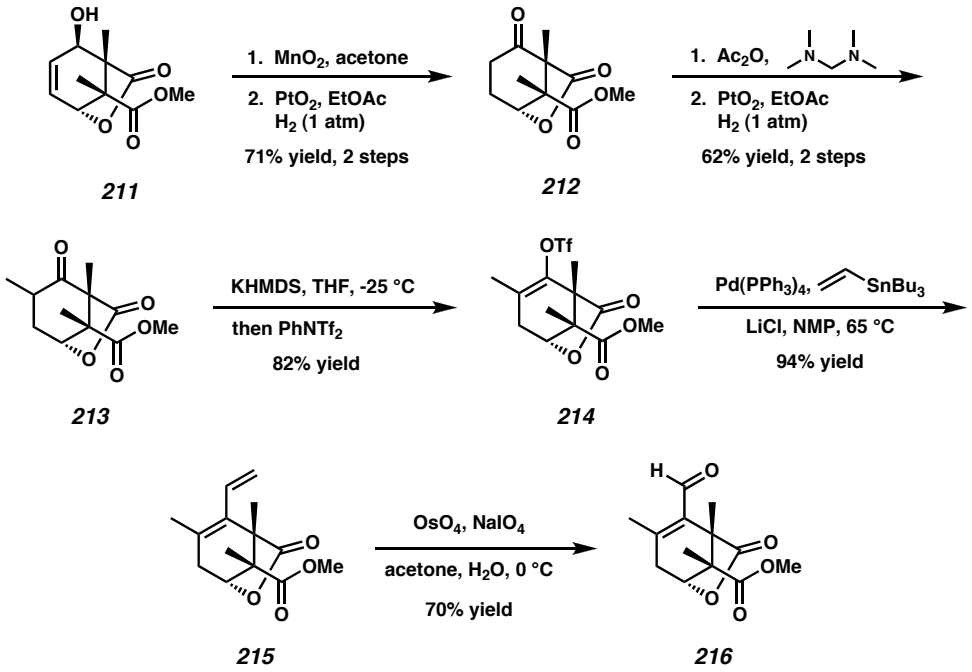

3.3.2 *A and C Ring Fragment Coupling*

Coupling of enal **216** with the A ring Grignard reagent **154** proved more difficult than anticipated (Scheme 3.8). Enal **216** was insoluble in the methylene chloride/ethyl ether mixtures that were found to give good diastereoselectivity for allylic alcohol **155** in

Chapter Two. Enal **216** did not undergo 1,2-addition when not dissolved. A large amount of tetrahydrofuran was required to dissolve enal **216** and, under those conditions, addition strongly favored the formation of allylic alcohol **217**, corresponding to the diastereomeric series at C(20), which did not undergo S_N' cyclization when exposed to TFA.[16] The assignment of allylic alcohol **217**'s C(20) stereocenter was made initially by comparison to ^{1}H NMR splitting patterns in allylic alcohol **155** and later confirmed by X-ray structure determination. Allylic alcohol **217** underwent smooth oxidation with Dess-Martin periodinane to give enone **218**. Attempts to generate allylic alcohol **219** for S_N' cyclization by either Mitsunobu inversion or reduction of enone **218** were unsuccessful.[17] As a result, S_N' cyclization strategy was not accessible with the lactone C ring synthon.

Scheme 3.8 Grignard Addition

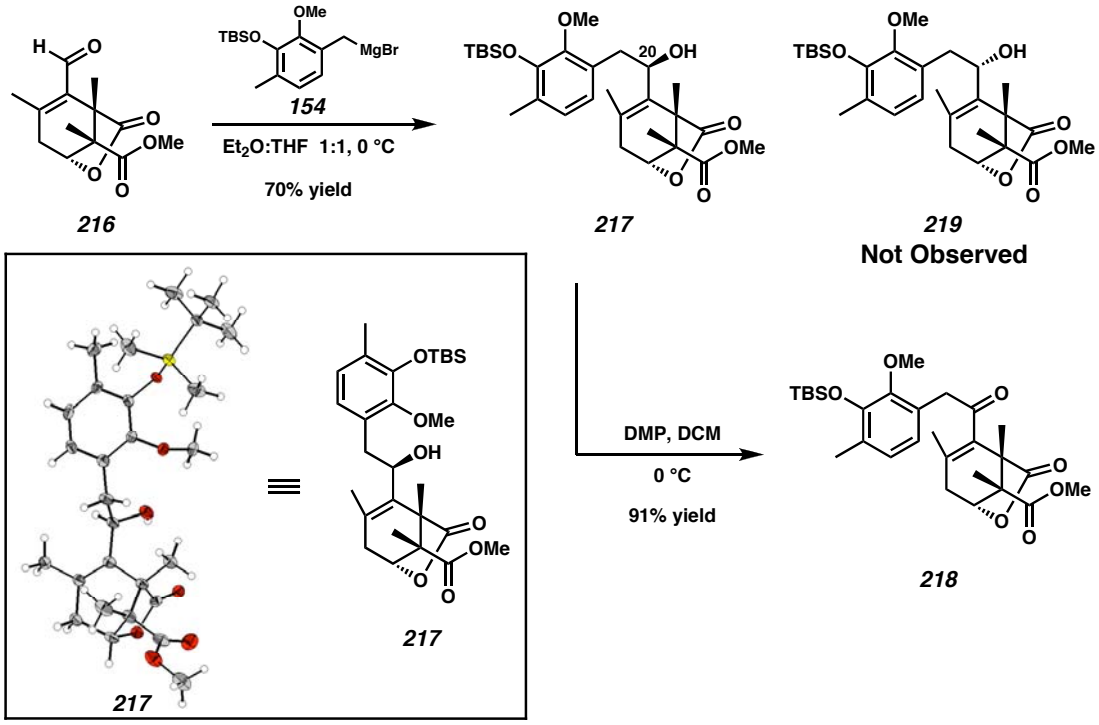

3.3.3 *Cyclization By Friedel-Crafts Conjugate Addition*

A number of Lewis and Brønsted acidic conditions are known to promote intramolecular conjugate addition of electron rich arenes into enones.[18] Enone **218** underwent only loss of the TBS group and decomposition when treated with TFA at 110 °C, $AlCl_3$ in toluene at 100 °C, or polyphosphoric acid at 100 °C. However, when treated with a mixture of formic acid and 85% phosphoric acid, enone **218** underwent an interesting cyclization reaction to afford the unusual caged bisacetoxyacetal **220** in 47% yield. Unfortunately, bisacetoxyacetal **220** exhibited the undesired relative stereochemistry between the newly formed C(12) stereocenter and the other quaternary stereocenters (C(9) and C(22)) as determined by X-ray structure analysis.

Scheme 3.9 Acid-Mediated Cyclization

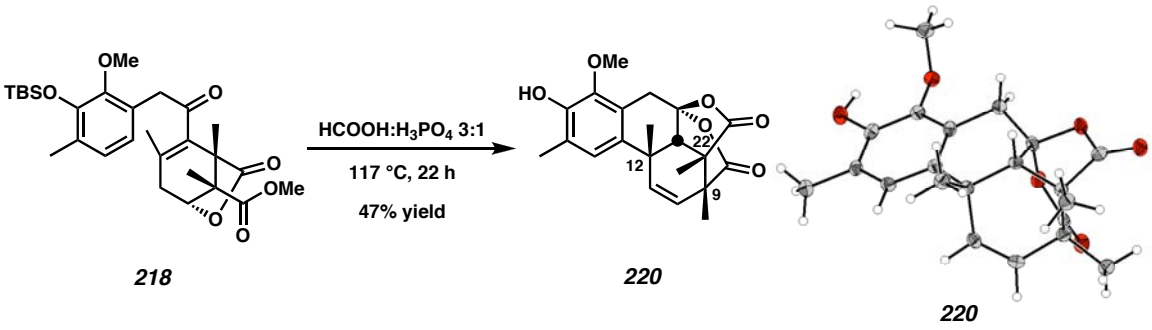

Unique to the formic acid/phosphoric acid conditions was an elimination to give the C(11)-C(12) olefin. This was likely crucial to the mechanism of the successful conjugate addition (Scheme 3.10). The formation of extended enol **221** may trigger the elimination of the carboxylic acid to give extended enone **222**. Protonation of enone **222** leads to resonance form **224**, which stabilizes the positive charge as a tertiary allylic

carbocation. The increased contribution of this resonance form encourages conjugate addition and explains the lack of cyclization in cases where no elimination took place. The complete selectivity for bisacetoxyacetal **220**, with the undesired C(12) stereochemistry, suggests that some preorganization involving the ketone moiety guides the outcome of the cyclization. Possibilities for preorganization include intramolecular hydrogen bonding (structure **225**) or hemiacetal formation (structure **226**). Encouraged by the bond-forming reactivity, we hoped to design a substrate that was disposed to generate the desired C(12) stereochemistry.

Scheme 3.10 Possible Mechanism for Enone Cyclization

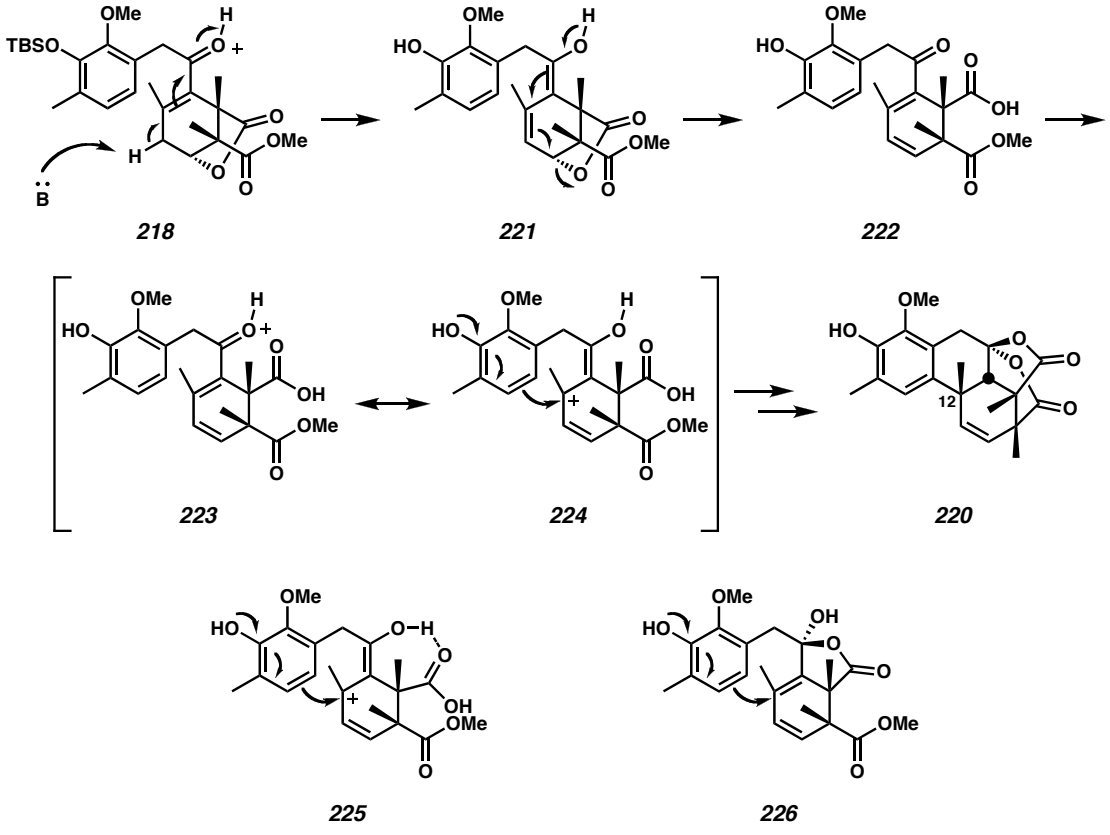

3.4 Studies Toward Elaborated C Ring Synthons

3.4.1 *Elaboration of Intermediate Allylic Alcohol **211***

Our attempts to synthesize more advanced substrates for cyclization had two goals: first, to better differentiate the lactone and methyl ester functionality in allylic alcohol **211** before cyclization, and second, to bias the cyclization toward the desired stereochemistry of the benzylic quaternary center. We began with intermediate allylic alcohol **211**, which was readily protected with TBSOTf to give silyl ether **227** (Scheme 3.11). Less reactive silylating agents (e.g., TBSCl) failed to give complete conversion to silyl ether **227** and demonstrated the challenges of performing even simple manipulations at neopentyl sites. Reduction of silyl ether **227** with LAH in THF afforded triol **228** in 83% yield over two steps. Differential protection of the triol presented a number of challenges. Strongly acidic conditions for acetonide formation removed the silyl protecting group. Anhydrous copper (II) sulfate in acetone showed good reactivity but gave a surprising mixture of 1,3-dioxepane **229** and acetonide **230**.[19,20] Although 1,3-dioxolane **230** is shown as the major product of the reaction, the ratio of the two products varied significantly.[21] While this mixture of products might seem undesirable on first consideration, both modes of protection proved useful in further elaboration.

Scheme 3.11 C Ring Elaboration

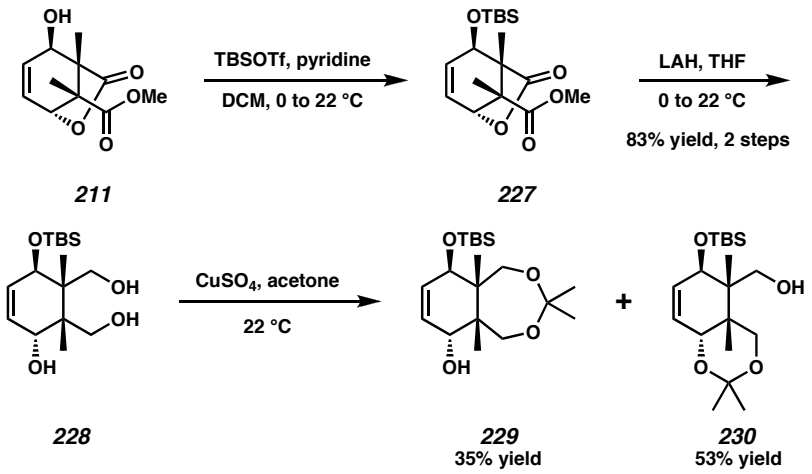

3.4.2 *Development of the 1,3-Dioxepane Containing C Ring Synthon*

1,3-Dioxepane **229** offered a serendipitous opportunity to construct a C ring fragment capable of elaboration to zoanthenol. Although we typically depict 1,3-dioxepane as enantiomer **229**, we have equally ready access to enantiomer **231** from our desymmetrization process (Scheme 3.12). When rotated by 180°, enantiomer **231** suggests the orientation of the C(9) and C(22) quaternary stereocenters shown. This perspective allowed us to construct a 1,3-dioxepane-containing C ring synthon in a manner analogous to our previous efforts with enal **145** and enal **216**. Conversion of allylic alcohol **231** to ketone **232** was accomplished in excellent yield by a two-step oxidation and hydrogenation sequence. Conventional methylation with LDA and methyl iodide afforded a combined 72% yield of separable methyl ketones **233**. Both ketone diastereomers were readily converted to triflate **234**. Pleasantly, triflate **234** was a good substrate for our palladium-catalyzed carbonylation and afforded a 65% yield of enal **235**, with the remaining material recovered as unreacted triflate.

Scheme 3.12 Completion of the 1,3-Dioxepane-Based C Ring Synthon

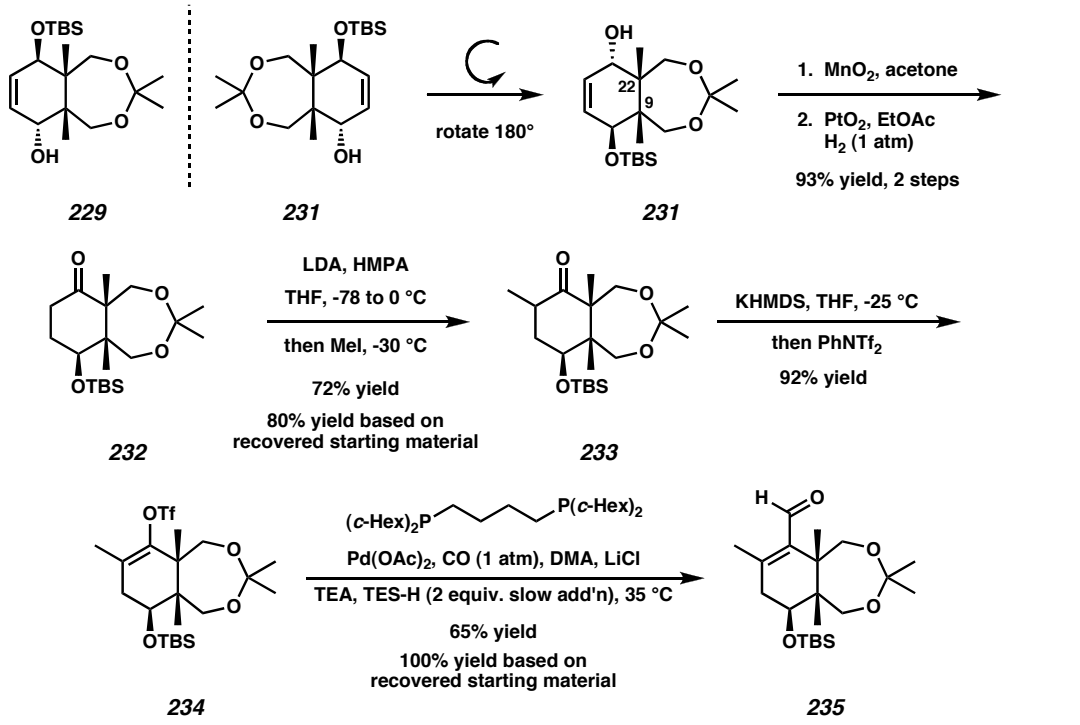

Addition of our A ring Grignard synthon gave a good yield of allylic alcohol **236** as a 10:1 mixture of diastereomers. The relative stereochemistry at C(20) of the major diastereomer was assigned by comparison of ^{1}H NMR splitting patterns. Oxidation of allylic alcohol **236** occurred without incident to give enone **237**.

Scheme 3.13 Completion of the 1,3-Dioxepane-Containing Cyclization Substrate

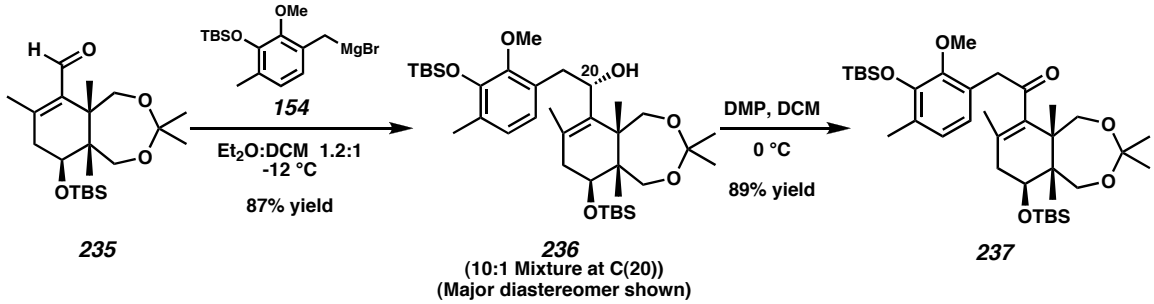

3.4.3 *Development of the 1,3-Dioxane-Containing C Ring Synthon*

Acetonide **230** was used as a starting material to develop an alternative C ring synthon (Scheme 3.14). The major advantage of this strategy was that it allowed us to consider several methods of homologation to install C(24). Hydrogenation of acetonide **230** with Adams catalyst gave clean conversion to primary alcohol **238**. This molecule had appropriately protected functionality to investigate strategies for homologation. One strategy involved oxidation of alcohol **238** to the corresponding aldehyde and reaction with various Wittig reagents. However, these reactions proved sluggish, and even with a large excess of reagents poor conversion occurred.[22] Another strategy for homologation was cyanide displacement of a leaving group. Although S_N2 displacements at neopentyl positions are difficult to achieve,[23] the opportunity to introduce C(24) in the correct oxidation state as a nitrile encouraged us to pursue the strategy. In the event, mesylation of alcohol **238** with mesyl chloride and TEA, followed immediately by treatment of the crude mesylate with potassium cyanide in DMSO at 80 °C, afforded a 76% yield of nitrile **239**.[24] This material was converted to ketone **240** by silyl ether cleavage and Swern oxidation. Intermediate ketone **240** was converted by standard means to enol triflate **241**. Unfortunately, enol triflate **241** failed to undergo palladium-catalyzed carbonylation, but was instead converted to enal **242** by Stille coupling with tributylvinyltin followed by oxidative cleavage.

Scheme 3.14 Completion of the Nitrile Homologated C Ring Synthon

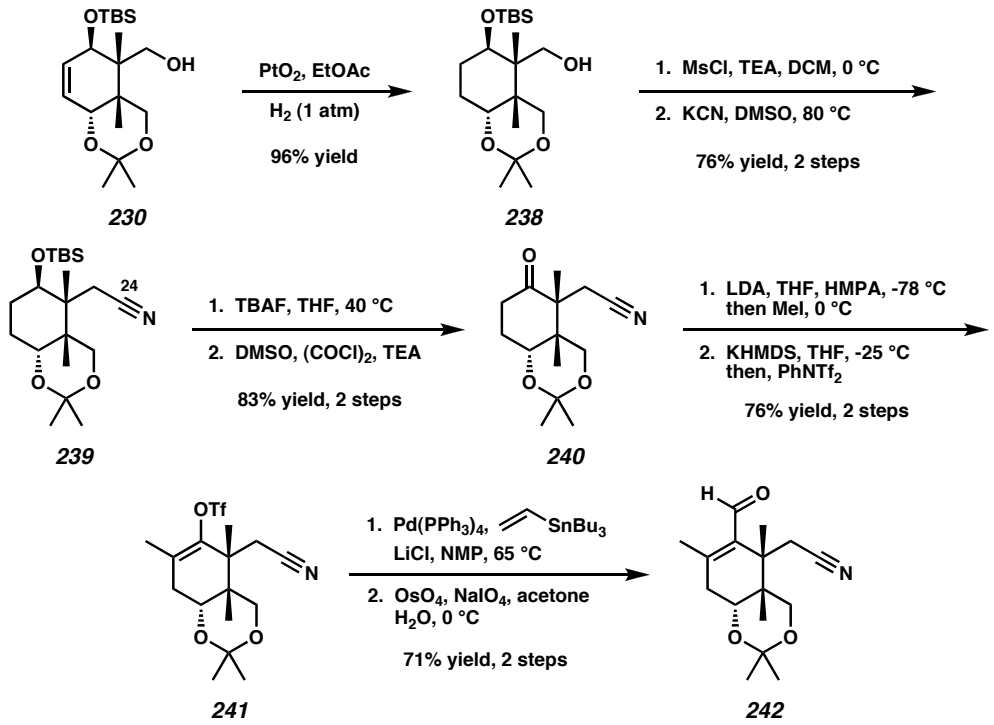

Fragment coupling with the A ring synthon and completion of enone **243** occurred as anticipated (Scheme 3.15). 1,2-Addition of Grignard reagent **154** afforded a good yield of a 3:1 mixture of diastereomeric allylic alcohols. This mixture was readily oxidized with Dess-Martin periodinane to give enone **243** in 85% yield for two steps.

Scheme 3.15 Completion of the Nitrile-Containing Cyclization Substrate

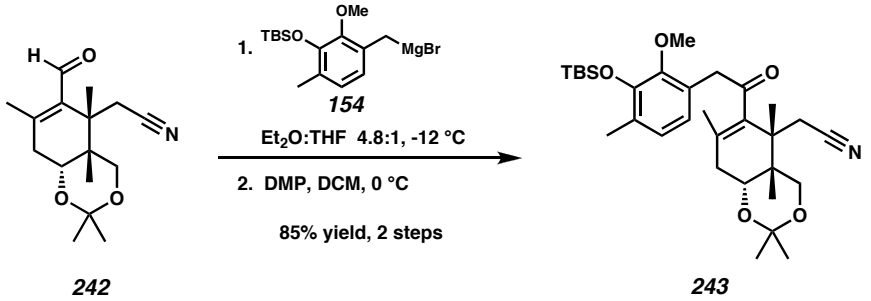

3.5 B Ring Formation Strategies for Advanced C Ring Synthons

3.5.1 *Cyclization Strategies for Substrates in the Alcohol Oxidation State at C(20)*

With ready access to several iterations of AC ring adducts, we turned our attention to finding reactions that would efficiently complete the B ring by forming the C(12)-C(13) bond. Directly inspired by our TFA-mediated cyclization of allylic alcohol **155**,[16] we attempted the same transformation with our advanced AC ring adducts (Scheme 3.16). We anticipated that the addition of the remote quaternary stereocenter at C(9) would have little impact on the reaction and that the additional alcohols deprotected during the reaction would be no more burdensome than the phenol present in the original reaction. We were disappointed to find that when either allylic alcohol **244** or acetate **245** were treated with trifluoroacetic acid at 65 °C, only a very small portion of the material exhibited an ^{1}H NMR spectra consistent with cyclization. The cyclized material represented only one of seven isolated products from the reaction, and was tentatively assigned as tetrahydrofuran **246** of the structures shown in Scheme 3.16. The low yield and likely formation of a tetrahydrofuran in structure **246** precluded the use of this strategy with 1,3-dioxepane substrates. Cyclizations of the analogous nitrile-containing AC ring adduct also failed.[25] We hypothesized that the difference in reactivity between allylic alcohols **155** and **244** might be caused by the different C(10) oxidation states. However, the C(10) ketone derived from allylic acetate **245** also failed to undergo significant S_N' cyclization.[26]

Scheme 3.16 Trifluoroacetic Acid-Mediated Cyclization

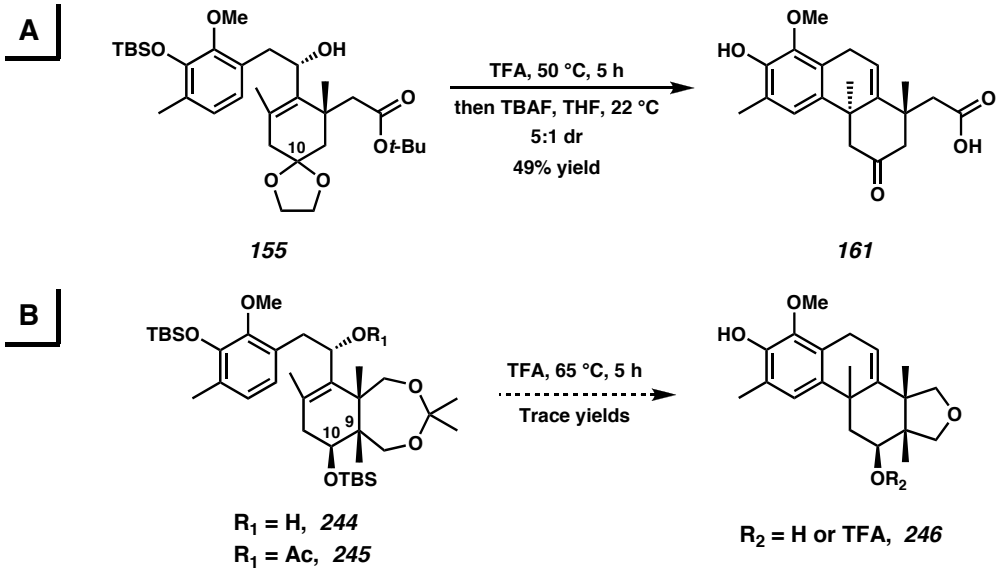

As an alternative, we explored reactions utilizing allylic leaving groups. Allylic alcohol **244** was converted to phenol acetates **247** and **248** by acylation and deprotection of the phenolic silyl group (Scheme 3.17). Fortuitously, the diastereomeric phenols were separable by column chromatography, and their relative stereochemistry was assigned by comparison to ^{1}H NMR spectra of analogous compounds.

Scheme 3.17 Derivatization and Separation of Allylic Alcohol **244**

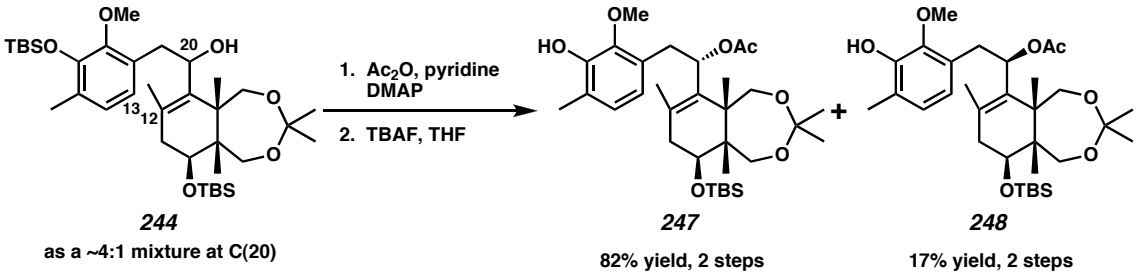

A straightforward strategy for cyclization relied on treatment of phenol acetates **247** and **248** with sodium hydride to generate phenoxides in situ (Scheme 3.18). We anticipated that these phenoxides might act as carbon nucleophiles in an S_N' process. In the event, treatment with sodium hydride in most solvents simply led to acetate cleavage near ambient temperature. However, in toluene the phenoxides did not show significant deacetylation until much higher temperatures. In the case of phenol **247**, which we anticipated would be more likely to undergo S_N' cyclization,[16] an interesting oxidative cleavage occurred to give enal **235**. No cyclization was observed for either phenoxide.

Scheme 3.18 Base-Promoted Cyclization Strategy

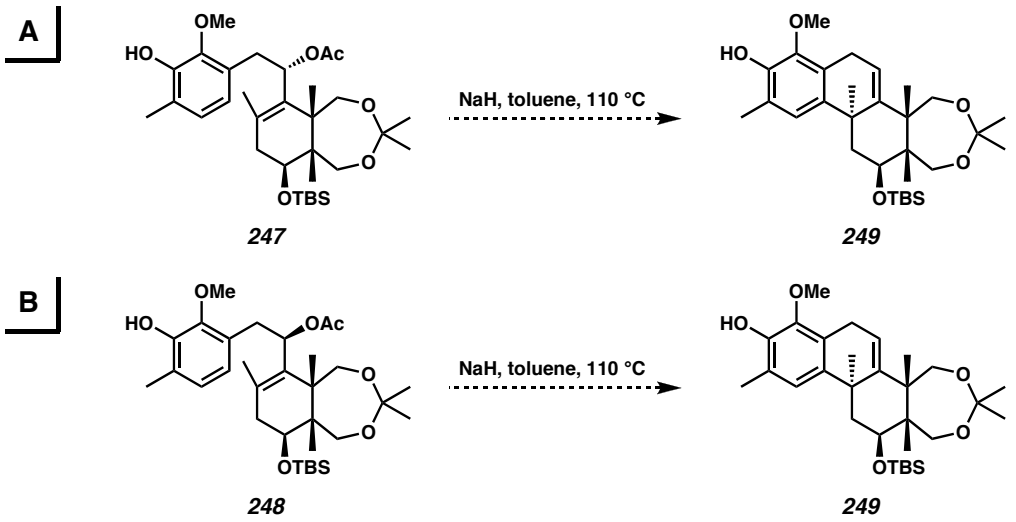

Another approach involved the use of palladium π-allyl complexes generated from the phenol acetates **247** and **248** as electrophiles (Scheme 3.19). In keeping with the double inversion mechanism of classical π-allyl chemistry, we anticipated isomer **248** would produce the desired stereochemistry at C(12).[27] Unfortunately, no evidence of oxidative addition into the allylic acetate was ever observed under any conditions. This

lack of reactivity was likely due to the number of sterically demanding substituents on the allyl portion of the molecule.

Scheme 3.19 Palladium π-Allyl Cyclization Strategy

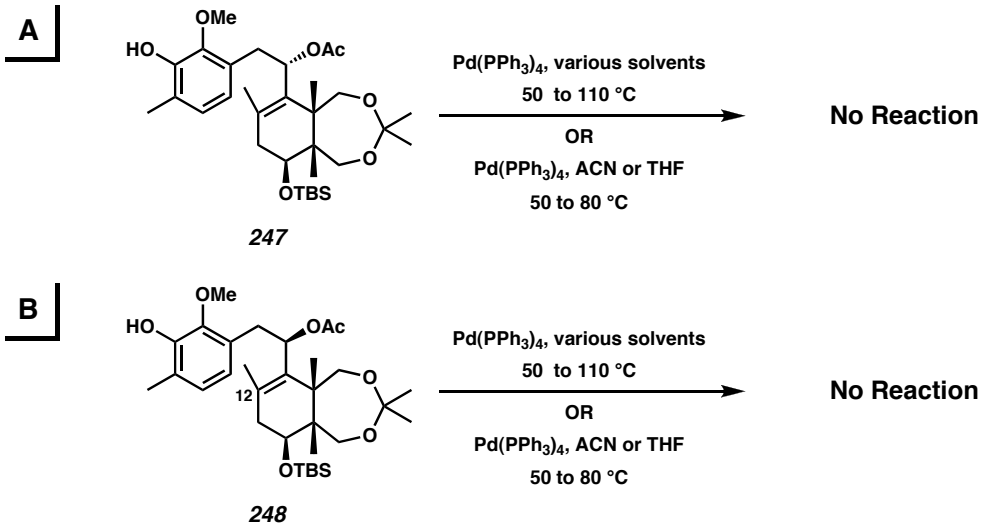

3.5.2 *Cyclization Strategies for Enone Substrates*

Another group of strategies for B ring formation used the AC ring adducts in the ketone oxidation state at C(20) as starting materials (Scheme 3.20). Upon exposure of enones **237** and **243** to trifluoroacetic acid, we anticipated elimination to form a C(10)-C(11) olefin in a manner similar to the formation of bisacetoxy acetal **220**. However, we anticipated that the different functionality of enones **237** and **243** would disrupt the preorganization of the substrate that led to the undesired stereochemistry at C(12) in bisacetoxy acetal **220**. Attempted trifluoroacetic acid cyclization of enone **237** led to a complex mixture of products. Although the majority of isolated products had ^{1}H NMR spectra consistent with cyclization, diastereoselectivity at C(12) appeared low and tetrahydrofuran formation seemed likely. Treatment of enone **243** with trifluoroacetic

acid at 60 °C led predominantly to a cyclized product, which was assigned as hemiacetal **250** by comparison to bisacetoxy acetal **220**. Unfortunately, selectivity was again obtained for the undesired C(12) stereochemistry.[28] Finally, cyclization of enone **243** with $AlCl_3$ in various solvents did not produce any cyclized products.

Scheme 3.20 Trifluoroacetic Acid-Mediated Enone Cyclizations

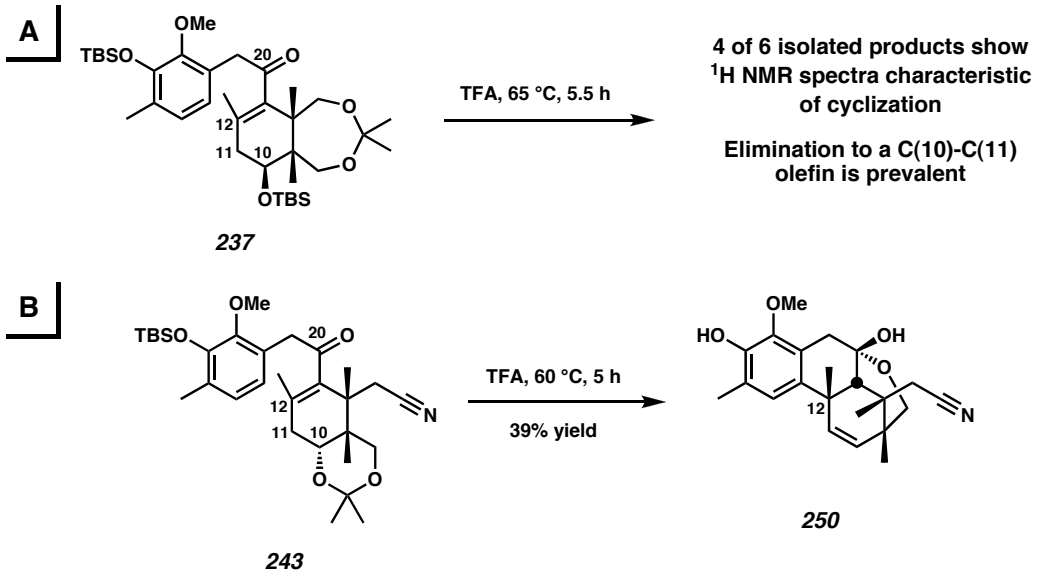

3.5.3 *Cyclization Strategies for Aryl Bromides*

In addition to cyclization strategies of our AC ring enones discussed above, we also considered cyclization strategies based on bromination of the arene nucleus at C(13) (Scheme 3.21). *N*-Bromosuccinimide (NBS) was well known to brominate *para* to electron releasing groups.[29] While there was little precedent for the superiority of silyl ethers over methoxy ethers as the directing group in this reaction, there was significant evidence that phenols were superior to methoxy ethers.[30] As a result, we carried out a three-step protocol to regioselectively produce aryl bromide **251**. Subsequently, we

found that direct bromination of enone **237** gave a favorable 4:1 mixture of bromide positional isomers in high yield. This mixture of bromide isomers was adequate for our investigations of cyclization reactions. Homologated enone **243** underwent both the regioselective three-step bromination and direct bromination with similar results to enone **237**.

Scheme 3.21 Bromination Methods for Enone **237** and **243**

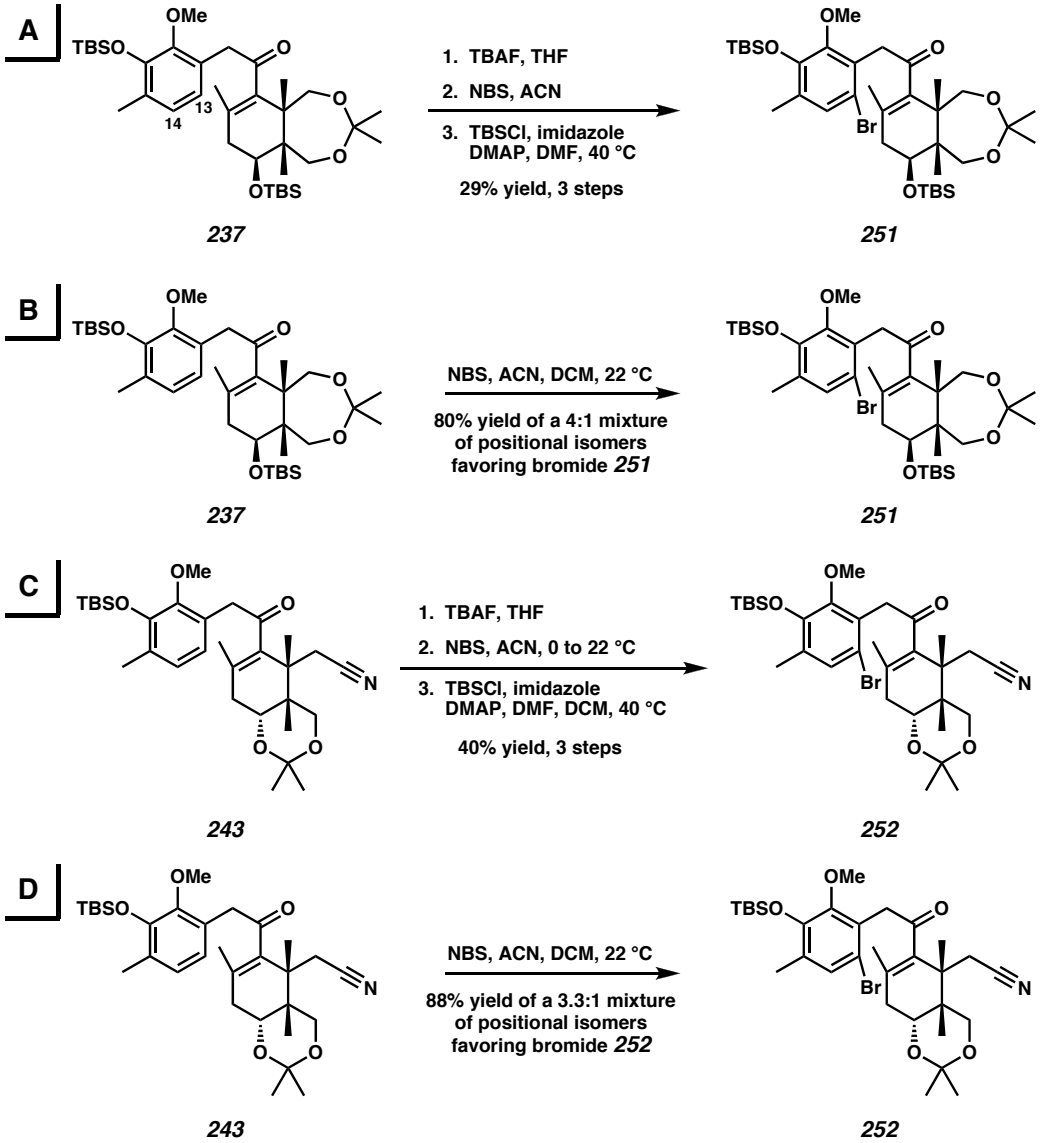

The synthesis of aryl bromides allowed us to investigate several metal-based strategies for the formation the B ring. Palladium-catalyzed 6-*exo* Heck cyclizations have been demonstrated to be efficient in forming the final bond (C(12)-C(13)) of the zoanthenol B ring.[31] In general, *exo*-Heck reactions are more favorable and much more common, but in certain cases 6-*endo* Heck cyclizations have been accomplished.[32] The intramolecular Heck reaction has been extensively reviewed.[33] We attempted 6-*endo* Heck cyclizations of bromoarene **251**, but recovered only debrominated material (Scheme 3.22).[34] Analogously, metal-halogen exchange with *tert*-butyl lithium at -78 °C was successful as judged by debromination, but the resulting anion failed to undergo conjugate addition, and led to the isolation of enone **237**.

Scheme 3.22 Heck and Metal-Halogen Exchange Strategies for Cyclization

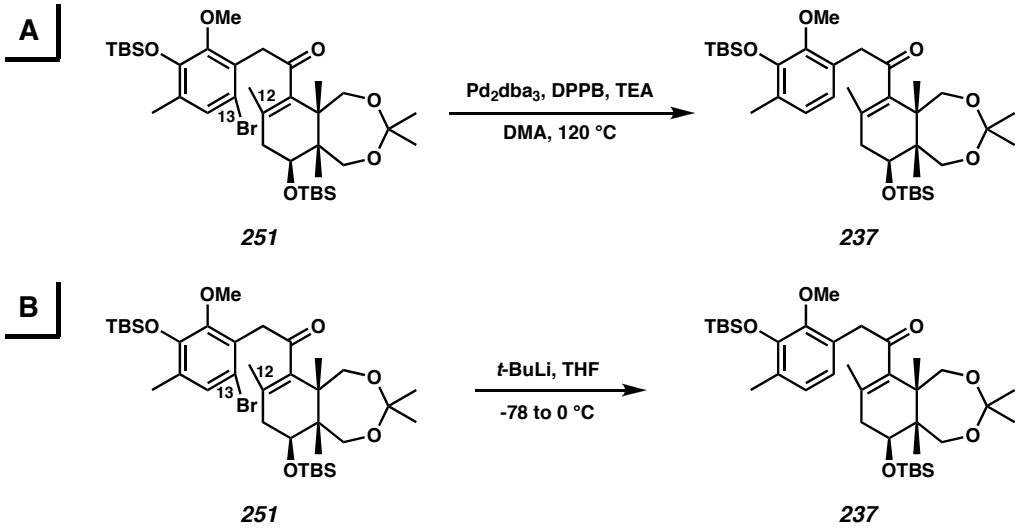

Another strategy that we investigated based on our bromoarenes was radical conjugate addition. As with Heck reactions, *endo* radical conjugate addition cyclization reactions are much less common than *exo* reactions.[35] However, a good precedent for

arene radical conjugate addition to make a quaternary center and a six-membered ring had been demonstrated.[36] To our delight, we found that in the presence of an azo radical initiator (e.g., AIBN) and a hydrogen atom donor (e.g., Bu_3SnH), aryl bromide **251** did form significant amounts of ketone **253** (Scheme 3.23). To date, our best conditions involve azo compound **254** (V-70) and slow addition of Ph_3SnH at 32 °C. In addition to the desired product, significant amounts of the debrominated enone **237** are obtained. The use of V-70 (**254**), which decomposes more readily ($t_{1/2}$ = ~10 h at 30 °C) than AIBN ($t_{1/2}$ = ~10 h at 80 °C), allows us to initiate the radical reaction at lower temperatures and reduces the amount of debrominated enone recovered. The stereochemical outcome of the radical-based cyclization was unambiguously confirmed by X-ray structure analysis of alcohol **255**, which was obtained from DIBAL-H reduction of ketone **255**.[37] While the yield of ketone **253** is still modest, our initial experiments in switching from AIBN to V-70 suggest that many reaction parameters will need to be further optimized (e.g., amounts of reagents, temperature, and rate of addition). We also plan to explore other avenues of optimization, such as the use of Lewis acids.[38]

Scheme 3.23 Radical Cyclization Methods for B Ring Formation

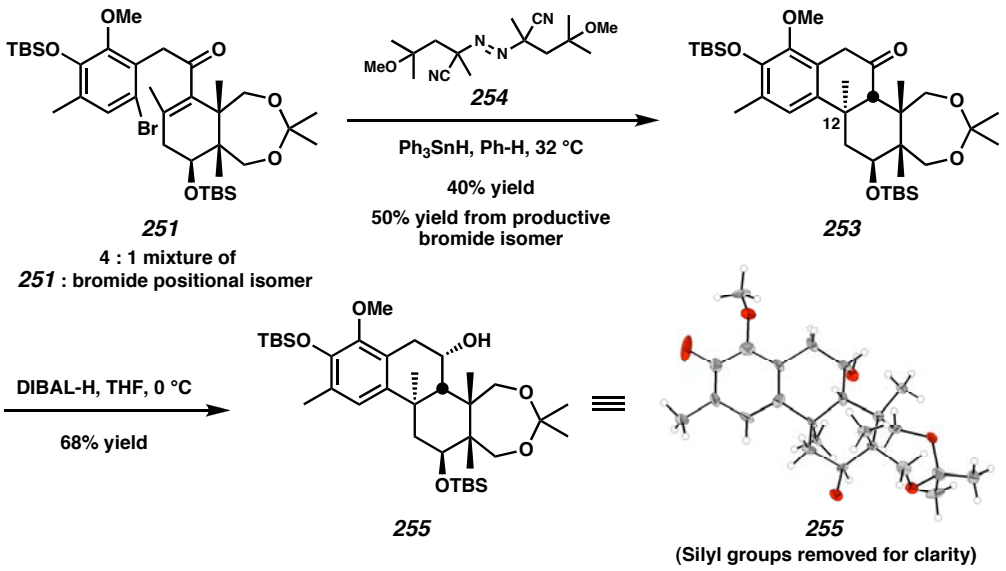

Currently, our efforts are directed at the optimization of the radical conjugate addition reaction conditions and employing the C(24) homologated series of compounds (e.g., aryl bromide **252**) as substrates for radical cyclization.[39] We believe that this radical cyclization strategy provides a novel, efficient, and functional group tolerant method to form the key C(12) quaternary stereocenter and close the B ring. The synthesis of the ABC ring fragments containing all three of zoanthenol's quaternary stereocenters represents an important milestone toward the total synthesis of this interesting alkaloid.

3.6 Model Studies for the Incorporation of the C(1)-C(6) Fragment

A final goal in validating our revised retrosynthetic plan was to model the fragment coupling between caprolactam **123** and the ABC ring fragment containing an alkyne. While alkynes are generally excellent nucleophiles, we judged it prudent to

model this reaction due the extremely crowded steric environment around the C ring and multiple sites of possible addition into caprolactam **123**. A similar alkyne addition strategy was employed in Miyashita's recent synthesis of norzoanthamine.[40]

The model alkyne we designed was intended to represent the worst case steric environment about the C ring (Scheme 3.24). Allyl ketone **256** was prepared in enantioenriched form by our asymmetric Tsuji allylation.[41] Isomerization of the allyl group was achieved with rhodium (III) chloride hydrate to give a 10:1 mixture favoring vinyl ketone **257**. Ketalization of vinyl ketone **258** under standard conditions followed by ozonolysis afforded aldehyde **259**. Conversion to the target alkyne **260** was accomplished using diazo compound **261** according to the Ohira-Bestmann modification of the Gilbert-Seyferth protocol.[42,43]

Scheme 3.24 Synthesis of C Ring Model Alkyne

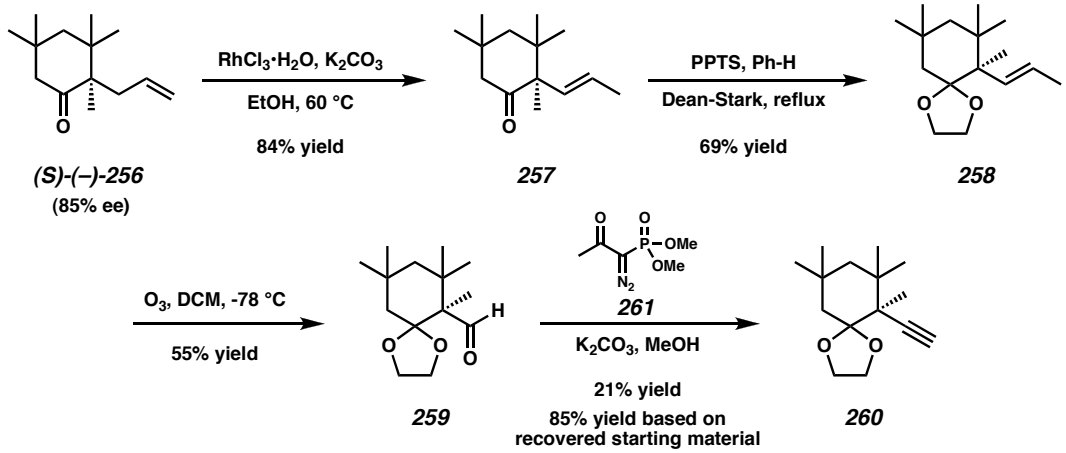

With alkyne **260** in hand we began coupling studies with caprolactam **123** (Scheme 3.25). KHMDS proved to be optimal as the base for the deprotonation of alkyne **260**.[44] While achieving high conversion to ynone **262** proved difficult, the alkyne

anion did cleanly add to the lactam carbonyl of caprolactam **123**.[45] This consistently low conversion is puzzling, as deuterium quenching experiments with the lithium salt of alkyne **260** showed >90% deuterium incorporation. However, the exclusive formation of ynone **262** validates the retrosynthetic disconnection as feasible. Hydrogenation of ynone **262** with Pd/C afforded ketone **263** as expected.

Scheme 3.25 Alkyne Fragment Coupling

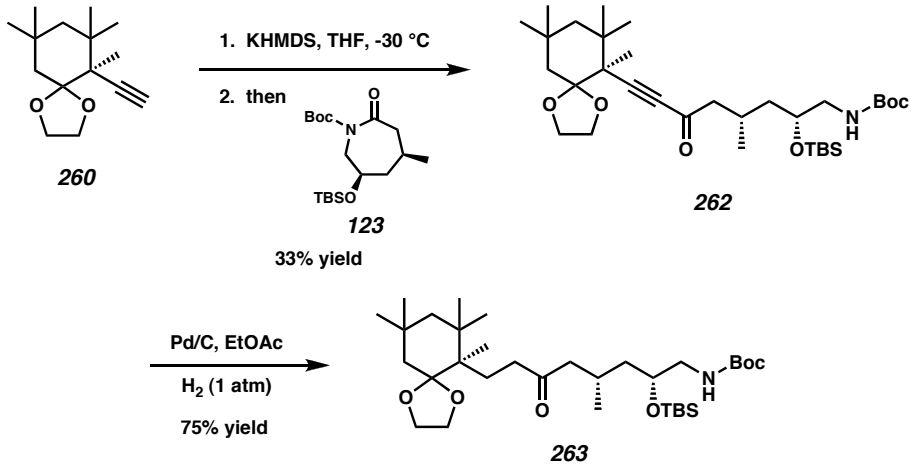

3.7 Concluding Remarks

We have demonstrated effective methods for the synthesis of a number of C ring synthons containing vicinal quaternary stereocenters. Our desymmetrization of *meso*-anhydride **203** affords access to either enantiomeric series of these synthons. Oxidation of our C ring intermediates was efficiently achieved by iodolactonization and S_N2' displacement. The resulting allylic alcohol **211** served as a branch point for the synthesis of three progressively more functionalized C ring synthons, the most elaborate of which includes homologation by cyanide displacement to install C(24).

Methods developed in Chapter Two allowed us to append each of these C ring synthons with an appropriately functionalized arene and explore methods to construct the challenging C(12) quaternary center by forming the C(12)-C(13) bond. Unfortunately, our previous S_N' and acid-mediated conjugate addition strategies proved unworkable when the cyclization substrates contained the additional quaternary center. The S_N' reactions gave only trace amounts of cyclized products, while the cyclized products generated by conjugate addition consistently had the undesired configuration at the formed quaternary stereocenter. However, a radical conjugate addition strategy was developed and demonstrated to form the benzylic C(12) quaternary stereocenter with high selectivity for the desired configuration. This radical cyclization approach has the significant advantage of using mild reaction conditions and being highly functional group tolerant. Products from the radical cyclization reactions are well poised to complete the synthesis. Finally, we showed our alkyne addition strategy for fragment coupling of the C(1)-C(6) portion of zoanthenol to be feasible even with extremely hindered alkynes.

3.8 Experimental Procedures

3.8.1 *Materials and Methods*

Unless otherwise stated, reactions were performed at ambient temperature (typically 19-24 °C) in flame-dried glassware under an argon or nitrogen atmosphere using dry, deoxygenated solvents. Solvents were dried by passage through an activated alumina column under argon. HMPA, TEA, DIPA, and pyridine were freshly distilled from CaH. KHMDS (95%) was purchased from Aldrich and stored in a glovebox until use. Trifluoroacetic acid (99%) was purchased from Aldrich. LiCl was flame-dried

under vacuum prior to use. Magnesium turnings were of 99.98% purity and purchased from Aldrich. TBSCl was purchased from Gelest. TBSOTf was freshly prepared by the method of Corey.[46] V-70 was purchased from Waco Chemicals. All other commercially obtained reagents were used as received. Reaction temperatures were controlled by an IKAmag temperature modulator. Thin-layer chromatography (TLC) was performed using E. Merck silica gel 60 F254 precoated plates (0.25 mm) and visualized by UV fluorescence quenching, anisaldehyde, $KMnO_4$, or CAM staining. ICN silica gel (particle size 0.032-0.063 mm) was used for flash chromatography. Optical rotations were measured with a Jasco P-1010 polarimeter at 589 nm. ^1H and ^{13}C NMR spectra were recorded on a Varian Mercury 300 (at 300 MHz and 75 MHz, respectively), or a Varian Inova 500 (at 500 MHz and 125 MHz, respectively) and are reported relative to Me_4Si (δ 0.0). Data for ^1H NMR spectra are reported as follows: chemical shift (δ ppm) (multiplicity, coupling constant (Hz), integration). Multiplicities are reported as follows: s = singlet, d = doublet, t = triplet, q = quartet, sept. = septet, m = multiplet, comp. m = complex multiplet, app. = apparent, bs = broad singlet. IR spectra were recorded on a Perkin Elmer Paragon 1000 spectrometer and are reported in frequency of absorption (cm^{-1}). High resolution mass spectra were obtained from the Caltech Mass Spectral Facility. Crystallographic analyses were performed at the California Institute of Technology Beckman Institute X-Ray Crystallography Laboratory. Crystallographic data have been deposited at the CCDC, 12 Union Road, Cambridge CB2 1EZ, UK, and copies can be obtained on request, free of charge, from the CCDC by quoting the publication citation and the deposition number (see individual structures for deposition numbers).

3.8.2 *Preparation of Compounds*

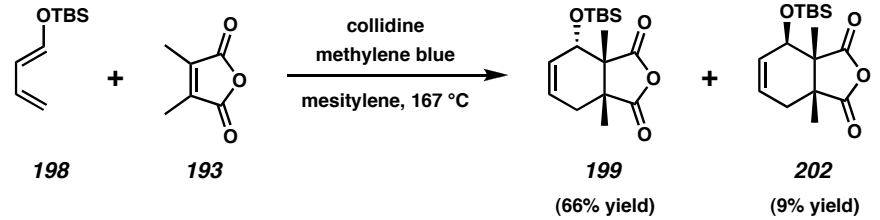

198 *193* *199* (66% yield) *202* (9% yield)

***Endo*-Diels-Alder adduct 199 and *Exo*-Diels-Alder adduct 202.** A mixture of diene **198** (67.3 g, 367.2 mmol, 1.00 equiv), 2,3-dimethylmaleic anhydride (46.3 g, 367.2 mmol, 1.00 equiv), collidine (2.91 mL, 22.0 mmol, 0.06 equiv), methylene blue (68.0 mg, 0.213 mmol, 0.000579 equiv), and mesitylene (80 mL) in a flamed-dried Ar filled Schlenk was sparged with Ar for 10 min, sealed, and heated to 167 °C for 3 d. Upon cooling, the reaction mixture was concentrated at 80 °C to give an oil, which was purified by flash chromatography on silica gel (1 to 10% EtOAc in hexanes) to give known *endo*-Diels-Alder adduct **199** (75.7 g, 66% yield), which solidified on standing: R_f 0.42 (15% EtOAc in hexanes) and *exo*-Diels-Alder adduct **202** (10.5 g, 9.2% yield) as an amorphous solid: : R_f 0.58 (15% EtOAc in hexanes); ^{1}H NMR (500 MHz, $CDCl_3$) δ 6.11 (m, 1H), 5.99 (m, 1H), 4.35 (d, J = 5.5 Hz, 1H), 2.61 (dd, J = 6.3, 16.3 Hz, 1H), 2.42 (app. dt, J = 3.3, 16.5 Hz, 1H), 1.42 (s, 3H), 1.39 (s, 3H), 0.88 (s, 9H), 0.10 (s, 3H), 0.04 (s, 3H); ^{13}C NMR (125 MHz, $CDCl_3$) δ 77.4, 175.1, 132.2, 129.8, 69.1, 53.8, 46.5, 34.2, 25.6, 21.6, 18.0, 17.6, -4.4, -5.2; IR (Neat film NaCl) 2952, 2930, 1774, 1250, 986, 1091, 986, 958, 914, 838, 778 cm^{-1}; HRMS (FAB) $[M+H]^+$ calc'd for $[C_{16}H_{26}SiO_4+H]^+$: m/z 311.1679, found 311.1671.

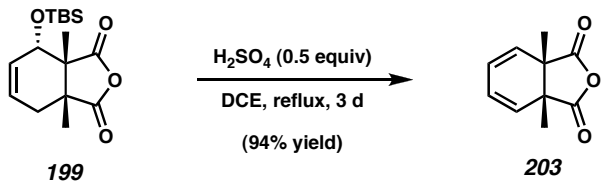

Diene 203. To a solution of *endo*-Diels-Alder adduct **199** (19.0 g, 61.4 mmol, 1.0 equiv) in DCE (614 mL) was added H_2SO_4 (1.71 mL, 30.7 mmol, 0.50 equiv), and the resulting solution was refluxed for 3 d. Upon cooling the reaction mixture was washed with sat. aq. $NaHCO_3$ (2 x 300 mL) [*Caution: gas evolution!*] and extracted with CH_2Cl_2 (2 x 120 mL). The combined organics from two such reactions were concentrated to give an oil and purified by flash chromatography on silica gel (1 to 10% EtOAc in hexanes) to give diene **203** (20.7 g, 94% yield) as a white solid: mp 61.5-62.5 °C; R_f 0.33 (15% EtOAc in hexanes); ^{1}H NMR (500 MHz, $CDCl_3$) δ 6.18-6.13 (m, 2H), 5.66-5.61 (m, 2H), 1.37 (s, 6H); ^{13}C NMR (125 MHz, $CDCl_3$) δ 75.1, 126.3, 124.5, 49.9, 18.6; IR (Neat film NaCl) 2984, 2940, 2848, 1856, 1785, 1233, 1196, 962, 912 cm^{-1}; HRMS (FAB) $[M+H]^+$ calc'd for $[C_{16}H_{26}SiO_4+H]^+$: *m/z* 311.1679, found 311.1671.

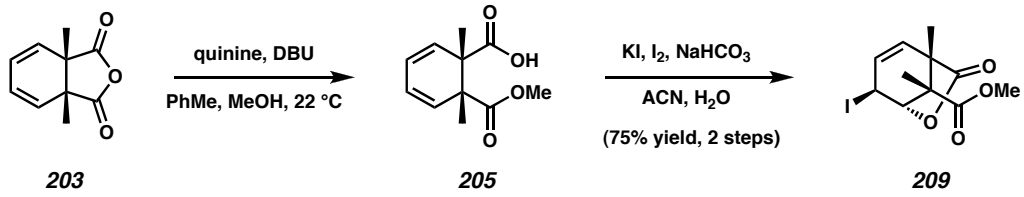

Iodolactone 209. To a solution of diene **203** (17.2 g, 96.6 mmol, 1.00 equiv), quinine (3.48 g, 9.66 mmol, 0.10 equiv), and DBU (15.9 mL, 106 mmol, 1.1 equiv) in toluene (483 mL) was added MeOH (39.1 mL, 966 mmol, 10.0 equiv). After 5 h, the reaction mixture was concentrated and the residue was diluted with EtOAc (1.00 L), washed with 2 M HCl (3 x 200 mL) and brine (1 x 200 mL), dried ($MgSO_4$), and

concentrated. Upon standing under vacuum, carboxylic acid **205** solidified and was typically used immediately in the next step without purification: R_f 0.19 (30% acetone in hexanes); ^{1}H NMR (500 MHz, $CDCl_3$) δ 5.80-5.45 (m, 4H), 3.66 (s, 3H), 1.46 (s, 3H), 1.45 (s, 3H); ^{13}C NMR (125 MHz, $CDCl_3$) δ 80.5, 175.1, 131.6, 131.5, 121.9, 121.8, 52.1, 48.4, 48.1, 20.2 (2C); IR (Neat film NaCl) 2985, 2954, 1731, 1700, 1258, 1240, 1132, 1102, 702 cm^{-1}; HRMS (EI) $[M]^+$ calc'd for $[C_{11}H_{14}O_4]^+$: *m/z* 210.0892, found 210.0898; $[\alpha]_D^{26}$ –10.94 (c 1.03, $CHCl_3$, 50% ee) from reaction with stoichiometric quinine. HPLC analysis (Chirapak AD 4.6 x 25 mm, 5.0% IPA in 95% hexane with 0.1% TFA, 1.0 mL/min, λ = 254 nm) of the asymmetric reaction performed with a catalytic amount of menthol derivative **208** showed carboxylic acid **205** to be of 85% ee (t_{fast} = 10.11 min, major; t_{slow} = 12.13 min, minor).

The above residue containing carboxylic acid **205** (theoretical yield: 96.6 mmol, 1.00 equiv) was dissolved in ACN (380 mL) and H_2O (380 mL) and treated with $NaHCO_3$ (24.3 g, 290 mmol, 3.00 equiv), KI (43.3 g, 261 mmol, 2.70 equiv), and I_2 (66.2 g, 261 mmol, 2.70 equiv) and the flask was wrapped in foil to exclude light. After 10 h, the reaction mixture was quenched in the dark with sat. aq. $Na_2S_2O_3$ until colorless, diluted with EtOAc (650 mL), extracted with EtOAc (2 x 300 mL), washed with brine (200 mL), dried ($MgSO_4$), and concentrated to an oil, which was purified by flash chromatography on silica gel (10 to 20% EtOAc in hexanes) to provide iodolactone **209** (24.4 g, 75% yield, 2 steps) as an unstable solid (typically used immediately in the next step): R_f 0.35 (50% EtOAc in hexanes); ^{1}H NMR (300 MHz, C_6D_6) δ 5.33 (ddd, *J* = 1.5, 3.0, 9.3 Hz, 1H), 4.86 (dd, *J* = 1.5, 9.3 Hz, 1H), 4.63 (app. t, *J* = 2.1 Hz, 1H), 4.29 (m, 1H), 3.13 (s, 3H), 1.34 (s, 3H), 1.27 (s, 3H); ^{13}C NMR (75 MHz, C_6D_6) δ 175.3, 173.0,

133.0, 130.1, 80.4, 53.6, 52.5, 47.0, 16.9, 16.0, 15.0; IR (Neat film NaCl) 2953, 1795, 1732, 1450, 1293, 1247, 1141, 1107, 1062, 969 cm^{-1}; HRMS (EI) $[M]^+$ calc'd for $[C_{11}H_{14}O_4I]^+$: m/z 336.9937, found 336.9930.

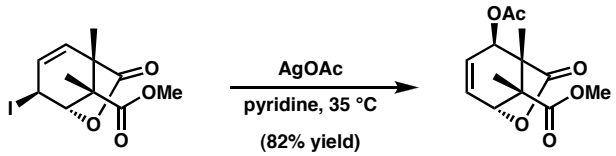

209 *210*

Allylic acetate 210. To a solution of iodolactone **209** (23.0 g, 68.5 mmol, 1.00 equiv) in pyridine (140 mL) was added AgOAc (34.3 g, 206 mmol, 3.00 equiv). The reaction mixture was wrapped in foil to exclude light and heated to 35 °C. After 3.5 d, the reaction mixture was concentrated (~5 torr at 50 °C), diluted with H_2O (500 mL) and CH_2Cl_2 (300 mL), and extracted with CH_2Cl_2 (7 x 150 mL). The combined organics were dried ($MgSO_4$), filtered, concentrated, and purified by flash chromatography on silica gel (15 to 35% EtOAc in hexanes) to provide allylic acetate **210** (15.2 g, 82% yield) as an oil: R_f 0.57 (50% EtOAc in hexanes); ^1H NMR (500 MHz, $CDCl_3$) δ 6.33 (ddd, J = 1.0, 5.6, 9.1 Hz, 1H), 5.98 (ddd, J = 1.0, 3.5, 9.0 Hz, 1H), 5.35 (dd, J = 1.5, 3.5 Hz, 1H), 4.85 (dd, J = 1.0, 6.0 Hz, 1H), 3.75 (s, 3H), 2.11 (s, 3H), 1.46 (s, 3H), 1.34 (s, 3H); ^{13}C NMR (125 MHz, $CDCl_3$) δ 177.2, 173.0, 169.6, 131.1, 129.5, 76.8, 69.9, 54.7, 52.7, 50.0, 20.7, 15.6, 13.6; IR (Neat film NaCl) 2986, 2953, 1788, 1735, 1373, 1257, 1219, 1024, 962 cm^{-1}; HRMS (FAB) $[M+H]^+$ calc'd for $[C_{13}H_{16}O_6+H]^+$: m/z 269.1025, found 269.1014.

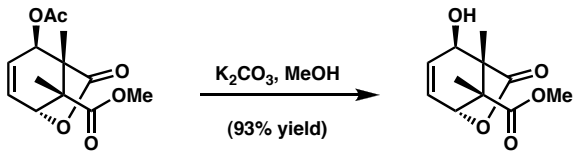

210 ***211***

Allylic alcohol 211. To a solution of allylic acetate **210** (15.2 g, 56.2, 1.00 equiv) in MeOH (275 mL) was added K_2CO_3 (1.55 g, 11.3 mmol, 0.20 equiv) and the reaction was vigorously stirred. After 10 min, TLC analysis indicated consumption of the starting material, and the reaction mixture was quenched with H_2O (200 mL), brine (300 mL), and CH_2Cl_2 (200 mL). The pH of the aqueous layer was adjusted to pH 7 with 3 M HCl (~8 mL) [*Caution: gas evolution!*] and extracted with CH_2Cl_2 (10 x 50 mL). The combined organics were washed with brine (100 mL), concentrated, and purified by flash chromatography on silica gel (25 to 35% EtOAc in hexanes) to provide allylic alcohol **211** (11.9 g, 93% yield) as a white solid. Crystals suitable for X-ray analysis were obtained by crystallization from Et_2O/heptanes at ambient temperature: mp 94.5-95.5 °C (Et_2O/heptane); R_f 0.38 (50% EtOAc in hexanes); ^{1}H NMR (500 MHz, $CDCl_3$) δ 6.22 (ddd, J = 1.5, 5.8, 9.3 Hz, 1H), 6.04 (ddd, J = 1.0, 3.3, 9.3 Hz, 1H), 4.79 (dd, J = 1.0, 5.5 Hz, 1H), 4.15 (dd, J = 1.0, 3.5 Hz, 1H), 3.72 (s, 3H), 1.43 (s, 3H), 1.41 (s, 3H); ^{13}C NMR (125 MHz, $CDCl_3$) δ 179.3, 173.6, 134.8, 127.3, 77.4, 69.8, 54.7, 52.6, 50.8, 15.5, 13.7; IR (Neat film NaCl) 3484, 2954, 1773, 1731, 1454, 1259, 1137, 1110, 1049, 1031, 983, 955 cm^{-1}; HRMS (FAB) $[M+H]^+$ calc'd for $[C_{11}H_{14}O_5+H]^+$: m/z 227.0919, found 227.0924.

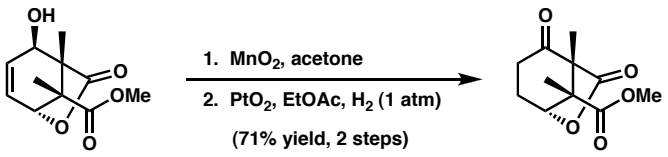

211 *212*

Ketone 212. To a solution of allylic alcohol **211** (2.23 g, 9.86 mmol, 1.00 equiv) in acetone (100 mL) was added activated MnO_2 (17.1 g, 197 mmol, 20.0 equiv) and the reaction mixture was stirred at ambient temperature for 1.25 h. The reaction mixture was filtered, washed with acetone, and concentrated to an oil.

To a solution of this crude material in EtOAc (60 mL) was added PtO_2 (67.1 mg, 0.296 mmol, 0.03 equiv), and the reaction mixture was sparged with H_2 (5 min) and stirred vigorously under an atmosphere of H_2 (balloon) for 1.5 h. The reaction mixture was flushed with N_2 and concentrated to an oil, which was purified by flash chromatography on silica gel (30 to 50% EtOAc in hexanes) to provide ketone **212** (1.59 g, 71% yield) as an amorphous solid: R_f 0.38 (50% EtOAc in hexanes); ^{1}H NMR (300 MHz, $CDCl_3$) δ 4.89 (dd, J = 1.2, 3.9 Hz, 1H), 3.75 (s, 3H), 2.62-2.56 (m, 2H), 2.47-2.37 (m, 1H), 2.15-2.01 (m, 1H), 1.23 (s, 3H), 1.20 (s, 3H); ^{13}C NMR (75 MHz, $CDCl_3$) δ 200.0, 173.4, 171.3, 79.4, 62.4, 56.5, 53.0, 33.9, 24.9, 14.3, 9.3; IR (Neat film NaCl) 2989, 2955, 1790, 1732, 1343, 1267, 1227, 1152, 1089, 1018, 966 cm^{-1}; HRMS (EI) $[M]^+$ calc'd for $[C_{11}H_{14}O_5]^+$: m/z 226.0841, found 226.0847.

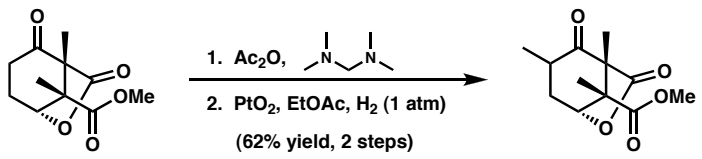

212 *213*

Methyl ketone 213. To a cooled (15 °C) solution of ketone **212** (1.31 g, 5.77 mmol, 1.00 equiv) and Ac_2O (6.55 mL, 69.3 mmol, 12.0 equiv) was added *N*,*N*,*N'*,*N'*-tetramethyldiaminomethane (4.73 mL, 34.6 mmol, 6.00 equiv) in a dropwise manner over 30 min. At the end of the addition, the reaction was allowed to come to ambient temperature. After 4 h, additional Ac_2O (6.00 mL, 63.5 mmol, 11.0 equiv) and *N*,*N*,*N'*,*N'*-tetramethyldiaminomethane (7.00 mL, 51.3 mmol, 8.89 equiv) were added and the reaction was warmed to 32 °C for 12 h. The reaction mixture was then cooled, concentrated in vacuo, quenched into water (40 mL), sat. aq. $NaHCO_3$ (20 mL), and ice (40 g), and extracted with CH_2Cl_2 (4 x 40 mL). The combined organics were dried (Na_2SO_4) and concentrated to give a crude solid that was used immediately in the next step.

To a solution of the crude material in EtOAc (100 mL) was added PtO_2 (131 mg, 0.577 mmol, 0.10 equiv), and the reaction mixture was sparged with H_2 (5 min) and stirred vigorously under an atmosphere of H_2 (balloon) for 5.5 h. The reaction mixture was flushed with N_2 and concentrated to an oil, which was purified by flash chromatography on silica gel (20 to 40% EtOAc in hexanes) to provide a single diastereomer of methyl ketone **213** (854 mg, 62% yield) as an amorphous solid: R_f 0.57, 0.29 (50% EtOAc in hexanes, 50% Et_2O in hexanes developed twice); ^{1}H NMR (300 MHz, $CDCl_3$) δ 4.87 (m, 1H), 3.75 (s, 3H), 2.75-2.56 (m, 2H), 1.82-1.66 (m, 1H), 1.27 (s, 3H), 1.14 (d, J = 6.3 Hz, 3H), 1.11 (s, 3H); ^{13}C NMR (75 MHz, $CDCl_3$) δ 202.3, 174.1,

171.3, 79.4, 62.0, 57.3, 53.0, 38.9, 34.0, 14.7, 13.9, 9.6; IR (Neat film NaCl) 2987, 2954, 1788, 1726, 1259, 1154, 1077, 1038 cm^{-1}; HRMS (EI) $[M]^+$ calc'd for $[C_{12}H_{16}O_5]^+$: m/z 240.0998, found 240.0996.

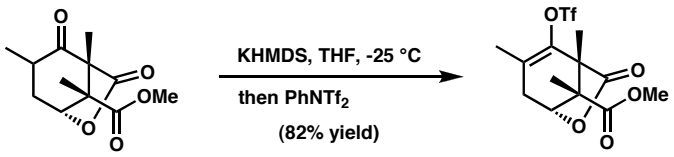

213 ***214***

Triflate 214. To a cooled (-25 °C) solution of KHMDS (339 mg, 1.70 mmol, 1.20 equiv) in THF (12 mL) was added methyl ketone **213** (340 mg, 1.42 mmol, 1.00 equiv) in THF (10 mL) in a dropwise manner over 10 min. After 1.5 h at -25 °C, $PhNTf_2$ (708 mg, 1.98 mmol, 1.40 equiv) in THF (5 mL) was added, and the reaction was maintained for an additional 30 min at -25°C. The reaction mixture was quenched into half-saturated brine (40 mL) and EtOAc (40 mL), and extracted with EtOAc (4 x 15 mL). The combined organics were washed with brine (2 x 20 mL), dried ($MgSO_4$), and concentrated to an oil, which was purified by flash chromatography on silica gel (15 to 40% EtOAc in hexanes) to provide triflate **214** (435 mg, 82% yield) as an oil: R_f 0.20 (50% Et_2O in hexanes developed twice); ^1H NMR (300 MHz, $CDCl_3$) δ 4.59 (app. t, J = 2.7 Hz, 1H), 3.75 (s, 3H), 2.63-2.47 (m, 2H), 1.86 (s, 3H), 1.42 (s, 3H), 1.33 (s, 3H); ^{13}C NMR (75 MHz, $CDCl_3$) δ 174.1, 172.1, 138.2, 128.2, 118.4 (app. d, $J_{C\text{-}F}$ = 319 Hz), 77.2, 54.6, 53.0, 50.4, 35.0, 17.2, 12.6, 10.0; IR (Neat film NaCl) 2956, 1790, 1727, 1408, 1208, 1138, 824 cm^{-1}; HRMS (EI) $[M+H]^+$ calc'd for $[C_{13}H_{15}O_7F_3S+H]^+$: m/z 373.0569, found 373.0550.

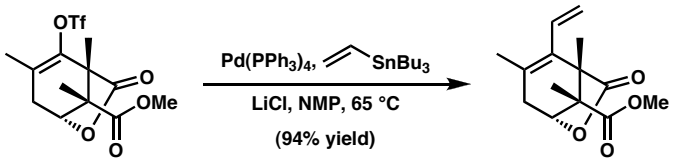

214 *215*

Diene 215. To a solution of triflate **214** (865 mg, 2.32 mmol, 1.00 equiv), $Pd(PPh_3)_4$ (134.2 mg, 0.116 mmol, 0.05 equiv), and LiCl (295 mg, 6.97 mmol, 3.00 equiv) in NMP (18 mL) was added tributyl(vinyl)tin (1.02 mL, 3.48 equiv, 1.50 equiv), and the mixture was heated to 65 °C for 9.5 h. The reaction mixture was cooled to ambient temperature, quenched with H_2O (50 mL) and Et_2O (50 mL), and extracted with Et_2O (5 x 30 mL). The combined organics were washed with brine (2 x 20 mL), dried ($MgSO_4$), and concentrated to an oil, which was purified by flash chromatography on silica gel (5 to 25% EtOAc in hexanes) to provide diene **215** (545 mg, 94% yield) as an oil: R_f 0.63, 0.80 (50% Et_2O in hexanes developed thrice, 50% EtOAc in hexanes developed twice); ^{1}H NMR (300 MHz, $CDCl_3$) δ 6.01 (ddd, J = 1.2, 11.3, 17.6 Hz, 1H), 5.34 (dd, J = 2.0, 11.3 Hz, 1H), 5.02 (dd, J = 2.3, 17.6 Hz, 1H), 4.53 (app. t, J = 2.7 Hz, 1H), 3.70 (s, 3H), 2.37 (s, 2H), 1.72 (s, 3H), 1.23 (s, 3H), 1.20 (s, 3H); ^{13}C NMR (75 MHz, $CDCl_3$) δ 176.7, 173.7, 132.3, 131.5, 130.2, 120.6, 77.7, 53.6, 52.5, 49.3, 35.3, 20.0, 12.9, 12.5; IR (Neat film NaCl) 2985, 2951, 2911, 1782, 1730, 1267, 1198, 1144, 1089, 1035, 972 cm^{-1}; HRMS (EI) $[M]^+$ calc'd for $[C_{14}H_{18}O_4]^+$: m/z 250.1205, found 250.1204.

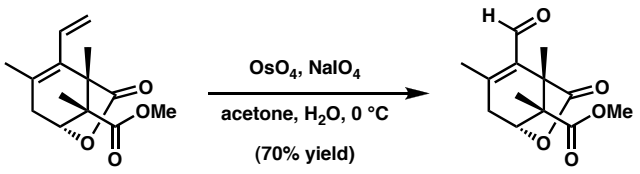

215 *216*

Enal 216. To a cooled (0 °C) solution of diene **215** (271 mg, 1.08 mmol, 1.00 equiv) in acetone (8.00 mL) and H_2O (8.00 mL) was added OsO_4 (27.5 mg, 0.108 mmol, 0.10 equiv) and $NaIO_4$ (511 mg, 2.38 mmol, 2.20 equiv). After 8.5 h at 0 °C, the reaction mixture was quenched with brine (30 mL) and EtOAc (30 mL), and extracted with EtOAc (5 x 30 mL). The combined organics were dried (Na_2SO_4) and concentrated to an oil, which was purified by flash chromatography on silica gel (25 to 50% EtOAc in hexanes) to provide enal **216** (191 mg, 70% yield) as a solid: R_f 0.48 (50% EtOAc in hexanes developed twice); ^{1}H NMR (300 MHz, $CDCl_3$) δ 9.88 (s, 1H), 4.54 (app. t, J = 2.4 Hz, 1H), 3.72 (s, 3H), 2.57 (d, J = 1.8 Hz, 2H), 2.07 (s, 3H), 1.49 (s, 2H), 1.21 (s, 3H); ^{13}C NMR (75 MHz, $CDCl_3$) δ 189.9, 176.0, 172.8, 151.0, 131.6, 76.7, 53.9, 52.7, 48.2, 37.5, 19.2, 12.5, 12.3; IR (Neat film NaCl) 2952, 1786, 1729, 1681, 1333, 1273, 1250, 1201, 1136, 1082, 1034, 969 cm^{-1}; HRMS (EI) $[M]^+$ calc'd for $[C_{13}H_{16}O_5]^+$: m/z 252.0998, found 252.0984.

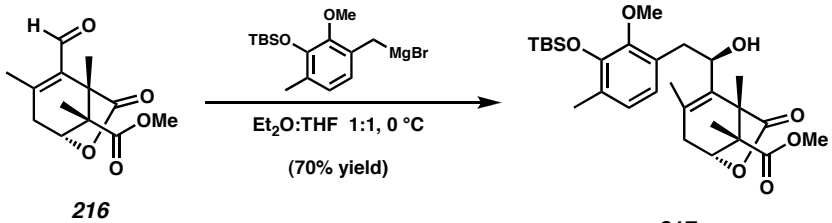

216 *217*

Allylic alcohol 217. A flame-dried two-neck round-bottom flask equipped with a reflux condenser and septum was charged with magnesium turnings (1.03 g, 42.4 mmol,

32.4 equiv) and Et_2O (12 mL) under an N_2 atmosphere and heated to reflux. To this mixture was added 1,2-dibromoethane (150 μL, 1.74 mmol, 1.33 equiv) in a dropwise manner [*Caution: gas evolution!*]. When gas evolution ceased, a solution of benzyl bromide **151** (677 mg, 1.96 mmol, 1.50 equiv) in Et_2O (7.0 mL) was added in a dropwise manner over 30 min and heating was continued for an additional 30 min. The Grignard reagent was then cooled (0 °C) and added to a cooled (0 °C) solution of enal **216** (330 mg, 1.31 mmol, 1.00 equiv) in Et_2O (10 mL) and THF (30 mL). After 1 h at 0 °C, the reaction mixture was allowed to come to ambient temperature, and after an additional 30 min, the reaction was quenched with ice cold H_2O (50 mL), 2 M HCl (2.0 mL), and Et_2O (20 mL), and extracted with Et_2O (4 x 40 mL). The combined organics were washed with brine (2 x 30 mL), dried ($MgSO_4$), and concentrated to an oil, which was purified by flash chromatography on silica gel (15 to 50% EtOAc in hexanes) to give allylic alcohol **217** (477 mg, 70% yield) as a white solid. Crystals suitable for X-ray analysis were obtained by crystallization from EtOAc/heptanes at ambient temperature: mp 154-155 °C (EtOAc/heptane); R_f 0.50 (35% EtOAc in hexanes developed twice); ^{1}H NMR (300 MHz, $CDCl_3$) δ 6.83 (d, J = 7.7 Hz, 1H), 6.71 (d, J = 7.5 Hz, 1H), 4.75 (bs, 1H), 4.52 (app. t, J = 2.6 Hz, 1H), 3.74 (s, 3H), 3.72 (s, 3H), 3.00-2.80 (m, 2H), 2.76-2.54 (bs, 1H), 2.36 (m, 2H), 2.20 (s, 3H), 1.78 (s, 3H), 1.50 (s, 3H), 1.29 (s, 3H), 1.02 (s, 9H), 0.15 (m, 6H); ^{13}C NMR (75 MHz, $CDCl_3$) δ 77.7, 173.8, 149.4, 147.1, 132.5, 131.8, 129.8, 129.6, 126.3, 123.5, 123.3, 72.0, 60.1, 54.4, 52.6, 50.0, 37.4, 37.0, 26.0, 19.4, 18.6, 17.1, 13.1, 12.9, -4.1; IR (Neat film NaCl) 3519, 2953, 2930, 2858, 1777, 1731, 1462, 1419, 1259, 1073, 840 cm^{-1}; HRMS (FAB) $[M+Na]^+$ calc'd for $[C_{28}H_{42}SiO_7+Na]^+$: m/z 541.2598, found 541.2571.

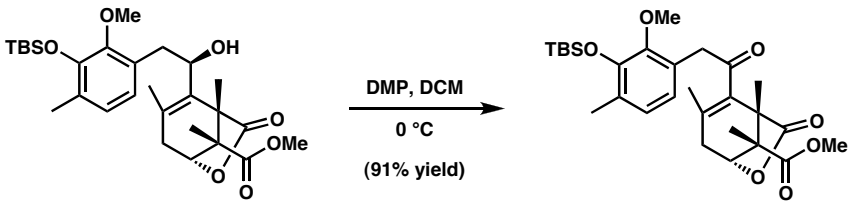

217 *218*

Enone 218. To a cooled (0 °C) solution of allylic alcohol **217** (129 mg, 0.248 mmol, 1.00 equiv) in CH_2Cl_2 (20 mL) was added Dess-Martin periodinane (210 mg, 0.496 mmol, 2.00 equiv) and the resulting mixture was stirred for 1 h. The reaction mixture was diluted with Et_2O (75 mL), filtered, and concentrated to an oil, which was purified by gradient flash chromatography on silica gel (15 to 40% EtOAc in hexanes) to give enone **218** (117 mg, 91% yield) as a foam: R_f 0.57 (35% EtOAc in hexanes developed twice); ^{1}H NMR (300 MHz, $CDCl_3$) δ 6.83 (d, J = 7.8 Hz, 1H), 6.64 (d, J = 8.1 Hz, 1H), 4.61 (app. t, J = 2.4 Hz, 1H), 3.94 (d, J = 17.7 Hz, 1H), 3.76 (d, J = 17.7 Hz, 1H), 3.75 (s, 3H), 3.65 (s, 3H), 2.46 (dd, J = 2.7, 18.9 Hz, 1H), 2.35 (dd, J = 1.5, 18.9 Hz, 1H), 2.20 (s, 3H), 1.66 (s, 3H), 1.29 (s, 3H), 1.28 (s, 3H), 1.02 (s, 9H), 0.15 (s, 6H); ^{13}C NMR (75 MHz, $CDCl_3$) δ 203.3, 176.2, 173.1, 150.0, 146.9, 135.4, 130.6, 130.0, 125.7, 124.4, 123.3, 77.8, 59.8, 53.5, 52.7, 47.8, 46.2, 34.3, 26.0, 18.8, 18.4, 17.0, 12.5, 11.7, -4.3; IR (Neat film NaCl) 2953, 2930, 2858, 1785, 1732, 1463, 1421, 1286, 1252, 1236, 840 cm^{-1}; HRMS (FAB) $[M+H]^+$ calc'd for $[C_{28}H_{40}SiO_7+H]^+$: m/z 517.2622, found 517.2631.

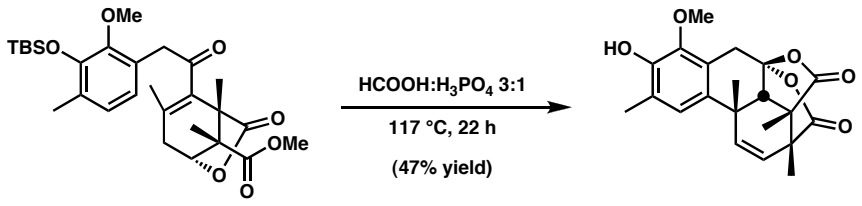

218 *220*

Bisacetoxyacetal 220. A solution of enone 218 (58.5 mg, 0.113 mmol, 1.00 equiv) in formic acid (2.40 mL) and 85% H_3PO_4 (800 μL) was fitted with a reflux condenser and heated at 117 °C for 22 h. The reaction mixture was cooled to ambient temperature, diluted with ice cold H_2O (60 mL) and extracted with Et_2O (5 x 15 mL). The combined organics were dried ($MgSO_4$) and concentrated to an oil, which was purified by flash chromatography on silica gel (10 to 40% EtOAc in hexanes) to give bisacetoxyacetal **220** (19.6 mg, 47% yield) as a white solid. Crystals suitable for X-ray analysis were obtained by crystallization from Et_2O/hexanes at ambient temperature: mp 185-190 °C decomp. (Et_2O/hexanes); R_f 0.32 (35% EtOAc in hexanes); ^{1}H NMR (300 MHz, $CDCl_3$) δ 6.92 (s, 1H), 6.14 (dd, J = 0.9, 9.3 Hz, 1H), 5.62 (bs, 1H), 5.42 (d, J = 9.3 Hz, 1H), 3.77 (s, 3H), 3.61 (d, J = 15.9 Hz, 1H), 3.02 (dd, J = 0.9, 15.9 Hz, 1H), 2.48 (s, 1H), 2.52 (s, 3H), 1.47 (s, 3H), 1.43 (s, 3H), 1.41 (s, 3H); ^{13}C NMR (75 MHz, $CDCl_3$) δ 175.6, 169.5, 145.9, 144.4, 137.4, 130.8, 126.0, 124.9, 124.7, 121.8, 105.7, 60.9, 53.0, 45.9, 38.0, 32.2, 31.5, 16.3, 16.2, 15.8; IR (Neat film NaCl) 3468, 2978, 2942, 1801, 1757, 1360, 1213, 1057, 937, 914, 732 cm^{-1}; HRMS (EI) $[M]^+$ calc'd for $[C_{21}H_{22}O_6]^+$: *m/z* 370.1416, found 370.1410.

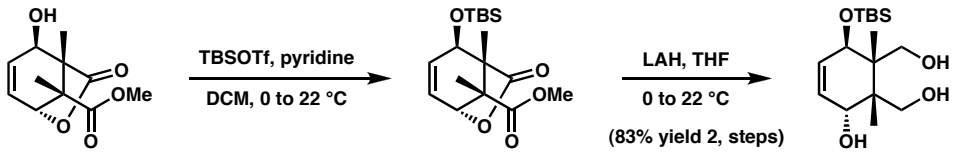

211 ***227*** ***228***

Triol 228. To cooled (0 °C) solution of allylic alcohol **211** (4.37 g, 19.3 mmol, 1.00 equiv) and pyridine (3.12 mL, 38.7 mmol, 2.00 equiv) in CH_2Cl_2 (19 mL) was added TBSOTf (6.66 mL, 29.0 mmol, 1.50 equiv) in a dropwise manner. At the end of the addition, the reaction was allowed to warm to ambient temperature and stirred for 15 h. The reaction mixture was diluted with CH_2Cl_2 (200 mL), quenched with sat. aq. NH_4Cl (75 mL), and extracted with CH_2Cl_2 (4 x 50 mL). The combined organics were dried ($MgSO_4$) and concentrated to give crude silyl ether **227**, which was typically used without purification in the next step: R_f 0.69 (50% EtOAc in hexanes); ^{1}H NMR (500 MHz, $CDCl_3$) δ 6.19 (ddd, J = 1.0, 6.0, 9.0 Hz, 1H), 5.89 (ddd, J = 1.0, 3.5, 9.0 Hz, 1H), 4.78 (d, J = 5.5 Hz, 1H), 4.08 (dd, J = 1.0, 3.5 Hz, 1H), 3.72 (s, 3H), 1.44 (s, 3H), 1.35 (s, 3H), 0.88 (s, 9H), 0.11 (s, 3H), 0.09 (s, 3H); ^{13}C NMR (125 MHz, $CDCl_3$) δ 178.9, 173.7, 134.8, 126.9, 77.3, 70.5, 54.9, 52.5, 51.3, 25.6, 17.9, 15.7, 14.7, -4.5, -5.1; IR (Neat film NaCl) 2952, 2933, 2857, 1779, 1737, 1725, 1454, 1374, 1254, 1095, 1065, 957, 841, 780 cm^{-1}; HRMS (FAB) $[M+H]^+$ calc'd for $[C_{17}H_{28}SiO_5+H]^+$: m/z 341.1784, found 341.1781.

The above residue containing silyl ether **227** (theoretical yield: 19.3 mmol, 1.00 equiv) was dissolved in THF (193 mL), cooled (0 °C), and treated with LAH (2.20 g, 58.0 mmol, 3.00 equiv) in portions. At the end of the addition, the reaction was allowed to come to ambient temperature and stirred for 18 h. The cooled (0 °C) reaction mixture was quenched by the careful dropwise addition of EtOAc (66 mL) until out gassing

ceased, addition of Celite (7.0 g), and, finally, careful addition of sat. aq. Na_2SO_4 (33 mL). The resulting slurry was filtered, dried (Na_2SO_4), and concentrated to give triol **228** (5.05 g, 83% yield, 2 steps) as a white solid of ~95% purity. Analytically pure material could be obtained by recrystallization from 1% EtOAc in benzene: mp 130.5-132.0 °C (EtOAc/benzene); R_f 0.22 (30% acetone in hexanes); ^{1}H NMR (500 MHz, $CDCl_3$) δ 5.68-5.62 (m, 2H), 4.45 (s, 1H), 4.20 (s, 1H), 3.91 (d, *J* = 11.5 Hz, 1H), 3.76 (d, *J* = 11.5 Hz, 1H), 3.69 (d, *J* = 11.5 Hz, 1H), 3.50 (d, *J* = 12.0 Hz, 1H), 1.15 (s, 3H), 0.89 (s, 9H), 0.84 (s, 3H), 0.11 (s, 3H), 0.10 (s, 3H); ^{13}C NMR (125 MHz, $CDCl_3$) δ 31.3, 129.1, 73.6, 69.3, 65.6, 63.7, 46.1, 45.2, 25.8, 18.0, 16.2, 13.6, -4.0, -5.0; IR (Neat film NaCl) 3255, 2955, 2929, 2886, 2857, 1472, 1253, 1076, 1049, 1026, 880, 835 cm^{-1}; HRMS (FAB) $[M+H]^+$ calc'd for $[C_{16}H_{32}SiO_4+H]^+$: *m/z* 317.2148, found 317.2162.

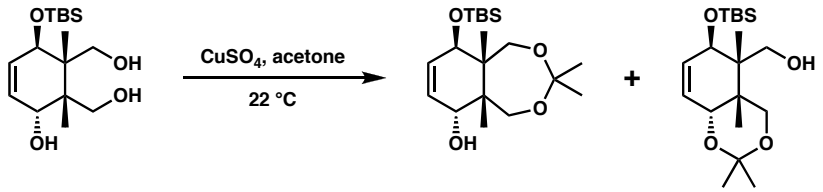

228 ***229*** (35% yield) ***230*** (53% yield)

1,3-Dioxepane 229 and Acetonide 230. To a solution of triol **228** (3.75 g, 11.9 mmol, 1.00 equiv) in acetone (120 mL) was added anhydrous $CuSO_4$ (9.46 g, 59.3 mmol, 5.00 equiv), and the reaction mixture was stirred for 40 min. An additional portion of $CuSO_4$ (1.89 g, 11.9 mmol, 1.00 equiv) was added to the reaction mixture, and after an additional 3 h of stirring, a final portion of $CuSO_4$ (1.00 g, 6.27 mmol, 0.53 equiv) was added. After 30 min, the reaction mixture was filtered, concentrated, and purified by flash chromatography on silica gel (5 to 15% EtOAc in hexanes) to give 1,3-dioxepane

229 (1.48 g, 35% yield) as a waxy solid: R_f 0.66 (35% EtOAc in hexanes); ^{1}H NMR (300 MHz, $CDCl_3$) δ 5.57 (dt, *J* = 2.1, 10.2 Hz, 1H), 5.49 (dt, *J* = 2.1, 10.2 Hz, 1H), 4.99 (s, 1H), 4.23 (app. q, *J* = 2.4 Hz, 1H), 3.73 (d, *J* = 12.3 Hz, 1H), 3.58 (d, *J* = 12.6 Hz, 1H), 3.56 (d, *J* = 12.6 Hz, 1H), 3.19 (d, *J* = 12.6 Hz, 1H), 1.33 (s, 3H), 1.30 (s, 3H), 0.90 (s, 9H), 0.71 (s, 3H), 0.10 (s, 3H), 0.09 (s, 3H); ^{13}C NMR (75 MHz, C_6D_6) δ 131.7, 129.2, 101.8, 73.5, 68.1, 63.8, 63.0, 46.9, 46.3, 26.5, 25.7, 25.4, 18.8, 18.7, 11.7, -3.7, -4.5; IR (Neat film NaCl) 3446, 2983, 2954, 2858, 1472, 1372, 1253, 1221, 1085, 1070, 1044, 835, 775 cm^{-1}; HRMS (FAB) [M-H_2+H]$^+$ calc'd for [$C_{19}H_{35}SiO_4$]$^+$: *m/z* 355.2305, found 355.2317 and acetonide **230** (2.25 g, 53% yield) as an oil: R_f 0.76 (35% EtOAc in hexanes); ^{1}H NMR (300 MHz, $CDCl_3$) δ 5.93 (dd, *J* = 4.4, 9.6 Hz, 1H), 5.69 (dd, *J* = 4.8, 9.9 Hz, 1H), 4.12 (d, *J* = 4.5 Hz, 1H), 4.01 (d, *J* = 12.9 Hz, 1H), 3.91 (s, 1H), 3.76 (d, *J* = 10.2 Hz, 1H), 3.64 (d, *J* = 10.2 Hz, 1H), 3.56 (d, *J* = 12.9 Hz, 1H), 1.49 (s, 3H), 1.43 (s, 3H), 1.04 (s, 3H), 0.98 (s, 3H), 0.88 (s, 9H), 0.09 (s, 3H), 0.08 (s, 3H); ^{13}C NMR (75 MHz, $CDCl_3$) δ 133.5, 124.4, 98.6, 71.7, 70.9, 68.9, 65.2, 43.8, 35.1, 28.4, 25.7, 20.9, 20.0 (bs), 17.9, 15.3, -4.1, -5.1; IR (Neat film NaCl) 3451, 2955, 2931, 2886, 2858, 1379, 1256, 1104, 1056, 836, 775 cm^{-1}; HRMS (FAB) [M+H]$^+$ calc'd for [$C_{19}H_{36}SiO_4$+H]$^+$: *m/z* 357.2461, found 357.2478.

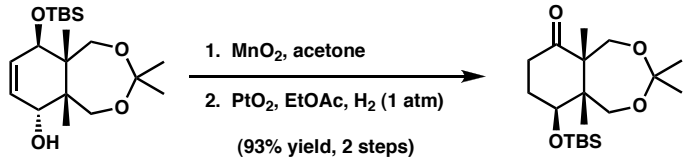

229 ***232***

Ketone 232. To a solution of 1,3-dioxepane **229** (798 mg, 2.24 mmol, 1.00 equiv) in acetone (23 mL) was added activated MnO_2 (3.89 g, 44.7 mmol, 20.0 equiv),

and the reaction mixture was stirred at ambient temperature for 1.5 h. The reaction mixture was filtered, washed with acetone, and concentrated to an oil.

To a solution of this crude material in EtOAc (28 mL) was added PtO_2 (16.0 mg, 67.2 μmol, 0.03 equiv), and the reaction mixture was sparged with H_2 (5 min) and stirred vigorously under an atmosphere of H_2 (balloon) for 1.5 h. The reaction mixture was flushed with N_2 and concentrated to an oil, which was purified by flash chromatography on silica gel (2.5 to 10% EtOAc in hexanes) to provide ketone **232** (744 mg, 93% yield, 2 steps) as an amorphous solid: R_f 0.52 (20% EtOAc in hexanes); ^{1}H NMR (300 MHz, $CDCl_3$) δ 4.59 (bs, 1H), 4.15 (bs, 1H), 3.40 (bs, 2H), 2.99 (bs, 1H), 2.31 (m, 2H), 2.10-1.70 (m, 2H), 1.33 (s, 3H), 1.32 (s, 3H), 1.09 (s, 3H), 0.89 (s, 9H), 0.64 (bs, 3H), 0.11 (s, 3H), 0.10 (s, 3H); ^{13}C NMR (75 MHz, $CDCl_3$) δ 212.7, 101.8, 67.3, 65.1, 64.0, 57.1, 47.2, 37.9, 29.4, 25.8, 24.8, 24.4, 18.0, 15.8, 11.5, -4.4, -5.1; IR (Neat film NaCl) 2954, 2857, 1709, 1220, 1096, 1073, 884, 836 cm^{-1}; HRMS (FAB) $[M+H]^+$ calc'd for $[C_{19}H_{36}O_4Si+H]^+$: m/z 357.2461, found 357.2473.

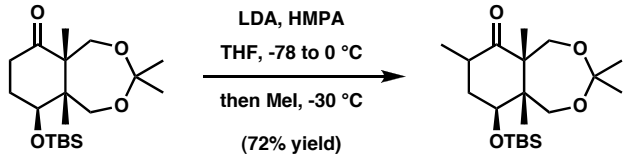

232 *233*

Methyl Ketones 233. A solution of LDA in THF was prepared by dropwise addition of 2.45 M *n*-BuLi solution in hexanes (1.21 mL, 2.96 mmol, 1.20 equiv) to diisopropylamine (519 μL, 3.70 mmol, 1.50 equiv) in THF (30.0 mL) at 0 °C, followed by stirring for 1 h. Upon cooling the solution to -78 °C, a solution of ketone **232** (879 mg, 2.47 mmol, 1.00 equiv) in THF (30.0 mL) was added in a dropwise manner, and the

reaction mixture was stirred at -78 °C for 30 min. HMPA (1.07 mL, 6.17 mmol, 2.50 equiv) was added and the reaction mixture brought to 0 °C for 1 h. After cooling again to -78 °C, the reaction mixture was treated with MeI (200 μL, 3.21 mmol, 1.30 equiv), and after 15 min allowed to warm to -30 °C. The reaction was allowed to warm to 0 °C slowly over 10 h, quenched with H_2O (150 mL) and EtOAc (75 mL), and extracted with EtOAc (4 x 50 mL). The combined organics were washed with brine (50 mL), dried (Na_2SO_4), and concentrated to an oil, which was purified by flash chromatography on silica gel (2.5 to 10% EtOAc in hexanes) to give recovered ketone **232** (90.9 mg, 10% yield), the high R_f diastereomer methyl ketone **233a** (219 mg, 24% yield) as an oil: R_f 0.65 (10% EtOAc in hexanes developed 2 times); ^{1}H NMR (300 MHz, $CDCl_3$) δ 4.70 (dd, J = 4.7, 12.2 Hz, 1H), 4.22 (d, J = 12.0 Hz, 1H), 3.49 (d, J = 12.6 Hz, 1H), 3.34 (d, J = 12.3 Hz, 1H), 2.93 (d, J = 11.7 Hz, 1H), 2.41 (dq, J = 6.3, 19.8 Hz, 1H), 1.98 (dt, J = 5.1, 12.9 Hz, 1H), 1.53 (d, J = 13.2 Hz, 1H), 1.34 (s, 3H), 1.10 (s, 3H), 1.01 (d, J = 6.6 Hz, 3H), 0.89 (s, 9H), 0.55 (s, 3H), 0.12 (s, 6H); ^{13}C NMR (75 MHz, $CDCl_3$) δ 213.4, 101.9, 67.0, 65.5, 63.9, 56.8, 48.1, 41.0, 38.6, 25.8, 24.8, 24.5, 18.0, 15.7, 14.7, 11.3, -4.3, -5.1; IR (Neat film NaCl) 2984, 2955, 2935, 2858, 1709, 1220, 1095, 1072, 1044, 868, 837, 776 cm^{-1}; HRMS (FAB) $[M+H]^+$ calc'd for $[C_{20}H_{38}O_4Si+H]^+$: m/z 371.2618, found 371.2607, and the low R_f diastereomer methyl ketone **233b** (436 mg, 48% yield) as an oil: R_f 0.36 (10% EtOAc in hexanes developed 2 times); ^{1}H NMR (300 MHz, $CDCl_3$) δ 3.80 (d, J = 12.6 Hz, 1H), 3.60 (d, J = 12.0 Hz, 1H), 3.58 (bs, 1H), 3.41 (d, J = 12.6 Hz, 1H), 3.02-2.80 (m, 2H), 1.91 (ddd, J = 4.2, 5.6, 14.0 Hz, 1H), 1.58 (m, 1H), 1.30 (s, 3H), 1.24 (s, 3H), 1.08 (s, 3H), 1.07 (s, 3H), 1.05 (s, 3H), 0.92 (s, 9H), 0.11 (s, 3H), 0.09 (s, 3H); ^{13}C NMR (75 MHz, $CDCl_3$) δ 214.6, 101.2, 73.0, 67.8, 64.3, 54.4, 47.0, 37.7, 35.3,

25.8, 25.0, 23.9, 19.4, 18.1, 16.9, 14.7, -4.6, -5.0; IR (Neat film NaCl) 2933, 2858, 1709, 1255, 1222, 1078, 1046, 838, 775 cm^{-1}; HRMS (FAB) $[M+H]^+$ calc'd for $[C_{20}H_{38}O_4Si+H]^+$: *m/z* 371.2618, found 371.2625.

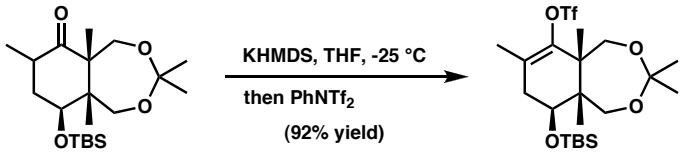

233 ***234***

Triflate 234. To a cooled (-25 °C) solution of KHMDS (668 mg, 3.35 mmol, 1.20 equiv) in THF (40 mL) was added the low R_f diastereomer methyl ketone **233b** (1.04 g, 2.79 mmol, 1.00 equiv) in THF (20 mL) in a dropwise manner over 10 min. After 2.0 h at -25 °C, $PhNTf_2$ (1.30 g, 3.63 mmol, 1.30 equiv) in THF (20 mL) was added, and the reaction was maintained for an additional 30 min at -25°C. The reaction mixture was quenched into half-saturated $NaHCO_3$ (50 mL) and EtOAc (50 mL), and extracted with EtOAc (5 x 50 mL). The combined organics were washed with brine (1 x 50 mL), dried (Na_2SO_4), and concentrated to an oil, which was purified by flash chromatography on silica gel (0 to 10% EtOAc in hexanes) to provide triflate **234** (1.30 g, 92% yield) as an oil: R_f 0.69 (10% Et_2O in hexanes); ^1H NMR (300 MHz, C_6D_6) δ 4.18 (dd, *J* = 6.3, 9.9 Hz, 1H), 3.79 (d, *J* = 12.3 Hz, 1H), 3.65 (d, *J* = 12.9 Hz, 1H), 3.41 (d, *J* = 12.3 Hz, 1H), 3.33 (d, *J* = 12.6 Hz, 1H), 2.08 (dd, *J* = 6.5, 17.6 Hz, 1H), 1.91 (ddd, *J* = 1.1, 9.9, 17.6 Hz, 1H), 1.61 (s, 3H), 1.20 (s, 3H), 1.17 (s, 3H), 1.16 (s, 3H), 0.98 (s, 9H), 0.49 (s, 3H), 0.15 (s, 3H), 0.05 (s, 3H); ^{13}C NMR (75 MHz, C_6D_6) δ 145.9, 127.1, 119.7 (q, $J_{C\text{-}F}$ = 318 Hz), 102.0, 65.4, 65.2, 62.7, 47.4, 45.9, 38.2, 26.5, 25.0, 24.9, 18.6, 18.3, 17.0, 11.0, -3.8,

-4.6; IR (Neat film NaCl) 2988, 2954, 2858, 1405, 1213, 1141, 1078, 879 cm^{-1}; HRMS (FAB) $[M+H]^+$ calc'd for $[C_{21}H_{37}SSiO_6F_3+H]^+$: m/z 503.2110, found 503.2094.

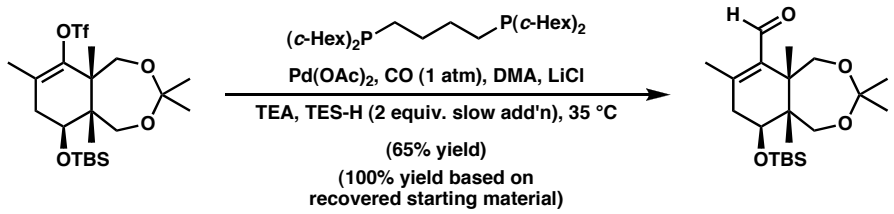

234 ***235***

Enal 235. A solution of flame-dried LiCl (433 mg, 10.2 mmol, 3.0 equiv), $Pd(OAc)_2$ (153 mg, 0.680 mmol, 0.20 equiv), and 1,4-bis-(dicyclohexylphosphino)butane (306 mg, 0.680 mmol, 0.20 equiv) in DMA (16 mL) was sparged with CO and warmed to 85 °C until a color change from red/orange to pale yellow was observed, at which point the reaction mixture was cooled to 40 °C. To the homogenous reaction mixture was added TEA (1.89 mL, 13.6 mmol, 4.00 equiv) and enol triflate **234** (1.71 g, 3.40 mmol, 1.00 equiv) in DMA (20 mL). A solution of Et_3SiH (1.09 mL, 6.80 mmol, 2.0 equiv) in DMA (10.0 mL) was added by syringe pump to the reaction over 10 h. After an additional 14 h at 40 °C, the reaction mixture was cooled to ambient temperature, poured into H_2O (100 mL) and Et_2O (100 mL), and extracted with Et_2O (5 x 50 mL). The combined organic layers were washed with H_2O (20 mL), brine (2 x 20 mL), dried (Na_2SO_4), and concentrated to give an oil, which was purified by flash chromatography on silica gel (2 to 10% EtOAc in hexanes) to give recovered triflate **234** (606 mg, 35% yield) and enal **235** (841 mg, 65% yield) as a pale yellow oil: R_f 0.50, 0.55 (10% EtOAc in hexanes developed twice, 25% Et_2O in hexanes); ^1H NMR (300 MHz, $CDCl_3$) δ 10.06 (s, 1H), 4.19 (dd, *J* = 7.1, 9.2 Hz, 1H), 3.73 (d, *J* = 12.3 Hz, 1H), 3.60 (d, *J* = 12.0 Hz, 1H), 3.57 (d, *J* = 12.3 Hz, 1H), 3.34 (d, *J* = 12.3 Hz, 1H), 2.32-2.22 (m, 2H), 2.09 (s, 3H),

1.31 (s, 3H), 1.24 (s, 6H), 0.89 (s, 9H), 0.53 (s, 3H), 0.08 (s, 6H); ^{13}C NMR (75 MHz, $CDCl_3$) δ 92.7, 154.2, 135.2, 101.0, 65.2, 65.0, 61.4, 45.2, 43.7, 41.3, 25.8, 24.6, 19.6, 18.0, 17.5, 10.7, -4.4, -5.1; IR (Neat film NaCl) 2986, 2953, 2888, 2857, 1677, 1371, 1221, 1101, 1073, 870, 837, 780 cm^{-1}; HRMS (FAB) $[M-H_2+H]^+$ calc'd for $[C_{20}H_{37}O_5]^+$: *m/z* 385.2410, found 385.2412.

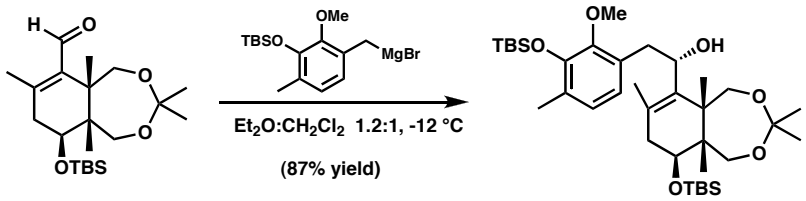

235 ***236***

Allylic alcohol 236. A flame-dried two-neck round-bottom flask equipped with a reflux condenser and septum was charged with magnesium turnings (3.00 g, 123 mmol, 56.1 equiv) and Et_2O (45 mL) under an N_2 atmosphere and heated to reflux. To this mixture was added 1,2-dibromoethane (75.0 μL, 0.870 mmol, 0.40 equiv) in a dropwise manner [*Caution: gas evolution!*]. When gas evolution ceased, a solution of benzyl bromide **151** (1.37 g, 3.96 mmol, 1.80 equiv) in Et_2O (18.0 mL) was added in a dropwise manner over 30 min and heating was continued for an additional 30 min. The Grignard reagent was then cooled (0 °C), and added to a cooled (-12 °C) solution of enal **235** (841 mg, 2.20 mmol, 1.00 equiv) in Et_2O (45 mL) and CH_2Cl_2 (90 mL). After 1 h at -12 °C, the reaction was quenched with H_2O (150 mL), 2 M citric acid (20 mL), brine (20 mL), and EtOAc (50 mL), and extracted with EtOAc (4 x 50 mL). The combined organics were washed with brine (2 x 50 mL), dried (Na_2SO_4), and concentrated to an oil, which was purified by flash chromatography on silica gel (2.5 to 12.5% Et_2O in hexanes) to give allylic alcohol **236** (1.24 g, 87% yield) as a foam consisting of a 10:1 mixture of

diastereomers. Only the major component (stereochemistry shown above) could be isolated in pure form: R_f 0.41, 0.29 (25% Et_2O in hexanes, 10% EtOAc in hexanes); ^1H NMR (300 MHz, $CDCl_3$) δ 6.84 (d, *J* = 7.5 Hz, 1H), 6.70 (d, *J* = 7.5 Hz, 1H), 4.46 (d, *J* = 10.2 Hz, 1H), 4.16 (dd, *J* = 7.1, 9.5 Hz, 1H), 3.71 (s, 3H), 3.62 (d, *J* = 12.6 Hz, 1H), 3.53 (d, *J* = 12.3 Hz, 1H), 3.39 (d, *J* = 12.3 Hz, 1H), 3.32 (bs, 1H), 3.27 (dd, *J* = 10.7, 14.0 Hz, 1H), 2.59 (dd, *J* = 3.0, 14.1 Hz, 1H), 2.46 (s, 1H), 2.20 (s, 3H), 2.10-2.00 (m, 2H), 1.98 (s, 3H), 1.31 (s, 3H), 1.26 (s, 3H), 1.21 (s, 3H), 1.03 (s, 9H), 0.90 (s, 9H), 0.56 (s, 3H), 0.19 (s, 3H), 0.16 (s, 3H), 0.10 (s, 6H); ^{13}C NMR (75 MHz, $CDCl_3$) δ 49.5, 147.2, 134.6, 132.2, 130.8, 129.4, 126.4, 123.1, 100.8, 72.6, 66.1, 65.7, 62.2, 60.0, 47.1, 43.6, 40.0, 38.4, 26.0, 25.9, 24.7(2C), 20.9, 18.6, 18.1, 17.8, 17.0, 10.9, -4.0, -4.2, -4.3, -5.1; IR (Neat film NaCl) 3479, 2955, 2931, 2858, 1463, 1253, 1221, 1074, 838, 780 cm^{-1}; HRMS (FAB) $[M\text{-}H_2+H]^+$ calc'd for $[C_{36}H_{63}Si_2O_6]^+$: *m/z* 647.4163, found 647.4156.

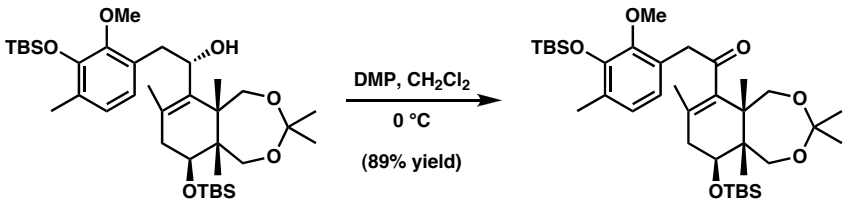

236 ***237***

Enone 237. To a cooled (0 °C) solution of allylic alcohol **236** (1.24 g, 1.91 mmol, 1.00 equiv) in CH_2Cl_2 (120 mL) was added Dess-Martin periodinane (1.21 g, 2.86 mmol, 1.50 equiv) and the resulting mixture was stirred for 2 h. The reaction mixture was concentrated to ~40 mL, diluted with Et_2O (250 mL), filtered, and concentrated to an oil, which was purified by gradient flash chromatography on silica gel (2.5 to 5% EtOAc in hexanes) to give enone **237** (1.10 g, 89% yield) as a foam: R_f 0.43, 0.69 (10% EtOAc in hexanes, 10% Et_2O in hexanes); ^1H NMR (300 MHz, $CDCl_3$) δ 6.83 (d, *J* = 7.5 Hz, 1H),

6.63 (d, *J* = 7.8 Hz, 1H), 4.28 (dd, *J* = 7.1, 9.5 Hz, 1H), 3.92 (d, *J* = 18.3 Hz, 1H), 3.80 (d, *J* = 18.0 Hz, 1H), 3.75 (d, *J* = 11.4 Hz, 1H), 3.64 (s, 3H), 3.52 (d, *J* = 12.6 Hz, 1H), 3.39 (d, *J* = 12.3 Hz, 1H), 2.20 (s, 3H), 2.12-1.98 (m, 2H), 1.72 (s, 3H), 1.31 (s, 3H), 1.27 (s, 3H), 1.13 (s, 3H), 1.02 (s, 9H), 0.90 (s, 9H), 0.66 (s, 3H), 0.15 (s, 6H), 0.09 (s, 3H), 0.08 (s, 6H); ^{13}C NMR (75 MHz, $CDCl_3$) δ 208.1, 150.1, 147.0, 138.2, 129.9 (2C), 125.8, 125.3, 123.2, 101.1, 65.9, 65.5, 61.5, 60.0, 47.1, 45.3, 42.9, 37.9, 26.1, 25.9, 24.7 (2C), 20.7, 18.6, 18.1, 17.1, 11.1, -4.2 (2C), -4.4, -5.1; IR (Neat film NaCl) 2954, 2930, 2858, 1699, 1463, 1252, 1221, 1099, 1073, 864, 836, 780 cm^{-1}; HRMS (FAB) $[M+H]^+$ calc'd for $[C_{36}H_{63}Si_2O_6+H]^+$: *m/z* 647.4163, found 647.4140.

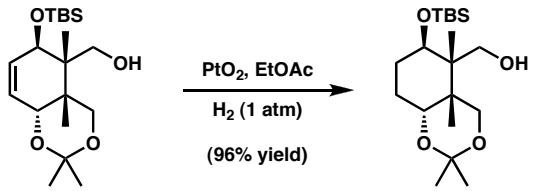

230 ***238***

Alcohol 238. To a solution of acetonide **230** (5.64 g, 15.8 mmol, 1.00 equiv) in EtOAc (198 mL) was added PtO_2 (108 mg, 0.475 mmol, 0.03 equiv), and the reaction mixture was sparged with a stream of H_2 gas for 4 h. The reaction mixture was concentrated (~10 mL), filtered through a plug of silica gel, and concentrated to give hydrogenated alcohol **238** (5.47 g, 96% yield) as an oil: R_f 0.76 (35% EtOAc in hexanes); ^{1}H NMR (500 MHz, $CDCl_3$) δ 4.43 (dd, *J* = 5.5, 12.0 Hz, 1H), 3.98 (dd, *J* = 5.0, 10.3 Hz, 1H), 3.88 (d, *J* = 13.0 Hz, 1H), 3.79 (app. t, *J* = 3.0 Hz, 1H), 3.45 (s, 1H), 3.32 (d, *J* = 12.0 Hz, 1H), 3.04 (app. t, *J* = 11.0 Hz, 1H), 2.12 (app. tt, *J* = 3.8, 14.3 Hz, 1H), 1.86 (app. tt, *J* = 3.0, 14.0 Hz, 1H), 1.48 (s, 3H), 1.47-1.37 (m, 1H), 1.42 (s, 3H), 0.97 (s, 3H), 0.93 (s, 3H), 0.90 (s, 9H), 0.05 (s, 3H), 0.04 (s, 3H); ^{13}C NMR (125 MHz,

$CDCl_3$) δ 98.5, 75.0, 74.4, 69.5, 66.8, 43.5, 35.0, 29.5, 25.9, 25.1, 21.9, 20.2, 18.8, 18.0, 17.2, -4.6, -5.0; IR (Neat film NaCl) 3497, 2953, 2936, 2883, 2858, 1472, 1379, 1257, 1196, 1083, 1060, 1034, 1005, 866, 834, 774 cm^{-1}; HRMS (FAB) $[M+H]^+$ calc'd for $[C_{19}H_{38}SiO_4+H]^+$: *m/z* 359.2618, found 359.2632.

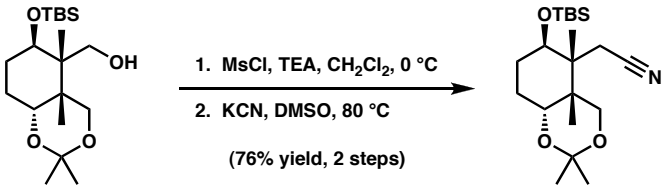

238 ***239***

Nitrile 239. To a cooled (0 °C) solution of alcohol **238** (880 mg, 2.45 mmol, 1.00) and TEA (1.02 mL, 7.36 mmol, 3.00 equiv) in CH_2Cl_2 (25 mL) was added methanesulfonyl chloride (228 μL, 2.95 mmol, 1.20 equiv) in a dropwise manner. After 30 min at 0 °C, the reaction mixture was diluted with CH_2Cl_2 (40 mL), ice cold H_2O (50 mL), and brine (25 mL), and extracted with CH_2Cl_2 (3 x 35 mL). The combined organics were washed with brine (30 mL), dried (Na_2SO_4), and concentrated to a waxy solid that was used in the next step immediately.

The above residue was dissolved in DMSO (25 mL) and treated with KCN (400 mg, 6.14 mmol, 2.50 equiv) at 80 °C for 4 h. The reaction mixture was cooled to ambient temperature, diluted with EtOAc (50 mL) and H_2O (150 mL), and extracted with EtOAc (7 x 40 mL). The combined organics were washed with brine (30 mL), dried (Na_2SO_4), concentrated, and purified by flash chromatography on silica gel (2.5 to 10% EtOAc in hexanes) to provide nitrile **239** (682 mg, 76% yield) as a solid : R_f 0.42 (20% EtOAc in hexanes); ^1H NMR (300 MHz, $CDCl_3$) δ 4.07 (d, *J* = 8.7 Hz, 1H), 3.83 (d, *J* = 8.4 Hz, 1H), 3.70-3.60 (m, 2H), 3.49 (d, *J* = 8.1 Hz, 1H), 3.46 (d, *J* = 8.7 Hz, 1H), 2.18-2.04 (m,

1H), 1.74-1.45 (m, 3H), 1.55 (s, 6H), 1.14 (s, 3H), 0.90 (s, 3H), 0.87 (s, 9H), 0.06 (s, 3H), 0.05 (s, 3H); ^{13}C NMR (75 MHz, $CDCl_3$) δ 121.7, 78.8, 76.1, 74.8, 71.0, 70.1, 50.8, 48.8, 28.8 (2C), 27.6 (2C), 25.8, 22.6, 18.0, 9.5, -3.9, -5.0; IR (Neat film NaCl) 2956, 2934, 2882, 2860, 1460, 1254, 1183, 1080, 1047, 916, 868, 835, 772 cm^{-1}; HRMS (FAB) [M-H_2+H]$^+$ calc'd for $[C_{20}H_{36}NO_3Si]^+$: *m/z* 366.2464, found 366.2459.

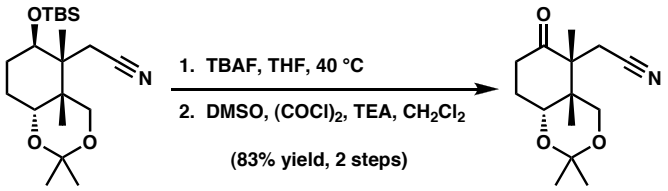

239 ***240***

Ketone 240. To a solution of nitrile **239** (1.13 g, 3.08 mmol, 1.00 equiv) in THF (18.5 mL) was added a 1.0 M solution of TBAF (9.23 mL, 9.23 mmol, 3.00 equiv) in THF, and the reaction mixture was heated to 40 °C for 7.5 h. An additional portion of a 1.0 M solution of TBAF (2.00 mL, 2.00 mmol, 0.65 equiv) in THF was added. After a further 1 h, the reaction mixture was cooled to ambient temperature, diluted with EtOAc (100 mL) and brine (75 mL), and extracted with EtOAc (5 x 75 mL). The combined organics were washed with brine (50 mL), dried (Na_2SO_4), and concentrated to an oil, which was used without further purification.

A solution of DMSO (1.75 mL, 24.6 mmol, 8.0 equiv) in CH_2Cl_2 (100 mL) was cooled (-78 °C) and oxalyl chloride (1.88 mL, 21.5 mmol, 7.00 equiv) was added in a dropwise manner. After 40 min at -78 °C, a solution of the crude alcohol generated above in CH_2Cl_2 (20 mL) was added in a dropwise manner down the wall of the flask over 13 min. After an additional 2.5 h at -78 °C, TEA (8.58 mL, 61.6 mmol, 20.0 equiv) was added and the reaction mixture was allowed to warm to ambient temperature over 3

h, diluted with half-saturated NH_4Cl (75 mL), and extracted with CH_2Cl_2 (4 x 50 mL). The combined organics were washed with saturated $NaHCO_3$ (30 mL), dried ($MgSO_4$), concentrated to an oil, and purified by flash chromatography on silica gel (2.5 to 35% EtOAc in hexanes) to provide ketone **240** (683 mg, 83% yield) as an oil: R_f 0.49 (50% EtOAc in hexanes); ^{1}H NMR (300 MHz, $CDCl_3$) δ 4.53 (d, J = 8.7 Hz, 1H), 4.01 (dd, J = 4.4, 10.7 Hz, 1H), 3.95 (d, J = 9.3 Hz, 1H), 3.50 (d, J = 9.3 Hz, 1H), 3.41 (d, J = 8.1 Hz, 1H), 2.68-2.41 (m, 2H), 2.41-2.24 (m, 1H), 2.10-1.90 (m, 1H), 1.61 (s, 6H), 1.23 (s, 3H), 1.14 (s, 3H), 0.87 (s, 9H), 0.06 (s, 3H), 0.05 (s, 3H); ^{13}C NMR (75 MHz, $CDCl_3$) δ 210.6, 121.3, 77.5, 75.0, 74.1, 70.7, 58.0, 50.4, 35.6, 28.6, 27.7, 27.5, 21.4, 16.7; IR (Neat film NaCl) 2983, 2881, 2254, 1714, 1387, 1373, 1171, 1052, 907, 729, 651 cm^{-1}; HRMS (EI) $[M]^+$ calc'd for $[C_{14}H_{21}NO_3]^+$: m/z 251.1521, found 251.1518.

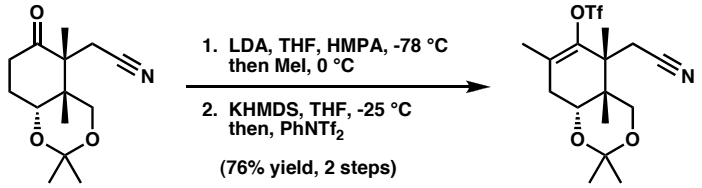

240 *241*

Triflate 241. A solution of LDA in THF was prepared by dropwise addition of 2.50 M *n*-BuLi solution in hexanes (580 μL, 1.45 mmol, 1.05 equiv) to diisopropylamine (252 μL, 1.79 mmol, 1.30 equiv) in THF (15.0 mL) at 0 °C, followed by stirring for 30 min. Upon cooling the solution to -78 °C, a solution of ketone **240** (347 mg, 1.38 mmol, 1.00 equiv) in THF (15.0 mL) was added in a dropwise manner, and the reaction mixture was stirred at -78 °C for 2 h. HMPA (552 μL, 3.18 mmol, 2.30 equiv) was added and the reaction mixture was brought to 0 °C for 1 h. After cooling again to -78 °C, the solution containing the enolate was added to a solution of MeI (258 μL, 4.14 mmol, 3.00 equiv) in

THF (4.00 mL) at -30 °C in a dropwise manner over 25 min. After 6 h at -25 °C, the reaction mixture was quenched with H_2O (30 mL) and CH_2Cl_2 (30 mL), and extracted with CH_2Cl_2 (5 x 30 mL). The combined organics were washed, dried ($MgSO_4$), and concentrated to an oil, which was purified by flash chromatography on silica gel (10 to 25% EtOAc in hexanes) to give to an inseparable mixture of diastereomeric methyl ketones (286 mg, 78% yield).

To a cooled (-25 °C) solution of KHMDS (300 mg, 1.50 mmol, 1.40 equiv) in THF (17 mL) was added the above mixture of methyl ketones (286 mg, 1.07 mmol, 1.00 equiv) in THF (15 mL) in a dropwise manner over 10 min. After 2.5 h at -25 °C, $PhNTf_2$ (614 mg, 1.72 mmol, 1.60 equiv) in THF (10.7 mL) was added, and the reaction maintained for an additional 30 min at -25°C. The reaction mixture was quenched into half-saturated $NaHCO_3$ (100 mL) and extracted with EtOAc (4 x 70 mL). The combined organics were dried (Na_2SO_4) and concentrated to an oil, which was purified by flash chromatography on silica gel (15 to 25% Et_2O in hexanes) to provide triflate **241** (420 mg, 98% yield, 76% yield for 2 steps) as an oil: R_f 0.41 (50% Et_2O in hexanes); ^1H NMR (300 MHz, C_6D_6) δ 4.16 (d, J = 8.7 Hz, 1H), 3.95 (d, J = 9.3 Hz, 1H), 3.52 (dd, J = 6.2, 8.6 Hz, 1H), 3.46 (d, J = 9.0 Hz, 1H), 3.36 (d, J = 9.0 Hz, 1H), 2.17 (dd, J = 6.0, 18.0 Hz, 1H), 1.95 (dd, J = 8.1, 18.0 Hz, 1H), 1.50 (s, 3H), 1.01 (s, 3H), 0.97 (s, 3H), 0.90 (s, 3H), 0.88 (s, 3H); ^{13}C NMR (75 MHz, C_6D_6) δ 145.7, 125.1, 121.5, 119.5 (app. d, $J_{C\text{-}F}$ = 296 Hz), 75.2, 74.7, 74.3, 71.0, 51.2, 50.4, 36.1, 28.2, 27.4, 21.6, 18.1, 16.4; IR (Neat film NaCl) 2988, 2942, 2884, 1403, 1211, 1141, 1053, 990, 874 cm^{-1}; HRMS (EI) $[M]^+$ calc'd for $[C_{16}H_{22}NO_5F_3S]^+$: m/z 397.1171, found 397.1179.

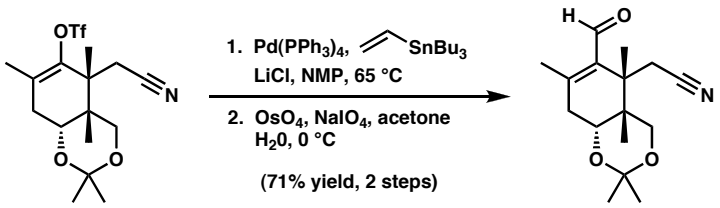

241 *242*

Enal 242. To a solution of triflate **241** (1.41 g, 3.54 mmol, 1.00 equiv), $Pd(PPh_3)_4$ (307 mg, 0.266 mmol, 0.075 equiv), and LiCl (450 mg, 10.6 mmol, 3.00 equiv) in NMP (59 mL) was added tributyl(vinyl)tin (1.55 mL, 5.31 equiv, 1.50 equiv), and the mixture was heated to 65 °C for 0.5 h. The reaction mixture was cooled to ambient temperature, quenched with H_2O (300 mL) and Et_2O (200 mL), and extracted with Et_2O (4 x 125 mL). The combined organics were washed with brine (170 mL), dried ($MgSO_4$), and concentrated to an oil, which was purified by flash chromatography on silica gel (2.5 to 10% EtOAc in hexanes) to provide the intermediate diene (1.04 g, quantitative yield) as a viscous oil containing a small amount of solvent.

To a cooled (0 °C) solution of the intermediate diene (116.7 mg, 0.42 mmol, 1.00 equiv) in acetone (5.30 mL) and H_2O (5.30 mL) was added OsO_4 (10.8 mg, 42.3 μmol, 0.10 equiv) and $NaIO_4$ (227 mg, 1.06 mmol, 2.50 equiv). After 3.5 h at 0 °C, the reaction mixture was diluted with H_2O (35 mL) and EtOAc (35 mL), and extracted with EtOAc (5 x 15 mL). The combined organics from four such reactions were washed with brine (200 mL), dried ($MgSO_4$), and concentrated to an oil, which was purified by flash chromatography on silica gel (20 to 35% EtOAc in hexanes) to provide enal **242** (332 mg, 71% yield, 2 steps) as an oil: R_f 0.28 (35% EtOAc in hexanes); ^{1}H NMR (300 MHz, $CDCl_3$) δ 10.10 (s, 1H), 4.21 (d, J = 9.0 Hz, 1H), 3.87 (d, J = 9.3 Hz, 1H), 3.85 (d, J = 8.4 Hz, 1H), 3.70 (d, J = 9.0 Hz, 1H), 3.51 (d, J = 8.7 Hz, 1H), 2.78 (dd, J = 6.0, 19.8 Hz, 1H), 2.49 (dd, J = 9.0, 19.8 Hz, 1H), 2.16 (s, 3H), 1.60 (s, 3H), 1.59 (s, 3H), 1.20 (s, 3H),

1.16 (s, 3H); ^{13}C NMR (75 MHz, $CDCl_3$) δ 191.0, 153.2, 136.8, 121.5, 76.0, 74.2, 74.1, 70.4, 48.7, 48.0, 38.7, 28.7, 27.3, 20.7, 19.0, 18.0; IR (Neat film NaCl) 2982, 2938, 2880, 1671, 1628, 1386, 1177, 1050 cm^{-1}; HRMS (EI) $[M]^+$ calc'd for $[C_{16}H_{23}NO_3]^+$: m/z 277.1678, found 277.1677.

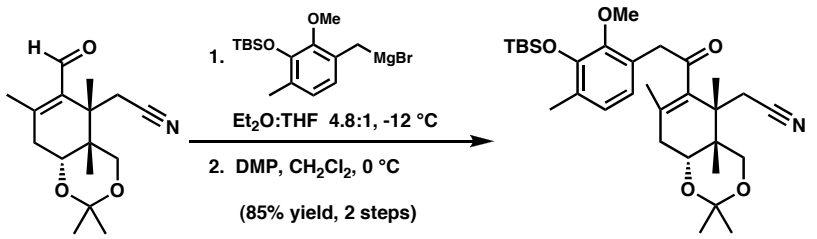

242 ***243***

Enone 243. A flame-dried two-neck round-bottom flask equipped with a reflux condenser and septum was charged with magnesium turnings (1.66 g, 68.4 mmol, 57.0 equiv) and Et_2O (27 mL) under an N_2 atmosphere and heated to reflux. To this mixture was added 1,2-dibromoethane (120 μL, 1.39 mmol, 1.16 equiv) in a dropwise manner [*Caution: gas evolution!*]. When gas evolution ceased, a solution of benzyl bromide **151** (1.24 g, 3.60 mmol, 3.00 equiv) in Et_2O (8.0 mL) was added in a dropwise manner over 30 min, and heating was continued for an additional 20 min. The Grignard reagent was then cooled (0 °C) and added to a cooled (0 °C) solution of enal **242** (332 mg, 1.20 mmol, 1.00 equiv) in THF (12 mL). After 1 h at 0 °C, the reaction was quenched with 0.5 M citric acid (40 mL) and EtOAc (40 mL), and extracted with EtOAc (5 x 25 mL). The combined organics were dried (Na_2SO_4) and concentrated to an oil, which was purified by flash chromatography on silica gel (10 to 25% EtOAc in hexanes) to give a separable 3:1 mixture of diastereomeric allylic alcohols (533.3 mg, 85% yield).

To a cooled (0 °C) solution of the above allylic alcohol (76.0 mg, 0.140 mmol, 1.00 equiv) in CH_2Cl_2 (5.0 mL) was added Dess-Martin periodinane (89.1 mg, 0.211 mmol, 1.50 equiv) and the resulting mixture was stirred for 2 h. The reaction mixture was diluted with Et_2O (35 mL), filtered, concentrated to an oil, and purified by flash chromatography on silica gel (5 to 20% EtOAc in hexanes) to give enone **243** (75.7 mg, 100% yield, 85% yield 2 steps) as an oil: R_f 0.47 (25% EtOAc in hexanes); ^{1}H NMR (300 MHz, $CDCl_3$) δ 6.85 (d, *J* = 7.8 Hz, 1H), 6.64 (d, *J* = 7.8 Hz, 1H), 4.16 (d, *J* = 8.7 Hz, 1H), 4.08 (d, *J* = 9.0 Hz, 1H), 3.87 (dd, *J* = 6.0, 8.4 Hz, 1H), 3.86 (s, 2H), 3.64 (s, 3H), 3.53 (d, *J* = 8.7 Hz, 1H), 3.52 (d, *J* = 9.0 Hz, 1H), 2.54 (dd, *J* = 6.0, 17.7 Hz, 1H), 2.30 (dd, *J* = 8.3, 18.2 Hz, 1H), 2.21 (s, 3H), 1.79 (s, 3H), 1.62 (s, 3H), 1.61 (s, 3H), 1.17 (s, 3H), 1.15 (s, 3H), 1.02 (s, 9H), 0.16 (s, 6H); ^{13}C NMR (75 MHz, $CDCl_3$) δ 207.4, 150.0, 147.0, 138.7, 130.0, 128.2, 125.8, 125.2, 123.3, 121.6, 75.5 (2C), 75.2, 70.5, 59.9, 49.7, 47.2, 47.1, 35.5, 28.7, 27.6, 26.0, 21.1, 20.8, 18.5, 18.2, 17.1, -4.2; IR (Neat film NaCl) 2932, 2859, 1699, 1464, 1422, 1286, 1073, 1047, 856, 841 cm^{-1}; HRMS (FAB) $[M+H]^+$ calc'd for $[C_{31}H_{47}NSiO_5+H]^+$: *m/z* 542.3302, found 542.3296.

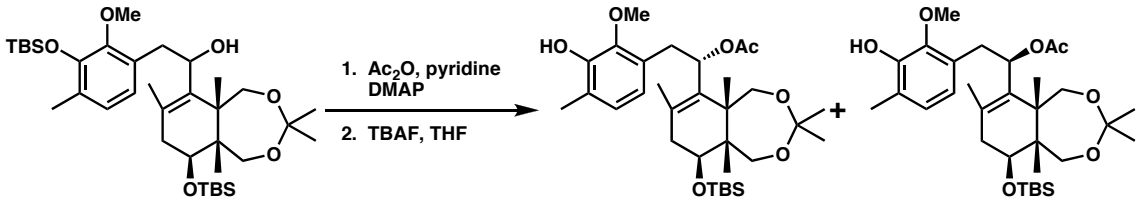

244 **as a ~4:1 mixture at C(20)** ***247*** **(82% yield 2 steps)** ***248*** **(17% yield 2 steps)**

Allylic acetates 247 and 248. To a solution of allylic alcohol **244** (120 mg, 0.185 mmol, 1.00 equiv) in Ac_2O (4.00 mL) and pyridine (1.00 mL) was added DMAP (11.3 mg, 92.4 μmol, 0.50 equiv). After 3 h, the reaction mixture was concentrated and

purified by flash chromatography on silica gel (2.5 to 10% Et_2O in hexanes) to give an inseparable mixture of intermediate acetates (122.1 mg).

To a solution of the above acetates in THF (4.00 mL) was added a 1.0 M solution of TBAF (1.06 mL, 1.06 mmol, 6.00 equiv). After a further 30 min, the reaction mixture was diluted with H_2O (30 mL) and CH_2Cl_2 (30 mL), and extracted with CH_2Cl_2 (6 x 30 mL). The combined organics were dried (Na_2SO_4), concentrated, and purified by flash chromatography on silica gel (5 to 20% EtOAc in hexanes) to give isomerically pure allylic acetate **248** (17.5 mg, 17% yield, two steps) as a white foam: R_f 0.34 (20% EtOAc in hexanes); ^{1}H NMR (300 MHz, $CDCl_3$) δ 6.78 (d, *J* = 7.5 Hz, 1H), 6.61 (d, *J* = 7.5 Hz, 1H), 5.64 (dd, *J* = 3.6, 10.8 Hz, 1H), 5.53 (s, 1H), 4.17 (dd, *J* = 7.1, 9.5 Hz, 1H), 3.79 (s, 3H), 3.55 (s, 2H), 3.52 (d, *J* = 12.6 Hz, 1H), 3.37 (d, *J* = 12.3 Hz, 1H), 3.13 (dd, *J* = 10.8, 14.4 Hz, 1H), 2.93 (dd, *J* = 3.6, 14.4 Hz, 1H), 2.21 (s, 3H), 2.12-2.00 (m, 2H), 1.96 (s, 3H), 1.82 (s, 3H), 1.31 (s, 3H), 1.24 (s, 3H), 1.17 (s, 3H), 0.89 (s, 9H), 0.55 (s, 3H), 0.08 (s, 6H); ^{13}C NMR (75 MHz, $CDCl_3$) δ 69.5, 147.0, 145.4, 133.8, 131.5, 128.0, 126.0, 123.4, 121.4, 101.0, 72.1, 65.5, 65.3, 61.9, 61.1, 46.7, 43.1, 40.0, 35.1, 25.9, 24.8, 24.6, 21.5, 20.9, 18.1, 16.9, 15.5, 11.1, -4.3, -5.1; IR (Neat film NaCl) 3448, 2950, 2856, 1739, 1463, 1373, 1248, 1220, 1067, 1039, 836 cm^{-1}; HRMS (FAB) $[M+H]^+$ calc'd for $[C_{32}H_{52}SiO_7+H]^+$: *m/z* 577.3561, found 577.3547, and allylic acetate **247** (83 mg, 82% yield, two steps) as a white foam: R_f 0.33 (20% EtOAc in hexanes); ^{1}H NMR (300 MHz, $CDCl_3$) δ 6.78 (d, *J* = 7.8 Hz, 1H), 6.58 (d, *J* = 7.8 Hz, 1H), 5.77 (bs, 1H), 5.59 (s, 3H), 4.09 (m, 1H), 3.81 (s, 3H), 3.50 (d, *J* = 12.3 Hz, 1H), 3.44-3.30 (m, 2H), 3.14 (dd, *J* = 9.6, 13.8 Hz, 1H), 2.99 (d, *J* = 12.0 Hz, 1H), 2.84 (dd, *J* = 5.1, 13.8 Hz, 1H), 2.20 (s, 3H), 2.12-2.00 (m, 2H), 1.98 (s, 3H), 1.89 (s, 3H), 1.28 (s, 3H), 1.19 (s, 3H), 1.14 (s, 3H), 0.89

(s, 9H), 0.51 (s, 3H), 0.09 (s, 3H), 0.08 (s, 3H); ^{13}C NMR (75 MHz, $CDCl_3$) δ 69.6, 147.1, 145.5, 134.8, 131.2, 128.0, 126.0, 123.6, 121.7, 100.8, 72.4, 65.8, 65.6, 62.0, 61.1, 47.0, 43.6, 40.0, 36.6, 35.4, 25.9, 24.6, 24.4, 21.3, 21.2, 18.1, 15.4, 10.9, -4.4, -5.1; IR (Neat film NaCl) 3418, 2985, 2952, 2857, 1741, 1464, 1371, 1248, 1221, 1067, 1040, 836, 777 cm^{-1}; HRMS (FAB) $[M\text{-}H_2\text{+}H]^+$ calc'd for $[C_{32}H_{51}SiO_7]^+$: *m/z* 575.3404, found 575.3405.

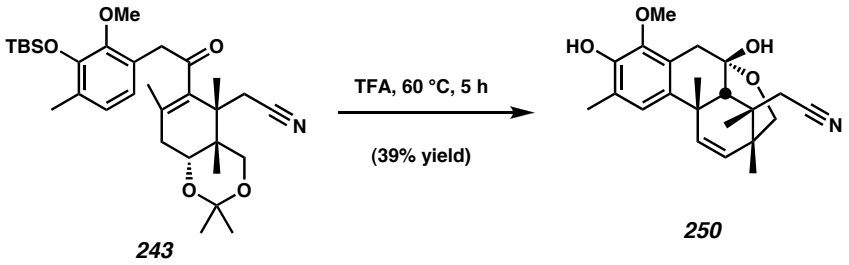

243 ***250***

Hemiacetal 250. A solution of enone **243** (29.9 mg, 55.2 μmol, 1.00 equiv) in trifluoroacetic acid (4.00 mL) was heated to 60 °C for 5 h. The reaction mixture was then cooled to ambient temperature, concentrated to an oil, and purified by flash chromatography on silica gel (5 to 50% EtOAc in hexanes) to give hemiacetal **250** (7.9 mg, 39% yield) as an off-white solid: R_f 0.30 (35% EtOAc in hexanes); ^{1}H NMR (500 MHz, $CDCl_3$) δ 6.95 (s, 1H), 5.97 (dd, *J* = 1.0, 9.5 Hz, 1H), 5.55 (s, 1H), 5.33 (d, *J* = 9.5 Hz, 1H), 4.18 (d, *J* = 8.5, 1H), 3.74 (s, 3H), 3.60 (d, *J* = 8.5 Hz, 1H), 3.55 (d, *J* = 11.5 Hz, 1H), 3.25 (d, *J* = 16.0, 1H), 3.09 (d, *J* = 11.5, 1H), 2.76 (d, *J* = 15.5, 1H), 2.23 (s, 3H), 1.76 (s, 1H), 1.42 (s, 3H), 1.15 (s, 3H), 0.87 (s, 3H); ^{13}C NMR (125 MHz, $CDCl_3$) δ 145.1, 144.1, 135.4, 135.1, 130.0, 124.7 (2C), 124.2, 123.1, 105.1, 75.1, 70.1, 60.5, 53.9, 41.7, 39.2, 35.3, 33.8, 31.6, 18.8, 17.7, 15.7; IR (Neat film NaCl) 3402, 2969, 2931, 2876, 2242, 1485, 1419, 1358, 1209, 1102, 1063, 981, 912, 732 cm^{-1}; MS (FAB) [M-

HCN]$^+$ calc'd for $[C_{21}H_{26}O_4]^+$: *m/z* 342.1831, found 342.2 (Hi-Res data not possible due to substrate fragmentation).

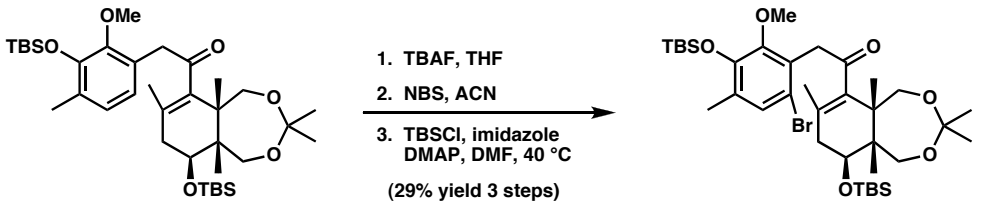

237 ***251***

Aryl bromide 251. To a solution of enone **237** (114 mg, 0.176 mmol, 1.00 equiv) in THF (8.0 mL) was added a 1.0 M solution of TBAF (176 μL, 0.176 mmol, 1.00 equiv) in THF. After 5 min, the reaction mixture was diluted with H_2O (50 mL) and CH_2Cl_2 (50 mL), and extracted with CH_2Cl_2 (4 x 25 mL). The combined organics were dried (Na_2SO_4), concentrated, and purified by flash chromatography on silica gel (5 to 25% EtOAc in hexanes) to give the intermediate phenol (91 mg, 97% yield).

To a solution of intermediate phenol (36.0 mg, 67.6 μmol, 1.00 equiv) in ACN (2.0 mL) was added NBS (18.0 mg, 101 μmol, 1.50 equiv). After 2.5 h, the reaction was diluted with H_2O (8 mL) and EtOAc (8 mL), and extracted with EtOAc (4 x 5 mL). The combined organics were dried (Na_2SO_4), concentrated, and purified by flash chromatography on silica gel (2.5 to 15% EtOAc in hexanes) to give the intermediate bromide (14.4 mg, 35% yield).

To a solution of intermediate bromide (14.4 mg, 23.5 μmol, 1.00 equiv), imidazole (36.0 mg, 0.530 mmol, 22.5 equiv), and TBSCl (26.6 mg, 0.177 mmol, 7.50 equiv) in DMF (2.5 mL) was added DMAP (21.5 mg, 0.176 mmol, 7.50 equiv) and the reaction was warmed to 40 °C. After 36 h, the reaction was diluted with H_2O (8 mL) and EtOAc (8 mL), and extracted with EtOAc (4 x 5 mL). The combined organics were dried

(Na_2SO_4), concentrated, and purified by flash chromatography on silica gel (1 to 5% Et_2O in hexanes) to give isomerically pure bromide **251** (14.5 mg, 85% yield, 29% yield for three steps) as a white foam: R_f 0.76, 0.79 (10% Et_2O in hexanes, 25% Et_2O in hexanes); ^{1}H NMR (300 MHz, $CDCl_3$) δ 7.13 (s, 1H), 4.29 (dd, *J* = 7.1, 9.5 Hz, 1H), 4.11 (d, *J* = 18.6 Hz, 1H), 4.00 (d, *J* = 18.6 Hz, 1H), 3.77 (d, *J* = 12.3 Hz, 1H), 3.62 (s, 3H), 3.55 (d, *J* = 12.9 Hz, 1H), 3.54 (d, *J* = 12.6 Hz, 1H), 3.39 (d, *J* = 12.3 Hz, 1H), 2.19 (s, 3H), 2.14-2.04 (m, 2H), 1.82 (s, 3H), 1.31 (s, 3H), 1.28 (s, 3H), 1.23 (s, 3H), 1.01 (s, 9H), 0.90 (s, 9H), 0.67 (s, 3H), 0.15 (s, 6H), 0.14 (s, 3H), 0.09 (s, 3H), 0.08 (s, 3H); ^{13}C NMR (75 MHz, $CDCl_3$) δ 206.1, 151.0, 146.4, 137.8, 131.4, 130.9, 129.4, 126.0, 116.4, 101.1, 66.0, 65.5, 61.5, 60.0, 48.0, 45.5, 43.0, 38.1, 26.0, 25.9, 24.7 (2C), 20.7, 18.5, 18.2, 18.1, 16.9, 11.1, -4.2, -4.3, -4.4, -5.1; IR (Neat film NaCl) 2954, 2930, 2858, 1700, 1471, 1404, 1233, 1220, 1099, 1075, 855, 837, 779 cm^{-1}; HRMS (FAB) $[M\text{-}H_2+H]^+$ calc'd for $[C_{36}H_{60}Si_2O_6Br]^+$: *m/z* 723.3112, found 723.3128.

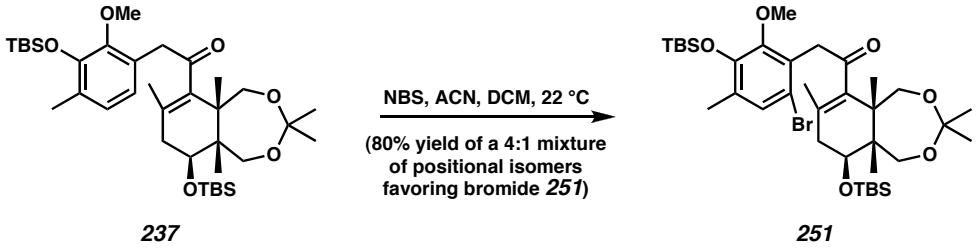

237 *251*

Aryl bromide 251 directly from enone **237**. To a solution of enone **237** (200 mg, 0.309 mmol, 1.00 equiv) in ACN (8.0 mL) and CH_2Cl_2 (1.2 mL) was added NBS (66.0 mg, 0.371 mmol, 1.20 equiv). After 2.5 h, the reaction was diluted with H_2O (30 mL) and EtOAc (15 mL), and extracted with EtOAc (5 x 15 mL). The combined organics were washed with brine (10 mL), dried (Na_2SO_4), concentrated, and purified by flash chromatography on silica gel (1 to 5% Et_2O in hexanes) to give aryl bromide **241** (179

mg, 80% yield) as a 4:1 mixture of bromide isomers favoring the desired aryl bromide **251**.

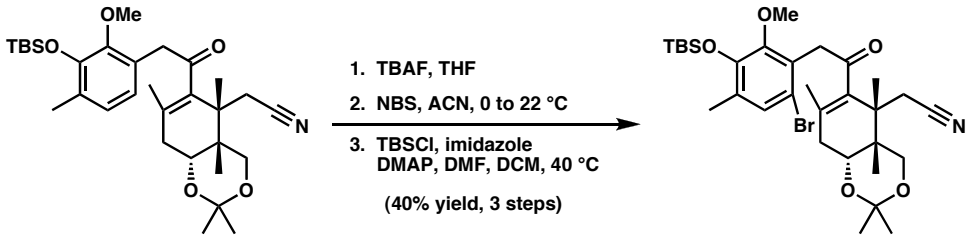

243 ***252***

Aryl bromide 252. To a solution of enone **243** (60.0 mg, 0.111 mmol, 1.00 equiv) in THF (3.7 mL) was added a 1.0 M solution of TBAF (166 μL, 0.166 mmol, 1.50 equiv) in THF. After 15 min, the reaction mixture was diluted with EtOAc (15 mL), H_2O (5 mL), and saturated aqueous NH_4Cl (5 mL), and extracted with EtOAc (5 x 20 mL). The combined organics were dried ($MgSO_4$), concentrated, and purified by flash chromatography on silica gel (20 to 30% EtOAc in hexanes) to give the intermediate phenol (40.0 mg, 85% yield).

To a cooled (0 °C) solution of intermediate phenol (33.7 mg, 78.8 μmol, 1.00 equiv) in ACN (1.6 mL) was added NBS (15.4 mg, 86.7 μmol, 1.10 equiv), and the reaction mixture was allowed to come to ambient temperature. After 5 h, the reaction was diluted with H_2O (10 mL) and EtOAc (20 mL), and extracted with EtOAc (5 x 10 mL). The combined organics were dried ($MgSO_4$), concentrated, and used without further purification in the next step.

To a solution of the above crude material (theory: 78.8 μmol, 1.00 equiv), imidazole (16.1 mg, 0.236 mmol, 3.00 equiv), TBSCl (17.8 mg, 0.118 mmol, 1.50 equiv) in DMF (200 μL) and CH_2Cl_2 (200 μL) was added DMAP (9.6 mg, 78.8 μmol, 1.00

equiv) and the reaction was stirred at ambient temperature for 24 h and then at 30 °C for 18 h. An additional portion of DMAP (10.0 mg, 81.9 μmol, 1.04 equiv) and TBSCl (20.0 mg, 132.7 μmol, 1.69 equiv) were added and the reaction mixture was heated at 40 °C for 4 h. The reaction was diluted with EtOAc (10 mL), washed with saturated aqueous NH_4Cl (3 x 5 mL), and extracted with EtOAc (3 x 10 mL). The combined organics were concentrated and purified by flash chromatography on silica gel (5 to 15% Et_2O in hexanes) to give isomerically pure bromide **252** (23.0 mg, 47% yield, 40% yield for three steps) as an amorphous white solid: R_f 043 (20% EtOAc in hexanes); ^{1}H NMR (500 MHz, $CDCl_3$) δ 7.13 (s, 1H), 4.29 (d, *J* = 8.5 Hz, 1H), 4.10 (d, *J* = 7.0 Hz, 1H), 4.07 (d, *J* = 7.0 Hz, 1H), 4.06 (d, *J* = 4.0 Hz, 1H), 3.88 (dd, *J* = 6.3, 8.8 Hz, 1H), 3.62 (s, 3H), 3.54 (app. t, *J* = 9.3 Hz, 1H), 2.55 (dd, *J* = 6.3, 17.8 Hz, 1H), 2.32 (dd, *J* = 8.5, 18.0 Hz, 1H), 2.18 (s, 3H), 1.87 (s, 3H), 1.62 (s, 3H), 1.61 (s, 3H), 1.21 (s, 3H), 1.17 (s, 3H), 1.01 (s, 9H), 0.14 (s, 6H); ^{13}C NMR (125 MHz, $CDCl_3$) δ 205.4, 150.9, 146.4, 138.3, 131.4, 129.3, 128.7, 126.0, 121.5, 116.3, 75.5, 75.3, 75.2, 70.5, 60.0, 49.7, 47.7, 47.2, 35.7, 28.7, 27.6, 26.0, 21.0, 20.8, 18.1, 16.8, -4.3; IR (Neat film NaCl) 2932, 2860, 2252, 1699, 1470, 1404, 1234, 1171, 1083, 1047, 853, 842, 734 cm^{-1}; HRMS (FAB) $[M+H]^+$ calc'd for $[C_{31}H_{46}NSiBrO_5+H]^+$: *m/z* 620.2407, found 620.2394.

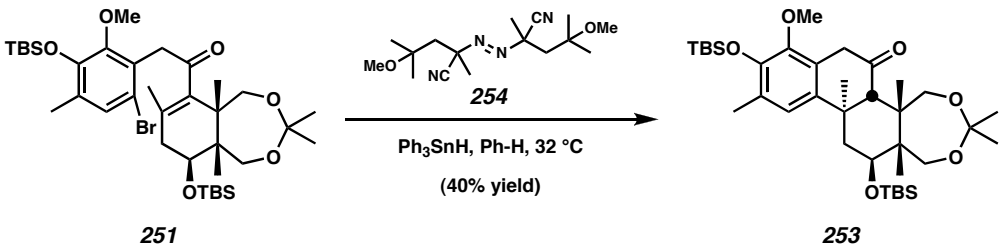

251 *253*

Cyclized ketone 253. To a solution of aryl bromide **251** (25.0 mg, 34.4 μmol, 1.00 equiv of a 4:1 mixture of isomers) and initiator V-70 (**254**) (15.9 mg, 51.7 μmol,

1.50 equiv) in benzene (2.0 mL) at 32 °C was added a solution of Ph_3SnH (24.2 mg, 68.8 μmol, 2.00 equiv) in benzene (0.5 mL) by syringe pump over 5 h. At the end of the addition, the reaction was cooled to ambient temperature, concentrated, and purified by flash chromatography on silica gel (2 to 7.5% Et_2O in hexanes) to give ketone **253** (8.9 mg, 40% yield, 50% yield based on the correct isomer of the starting material) as an oil: R_f 0.52 (25% Et_2O in hexanes); ^1H NMR (500 MHz, $CDCl_3$) δ 6.77 (s, 1H), 4.53 (d, J = 12.0 Hz, 1H), 4.43 (dd, J = 4.5, 12.5 Hz, 1H), 3.97 (d, J = 12.5 Hz, 1H), 3.66 (d, J = 22.0 Hz, 1H), 3.64 (s, 3H), 3.55 (d, J = 12.5 Hz, 1H), 3.39 (d, J = 22.0 Hz, 1H), 3.33 (d, J = 12.5 Hz, 1H), 2.84 (s, 1H), 2.22 (s, 3H), 2.18 (dd, J = 4.5, 12.5 Hz, 1H), 1.92 (app. t, J = 12.5 1H), 1.33 (s, 3H), 1.31 (s, 3H), 1.16 (s, 3H), 1.14 (s, 3H), 1.03 (s, 9H), 0.94 (s, 9H), 0.57 (s, 3H), 0.19 (s, 6H), 0.18 (s, 3H), 0.15 (s, 3H), 0.14 (s, 3H); ^{13}C NMR (125 MHz, $CDCl_3$) δ 209.3, 147.8, 145.1, 141.5, 129.0, 123.8, 120.8, 100.9, 65.8, 62.2, 62.1, 59.3, 58.8, 44.7, 43.5, 42.5, 41.2, 41.0, 27.4, 26.0 (2C), 24.8, 24.6, 20.0, 18.6, 18.2, 17.6, 10.1, -4.0, -4.2 (2C), -4.9; IR (Neat film NaCl) 2954, 2929, 2857, 1715, 1472, 1462, 1254, 1221, 1088, 1071, 838 cm^{-1}; HRMS (FAB) $[M-H_2+H]^+$ calc'd for $[C_{36}H_{61}Si_2O_6]^+$: m/z 645.4007, found 645.4007.

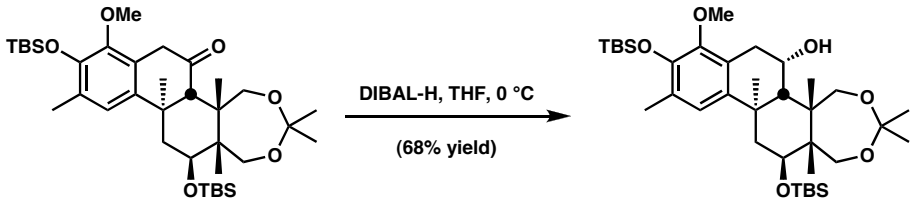

253 *255*

Alcohol 255. To a cooled (0 °C) solution of ketone **253** (19.9 mg, 30.8 μmol, 1.00 equiv) in THF (5.0 mL) was added a 1.0 M solution of DIBAL-H (250 μL, 0.250 mmol, 8.12 equiv) in toluene. After 4 h, an additional portion of DIBAL-H (100 μL,

0.100 mmol, 3.25 equiv) in toluene was added. After an additional 1 h at 0 °C, the reaction mixture was quenched with Na_2SO_4•$10H_2O$ (300 mg) in a portionwise manner, filtered, washed (CH_2Cl_2), concentrated, and purified by flash chromatography on silica gel (10 to 40% Et_2O in hexanes) to give alcohol **255** (13.6 mg, 68% yield) as a white solid. Crystals suitable for X-ray analysis were obtained by crystallization from CH_2Cl_2 at ambient temperature: mp 185-190 °C decomp. (CH_2Cl_2); R_f 0.21 (25% Et_2O in hexanes); ^{1}H NMR (500 MHz, $CDCl_3$) δ 6.78 (s, 1H), 4.68 (s, 1H), 4.47 (dd, *J* = 3.8, 12.3 Hz, 1H), 4.28 (d, *J* = 12.5 Hz, 1H), 3.93 (d, *J* = 13.0 Hz, 1H), 3.65 (s, 3H), 3.53 (d, *J* = 12.0 Hz, 1H), 3.37 (d, *J* = 12.5 Hz, 1H), 2.95 (s, 1H), 2.94 (s, 1H), 2.20 (s, 3H), 2.07 (dd, *J* = 4.0, 12.5 Hz, 1H), 1.66 (s, 1H), 1.62 (d, *J* = 12.0 Hz, 1H), 1.58 (s, 3H), 1.33 (s, 3H), 1.32 (s, 3H), 1.20 (bs, 1H), 1.11 (s, 3H), 1.03 (s, 9H), 0.92 (s, 9H), 0.57 (s, 3H), 0.19 (s, 3H), 0.17 (s, 6H), 0.14 (s, 3H); ^{13}C NMR (125 MHz, $CDCl_3$) δ 148.6, 144.4, 141.8, 128.3, 122.8, 122.1, 100.9, 66.4, 65.4, 65.3, 63.0, 59.2, 48.6, 45.7, 45.4, 44.6, 37.5, 36.7, 29.6, 26.1, 26.0, 25.0, 24.6, 22.2, 18.6, 18.1, 17.5, 10.4, -4.0 (2C), -4.1, -4.9; IR (Neat film NaCl) 3454, 2954, 2930, 2858, 1473, 1252, 1220, 1089, 1061, 836 cm^{-1}; HRMS (FAB) [M-H_2+H]$^+$ calc'd for $[C_{36}H_{63}Si_2O_6]^+$: *m/z* 647.4163, found 647.4162.

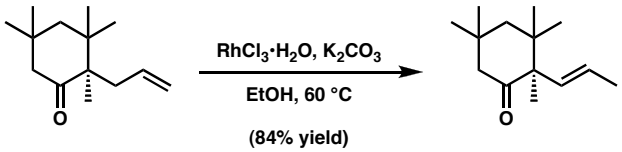

256
(85% ee)

257

Vinyl ketone 257. To a solution of allyl ketone **256** (905 mg, 4.35 mmol, 1.00 equiv) in EtOH (45 mL) in a sealable Schlenk flask (100 mL) was added K_2CO_3 (601 mg, 4.35 mmol, 1.00 equiv) and $RhCl_3$•H_2O (49.4 mg, 0.218 mmol, 0.05 equiv). The reaction

mixture was sparged with Ar for 10 min, sealed and heated to 60 °C for 12 h. After cooling to ambient temperature, the reaction mixture was filtered, washed with EtOH, concentrated, and purified by flash chromatography on silica gel (7.5 to 10% Et_2O in pentane) to give vinyl ketone **257** (759 mg, 84% yield of a 10:1 mixture containing allyl ketone **256** as the minor component) as an amorphous solid: R_f 0.67, 0.46 (25% Et_2O in hexanes, 5% Et_2O in hexanes developed twice); ^{1}H NMR (300 MHz, $CDCl_3$) δ 5.88 (dq, J = 1.8, 15.5 Hz, 1H), 5.42 (dq, J = 6.3, 15.3 Hz, 1H), 2.53 (d, J = 13.2 Hz, 1H), 2.11 (dd, J = 1.8, 13.5 Hz, 1H), 1.85 (d, J = 14.4 Hz, 1H), 1.71 (dd, J = 1.7, 6.5 Hz, 3H), 1.42 (dd, J = 1.8, 14.4 Hz, 1H), 1.09 (s, 3H), 1.04 (s, 3H), 1.01 (s, 3H), 0.90 (s, 6H); ^{13}C NMR (75 MHz, $CDCl_3$) δ 214.1, 132.5, 126.2, 56.4, 50.7, 49.6, 40.6, 35.4, 33.7, 30.2, 26.9, 26.8, 18.6, 15.6; IR (Neat film NaCl) 2957, 1707, 1458, 1391, 1370, 1283, 977 cm^{-1}; HRMS (EI) $[M]^+$ calc'd for $[C_{14}H_{24}O]^+$: m/z 208.1827, found 208.1820; $[\alpha]_D^{25}$ –59.07 (c 1.04, $CHCl_3$, 85% ee).

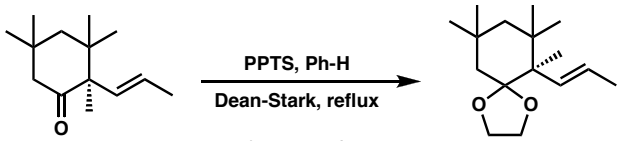

257 ***258***

Ketal 258. A solution of the vinyl ketone **257** (700 mg, 3.36 mmol, 1.00 equiv), ethylene glycol (1.30 mL, 23.5 mmol, 7.00 equiv), and pyridinium *p*-toluenesulfonate (211 mg, 0.84 mmol, 0.25 equiv) in benzene (70 mL) was fitted with a Dean-Stark apparatus and refluxed at 100 °C for 30 h. The reaction mixture was cooled to ambient temperature, diluted with saturated aqueous $NaHCO_3$ (40 mL), and extracted with Ph-H (3 x 30 mL). The combined organics were washed with brine (20 mL), dried (Na_2SO_4),

concentrated, and purified by flash chromatography on silica gel (1 to 2% Et_2O in hexane) to give acetal **258** (585 mg, 70% yield) as an oil: R_f 0.61, 0.67 (5% Et_2O in hexanes developed twice, 25% Et_2O in hexanes); ^1H NMR (300 MHz, $CDCl_3$) δ 5.74 (dq, *J* = 1.5, 15.8 Hz, 1H), 5.44 (dq, *J* = 6.3, 15.8 Hz, 1H), 3.92-3.78 (m, 4H), 1.72 (dd, *J* = 1.7, 6.5 Hz, 3H), 1.52 (s, 2H), 1.37 (d, *J* = 14.1 Hz, 1H), 1.30 (d, *J* = 14.1 Hz, 1H), 1.03 (s, 6H), 1.02 (s, 3H), 0.96 (s, 3H), 0.95 (s, 3H); ^{13}C NMR (75 MHz, $CDCl_3$) δ 133.7, 124.3, 113.8, 64.6, 64.4, 49.8, 48.6, 42.2, 38.0, 32.3, 32.0, 31.5, 28.3, 27.7, 18.7, 14.2; IR (Neat film NaCl) 2952, 1455, 1388, 1225, 1146, 1124, 1078, 981 cm^{-1}; HRMS (EI) $[M]^+$ calc'd for $[C_{16}H_{28}O]^+$: m/z 252.2089, found 252.2090; $[\alpha]_D^{24}$ +1.51 (c 1.11, $CHCl_3$, 85% ee).

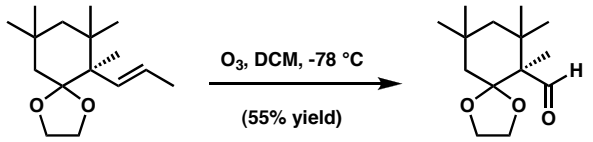

258 ***259***

Aldehyde 259. Through a cooled (-78 °C) solution of acetal **258** (252 mg, 1.00 mmol, 1.00 equiv) in CH_2Cl_2 (25 mL) was bubbled a stream of ozone until the reaction mixture turned blue. The reaction mixture was quenched with dimethyl sulfide (0.20 mL), allowed to warm to ambient temperature, concentrated to an oil, and purified by flash chromatography on silica gel (2.5 to 10% Et_2O in hexane) to give aldehyde **259** (132 mg, 55% yield) as an oil: R_f 0.41, 0.29 (25% Et_2O in hexanes, 5% Et_2O in hexanes developed twice); ^1H NMR (300 MHz, $CDCl_3$) δ 9.93 (s, 1H), 3.98-3.85 (m, 4H), 1.69 (d, *J* = 14.4 Hz, 3H), 1.57 (dd, *J* = 1.2, 14.4 Hz, 1H), 1.50 (d, *J* = 14.4 Hz, 1H), 1.37 (dd, *J* = 1.2, 14.4 Hz, 1H), 1.08 (s, 3H), 1.07 (s, 3H), 1.06 (s, 3H), 1.04 (s, 3H), 1.03 (s, 3H); ^{13}C

NMR (75 MHz, $CDCl_3$) δ 206.2, 112.1, 64.5, 64.3, 58.0, 50.3, 43.0, 38.1, 32.9, 31.6, 30.6, 27.8, 27.7, 11.1; IR (Neat film NaCl) 2954, 2899, 1722, 1241, 1110, 1075, 964 cm^{-1}; HRMS (EI) $[M]^+$ calc'd for $[C_{14}H_{24}O_3]^+$: m/z 240.1726, found 240.1720; $[\alpha]_D^{24}$ –39.53 (c 0.385, $CHCl_3$, 85% ee).

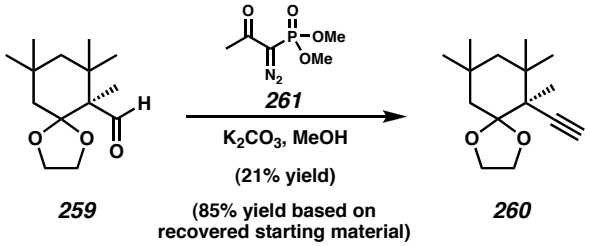

Alkyne 260. To a solution of aldehyde **259** (75.0 mg, 0.312 mmol, 1.00 equiv), and K_2CO_3 (108 mg, 0.780 mmol, 2.50 equiv) in MeOH (3.10 mL) was added diazoketone **261** (89.9 mg, 0.468 mmol, 1.5 equiv). After 1 h, an additional portion of K_2CO_3 (214 mg, 1.56 mmol, 5.00 equiv) and of diazoketone **261** (150 mg, 0.780 mmol, 2.5 equiv) were added. After a further 4 h, a final portion of K_2CO_3 (200 mg, 1.45 mmol, 4.65 equiv) and of diazoketone **261** (200 mg, 1.05 mmol, 3.37 equiv) were added. After stirring for 20 h, the reaction mixture was diluted with H_2O (10 mL), extracted with CH_2Cl_2 (8 x 5 mL), dried ($MgSO_4$), concentrated, and purified by flash chromatography on silica gel (1 to 7% Et_2O in hexanes) to give recovered aldehyde **259** (55.6 mg, 74% yeld) and alkyne **260** (15.5 mg, 21% yield, 85% yield based on recovered aldehyde **259**) as an oil: R_f 0.40 (5% Et_2O in hexanes developed twice); ^1H NMR (300 MHz, C_6D_6) δ 3.62-3.40 (m, 4H), 2.01 (d, J = 14.1 Hz, 1H), 1.93 (s, 1H), 1.72 (d, J = 14.1 Hz, 1H), 1.47 (dd, J = 1.8, 13.8 Hz, 1H), 1.36 (s, 3H), 1.34 (s, 3H), 1.22 (s, 3H), 1.17 (dd, J = 1.7, 14.3 Hz, 1H), 1.10 (s, 3H), 1.04 (s, 3H); ^{13}C NMR (75 MHz, $CDCl_3$) δ 112.5, 89.1, 76.6, 70.7,

65.5, 64.2, 49.8, 47.3, 42.5, 38.0, 34.6, 31.4, 29.8, 28.8, 24.9, 16.2; IR (Neat film NaCl) 3309, 2954, 2911, 2111, 1454, 1390, 1367, 1235, 1148, 1088, 1073, 984 cm^{-1}; HRMS (EI) $[M]^+$ calc'd for $[C_{15}H_{24}O_2]^+$: m/z 236.1776, found 236.1786; $[\alpha]_D^{26}$ –20.35 (c 1.25, CH_2Cl_2, 85% ee).

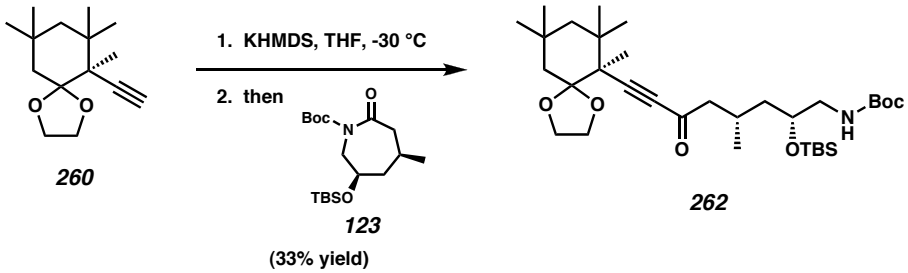

Ynone 262. To a cooled (-30 °C) solution of KHMDS (24.1 mg, 0.121 mmol, 2.20 equiv) in THF (1.00 mL) was added alkyne **260** (13.0 mg, 0.055 mmol, 1.00 equiv) in THF (1.00 mL). The solution was maintained for 30 min each at -30 °C, 0 °C, and 22 °C. The alkyne anion was cooled to -78 °C, and caprolactam **123** (23.6 mg, 0.066 mmol, 1.2 equiv) in THF (1.00 mL) was added. After 1 h, additional KHMDS (12.0 mg, 0.061 mmol, 1.10 equiv) in THF (0.50 mL) was added. After a further 5 h, the reaction mixture was quenched with saturated aqueous $NaHCO_3$ (0.50 mL), diluted with H_2O (2 mL), brine (4 mL), and Et_2O (4 mL), and extracted with Et_2O (6 x 4 mL) and CH_2Cl_2 (2 x 2 mL). The combined organics were dried (Na_2SO_4) and concentrated to an oil, which was purified by flash chromatography on silica gel (2.5 to 15% EtOAc in hexanes) to give ynone **262** (10.9 mg, 33% yield) as a oil: R_f 0.24, 0.50 (10% EtOAc in hexanes developed twice, 20% EtOAc in hexanes); ^1H NMR (500 MHz, $CDCl_3$) δ 4.78 (s, 1H), 4.07-4.02 (m, 1H), 4.00-3.94 (m, 3H), 3.84 (bs, 1H), 3.38-3.30 (m, 1H), 2.97 (dt, J = 6.0, 14.5 Hz, 1H), 2.58 (dd, J = 5.5, 15.5 Hz, 1H), 2.38 (dd, J = 8.0, 15.5 Hz, 1H), 2.26-2.16

(m, 1H), 1.76 (d, J = 14.0 Hz, 1H), 1.62-1.44 (comp. m, 4H), 1.46 (s, 9H), 1.40-1.30 (m, 1H), 1.26 (s, 3H), 1.17 (s, 3H), 1.14 (s, 3H), 1.07 (s, 3H), 1.01 (s, 3H), 1.00 (s, 3H), 0.91 (s, 9H), 0.09 (s, 3H), 0.08 (s, 3H); ^{13}C NMR (125 MHz, $CDCl_3$) δ 87.2, 155.9, 112.1, 98.7, 83.7, 79.1, 69.4, 65.5, 64.6, 53.2, 49.8, 48.1, 45.9, 43.0, 42.2, 38.7, 33.8, 31.4, 29.7, 29.6, 28.4, 28.0, 26.3, 25.9, 25.6, 20.2, 18.0, -4.5, -4.6; IR (Neat film NaCl) 3383, 2955, 2930, 2208, 1716, 1673, 1504, 1391, 1366, 1252, 1171, 1090, 836 cm^{-1}; HRMS (FAB) $[M+H]^+$ calc'd for $[C_{33}H_{59}NO_6Si+H]^+$: m/z 594.4190, found 594.4208; $[\alpha]_D^{26}$ –36.12 (c 0.545, EtOAc).

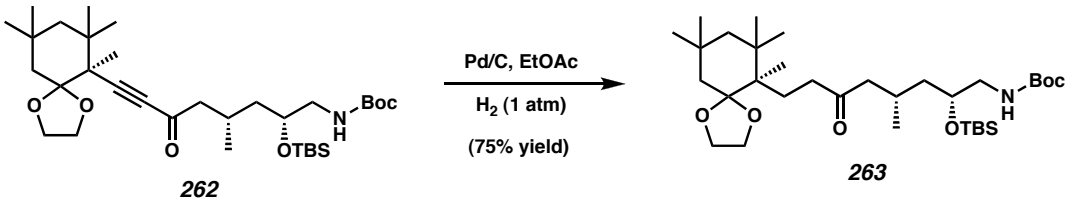

Ketone 263. To a solution of ynone **262** (10.9 mg, 18.3 μmol, 1.00 equiv) in EtOAc (6 mL) was added 10% Pd/C (4.0 mg), and the reaction mixture was sparged with H_2 (5 min). After 18 h of vigorous stirring under an atmosphere of H_2 (balloon), the reaction mixture was concentrated and purified by flash chromatography on silica gel (5 to 10% EtOAc in hexanes). NMR analysis of the chromatographed product indicated the presence of some partially hydrogenated material. A solution of this material in EtOAc (5 mL) was treated again with 10% Pd/C (5.0 mg) under an atmosphere of H_2 (balloon) for 4 h. The reaction mixture was concentrated to an oil and purified by flash chromatography on silica gel (5 to 10% EtOAc in hexanes) to give ketone **263** (8.2 mg, 75% yield) as a oil: R_f 0.53 (20% EtOAc in hexanes); ^{1}H NMR (500 MHz, $CDCl_3$) δ 4.79 (s, 1H), 3.96 (app. t, J = 6.8 Hz, 1H), 3.83 (app. q, J = 7.0 Hz, 1H), 3.79 (bs, 1H),

3.74 (app. q, *J* = 7.0 Hz, 1H), 3.34-3.26 (m, 1H), 2.98 (dt, *J* = 6.5, 13.5 Hz, 1H), 2.60-2.50 (m, 1H), 2.48-2.36 (m 2H), 2.20 (dd, *J* = 7.8, 16.3 Hz, 1H), 2.12-2.02 (m, 1H), 2.00-1.92 (m, 1H), 1.56-1.24 (comp. m, 9H), 1.44 (s, 9H), 1.15 (d, *J* = 14.0 Hz, 1H), 1.11 (s, 3H), 1.05 (s, 3H), 0.96 (s, 3H), 0.92-0.89 (m, 6H), 0.89 (s, 9H), 0.07 (s, 3H), 0.06 (s, 3H); ^{13}C NMR (125 MHz, $CDCl_3$) δ 211.9, 156.2, 115.2, 79.3, 69.8, 64.9, 62.6, 50.6, 50.5, 46.2, 44.2, 42.7, 41.4, 40.9, 39.1, 34.7, 31.5, 30.0, 29.4, 28.7, 28.3, 26.8, 26.1, 26.0, 24.4, 20.6, 18.3, 16.8, -4.3; IR (Neat film NaCl) 3391, 2953, 2930, 1714, 1503, 1366, 1253, 1173, 1076, 836, 776 cm^{-1}; HRMS (FAB) $[M+H]^+$ calc'd for $[C_{33}H_{63}NO_6Si+H]^+$: *m/z* 598.4503, found 598.4489; $[\alpha]_D^{26}$ 9.33 (c 0.105, CH_2Cl_2).

3.9 Notes and Citations

---

(1) Bagdanoff, J. T. Development of the Enantioselective Oxidation of Secondary Alcohols and Natural Products Total Synthesis. Ph.D., California Institute of Technology, Pasadena, CA, August 2005.

(2) For limitations of DMMA Diels-Alder reactions, see: (a) Rae, I. D.; Serelis, A. K. *Aust. J. Chem.* **1990**, *43*, 1941-1948. (b) Ziegler, K.; Flaig, W.; Velling, G. *Justus Liebig Ann. Chem.* **1950**, *567*, 204-214.

(3) For synthesis of dihydrothiophene **195**, see: (a) Baker, B. R.; Querry, M. V.; Kadish, A. F. *J. Am. Chem. Soc.* **1980**, *102*, 6893-6894. (b) Dauben, W. G.; Gerdes, J. M.; Smith, D. B. *J. Org. Chem.* **1985**, *50*, 2576-2578.

(4) (a) Dauben, W. G.; Kessel, C. R.; Takemura, K. H. *J. Am. Chem. Soc.* **1980**, *102*, 6894-6896.

(5) Birman, V. B.; Danishefsky, S. J. *J. Am. Chem. Soc.* **2002**, *124*, 2080-2081.

(6) For the synthesis of known diene **200,** see: Duke, R. K.; Rickards, R. W. *J. Org. Chem.* **1984**, *49*, 1898-1904.

(7) Diene **198** is readily available in one step from crotonaldehyde and TBSOTf, see: Trost, B. M.; Chupak, L. S.; Lübbers, T. *J. Org. Chem.* **1997**, *62*, 736-737.

(8) DMMA is commercially available, but on scale is readily and more economically made from maleic anhydride, see: Baumann, M. E.; Bosshard, H.; Breitenstein, W.; Rihs, G.; Winkler, T. *Helv. Chim. Acta* **1984**, *67*, 1897-1905.

(9) Shimizu, M.; Matsukawa, K.; Fujisawa, T. *Bull. Chem. Soc. Jpn.* **1993**, *66*, 2128-2130.

(10) Bolm, C.; Schiffers, I.; Dinter, C. L.; Gerlach, A. *J. Org. Chem.* **2000**, *65*, 6984-6991.

(11) (a) Chen, Y.; Tian, S.-K.; Deng, L. *J. Am. Chem. Soc.* **2000**, *122*, 9542-9543. (b) Chen, Y.; Deng, L. *J. Am. Chem. Soc.* **2001**, *123*, 11302-11303.

(12) (a) Chen, Y.; McDaid, P.; Deng, L. *Chem. Rev.* **2003**, *103*, 2965-2983. (b) Tian, S.-K.; Chen, Y.; Hang, J.; Tang, L.; McDaid, P.; Deng, L. *Acc. Chem. Res.* **2004**, *37*, 621-631.

(13) We acknowledge Thomas C. Scotton for the synthesis and testing of **207**. Menthol derivative **208** was a generous gift from Prof. Deng.

(14) Analysis of samples taken early during the reaction suggest that iodolactone **209** is a thermodynamic sink as other isomers appear to be initially formed.

(15) The most isomerization to ketone **212** (~30%) was observed with $RhI_3 \bullet H_2O$ in EtOH at 80 °C.

(16) See Chapter Two for details.

(17) Standard Mitsunobu conditions do not give reactivity, likely due to steric difficulties caused by nearby quaternary centers. For Mitsunobu protocol, see: Majetich, G.; Defauw, J.; Ringold, C. *J. Org. Chem.* **1988**, *53*, 50-68.

Reduction of enone **218** with $NaBH_4$ gave selective reduction of the methyl ester. Reduction under Luche conditions afforded only the undesired diastereomer **217**.

(18) See Chapter Two for more examples and discussion.

(19) The purity of triol **228** drastically modulates the efficacy of $CuSO_4$ in the acetonide forming reaction. Chromatography or recrystallization is required to remove what

are likely hydrated aluminum salts. Without purification of triol **228**, the reaction often fails to progress to more than 20% conversion.

(20) For other examples of favorable 1,3-dioxepane formation in synthesis, see: (a) Ritter, T.; Zarotti, P.; Carreira, E. M. *Org. Lett.* **2004**, *6*, 4371-4374. (b) Brewster, A. G.; Leach, A. *Tetrahedron Lett.* **1986**, *27*, 2539-2542.

(21) The ratio of products seemed to depend most on the duration of the reaction, suggesting that some equilibration was possible between the products. On a number of occasions 1,3-dioxepane **229** was the major product (e.g., 44% yield of 1,3-dioxepane **229**, and 41% yield of 1,3-dioxolane **230**).

(22) Reaction with the methoxy methylene Wittig reagent gave ~25-40% yields.

(23) For recent examples, see: (a) Sano, S.; Kenji, M. *Eur. J. Org. Chem.* **1999**, *7*, 1679-1686. (b) Hamilton, J. G. C.; Hooper, A. M.; Mori, K.; Pickett, J. A.; Sano, S. *Chem. Commun.* **1999**, 355-356. (c) Hoffman, H. M. R.; Eggert, U.; Gibbels, U.; Giesel, K.; Koch, O.; Lies, R.; Rabe, J. *Tetrahedron* **1988**, *44*, 3899-3918.

(24) DMSO was uniquely effective among polar solvents used in optimization trials of the KCN displacement reactions. ACN, DMF, NMP, and HMPA all proved to be grossly inferior. The addition of 18-C-6 did not improve the yield of the reaction.

(25) Attempts to carry out S_N' cyclization of allylic alcohol **xxiii** gave mostly styrene elimination products.

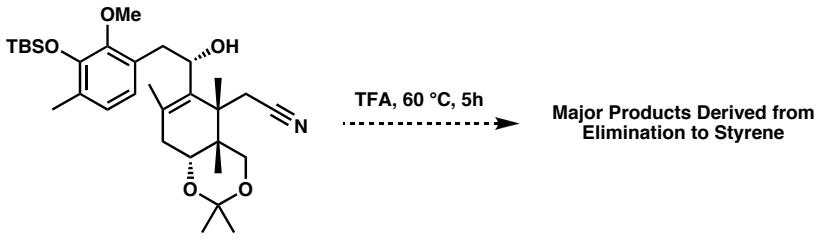

xxiii

(26) Synthesis of keto allylic acetate **247** was completed in several steps as shown below. The attempted S_N' cyclization of keto allylic acetate **xxvii** qualitatively gave less cyclized material and many more byproducts than either allylic alcohol **244** or allylic acetate **255**.

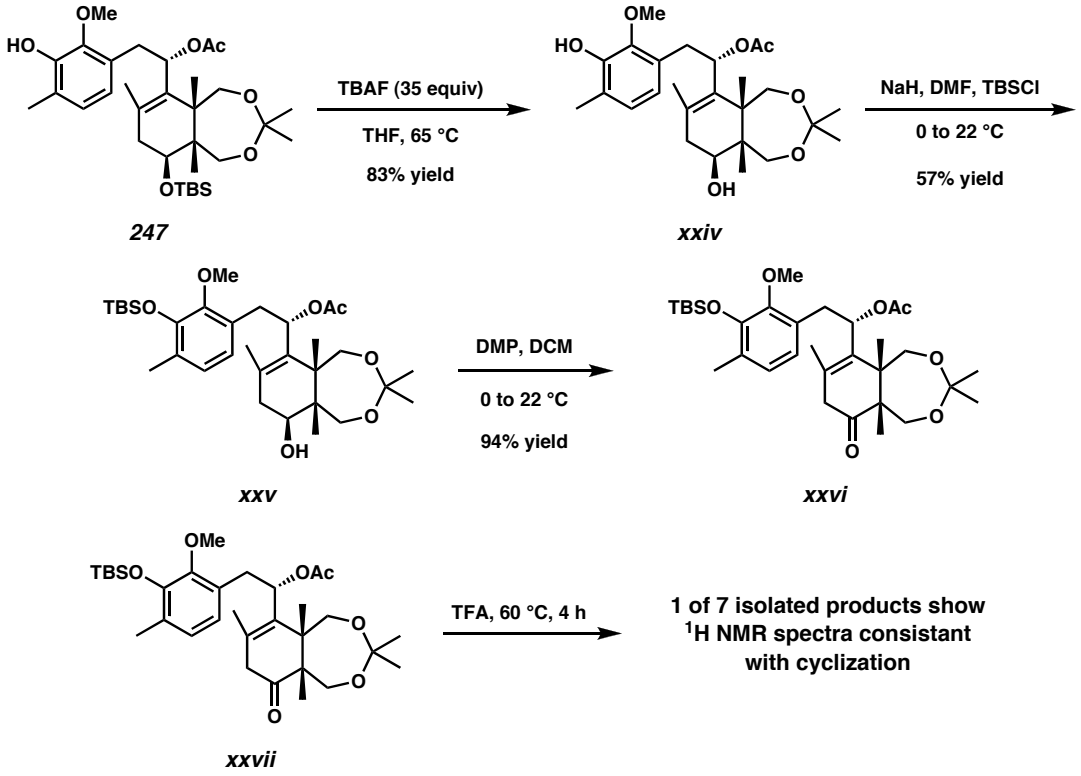

(27) Both C(20) stereoisomers were tried in parallel because the identity of each isomer had not been rigorously proven.

(28) Trifluoroacetic acid cyclization of the related enone **xxviii** afforded the related mixed acetal **xxix**.

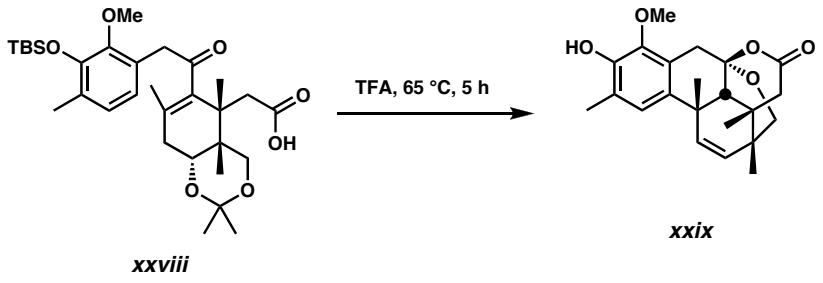

(29) (a) Carreno, M. C.; Ruano, J. L. G.; Sanz, G.; Toledo, M. A.; Urbano, A. *J. Org. Chem.* **1995**, *60*, 5328-5331. (b) Berthelot, J.; Guette, C.; Desbène, P.-J.; Basselier, J.-J. *Can. J. Chem.* **1989**, *67*, 2061-2066.

(30) Carreno, M. C.; Ruano, J. L. G.; Sanz, G.; Toledo, M. A.; Urbano, A. *Synlett.* **1997**, 1241-1242.

(31) (a) Hirai, G.; Koizumi, Y.; Moharram, S. M.; Oguri, H.; Hirama, M. *Org. Lett.* **2002**, *4*, 1627-1630. (b) Hirai, G.; Oguri, H.; Moharram, S. M.; Koyama, K.; Hirama, M. *Tetrahedron Lett.* **2001**, *42*, 5783-5787.

(32) (a) Rigby, J. H.; Hughes, R. C.; Heeg, M. J. *J. Am. Chem. Soc.* **1995**, *117*, 7834-7835. (b) Dankwardt, J. W.; Flippin, L. A. *J. Org. Chem.* **1995**, *60*, 2312-2313. (c) Gibson, S.E.; Middleton, R. J. *J. Chem. Soc., Chem. Commun.* **1995**, 1743-1744. (d) Gibson, S.E.; Guillo, N.; Tozer, M. J. *Chem. Commun.* **1997**, 637-638.

(33) (a) Link, J. T. The Intramolecular Heck Reaction. In *Organic Reactions*; Overman, L. E., Ed.; John Wiley & Sons: New York, 2002, 60, pp 157-325. (b) Bräse, S.; De Meijee A. Intramolecular Heck Reaction. In *Handbook of Organopalladium Chemistry for Organic Synthesis*; Negishi, E., Ed.; John Wiley & Sons: New York, 2002, pp 1223-1254.

(34) Attempted Heck reactions from substrates with the C(20) alcohol oxidation also resulted in debrominated material.

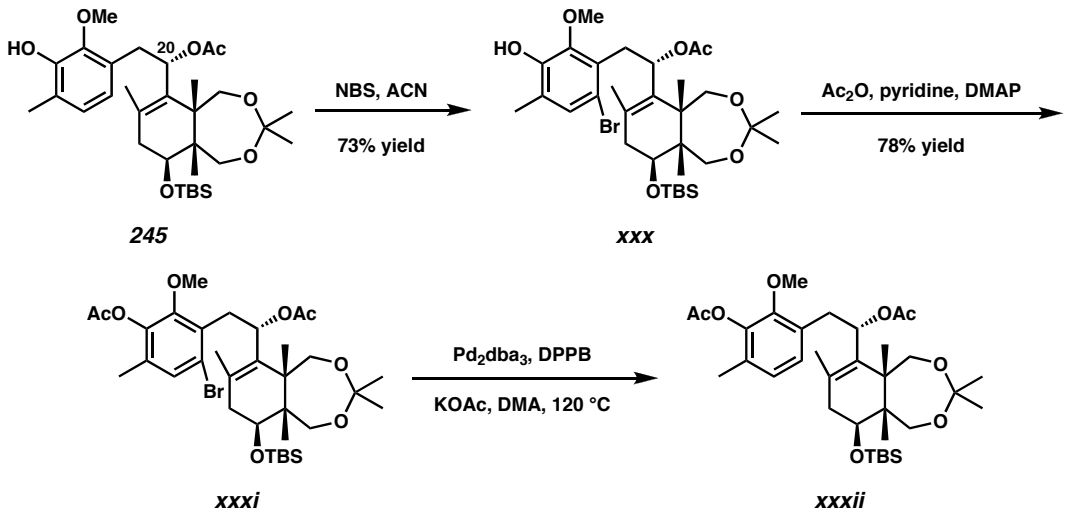

(35) For an excellent review of intramolecular radical conjugate addition, see: Zhang, W. *Tetrahedron* **2001**, *57*, 7237-7262.

(36) Rajamannar, T.; Balasubramanian, K. K. *J. Chem. Soc., Chem. Commun.* **1994**, 25-26.

(37) TBS groups removed from the figure for clarity.

(38) Lewis acids have been used numerous times to promote radical conjugate additions, see: (a) Sibi, M. P.; Ji, J.; Sausker, J. B.; Jasperse, C. P. *J. Am. Chem. Soc*. **1999**, *121*, 7517-7526. (b) Iserloh, U.; Curran, D. P.; Kanemasa, S. *Tetrahedron: Asymmetry* **1999**, *10*, 2417-2428. (c) Murakata, M.; Tsutsui, H.; Hoshino, O, *Org. Lett*. **2001**, *3*, 299-302. (d) Sibi, M. P.; Manyem, S. *Org. Lett*. **2002**, *4*, 2929-2932.

(39) Preliminary studies with aryl bromide **252** suggest that cyclized products with both C(12) relative stereochemistries are formed. Our conjecture at this time is that the C(10) stereocenter may play a crucial role in determining the stereochemical

outcome of the radical conjugate addition reaction due to the additional 1,3-diaxial interactions that occur formed in the products.

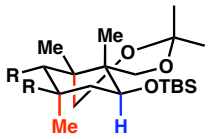

Cyclization product from aryl bromide *251* experiences only 1 new 1,3-diaxial interaction

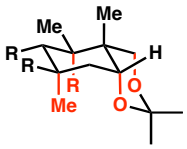

Cyclization product from aryl bromide *252* experiences several new 1,3-diaxial interactions

(40) Miyashita, M.; Sasaki, M.; Hattori, I.; Sakai, M.; Tanino, K. *Science* **2004**, *305*, 495-499.

(41) See Chapter Four for details.

(42) (a) Ohira, S. *Synth. Commun.* **1989**, *19*, 561-564. (b) Müller, S.; Liepold, B.; Ruth, G. J.; Bestmann, H. J. *Synlett* **1996**, 521-522.

(43) Complete consumption of aldehyde **259** is observed by TLC during the reaction. However, it reappears again upon workup, suggesting that the collapse of the intermediate addition adduct to the olefin is slow. Attempts to drive the reaction to completion with heat or additional equivalents of phosphate **261** were unsuccessful. Reaction of aldehyde **259** with lithiated TMS diazomethane gave a slightly higher yield (~35%), but no aldehyde could be recovered.

(44) KHMDS caused significantly less degradation of caprolactam **123** than potassium *t*-butoxide, or LDA.

(45) It should be noted that ynone **262** is diastereomeric to an exact zoanthenol model. (*R*)-Alkyne **260** would be required to model the correct absolute stereochemistry of the natural product. Caprolactam **123** is of the correct enantiomeric series for completion of the natural product.

(46) Corey, E. J.; Cho, H.; Rucker, C.; Hua, D. H. *Tetrahedron Lett.* **1981**, *22*, 3455-3458.

APPENDIX FOUR

Synthetic Summary of Approaches Toward Advanced Zoanthenol ABC Ring Systems Containing Three Quaternary Stereocenters

Scheme A4.1: Synthesis of C Ring Precursor with Vicinal Quaternary Centers

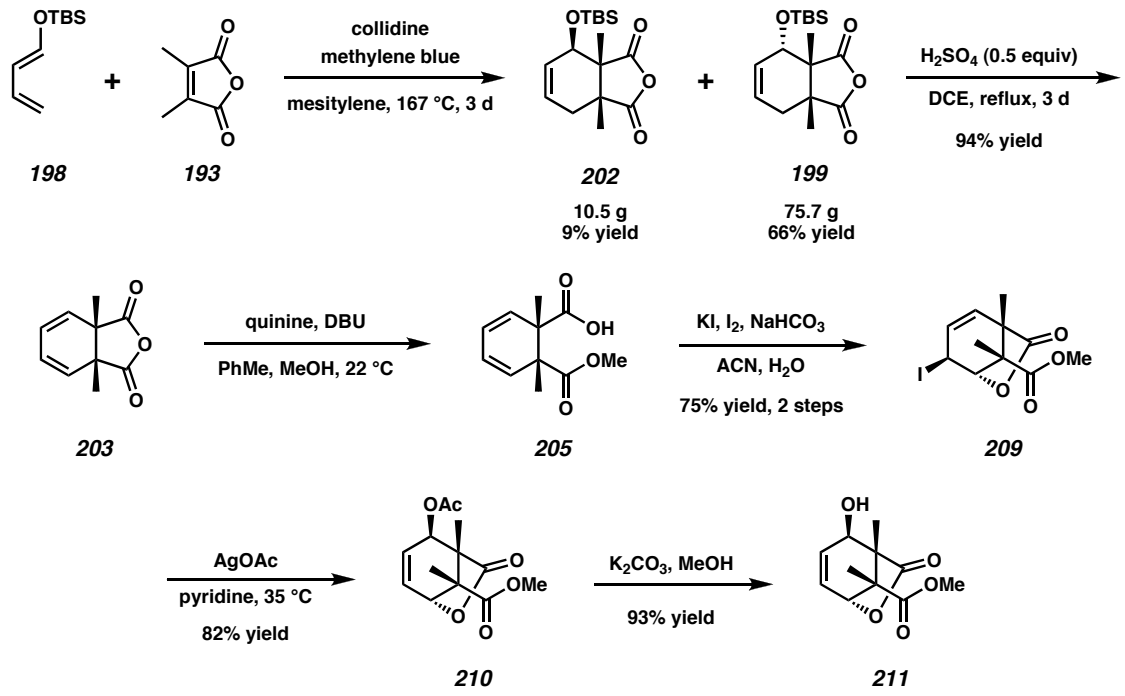

Scheme A4.2 Elaboration of the Lactone C Ring Synthon

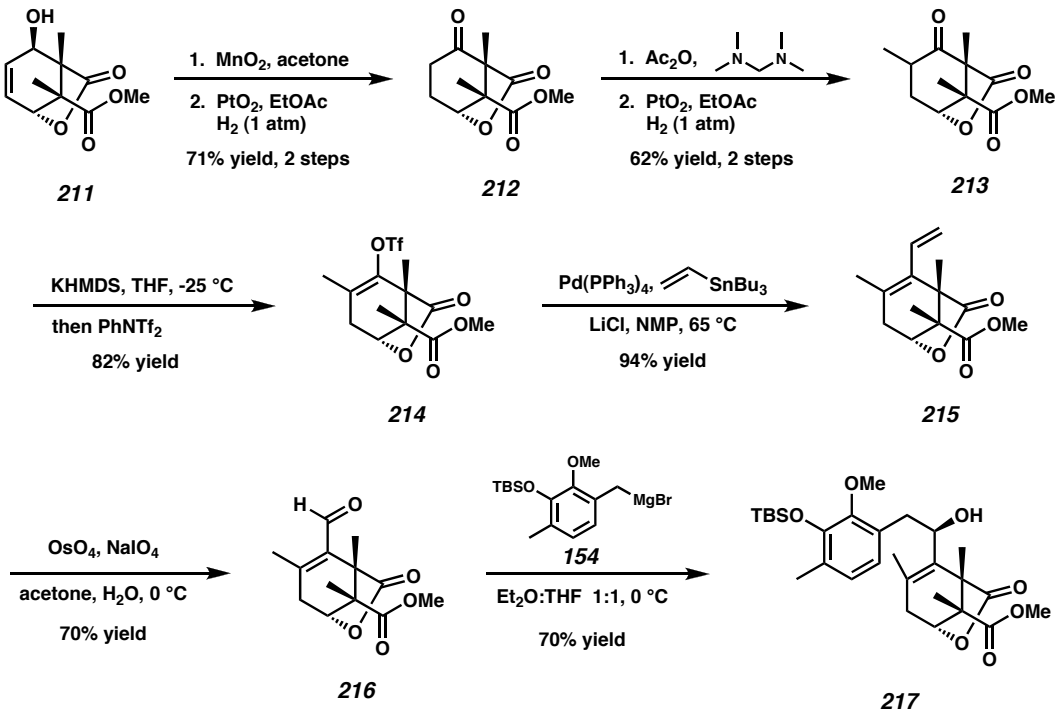

Scheme A4.3 Completion and Cyclization of the Lactone C Ring Synthon

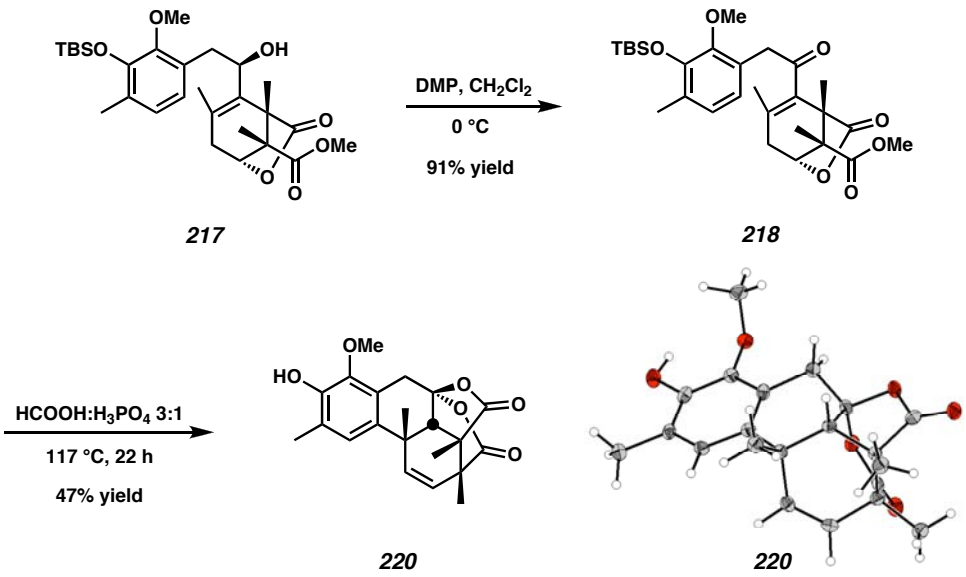

Scheme A4.4 Common Steps of the 1,3-Dioxepane and Acetonide C Ring Synthon Syntheses

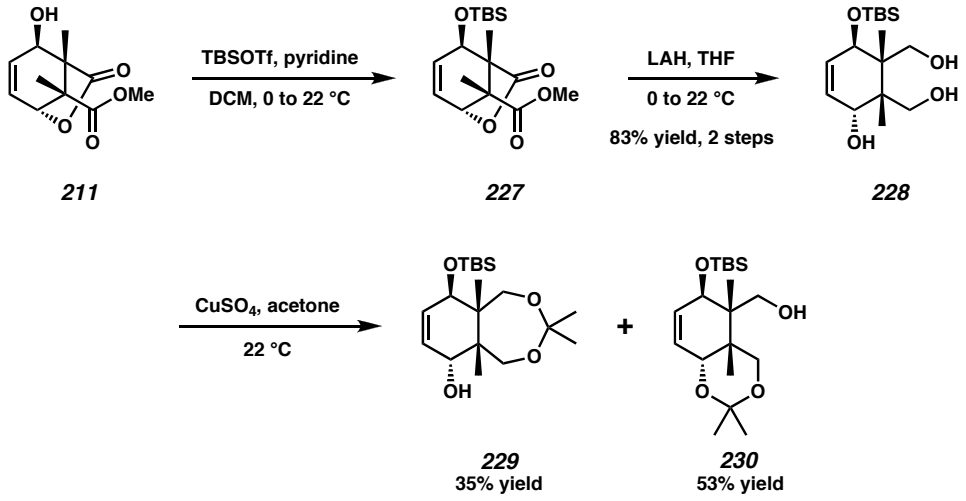

Scheme A4.5 Synthesis and Cyclization of the 1,3-Dioxepane C Ring Synthon

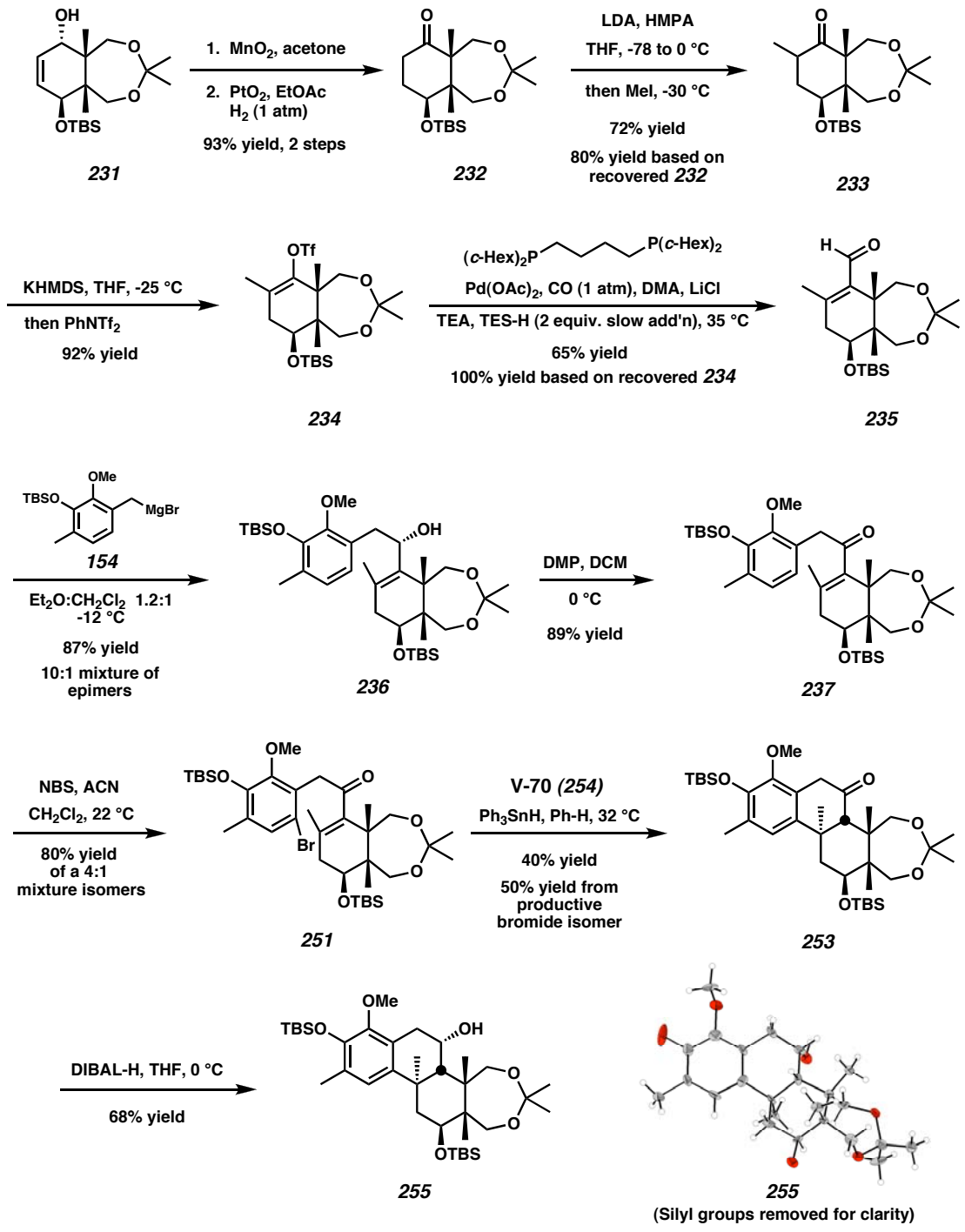

Scheme A4.6 Synthesis of the Nitrile Acetonide C Ring Synthon

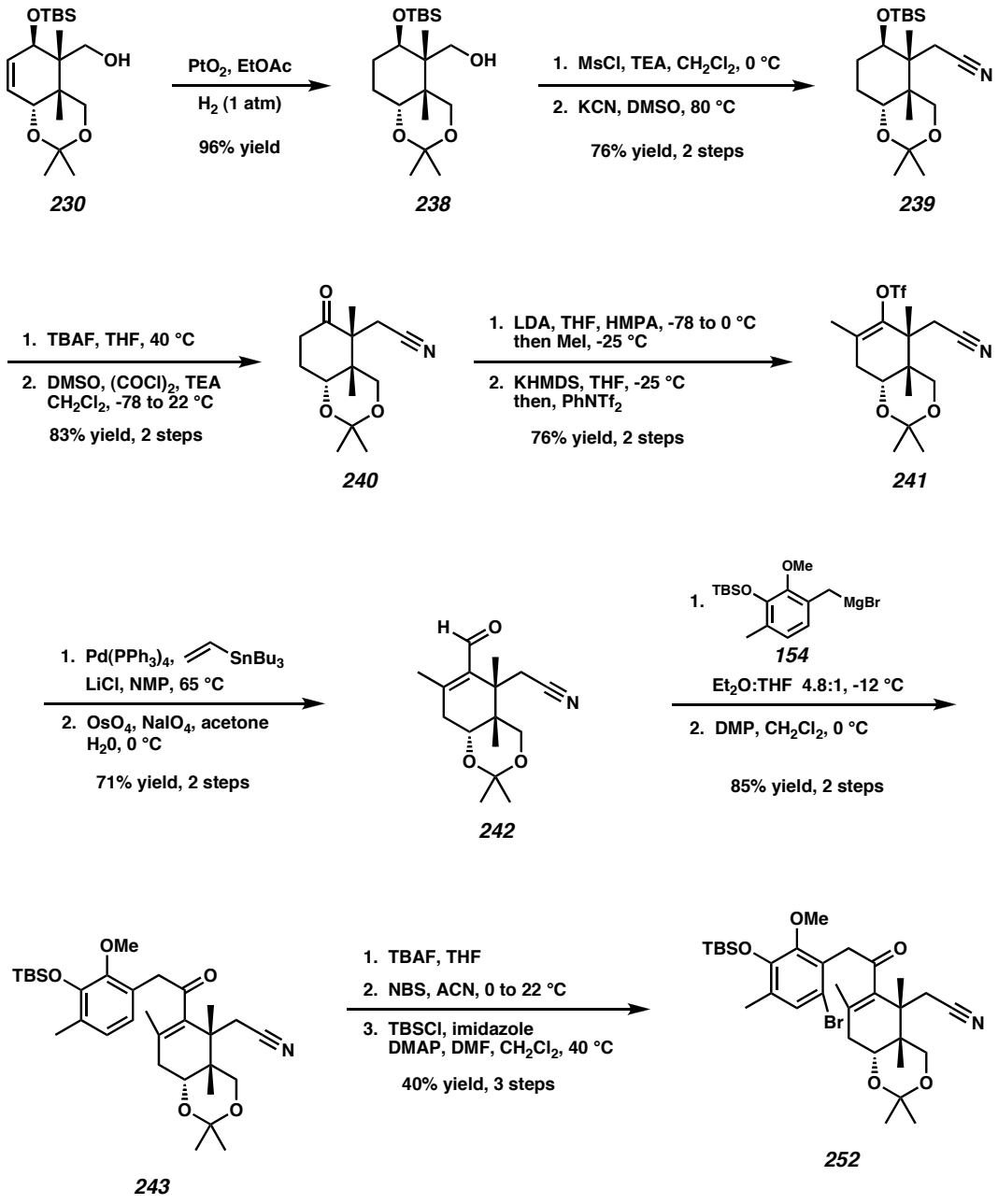

Scheme A4.7 Model C(1)-C(6) Fragment Coupling

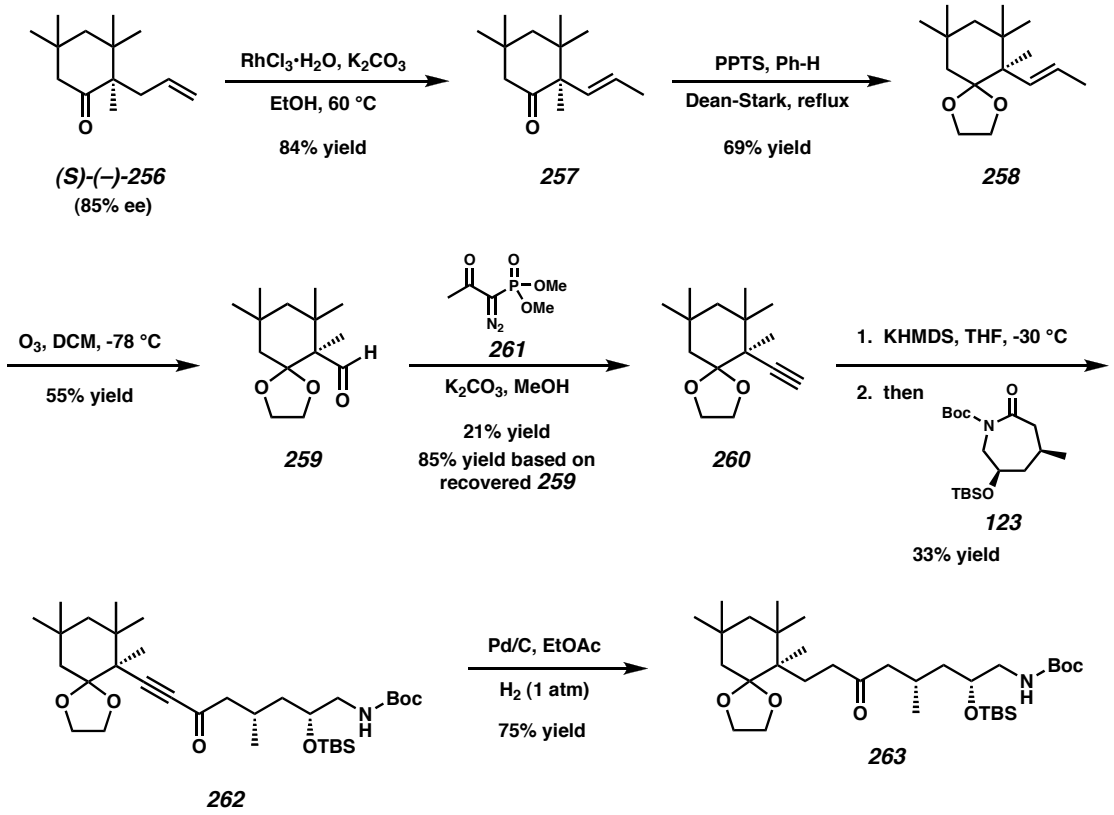

APPENDIX FIVE

Spectra of Compounds Relevant to Chapter Three

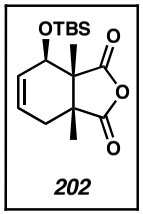

Figure A5.1 ^{1}H NMR of compound **202** (500 MHz, $CDCl_3$)

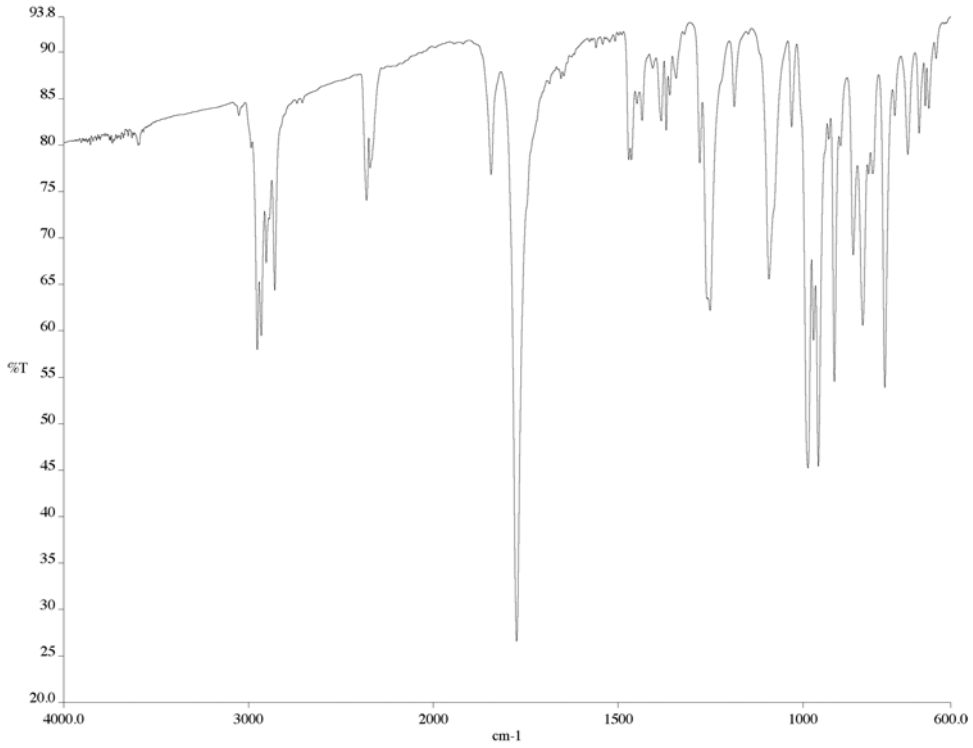

Figure A5.2 IR of compound **202** (NaCl/film)

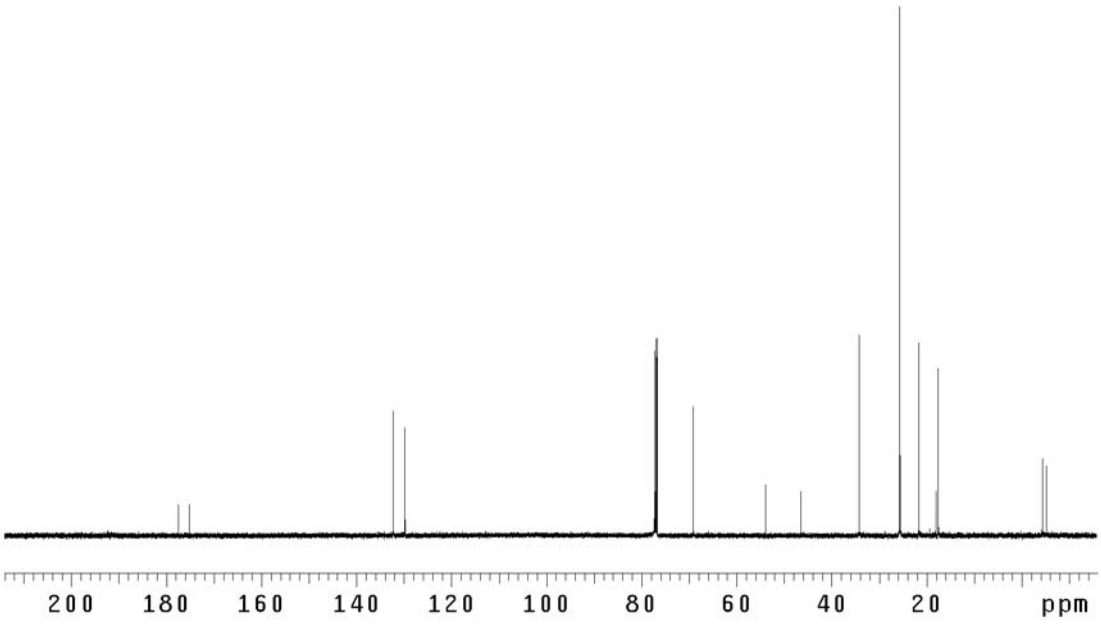

Figure A5.3 ^{13}C NMR of compound **202** (125 MHz, $CDCl_3$)

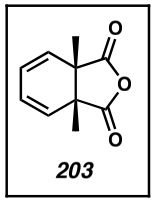

Figure A5.4 ^{1}H NMR of compound **203** (500 MHz, $CDCl_3$)

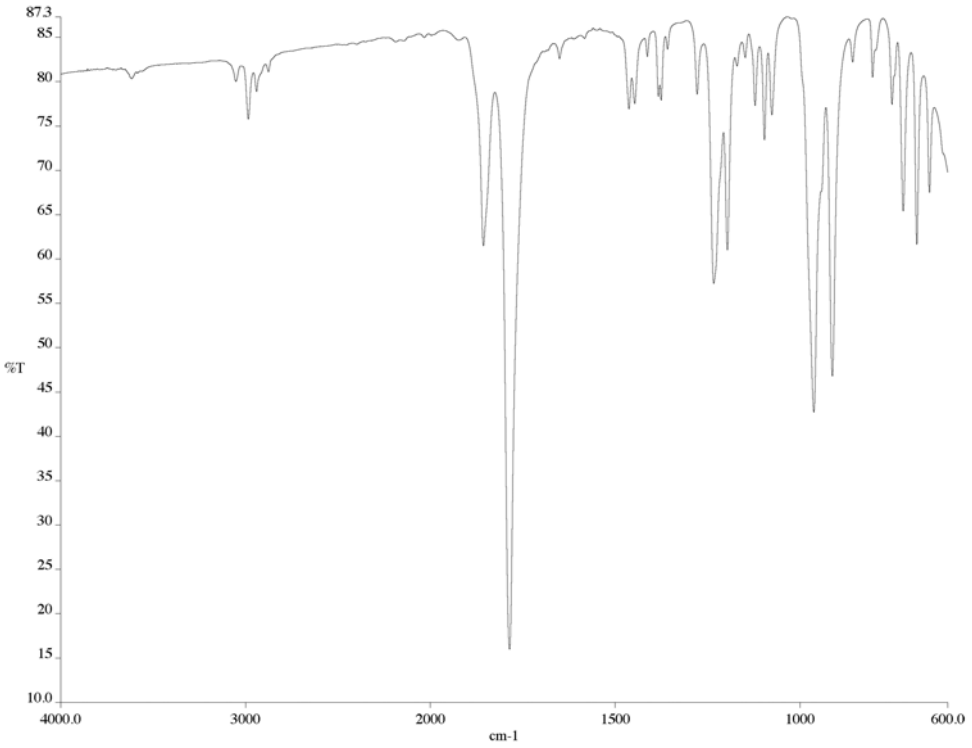

Figure A5.5 IR of compound **203** (NaCl/film)

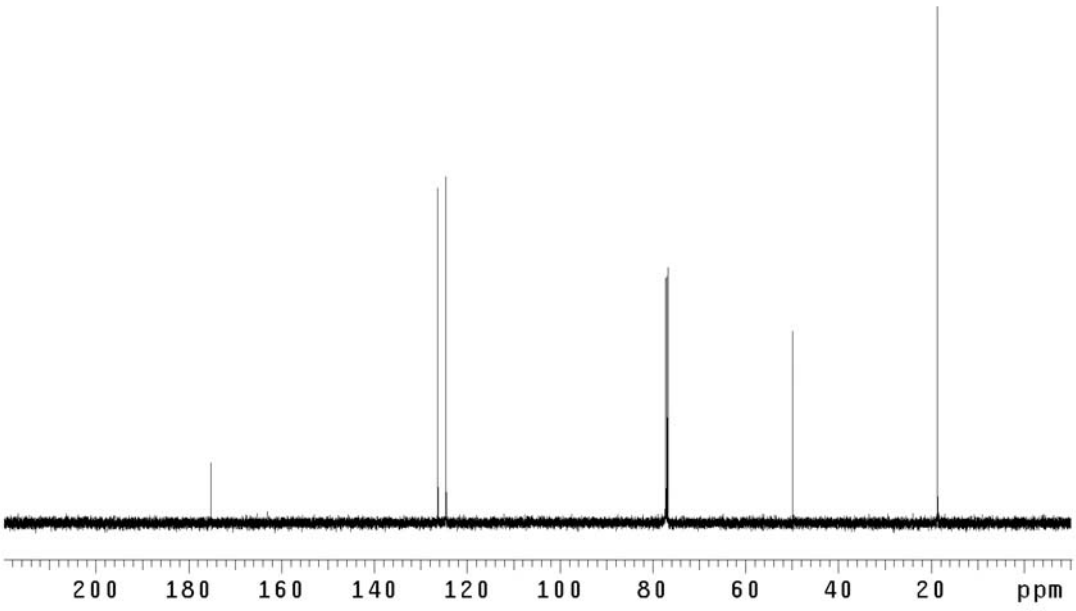

Figure A5.6 ^{13}C NMR of compound **203** (125 MHz, $CDCl_3$)

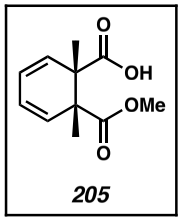

205

Figure A5.7 ^{1}H NMR of compound **205** (500 MHz, $CDCl_3$)

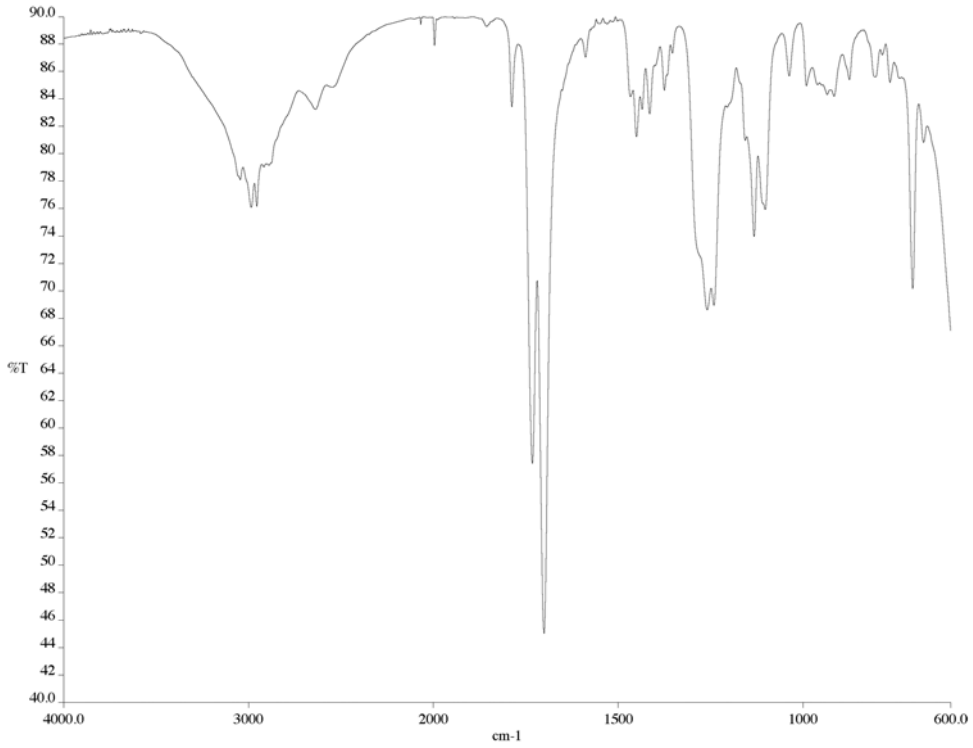

Figure A5.8 IR of compound **205** (NaCl/film)

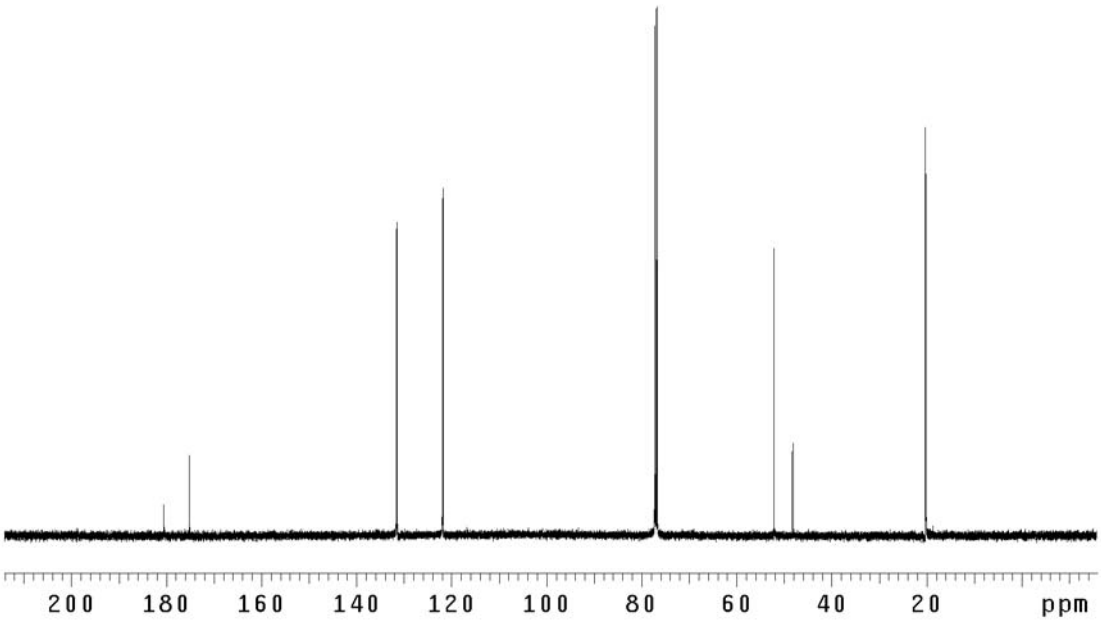

Figure A5.9 ^{13}C NMR of compound **205** (125 MHz, $CDCl_3$)

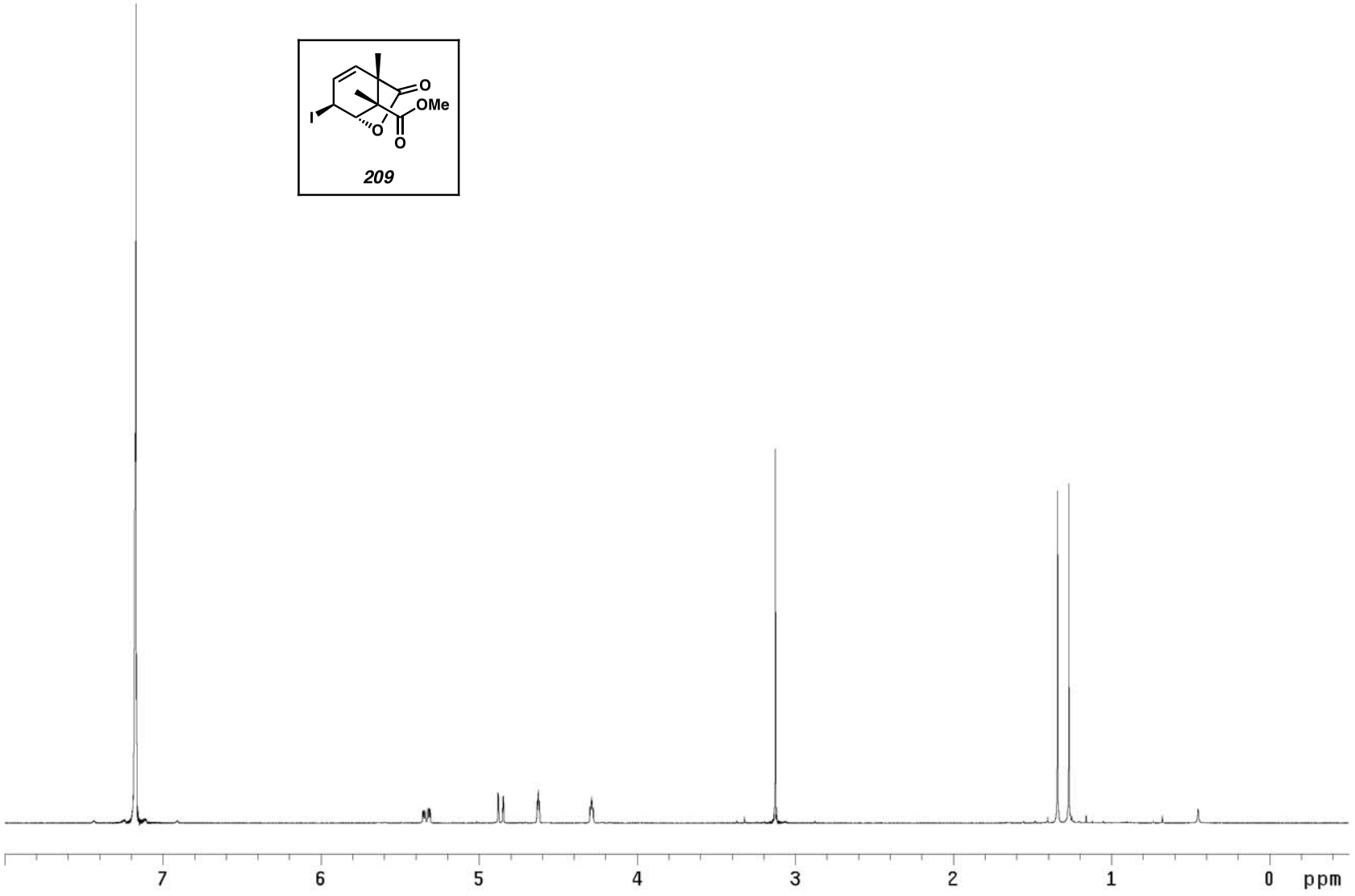

Figure A5.10 ^{1}H NMR of compound **209** (300 MHz, C_6D_6)

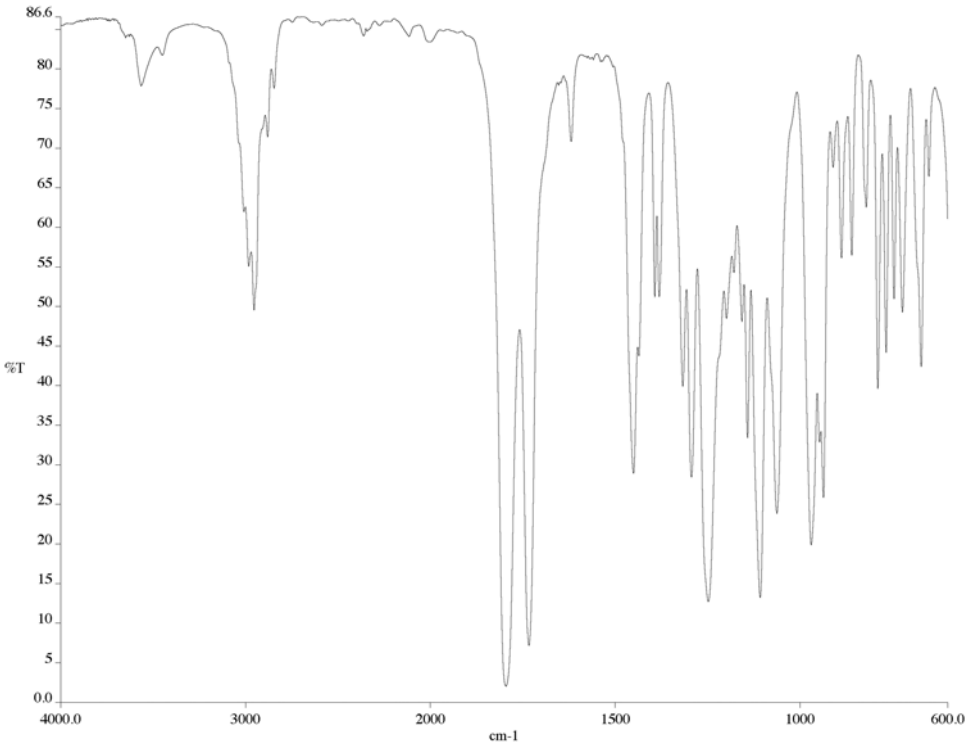

Figure A5.11 IR of compound **209** (NaCl/film)

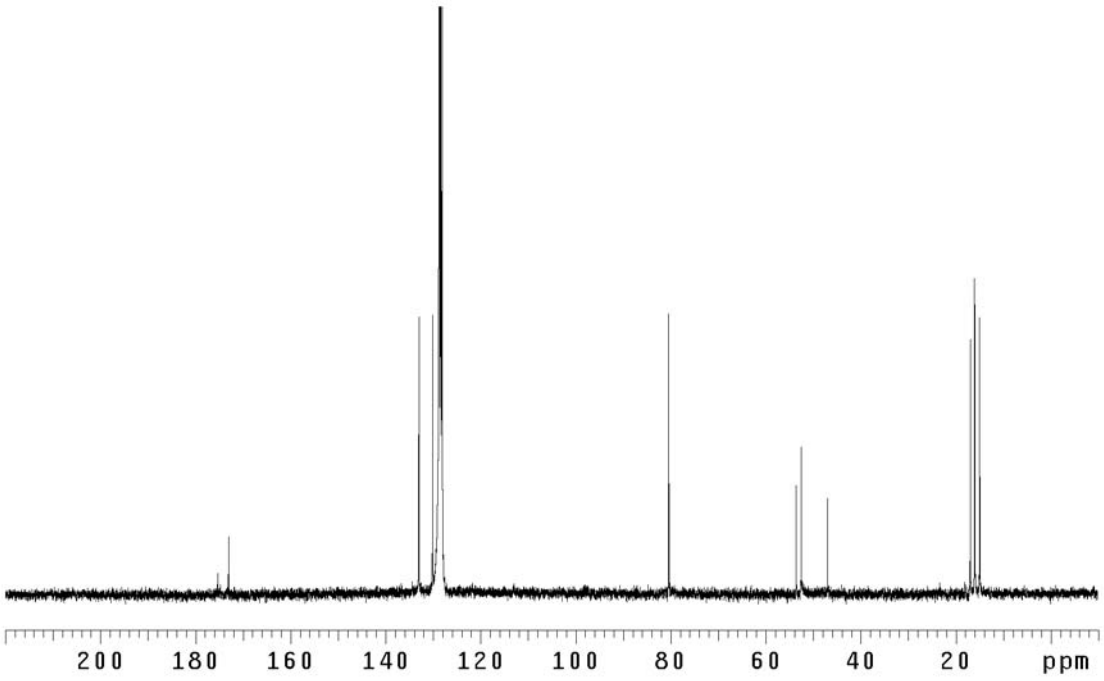

Figure A5.12 ^{13}C NMR of compound **209** (75 MHz, C_6D_6)

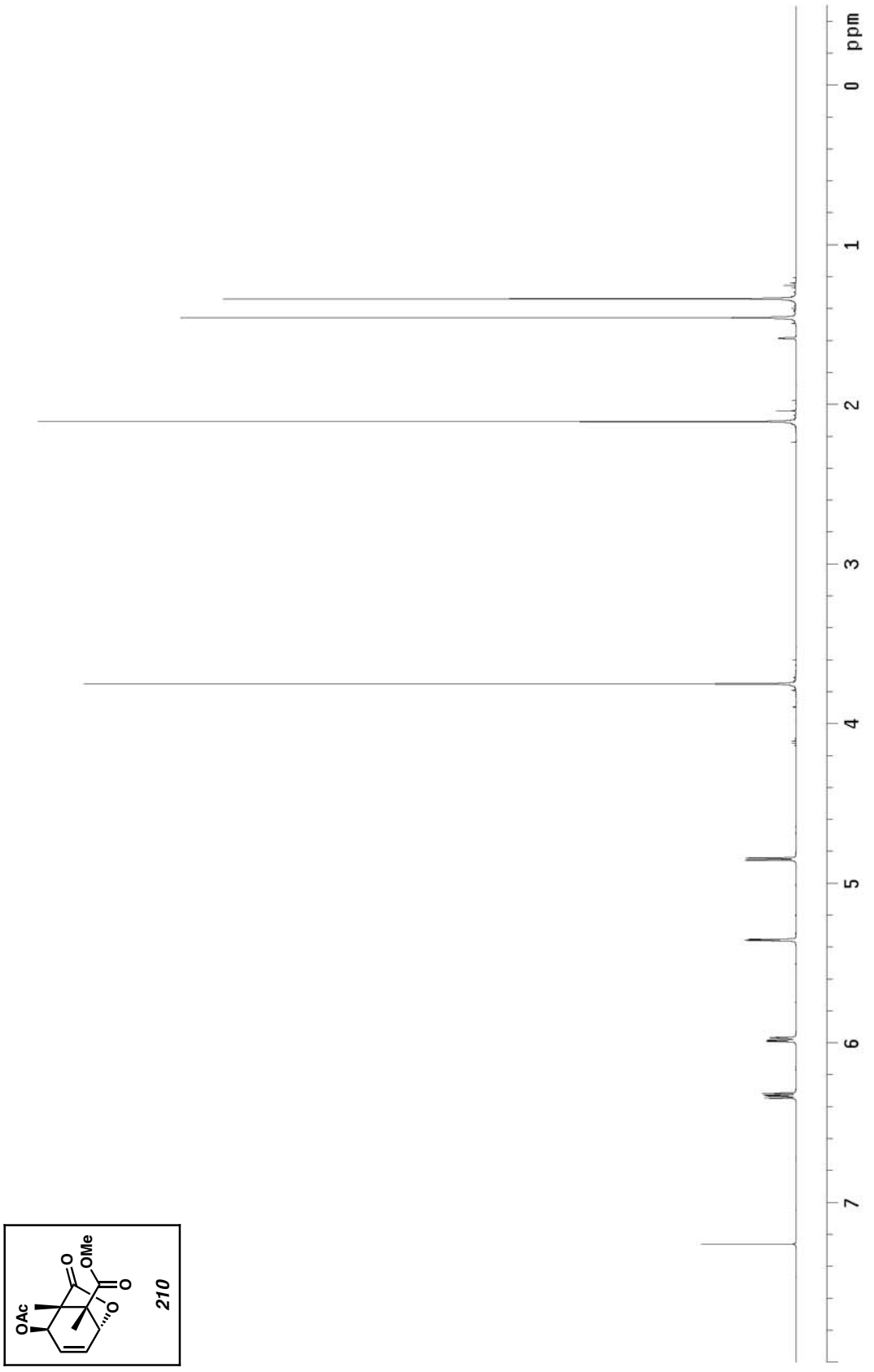

Figure A5.13 ^{1}H NMR of compound **210** (500 MHz, $CDCl_3$)

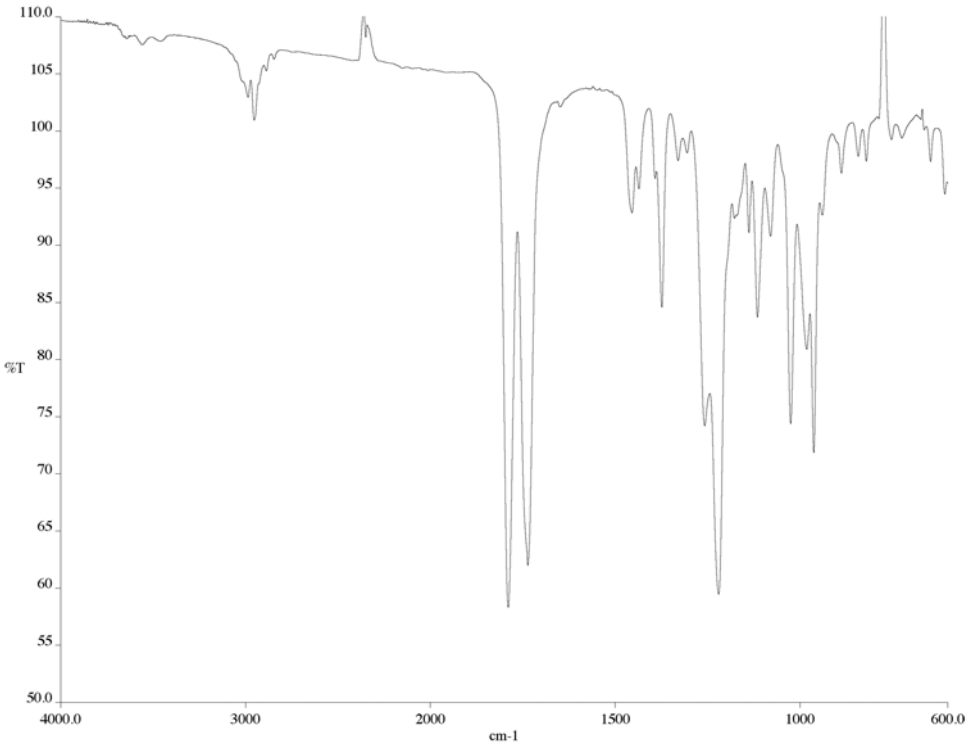

Figure A5.14 IR of compound **210** (NaCl/film)

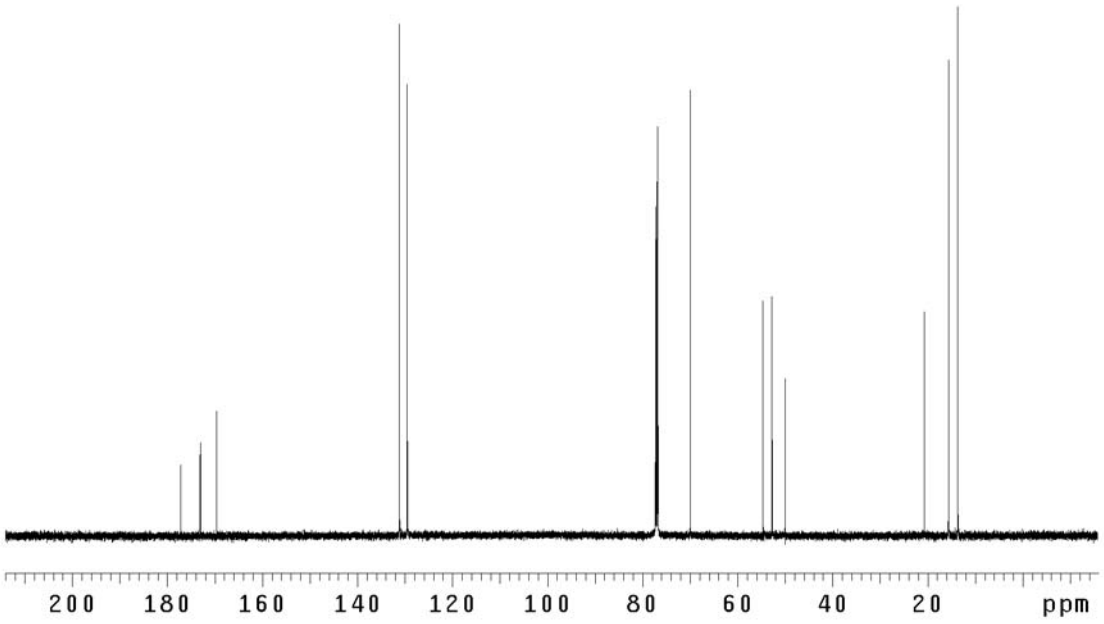

Figure A5.15 ^{13}C NMR of compound **210** (125 MHz, $CDCl_3$)

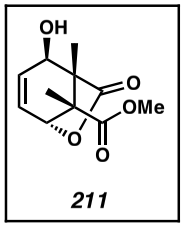

Figure A5.16 ^{1}H NMR of compound **211** (500 MHz, $CDCl_3$)

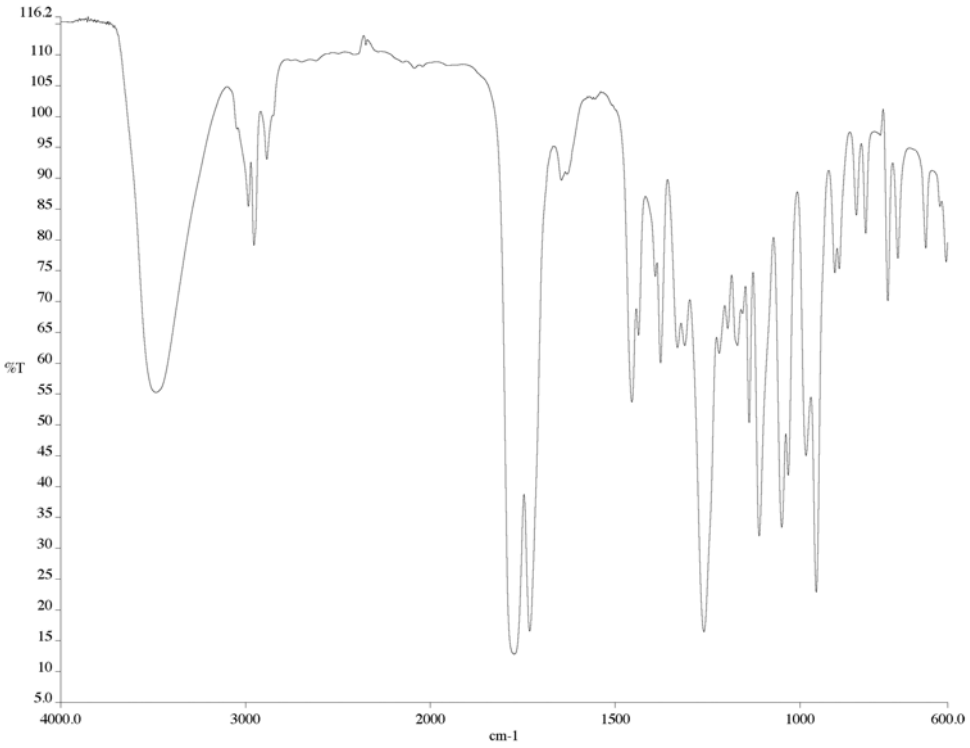

Figure A5.17 IR of compound **211** (NaCl/film)

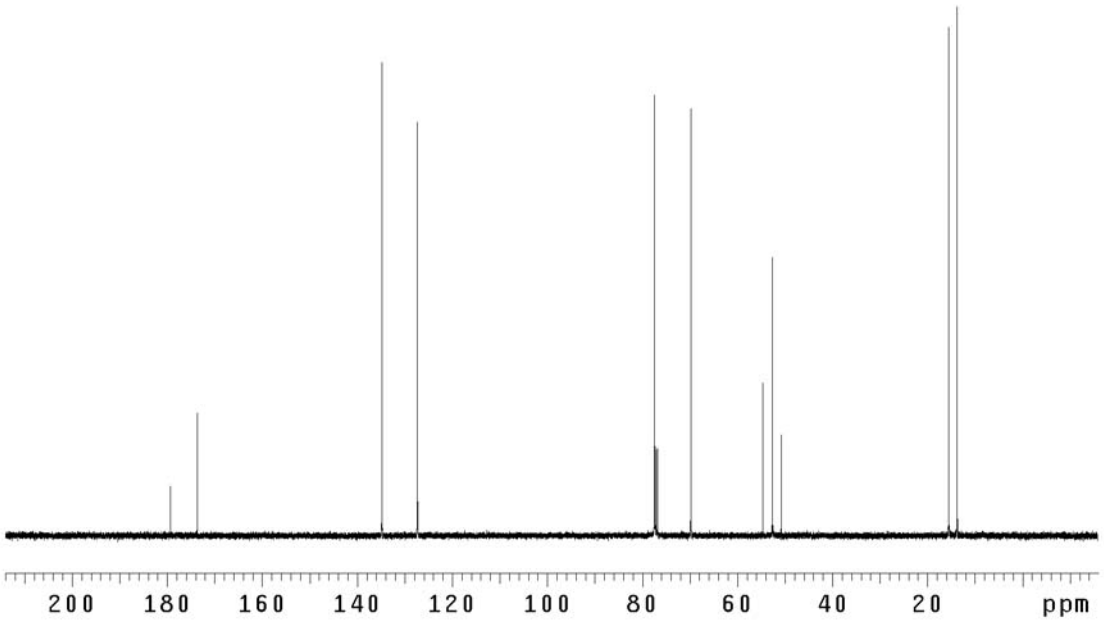

Figure A5.18 ^{13}C NMR of compound **211** (125 MHz, $CDCl_3$)

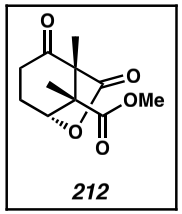

Figure A5.19 ^{1}H NMR of compound **212** (300 MHz, $CDCl_3$)

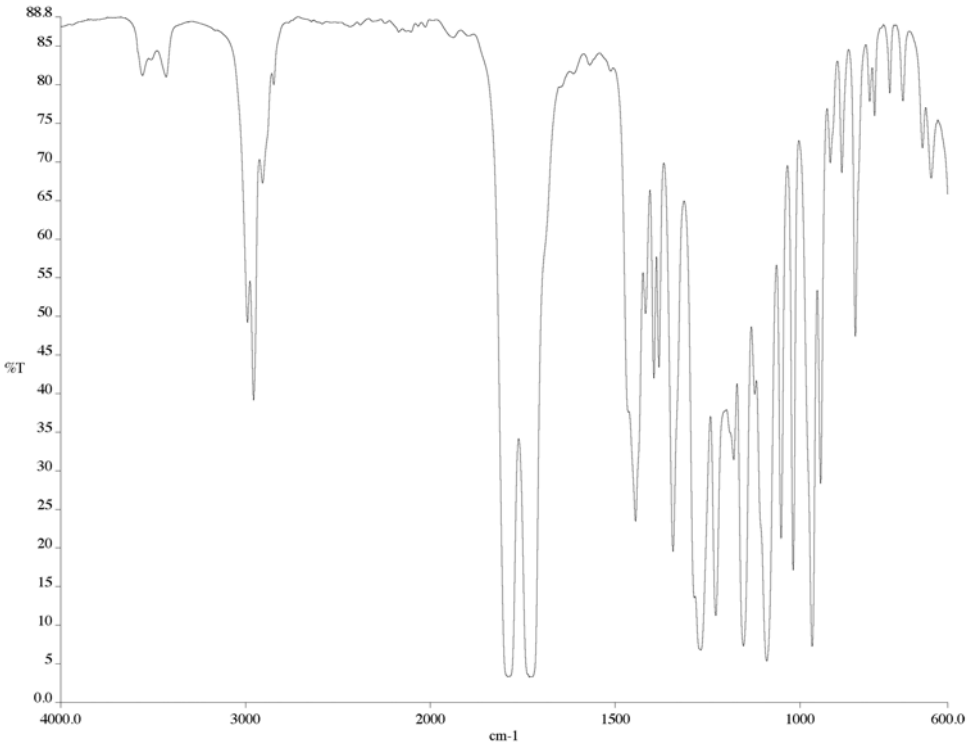

Figure A5.20 IR of compound **212** (NaCl/film)

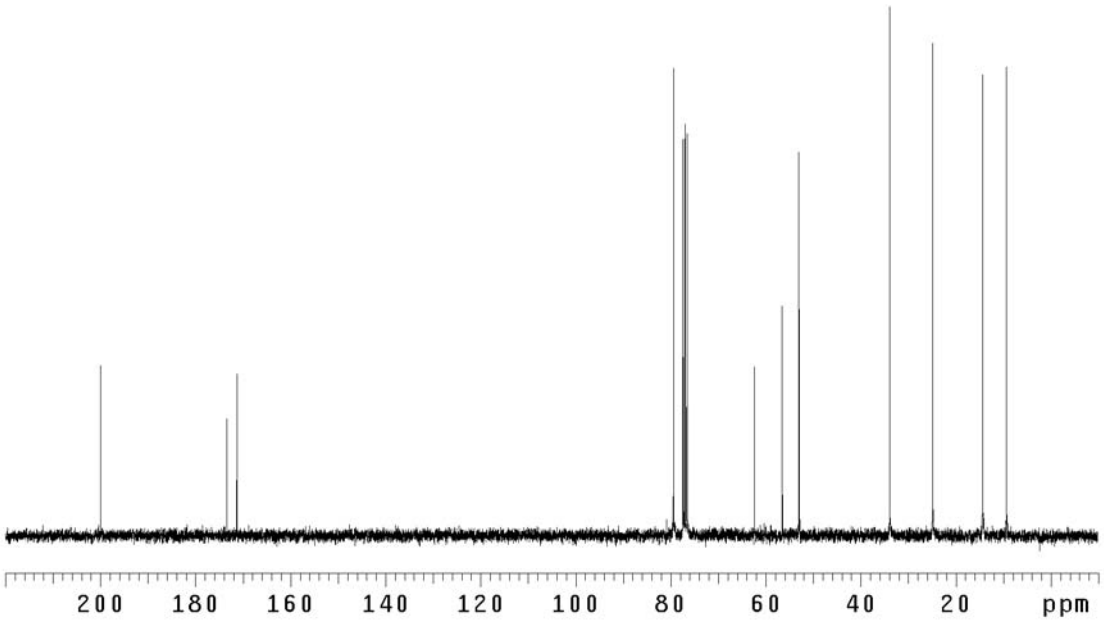

Figure A5.21 ^{13}C NMR of compound **212** (75 MHz, $CDCl_3$)

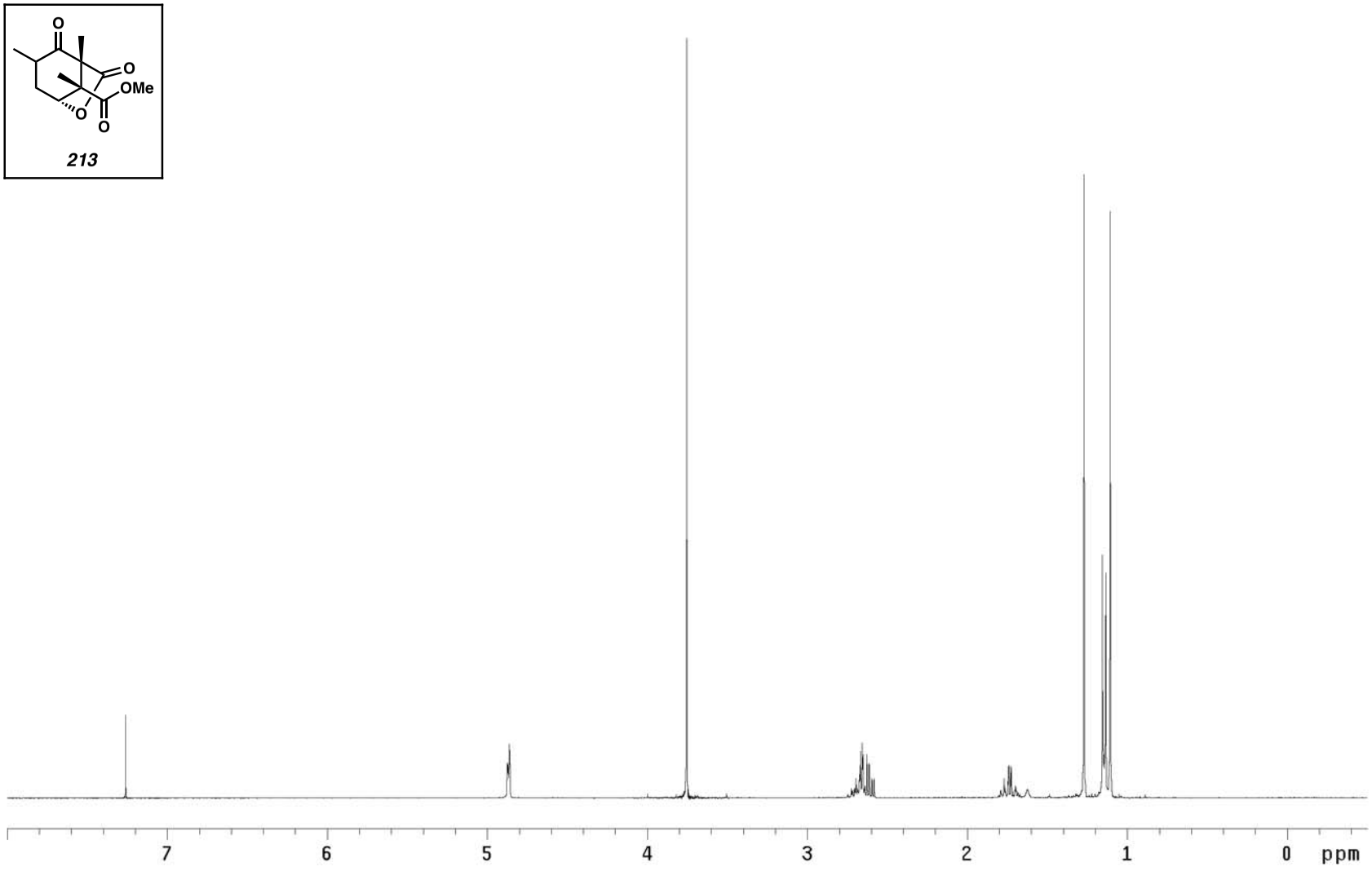

Figure A5.22 ^{1}H NMR of compound **213** (300 MHz, $CDCl_3$)

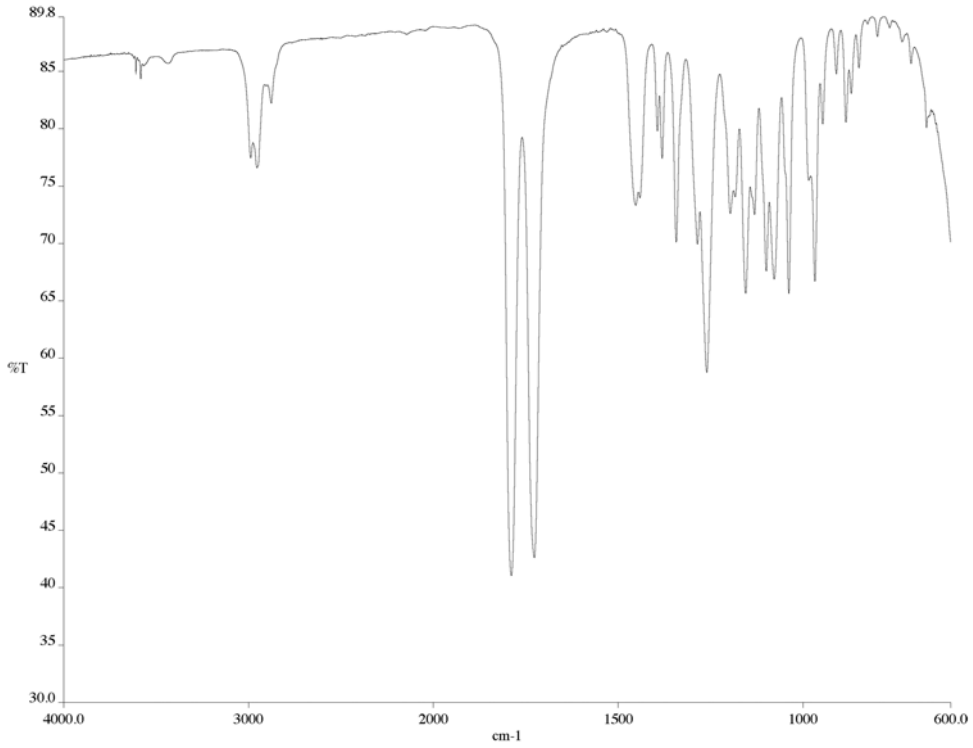

Figure A5.23 IR of compound **213** (NaCl/film)

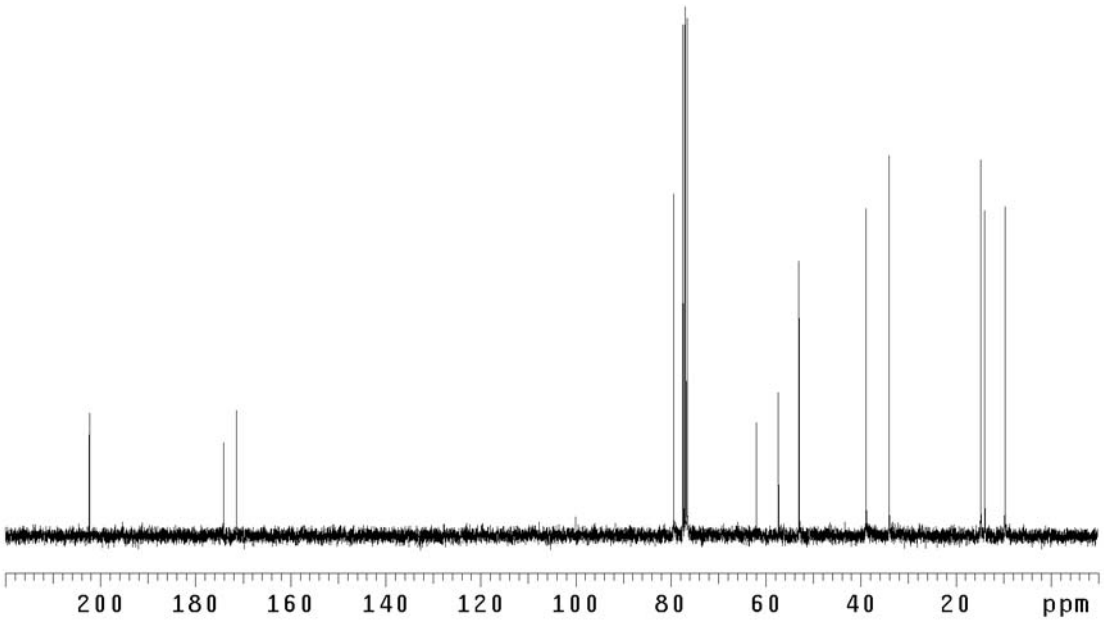

Figure A5.24 ^{13}C NMR of compound **213** (75 MHz, $CDCl_3$)

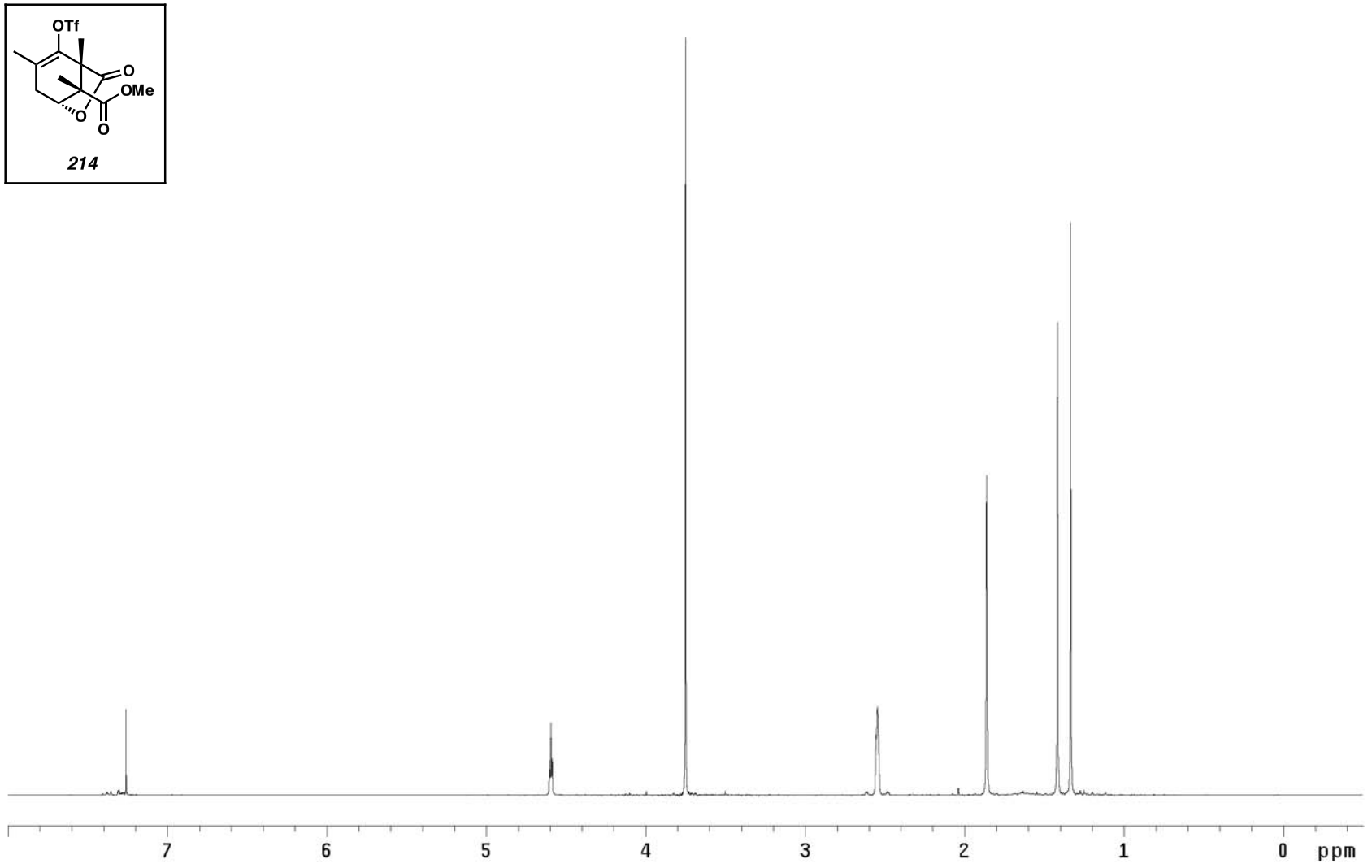

Figure A5.25 ^{1}H NMR of compound **214** (300 MHz, $CDCl_3$)

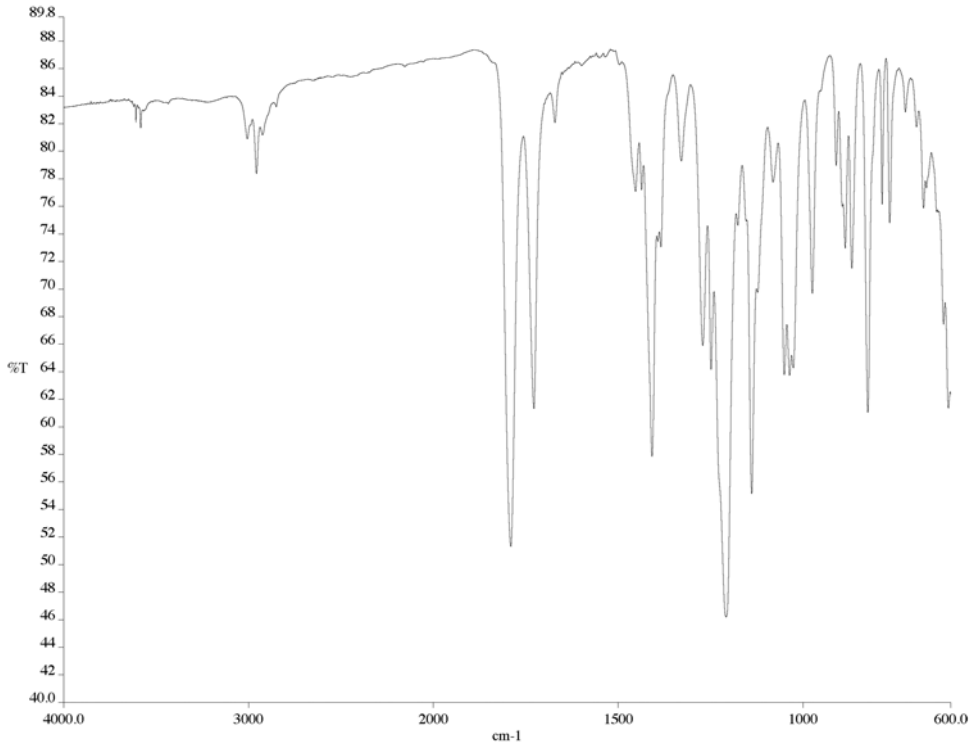

Figure A5.26 IR of compound **214** (NaCl/film)

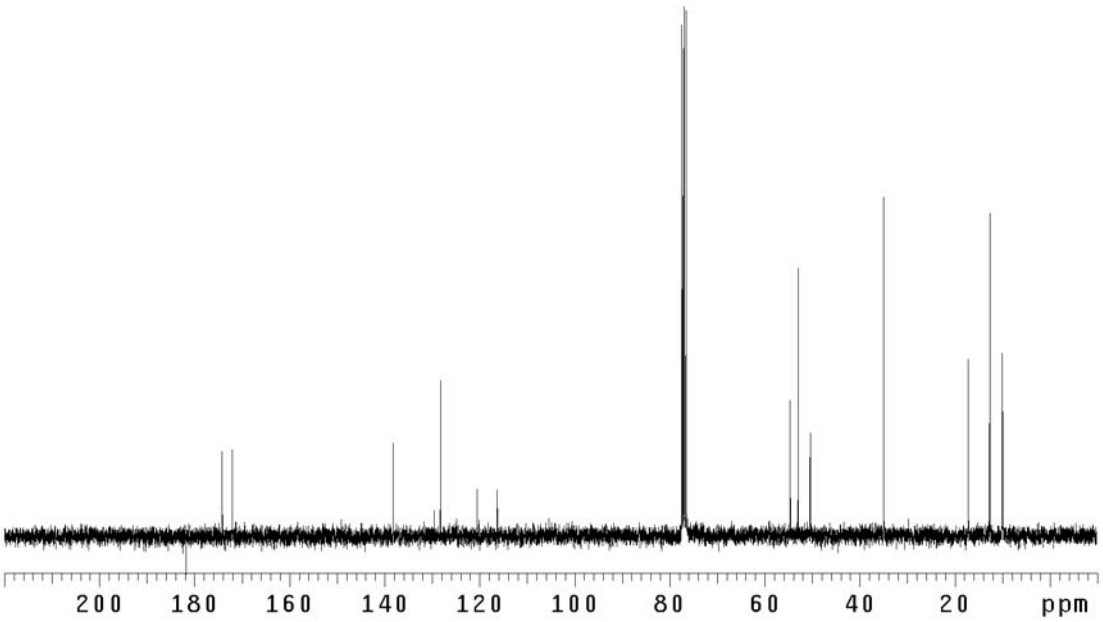

Figure A5.27 ^{13}C NMR of compound **214** (75 MHz, $CDCl_3$)

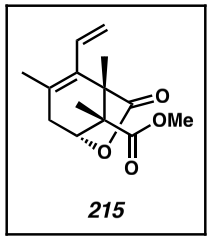

215

Figure A5.28 ^{1}H NMR of compound **215** (300 MHz, $CDCl_3$)

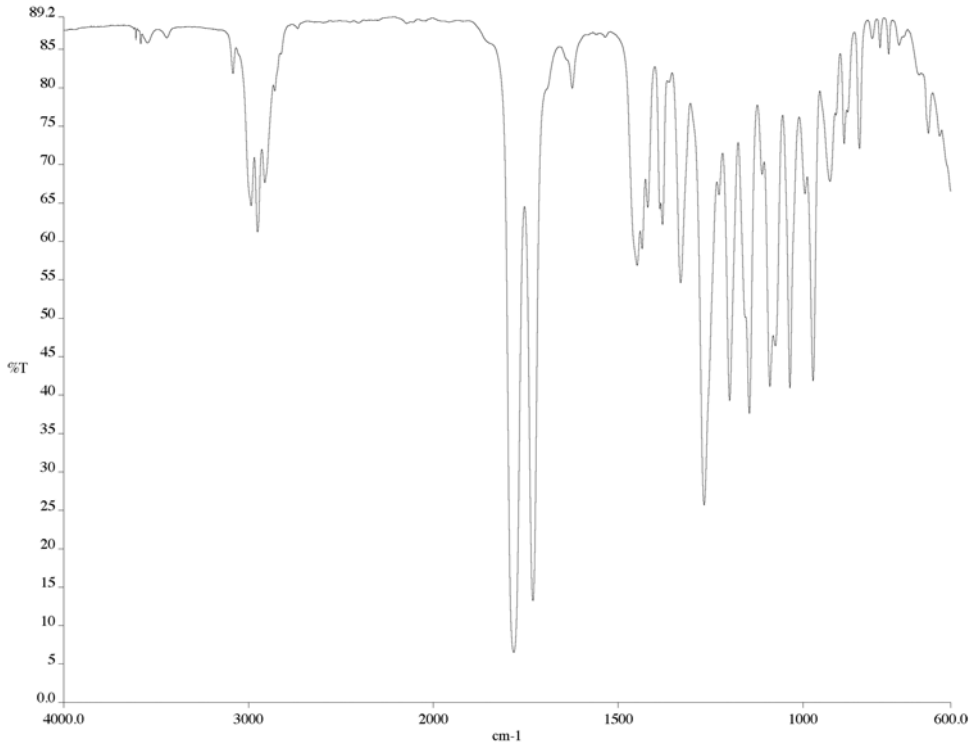

Figure A5.29 IR of compound **215** (NaCl/film)

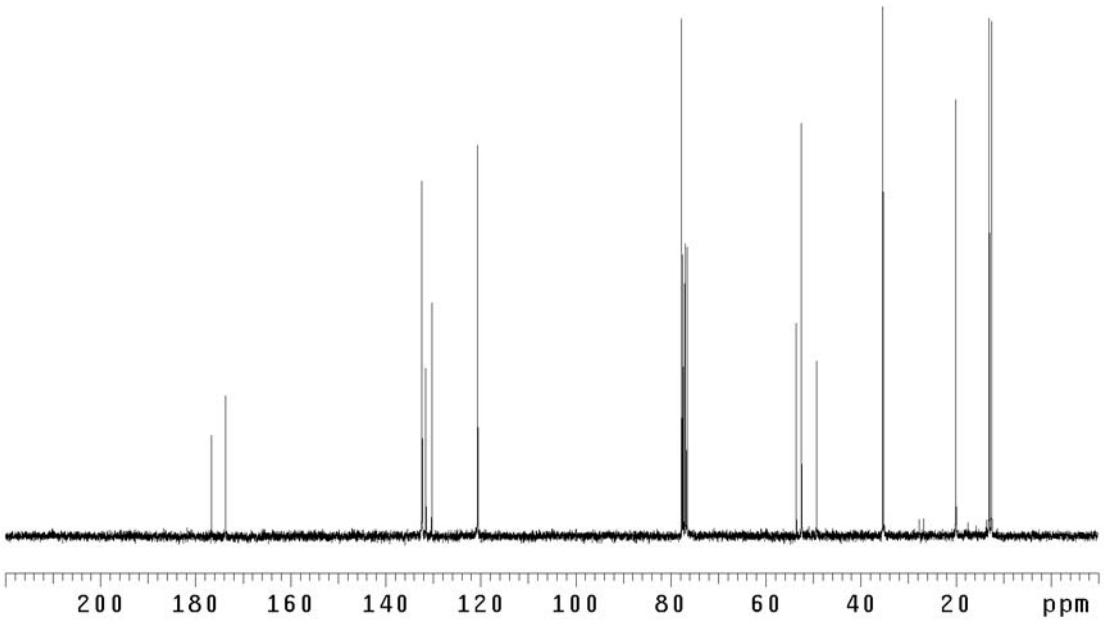

Figure A5.30 ^{13}C NMR of compound **215** (75 MHz, $CDCl_3$)

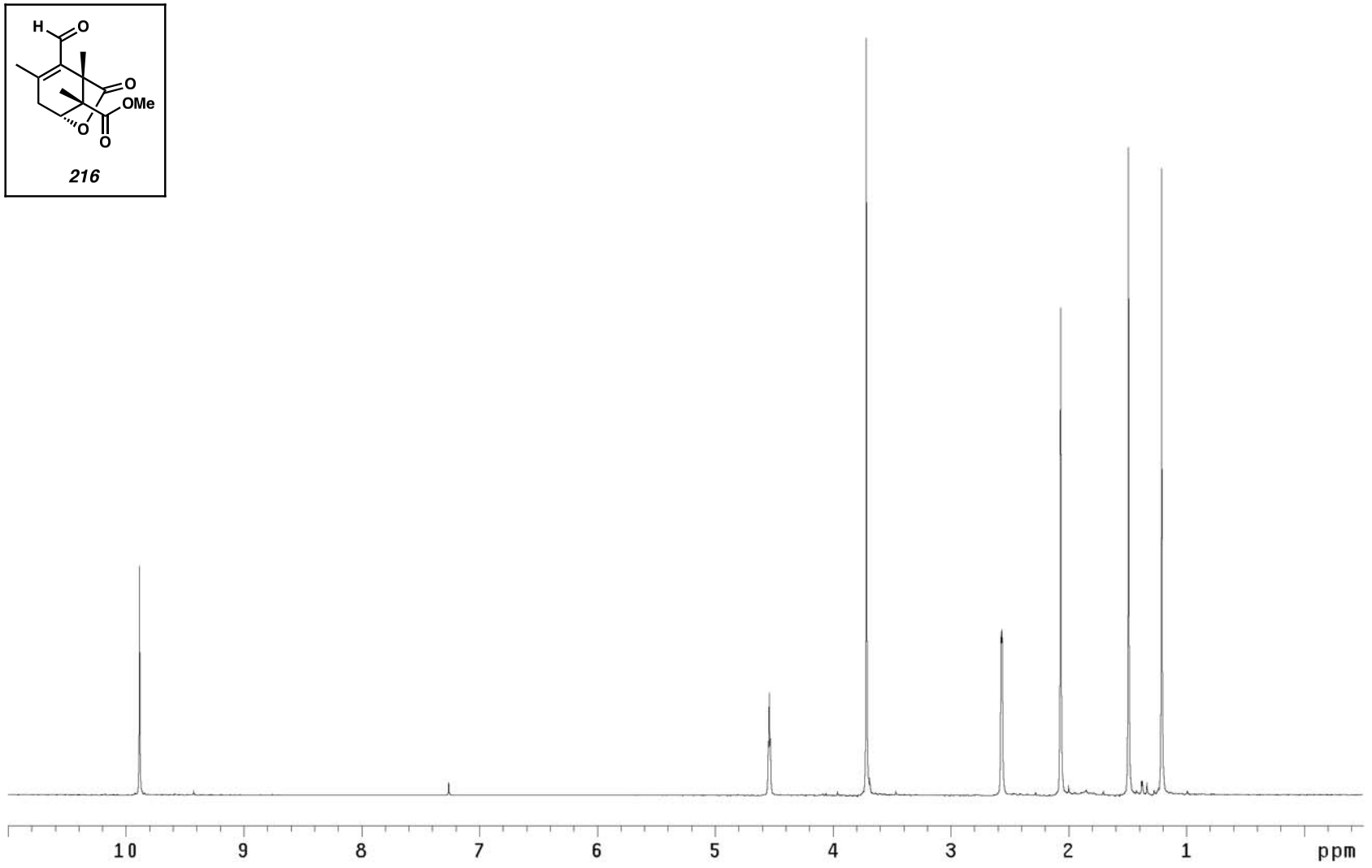

Figure A5.31 ^{1}H NMR of compound **216** (300 MHz, $CDCl_3$)

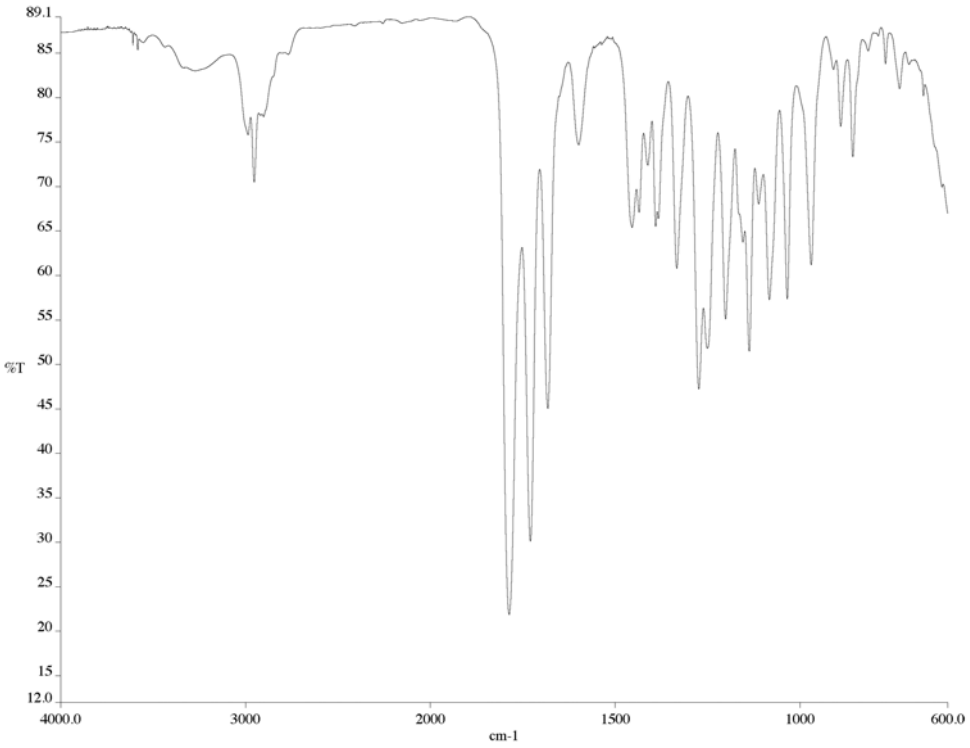

Figure A5.32 IR of compound **216** (NaCl/film)

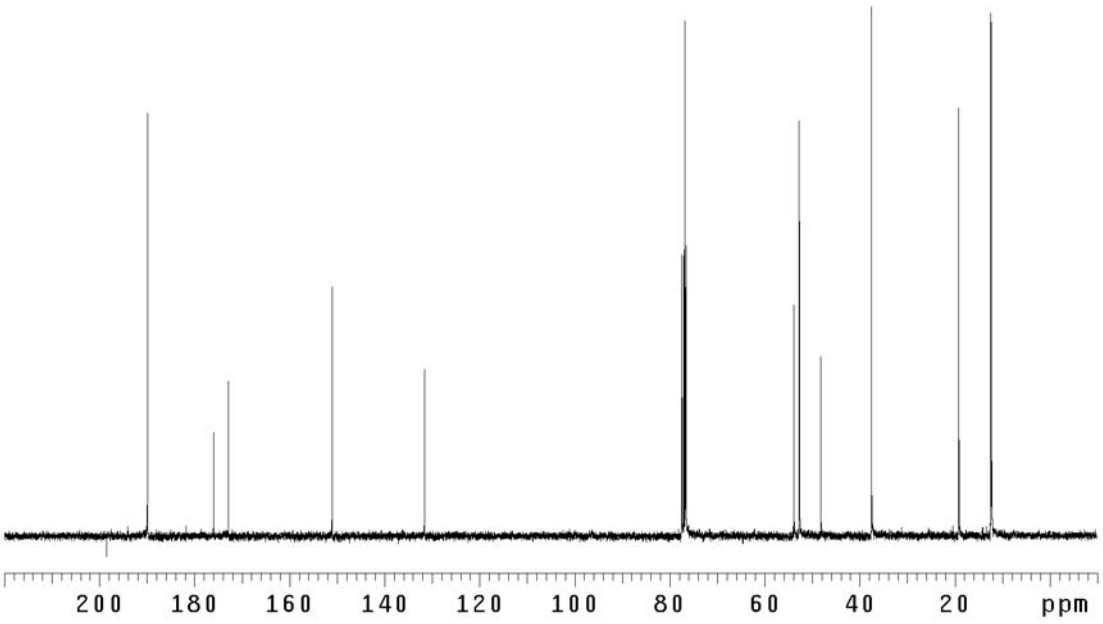

Figure A5.33 ^{13}C NMR of compound **216** (75 MHz, $CDCl_3$)

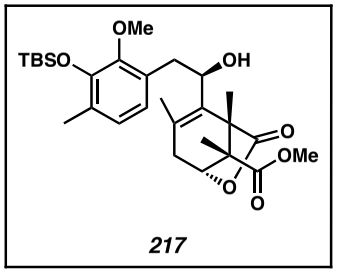

Figure A5.34 ^{1}H NMR of compound **217** (300 MHz, $CDCl_3$)

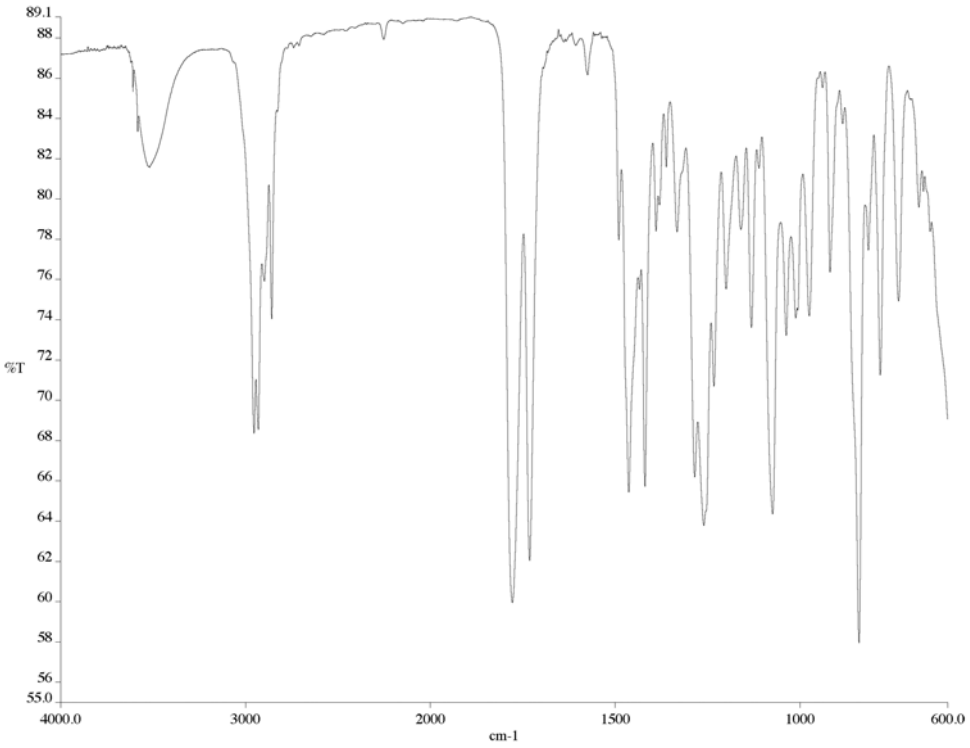

Figure A5.35 IR of compound **217** (NaCl/film)

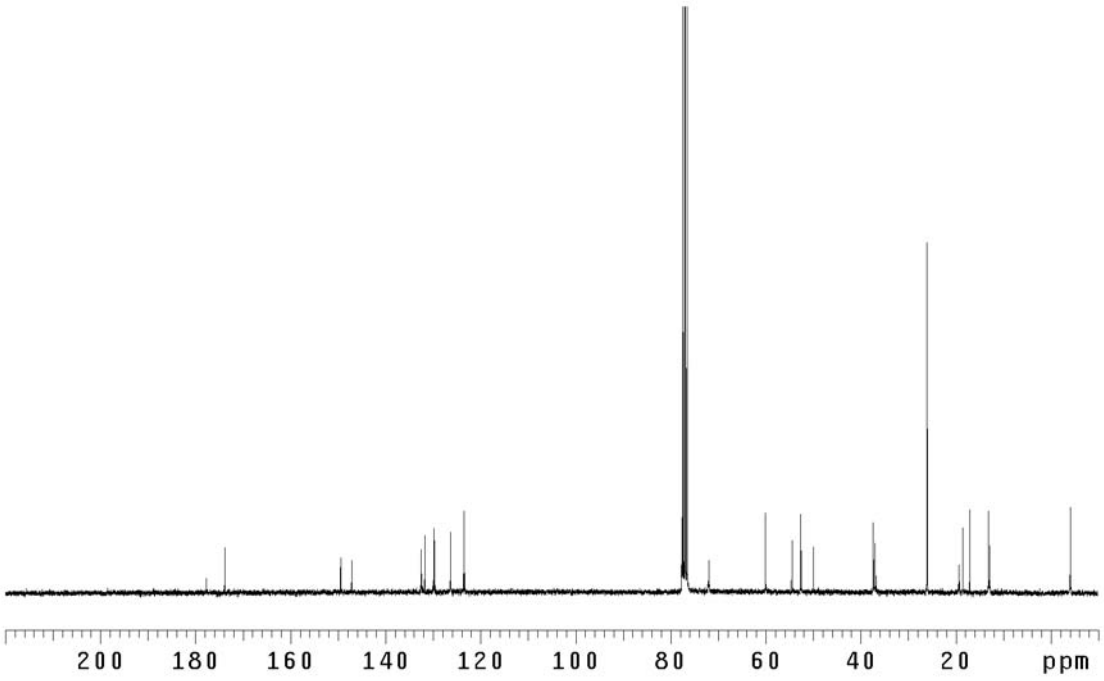

Figure A5.36 ^{13}C NMR of compound **217** (75 MHz, $CDCl_3$)

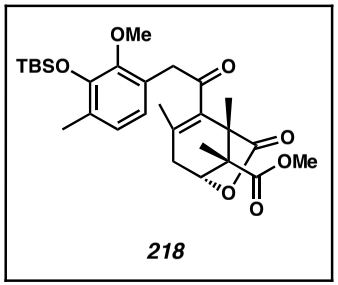

218

Figure A5.37 ^{1}H NMR of compound **218** (300 MHz, $CDCl_3$)

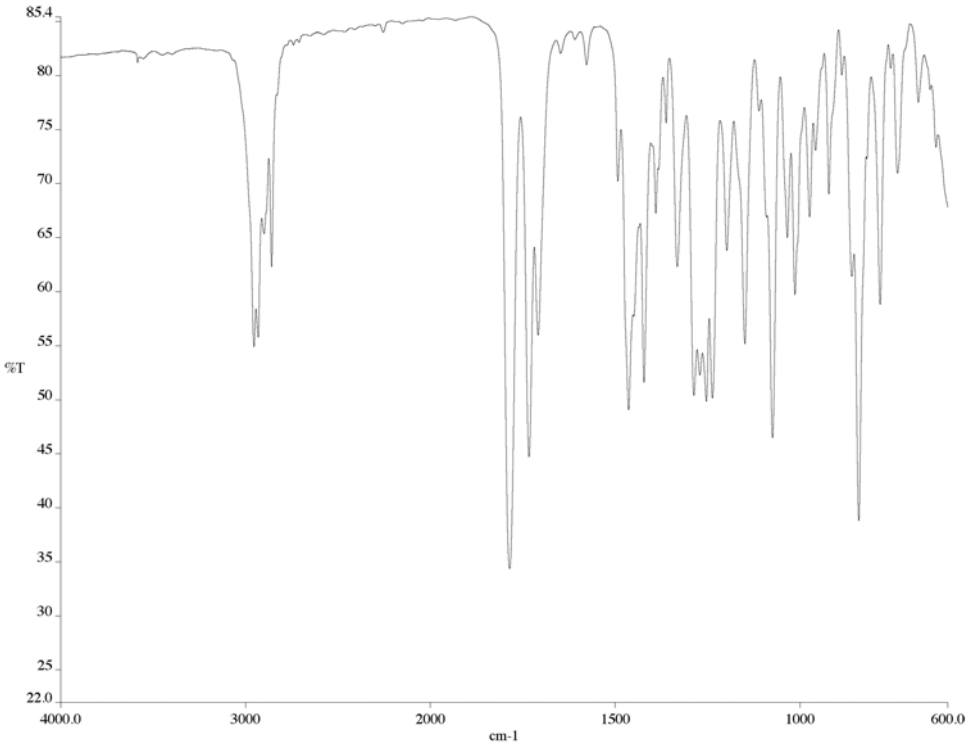

Figure A5.38 IR of compound **218** (NaCl/film)

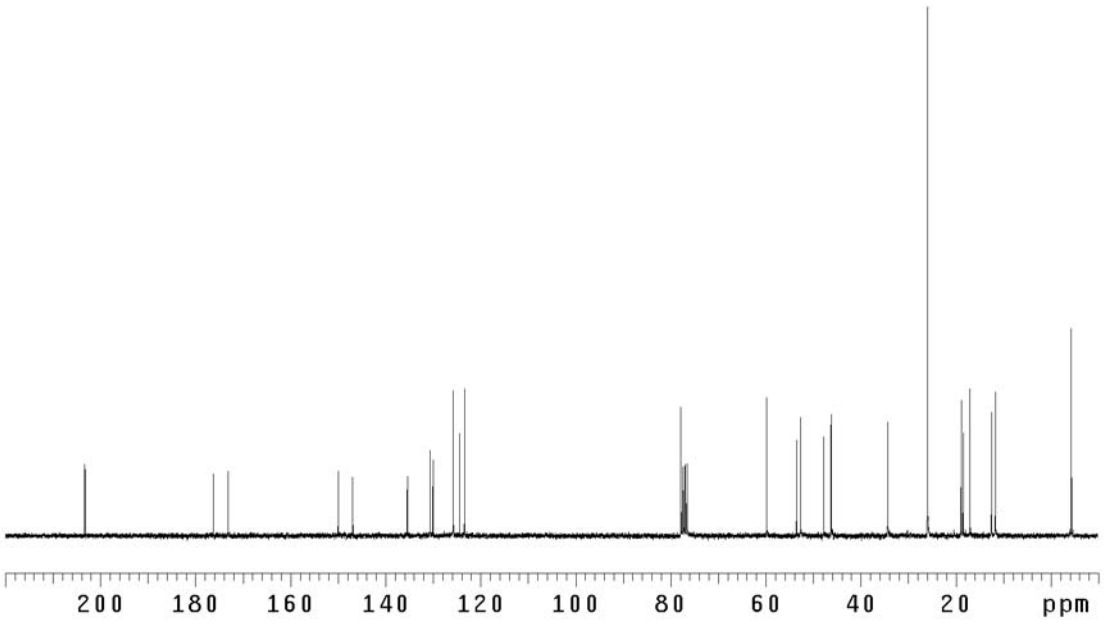

Figure A5.39 ^{13}C NMR of compound **218** (75 MHz, $CDCl_3$)

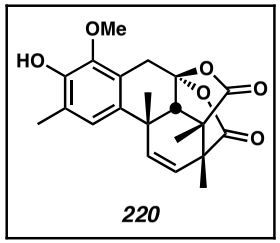

220

Figure A5.40 ^{1}H NMR of compound **220** (300 MHz, $CDCl_3$)

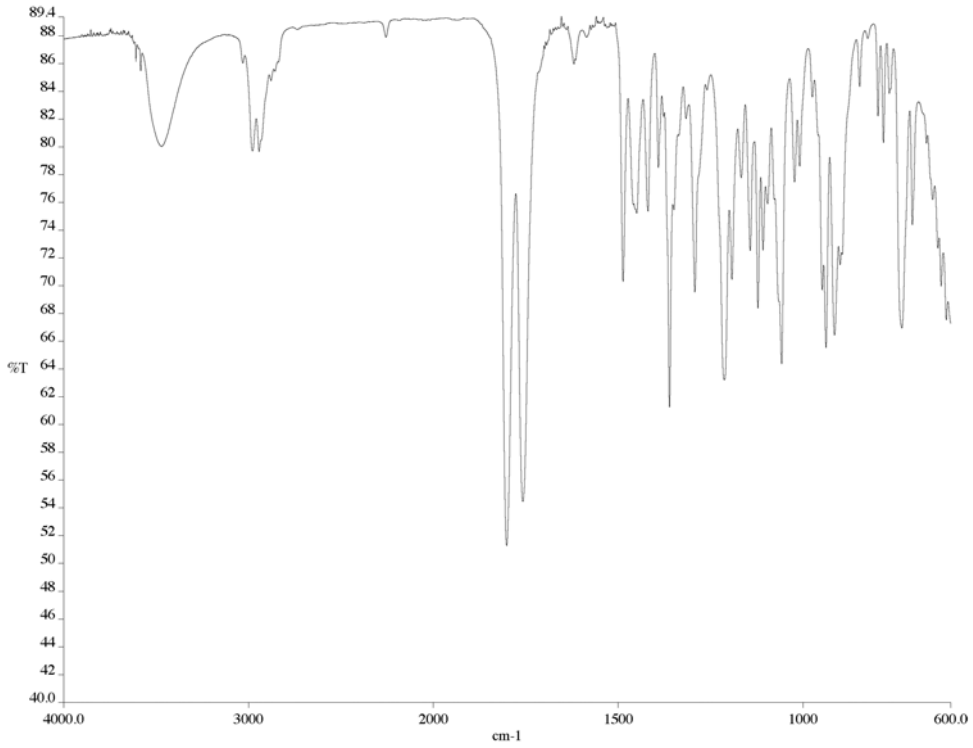

Figure A5.41 IR of compound **220** (NaCl/film)

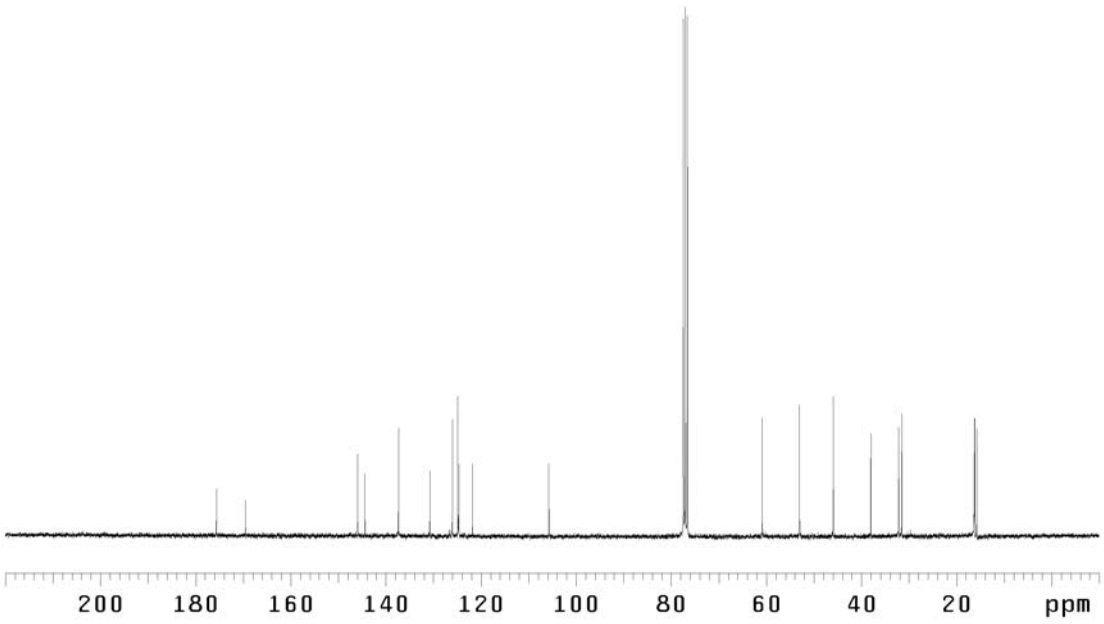

Figure A5.42 ^{13}C NMR of compound **220** (75 MHz, $CDCl_3$)

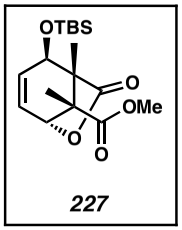

227

Figure A5.43 ^{1}H NMR of compound **227** (500 MHz, $CDCl_3$)

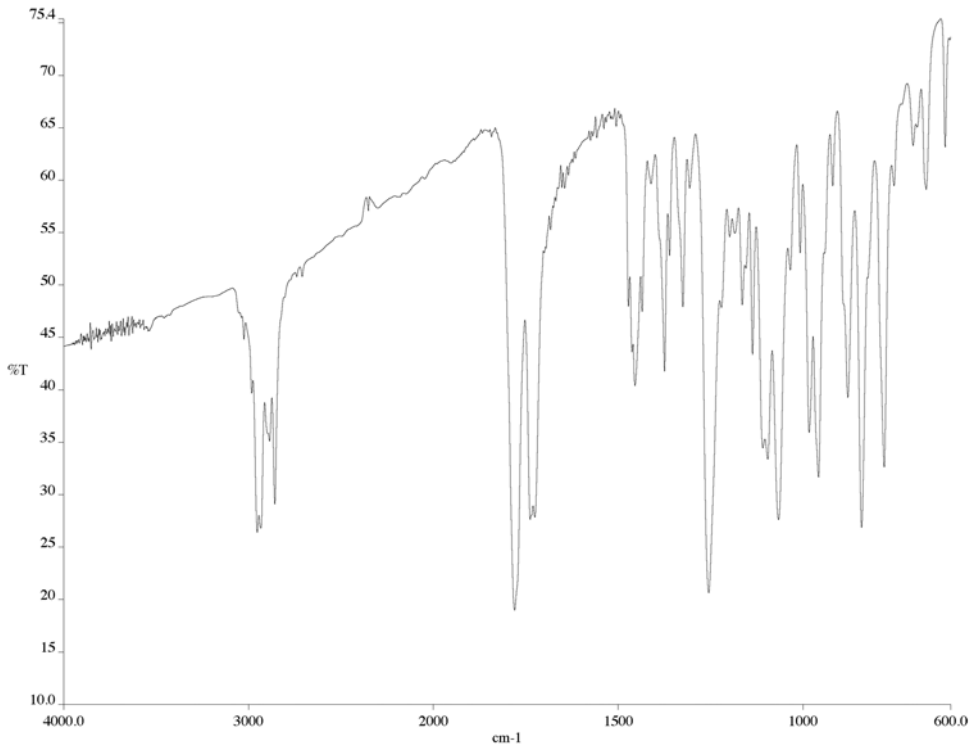

Figure A5.44 IR of compound **227** (NaCl/film)

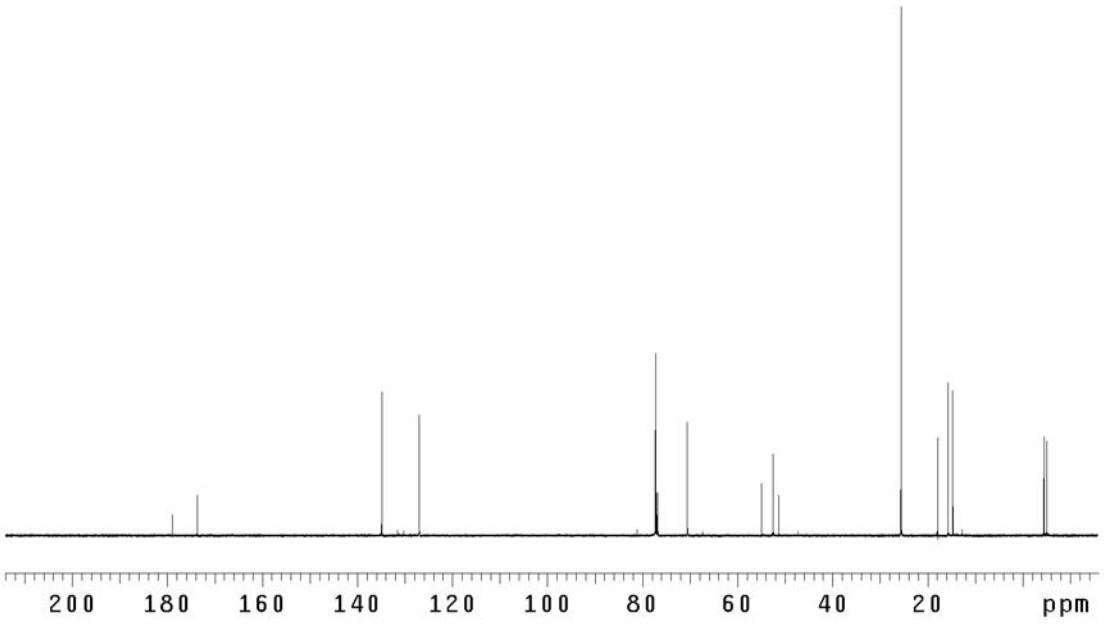

Figure A5.45 ^{13}C NMR of compound **227** (125 MHz, $CDCl_3$)

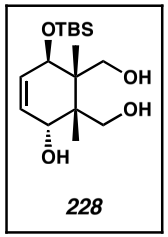

Figure A5.46 ^{1}H NMR of compound **228** (500 MHz, $CDCl_3$)

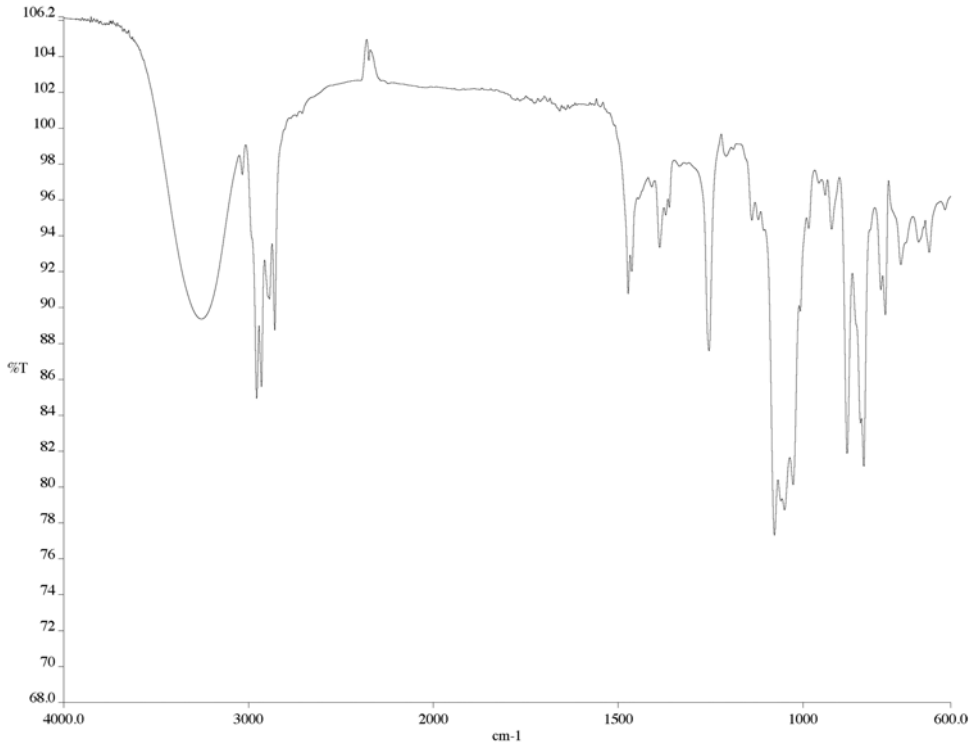

Figure A5.47 IR of compound **228** (NaCl/film)

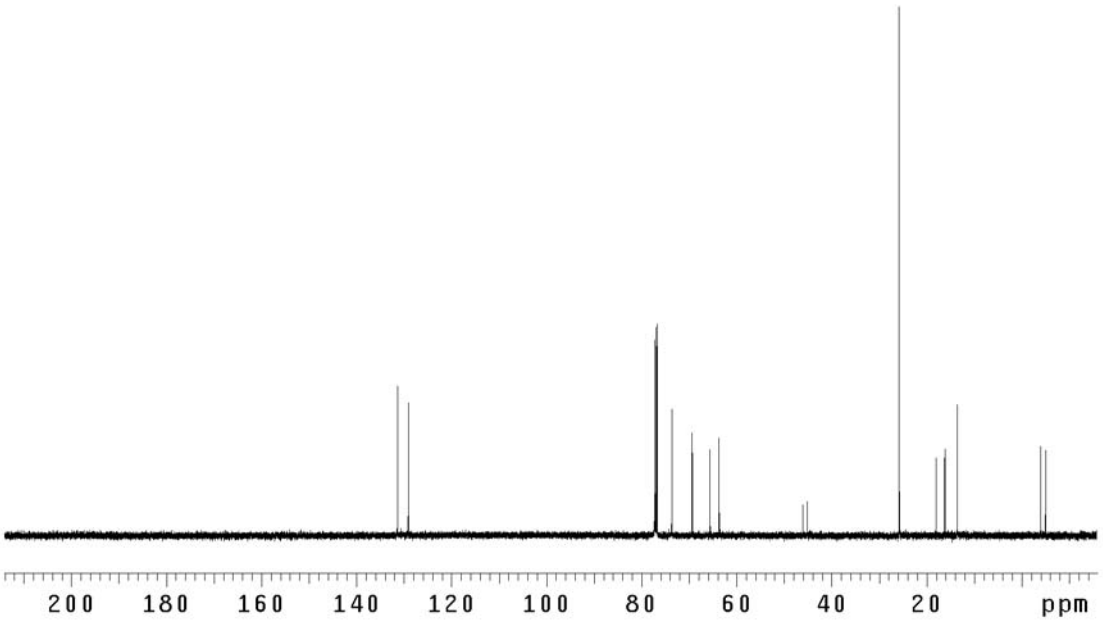

Figure A5.48 ^{13}C NMR of compound **228** (125 MHz, $CDCl_3$)

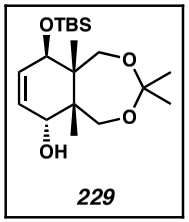

Figure A5.49 ^{1}H NMR of compound **229** (300 MHz, $CDCl_3$)

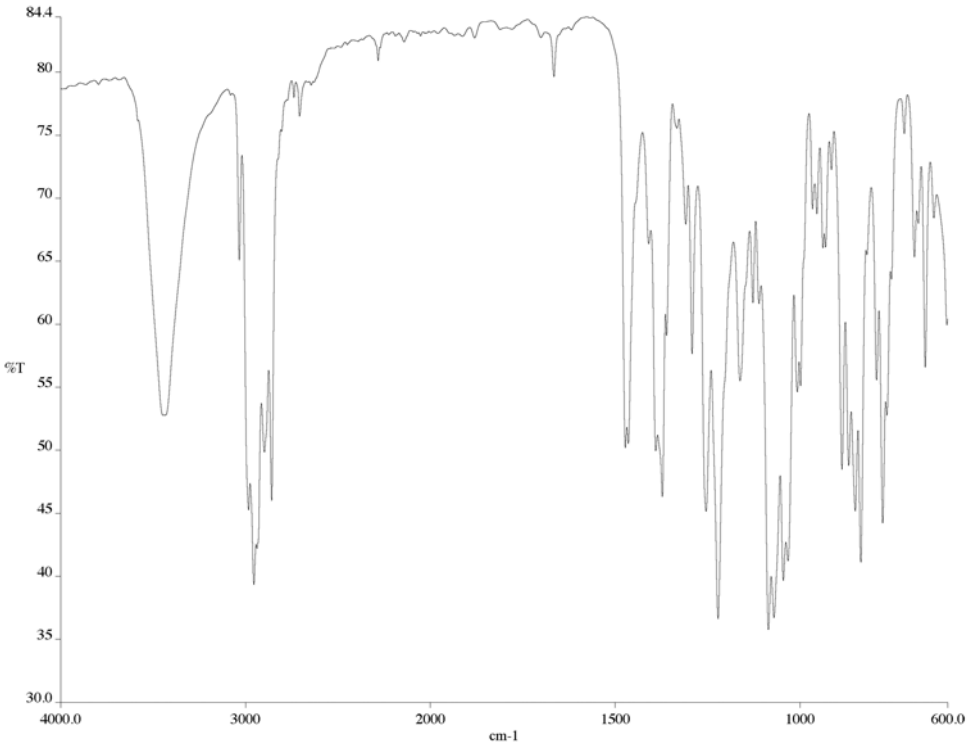

Figure A5.50 IR of compound **229** (NaCl/film)

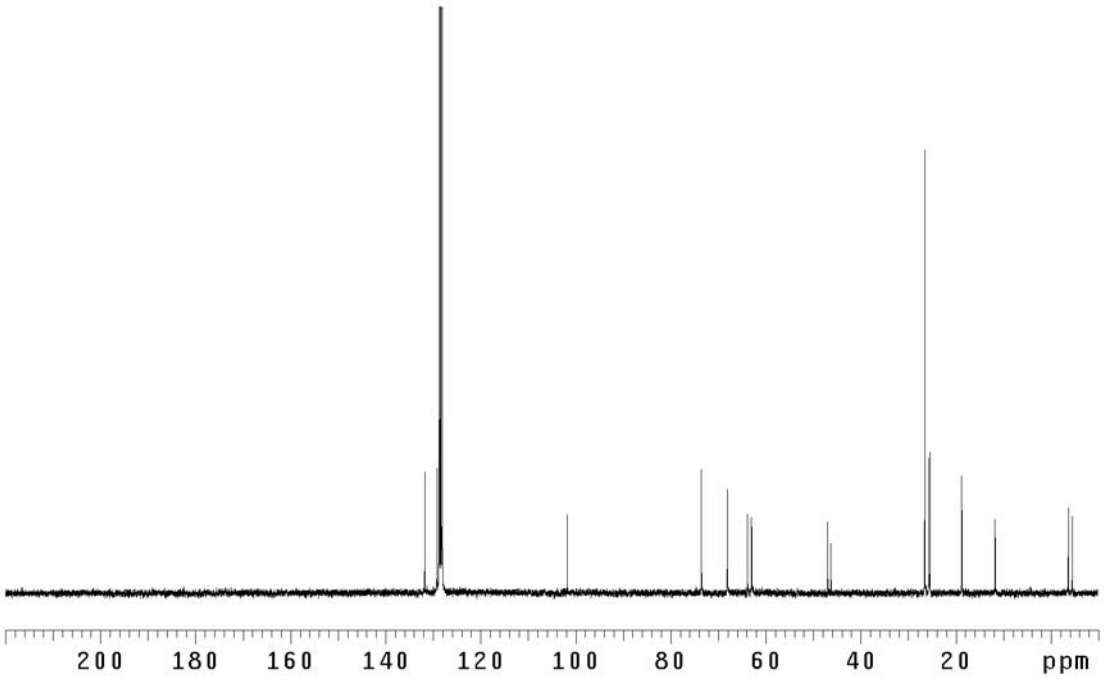

Figure A5.51 ^{13}C NMR of compound **229** (75 MHz, C_6D_6)

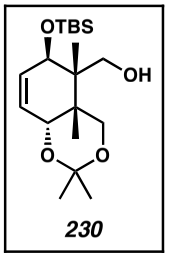

Figure A5.52 ^{1}H NMR of compound **230** (300 MHz, $CDCl_3$)

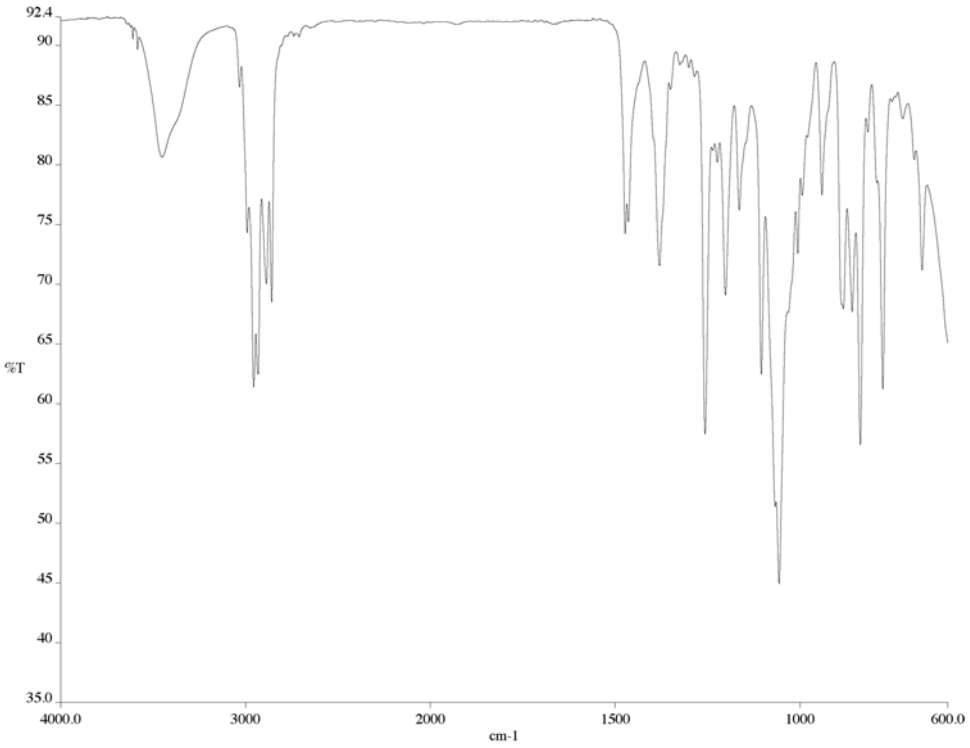

Figure A5.53 IR of compound **230** (NaCl/film)

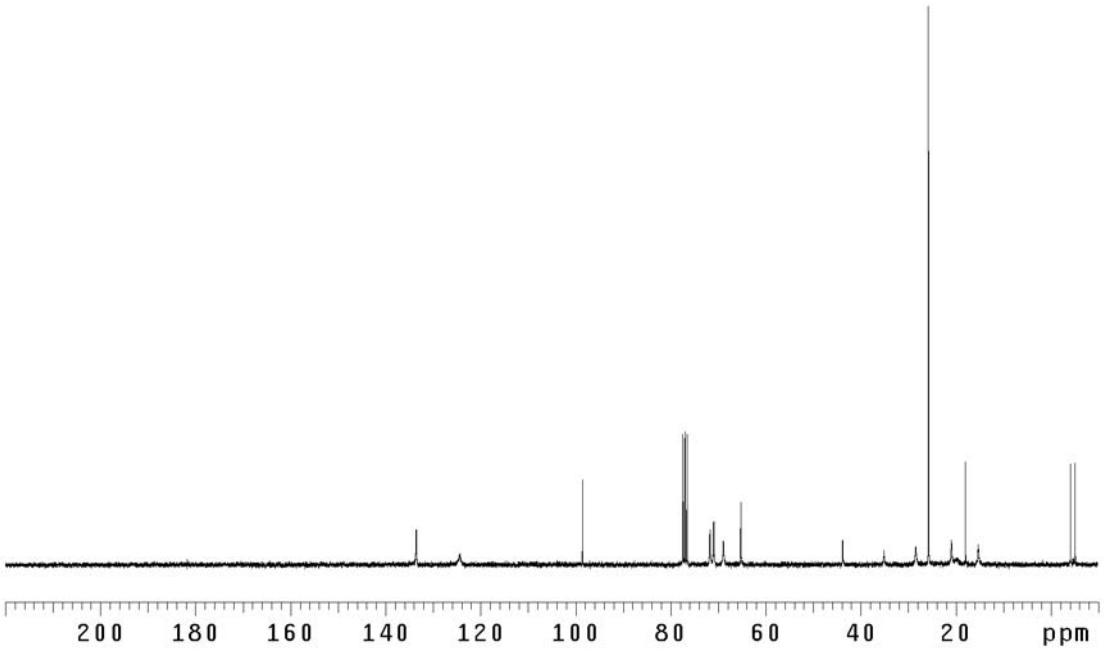

Figure A5.54 ^{13}C NMR of compound **230** (75 MHz, $CDCl_3$)

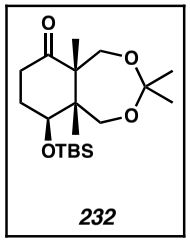

232

Figure A5.55 ^{1}H NMR of compound **232** (300 MHz, $CDCl_3$)

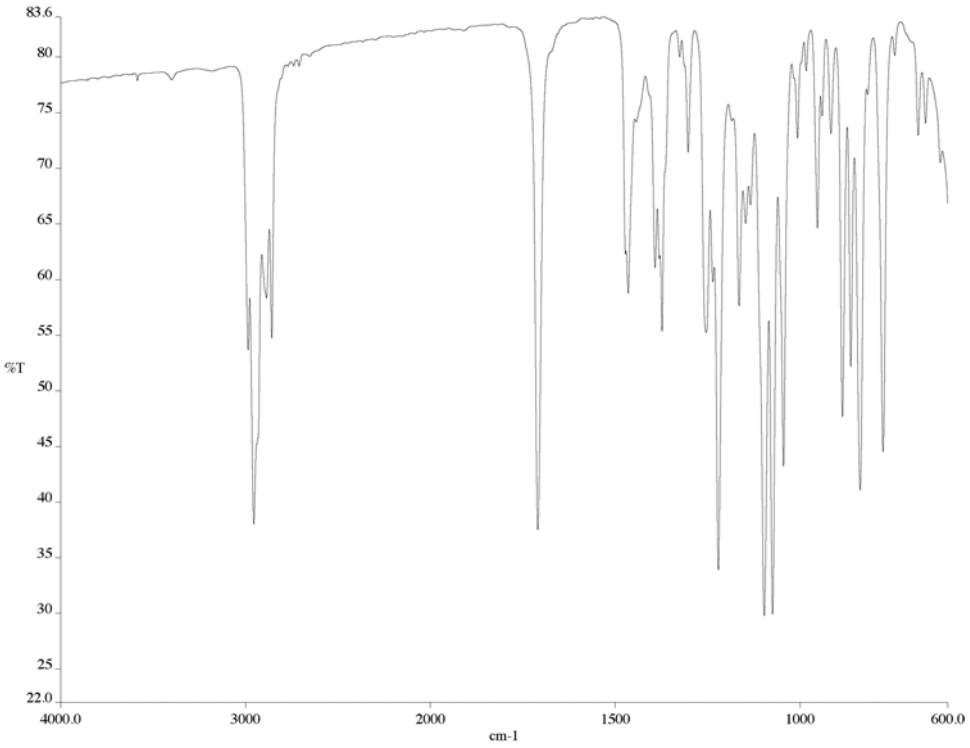

Figure A5.56 IR of compound **232** (NaCl/film)

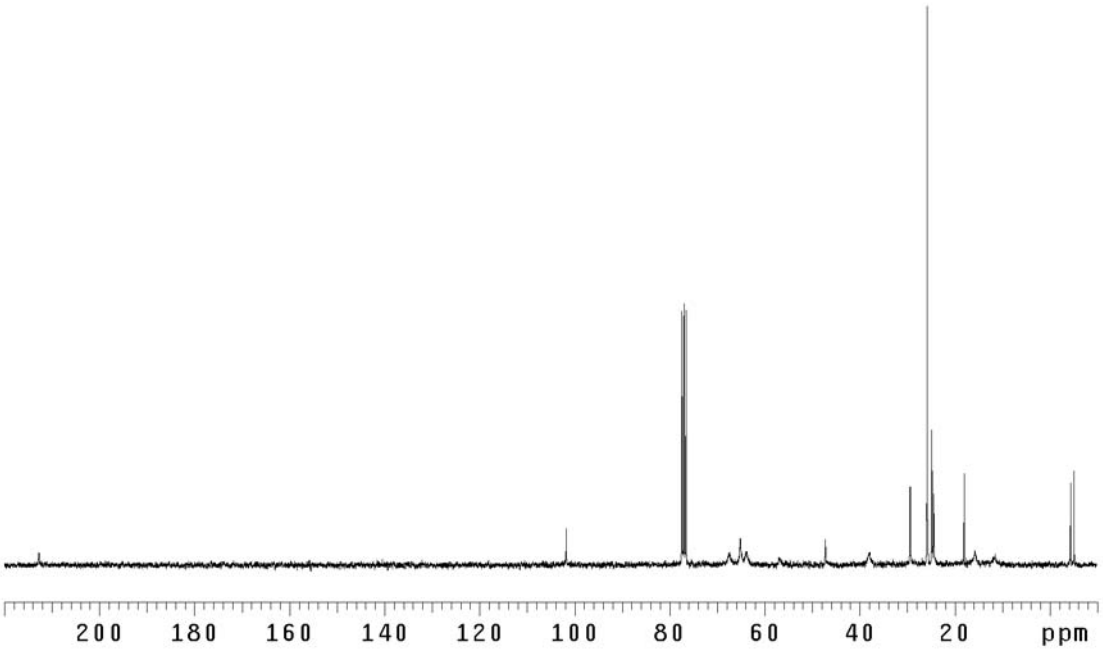

Figure A5.57 ^{13}C NMR of compound **232** (75 MHz, $CDCl_3$)

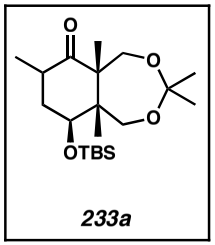

233a

Figure A5.58 ^{1}H NMR of compound **233a** (300 MHz, $CDCl_3$)

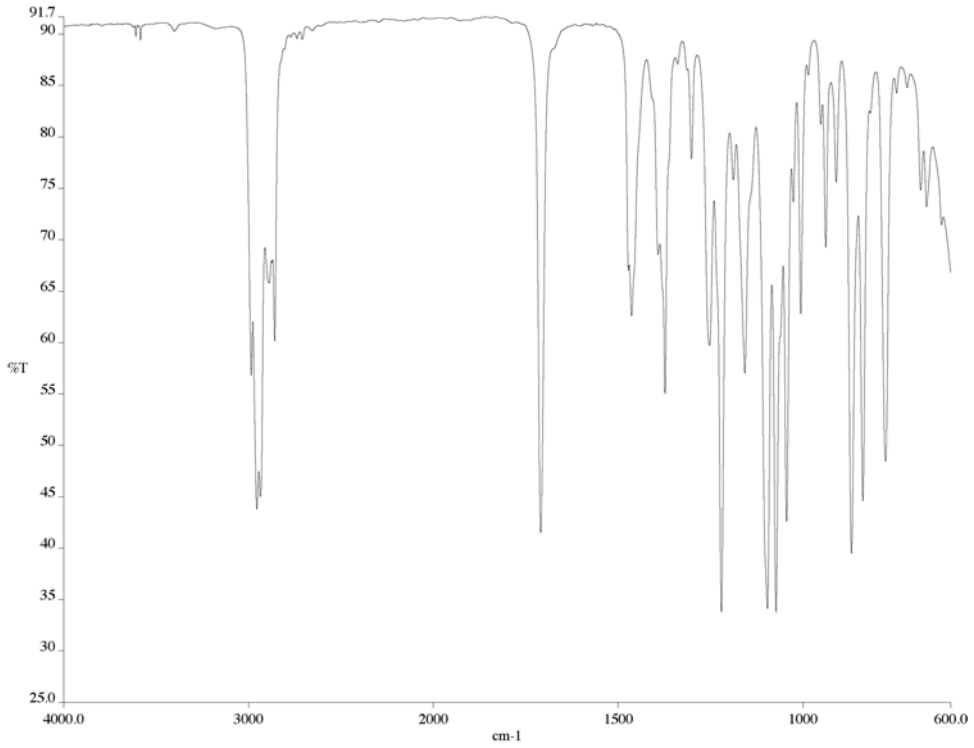

Figure A5.59 IR of compound **233a** (NaCl/film)

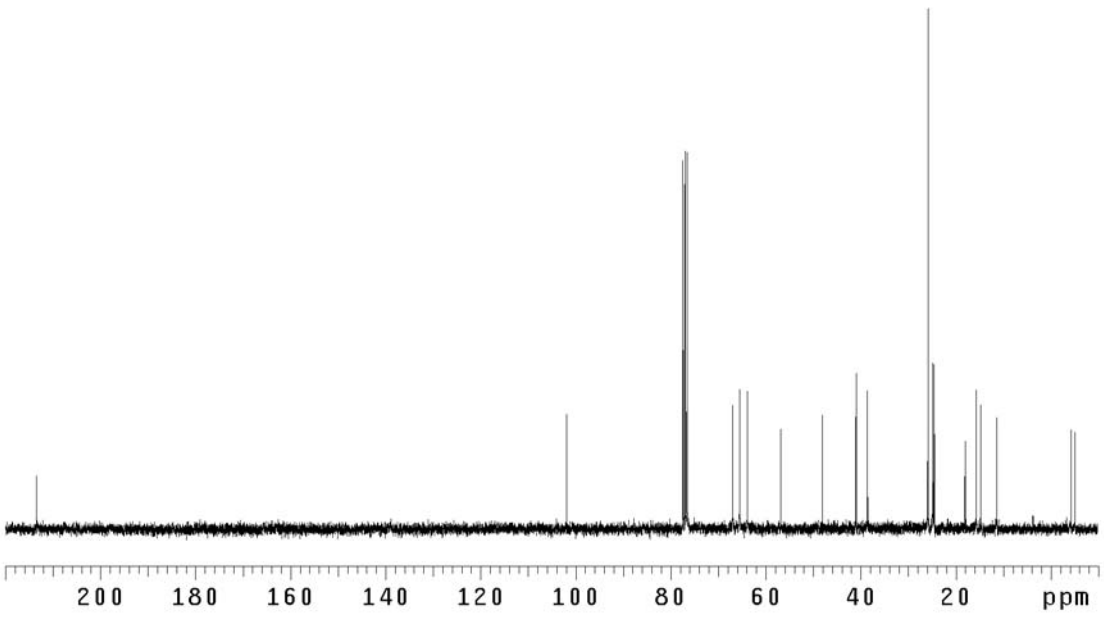

Figure A5.60 ^{13}C NMR of compound **233a** (75 MHz, $CDCl_3$)

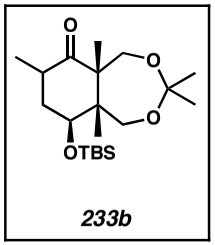

233b

Figure A5.61 ^{1}H NMR of compound **233b** (300 MHz, $CDCl_3$)

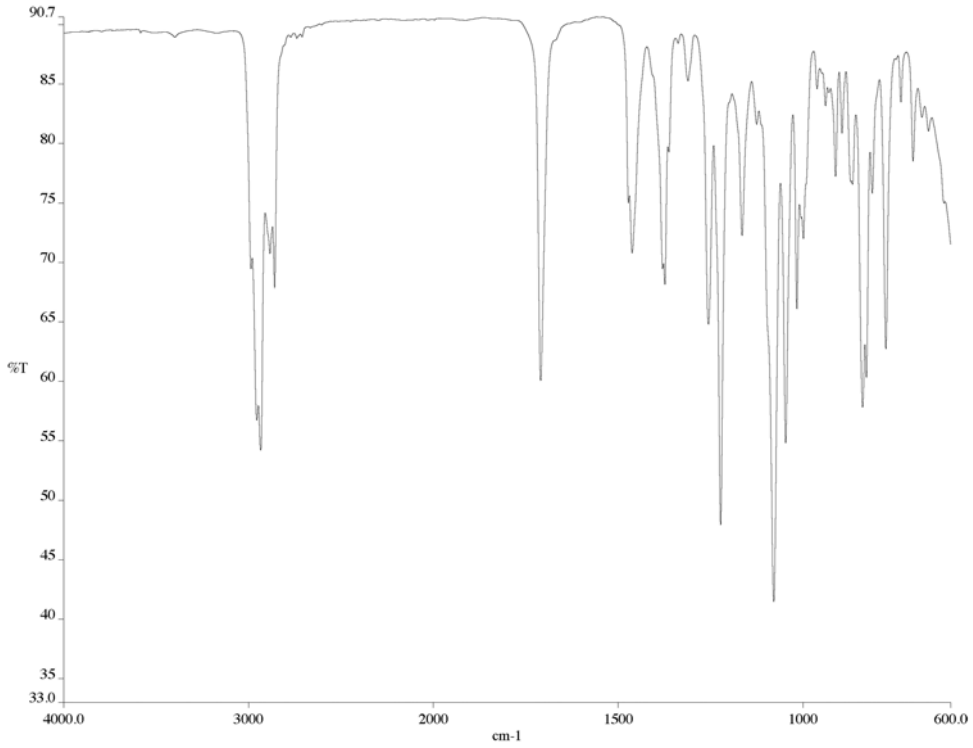

Figure A5.62 IR of compound **233b** (NaCl/film)

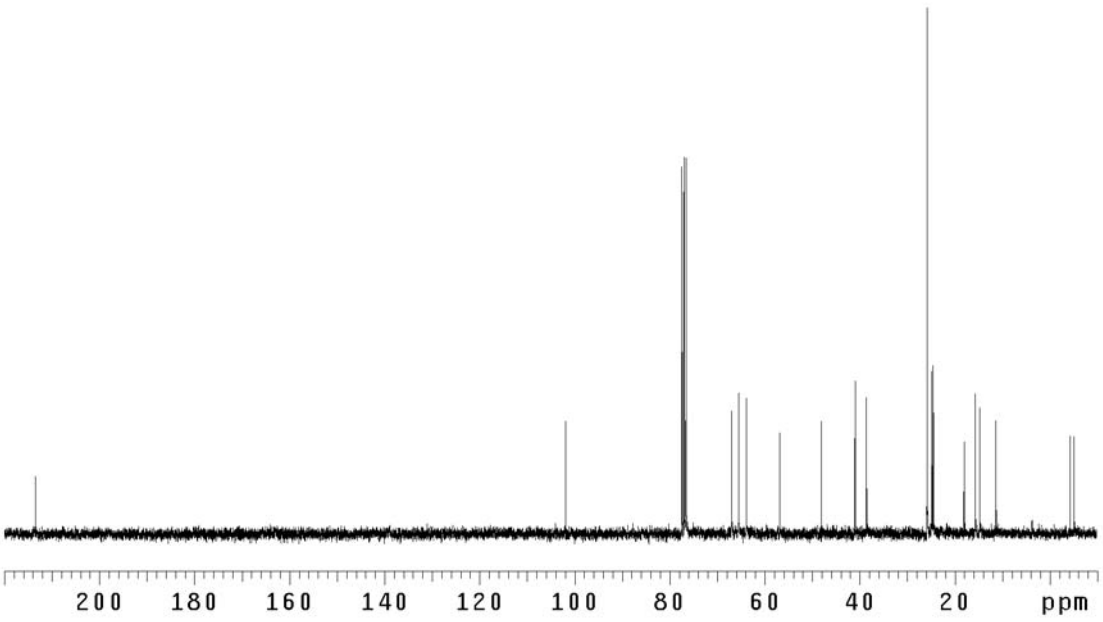

Figure A5.63 ^{13}C NMR of compound **233b** (75 MHz, $CDCl_3$)

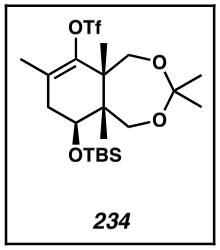

234

Figure A5.64 ^{1}H NMR of compound **234** (300 MHz, C_6D_6)

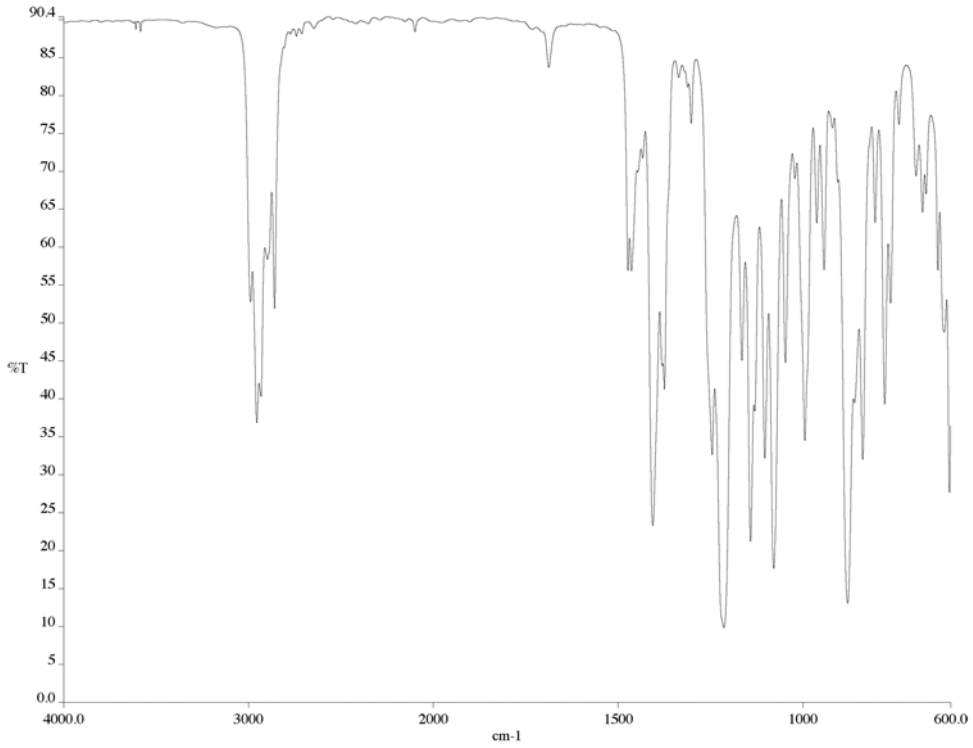

Figure A5.65 IR of compound **234** (NaCl/film)

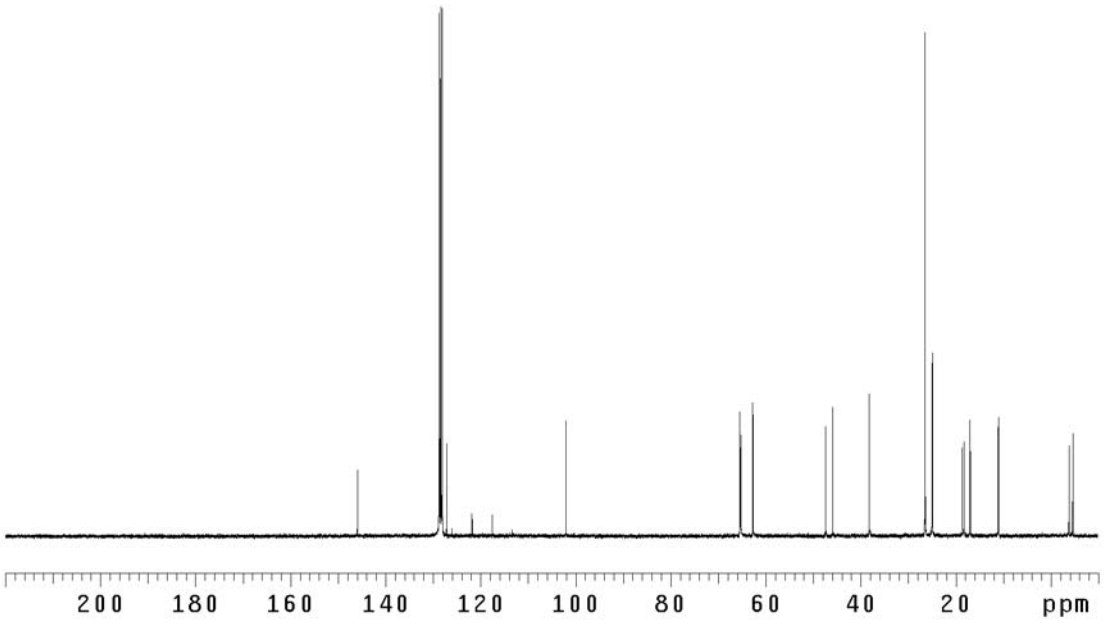

Figure A5.66 ^{13}C NMR of compound **234** (75 MHz, C_6D_6)

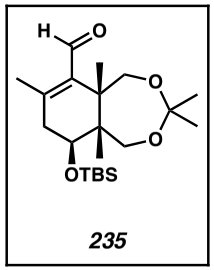

235

Figure A5.67 ^{1}H NMR of compound **235** (300 MHz, $CDCl_3$)

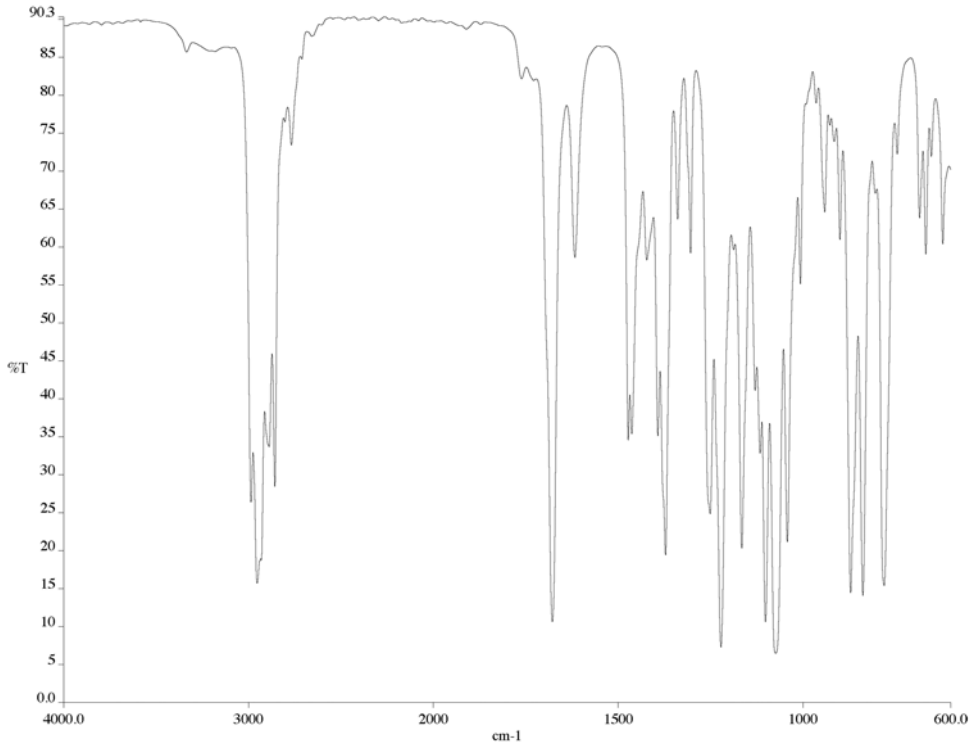

Figure A5.68 IR of compound **235** (NaCl/film)

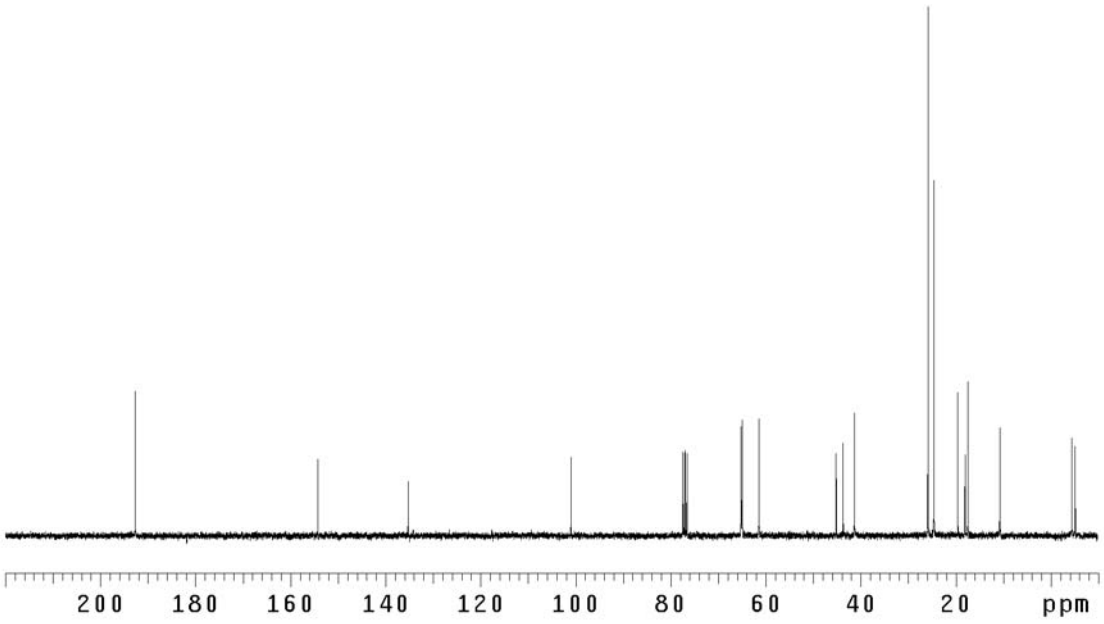

Figure A5.69 ^{13}C NMR of compound **235** (75 MHz, $CDCl_3$)

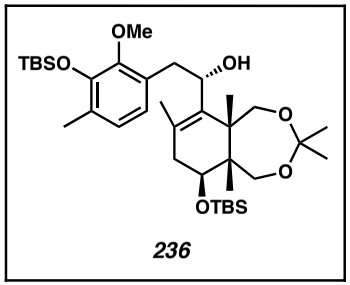

236

Figure A5.70 ^{1}H NMR of compound **236** (300 MHz, $CDCl_3$)

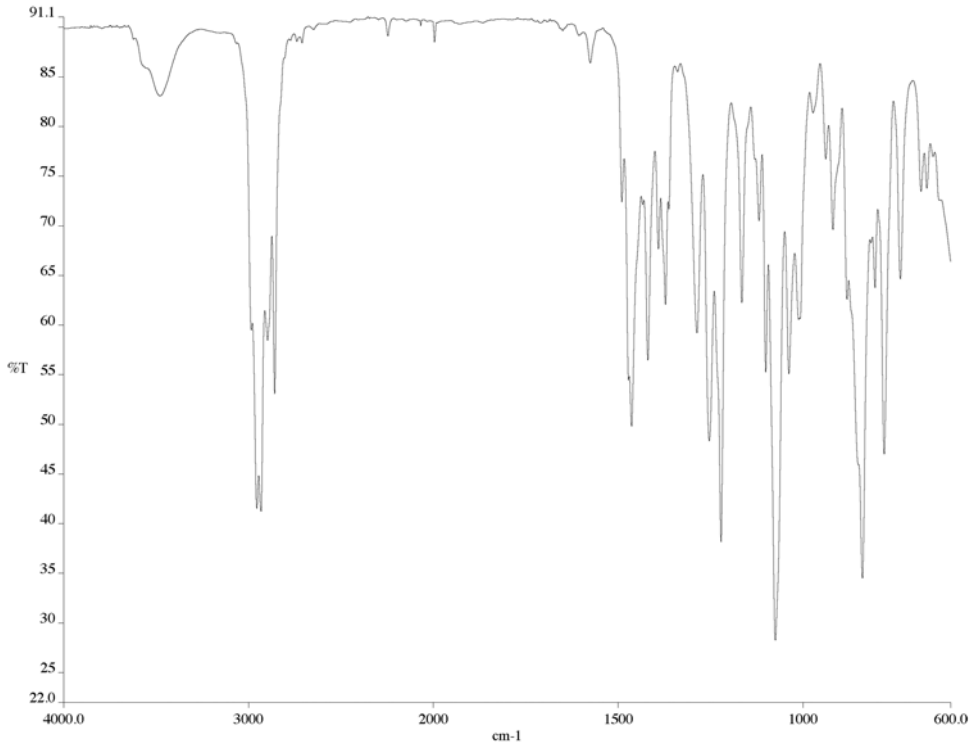

Figure A5.71 IR of compound **236** (NaCl/film)

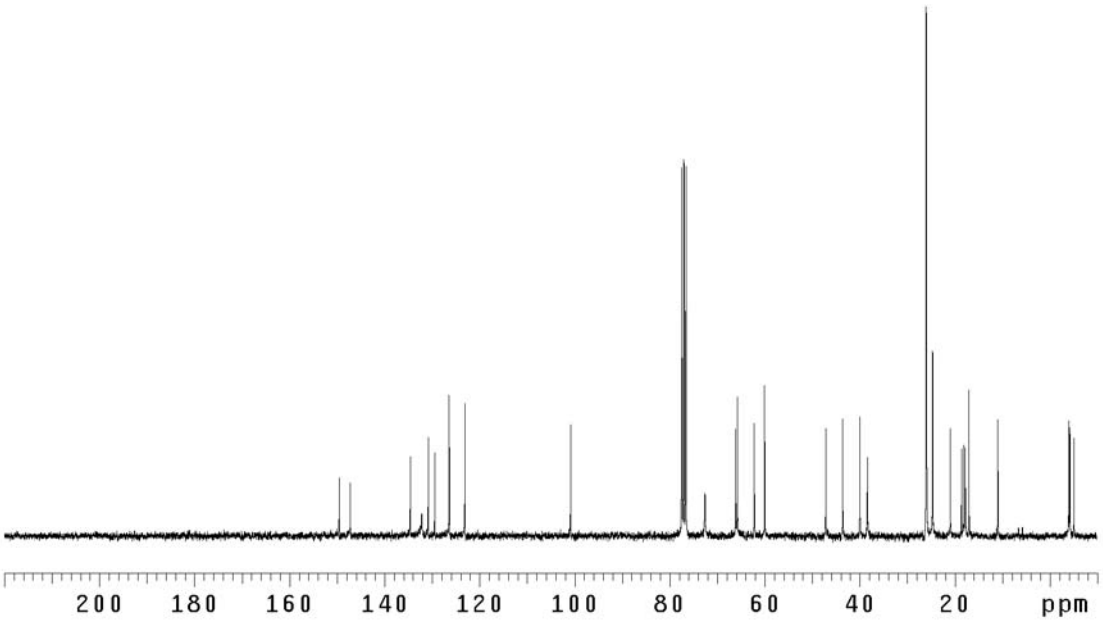

Figure A5.72 ^{13}C NMR of compound **236** (75 MHz, $CDCl_3$)

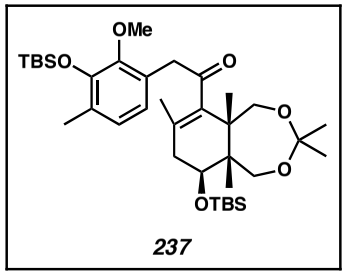

237

Figure A5.73 ^{1}H NMR of compound **237** (300 MHz, $CDCl_3$)

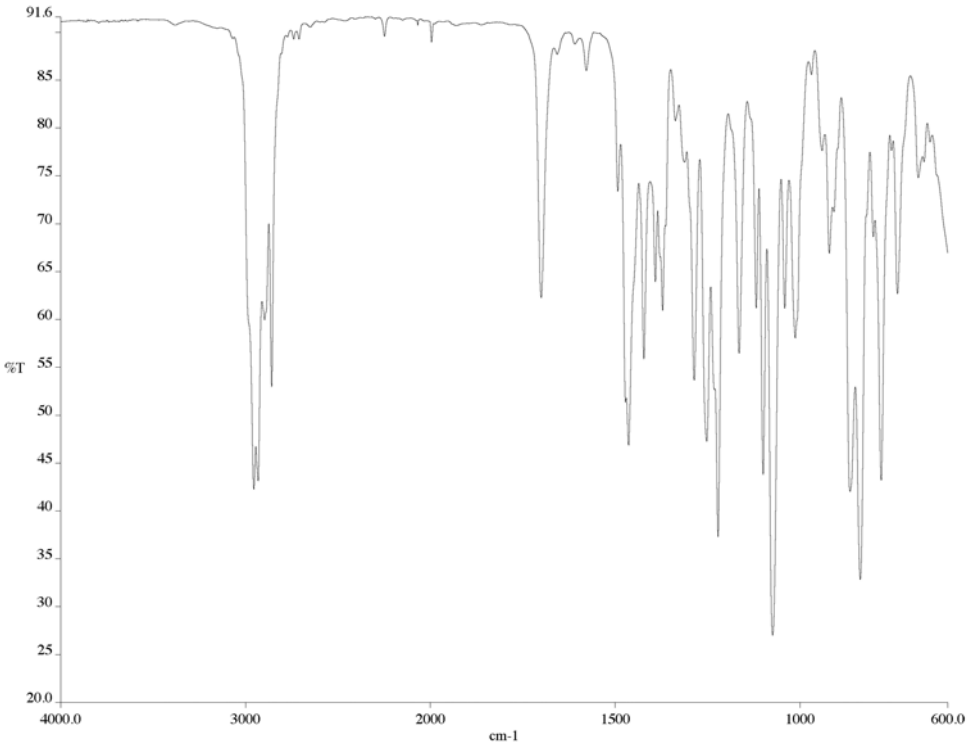

Figure A5.74 IR of compound **237** (NaCl/film)

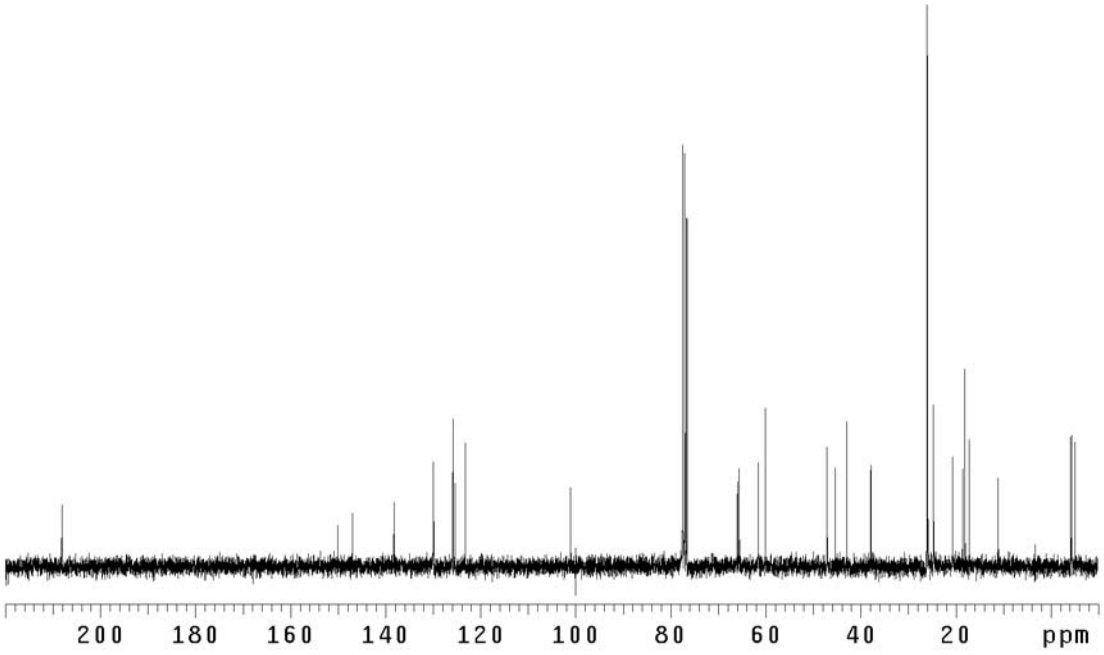

Figure A5.75 ^{13}C NMR of compound **237** (75 MHz, $CDCl_3$)

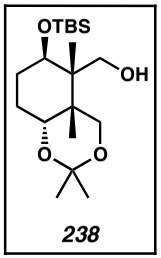

Figure A5.76 ^{1}H NMR of compound **238** (500 MHz, $CDCl_3$)

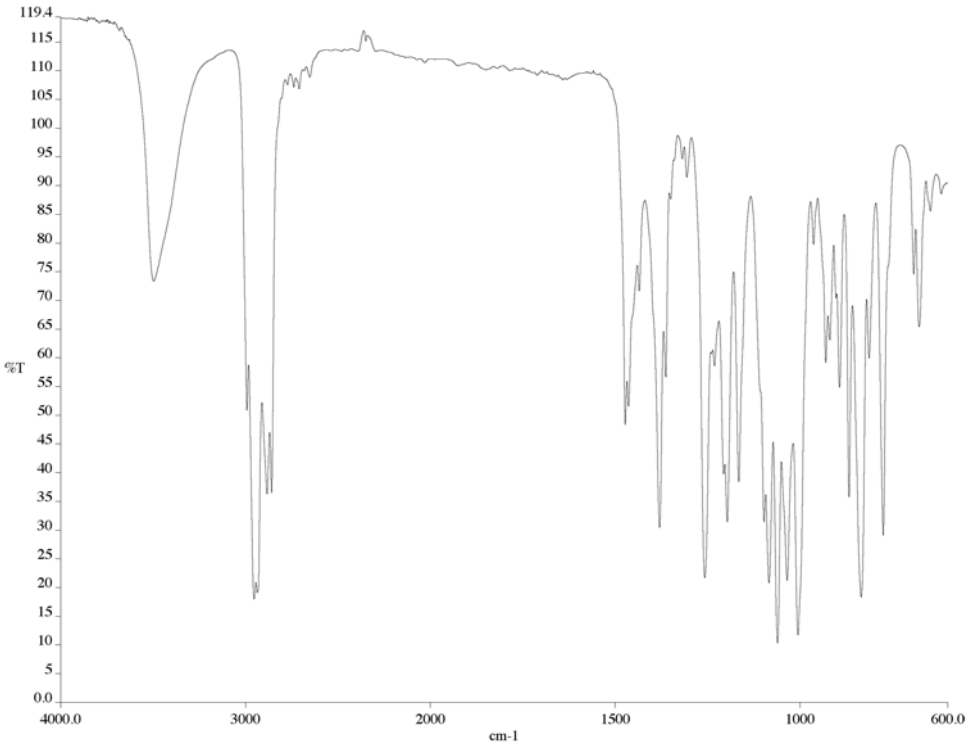

Figure A5.77 IR of compound **238** (NaCl/film)

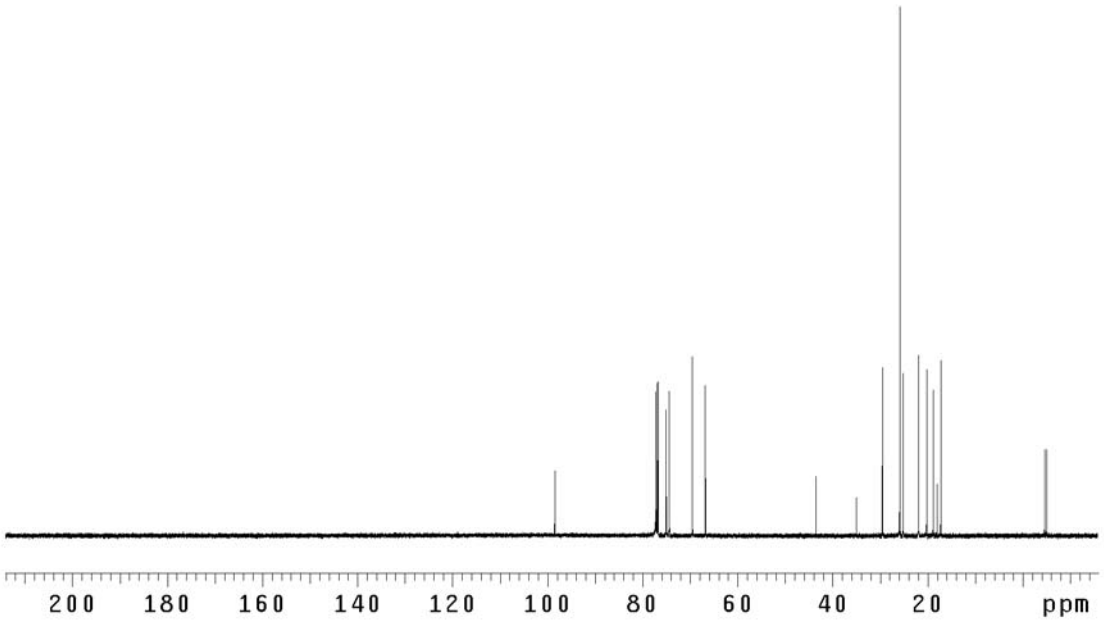

Figure A5.78 ^{13}C NMR of compound **238** (125 MHz, $CDCl_3$)

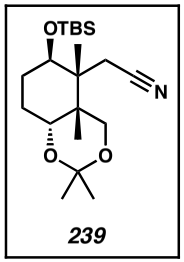

Figure A5.79 ^{1}H NMR of compound **239** (300 MHz, $CDCl_3$)

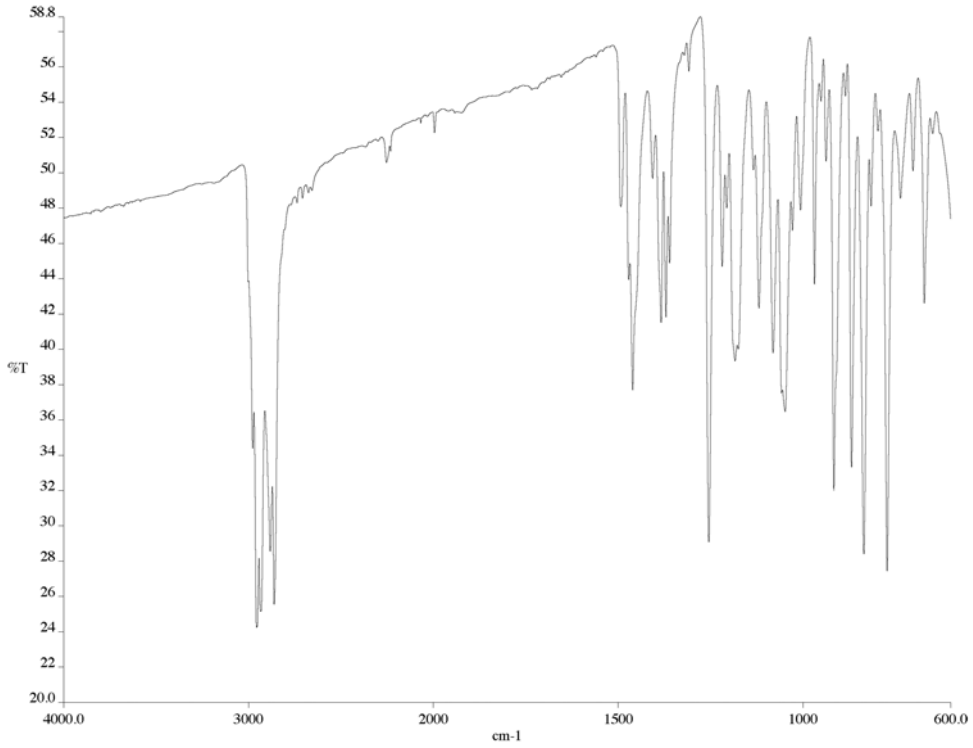

Figure A5.80 IR of compound **239** (NaCl/film)

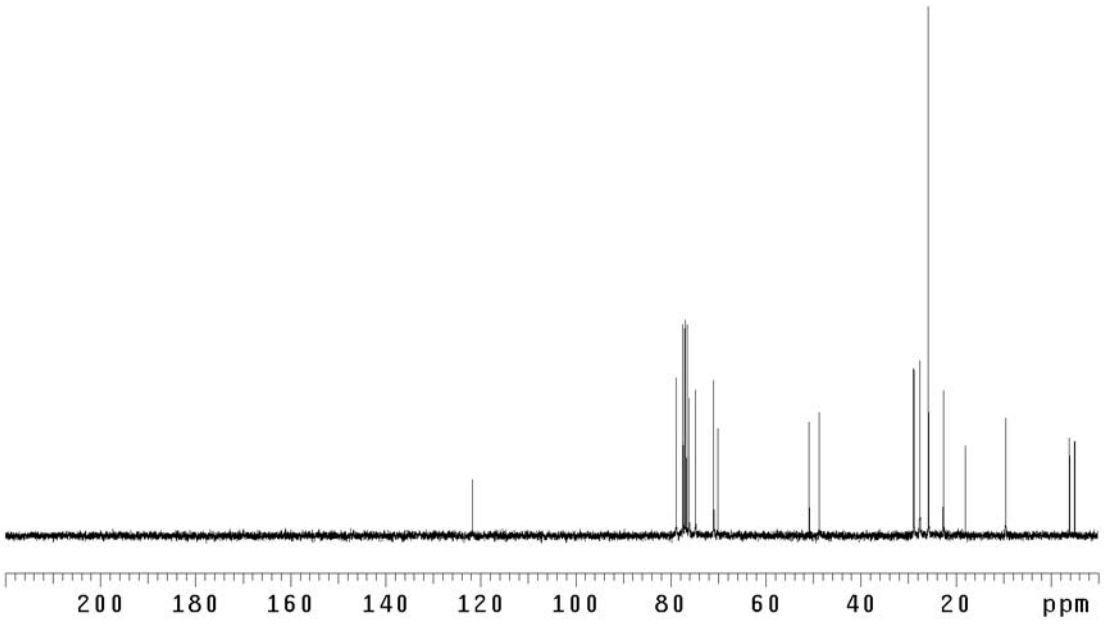

Figure A5.81 ^{13}C NMR of compound **239** (75 MHz, $CDCl_3$)

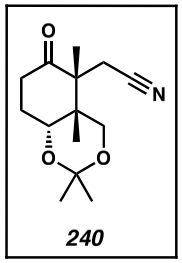

Figure A5.82 ^{1}H NMR of compound **240** (300 MHz, $CDCl_3$)

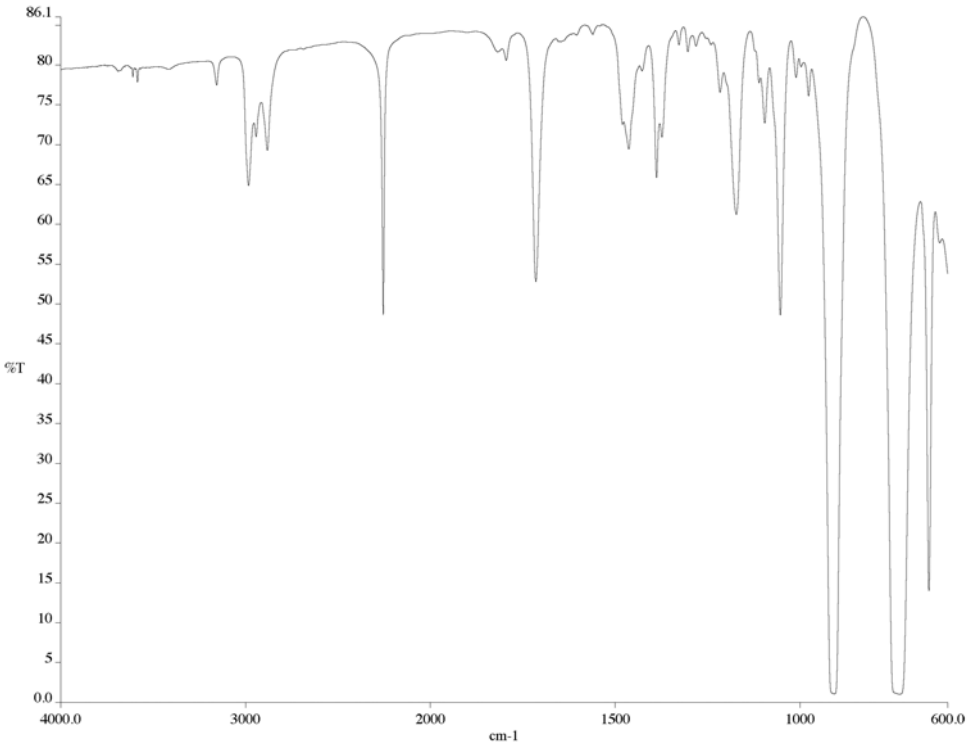

Figure A5.83 IR of compound **240** (NaCl/film)

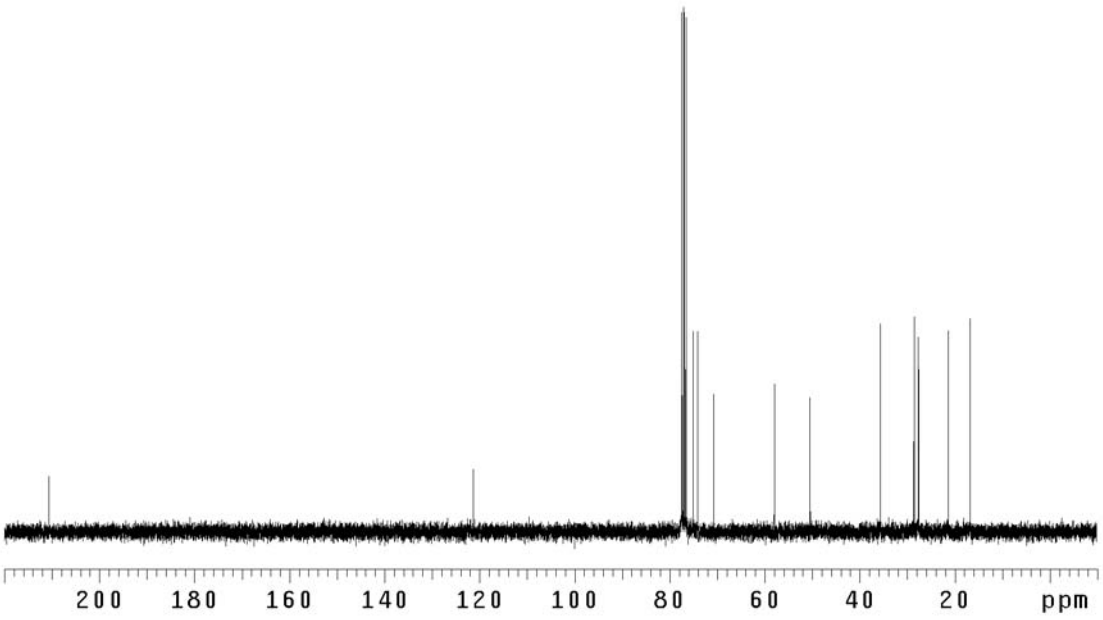

Figure A5.84 ^{13}C NMR of compound **240** (75 MHz, $CDCl_3$)

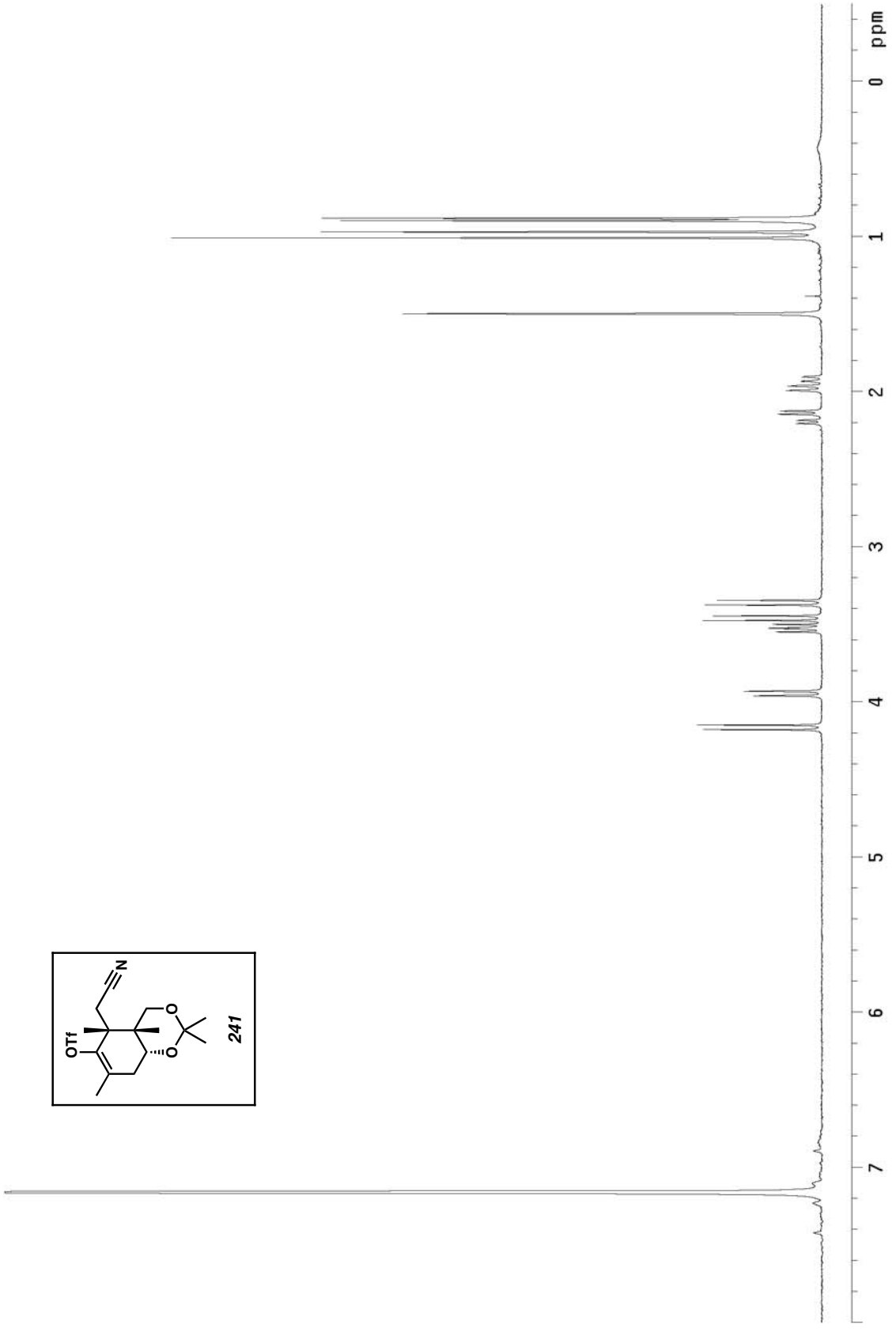

Figure A5.85 ^{1}H NMR of compound **241** (300 MHz, C_6D_6)

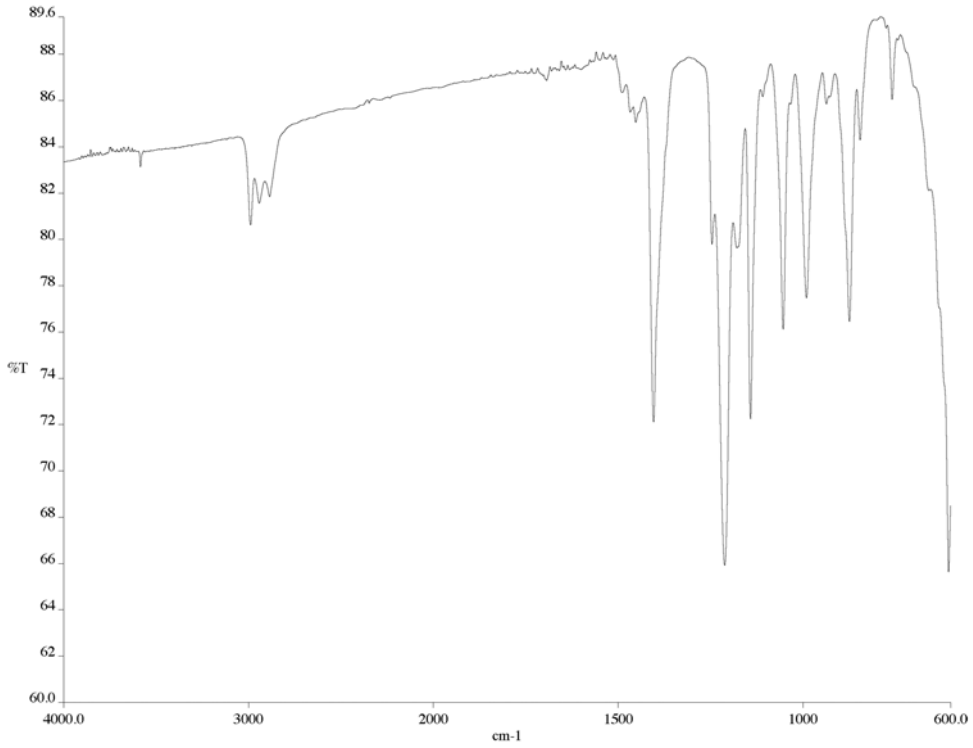

Figure A5.86 IR of compound **241** (NaCl/film)

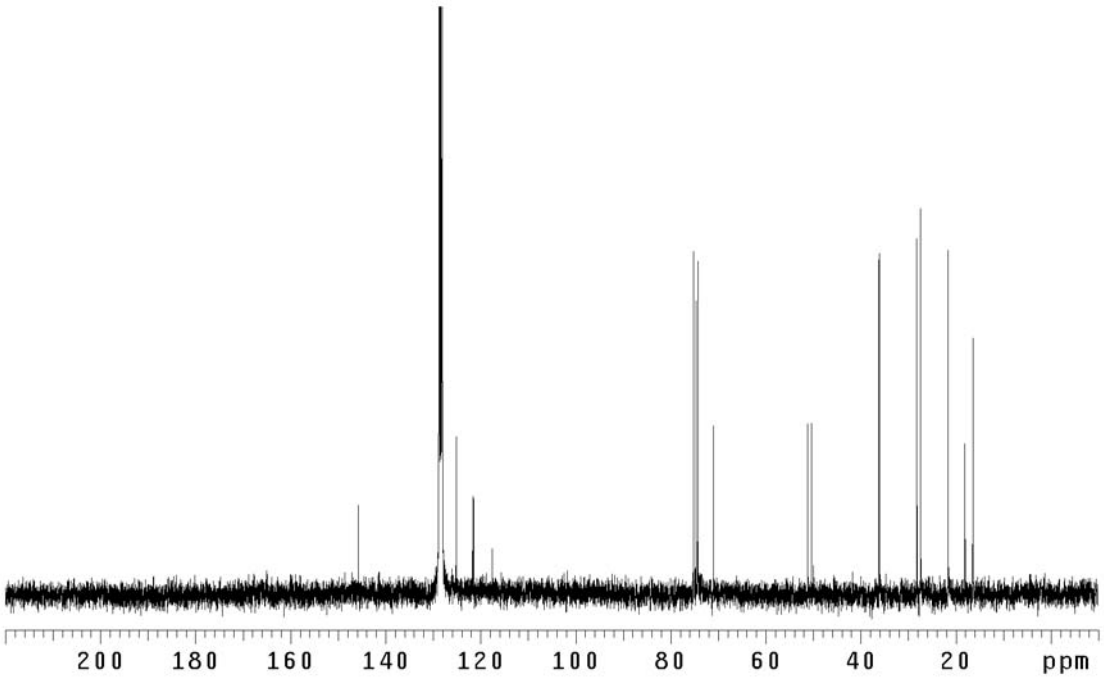

Figure A5.87 ^{13}C NMR of compound **241** (75 MHz, C_6D_6)

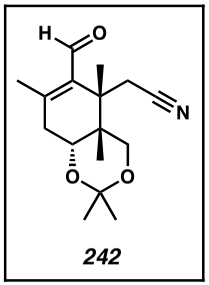

Figure A5.88 ^{1}H NMR of compound **242** (300 MHz, $CDCl_3$)

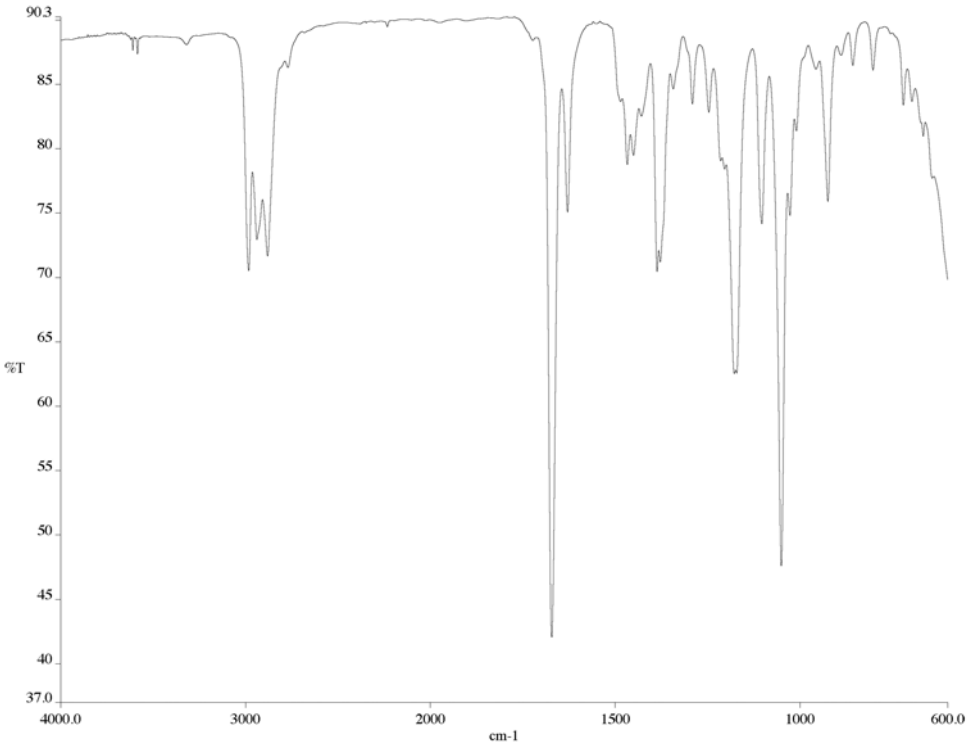

Figure A5.89 IR of compound **242** (NaCl/film)

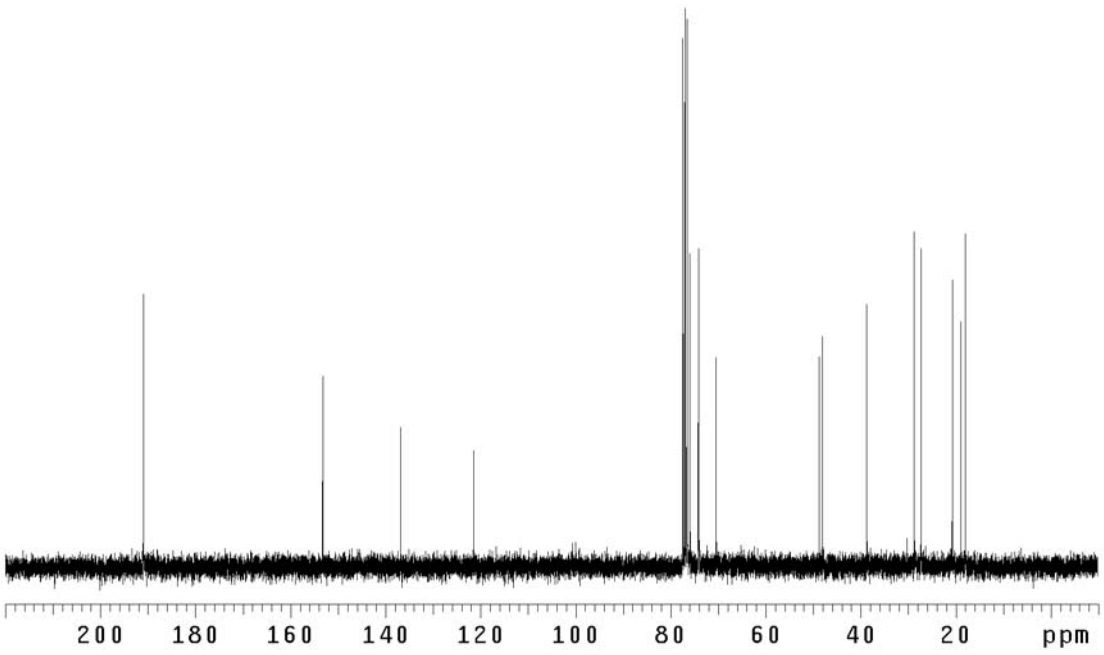

Figure A5.90 ^{13}C NMR of compound **242** (75 MHz, $CDCl_3$)

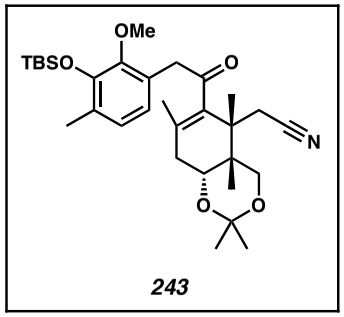

Figure A5.91 ^{1}H NMR of compound **243** (300 MHz, $CDCl_3$)

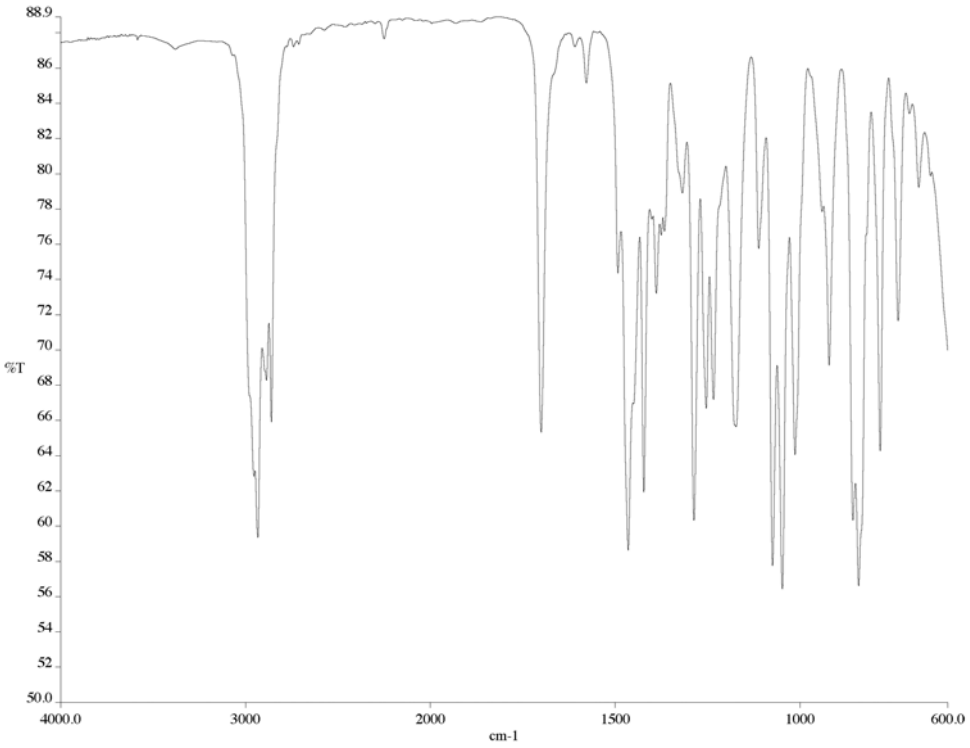

Figure A5.92 IR of compound **243** (NaCl/film)

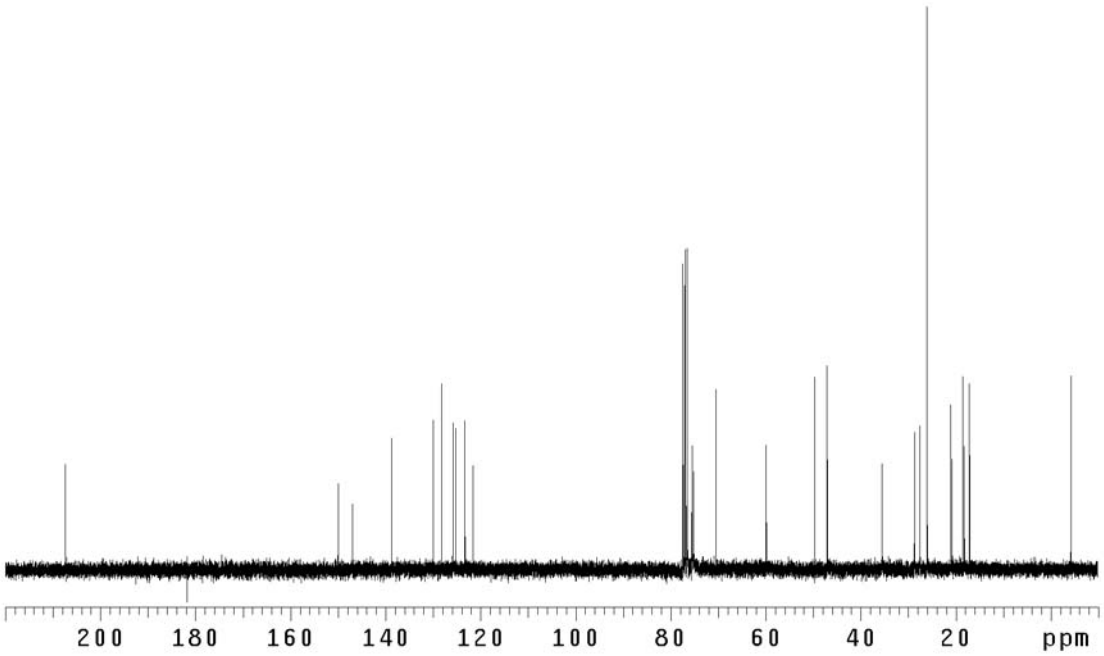

Figure A5.93 ^{13}C NMR of compound **243** (75 MHz, $CDCl_3$)

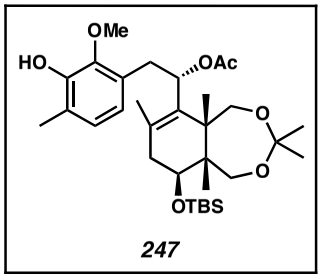

Figure A5.94 ^{1}H NMR of compound **247** (300 MHz, $CDCl_3$)

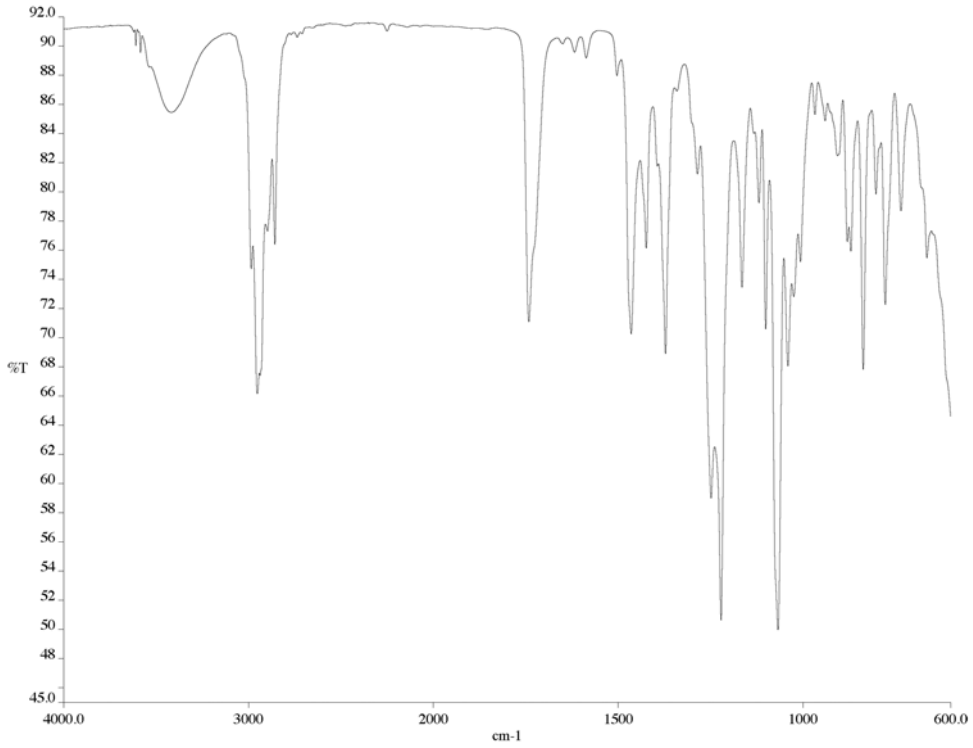

Figure A5.95 IR of compound **247** (NaCl/film)

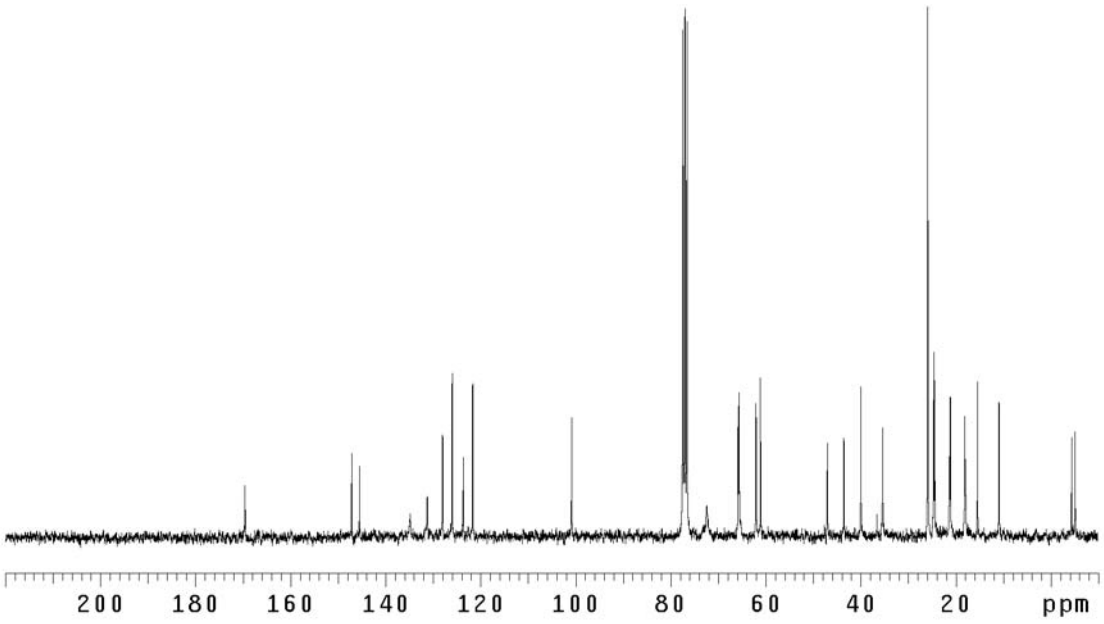

Figure A5.96 ^{13}C NMR of compound **247** (75 MHz, $CDCl_3$)

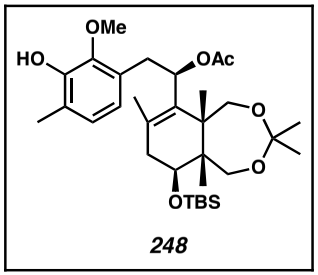

Figure A5.97 ^{1}H NMR of compound **248** (300 MHz, $CDCl_3$)

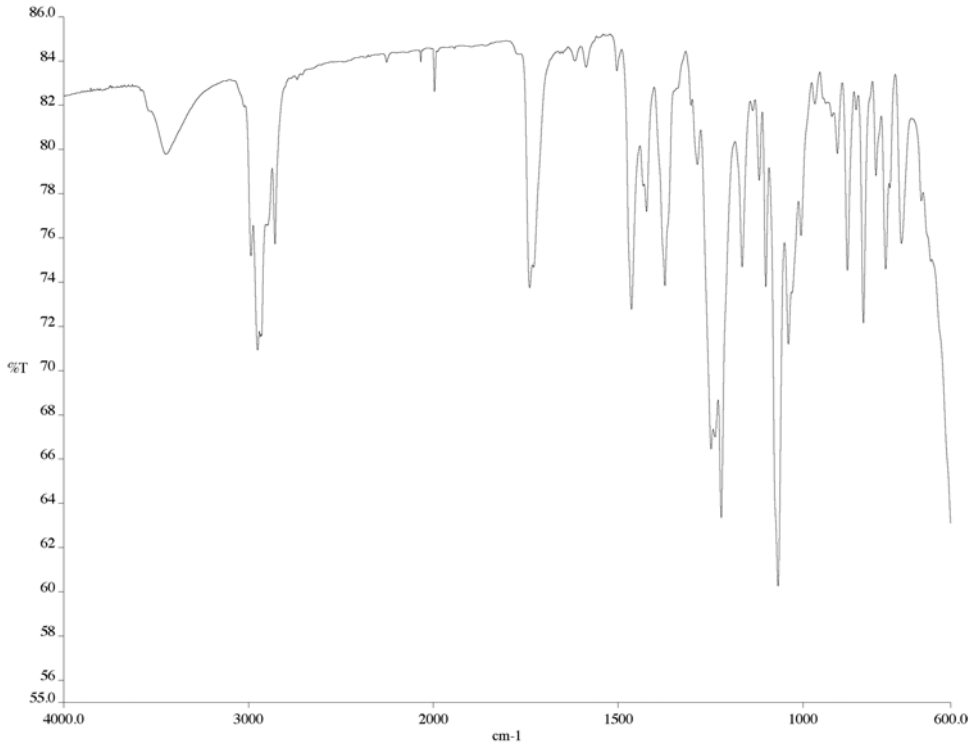

Figure A5.98 IR of compound **248** (NaCl/film)

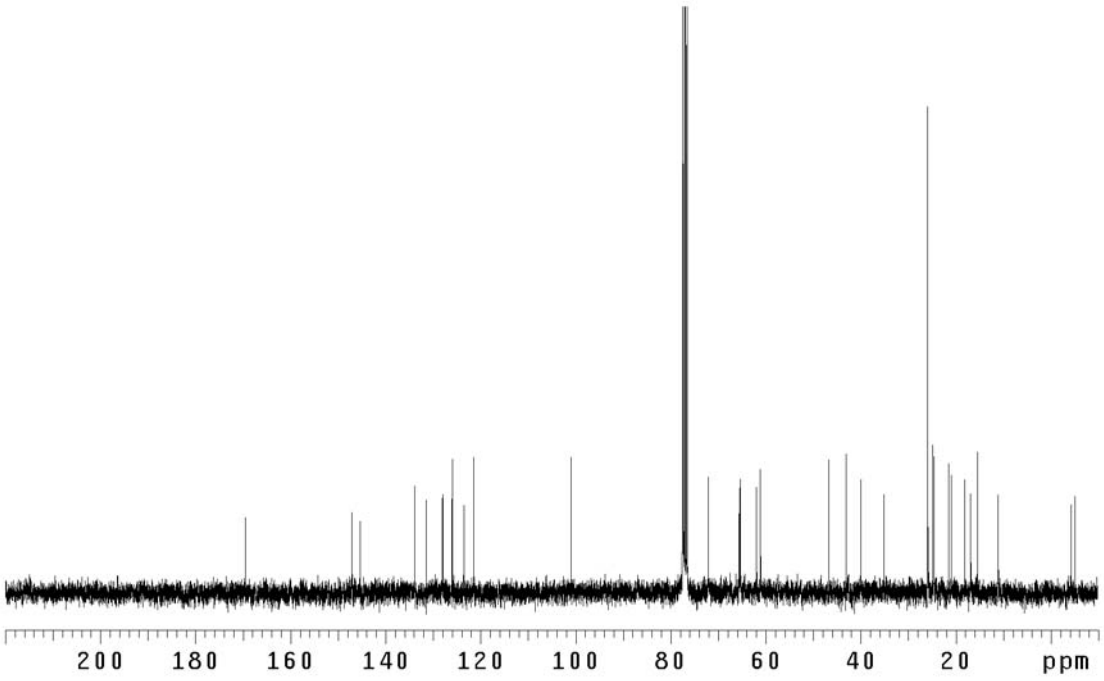

Figure A5.99 ^{13}C NMR of compound **248** (75 MHz, $CDCl_3$)

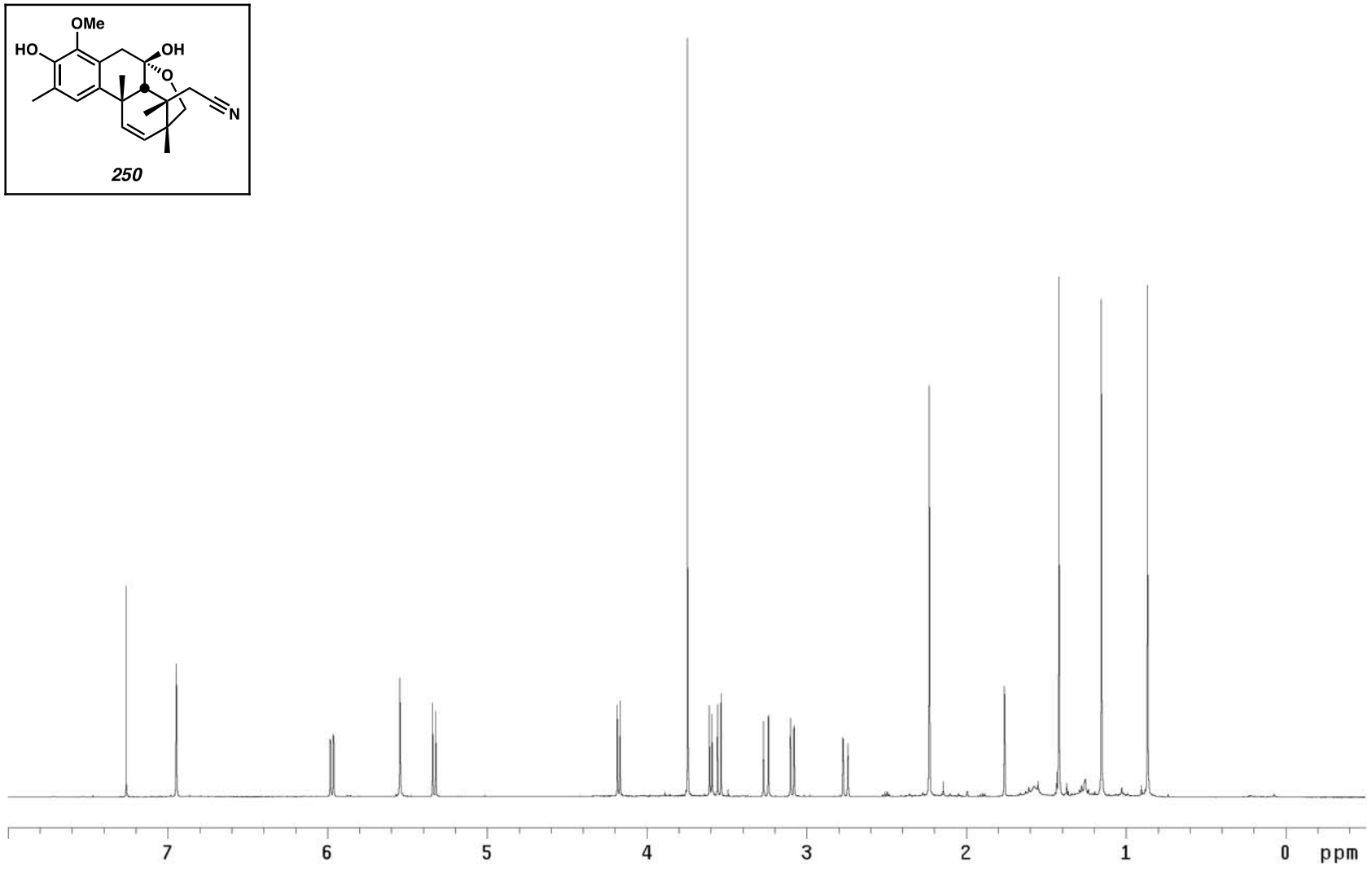

Figure A5.100 ^{1}H NMR of compound **250** (500 MHz, $CDCl_3$)

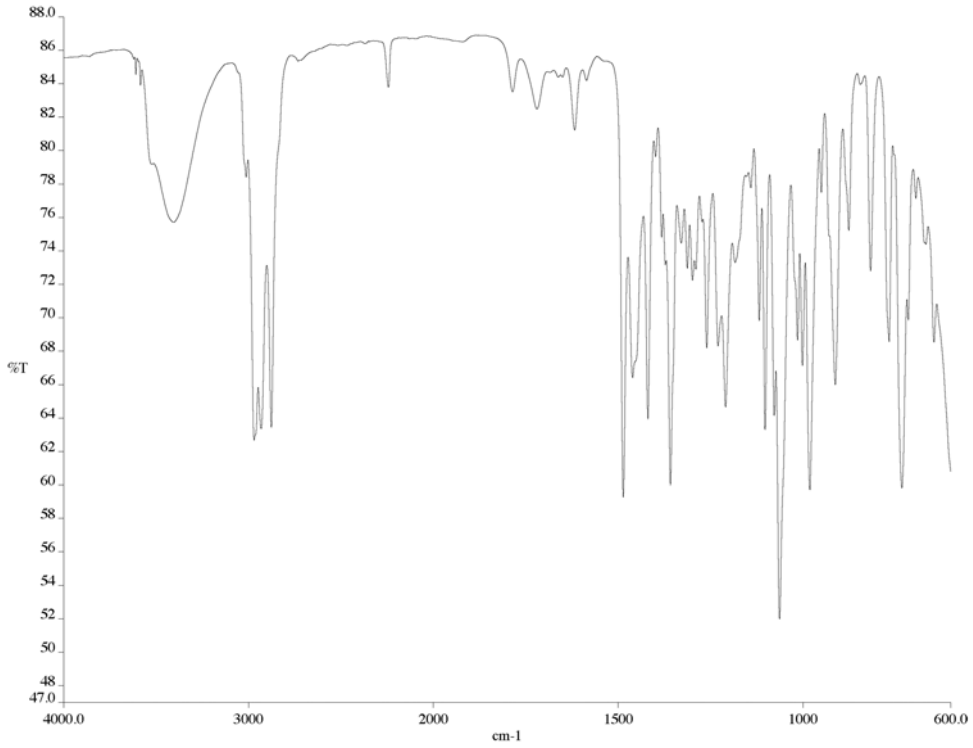

Figure A5.101 IR of compound **250** (NaCl/film)

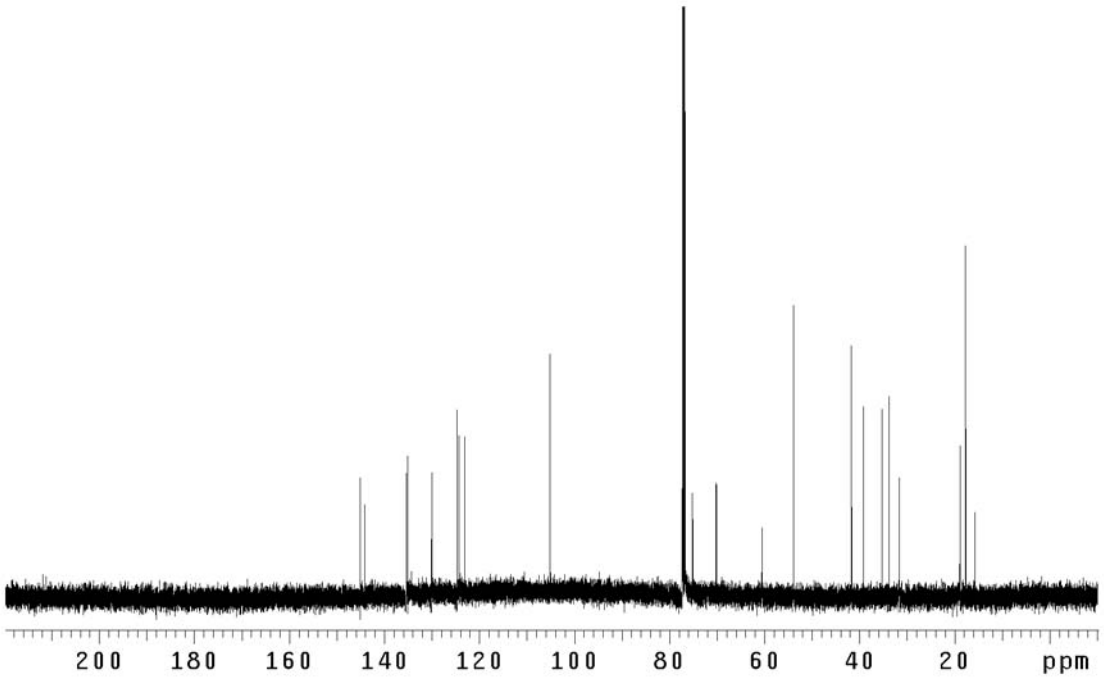

Figure A5.102 ^{13}C NMR of compound **250** (125 MHz, $CDCl_3$)

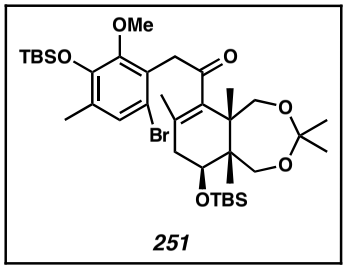

Figure A5.103 ^{1}H NMR of compound **251** (300 MHz, $CDCl_3$)

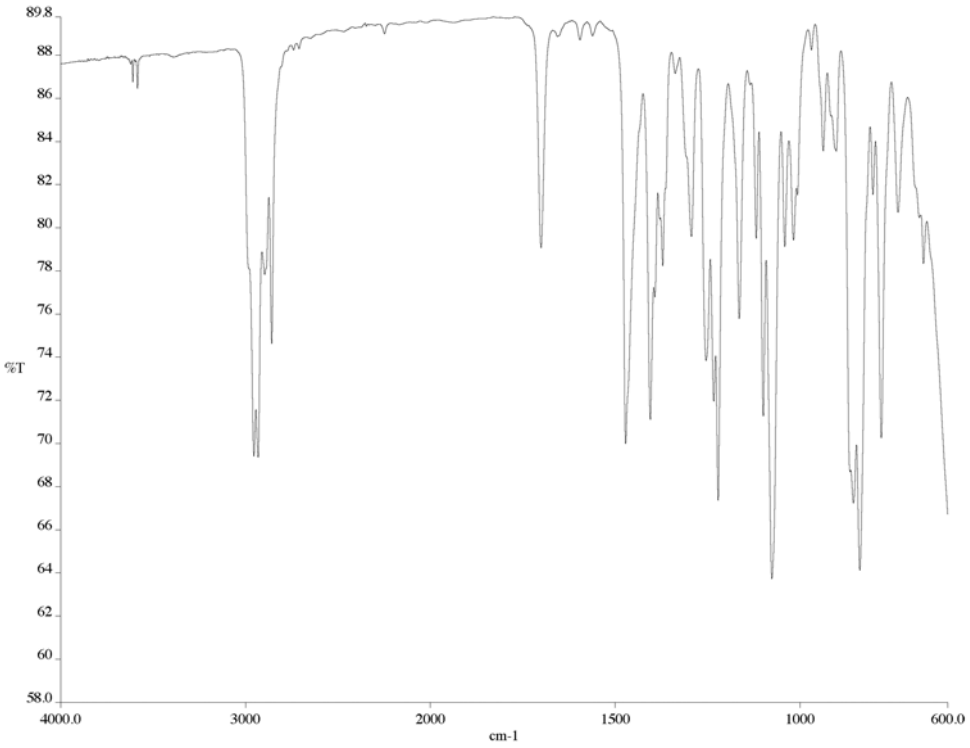

Figure A5.104 IR of compound **251** (NaCl/film)

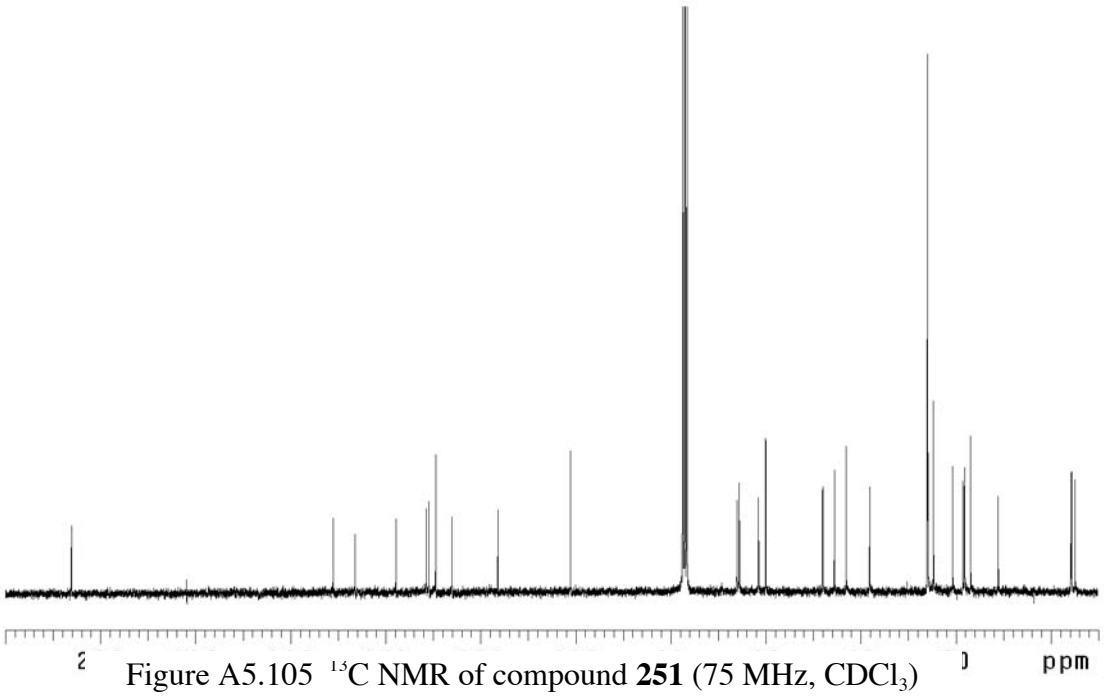

Figure A5.105 ^{13}C NMR of compound **251** (75 MHz, $CDCl_3$)

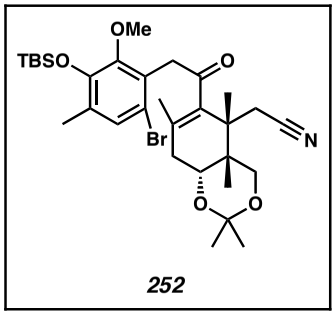

Figure A5.106 ^{1}H NMR of compound **252** (500 MHz, $CDCl_3$)

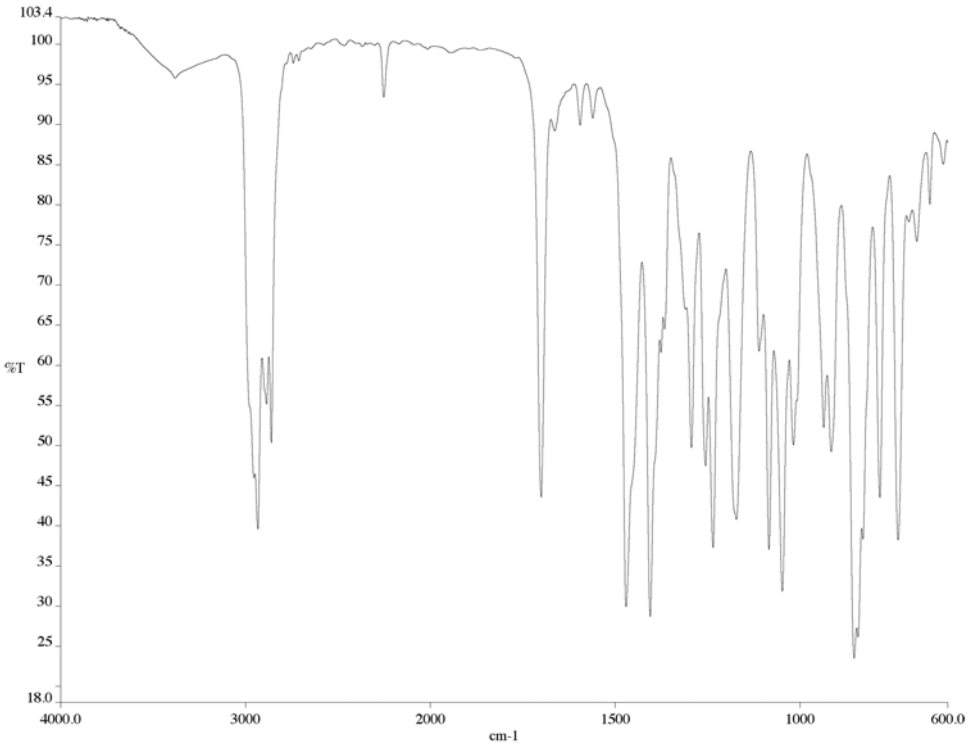

Figure A5.107 IR of compound **252** (NaCl/film)

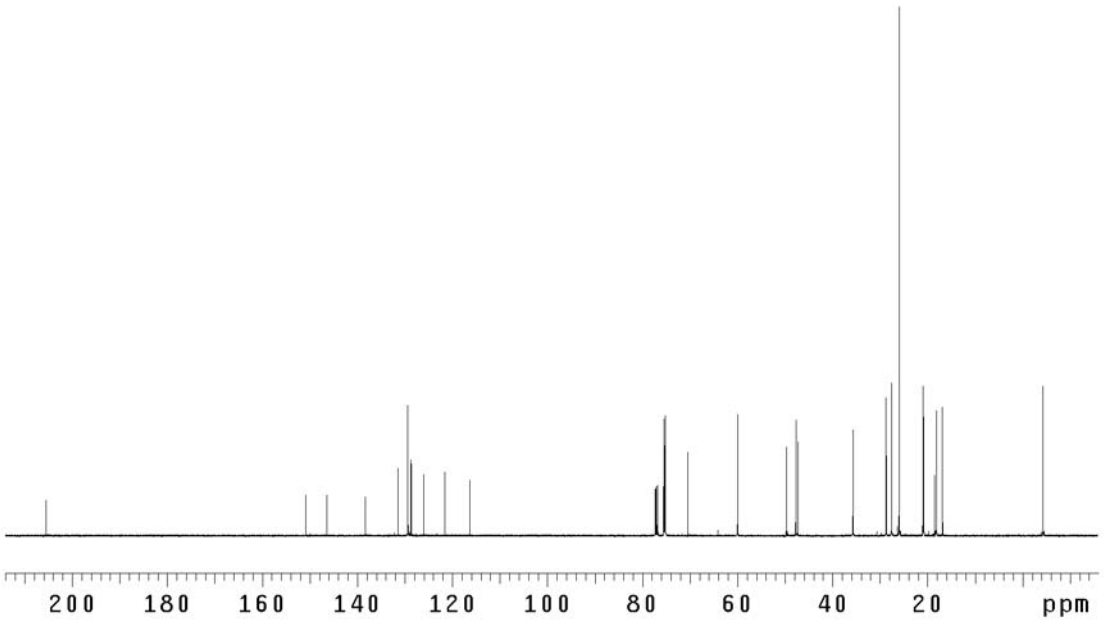

Figure A5.108 ^{13}C NMR of compound **252** (125 MHz, $CDCl_3$)

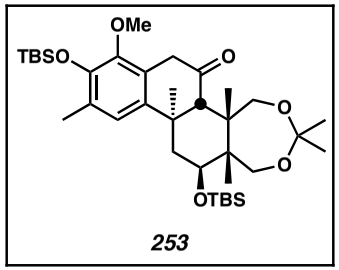

253

Figure A5.109 ^{1}H NMR of compound **253** (500 MHz, $CDCl_3$)

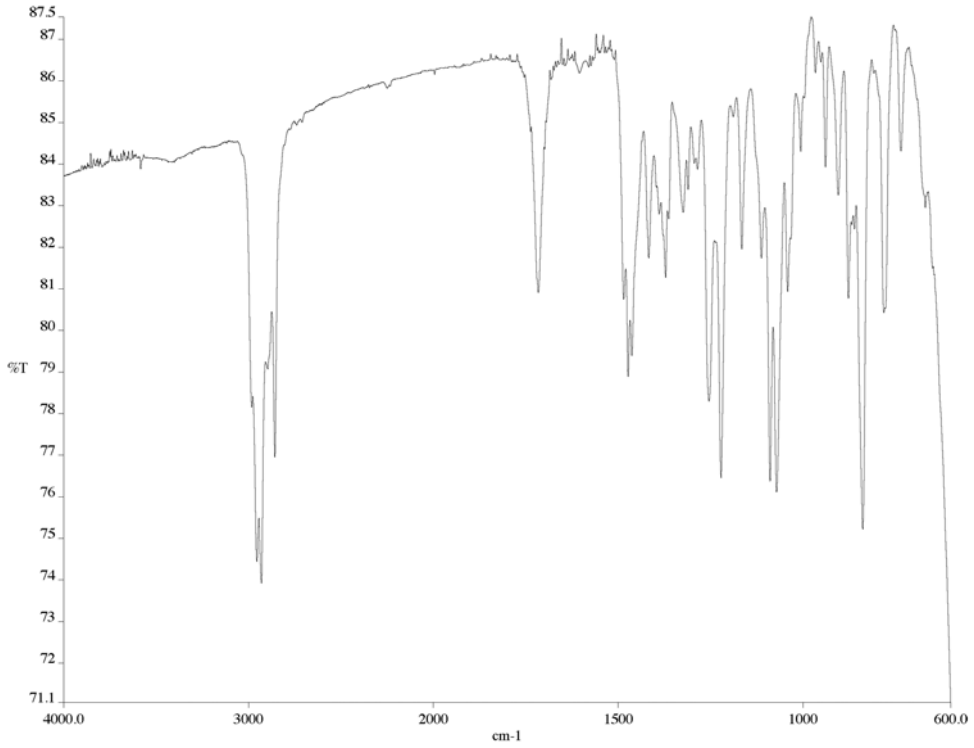

Figure A5.110 IR of compound **253** (NaCl/film)

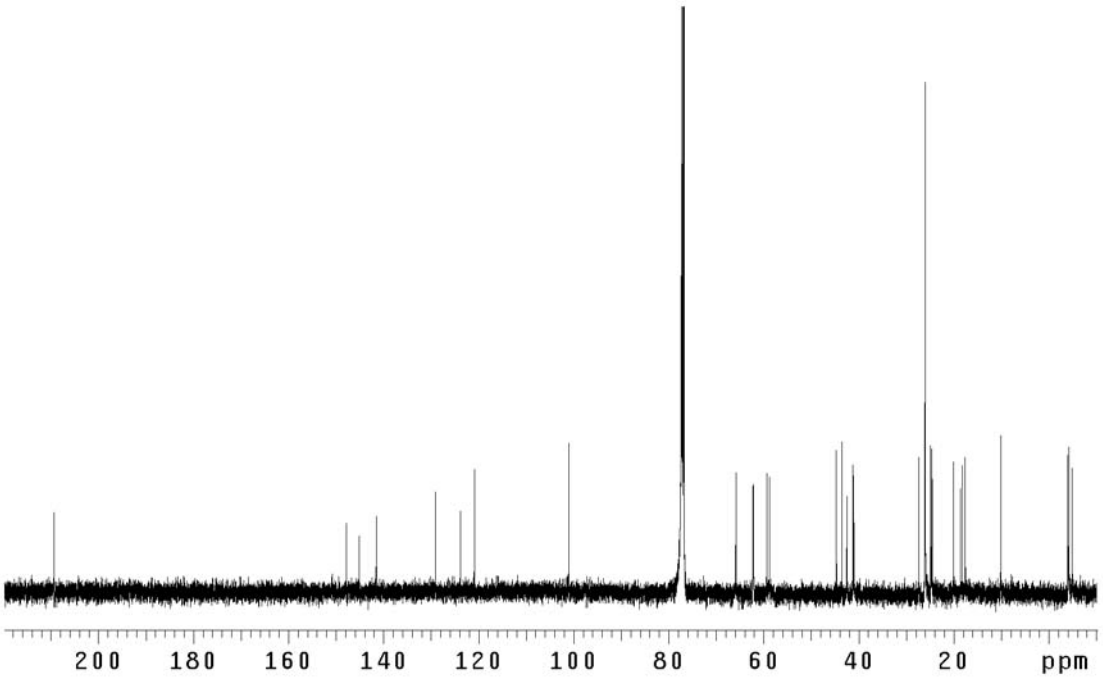

Figure A5.111 ^{13}C NMR of compound **253** (125 MHz, $CDCl_3$)

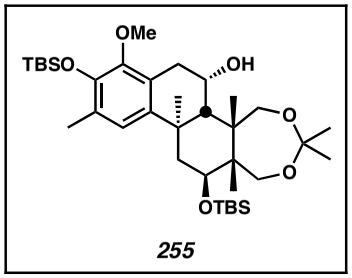

Figure A5.112 ^{1}H NMR of compound **255** (500 MHz, $CDCl_3$)

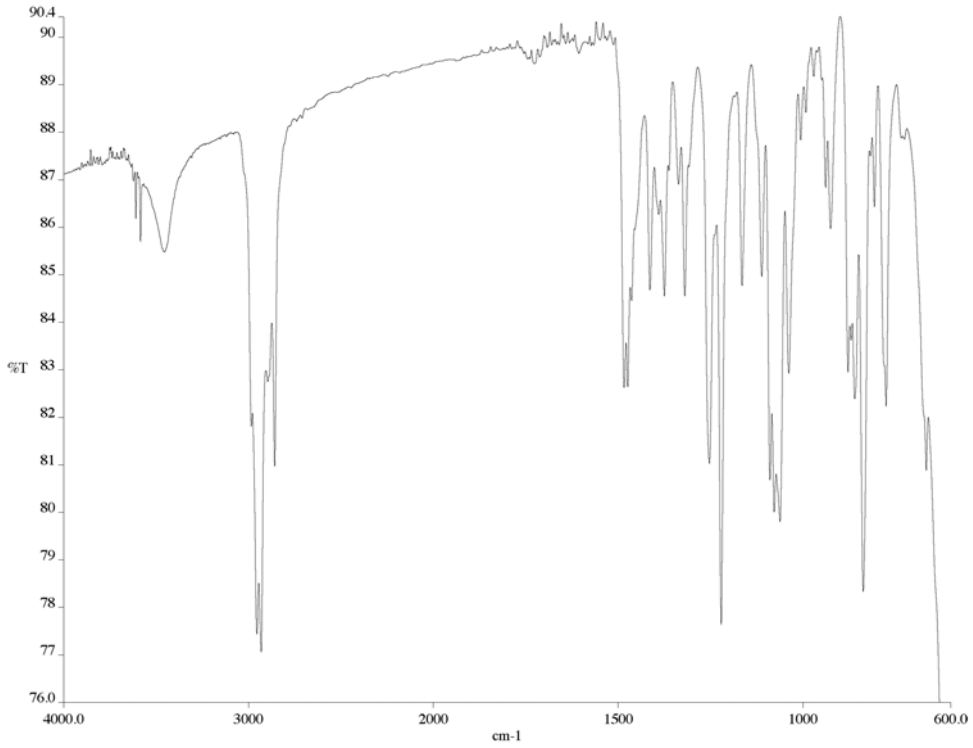

Figure A5.113 IR of compound **255** (NaCl/film)

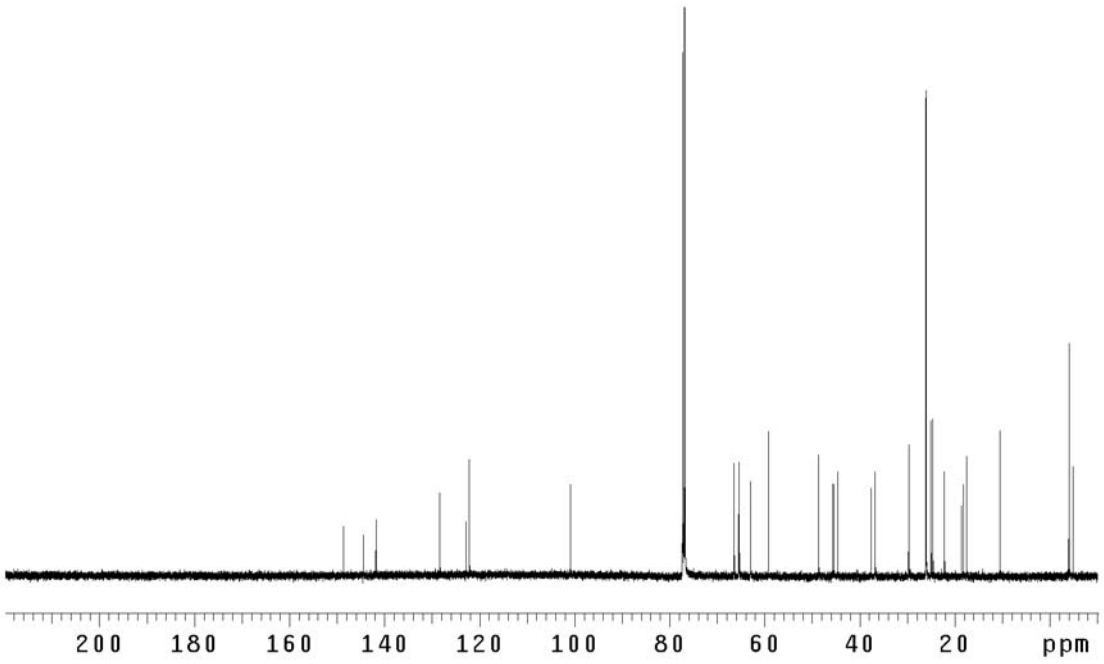

Figure A5.114 ^{13}C NMR of compound **255** (125 MHz, $CDCl_3$)

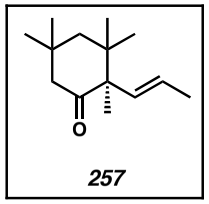

Figure A5.115 ^{1}H NMR of compound **257** (300 MHz, $CDCl_3$)

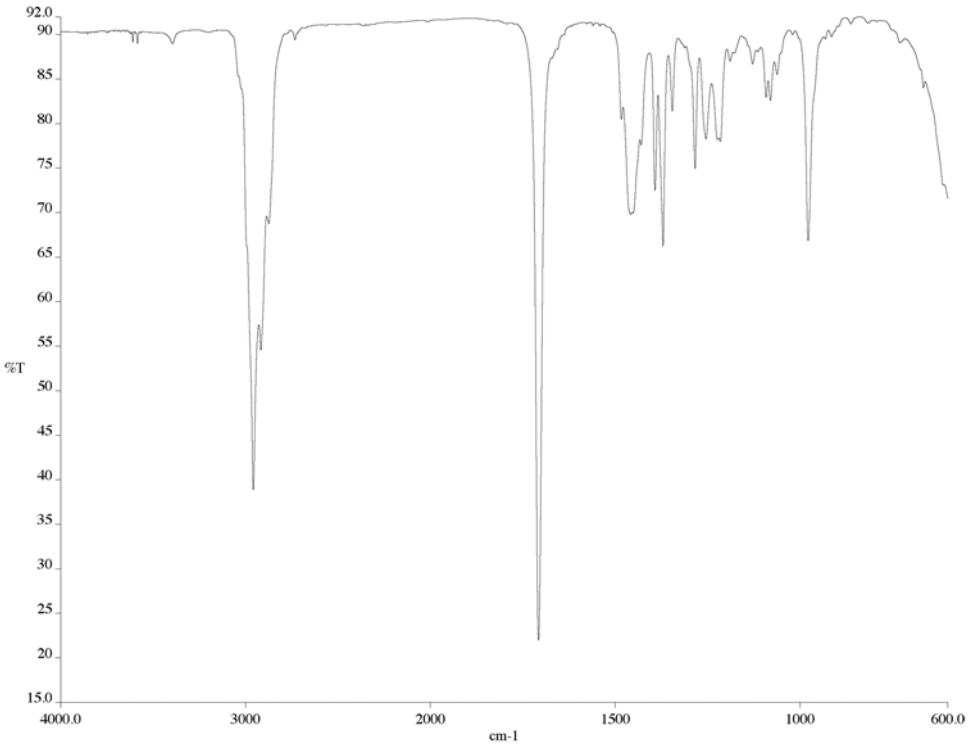

Figure A5.116 IR of compound ***257*** (NaCl/film)

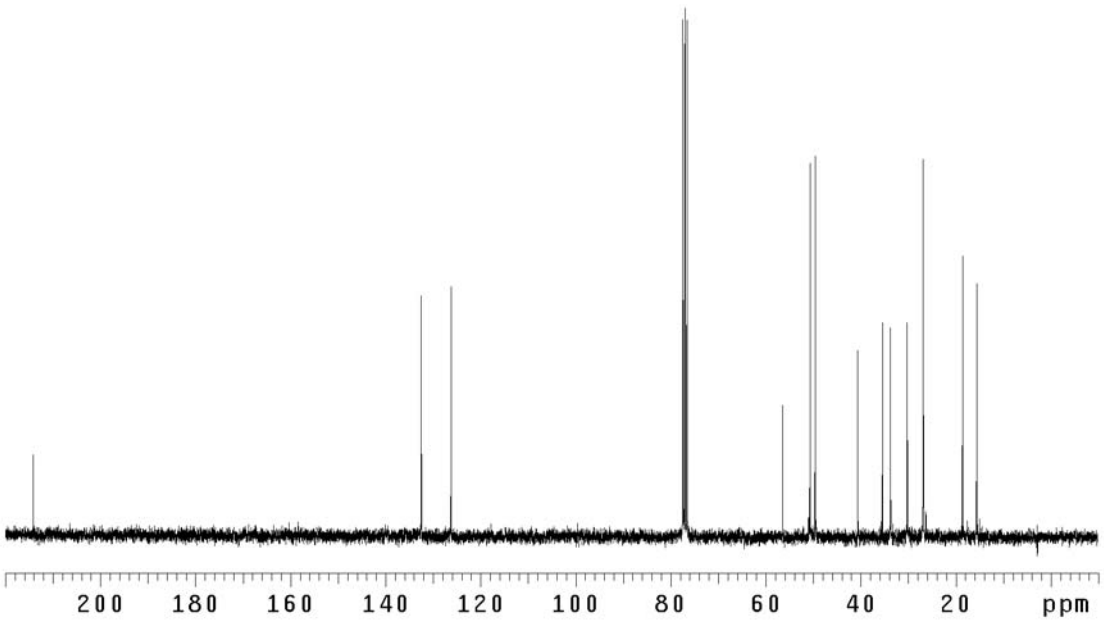

Figure A5.117 ^{13}C NMR of compound ***257*** (75 MHz, $CDCl_3$)

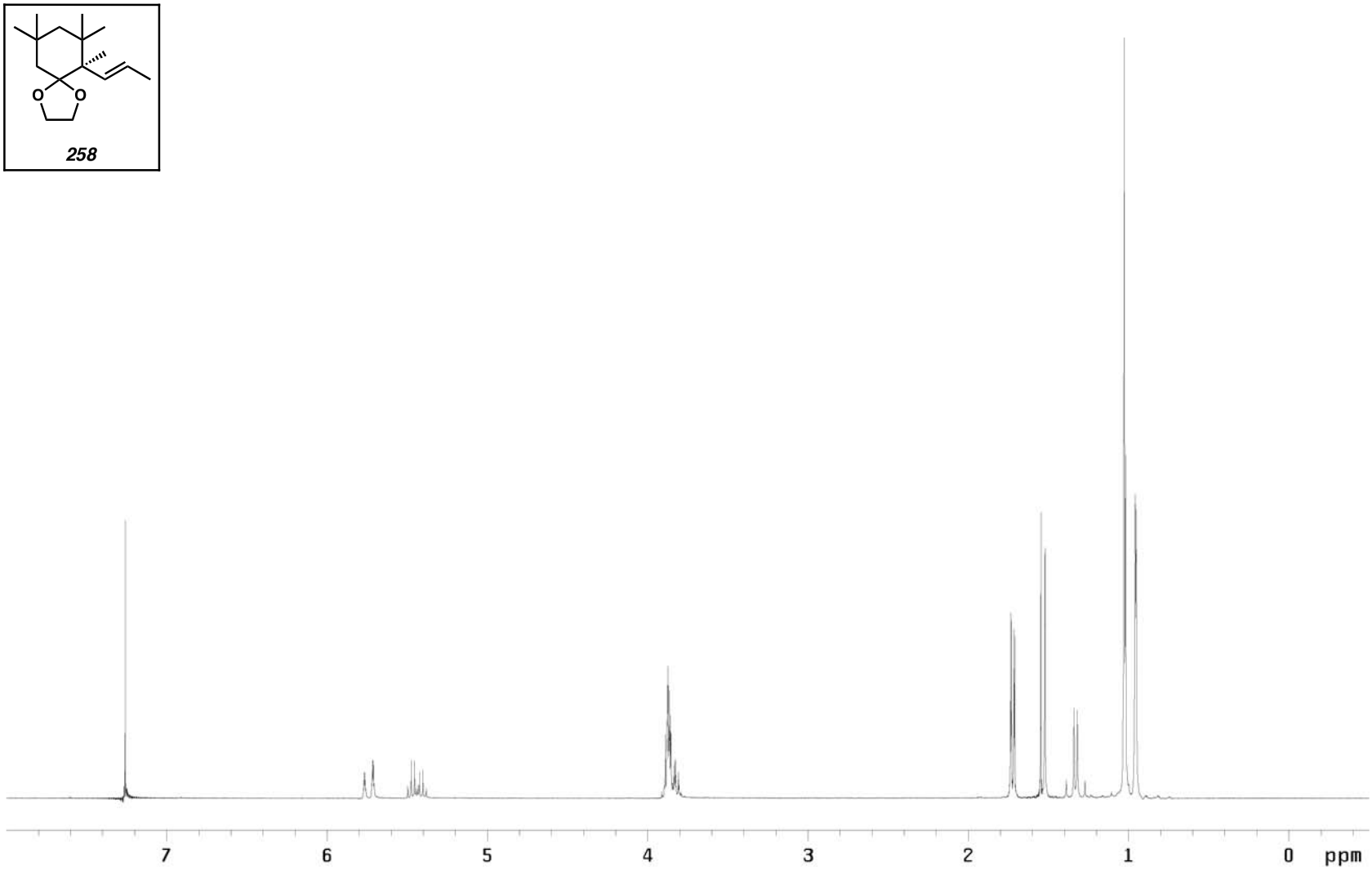

Figure A5.118 ^{1}H NMR of compound **258** (300 MHz, $CDCl_3$)

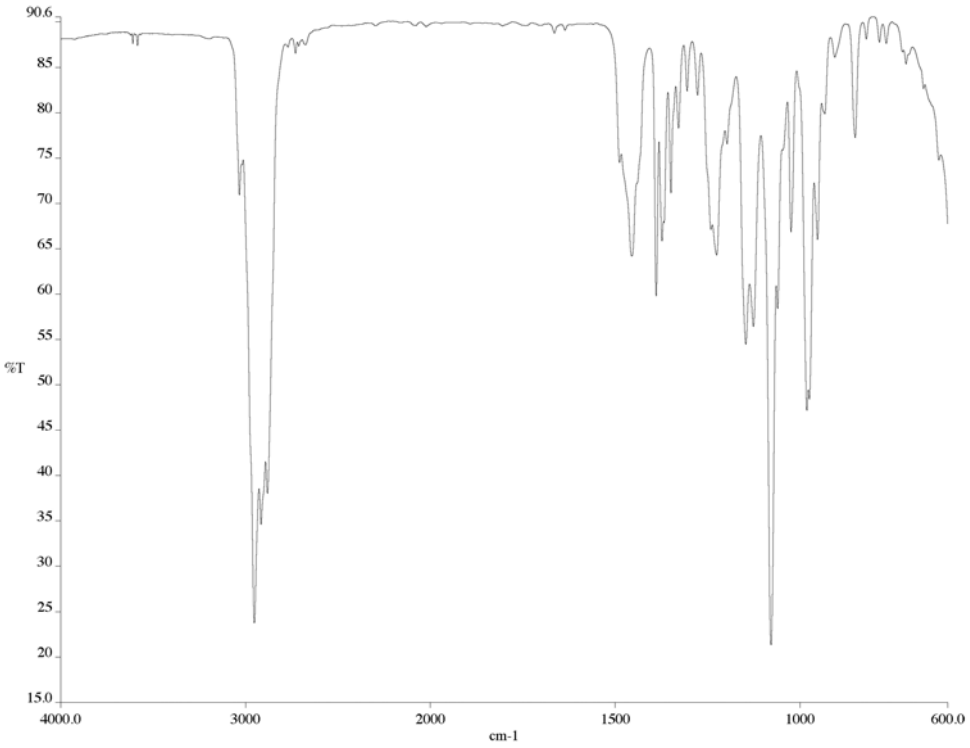

Figure A5.119 IR of compound **258** (NaCl/film)

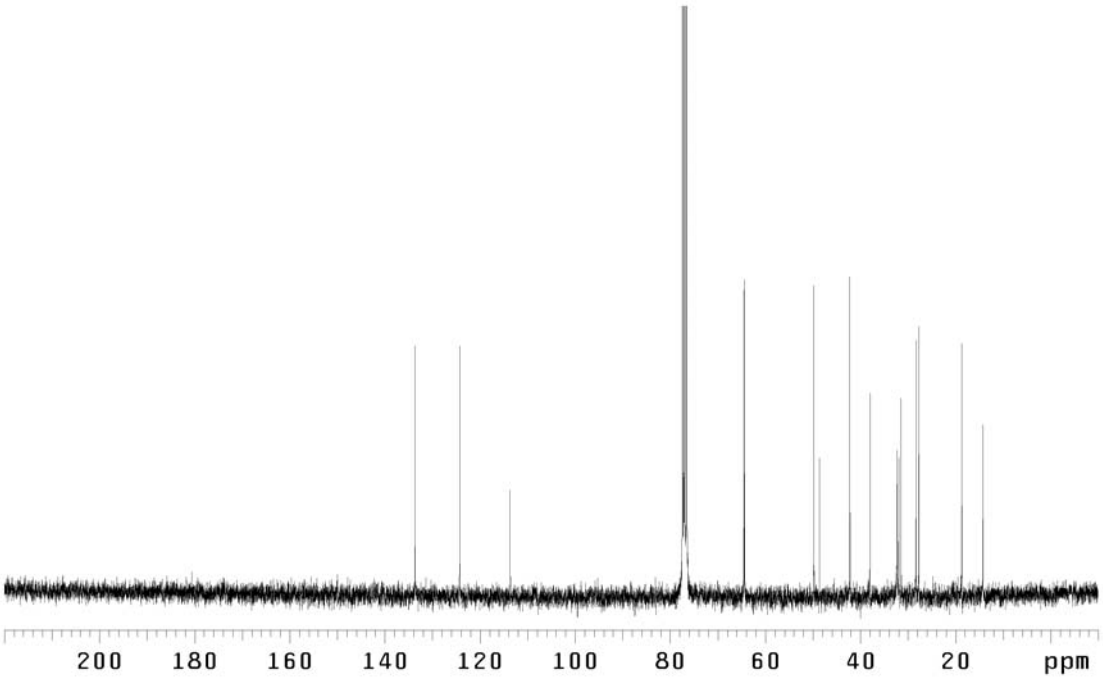

Figure A5.120 ^{13}C NMR of compound **258** (75 MHz, $CDCl_3$)

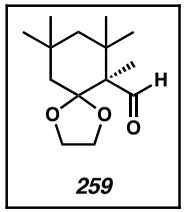

259

Figure A5.121 ^{1}H NMR of compound **259** (300 MHz, $CDCl_3$)

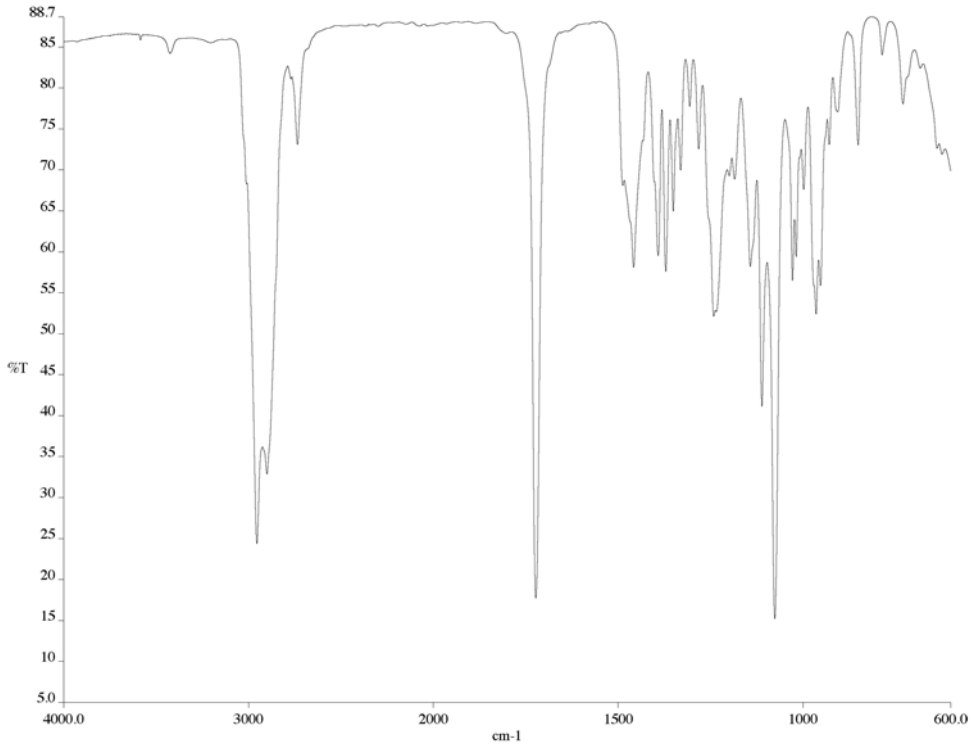

Figure A5.122 IR of compound **259** (NaCl/film)

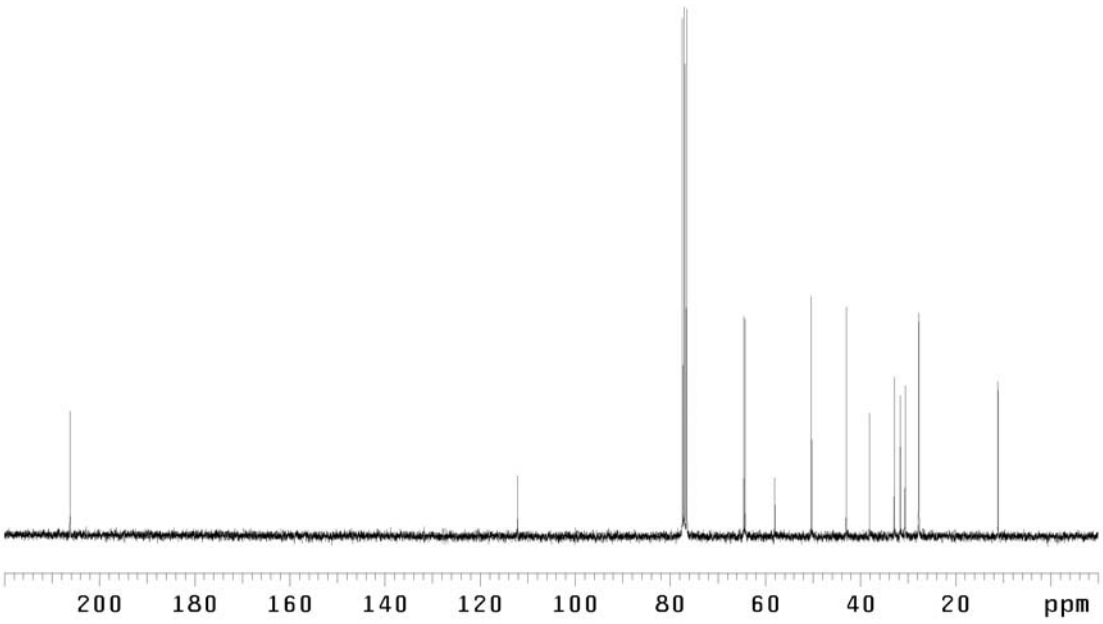

Figure A5.123 ^{13}C NMR of compound **259** (75 MHz, $CDCl_3$)

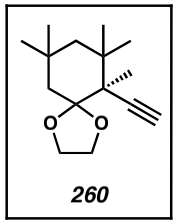

Figure A5.124 ^{1}H NMR of compound **260** (300 MHz, $CDCl_3$)

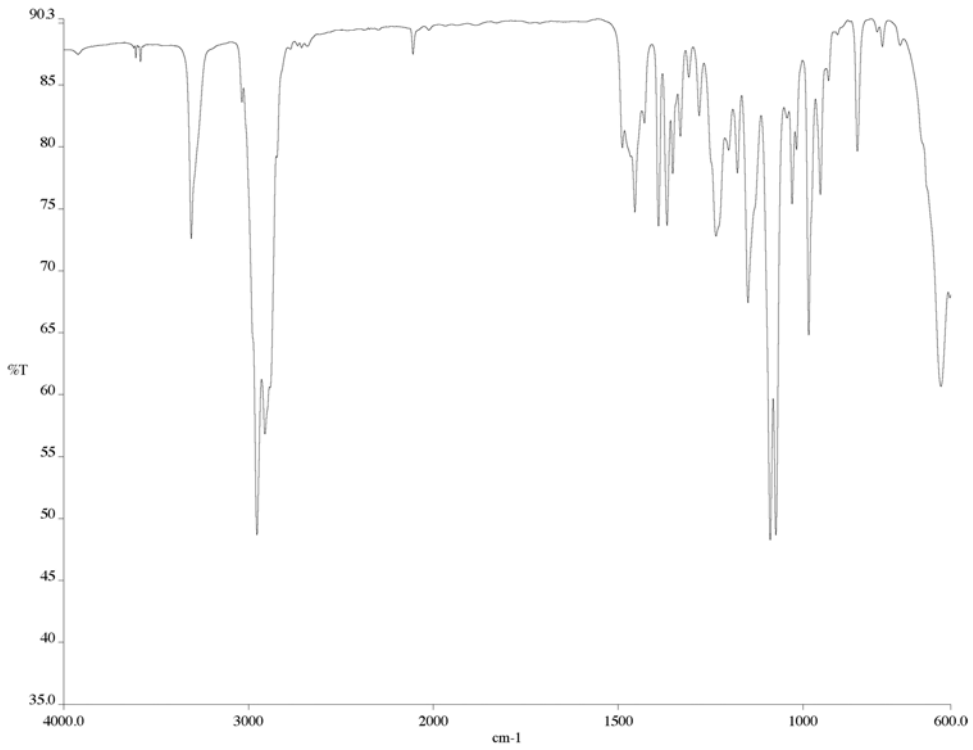

Figure A5.125 IR of compound **260** (NaCl/film)

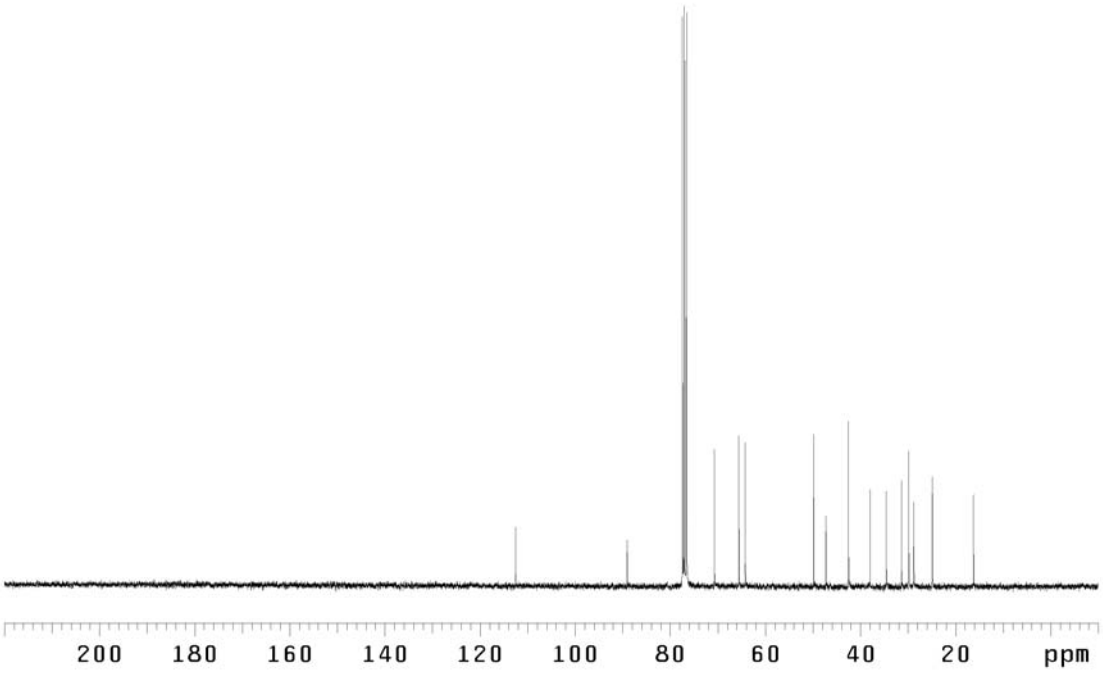

Figure A5.126 ^{13}C NMR of compound **260** (75 MHz, $CDCl_3$)

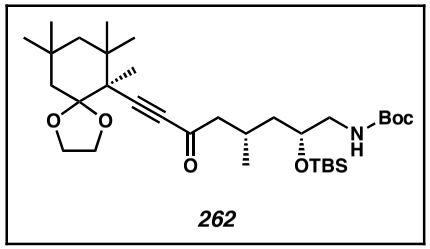

262

Figure A5.127 ^{1}H NMR of compound **262** (500 MHz, $CDCl_3$)

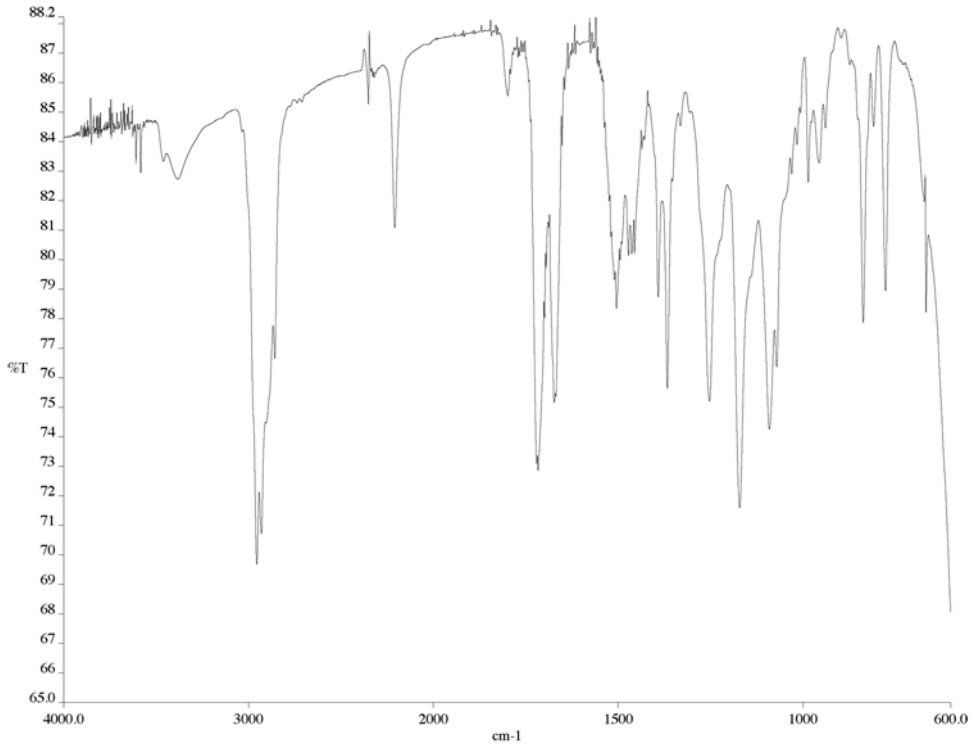

Figure A5.128 IR of compound **262** (NaCl/film)

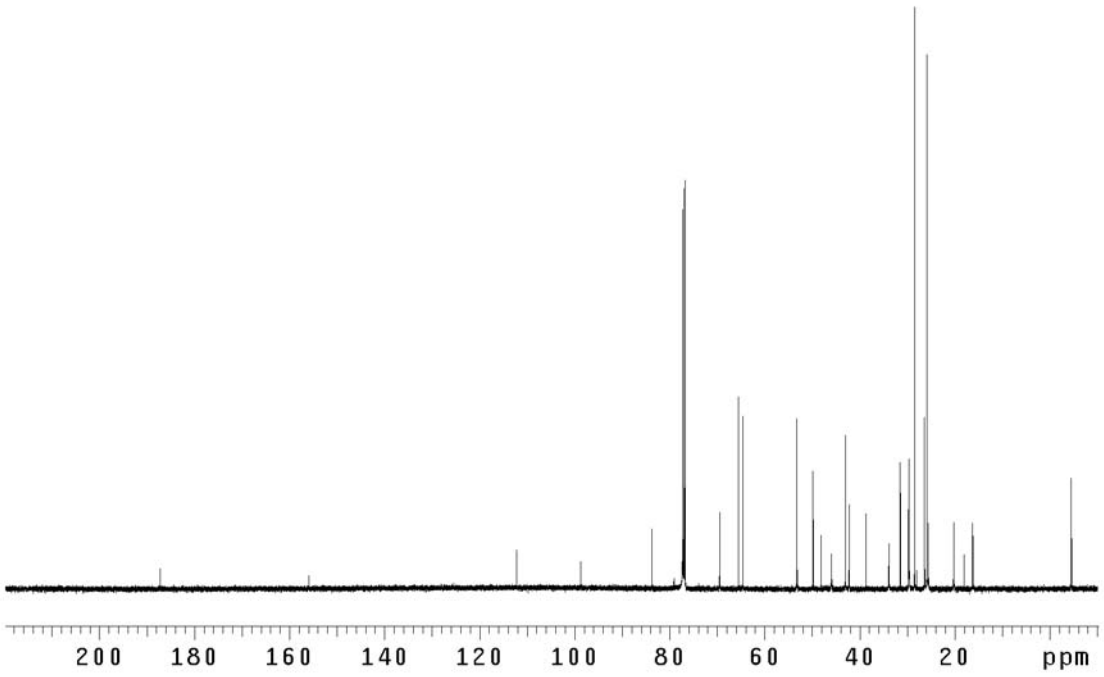

Figure A5.129 ^{13}C NMR of compound **262** (125 MHz, $CDCl_3$)

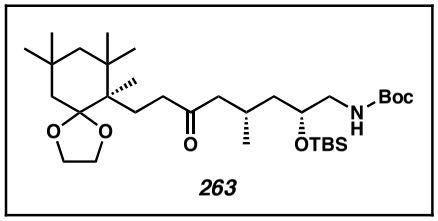

263

Figure A5.130 ^{1}H NMR of compound **263** (500 MHz, $CDCl_3$)

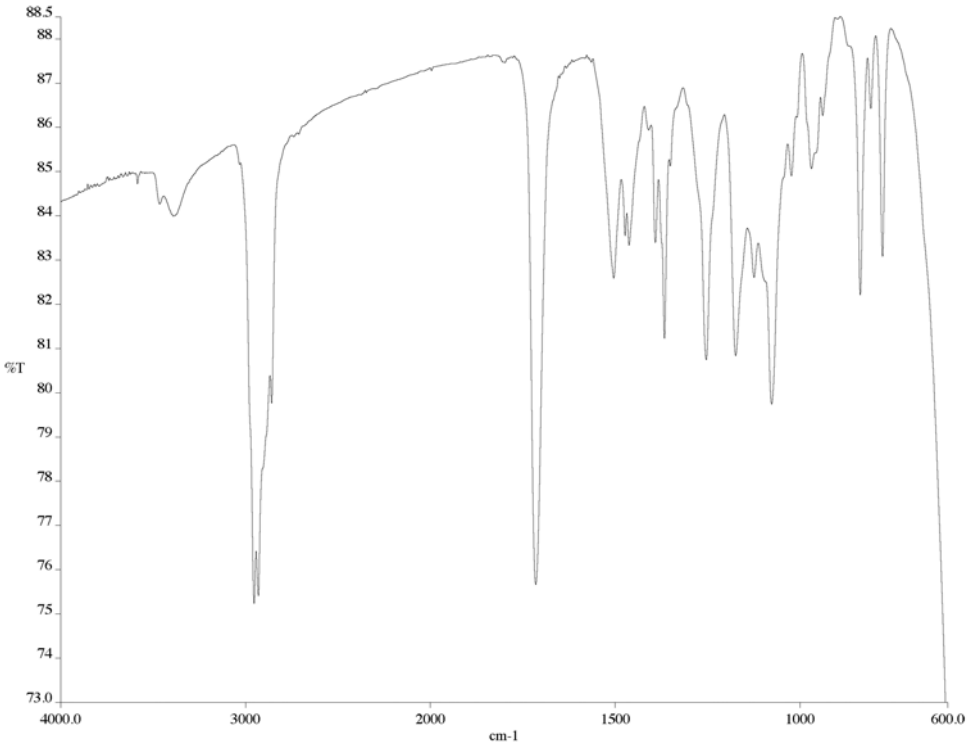

Figure A5.131 IR of compound **263** (NaCl/film)

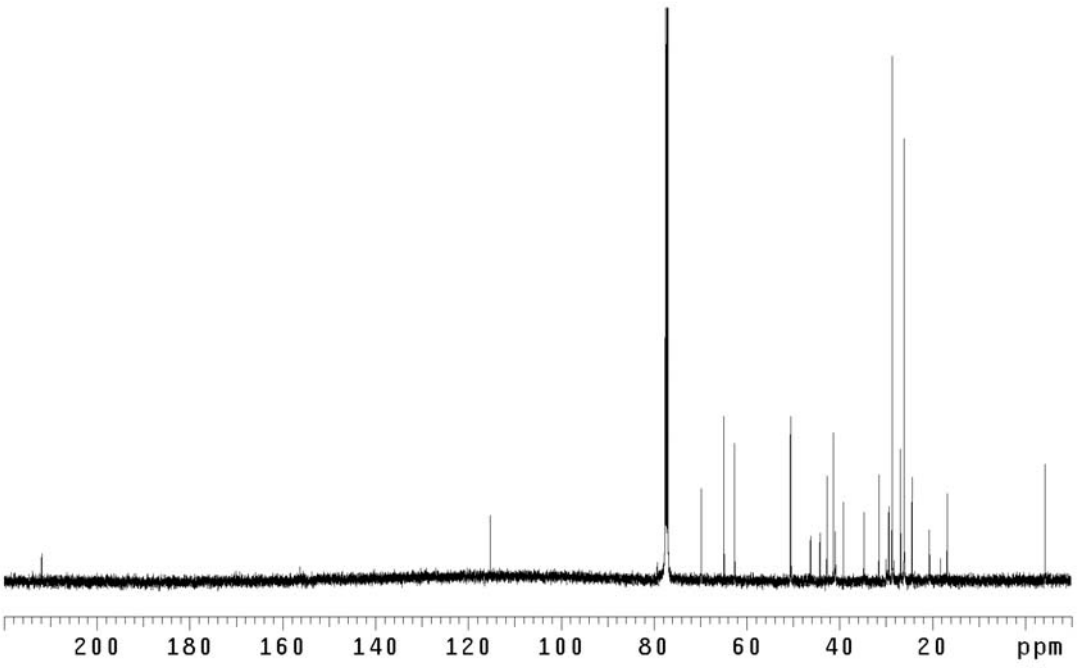

Figure A5.132 ^{13}C NMR of compound **263** (125 MHz, $CDCl_3$)

APPENDIX SIX

X-Ray Crystallographic Data Relevant to Chapter Three

CALIFORNIA INSTITUTE OF TECHNOLOGY

BECKMAN INSTITUTE

X-RAY CRYSTALLOGRAPHY LABORATORY

Crystal Structure Analysis of:

Allylic Alcohol 211 (DCB30)

(CCDC 277462)

Contents:

Figure A6.1 Representation of Allylic Alcohol **211**

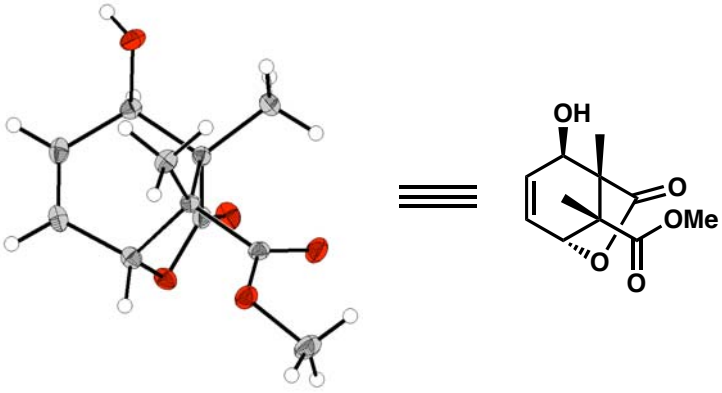

Table 1. Crystal data and structure refinement for DCB30 (CCDC 277462).

Empirical formula	$C_{11}H_{14}O_5$
Formula weight	226.22
Crystallization Solvent	Heptane/diethylether
Crystal Habit	Fragment
Crystal size	0.41 x 0.24 x 0.16 mm^3
Crystal color	Colorless

Data Collection

Type of diffractometer	Bruker SMART 1000
Wavelength	0.71073 Å MoKα
Data Collection Temperature	100(2) K
θ range for 8068 reflections used in lattice determination	2.74 to 39.14°
Unit cell dimensions	a = 8.5469(4) Å b = 8.7203(4) Å c = 14.1988(6) Å
Volume	1058.26(8) $Å^3$
Z	4
Crystal system	Orthorhombic
Space group	$P2_12_12_1$
Density (calculated)	1.420 Mg/m^3
F(000)	480
Data collection program	Bruker SMART v5.630
θ range for data collection	2.74 to 40.70°
Completeness to θ = 40.70°	92.3 %
Index ranges	$-15 \le h \le 13$, $-15 \le k \le 15$, $-25 \le l \le 23$
Data collection scan type	ω scans at 5 ϕ settings
Data reduction program	Bruker SAINT v6.45A
Reflections collected	19516
Independent reflections	6114 [R_{int}= 0.0607]
Absorption coefficient	0.113 mm^{-1}
Absorption correction	None
Max. and min. transmission	0.9822 and 0.9553

Table 1 (cont.)

Structure solution and Refinement

Structure solution program	Bruker XS v6.12
Primary solution method	Direct methods
Secondary solution method	Difference Fourier map
Hydrogen placement	Difference Fourier map
Structure refinement program	Bruker XL v6.12
Refinement method	Full matrix least-squares on F^2
Data / restraints / parameters	6114 / 0 / 201
Treatment of hydrogen atoms	Unrestrained
Goodness-of-fit on F^2	1.304
Final R indices [I>2σ(I), 4485 reflections]	R1 = 0.0415, *w*R2 = 0.0690
R indices (all data)	R1 = 0.0621, *w*R2 = 0.0715
Type of weighting scheme used	Sigma
Weighting scheme used	$w=1/\sigma^2(Fo^2)$
Max shift/error	0.001
Average shift/error	0.000
Absolute structure determination	Not possible to reliably determine absolute configuration
Absolute structure parameter	-0.2(6)
Largest diff. peak and hole	0.427 and -0.273 e.Å^{-3}

Special Refinement Details

Refinement of F^2 against ALL reflections. The weighted R-factor (*w*R) and goodness of fit (S) are based on F^2, conventional R-factors (R) are based on F, with F set to zero for negative F^2. The threshold expression of $F^2 > 2\sigma(F^2)$ is used only for calculating R-factors(gt) etc. and is not relevant to the choice of reflections for refinement. R-factors based on F^2 are statistically about twice as large as those based on F, and R-factors based on ALL data will be even larger.

All esds (except the esd in the dihedral angle between two l.s. planes) are estimated using the full covariance matrix. The cell esds are taken into account individually in the estimation of esds in distances, angles and torsion angles; correlations between esds in cell parameters are only used when they are defined by crystal symmetry. An approximate (isotropic) treatment of cell esds is used for estimating esds involving l.s. planes.

Table 2. Atomic coordinates (x 10^4) and equivalent isotropic displacement parameters ($Å^2$x 10^3) for DCB30 (CCDC 277462). U(eq) is defined as the trace of the orthogonalized U^{ij} tensor.

	x	y	z	U_{eq}
O(1)	1165(1)	11191(1)	7918(1)	16(1)
O(2)	1872(1)	13004(1)	8946(1)	21(1)
O(3)	4173(1)	9617(1)	8803(1)	21(1)
O(4)	3237(1)	7678(1)	7931(1)	18(1)
O(5)	-878(1)	9680(1)	10618(1)	19(1)
C(1)	-1241(1)	9774(1)	8195(1)	17(1)
C(2)	492(1)	9626(1)	8002(1)	15(1)
C(3)	1380(1)	8989(1)	8868(1)	12(1)
C(4)	1180(1)	10414(1)	9520(1)	12(1)
C(5)	-565(1)	10628(1)	9813(1)	14(1)
C(6)	-1706(1)	10259(1)	9031(1)	17(1)
C(7)	1471(1)	11701(1)	8802(1)	14(1)
C(8)	2214(1)	10544(1)	10395(1)	16(1)
C(9)	763(1)	7465(1)	9253(1)	16(1)
C(10)	3095(1)	8815(1)	8558(1)	14(1)
C(11)	4809(1)	7460(1)	7566(1)	23(1)

Table 3. Bond lengths [Å] and angles [°] for DCB30 (CCDC 277462).

O(1)-C(7)	1.3559(11)	C(8)-C(4)-C(7)	113.05(7)
O(1)-C(2)	1.4855(11)	C(8)-C(4)-C(3)	118.58(7)
O(2)-C(7)	1.2050(11)	C(7)-C(4)-C(3)	99.84(6)
O(3)-C(10)	1.2082(11)	C(8)-C(4)-C(5)	109.06(7)
O(4)-C(10)	1.3387(11)	C(7)-C(4)-C(5)	104.16(7)
O(4)-C(11)	1.4519(12)	C(3)-C(4)-C(5)	111.03(7)
O(5)-C(5)	1.4350(11)	O(5)-C(5)-C(6)	110.00(7)
O(5)-H(5A)	0.783(13)	O(5)-C(5)-C(4)	108.75(7)
C(1)-C(6)	1.3223(13)	C(6)-C(5)-C(4)	113.26(7)
C(1)-C(2)	1.5115(13)	O(5)-C(5)-H(5)	109.9(6)
C(1)-H(1)	0.973(11)	C(6)-C(5)-H(5)	108.8(6)
C(2)-C(3)	1.5486(12)	C(4)-C(5)-H(5)	106.0(6)
C(2)-H(2)	0.989(9)	C(1)-C(6)-C(5)	122.26(8)
C(3)-C(9)	1.5301(12)	C(1)-C(6)-H(6)	120.8(6)
C(3)-C(10)	1.5380(13)	C(5)-C(6)-H(6)	116.9(6)
C(3)-C(4)	1.5586(12)	O(2)-C(7)-O(1)	121.44(8)
C(4)-C(8)	1.5294(12)	O(2)-C(7)-C(4)	128.47(8)
C(4)-C(7)	1.5365(12)	O(1)-C(7)-C(4)	110.07(7)
C(4)-C(5)	1.5600(12)	C(4)-C(8)-H(8A)	108.8(6)
C(5)-C(6)	1.5120(13)	C(4)-C(8)-H(8B)	108.5(7)
C(5)-H(5)	0.994(11)	H(8A)-C(8)-H(8B)	109.1(9)
C(6)-H(6)	0.951(10)	C(4)-C(8)-H(8C)	112.1(7)
C(8)-H(8A)	1.025(12)	H(8A)-C(8)-H(8C)	105.7(10)
C(8)-H(8B)	0.977(11)	H(8B)-C(8)-H(8C)	112.6(10)
C(8)-H(8C)	0.976(12)	C(3)-C(9)-H(9A)	110.7(6)
C(9)-H(9A)	0.987(11)	C(3)-C(9)-H(9B)	111.9(7)
C(9)-H(9B)	0.952(11)	H(9A)-C(9)-H(9B)	104.0(9)
C(9)-H(9C)	0.952(12)	C(3)-C(9)-H(9C)	110.2(7)
C(11)-H(11A)	0.967(12)	H(9A)-C(9)-H(9C)	108.6(9)
C(11)-H(11B)	0.940(13)	H(9B)-C(9)-H(9C)	111.2(10)
C(11)-H(11C)	0.962(12)	O(3)-C(10)-O(4)	123.45(8)
		O(3)-C(10)-C(3)	125.99(8)
C(7)-O(1)-C(2)	107.57(7)	O(4)-C(10)-C(3)	110.48(7)
C(10)-O(4)-C(11)	114.73(8)	O(4)-C(11)-H(11A)	107.9(7)
C(5)-O(5)-H(5A)	104.1(10)	O(4)-C(11)-H(11B)	106.0(8)
C(6)-C(1)-C(2)	119.00(8)	H(11A)-C(11)-H(11B)	111.7(10)
C(6)-C(1)-H(1)	122.2(6)	O(4)-C(11)-H(11C)	108.7(7)
C(2)-C(1)-H(1)	118.8(6)	H(11A)-C(11)-H(11C)	111.6(9)
O(1)-C(2)-C(1)	108.39(7)	H(11B)-C(11)-H(11C)	110.6(10)
O(1)-C(2)-C(3)	101.75(7)		
C(1)-C(2)-C(3)	111.51(7)		
O(1)-C(2)-H(2)	105.7(6)		
C(1)-C(2)-H(2)	112.9(6)		
C(3)-C(2)-H(2)	115.6(5)		
C(9)-C(3)-C(10)	110.19(7)		
C(9)-C(3)-C(2)	115.23(8)		
C(10)-C(3)-C(2)	105.96(7)		
C(9)-C(3)-C(4)	116.29(7)		
C(10)-C(3)-C(4)	110.65(7)		
C(2)-C(3)-C(4)	97.55(7)		

Table 4. Anisotropic displacement parameters ($Å^2 x 10^4$) for DCB30 (CCDC 277462). The anisotropic displacement factor exponent takes the form: $-2\pi^2 [h^2 a^{*2} U^{11} + ... + 2 h k a^* b^* U^{12}]$

	U^{11}	U^{22}	U^{33}	U^{23}	U^{13}	U^{12}
O(1)	203(3)	149(3)	142(3)	30(2)	-26(3)	-27(3)
O(2)	239(4)	146(3)	239(3)	28(3)	-42(3)	-47(3)
O(3)	154(3)	239(4)	236(3)	-25(3)	30(3)	-54(3)
O(4)	154(3)	204(3)	196(3)	-37(3)	29(3)	16(3)
O(5)	178(3)	213(3)	185(3)	47(3)	60(3)	34(3)
C(1)	159(4)	156(4)	203(4)	11(3)	-58(3)	-11(4)
C(2)	167(4)	130(4)	149(4)	-4(3)	-18(3)	-17(4)
C(3)	129(4)	116(4)	122(3)	8(3)	3(3)	-2(3)
C(4)	120(4)	119(4)	124(3)	11(3)	-4(3)	0(3)
C(5)	147(4)	127(4)	144(4)	9(3)	21(3)	14(3)
C(6)	129(4)	162(4)	230(4)	24(3)	-19(3)	10(4)
C(7)	118(4)	149(4)	157(4)	18(3)	-10(3)	3(3)
C(8)	163(4)	190(5)	138(4)	6(3)	-24(3)	-5(4)
C(9)	154(4)	117(4)	201(4)	11(3)	21(4)	-5(4)
C(10)	148(4)	151(4)	120(4)	32(3)	18(3)	10(4)
C(11)	191(5)	259(6)	230(5)	-5(4)	75(4)	52(4)

Table 5. Hydrogen coordinates (x 10^4) and isotropic displacement parameters ($Å^2$x 10^3) for DCB30 (CCDC 277462).

	x	y	z	U_{iso}
H(5A)	-1603(15)	10067(15)	10856(9)	35(4)
H(1)	-1977(13)	9484(13)	7703(7)	18(3)
H(2)	719(11)	9112(11)	7397(7)	6(2)
H(5)	-680(12)	11727(13)	9986(7)	15(3)
H(6)	-2786(12)	10404(12)	9164(7)	14(3)
H(8A)	1942(13)	11540(14)	10742(8)	23(3)
H(8B)	1993(13)	9673(14)	10807(7)	23(3)
H(8C)	3321(14)	10627(15)	10235(8)	29(3)
H(9A)	1386(12)	7128(12)	9800(8)	17(3)
H(9B)	-271(13)	7561(12)	9496(8)	17(3)
H(9C)	815(14)	6693(14)	8779(8)	27(3)
H(11A)	5491(14)	7243(13)	8093(8)	20(3)
H(11B)	4748(14)	6625(15)	7148(9)	29(3)
H(11C)	5121(13)	8376(14)	7239(8)	20(3)

Table 6. Hydrogen bonds for DCB30 (CCDC 277462) [Å and °].

D-H...A	d(D-H)	d(H...A)	d(D...A)	<(DHA)
O(5)-H(5A)...O(2)#1	0.783(13)	2.147(13)	2.8567(10)	151.0(13)

Symmetry transformations used to generate equivalent atoms:
#1 x-1/2,-y+5/2,-z+2

CALIFORNIA INSTITUTE OF TECHNOLOGY

BECKMAN INSTITUTE

X-RAY CRYSTALLOGRAPHY LABORATORY

Crystal Structure Analysis of:

Allylic Alcohol 217 (DCB31)

(CCDC 283708)

Contents:

Figure A6.2 Representation of Allylic Alcohol **217**

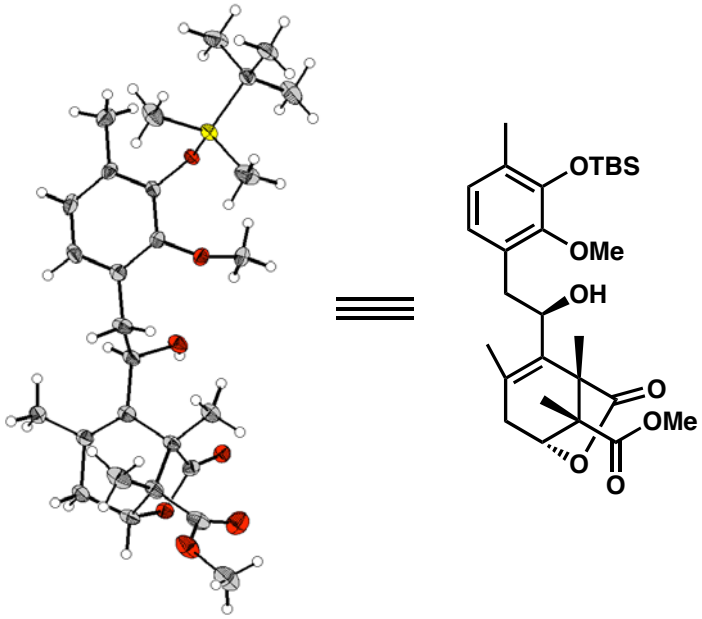

Table 1. Crystal data and structure refinement for DCB31 (CCDC 283708).

Empirical formula	$C_{28}H_{42}O_7$ Si	
Formula weight	518.71	
Crystallization Solvent	EtOAc/heptane	
Crystal Habit	Block	
Crystal size	0.32 x 0.31 x 0.22 mm^3	
Crystal color	Colorless	

Data Collection

Type of diffractometer	Bruker SMART 1000	
Wavelength	0.71073 Å MoKα	
Data Collection Temperature	100(2) K	
θ range for 15772 reflections used in lattice determination	2.32 to 28.21°	
Unit cell dimensions	a = 12.6604(8) Å b = 15.4100(10) Å c = 15.7147(10) Å	α= 81.0750(10)° β= 66.6280(10)° γ = 87.6100(10)°
Volume	2779.6(3) $Å^3$	
Z	4	
Crystal system	Triclinic	
Space group	P-1	
Density (calculated)	1.240 Mg/m^3	
F(000)	1120	
Data collection program	Bruker SMART v5.630	
θ range for data collection	1.75 to 28.27°	
Completeness to θ = 28.27°	92.1 %	
Index ranges	$-16 \le h \le 16, -20 \le k \le 19, -20 \le l \le 20$	
Data collection scan type	ω scans at 7 ϕ settings	
Data reduction program	Bruker SAINT v6.45A	
Reflections collected	56601	
Independent reflections	12691 [R_{int}= 0.0626]	
Absorption coefficient	0.127 mm^{-1}	
Absorption correction	None	
Max. and min. transmission	0.9725 and 0.9604	

Table 1 (cont.)

Structure solution and Refinement

Structure solution program	SHELXS-97 (Sheldrick, 1990)
Primary solution method	Direct methods
Secondary solution method	Difference Fourier map
Hydrogen placement	Difference Fourier map
Structure refinement program	SHELXL-97 (Sheldrick, 1997)
Refinement method	Full matrix least-squares on F^2
Data / restraints / parameters	12691 / 0 / 985
Treatment of hydrogen atoms	Unrestrained
Goodness-of-fit on F^2	1.502
Final R indices [$I>2\sigma(I)$, 7901 reflections]	R1 = 0.0455, *w*R2 = 0.0721
R indices (all data)	R1 = 0.0839, *w*R2 = 0.0763
Type of weighting scheme used	Sigma
Weighting scheme used	$w=1/\sigma^2(Fo^2)$
Max shift/error	0.003
Average shift/error	0.000
Largest diff. peak and hole	0.492 and -0.382 e.Å^{-3}

Special Refinement Details

Refinement of F^2 against ALL reflections. The weighted R-factor (*w*R) and goodness of fit (S) are based on F^2, conventional R-factors (R) are based on F, with F set to zero for negative F^2. The threshold expression of $F^2 > 2\sigma(F^2)$ is used only for calculating R-factors(gt) etc. and is not relevant to the choice of reflections for refinement. R-factors based on F^2 are statistically about twice as large as those based on F, and R-factors based on ALL data will be even larger.

All esds (except the esd in the dihedral angle between two l.s. planes) are estimated using the full covariance matrix. The cell esds are taken into account individually in the estimation of esds in distances, angles and torsion angles; correlations between esds in cell parameters are only used when they are defined by crystal symmetry. An approximate (isotropic) treatment of cell esds is used for estimating esds involving l.s. planes.

Table 2. Atomic coordinates (x 10^4) and equivalent isotropic displacement parameters ($Å^2$x 10^3) for DCB31 (CCDC 283708). U(eq) is defined as the trace of the orthogonalized U^{ij} tensor.

	x	y	z	U_{eq}
Si(1)	-42(1)	510(1)	2060(1)	21(1)
O(1A)	816(1)	1084(1)	2346(1)	19(1)
O(2A)	1297(1)	2515(1)	937(1)	23(1)
O(3A)	3033(1)	4131(1)	770(1)	26(1)
O(4A)	3980(1)	6315(1)	-2542(1)	37(1)
O(5A)	2422(1)	7069(1)	-2515(1)	38(1)
O(6A)	4208(1)	6810(1)	-903(1)	21(1)
O(7A)	4924(1)	5456(1)	-917(1)	22(1)
C(1A)	646(1)	1925(1)	2572(1)	18(1)
C(2A)	899(1)	2648(1)	1864(1)	18(1)
C(3A)	719(1)	3501(1)	2073(1)	21(1)
C(4A)	306(2)	3607(1)	3011(1)	27(1)
C(5A)	107(2)	2895(1)	3709(1)	26(1)
C(6A)	276(1)	2039(1)	3508(1)	20(1)
C(7A)	81(2)	1260(1)	4263(1)	29(1)
C(8A)	2448(2)	2186(2)	597(2)	28(1)
C(9A)	166(2)	811(2)	810(2)	38(1)
C(10A)	-1553(2)	709(2)	2806(2)	35(1)
C(11A)	375(1)	-659(1)	2268(1)	22(1)
C(12A)	-338(2)	-1258(1)	1990(2)	30(1)
C(13A)	1656(2)	-771(2)	1691(2)	37(1)
C(14A)	138(2)	-938(1)	3311(1)	34(1)
C(15A)	999(2)	4291(1)	1317(1)	25(1)
C(16A)	2140(1)	4736(1)	1130(1)	21(1)
C(17A)	2349(1)	5629(1)	503(1)	20(1)
C(18A)	2866(1)	5673(1)	-583(1)	20(1)
C(19A)	2473(1)	6519(1)	-1042(1)	24(1)
C(20A)	3079(2)	7190(1)	-749(1)	24(1)
C(21A)	2454(2)	7262(1)	276(1)	24(1)
C(22A)	2158(1)	6374(1)	879(1)	22(1)
C(23A)	1640(2)	6435(1)	1910(1)	29(1)
C(24A)	2706(2)	4851(1)	-947(1)	25(1)
C(25A)	4114(2)	5923(1)	-833(1)	20(1)
C(26A)	1171(2)	6613(2)	-701(2)	35(1)
C(27A)	3055(2)	6601(1)	-2107(1)	28(1)
C(28A)	2900(3)	7207(2)	-3527(2)	44(1)
Si(2)	5149(1)	9590(1)	2638(1)	21(1)
O(1B)	4218(1)	9004(1)	2444(1)	20(1)
O(2B)	3743(1)	7599(1)	3860(1)	24(1)
O(3B)	1918(1)	5944(1)	4116(1)	26(1)
O(4B)	1344(1)	3774(1)	7408(1)	34(1)
O(5B)	2918(1)	2985(1)	7232(1)	32(1)
O(6B)	863(1)	3261(1)	5877(1)	21(1)
O(7B)	126(1)	4607(1)	5934(1)	23(1)
C(1B)	4350(1)	8159(1)	2224(1)	17(1)
C(2B)	4097(1)	7444(1)	2943(1)	18(1)

C(3B)	4225(1)	6587(1)	2749(1)	21(1)
C(4B)	4584(1)	6466(1)	1817(1)	24(1)
C(5B)	4779(1)	7171(1)	1112(1)	24(1)
C(6B)	4666(1)	8032(1)	1295(1)	19(1)
C(7B)	4854(2)	8801(1)	525(1)	26(1)
C(8B)	2574(2)	7893(1)	4228(1)	29(1)
C(9B)	5680(2)	8968(1)	3484(2)	29(1)
C(10B)	6404(2)	9919(2)	1510(2)	33(1)
C(11B)	4327(2)	10573(1)	3092(1)	25(1)
C(12B)	5122(2)	11175(1)	3282(2)	32(1)
C(13B)	3289(2)	10289(2)	4020(2)	46(1)
C(14B)	3894(2)	11088(2)	2385(2)	46(1)
C(15B)	3966(2)	5805(1)	3514(1)	25(1)
C(16B)	2821(1)	5350(1)	3733(1)	19(1)
C(17B)	2636(1)	4457(1)	4354(1)	19(1)
C(18B)	2219(1)	4416(1)	5438(1)	19(1)
C(19B)	2690(1)	3582(1)	5839(1)	22(1)
C(20B)	2018(2)	2897(1)	5624(1)	22(1)
C(21B)	2507(2)	2827(1)	4603(1)	22(1)
C(22B)	2764(1)	3713(1)	3988(1)	20(1)
C(23B)	3189(2)	3634(1)	2963(1)	26(1)
C(24B)	2419(2)	5244(1)	5771(1)	23(1)
C(25B)	955(2)	4150(1)	5785(1)	19(1)
C(26B)	3999(2)	3506(2)	5394(2)	29(1)
C(27B)	2231(2)	3484(1)	6908(1)	25(1)
C(28B)	2541(2)	2794(2)	8236(1)	35(1)

Table 3. Bond lengths [Å] and angles [°] for DCB31 (CCDC 283708).

Si(1)-O(1A)	1.6602(11)	C(15A)-H(15B)	1.012(16)
Si(1)-C(10A)	1.847(2)	C(16A)-C(17A)	1.529(2)
Si(1)-C(9A)	1.860(2)	C(16A)-H(16A)	1.032(13)
Si(1)-C(11A)	1.8719(17)	C(17A)-C(22A)	1.342(2)
O(1A)-C(1A)	1.3834(18)	C(17A)-C(18A)	1.559(2)
O(2A)-C(2A)	1.3854(18)	C(18A)-C(25A)	1.520(2)
O(2A)-C(8A)	1.440(2)	C(18A)-C(24A)	1.519(2)
O(3A)-C(16A)	1.4266(19)	C(18A)-C(19A)	1.552(2)
O(3A)-H(3A)	0.92(2)	C(19A)-C(26A)	1.525(2)
O(4A)-C(27A)	1.203(2)	C(19A)-C(27A)	1.525(2)
O(5A)-C(27A)	1.337(2)	C(19A)-C(20A)	1.538(2)
O(5A)-C(28A)	1.442(2)	C(20A)-C(21A)	1.506(2)
O(6A)-C(25A)	1.3611(19)	C(20A)-H(20A)	1.015(16)
O(6A)-C(20A)	1.4637(19)	C(21A)-C(22A)	1.505(2)
O(7A)-C(25A)	1.2020(18)	C(21A)-H(21A)	0.976(15)
C(1A)-C(2A)	1.394(2)	C(21A)-H(21B)	1.002(16)
C(1A)-C(6A)	1.393(2)	C(22A)-C(23A)	1.505(2)
C(2A)-C(3A)	1.392(2)	C(23A)-H(23A)	0.95(2)
C(3A)-C(4A)	1.389(2)	C(23A)-H(23B)	0.963(19)
C(3A)-C(15A)	1.508(2)	C(23A)-H(23C)	0.98(2)
C(4A)-C(5A)	1.378(2)	C(24A)-H(24A)	0.973(16)
C(4A)-H(4A)	0.933(16)	C(24A)-H(24B)	1.022(16)
C(5A)-C(6A)	1.392(2)	C(24A)-H(24C)	0.984(16)
C(5A)-H(5A)	0.918(15)	C(26A)-H(26A)	1.042(16)
C(6A)-C(7A)	1.504(2)	C(26A)-H(26B)	0.994(18)
C(7A)-H(7A1)	0.978(19)	C(26A)-H(26C)	0.944(18)
C(7A)-H(7A2)	0.991(17)	C(28A)-H(28A)	0.96(2)
C(7A)-H(7A3)	0.977(17)	C(28A)-H(28B)	1.00(2)
C(8A)-H(8A1)	0.96(2)	C(28A)-H(28C)	0.95(2)
C(8A)-H(8A2)	0.96(2)	Si(2)-O(1B)	1.6614(12)
C(8A)-H(8A3)	0.980(18)	Si(2)-C(9B)	1.844(2)
C(9A)-H(9A1)	0.96(2)	Si(2)-C(10B)	1.864(2)
C(9A)-H(9A2)	0.99(2)	Si(2)-C(11B)	1.8712(17)
C(9A)-H(9A3)	1.04(2)	O(1B)-C(1B)	1.3842(18)
C(10A)-H(10A)	1.032(18)	O(2B)-C(2B)	1.3868(18)
C(10A)-H(10B)	0.95(2)	O(2B)-C(8B)	1.441(2)
C(10A)-H(10C)	0.91(2)	O(3B)-C(16B)	1.4298(19)
C(11A)-C(13A)	1.530(2)	O(3B)-H(3B)	0.98(3)
C(11A)-C(14A)	1.537(2)	O(4B)-C(27B)	1.2025(19)
C(11A)-C(12A)	1.539(2)	O(5B)-C(27B)	1.3347(19)
C(12A)-H(12A)	0.995(16)	O(5B)-C(28B)	1.441(2)
C(12A)-H(12B)	1.002(16)	O(6B)-C(25B)	1.3590(19)
C(12A)-H(12C)	0.939(17)	O(6B)-C(20B)	1.4668(19)
C(13A)-H(13A)	0.986(18)	O(7B)-C(25B)	1.2030(18)
C(13A)-H(13B)	0.990(17)	C(1B)-C(6B)	1.396(2)
C(13A)-H(13C)	1.072(16)	C(1B)-C(2B)	1.396(2)
C(14A)-H(14A)	1.043(18)	C(2B)-C(3B)	1.389(2)
C(14A)-H(14B)	1.016(17)	C(3B)-C(4B)	1.391(2)
C(14A)-H(14C)	0.982(18)	C(3B)-C(15B)	1.509(2)
C(15A)-C(16A)	1.525(2)	C(4B)-C(5B)	1.378(2)
C(15A)-H(15A)	0.967(16)	C(4B)-H(4B)	0.941(15)

C(5B)-C(6B)	1.391(2)	C(26B)-H(26F)	0.902(18)
C(5B)-H(5B)	0.956(15)	C(28B)-H(28D)	0.973(19)
C(6B)-C(7B)	1.508(2)	C(28B)-H(28E)	1.01(2)
C(7B)-H(7B1)	0.984(18)	C(28B)-H(28F)	1.005(18)
C(7B)-H(7B2)	0.973(18)		
C(7B)-H(7B3)	0.959(18)	O(1A)-Si(1)-C(10A)	108.83(9)
C(8B)-H(8B1)	0.994(16)	O(1A)-Si(1)-C(9A)	112.73(9)
C(8B)-H(8B2)	0.949(17)	C(10A)-Si(1)-C(9A)	108.59(12)
C(8B)-H(8B3)	0.976(19)	O(1A)-Si(1)-C(11A)	104.53(7)
C(9B)-H(9B1)	1.021(19)	C(10A)-Si(1)-C(11A)	112.83(9)
C(9B)-H(9B2)	0.968(18)	C(9A)-Si(1)-C(11A)	109.35(9)
C(9B)-H(9B3)	0.910(18)	C(1A)-O(1A)-Si(1)	126.87(10)
C(10B)-H(10D)	0.929(19)	C(2A)-O(2A)-C(8A)	112.94(13)
C(10B)-H(10E)	0.972(19)	C(16A)-O(3A)-H(3A)	109.0(14)
C(10B)-H(10F)	1.041(19)	C(27A)-O(5A)-C(28A)	116.14(17)
C(11B)-C(14B)	1.529(3)	C(25A)-O(6A)-C(20A)	108.79(12)
C(11B)-C(12B)	1.537(3)	O(1A)-C(1A)-C(2A)	119.97(14)
C(11B)-C(13B)	1.541(3)	O(1A)-C(1A)-C(6A)	119.17(14)
C(12B)-H(12D)	0.961(18)	C(2A)-C(1A)-C(6A)	120.77(16)
C(12B)-H(12E)	0.976(16)	O(2A)-C(2A)-C(3A)	119.27(15)
C(12B)-H(12F)	1.036(18)	O(2A)-C(2A)-C(1A)	119.52(15)
C(13B)-H(13D)	0.99(2)	C(3A)-C(2A)-C(1A)	121.17(15)
C(13B)-H(13E)	0.97(2)	C(4A)-C(3A)-C(2A)	117.57(16)
C(13B)-H(13F)	0.988(19)	C(4A)-C(3A)-C(15A)	120.43(17)
C(14B)-H(14D)	1.009(19)	C(2A)-C(3A)-C(15A)	121.96(16)
C(14B)-H(14E)	0.99(2)	C(5A)-C(4A)-C(3A)	121.26(18)
C(14B)-H(14F)	1.010(19)	C(5A)-C(4A)-H(4A)	120.0(10)
C(15B)-C(16B)	1.526(2)	C(3A)-C(4A)-H(4A)	118.7(10)
C(15B)-H(15C)	0.983(16)	C(4A)-C(5A)-C(6A)	121.60(17)
C(15B)-H(15D)	0.969(15)	C(4A)-C(5A)-H(5A)	120.6(10)
C(16B)-C(17B)	1.527(2)	C(6A)-C(5A)-H(5A)	117.8(10)
C(16B)-H(16B)	1.061(14)	C(5A)-C(6A)-C(1A)	117.47(16)
C(17B)-C(22B)	1.336(2)	C(5A)-C(6A)-C(7A)	121.95(16)
C(17B)-C(18B)	1.562(2)	C(1A)-C(6A)-C(7A)	120.58(16)
C(18B)-C(24B)	1.519(2)	C(6A)-C(7A)-H(7A1)	113.2(11)
C(18B)-C(25B)	1.524(2)	C(6A)-C(7A)-H(7A2)	110.5(10)
C(18B)-C(19B)	1.545(2)	H(7A1)-C(7A)-H(7A2)	109.8(14)
C(19B)-C(27B)	1.528(2)	C(6A)-C(7A)-H(7A3)	111.4(10)
C(19B)-C(26B)	1.530(2)	H(7A1)-C(7A)-H(7A3)	105.1(15)
C(19B)-C(20B)	1.538(2)	H(7A2)-C(7A)-H(7A3)	106.4(13)
C(20B)-C(21B)	1.494(2)	O(2A)-C(8A)-H(8A1)	109.8(11)
C(20B)-H(20B)	0.966(15)	O(2A)-C(8A)-H(8A2)	107.6(11)
C(21B)-C(22B)	1.511(2)	H(8A1)-C(8A)-H(8A2)	113.2(16)
C(21B)-H(21C)	1.005(15)	O(2A)-C(8A)-H(8A3)	111.8(10)
C(21B)-H(21D)	0.945(15)	H(8A1)-C(8A)-H(8A3)	106.8(15)
C(22B)-C(23B)	1.505(2)	H(8A2)-C(8A)-H(8A3)	107.7(15)
C(23B)-H(23D)	1.002(18)	Si(1)-C(9A)-H(9A1)	110.4(11)
C(23B)-H(23E)	0.977(19)	Si(1)-C(9A)-H(9A2)	110.6(11)
C(23B)-H(23F)	0.991(17)	H(9A1)-C(9A)-H(9A2)	107.4(16)
C(24B)-H(24D)	0.991(16)	Si(1)-C(9A)-H(9A3)	112.4(11)
C(24B)-H(24E)	0.985(17)	H(9A1)-C(9A)-H(9A3)	108.1(16)
C(24B)-H(24F)	0.994(16)	H(9A2)-C(9A)-H(9A3)	107.9(16)
C(26B)-H(26D)	1.02(2)	Si(1)-C(10A)-H(10A)	108.2(10)
C(26B)-H(26E)	1.022(17)	Si(1)-C(10A)-H(10B)	108.1(11)

H(10A)-C(10A)-H(10B)	104.5(15)	C(20A)-C(19A)-C(18A)	97.74(13)
Si(1)-C(10A)-H(10C)	108.5(13)	O(6A)-C(20A)-C(21A)	109.08(14)
H(10A)-C(10A)-H(10C)	115.9(16)	O(6A)-C(20A)-C(19A)	103.63(13)
H(10B)-C(10A)-H(10C)	111.3(17)	C(21A)-C(20A)-C(19A)	110.94(15)
C(13A)-C(11A)-C(14A)	108.50(17)	O(6A)-C(20A)-H(20A)	107.1(9)
C(13A)-C(11A)-C(12A)	109.27(16)	C(21A)-C(20A)-H(20A)	112.5(9)
C(14A)-C(11A)-C(12A)	108.78(16)	C(19A)-C(20A)-H(20A)	113.0(9)
C(13A)-C(11A)-Si(1)	110.65(13)	C(22A)-C(21A)-C(20A)	112.11(15)
C(14A)-C(11A)-Si(1)	110.17(12)	C(22A)-C(21A)-H(21A)	108.0(9)
C(12A)-C(11A)-Si(1)	109.44(13)	C(20A)-C(21A)-H(21A)	111.1(9)
C(11A)-C(12A)-H(12A)	110.6(9)	C(22A)-C(21A)-H(21B)	111.3(9)
C(11A)-C(12A)-H(12B)	110.9(9)	C(20A)-C(21A)-H(21B)	107.9(9)
H(12A)-C(12A)-H(12B)	109.3(13)	H(21A)-C(21A)-H(21B)	106.3(13)
C(11A)-C(12A)-H(12C)	109.0(11)	C(17A)-C(22A)-C(21A)	121.63(16)
H(12A)-C(12A)-H(12C)	110.9(14)	C(17A)-C(22A)-C(23A)	125.70(16)
H(12B)-C(12A)-H(12C)	106.0(14)	C(21A)-C(22A)-C(23A)	112.67(16)
C(11A)-C(13A)-H(13A)	109.7(10)	C(22A)-C(23A)-H(23A)	115.5(12)
C(11A)-C(13A)-H(13B)	111.0(9)	C(22A)-C(23A)-H(23B)	108.7(11)
H(13A)-C(13A)-H(13B)	106.6(14)	H(23A)-C(23A)-H(23B)	102.7(15)
C(11A)-C(13A)-H(13C)	107.1(9)	C(22A)-C(23A)-H(23C)	113.8(11)
H(13A)-C(13A)-H(13C)	113.9(14)	H(23A)-C(23A)-H(23C)	108.7(17)
H(13B)-C(13A)-H(13C)	108.6(13)	H(23B)-C(23A)-H(23C)	106.5(16)
C(11A)-C(14A)-H(14A)	111.0(10)	C(18A)-C(24A)-H(24A)	112.1(10)
C(11A)-C(14A)-H(14B)	108.8(9)	C(18A)-C(24A)-H(24B)	110.3(9)
H(14A)-C(14A)-H(14B)	107.3(14)	H(24A)-C(24A)-H(24B)	107.2(13)
C(11A)-C(14A)-H(14C)	110.1(10)	C(18A)-C(24A)-H(24C)	111.6(9)
H(14A)-C(14A)-H(14C)	111.2(14)	H(24A)-C(24A)-H(24C)	107.9(13)
H(14B)-C(14A)-H(14C)	108.3(14)	H(24B)-C(24A)-H(24C)	107.4(13)
C(3A)-C(15A)-C(16A)	112.34(15)	O(7A)-C(25A)-O(6A)	121.67(15)
C(3A)-C(15A)-H(15A)	110.7(9)	O(7A)-C(25A)-C(18A)	129.29(16)
C(16A)-C(15A)-H(15A)	105.5(9)	O(6A)-C(25A)-C(18A)	108.93(14)
C(3A)-C(15A)-H(15B)	110.2(9)	C(19A)-C(26A)-H(26A)	110.5(9)
C(16A)-C(15A)-H(15B)	110.8(9)	C(19A)-C(26A)-H(26B)	107.7(10)
H(15A)-C(15A)-H(15B)	107.2(13)	H(26A)-C(26A)-H(26B)	107.1(13)
O(3A)-C(16A)-C(15A)	107.75(15)	C(19A)-C(26A)-H(26C)	109.7(11)
O(3A)-C(16A)-C(17A)	112.97(13)	H(26A)-C(26A)-H(26C)	109.4(14)
C(15A)-C(16A)-C(17A)	113.83(14)	H(26B)-C(26A)-H(26C)	112.4(15)
O(3A)-C(16A)-H(16A)	99.6(7)	O(4A)-C(27A)-O(5A)	123.21(17)
C(15A)-C(16A)-H(16A)	112.7(7)	O(4A)-C(27A)-C(19A)	125.58(16)
C(17A)-C(16A)-H(16A)	109.1(7)	O(5A)-C(27A)-C(19A)	111.16(16)
C(22A)-C(17A)-C(16A)	120.51(15)	O(5A)-C(28A)-H(28A)	110.6(12)
C(22A)-C(17A)-C(18A)	119.78(15)	O(5A)-C(28A)-H(28B)	103.5(13)
C(16A)-C(17A)-C(18A)	119.58(15)	H(28A)-C(28A)-H(28B)	109.6(18)
C(25A)-C(18A)-C(24A)	114.37(15)	O(5A)-C(28A)-H(28C)	110.8(11)
C(25A)-C(18A)-C(19A)	100.28(13)	H(28A)-C(28A)-H(28C)	112.4(17)
C(24A)-C(18A)-C(19A)	113.17(14)	H(28B)-C(28A)-H(28C)	109.6(17)
C(25A)-C(18A)-C(17A)	101.39(12)	O(1B)-Si(2)-C(9B)	112.15(8)
C(24A)-C(18A)-C(17A)	116.05(14)	O(1B)-Si(2)-C(10B)	109.07(9)
C(19A)-C(18A)-C(17A)	109.92(14)	C(9B)-Si(2)-C(10B)	108.51(10)
C(26A)-C(19A)-C(27A)	112.09(16)	O(1B)-Si(2)-C(11B)	104.44(7)
C(26A)-C(19A)-C(20A)	114.62(16)	C(9B)-Si(2)-C(11B)	111.62(9)
C(27A)-C(19A)-C(20A)	106.69(14)	C(10B)-Si(2)-C(11B)	111.00(9)
C(26A)-C(19A)-C(18A)	114.66(15)	C(1B)-O(1B)-Si(2)	127.35(10)
C(27A)-C(19A)-C(18A)	109.97(14)	C(2B)-O(2B)-C(8B)	112.18(13)

C(16B)-O(3B)-H(3B)	107.7(14)	C(11B)-C(12B)-H(12F)	112.8(10)
C(27B)-O(5B)-C(28B)	116.43(15)	H(12D)-C(12B)-H(12F)	105.8(14)
C(25B)-O(6B)-C(20B)	108.58(13)	H(12E)-C(12B)-H(12F)	110.6(14)
O(1B)-C(1B)-C(6B)	119.68(14)	C(11B)-C(13B)-H(13D)	109.3(12)
O(1B)-C(1B)-C(2B)	119.45(14)	C(11B)-C(13B)-H(13E)	110.6(12)
C(6B)-C(1B)-C(2B)	120.76(16)	H(13D)-C(13B)-H(13E)	108.2(17)
O(2B)-C(2B)-C(3B)	119.92(14)	C(11B)-C(13B)-H(13F)	108.0(10)
O(2B)-C(2B)-C(1B)	118.93(15)	H(13D)-C(13B)-H(13F)	110.4(16)
C(3B)-C(2B)-C(1B)	121.12(15)	H(13E)-C(13B)-H(13F)	110.3(16)
C(2B)-C(3B)-C(4B)	117.72(16)	C(11B)-C(14B)-H(14D)	109.6(10)
C(2B)-C(3B)-C(15B)	121.99(16)	C(11B)-C(14B)-H(14E)	110.8(12)
C(4B)-C(3B)-C(15B)	120.27(17)	H(14D)-C(14B)-H(14E)	105.5(15)
C(5B)-C(4B)-C(3B)	121.15(17)	C(11B)-C(14B)-H(14F)	108.6(12)
C(5B)-C(4B)-H(4B)	119.8(9)	H(14D)-C(14B)-H(14F)	115.0(16)
C(3B)-C(4B)-H(4B)	119.0(9)	H(14E)-C(14B)-H(14F)	107.3(17)
C(4B)-C(5B)-C(6B)	121.71(17)	C(3B)-C(15B)-C(16B)	112.59(15)
C(4B)-C(5B)-H(5B)	120.8(10)	C(3B)-C(15B)-H(15C)	108.3(10)
C(6B)-C(5B)-H(5B)	117.5(10)	C(16B)-C(15B)-H(15C)	110.0(9)
C(5B)-C(6B)-C(1B)	117.39(16)	C(3B)-C(15B)-H(15D)	110.1(9)
C(5B)-C(6B)-C(7B)	121.52(16)	C(16B)-C(15B)-H(15D)	107.5(9)
C(1B)-C(6B)-C(7B)	121.08(16)	H(15C)-C(15B)-H(15D)	108.3(13)
C(6B)-C(7B)-H(7B1)	113.2(10)	O(3B)-C(16B)-C(17B)	112.54(13)
C(6B)-C(7B)-H(7B2)	112.6(10)	O(3B)-C(16B)-C(15B)	108.21(14)
H(7B1)-C(7B)-H(7B2)	104.5(15)	C(17B)-C(16B)-C(15B)	114.24(14)
C(6B)-C(7B)-H(7B3)	111.5(11)	O(3B)-C(16B)-H(16B)	98.2(7)
H(7B1)-C(7B)-H(7B3)	109.7(14)	C(17B)-C(16B)-H(16B)	110.5(8)
H(7B2)-C(7B)-H(7B3)	104.8(14)	C(15B)-C(16B)-H(16B)	112.1(7)
O(2B)-C(8B)-H(8B1)	110.8(9)	C(22B)-C(17B)-C(16B)	120.84(15)
O(2B)-C(8B)-H(8B2)	107.1(10)	C(22B)-C(17B)-C(18B)	119.74(14)
H(8B1)-C(8B)-H(8B2)	110.8(14)	C(16B)-C(17B)-C(18B)	119.31(14)
O(2B)-C(8B)-H(8B3)	109.1(11)	C(24B)-C(18B)-C(25B)	113.84(15)
H(8B1)-C(8B)-H(8B3)	107.0(14)	C(24B)-C(18B)-C(19B)	113.46(14)
H(8B2)-C(8B)-H(8B3)	112.0(14)	C(25B)-C(18B)-C(19B)	100.43(13)
Si(2)-C(9B)-H(9B1)	110.4(11)	C(24B)-C(18B)-C(17B)	116.12(14)
Si(2)-C(9B)-H(9B2)	109.6(10)	C(25B)-C(18B)-C(17B)	102.22(12)
H(9B1)-C(9B)-H(9B2)	106.8(15)	C(19B)-C(18B)-C(17B)	109.14(13)
Si(2)-C(9B)-H(9B3)	109.9(11)	C(27B)-C(19B)-C(26B)	112.00(15)
H(9B1)-C(9B)-H(9B3)	110.6(15)	C(27B)-C(19B)-C(20B)	105.71(14)
H(9B2)-C(9B)-H(9B3)	109.6(15)	C(26B)-C(19B)-C(20B)	114.79(16)
Si(2)-C(10B)-H(10D)	109.2(11)	C(27B)-C(19B)-C(18B)	110.73(14)
Si(2)-C(10B)-H(10E)	110.5(10)	C(26B)-C(19B)-C(18B)	114.56(14)
H(10D)-C(10B)-H(10E)	107.8(15)	C(20B)-C(19B)-C(18B)	97.96(13)
Si(2)-C(10B)-H(10F)	113.3(10)	O(6B)-C(20B)-C(21B)	108.63(14)
H(10D)-C(10B)-H(10F)	108.2(15)	O(6B)-C(20B)-C(19B)	103.56(13)
H(10E)-C(10B)-H(10F)	107.7(14)	C(21B)-C(20B)-C(19B)	111.22(14)
C(14B)-C(11B)-C(12B)	109.06(17)	O(6B)-C(20B)-H(20B)	107.2(9)
C(14B)-C(11B)-C(13B)	108.9(2)	C(21B)-C(20B)-H(20B)	112.0(9)
C(12B)-C(11B)-C(13B)	108.43(17)	C(19B)-C(20B)-H(20B)	113.7(9)
C(14B)-C(11B)-Si(2)	111.31(14)	C(20B)-C(21B)-C(22B)	112.67(15)
C(12B)-C(11B)-Si(2)	108.80(13)	C(20B)-C(21B)-H(21C)	110.0(8)
C(13B)-C(11B)-Si(2)	110.29(13)	C(22B)-C(21B)-H(21C)	110.7(8)
C(11B)-C(12B)-H(12D)	110.8(11)	C(20B)-C(21B)-H(21D)	108.8(9)
C(11B)-C(12B)-H(12E)	111.3(10)	C(22B)-C(21B)-H(21D)	110.2(9)
H(12D)-C(12B)-H(12E)	105.1(14)	H(21C)-C(21B)-H(21D)	104.2(12)

C(17B)-C(22B)-C(23B)	126.52(16)
C(17B)-C(22B)-C(21B)	121.36(15)
C(23B)-C(22B)-C(21B)	112.11(15)
C(22B)-C(23B)-H(23D)	115.8(10)
C(22B)-C(23B)-H(23E)	113.2(10)
H(23D)-C(23B)-H(23E)	108.1(14)
C(22B)-C(23B)-H(23F)	108.3(9)
H(23D)-C(23B)-H(23F)	104.7(13)
H(23E)-C(23B)-H(23F)	105.9(14)
C(18B)-C(24B)-H(24D)	113.2(9)
C(18B)-C(24B)-H(24E)	110.4(10)
H(24D)-C(24B)-H(24E)	108.6(13)
C(18B)-C(24B)-H(24F)	110.5(9)
H(24D)-C(24B)-H(24F)	108.5(13)
H(24E)-C(24B)-H(24F)	105.3(13)
O(7B)-C(25B)-O(6B)	121.65(16)
O(7B)-C(25B)-C(18B)	129.16(16)
O(6B)-C(25B)-C(18B)	109.13(14)
C(19B)-C(26B)-H(26D)	109.0(11)
C(19B)-C(26B)-H(26E)	109.2(9)
H(26D)-C(26B)-H(26E)	111.8(14)
C(19B)-C(26B)-H(26F)	110.8(11)
H(26D)-C(26B)-H(26F)	105.9(15)
H(26E)-C(26B)-H(26F)	110.2(15)
O(4B)-C(27B)-O(5B)	123.36(17)
O(4B)-C(27B)-C(19B)	125.61(16)
O(5B)-C(27B)-C(19B)	110.94(15)
O(5B)-C(28B)-H(28D)	112.0(11)
O(5B)-C(28B)-H(28E)	107.3(11)
H(28D)-C(28B)-H(28E)	117.1(16)
O(5B)-C(28B)-H(28F)	112.6(10)
H(28D)-C(28B)-H(28F)	96.4(14)
H(28E)-C(28B)-H(28F)	111.3(15)

Table 4. Anisotropic displacement parameters ($Å^2 x\ 10^4$) for DCB31 (CCDC 283708). The anisotropic displacement factor exponent takes the form: $-2\pi^2$ [$h^2 a^{*2} U^{11}$ + ... + 2 h k a* b* U^{12}]

	U^{11}	U^{22}	U^{33}	U^{23}	U^{13}	U^{12}
Si(1)	246(3)	166(3)	247(3)	-46(2)	-122(2)	20(2)
O(1A)	218(7)	140(6)	209(6)	-42(5)	-89(5)	25(5)
O(2A)	235(7)	253(7)	173(6)	-30(5)	-67(5)	39(6)
O(3A)	198(7)	203(7)	373(8)	-42(6)	-118(6)	22(6)
O(4A)	350(8)	465(9)	301(8)	4(7)	-165(6)	64(7)
O(5A)	562(9)	293(8)	437(9)	-82(7)	-372(7)	140(7)
O(6A)	189(7)	196(7)	260(7)	-20(5)	-99(5)	-15(5)
O(7A)	170(7)	244(7)	230(7)	-32(5)	-82(5)	31(6)
C(1A)	140(9)	163(10)	236(10)	-59(8)	-64(8)	2(8)
C(2A)	125(9)	219(10)	200(10)	-34(8)	-58(7)	3(8)
C(3A)	99(9)	196(10)	304(11)	-37(8)	-44(8)	0(8)
C(4A)	175(10)	184(11)	378(12)	-115(10)	-14(9)	-18(8)
C(5A)	205(10)	327(12)	211(11)	-121(9)	0(8)	-51(9)
C(6A)	156(9)	238(11)	176(10)	-32(8)	-27(8)	-46(8)
C(7A)	308(13)	319(13)	205(11)	-27(9)	-78(9)	-47(11)
C(8A)	227(12)	296(13)	235(12)	-65(10)	4(9)	37(10)
C(9A)	642(18)	241(13)	365(13)	-23(10)	-322(13)	-22(12)
C(10A)	281(12)	289(13)	538(16)	-137(12)	-195(11)	40(10)
C(11A)	254(10)	188(10)	231(10)	-56(8)	-103(8)	11(8)
C(12A)	390(14)	169(12)	358(13)	-41(10)	-182(11)	1(10)
C(13A)	351(13)	250(13)	550(16)	-136(11)	-187(12)	57(10)
C(14A)	506(15)	206(12)	379(13)	22(10)	-264(12)	-19(11)
C(15A)	157(10)	174(11)	395(13)	2(9)	-100(9)	-11(8)
C(16A)	163(10)	150(10)	287(11)	-20(8)	-78(8)	13(8)
C(17A)	116(9)	190(10)	297(10)	-27(8)	-78(8)	-11(8)
C(18A)	178(10)	160(10)	270(10)	-26(8)	-103(8)	10(8)
C(19A)	222(10)	189(10)	341(11)	-43(8)	-145(9)	34(8)
C(20A)	242(11)	139(10)	339(11)	8(9)	-143(9)	4(8)
C(21A)	213(11)	162(10)	324(11)	-52(9)	-93(9)	17(9)
C(22A)	140(9)	178(10)	300(11)	-25(8)	-48(8)	10(8)
C(23A)	272(12)	208(12)	307(12)	-50(10)	-27(10)	10(10)
C(24A)	238(12)	217(11)	321(12)	-52(9)	-141(10)	12(9)
C(25A)	220(10)	213(11)	163(9)	-8(8)	-94(8)	-19(8)
C(26A)	263(12)	263(13)	599(16)	-47(12)	-252(12)	52(10)
C(27A)	365(12)	184(11)	394(12)	-14(9)	-269(10)	-28(9)
C(28A)	750(20)	329(15)	444(15)	-103(12)	-428(14)	111(14)
Si(2)	224(3)	166(3)	247(3)	-30(2)	-96(2)	14(2)
O(1B)	223(7)	140(7)	237(7)	-21(5)	-98(5)	13(5)
O(2B)	255(7)	269(7)	176(7)	0(6)	-64(5)	-3(6)
O(3B)	237(8)	179(7)	385(8)	-45(6)	-133(6)	34(6)
O(4B)	300(8)	425(9)	267(7)	-10(6)	-100(6)	72(7)
O(5B)	431(8)	303(8)	273(7)	-35(6)	-207(6)	95(6)
O(6B)	175(7)	173(7)	257(7)	-21(5)	-58(5)	-15(5)
O(7B)	179(7)	243(7)	246(7)	-58(6)	-74(5)	33(6)
C(1B)	149(9)	135(9)	218(10)	-21(8)	-63(8)	1(7)
C(2B)	141(9)	212(10)	167(9)	1(8)	-48(7)	7(8)

C(3B)	121(9)	188(10)	273(10)	15(8)	-54(8)	-24(8)
C(4B)	182(10)	150(11)	346(12)	-63(9)	-58(9)	-11(8)
C(5B)	171(10)	289(12)	213(11)	-96(9)	-15(8)	-23(8)
C(6B)	149(9)	212(10)	178(9)	-1(8)	-37(7)	-24(8)
C(7B)	294(12)	270(12)	189(11)	31(9)	-89(9)	-29(10)
C(8B)	303(13)	269(13)	222(12)	-62(10)	-26(9)	15(10)
C(9B)	321(13)	249(12)	356(13)	-55(10)	-177(11)	25(10)
C(10B)	290(12)	329(13)	334(13)	-78(11)	-82(10)	-43(11)
C(11B)	242(10)	183(10)	341(11)	-73(8)	-111(9)	19(8)
C(12B)	332(13)	219(12)	412(14)	-126(10)	-134(11)	19(10)
C(13B)	329(14)	304(14)	624(18)	-215(13)	7(12)	17(12)
C(14B)	586(17)	253(13)	755(19)	-156(13)	-461(16)	154(13)
C(15B)	181(11)	171(11)	348(12)	48(9)	-92(9)	-14(9)
C(16B)	171(10)	135(10)	264(10)	2(8)	-92(8)	-13(8)
C(17B)	128(9)	179(10)	227(10)	0(8)	-58(8)	-16(8)
C(18B)	186(10)	141(10)	236(10)	-8(8)	-88(8)	-2(8)
C(19B)	231(10)	186(10)	232(10)	-4(8)	-93(8)	9(8)
C(20B)	213(10)	139(10)	267(11)	27(8)	-74(8)	0(8)
C(21B)	215(11)	154(10)	265(11)	-55(8)	-66(9)	22(9)
C(22B)	169(10)	174(10)	218(10)	-17(8)	-50(8)	-14(8)
C(23B)	279(12)	219(12)	218(11)	-32(9)	-31(9)	14(10)
C(24B)	243(12)	193(11)	284(12)	-45(9)	-124(9)	-5(9)
C(25B)	231(10)	207(10)	142(9)	-28(8)	-79(8)	-4(9)
C(26B)	214(11)	284(13)	350(13)	20(10)	-119(10)	53(10)
C(27B)	272(11)	193(10)	312(11)	-10(9)	-156(9)	-17(9)
C(28B)	468(15)	337(13)	264(12)	-40(10)	-188(11)	62(12)

Table 5. Hydrogen coordinates (x 10^4) and isotropic displacement parameters ($Å^2$x 10^3) for DCB31 (CCDC 283708).

	x	y	z	U_{iso}
H(3A)	3688(19)	4314(14)	814(14)	78(8)
H(4A)	201(13)	4175(11)	3162(11)	30(5)
H(5A)	-132(13)	2974(10)	4325(11)	25(5)
H(7A1)	-544(16)	867(12)	4330(12)	46(6)
H(7A2)	-69(13)	1455(11)	4872(12)	32(5)
H(7A3)	760(15)	894(11)	4127(11)	40(6)
H(8A1)	2967(16)	2594(13)	644(12)	53(7)
H(8A2)	2642(16)	2081(13)	-37(14)	60(7)
H(8A3)	2505(14)	1627(12)	968(12)	41(6)
H(9A1)	45(16)	1427(14)	673(13)	59(7)
H(9A2)	-397(16)	488(13)	676(13)	58(7)
H(9A3)	985(18)	670(14)	351(14)	71(8)
H(10A)	-1676(14)	505(12)	3497(13)	46(6)
H(10B)	-2032(17)	324(13)	2692(13)	55(7)
H(10C)	-1708(17)	1284(14)	2659(14)	66(8)
H(12A)	-171(13)	-1113(10)	1309(12)	28(5)
H(12B)	-1181(15)	-1199(10)	2360(11)	29(5)
H(12C)	-170(14)	-1847(12)	2143(11)	33(5)
H(13A)	1874(15)	-1379(12)	1840(12)	45(6)
H(13B)	2135(14)	-385(11)	1849(11)	29(5)
H(13C)	1796(13)	-581(11)	968(12)	34(5)
H(14A)	-721(16)	-845(12)	3734(12)	49(6)
H(14B)	627(14)	-554(11)	3490(11)	31(5)
H(14C)	355(14)	-1552(12)	3421(12)	43(6)
H(15A)	425(13)	4736(10)	1503(10)	25(5)
H(15B)	998(13)	4120(11)	721(11)	30(5)
H(16A)	2236(11)	4803(8)	1738(9)	3(4)
H(20A)	3219(13)	7783(11)	-1165(11)	34(5)
H(21A)	2915(13)	7589(10)	494(10)	21(5)
H(21B)	1745(13)	7611(10)	350(10)	26(5)
H(23A)	1387(17)	5894(14)	2315(14)	64(7)
H(23B)	941(17)	6760(13)	2048(12)	54(7)
H(23C)	2132(17)	6743(13)	2117(13)	60(7)
H(24A)	3128(14)	4891(11)	-1621(12)	33(5)
H(24B)	1857(15)	4754(10)	-810(11)	32(5)
H(24C)	2960(13)	4324(11)	-645(11)	28(5)
H(26A)	782(14)	6455(11)	27(12)	33(5)
H(26B)	880(14)	6179(12)	-967(11)	39(6)
H(26C)	997(14)	7196(12)	-883(12)	40(6)
H(28A)	3459(16)	7683(14)	-3771(13)	55(7)
H(28B)	2220(20)	7377(15)	-3685(15)	87(9)
H(28C)	3208(16)	6680(13)	-3761(13)	53(7)
H(3B)	1220(20)	5723(16)	4087(17)	114(10)
H(4B)	4665(12)	5890(10)	1672(10)	19(5)
H(5B)	5010(13)	7083(10)	475(11)	26(5)
H(7B1)	5590(16)	9117(12)	338(12)	44(6)
H(7B2)	4273(15)	9247(12)	709(12)	45(6)

H(7B3)	4798(14)	8624(11)	-15(12)	39(6)
H(8B1)	2458(13)	8392(11)	3792(11)	29(5)
H(8B2)	2434(13)	8067(11)	4816(12)	32(5)
H(8B3)	2056(16)	7416(13)	4285(12)	51(6)
H(9B1)	5015(17)	8795(12)	4117(14)	58(7)
H(9B2)	6204(15)	9337(12)	3590(11)	43(6)
H(9B3)	6052(15)	8483(12)	3257(12)	41(6)
H(10D)	6756(15)	9418(13)	1273(12)	47(6)
H(10E)	6969(15)	10252(12)	1610(12)	45(6)
H(10F)	6179(15)	10302(12)	1002(13)	52(6)
H(12D)	4742(15)	11708(12)	3470(12)	43(6)
H(12E)	5801(14)	11364(11)	2713(12)	30(5)
H(12F)	5359(15)	10891(12)	3820(13)	47(6)
H(13D)	3564(17)	9949(14)	4480(14)	66(8)
H(13E)	2761(17)	9917(13)	3923(13)	60(7)
H(13F)	2901(15)	10825(12)	4254(12)	44(6)
H(14D)	3408(15)	11588(12)	2666(12)	48(6)
H(14E)	3379(17)	10716(13)	2251(13)	62(7)
H(14F)	4577(18)	11267(13)	1777(14)	62(8)
H(15C)	3961(13)	6006(11)	4080(11)	29(5)
H(15D)	4563(13)	5374(10)	3328(10)	20(5)
H(16B)	2690(11)	5298(9)	3116(10)	13(4)
H(20B)	1938(12)	2330(10)	6009(10)	21(5)
H(21C)	1972(13)	2468(10)	4457(10)	21(5)
H(21D)	3183(13)	2494(10)	4462(10)	19(5)
H(23D)	3419(14)	4199(12)	2518(12)	43(6)
H(23E)	2648(16)	3318(12)	2812(12)	47(6)
H(23F)	3899(15)	3285(11)	2794(11)	34(5)
H(24D)	2117(13)	5778(11)	5512(10)	26(5)
H(24E)	3246(15)	5340(11)	5603(11)	34(5)
H(24F)	2058(13)	5180(10)	6467(12)	29(5)
H(26D)	4364(16)	3949(13)	5623(12)	55(7)
H(26E)	4271(14)	3613(11)	4680(12)	42(6)
H(26F)	4218(15)	2973(12)	5585(12)	39(6)
H(28D)	2178(16)	3296(13)	8539(13)	51(6)
H(28E)	3210(17)	2533(13)	8372(13)	60(7)
H(28F)	1846(15)	2391(12)	8536(12)	41(6)

Table 6. Hydrogen bonds for DCB31 (CCDC 283708) [Å and °].

D-H...A	d(D-H)	d(H...A)	d(D...A)	<(DHA)
O(3A)-H(3A)...O(7A)#1	0.92(2)	1.88(2)	2.7946(17)	173(2)
O(3B)-H(3B)...O(7B)#2	0.98(3)	1.81(3)	2.7910(17)	176(2)

Symmetry transformations used to generate equivalent atoms:
#1 -x+1,-y+1,-z
#2 -x,-y+1,-z+1

CALIFORNIA INSTITUTE OF TECHNOLOGY

BECKMAN INSTITUTE

X-RAY CRYSTALLOGRAPHY LABORATORY

Crystal Structure Analysis of:

Bisacetoxyacetal 220 (DCB32)

(CCDC 289914)

Contents:

Figure A6.3 Representation of Bisacetoxyacetal **220**

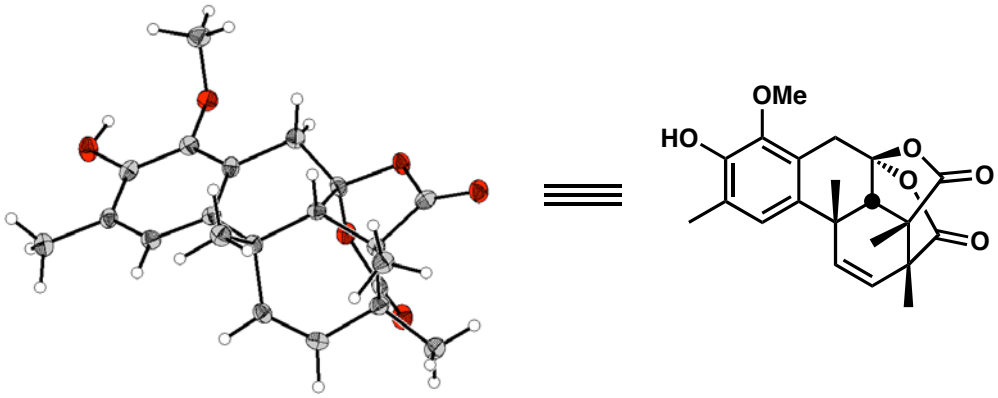

Table 1. Crystal data and structure refinement for DCB32 (CCDC 289914).

Empirical formula	$C_{21}H_{22}O_6$
Formula weight	370.39
Crystallization Solvent	Et_2O/hexanes
Crystal Habit	Needle
Crystal size	0.39 x 0.22 x 0.19 mm^3
Crystal color	Colorless

Data Collection

Type of diffractometer	Bruker SMART 1000
Wavelength	0.71073 Å MoKα
Data Collection Temperature	100(2) K
θ range for 13215 reflections used in lattice determination	2.27 to 28.03°
Unit cell dimensions	a = 21.9617(16) Å b = 8.5236(6) Å c = 19.6358(14) Å
Volume	3675.7(5) $Å^3$
Z	8
Crystal system	Orthorhombic
Space group	Pbcn
Density (calculated)	1.339 Mg/m^3
F(000)	1568
Data collection program	Bruker SMART v5.630
θ range for data collection	1.85 to 28.38°
Completeness to θ = 28.38°	94.2 %
Index ranges	$-28 \le h \le 28$, $-11 \le k \le 11$, $-24 \le l \le 26$
Data collection scan type	ω scans at 5 ϕ settings
Data reduction program	Bruker SAINT v6.45A
Reflections collected	50823
Independent reflections	4344 [R_{int}= 0.0809]
Absorption coefficient	0.098 mm^{-1}
Absorption correction	None
Max. and min. transmission	0.9816 and 0.9628

Table 1 (cont.)

Structure solution and Refinement

Structure solution program	Bruker XS v6.12
Primary solution method	Direct methods
Secondary solution method	Difference Fourier map
Hydrogen placement	Difference Fourier map
Structure refinement program	Bruker XL v6.12
Refinement method	Full matrix least-squares on F^2
Data / restraints / parameters	4344 / 0 / 332
Treatment of hydrogen atoms	Unrestrained
Goodness-of-fit on F^2	1.880
Final R indices [I>2σ(I), 3001 reflections]	R1 = 0.0466, *w*R2 = 0.0611
R indices (all data)	R1 = 0.0778, *w*R2 = 0.0633
Type of weighting scheme used	Sigma
Weighting scheme used	$w=1/\sigma^2(Fo^2)$
Max shift/error	0.001
Average shift/error	0.000
Largest diff. peak and hole	0.331 and -0.276 e.Å^{-3}

Special Refinement Details

Refinement of F^2 against ALL reflections. The weighted R-factor (*w*R) and goodness of fit (S) are based on F^2, conventional R-factors (R) are based on F, with F set to zero for negative F^2. The threshold expression of $F^2 > 2\sigma(F^2)$ is used only for calculating R-factors(gt) etc. and is not relevant to the choice of reflections for refinement. R-factors based on F^2 are statistically about twice as large as those based on F, and R-factors based on ALL data will be even larger.

All esds (except the esd in the dihedral angle between two l.s. planes) are estimated using the full covariance matrix. The cell esds are taken into account individually in the estimation of esds in distances, angles and torsion angles; correlations between esds in cell parameters are only used when they are defined by crystal symmetry. An approximate (isotropic) treatment of cell esds is used for estimating esds involving l.s. planes.

Table 2. Atomic coordinates (x 10^4) and equivalent isotropic displacement parameters ($Å^2$x 10^3) for DCB32 (CCDC 289914). U(eq) is defined as the trace of the orthogonalized U^{ij} tensor.

	x	y	z	U_{eq}
O(1)	2750(1)	8498(1)	11657(1)	20(1)
O(2)	3463(1)	6194(1)	12216(1)	22(1)
O(3)	4347(1)	12923(1)	9814(1)	24(1)
O(4)	3652(1)	11114(1)	10020(1)	19(1)
O(5)	2849(1)	12317(1)	8276(1)	22(1)
O(6)	2812(1)	11335(1)	9329(1)	18(1)
C(1)	3243(1)	8168(2)	10565(1)	16(1)
C(2)	3171(1)	7737(2)	11243(1)	16(1)
C(3)	3539(1)	6609(2)	11548(1)	17(1)
C(4)	3993(1)	5863(2)	11174(1)	17(1)
C(5)	4067(1)	6316(2)	10500(1)	17(1)
C(6)	3705(1)	7443(2)	10182(1)	16(1)
C(7)	3834(1)	7839(2)	9427(1)	15(1)
C(8)	3386(1)	9079(2)	9173(1)	15(1)
C(9)	3172(1)	10217(2)	9710(1)	17(1)
C(10)	2832(1)	9437(2)	10272(1)	18(1)
C(11)	2149(1)	7822(2)	11619(1)	25(1)
C(12)	4388(1)	4633(2)	11498(1)	24(1)
C(13)	3759(1)	6327(2)	8998(1)	20(1)
C(14)	4480(1)	8405(2)	9339(1)	18(1)
C(15)	4634(1)	9789(2)	9089(1)	19(1)
C(16)	4175(1)	11058(2)	8904(1)	18(1)
C(17)	3586(1)	10261(2)	8630(1)	15(1)
C(18)	4452(1)	12247(2)	8416(1)	23(1)
C(19)	3652(1)	9638(2)	7907(1)	21(1)
C(20)	4062(1)	11828(2)	9598(1)	19(1)
C(21)	3057(1)	11422(2)	8689(1)	17(1)

Table 3. Bond lengths [Å] and angles [°] for DCB32 (CCDC 289914).

O(1)-C(2)	1.3917(16)	C(19)-H(19B)	1.006(15)
O(1)-C(11)	1.4405(18)	C(19)-H(19C)	0.974(17)
O(2)-C(3)	1.3695(17)		
O(2)-H(2)	0.887(19)	C(2)-O(1)-C(11)	113.13(12)
O(3)-C(20)	1.2002(16)	C(3)-O(2)-H(2)	108.0(13)
O(4)-C(20)	1.3677(17)	C(20)-O(4)-C(9)	117.64(11)
O(4)-C(9)	1.4373(16)	C(21)-O(6)-C(9)	107.19(11)
O(5)-C(21)	1.2031(16)	C(2)-C(1)-C(6)	118.61(13)
O(6)-C(21)	1.3697(16)	C(2)-C(1)-C(10)	118.79(13)
O(6)-C(9)	1.4462(16)	C(6)-C(1)-C(10)	122.58(13)
C(1)-C(2)	1.3899(19)	C(1)-C(2)-C(3)	121.92(13)
C(1)-C(6)	1.4059(19)	C(1)-C(2)-O(1)	120.79(13)
C(1)-C(10)	1.521(2)	C(3)-C(2)-O(1)	117.17(13)
C(2)-C(3)	1.3915(19)	O(2)-C(3)-C(2)	121.36(13)
C(3)-C(4)	1.3917(19)	O(2)-C(3)-C(4)	118.33(13)
C(4)-C(5)	1.388(2)	C(2)-C(3)-C(4)	120.30(13)
C(4)-C(12)	1.503(2)	C(5)-C(4)-C(3)	117.36(14)
C(5)-C(6)	1.3954(19)	C(5)-C(4)-C(12)	122.04(14)
C(5)-H(5)	0.960(12)	C(3)-C(4)-C(12)	120.60(14)
C(6)-C(7)	1.546(2)	C(4)-C(5)-C(6)	123.54(14)
C(7)-C(14)	1.5080(19)	C(4)-C(5)-H(5)	118.2(7)
C(7)-C(8)	1.5268(19)	C(6)-C(5)-H(5)	118.2(7)
C(7)-C(13)	1.548(2)	C(5)-C(6)-C(1)	118.25(14)
C(8)-C(9)	1.5086(19)	C(5)-C(6)-C(7)	118.43(13)
C(8)-C(17)	1.5300(19)	C(1)-C(6)-C(7)	123.32(13)
C(8)-H(8)	0.966(13)	C(14)-C(7)-C(8)	110.30(12)
C(9)-C(10)	1.490(2)	C(14)-C(7)-C(6)	110.57(12)
C(10)-H(10A)	1.027(14)	C(8)-C(7)-C(6)	110.27(12)
C(10)-H(10B)	0.976(14)	C(14)-C(7)-C(13)	107.68(12)
C(11)-H(11A)	1.018(15)	C(8)-C(7)-C(13)	109.33(12)
C(11)-H(11B)	0.941(14)	C(6)-C(7)-C(13)	108.64(12)
C(11)-H(11C)	1.017(15)	C(9)-C(8)-C(7)	114.69(12)
C(12)-H(12A)	0.965(18)	C(9)-C(8)-C(17)	98.80(11)
C(12)-H(12B)	0.994(18)	C(7)-C(8)-C(17)	119.94(12)
C(12)-H(12C)	0.989(17)	C(9)-C(8)-H(8)	106.2(8)
C(13)-H(13A)	1.003(14)	C(7)-C(8)-H(8)	107.8(8)
C(13)-H(13B)	0.988(15)	C(17)-C(8)-H(8)	108.4(8)
C(13)-H(13C)	0.996(14)	O(4)-C(9)-O(6)	105.61(11)
C(14)-C(15)	1.323(2)	O(4)-C(9)-C(10)	106.90(12)
C(14)-H(14)	0.975(13)	O(6)-C(9)-C(10)	113.83(12)
C(15)-C(16)	1.523(2)	O(4)-C(9)-C(8)	114.14(12)
C(15)-H(15)	0.987(11)	O(6)-C(9)-C(8)	103.46(11)
C(16)-C(18)	1.520(2)	C(10)-C(9)-C(8)	112.83(13)
C(16)-C(20)	1.533(2)	C(9)-C(10)-C(1)	107.47(13)
C(16)-C(17)	1.5582(19)	C(9)-C(10)-H(10A)	107.7(7)
C(17)-C(19)	1.523(2)	C(1)-C(10)-H(10A)	113.2(8)
C(17)-C(21)	1.530(2)	C(9)-C(10)-H(10B)	111.0(8)
C(18)-H(18A)	0.989(14)	C(1)-C(10)-H(10B)	110.6(8)
C(18)-H(18B)	0.977(15)	H(10A)-C(10)-H(10B)	106.9(11)
C(18)-H(18C)	1.001(16)	O(1)-C(11)-H(11A)	111.2(8)
C(19)-H(19A)	0.956(14)	O(1)-C(11)-H(11B)	104.9(8)

H(11A)-C(11)-H(11B)	109.5(11)
O(1)-C(11)-H(11C)	111.2(8)
H(11A)-C(11)-H(11C)	110.5(12)
H(11B)-C(11)-H(11C)	109.4(12)
C(4)-C(12)-H(12A)	112.6(11)
C(4)-C(12)-H(12B)	111.6(10)
H(12A)-C(12)-H(12B)	104.8(14)
C(4)-C(12)-H(12C)	112.2(10)
H(12A)-C(12)-H(12C)	108.5(14)
H(12B)-C(12)-H(12C)	106.7(14)
C(7)-C(13)-H(13A)	109.3(8)
C(7)-C(13)-H(13B)	111.2(8)
H(13A)-C(13)-H(13B)	109.6(11)
C(7)-C(13)-H(13C)	108.8(8)
H(13A)-C(13)-H(13C)	110.4(11)
H(13B)-C(13)-H(13C)	107.5(11)
C(15)-C(14)-C(7)	124.68(14)
C(15)-C(14)-H(14)	118.8(8)
C(7)-C(14)-H(14)	116.5(7)
C(14)-C(15)-C(16)	123.55(14)
C(14)-C(15)-H(15)	119.1(7)
C(16)-C(15)-H(15)	117.2(7)
C(18)-C(16)-C(15)	111.10(13)
C(18)-C(16)-C(20)	109.81(13)
C(15)-C(16)-C(20)	101.49(11)
C(18)-C(16)-C(17)	113.92(13)
C(15)-C(16)-C(17)	108.83(12)
C(20)-C(16)-C(17)	111.00(12)
C(19)-C(17)-C(21)	111.62(12)
C(19)-C(17)-C(8)	116.54(13)
C(21)-C(17)-C(8)	99.01(11)
C(19)-C(17)-C(16)	113.21(12)
C(21)-C(17)-C(16)	108.81(12)
C(8)-C(17)-C(16)	106.55(11)
C(16)-C(18)-H(18A)	107.5(8)
C(16)-C(18)-H(18B)	111.6(8)
H(18A)-C(18)-H(18B)	110.3(12)
C(16)-C(18)-H(18C)	108.8(9)
H(18A)-C(18)-H(18C)	111.5(12)
H(18B)-C(18)-H(18C)	107.2(12)
C(17)-C(19)-H(19A)	107.7(8)
C(17)-C(19)-H(19B)	110.6(8)
H(19A)-C(19)-H(19B)	111.7(12)
C(17)-C(19)-H(19C)	113.5(9)
H(19A)-C(19)-H(19C)	104.7(12)
H(19B)-C(19)-H(19C)	108.6(12)
O(3)-C(20)-O(4)	118.39(14)
O(3)-C(20)-C(16)	124.22(14)
O(4)-C(20)-C(16)	117.06(13)
O(5)-C(21)-O(6)	120.27(13)
O(5)-C(21)-C(17)	130.33(14)
O(6)-C(21)-C(17)	109.40(12)

Table 4. Anisotropic displacement parameters ($Å^2 x\ 10^4$) for DCB32 (CCDC 289914). The anisotropic displacement factor exponent takes the form: $-2\pi^2$ [$h^2 a^{*2} U^{11}$ + ... + 2 h k a* b* U^{12}]

	U^{11}	U^{22}	U^{33}	U^{23}	U^{13}	U^{12}
O(1)	219(6)	189(6)	191(6)	-17(5)	52(5)	31(5)
O(2)	300(7)	204(6)	154(6)	14(5)	13(5)	46(5)
O(3)	273(6)	157(6)	288(7)	-25(5)	-80(5)	-20(5)
O(4)	233(6)	155(6)	172(6)	-15(5)	-14(5)	-8(5)
O(5)	248(6)	236(6)	179(6)	56(5)	-2(5)	32(5)
O(6)	215(6)	187(6)	141(6)	24(5)	18(5)	52(5)
C(1)	198(9)	125(8)	164(8)	-5(7)	-11(7)	-4(7)
C(2)	186(8)	133(8)	168(9)	-39(7)	23(7)	0(7)
C(3)	227(9)	148(9)	130(9)	-8(7)	-8(7)	-46(7)
C(4)	201(9)	112(8)	200(9)	-4(7)	-20(7)	-16(7)
C(5)	172(9)	147(8)	204(9)	-35(7)	31(7)	20(7)
C(6)	172(8)	139(8)	166(8)	-26(7)	1(7)	-13(7)
C(7)	156(8)	139(8)	161(8)	-18(7)	3(7)	18(7)
C(8)	136(8)	152(8)	162(9)	-18(7)	-2(7)	-18(7)
C(9)	166(8)	156(8)	183(8)	15(7)	-40(7)	20(7)
C(10)	211(9)	175(9)	157(9)	1(7)	36(8)	24(7)
C(11)	232(10)	239(10)	269(11)	-6(9)	92(9)	14(8)
C(12)	245(10)	208(10)	272(11)	45(8)	2(8)	35(8)
C(13)	221(10)	182(9)	205(10)	-34(8)	4(8)	11(8)
C(14)	179(9)	198(9)	159(9)	-11(7)	3(7)	40(7)
C(15)	141(8)	234(9)	180(9)	-23(7)	3(7)	0(7)
C(16)	168(8)	170(8)	188(9)	-1(7)	3(7)	-14(7)
C(17)	167(8)	146(8)	148(8)	-11(7)	10(7)	7(7)
C(18)	228(10)	218(10)	249(10)	30(8)	2(8)	-26(8)
C(19)	239(10)	241(10)	159(9)	7(8)	3(8)	-8(9)
C(20)	178(9)	154(9)	228(9)	32(7)	-44(7)	41(7)
C(21)	188(9)	169(8)	159(9)	-30(7)	-2(7)	-52(7)

Table 5. Hydrogen coordinates (x 10^4) and isotropic displacement parameters ($Å^2$x 10^3) for DCB32 (CCDC 289914).

	x	y	z	U_{iso}
H(2)	3183(9)	6820(20)	12395(10)	66(7)
H(5)	4383(6)	5822(14)	10239(6)	7(3)
H(8)	3027(6)	8542(15)	9011(6)	11(4)
H(10A)	2434(6)	9003(15)	10073(7)	16(4)
H(10B)	2719(6)	10191(17)	10624(7)	21(4)
H(11A)	1959(6)	8003(17)	11152(8)	27(4)
H(11B)	1921(6)	8358(16)	11952(7)	15(4)
H(11C)	2158(6)	6658(19)	11731(7)	26(4)
H(12A)	4187(8)	3630(20)	11532(9)	59(6)
H(12B)	4495(7)	4910(20)	11975(9)	56(6)
H(12C)	4777(8)	4488(19)	11252(8)	49(5)
H(13A)	4066(6)	5529(17)	9151(7)	26(4)
H(13B)	3815(6)	6542(16)	8508(8)	22(4)
H(13C)	3338(7)	5917(15)	9061(7)	22(4)
H(14)	4801(6)	7679(15)	9475(6)	12(4)
H(15)	5070(5)	10055(15)	9044(6)	9(4)
H(18A)	4804(6)	12732(16)	8649(7)	23(4)
H(18B)	4157(7)	13051(17)	8286(7)	29(4)
H(18C)	4578(6)	11692(17)	7990(8)	32(5)
H(19A)	3300(6)	9017(16)	7809(7)	20(4)
H(19B)	4038(7)	9014(17)	7859(7)	30(5)
H(19C)	3650(6)	10458(19)	7561(8)	36(5)

Table 6. Hydrogen bonds for DCB32 (CCDC 289914) [Å and °].

D-H...A	d(D-H)	d(H...A)	d(D...A)	<(DHA)
O(2)-H(2)...O(5)#1	0.887(19)	2.02(2)	2.7848(15)	144.2(17)
O(2)-H(2)...O(1)	0.887(19)	2.248(19)	2.7418(14)	114.8(15)

Symmetry transformations used to generate equivalent atoms:
#1 x,-y+2,z+1/2

CALIFORNIA INSTITUTE OF TECHNOLOGY

BECKMAN INSTITUTE

X-RAY CRYSTALLOGRAPHY LABORATORY

Crystal Structure Analysis of:

Alcohol 255 (DCB34)

Contents:

Figure A6.4 Representation of Alcohol **255**

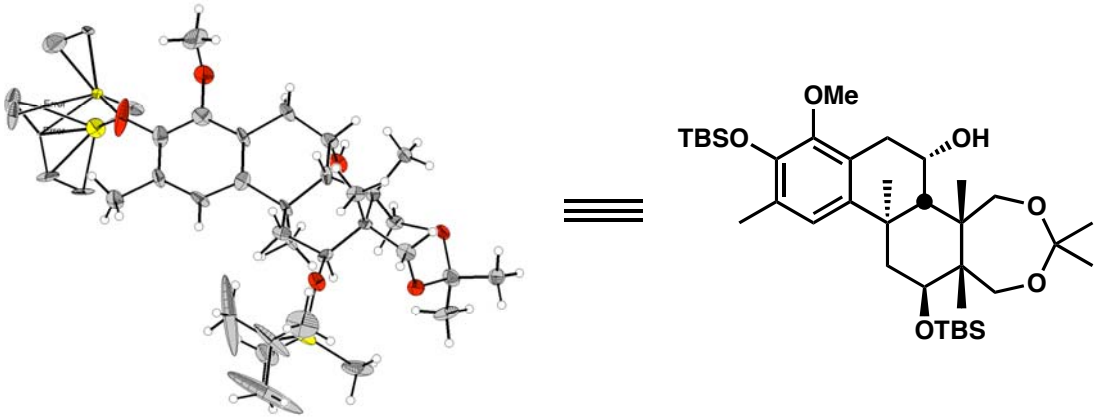

Table 1. Crystal data and structure refinement for dcb34.

Empirical formula	C36 H49 O6 Si2
Formula weight	633.93
Crystallization Solvent	Methylene Chloride
Crystal Habit	Fragment
Crystal size	0.45 x 0.20 x 0.19 mm^3
Crystal color	Colorless

Data Collection

Preliminary Photos		
Type of diffractometer	Bruker SMART 1000	
Wavelength	0.71073 Å MoKα	
Data Collection Temperature	100(2) K	
θ range for 2391 reflections used in lattice determination	2.25 to 25.75°	
Unit cell dimensions	a = 8.012(3) Å b = 12.103(5) Å c = 21.064(8) Å	α= 104.652(5)° β= 92.405(7)° γ = 98.610(6)°
Volume	1947.0(12) $Å^3$	
Z	2	
Crystal system	Triclinic	
Space group	P-1	
Density (calculated)	1.081 Mg/m^3	
F(000)	682	
θ range for data collection	1.76 to 27.12°	
Completeness to θ = 27.12°	78.9 %	
Index ranges	-10<=h<=8, -15<=k<=15, -26<=l<=12	
Data collection scan type	scans at 3 settings	
Reflections collected	8155	
Independent reflections	6807 [R_{int}= 0.0961; GOF_{merge}=]	
Absorption coefficient	0.129 mm^{-1}	
Absorption correction	None	

Table 1 (cont.)

Structure solution and Refinement

Structure solution program	SHELXS-97 (Sheldrick, 1990)
Primary solution method	direct
Secondary solution method	difmap
Hydrogen placement	geom
Structure refinement program	SHELXL-97 (Sheldrick, 1997)
Refinement method	Full-matrix least-squares on F^2
Data / restraints / parameters	6807 / 0 / 456
Treatment of hydrogen atoms	mixed
Goodness-of-fit on F^2	2.722
Final R indices [I>2σ(I), 4077 reflections]	R1 = 0.1484, wR2 = 0.1836
R indices (all data)	R1 = 0.2120, wR2 = 0.1890
Type of weighting scheme used	calc
Weighting scheme used	calc w=1/[^2^(Fo^2^)+(0.0000P)^2^+0.0000P] where P=(Fo^2^+2Fc^2^)/3
Max shift/error	1.254
Average shift/error	0.004
Largest diff. peak and hole	0.655 and -0.594 e.$Å^{-3}$

Table 2. Atomic coordinates (x 10^4) and equivalent isotropic displacement parameters ($Å^2$x 10^3) for dcb34. U(eq) is defined as the trace of the orthogonalized U^{ij} tensor.

	x	y	z	U_{eq}	Occ
Si(2A)	11898(6)	1267(5)	4132(2)	15(2)	0.480(9)
Si(2B)	12395(6)	2036(5)	4004(2)	32(2)	0.520(9)
O(6)	2561(6)	4434(4)	2066(2)	26(1)	1
O(4)	3040(6)	1577(4)	-102(2)	21(1)	1
O(3)	7053(6)	620(4)	947(2)	27(1)	1
O(5)	2281(6)	3355(4)	432(2)	24(1)	1
O(1A)	10070(40)	1775(16)	4115(16)	23(7)	0.480(9)
C(1)	2380(8)	2466(5)	1362(3)	16(2)	1
O(2)	8803(7)	-67(4)	2989(3)	41(2)	1
C(2)	4738(9)	3387(6)	2278(3)	23(2)	1
C(3)	4299(8)	1754(6)	459(3)	21(2)	1
C(4)	4798(8)	1409(6)	1584(3)	20(2)	1
C(5)	5795(9)	384(6)	1376(3)	23(2)	1
C(6)	5952(8)	2528(5)	1996(3)	19(2)	1
C(7)	7591(9)	3162(6)	3129(4)	25(2)	1
C(8)	7268(8)	3098(6)	1588(3)	21(2)	1
C(9)	3425(8)	1492(6)	1051(3)	16(2)	1
C(10)	3552(8)	3555(5)	1752(3)	19(2)	1
C(11)	8602(9)	3023(6)	3647(3)	24(2)	1
C(12)	6986(9)	2280(7)	2562(3)	24(2)	1
C(13)	7315(8)	1161(6)	2542(3)	22(2)	1
C(14)	1097(8)	2053(6)	1829(3)	20(2)	1
C(15)	1296(8)	2793(6)	853(3)	22(2)	1
C(16)	8395(9)	1028(6)	3049(4)	30(2)	1
C(17)	9097(10)	1930(7)	3580(4)	30(2)	1
C(18)	976(8)	2272(6)	-653(3)	25(2)	1
C(19)	2236(8)	320(5)	817(3)	23(2)	1
C(20)	6564(9)	111(6)	1978(3)	24(2)	1
C(21)	9165(10)	4017(6)	4246(3)	38(2)	1
C(22)	2536(10)	2627(6)	-208(4)	28(2)	1
C(23)	5312(9)	6404(7)	2242(4)	45(2)	1
C(24)	3956(9)	3325(6)	-466(4)	34(2)	1
C(25)	2088(11)	6074(7)	1347(5)	71(3)	1
C(26)	26(11)	6041(8)	2774(4)	64(3)	1
C(27)	2062(17)	7851(9)	2892(9)	241(12)	1
C(28)	1911(11)	6533(7)	2886(6)	80(4)	1
C(29)	2709(15)	6347(16)	3472(5)	225(13)	1
C(30)	7871(15)	-666(8)	3383(5)	95(5)	1
C(34)	15112(10)	2027(7)	4889(4)	39(2)	1
C(33)	12570(10)	2764(7)	5392(3)	43(2)	1
C(32)	13620(60)	2710(70)	4690(20)	330(60)	0.480(9)
O(1B)	10270(40)	1780(20)	4019(18)	67(10)	0.520(9)
C(37)	13940(30)	3570(18)	4427(13)	49(8)	0.480(9)
C(38)	12530(30)	502(17)	4794(9)	62(7)	0.520(9)
C(39)	13340(30)	2090(30)	4776(15)	42(7)	0.520(9)
C(42)	12884(10)	1006(6)	3290(3)	33(2)	1
C(40)	11720(20)	-94(12)	4414(8)	21(4)	0.480(9)

C(41)	13220(20)	3598(12)	3960(8)	30(4)	0.520(9)
Si(1)	2960(3)	5826(2)	2116(1)	36(1)	1

Table 3. Bond lengths [Å] and angles [°] for dcb34.

Si(2A)-O(1A)	1.68(3)	C(14)-H(14A)	0.9800
Si(2A)-C(40)	1.876(15)	C(14)-H(14B)	0.9800
Si(2A)-C(42)	1.943(8)	C(14)-H(14C)	0.9800
Si(2A)-C(32)	2.11(7)	C(15)-H(15A)	0.9900
Si(2B)-O(1B)	1.69(3)	C(15)-H(15B)	0.9900
Si(2B)-C(39)	1.75(3)	C(16)-C(17)	1.381(10)
Si(2B)-C(42)	1.793(8)	C(17)-O(1B)	1.35(3)
Si(2B)-C(41)	1.934(15)	C(18)-C(22)	1.470(9)
O(6)-C(10)	1.464(7)	C(18)-H(18A)	0.9800
O(6)-Si(1)	1.643(5)	C(18)-H(18B)	0.9800
O(4)-C(22)	1.456(8)	C(18)-H(18C)	0.9800
O(4)-C(3)	1.471(7)	C(19)-H(19A)	0.9800
O(3)-C(5)	1.426(8)	C(19)-H(19B)	0.9800
O(3)-H(3)	0.8400	C(19)-H(19C)	0.9800
O(5)-C(15)	1.441(7)	C(20)-H(20A)	0.9900
O(5)-C(22)	1.454(8)	C(20)-H(20B)	0.9900
O(1A)-C(17)	1.41(3)	C(21)-H(21A)	0.9800
C(1)-C(15)	1.516(9)	C(21)-H(21B)	0.9800
C(1)-C(10)	1.520(9)	C(21)-H(21C)	0.9800
C(1)-C(14)	1.567(9)	C(22)-C(24)	1.516(9)
C(1)-C(9)	1.572(8)	C(23)-Si(1)	1.892(8)
O(2)-C(16)	1.388(8)	C(23)-H(23A)	0.9800
O(2)-C(30)	1.403(11)	C(23)-H(23B)	0.9800
C(2)-C(10)	1.502(8)	C(23)-H(23C)	0.9800
C(2)-C(6)	1.554(8)	C(24)-H(24A)	0.9800
C(2)-H(2A)	0.9900	C(24)-H(24B)	0.9800
C(2)-H(2B)	0.9900	C(24)-H(24C)	0.9800
C(3)-C(9)	1.535(9)	C(25)-Si(1)	1.847(8)
C(3)-H(3A)	0.9900	C(25)-H(25A)	0.9800
C(3)-H(3B)	0.9900	C(25)-H(25B)	0.9800
C(4)-C(6)	1.551(9)	C(25)-H(25C)	0.9800
C(4)-C(5)	1.556(8)	C(26)-C(28)	1.523(11)
C(4)-C(9)	1.570(9)	C(26)-H(26A)	0.9800
C(4)-H(4)	1.0000	C(26)-H(26B)	0.9800
C(5)-C(20)	1.519(9)	C(26)-H(26C)	0.9800
C(5)-H(5)	1.0000	C(27)-C(28)	1.578(15)
C(6)-C(12)	1.540(9)	C(27)-H(27A)	0.9800
C(6)-C(8)	1.576(9)	C(27)-H(27B)	0.9800
C(7)-C(11)	1.391(9)	C(27)-H(27C)	0.9800
C(7)-C(12)	1.397(9)	C(28)-C(29)	1.449(17)
C(7)-H(7)	0.9500	C(28)-Si(1)	1.923(9)
C(8)-H(8A)	0.9800	C(29)-H(29A)	0.9800
C(8)-H(8B)	0.9800	C(29)-H(29B)	0.9800
C(8)-H(8C)	0.9800	C(29)-H(29C)	0.9800
C(9)-C(19)	1.537(9)	C(30)-H(30A)	0.9800
C(10)-H(10)	1.0000	C(30)-H(30B)	0.9800
C(11)-C(17)	1.412(10)	C(30)-H(30C)	0.9800
C(11)-C(21)	1.505(9)	C(34)-C(39)	1.45(3)
C(12)-C(13)	1.410(9)	C(34)-C(32)	1.65(5)
C(13)-C(16)	1.402(9)	C(33)-C(39)	1.55(3)
C(13)-C(20)	1.528(8)	C(33)-C(32)	1.73(5)

C(32)-C(37)	1.29(9)
C(38)-C(39)	1.94(4)
O(1A)-Si(2A)-C(40)	113.4(11)
O(1A)-Si(2A)-C(42)	112.9(13)
C(40)-Si(2A)-C(42)	108.8(5)
O(1A)-Si(2A)-C(32)	103.6(15)
C(40)-Si(2A)-C(32)	117(2)
C(42)-Si(2A)-C(32)	100.4(15)
O(1B)-Si(2B)-C(39)	109.1(16)
O(1B)-Si(2B)-C(42)	106.2(11)
C(39)-Si(2B)-C(42)	119.3(11)
O(1B)-Si(2B)-C(41)	112.0(12)
C(39)-Si(2B)-C(41)	99.8(12)
C(42)-Si(2B)-C(41)	110.5(6)
C(10)-O(6)-Si(1)	126.8(4)
C(22)-O(4)-C(3)	115.3(5)
C(5)-O(3)-H(3)	109.5
C(15)-O(5)-C(22)	116.3(5)
C(17)-O(1A)-Si(2A)	130(2)
C(15)-C(1)-C(10)	107.9(5)
C(15)-C(1)-C(14)	104.9(5)
C(10)-C(1)-C(14)	108.9(5)
C(15)-C(1)-C(9)	113.1(6)
C(10)-C(1)-C(9)	110.7(5)
C(14)-C(1)-C(9)	111.1(5)
C(16)-O(2)-C(30)	112.3(6)
C(10)-C(2)-C(6)	112.6(5)
C(10)-C(2)-H(2A)	109.1
C(6)-C(2)-H(2A)	109.1
C(10)-C(2)-H(2B)	109.1
C(6)-C(2)-H(2B)	109.1
H(2A)-C(2)-H(2B)	107.8
O(4)-C(3)-C(9)	110.2(5)
O(4)-C(3)-H(3A)	109.6
C(9)-C(3)-H(3A)	109.6
O(4)-C(3)-H(3B)	109.6
C(9)-C(3)-H(3B)	109.6
H(3A)-C(3)-H(3B)	108.1
C(6)-C(4)-C(5)	112.0(5)
C(6)-C(4)-C(9)	119.5(6)
C(5)-C(4)-C(9)	115.5(5)
C(6)-C(4)-H(4)	102.2
C(5)-C(4)-H(4)	102.2
C(9)-C(4)-H(4)	102.2
O(3)-C(5)-C(20)	111.5(6)
O(3)-C(5)-C(4)	111.1(6)
C(20)-C(5)-C(4)	110.5(6)
O(3)-C(5)-H(5)	107.9
C(20)-C(5)-H(5)	107.9
C(4)-C(5)-H(5)	107.9
C(12)-C(6)-C(4)	110.9(6)
C(12)-C(6)-C(2)	110.1(5)
C(4)-C(6)-C(2)	105.8(5)
C(12)-C(6)-C(8)	106.6(6)
C(4)-C(6)-C(8)	113.9(5)
C(2)-C(6)-C(8)	109.6(5)
C(11)-C(7)-C(12)	124.2(7)
C(11)-C(7)-H(7)	117.9
C(12)-C(7)-H(7)	117.9
C(6)-C(8)-H(8A)	109.5
C(6)-C(8)-H(8B)	109.5
H(8A)-C(8)-H(8B)	109.5
C(6)-C(8)-H(8C)	109.5
H(8A)-C(8)-H(8C)	109.5
H(8B)-C(8)-H(8C)	109.5
C(3)-C(9)-C(19)	108.6(5)
C(3)-C(9)-C(4)	109.4(5)
C(19)-C(9)-C(4)	108.9(5)
C(3)-C(9)-C(1)	110.8(5)
C(19)-C(9)-C(1)	109.7(5)
C(4)-C(9)-C(1)	109.4(5)
O(6)-C(10)-C(2)	107.6(5)
O(6)-C(10)-C(1)	110.2(5)
C(2)-C(10)-C(1)	115.2(6)
O(6)-C(10)-H(10)	107.9
C(2)-C(10)-H(10)	107.9
C(1)-C(10)-H(10)	107.9
C(7)-C(11)-C(17)	117.5(7)
C(7)-C(11)-C(21)	120.5(6)
C(17)-C(11)-C(21)	122.0(7)
C(7)-C(12)-C(13)	117.3(6)
C(7)-C(12)-C(6)	120.7(6)
C(13)-C(12)-C(6)	121.9(6)
C(16)-C(13)-C(12)	118.3(6)
C(16)-C(13)-C(20)	120.0(6)
C(12)-C(13)-C(20)	121.7(6)
C(1)-C(14)-H(14A)	109.5
C(1)-C(14)-H(14B)	109.5
H(14A)-C(14)-H(14B)	109.5
C(1)-C(14)-H(14C)	109.5
H(14A)-C(14)-H(14C)	109.5
H(14B)-C(14)-H(14C)	109.5
O(5)-C(15)-C(1)	113.0(6)
O(5)-C(15)-H(15A)	109.0
C(1)-C(15)-H(15A)	109.0
O(5)-C(15)-H(15B)	109.0
C(1)-C(15)-H(15B)	109.0
H(15A)-C(15)-H(15B)	107.8
C(17)-C(16)-O(2)	119.7(7)
C(17)-C(16)-C(13)	123.3(7)
O(2)-C(16)-C(13)	117.0(7)
O(1B)-C(17)-C(16)	120.7(14)
O(1B)-C(17)-O(1A)	11(3)
C(16)-C(17)-O(1A)	123.0(10)
O(1B)-C(17)-C(11)	120.6(14)
C(16)-C(17)-C(11)	118.6(7)
O(1A)-C(17)-C(11)	117.5(11)

C(22)-C(18)-H(18A)	109.5	H(26A)-C(26)-H(26B)	109.5
C(22)-C(18)-H(18B)	109.5	C(28)-C(26)-H(26C)	109.5
H(18A)-C(18)-H(18B)	109.5	H(26A)-C(26)-H(26C)	109.5
C(22)-C(18)-H(18C)	109.5	H(26B)-C(26)-H(26C)	109.5
H(18A)-C(18)-H(18C)	109.5	C(28)-C(27)-H(27A)	109.5
H(18B)-C(18)-H(18C)	109.5	C(28)-C(27)-H(27B)	109.5
C(9)-C(19)-H(19A)	109.5	H(27A)-C(27)-H(27B)	109.5
C(9)-C(19)-H(19B)	109.5	C(28)-C(27)-H(27C)	109.5
H(19A)-C(19)-H(19B)	109.5	H(27A)-C(27)-H(27C)	109.5
C(9)-C(19)-H(19C)	109.5	H(27B)-C(27)-H(27C)	109.5
H(19A)-C(19)-H(19C)	109.5	C(29)-C(28)-C(26)	112.9(11)
H(19B)-C(19)-H(19C)	109.5	C(29)-C(28)-C(27)	113.7(11)
C(5)-C(20)-C(13)	115.6(6)	C(26)-C(28)-C(27)	106.1(9)
C(5)-C(20)-H(20A)	108.4	C(29)-C(28)-Si(1)	110.7(7)
C(13)-C(20)-H(20A)	108.4	C(26)-C(28)-Si(1)	107.6(6)
C(5)-C(20)-H(20B)	108.4	C(27)-C(28)-Si(1)	105.4(8)
C(13)-C(20)-H(20B)	108.4	C(28)-C(29)-H(29A)	109.5
H(20A)-C(20)-H(20B)	107.5	C(28)-C(29)-H(29B)	109.5
C(11)-C(21)-H(21A)	109.5	H(29A)-C(29)-H(29B)	109.5
C(11)-C(21)-H(21B)	109.5	C(28)-C(29)-H(29C)	109.5
H(21A)-C(21)-H(21B)	109.5	H(29A)-C(29)-H(29C)	109.5
C(11)-C(21)-H(21C)	109.5	H(29B)-C(29)-H(29C)	109.5
H(21A)-C(21)-H(21C)	109.5	O(2)-C(30)-H(30A)	109.5
H(21B)-C(21)-H(21C)	109.5	O(2)-C(30)-H(30B)	109.5
O(5)-C(22)-O(4)	107.4(5)	H(30A)-C(30)-H(30B)	109.5
O(5)-C(22)-C(18)	112.5(6)	O(2)-C(30)-H(30C)	109.5
O(4)-C(22)-C(18)	107.1(6)	H(30A)-C(30)-H(30C)	109.5
O(5)-C(22)-C(24)	105.3(6)	H(30B)-C(30)-H(30C)	109.5
O(4)-C(22)-C(24)	111.1(6)	C(39)-C(34)-C(32)	30(4)
C(18)-C(22)-C(24)	113.4(7)	C(39)-C(33)-C(32)	28(3)
Si(1)-C(23)-H(23A)	109.5	C(37)-C(32)-C(34)	123(4)
Si(1)-C(23)-H(23B)	109.5	C(37)-C(32)-C(33)	124(4)
H(23A)-C(23)-H(23B)	109.5	C(34)-C(32)-C(33)	96(4)
Si(1)-C(23)-H(23C)	109.5	C(37)-C(32)-Si(2A)	116(3)
H(23A)-C(23)-H(23C)	109.5	C(34)-C(32)-Si(2A)	99(4)
H(23B)-C(23)-H(23C)	109.5	C(33)-C(32)-Si(2A)	93(3)
C(22)-C(24)-H(24A)	109.5	C(17)-O(1B)-Si(2B)	127(3)
C(22)-C(24)-H(24B)	109.5	C(34)-C(39)-C(33)	113.8(18)
H(24A)-C(24)-H(24B)	109.5	C(34)-C(39)-Si(2B)	123(2)
C(22)-C(24)-H(24C)	109.5	C(33)-C(39)-Si(2B)	117(2)
H(24A)-C(24)-H(24C)	109.5	C(34)-C(39)-C(38)	95.0(19)
H(24B)-C(24)-H(24C)	109.5	C(33)-C(39)-C(38)	100.8(16)
Si(1)-C(25)-H(25A)	109.5	Si(2B)-C(39)-C(38)	98.6(14)
Si(1)-C(25)-H(25B)	109.5	Si(2B)-C(42)-Si(2A)	32.6(2)
H(25A)-C(25)-H(25B)	109.5	O(6)-Si(1)-C(25)	108.9(3)
Si(1)-C(25)-H(25C)	109.5	O(6)-Si(1)-C(23)	111.8(3)
H(25A)-C(25)-H(25C)	109.5	C(25)-Si(1)-C(23)	109.2(4)
H(25B)-C(25)-H(25C)	109.5	O(6)-Si(1)-C(28)	104.3(4)
C(28)-C(26)-H(26A)	109.5	C(25)-Si(1)-C(28)	113.9(5)
C(28)-C(26)-H(26B)	109.5	C(23)-Si(1)-C(28)	108.8(4)